DOE/METC-93/6132
(CONF-930893)
(DE93011308)

# Proceedings of the Joint Contractors Meeting: FE/EE Advanced Turbine Systems Conference FE Fuel Cells and Coal-Fired Heat Engines Conference

Editor
Donald W. Geiling

Sponsored by
U.S. Department of Energy
Office of Fossil Energy
Morgantown Energy Technology Center
P.O. Box 880
Morgantown, West Virginia 26507-0880
(304) 291-4764
FAX (304 291-4403/4469

August 3-5, 1993

MASTER

DISTRIBUTION OF THIS DOCUMENT IS UNLIMITED

## DISCLAIMER

This report was prepared as an account of work sponsored by an agency of the United States Government. Neither the United States Government nor any agency thereof, nor any of their employees, make any warranty, express or implied, or assumes any legal liability or responsibility for the accuracy, completeness, or usefulness of any information, apparatus, product, or process disclosed, or represents that its use would not infringe privately owned rights. Reference herein to any specific commercial product, process, or service by trade name, trademark, manufacturer, or otherwise does not necessarily constitute or imply its endorsement, recommendation, or favoring by the United States Government or any agency thereof. The views and opinions of authors expressed herein do not necessarily state or reflect those of the United States Government or any agency thereof.

DISCLAIMER

Portions of this document may be illegible in electronic image products. Images are produced from the best available original document.

# Contents

## FE/EE Advanced Turbine Systems Conference

### Session 1 -- Studies and Conceptual Design


1.1 Development of Advanced Gas Turbine Systems -- Ronald L. Bannister, David A. Little, and Benjamin C. Wiant . . . . . 3

1.2 GE Power Generation Technology Challenges for Advanced Gas Turbines -- Dr. Charles S. Cook and John G. Nourse . . . . . 16

1.3 Gas Fired Advanced Turbine System -- Richard T. LeCren and David J. White . . . . . 26

1.4 Advanced Turbine Systems Program -- Colin Wilkes, Dale W. Mukavetz, T.K. Knickerbocker, and Dr. Sy A. Ali . . . . . 33

1.5 Advanced Turbine Systems - Studies and Conceptual Design -- Septimus van der Linden, Gregor Gnaedig, and Franz Kreitmeier . . . . . 42

1.6 METC Combustion Research Facility -- John S. Halow, Daniel J. Maloney, and George A. Richards . . . . . 67


### Session 2 -- Industrial Systems


2.1 Ceramic Retrofit Program -- Mark van Roode, Paul F. Norton, and William D. Brentnall . . . . . 77

2.2 Materials/Manufacturing Element of the Advanced Turbine System Program -- Michael A. Karnitz, Jack H. De Van, Robert S. Holcomb, and Arvid E. Pasto . . . . . 94


### Session 3 -- Related Programs


3.1 Collaborative Advanced Gas Turbine Program -- Arthur Cohn . . . . . 103

3.2 U.S. Navy Intercooled Recuperated (ICR) Engine -- Thomas L. Bowen . . . . . 109

3.4 Industry/University Consortium for ATS Research -- R.P. Allen and L.P. Golan . . . . . 119

# Contents
(Continued)

## ATS University Workshop

Welcome - ATS University Workshop -- R.P. Allen and L.P. Golan . . . . . 125

University Participation in the ATS Program -- Roy P. Allen and Lawrence P. Golan . . . . . 127

## University Presentations

W2 Ultra-Low Gas Turbine Emissions Using Catalytic and Noncatalytic Porous Combustors -- Roy P. Allen, Robert W. Dibble, Juh-Yuan Chen, and Robert F. Sawyer . . . . . 137

W3 Reduction of Turbine Endwall Total Pressure Loss and Heat Transfer Using the Iceformation Design Method -- Roy P. Allen and Dr. Ronald S. LaFleur . . . . 139

W4 Functionally Gradient Materials For Thermal Barrier Coatings In Advanced Gas Turbine Systems -- Roy P. Allen and Dr. Arnold R. Marder . . . . . 140

W5 Vortex-Generator Induced Enhanced Heat Transfer in Gas Turbine Blade Coolant Channels With Rotation -- Roy P. Allen, Sumanta Acharya, Tod A. Myrum, Dimitris Nikitopoulos, and Joel Tohline . . . . . 142

W6 Life Prediction of Advanced Materials for Gas Turbine Applications -- Roy P. Allen, Sam Y. Zamrik, Asok Ray, and Donald A. Koss . . . . . 144

W7 $NO_x$ Abatement in Advanced Gas Turbines -- Roy P. Allen, P.E. Sojka, J.P. Gore, and N.M. Laurendeau . . . . . 146

# FE Coal-Fired Heat Engines Conference

## Session 1 -- Coal-Fueled Turbines

1.1 Interface Between a Gas Turbine and PFBC -- Ronald L. Bannister, Arthur W. McGuigan, James A. Christenson, Ivan L. Howell, Ezio Marson, Michael V. Post, Thomas P. Risley, and Terry L. Vota . . . . . 151

# Contents
(Continued)

1.2 Full-Scale and Bench-Scale Testing of a Coal-Fueled Gas Turbine System -- Peter B. Roberts, Richard T. LeCren, Luke H. Cowell, Marlene A. Galica, Michael D. Stephenson, and Chaur S. Wen . . . . . 165

1.3 High Pressure Ceramic Air Heater for Indirectly-Fired Gas Turbine Applications -- Paul G. LaHaye, Gwynne F. Briggs, Nelson J. Orozco, and John L. Seger . . . . . 167

1.4 Direct Coal-Fired Gas Turbines for Combined Cycle Plants -- John Rothrock, Richard Wenglarz, Peter Hart, and Hukam Mongia . . . . . 178

1.5 Heavy Duty Gas Turbine Combustion Tests With Simulated Low BTU Coal Gas -- Thomas E. Ekstrom, Robert A. Battista, Frank H. Belisle, and Gregory P. Maxwell . . . . . 186

1.6 Combustion Tests of a Turbine Simulator Burning Low Btu Fuel From a Fixed Bed Gasifier -- Charles S. Cook, Nesim Abuaf, Alan S. Feitelberg, Stephen L. Hung, David J. Najewicz, and Martin S. Samuels . . . . . 199

## Session 2 -- Coal-Fueled Diesels

2.1 Commercialization of Coal Diesel Engines for Non-Utility and Export Power Markets -- Robert P. Wilson, Kam Rao, Eric N. Balles, Karen R. Benedek, Charles E. Benson, Ronald A. Mayville, Daniel Itse, Jack Kimberley, and James Parkinson . . . . . 211

2.2 Coal-Fueled Diesel Engines for Locomotive Applications -- Bertrand D. Hsu, David J. Najewicz, and Charles S. Cook . . . . . 222

# FE Fuel Cells Conference

## Session 1 -- Molten Carbonate Fuel Cells

1.1 Overview of ERC's Carbonate Fuel Cell Development Program -- Bernard S. Baker, Christopher R. Bentley, and Donald R. Glenn . . . . . 239

1.2 Overview of M-C Power's MCFC Power Generation System -- Thomas G. Benjamin and Richard R. Woods . . . . . 250

# Contents
(Continued)

1.3 MCFC Product Development Test -- Ashok K. Kush, Anthony J. Leo, and Thomas P. O'Shea . . . . . 255

1.4 Molten Carbonate Fuel Cell Product Development Test -- Joseph A. Scroppo, Elias H. Cámara, and R. Al Figueroa . . . . . 263

1.5 MCFC Power Plant System Verification -- Mohammad Farooque, R. Bernard, J. Doyon, L. Paetsch, P. Patel, A. Skok, and C. Yuh . . . . . 280

1.6 Simulated Coal Gas MCFC Power Plant System Verification -- Elias H. Cámara, Thomas G. Benjamin, Leonard G. Marianowski, Vincent J. Petraglia, and René M. Laurens . . . . . 288

## Session 2 -- Solid Oxide Fuel Cells

2.1 High Temperature Solid Oxide Fuel Cell Development Activities -- Emerson R. Ray . . . . . 293

2.2 MSOFC Development Status -- Dr. Richard A. Gibson and Dr. Nguyen Q. Minh . . . . . 299

2.3 High Temperature Solid Oxide Fuel Cell - Customer Test Units -- Emerson R. Ray and Stephen E. Veyo . . . . . 304

2.4 Contaminant Effects in Solid Oxide Fuel Cells -- Emerson R. Ray and Nicholas J. Maskalick . . . . . 313

Commercialization of Fuel Cells in the 21st Century -- R.A. Figueroa . . . . . 323
(Presented as part of panel discussion)

## Poster Session
## Heat Engines and Fuel Cells

P1 Particulate Control for Coal-Fueled Diesel Engine Exhaust -- Dr. Leo A. Smolensky and Dr. Bruce H. Easom . . . . . 327

P3 Sub-Scale Development of an Acoustically Enhanced Cyclone for PFBC -- Marlene A. Galica . . . . . 334

# Contents
(Continued)


P4 Air Extraction in Gas Turbines Burning Coal-Derived Gas -- Tah-teh Yang, Ajay K. Agrawal, and Jayanta S. Kapat . . . . . 335

P5 Development of a Dry-Feed System for a Coal-Fired Gas Turbine -- John W. Rothrock Jr. and Craig F. Smith . . . . . 345

P6 METC Research on Coal-Fired Diesels -- Michael H. McMillian, Edward H. Robey, and Richard E. Addis . . . . . 355

P7 Pressure-Gain Combustion -- George A. Richards, Joseph Yip, Randall S. Gemmen, Michael C. Janus, Thomas Norton, and William A. Rogers . . . . . 366

P8 Pressurized Burner Test Facility -- Daniel J. Maloney, Thomas S. Norton, and Mark A. Hadley . . . . . 373

P9 Premixed Burner Studies of $NO_x$ Formation and Control -- Kent H. Casleton, Doug L. Straub, Colleen Moran, and James W. Stephens . . . . . 376

P10 The DOE NEPA Process -- Suellen A. Van Ooteghem . . . . . 383

P11 Research and Development of Alternative Components at Argonne National Laboratory for Molten Carbonate Fuel Cells -- K.M. Myles, M. Krumpelt, G.H. Kucera, M. Roche, and E. Indacochea . . . . . 386

P12 Sealant Research for Solid Oxide Fuel Cells -- Kevin M. Myles, Ira Bloom, Michael Krumpelt, Kevin L. Ley, Stephen E. Dorris, and Arun S. Wagh . . . . 393

P13 Alternative Materials for Solid Oxide Fuel Cells: Processing and Interactions of Materials -- Dr. J. Lambert Bates, Dr. Timothy R. Armstrong, and Dr. Larry A. Chick . . . . . 398

P14 Low Cost, Radial Flow, Solid Oxide Fuel Cell -- Michael A. Petrik . . . . . 409

P15 Processing of $LaCrO_3$ for Solid Oxide Fuel Cell Applications -- Wayne Huebner, Magdi M. Nasrallah, and Harlan U. Anderson . . . . . 415

P17 Advanced Research and Technology Development of MCFCs -- Thomas G. Benjamin, Robert J. Remick, and Rafael A. Donado . . . . . 425

P18 Fuel Cell Handbook Update -- William R. Owens, John H. Hirschenhofer, Ronald R. Engleman Jr., and David B. Stauffer . . . . . 432

# Contents
(Continued)

P19 Macrocyclic Redox Promoters for Methanol Oxidation -- Shantha Sarangapani . . . 437

P20 Optical Sensor Development for MCFCs: HCl Detection Through Wavelength Modulation Diode Laser Absorption Spectroscopy -- Robert Hanold, David J. Funk, Byron A. Palmer, and Richard C. Oldenborg . . . . . 446

P21 Perovskite Solid Electrolytes for SOFC -- Anthony F. Sammells . . . . . 456

## Appendices

Appendix A. Agenda . . . . . 463

Appendix B. Meeting Participants . . . . . 476

Appendix C. METC Participants . . . . . 497

# FE/EE Advanced Turbine Systems Conference

## Session 1

## *Studies and Conceptual Design*

## 1.1 Development of Advanced Gas Turbine Systems

### CONTRACT INFORMATION

| | |
|---|---|
| **Contract Number** | DE-AC21-86MC23167 |
| **Contractor** | Westinghouse Electric Corporation<br>4400 Alafaya Trail<br>Orlando, Florida 32826-2399<br>(407) 281-3270 |
| **Contractor Project Manager** | Ronald L. Bannister |
| **Principal Investigators** | David A. Little<br>Benjamin C. Wiant |
| **METC Project Manager** | Donald W. Geiling |
| **Period of Performance** | July 24, 1986 to August 15, 1993 |

### OBJECTIVES

The objective of the Advanced Turbine Systems study is to investigate innovative natural gas fired cycle developments to determine the feasibility of achieving 60% efficiency within a 8-year time frame. The potential system was to be environmentally superior, cost competitive and adaptable to coal-derived fuels.

### BACKGROUND INFORMATION

The National Energy Strategy (NES) calls for a balanced program of greater energy efficiency, use of alterative fuels, and the environmentally responsible development of all U.S. energy resources. Consistent with the NES, a Department of Energy (DOE) program has been created to develop Advanced Turbine Systems (ATS). The technical ATS requiremens are based upon two workshops held in Greenville, SC that were sponsored by DOE and hosted by Clemson University. The objective of this 8-year program, managed jointly by DOE's Office of Fossil Energy and Office of Energy Efficiency and Renewable Energy, is to develop natural gas fired base load power plants that will have cycle efficiencies greater than 60% (LHV), be environmentally superior to current technology, and also be cost competitive. The program will include work to transfer advanced technology to the coal-and biomass-fueled systems being developed in other DOE programs.

The Advanced Turbine Systems program is structured into four elements:

- Innovative Cycle Development
- Utility Advanced Turbine Systems
- Industrial Advanced Turbine Systems
- Technology Base

Within each program element there are several planned phases. The Innovative Cycle Studies element includes two phases:

- Program Definition/Planning Studies
- Concept Development

This paper describes the response of the Westinghouse Electric Corporation to Phase I, Program Definition/Planning Studies of the Innovative Cycle Studies Element.

## INTRODUCTION

The gas turbine combined cycle, a synergistic combination of the Brayton and the Rankine cycle, was developed to increase overall cycle efficiency. Heat rejected by the higher temperature topping cycle is recovered in the lower temperature bottoming cycle to produce additional power from the energy initially released by the fuel. In the last 25 years combined cycle efficiency has increased, primarily driven by the escalation in gas turbine inlet temperature.

Today, with a turbine inlet temperature of about 2460°F (2300°F rotor inlet temperature), natural gas combined cycles are in the range of 54 to 55%.

The target of 60% combined cycle efficiency by the year 2000 seems beyond reach if the inlet temperature is raised and the combined cycle configuration is basically unchanged. In this study, innovative changes to the combined cycle were investigated to see if the 60% plant cycle efficienty can be attained.

## CYCLE STUDIES

Intercooling between compressor stages to reduce compression power has long been a feature of centrifugal compressor installations. Thus, inclusion of intercooling by splitting the single axial compressor into a low pressure (LP) and a high pressure (HP) section was an obvious suggestion. Since HP compressor delivery temperature is greatly decreased with intercooling, additional benefits accrue to the cooling air system. The traditional rotor air cooler which supplies 475°F air can be eliminated, and to maintain the same cooled vane metal temperatures, less (uncooled) compressor delivery air can be used.

The lower compressor delivery temperature also leads logically into another idea, that of exhaust gas recuperation. Westinghouse has a long history of recuperative turbine (W52, W62, W92) installations, the most recent of which was the CW352RM (35,000 hp, 2 shaft, mechanical drive), where higher gas turbine efficiency was achieved by recuping hot exhaust gas energy. Heat exchange between exhaust gas and compressor delivery air significantly reduces the quantity of fuel required to achieve a specified turbine inlet temperature. With intercooling, compressor delivery air temperature would be much lower, thus there would be an even greater flow of exhaust energy back into the Brayton cycle through the recuperator.

In the combined cycle configuration, the effect of recuperation on efficiency is not quite as obvious because exhaust gases leave the cycle at stack gas temperature (typically 220°F) whether or not recuperation is employed. Recuperation redirects exhaust energy from the bottoming, Rankine cycle into the topping, Brayton cycle, thus as long as the Brayton cycle is more efficient than the Rankine cycle, recuperation should benefit cycle efficiency.

The intercooled, recuperative combined cycle (ICRCC), shown in Figure 1, was analyzed and compared to the base cycle in Figure 2. At the same rotor inlet temperature, and the same turbine expansion ratio (≈ 18:1), combined cycle efficiency was found to increase a very significant 1.5 to 2.0 percentage points.

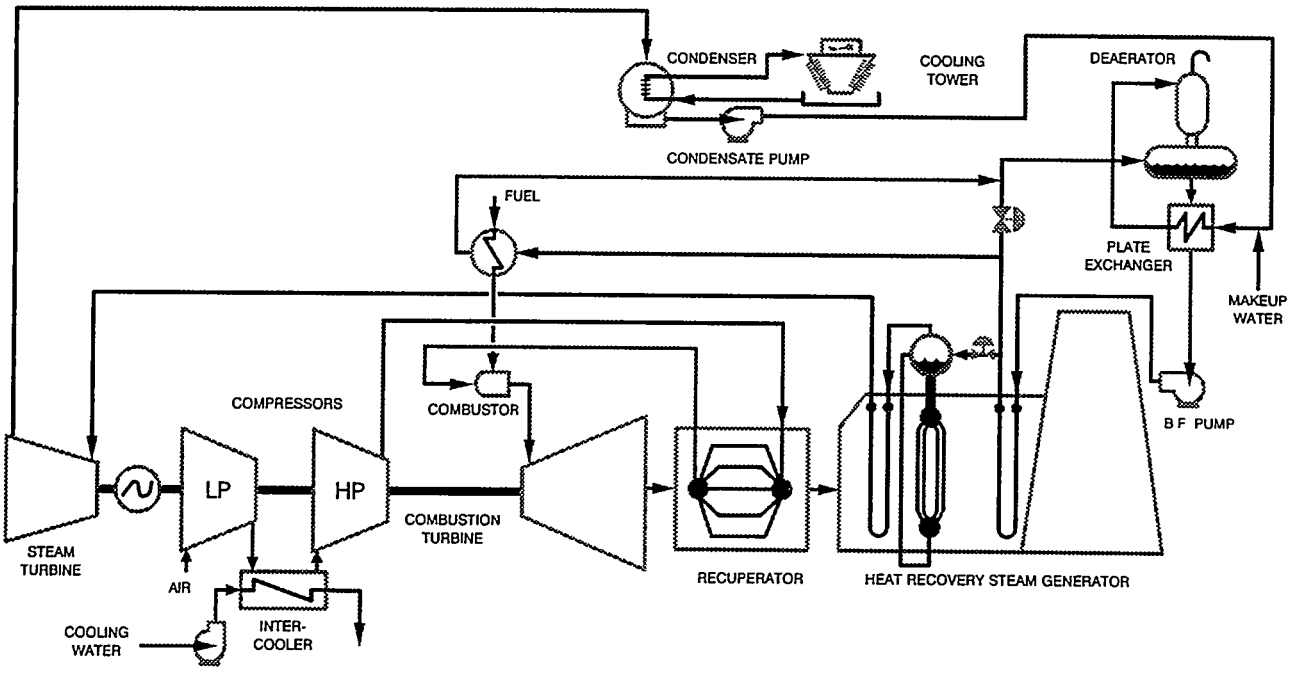


**Figure 1. Intercooled, Recuperative Combined Cycle**

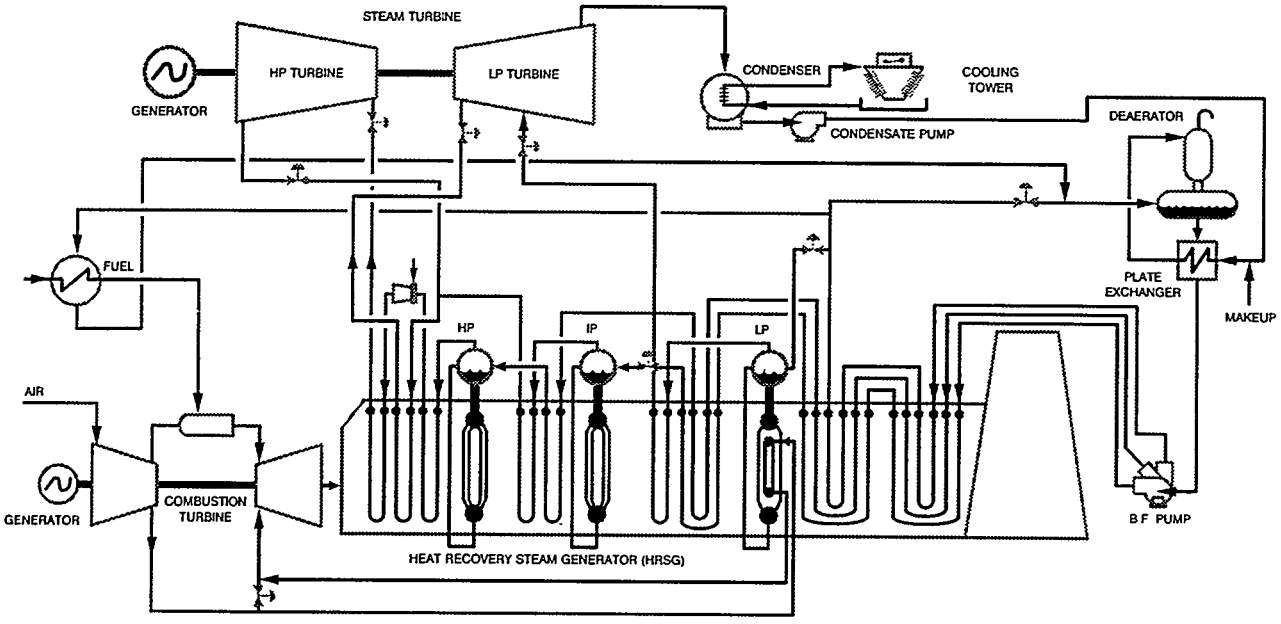


**Figure 2. 501F Based, Natural Gas Fired, Combined Cycle Plant**

The turbomachinery for the ICRCC, illustrated in Figure 1, is directly coupled to form a single shaft operating at 3600 RPM. The HP compressor and gas turbine would be a two bearing rotor in a single housing. The LP compressor, generator and steam turbine would have individual rotors in separate housings. The generator rotor would be double ended so that it can be driven from both ends. The steam and gas turbines would probably have their own thrust bearings to maintain proper axial position of the rotors relative to stationary parts.

Westinghouse's experience using single-shaft designed mechanical drive gas turbines directly coupled to steam turbines will be utilized. Steam system and/or gas turbine transients are not considered to be an operational problem. The overall control system is simpler for single shaft versus multishaft plant designs for similar ratings.

Within the basic intercooled, recuperative combined cycle configuration, the broad question of water vapor addition to the Brayton cycle and its effect on efficiency was also investigated. Evaporative cooling of inlet air has long been a technique employed to increase gas turbine and combined cycle power when inlet air is hot and dry. Steam injection into compressor delivery air for power augumentation has be incorporated into many gas turbines over the years. Water spray evaporative intercooling was designed for the Japanese Advanced Reheat Gas Turbine pilot plant project (Moonlight) in the late 70s, early 80s. The Humid Air Turbine (HAT) cycle entirely eliminates the steam turbine bottoming cycle, and instead uses recuperator exhaust energy to heat water for humidification of compressor delivery air.

The first alternative considered is shown in Figure 3, where an evaporative aftercooler is incorporated within the basic ICRCC. HP compressor delivery air is cooled as it evaporates preheated intercooler water, thus allowing more heat transfer from turbine exhaust gas into aftercooler exit air through the recuperator. Gas turbine power increases considerably since additional mass (water vapor) is now available for expansion through the turbine while the compressor's mass flow has not changed. Bottoming cycle power decreases, but by only 1/3 of the gas turbine's power increase. However, gas turbine fuel consumption also increases because the additional water vapor flowing through the combustors is heated to turbine inlet temperature. The net effect on combined cycle efficiency is not clear, and conflicting results have been calculated, depending on cycle assumptions. Further study will be needed to clarify the potential for this type of humidification. The intercooler shown in Figures 1 and 3 could also take the form of spray cooling (humidification), instead of surface heat transfer.

The ultimate form of intercooling is continual evaporative cooling of the compression process (Figure 4) through the introduction of a fine water mist into each compressor stage. Preheated water droplets about 5 microns in diameter would possibly evaporate in each stage providing a continuous reduction in the heat of compression. Initial cycle calculations show that this concept may provide a significant boost to cycle efficiency.

A preliminary analysis of this concept indicates a 25 to 30% reduction in the work of the compressor; a corresponding reduction in the temperature increase over the compressor; and, perhaps a reduction in the water used over a staged inter-and after-cooler process.

Continual or staged evaporation of water into the recuperator air stream is yet another idea investigated in this preliminary phase. Recuperator gas side exit temperature will be lowered by this technique leaving less energy for the lower efficiency bottoming cycle. Preliminary indications are that combined cycle efficiency will be enhanced by the additional transfer of exhaust energy into the topping cycle.

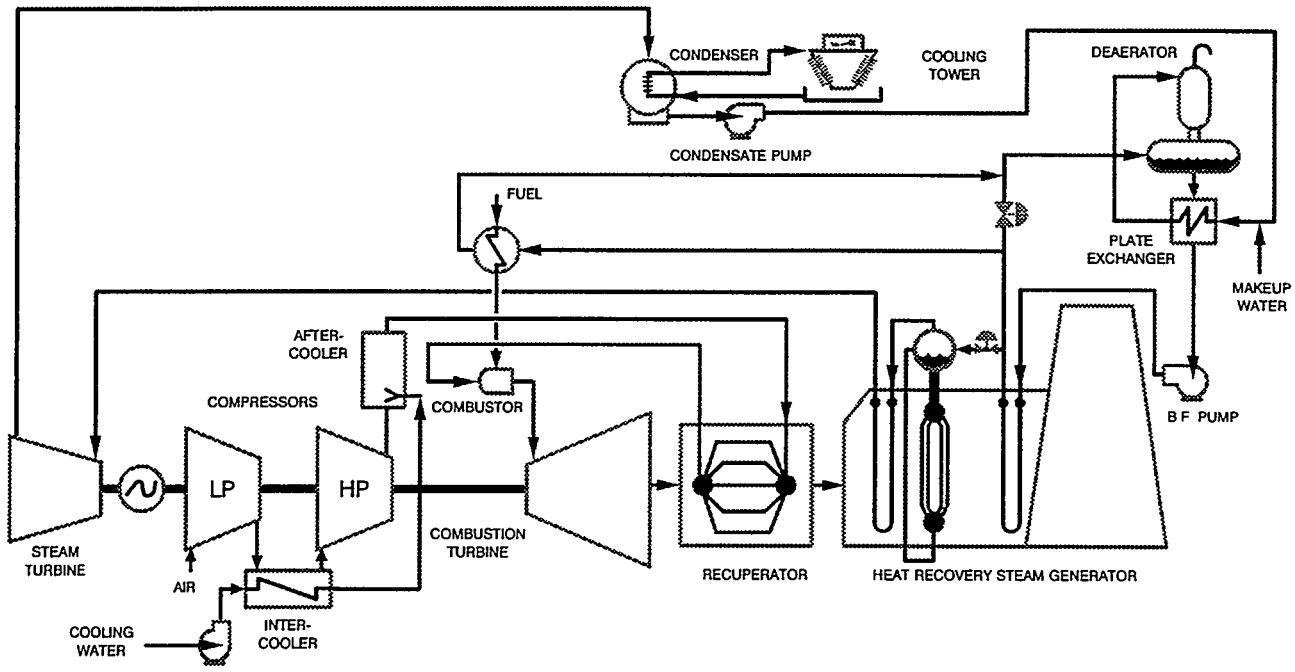


**Figure 3. Intercooled, Aftercooled (Evaporative), Recuperative Combined Cycle**

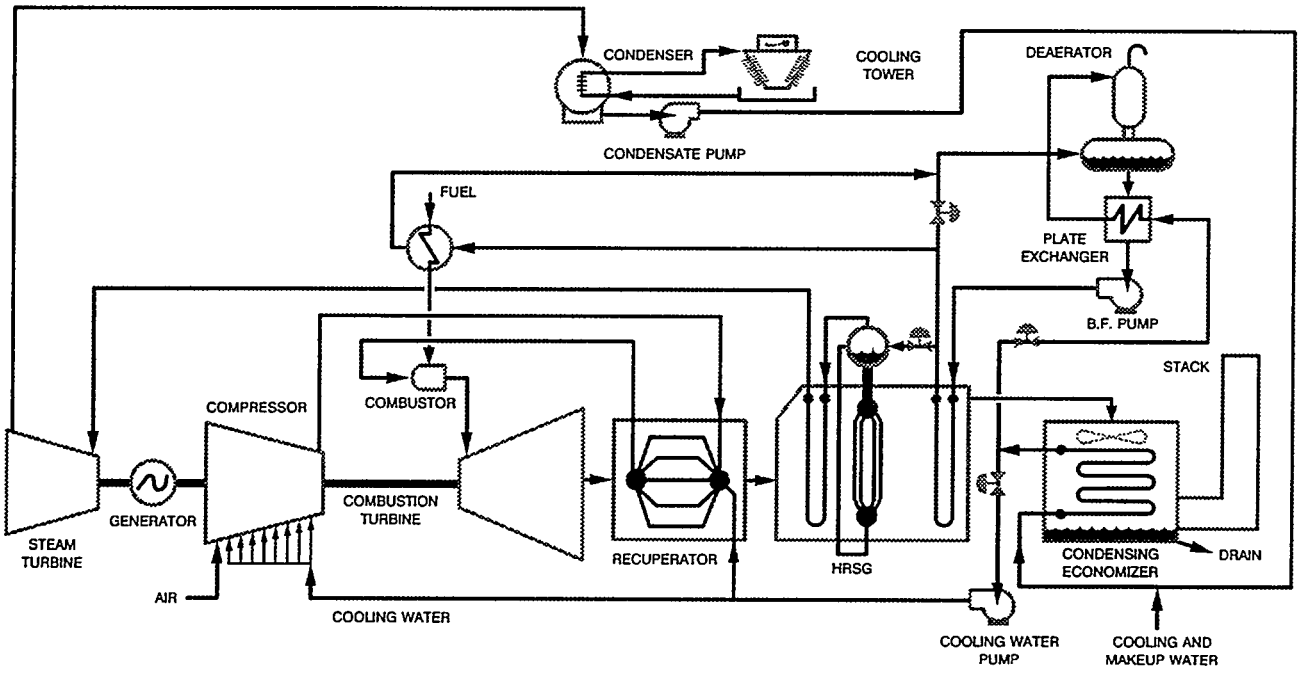


**Figure 4. Condensing Economizer in Humidified ICRCC**

With evaporation of water into the open Brayton cycle, all the latent heat of vaporization which has been supplied by the cycle is rejected to atmosphere. Cycle efficiency can be raised by condensing a portion of the exhaust vapor in a condensing economizer as long as the very low grade heat (<212°F) is returned to the cycle. A teflon coated condensing economizer, heating evaporation water from 59° to 200°F by condensing and cooling the stack gases, would recover about 16% of the heat required to evaporate water into the gas turbine.

Another innovation in the combined Brayton and Rankine cycles which will provide increased cycle efficiency at constant rotor inlet temperature is closed loop steam cooling. Closed loop steam cooling involves directing a portion of the dry steam raised in the HRSG through the walls of stationary hot end components, such as combustor baskets, transitions, and vanes, prior to expanding it through the steam turbine. The steam, which is superheated as it removes heat radiated and convected from the hot gas path, is supplied to the steam turbine.

By comparing steam turbine output with, and without, closed loop steam cooling, it was found that additional power, equivalent to 35% to 40% of the heat absorbed by the steam in the gas turbine, would be generated. For row 1 vane cooling alone, this could raise overall efficiency about 0.8 percentage points.

Closed loop steam cooling of stationary rows 2, 3 (and 4) could provide another 0.5 percentage point or more in increased cycle efficiency, since in addition to the extra steam superheat, turbine exhaust temperature will increase significantly, thus enhancing the effectiveness of both the recuperator and the HRSG.

Thermochemical recuperation of gas turbine exhaust energy, as shown in Figure 5, was also considered. Here only the gas turbine would produce power (no longer a combined cycle) by burning reformed, recuperated fuel. Methane and sufficient steam in the presence of a catalyst, and at appropriate temperature, will reform into a low Btu fuel consisting of $H_2$ and CO. None of the latent heat of vaporization of steam generated in the HRSG is lost to the cycle, and so the potential exists for efficient exhaust energy recuperation. In current reforming technology, methane conversion efficiency is a function of pressure, temperature and excess steam/methane ratio.

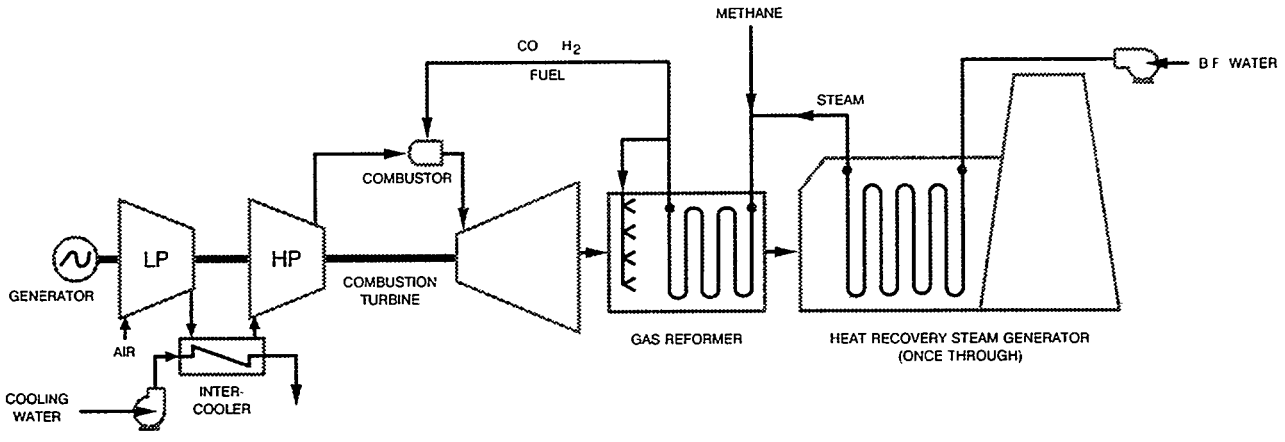


**Figure 5. Thermo Chemical Recuperation Cycle**

One final reconfiguration of the combined cycle with the turbine split to allow reheat after partial expansion, as shown in Figure 6, was studied. At a cycle pressure ratio of approximately 20:1, it was found that combined cycle efficiency dropped about 4.0 percentage points when compared to the ICRCC of Figure 4, therefore the idea was dropped.

be determined, however, due to the preliminary nature of the studies.

Reinforcing the selection of the ICRCC as the reference ATS, is the award by the U.S. Navy to Westinghouse's Marine Division to develop an ICR engine system. The Westinghouse-Rolls, WR21, engine will use all the major components (LP and HP compressors, combustor, HP, LP and

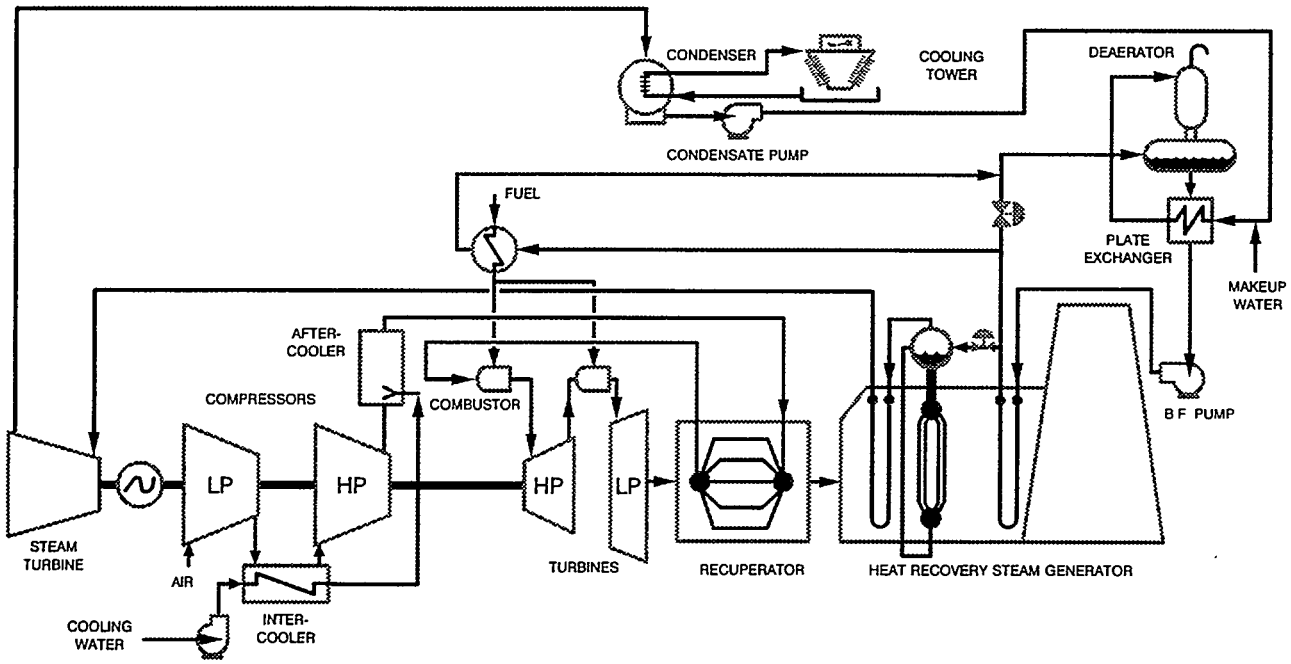


**Figure 6. Reheat Combined Cycle**

The conclusion reached from Phase I cycle studies was that compressor intercooling, combined with exhaust recuperation and closed loop steam cooling should be considered as the reference cycle for ATS in Phase I. The optimal types of intercooling and recuperation could not

power turbine) of the RB211 aircraft engine in combination with a compact AiResearch surface intercooler and recuperator. The aggressive development schedule targeting initial engine demonstration in early 1994, will allow lessons learned from system integration, component

testing, and engine testing to be applied to the reference ATS.

## EFFICIENCY ENHANCEMENT WITHIN THE ADVANCED CYCLE

Within the framework of the ICRCC, cycle efficiency will be further increased by:

- Raising firing temperature
- Reducing cooling air requirement
- Using pressure gain pulse combustion
- Increasing component aerodynamic efficiencies, and
- Reducing clearances and leakages

Raising the rotor inlet temperature from its current, 2300°F level in the 501F is necessary for the advanced turbine system to achieve its 60% (LHV) target. If turbine inlet temperature increase on its own is considered, while holding metal temperatures in the hot gas path components constant through the use of additional quantities of cooling air, the increase in cycle efficiency of only 1.2 percentage points is all than can be expected for a 200°F increase in the rotor inlet temperature.

It is anticipated that an increase in rotor inlet temperature of about 300°F will be necessary within the ATS to allow achievement of target efficiency. Turbine inlet temperature on the other hand, would increase only about 150°F if closed loop steam cooling of the row 1 vane is incorporated. This is because the 150°F drop in gas path temperature, when row 1 vane cooling air is mixed in upstream of the row 1 blade, would no longer exist.

As rotor inlet temperaure increases, the cooling air quantity required to hold metal temperature also increases significantly. Reducing this cooling air requirement is an extremely effective method for increasing cycle efficiency, since more of the air which has absorbed work in the compressor can now be brought to the turbine and expanded through all four stages of the turbine. Because exhaust temperature increases, heat transfer through the recuperator into the compressor air stream is enhanced, requiring less fuel/lb of air, and more heat is available to the bottoming cycle. At ATS conditions, each reduction in cooling air requirement of 1% of compressor inlet flow would increase cycle efficiency approximately 0.2 percentage points.

As discussed previously, closed loop stream cooling of stationary vanes is the most effective method of eliminating cooling air, since cooling air is replaced by steam (which doesn't enter the gas path).

Another benefit of cycle innovation is the decrease in compressor temperatures accompanying intercooling. Less, lower temperature cooling air will be required to hold specified metal temperatures. When spray evaporation into, between, and/or after the compressors is incorporated, even less cooling air will be required due to the higher specific heat of the water vapor/air mixture.

Increasing the Mach No. through the first row vane by opening the throats of subsequent rows will reduce gas path temperatures into downstream rows, and subsequently reduce the cooling demand. Regauging will affect aerodynamic efficiency, so the optimum cooling flow - efficiency combination must be found.

The application of thermal barrier coatings (10 to 30 mils) to the outside aerofoil surfaces will reduce conduction of heat from the hot gas

path into the cooled aerofoil, and thus reduce the amount of cooling air required. Ensuing good bonding to the substrate, fatigue resistance, and surface smoothness will be prerequisites to this method of cooling air reduction.

Currently the last 3 (of 4) stages in the 501F are cooled. First stage vane cooling is accomplished by a combination of impingement, film and convective cooling. First stage blade cooling incorporates serpentine, ribbed, pin fin passages with external film. Both of these highly complex cooling schemes may be further refined, but potential gains are small. Alternatively, several approaches which have been investigated in the past may be reconsidered.

One of the most promising of these is shell/spar construction. Shell/spar vanes and blades may be formed by bonding a thin non-porous aerofoil shaped metal sheet (the shell) to an inner hollow cast support member (the spar), or by casting. Cooling air for the assembly is supplied from alternate cavities within the spar (the supply cavities). It flows along chordwise convection cooling channels between the spar and the shell and returns to the remaining spar cavities (the discharge cavities). The heated or spent cooling air is then routed from the discharge cavities to the main gas stream through exit holes in the shrouds or areofoil.

Another approach identified by Westinghouse with Allison/GM under the High Temperature Turbine Technology (HTTT) program was advanced transpiration type cooling. This transpiration design consists of two layers of sheet material diffusion bonded to a hollow, cast spar. In the leading edge region, the sheet is solid to minimize susceptibility to erosion and deposition and is cooled by a multiple diffusion bonded scheme. In the trailing edge region, the outer layer of the sheet material is solid for aerodynamic and fabrication reasons and is cooled via chordwise channels located in the inner layer of the skin. Over the rest of the airfoil, the skin is tangential injection Lamilloy) which is a porous material that produces quasi-transpiration cooling. Preliminary studies have demonstrated the improved heat transfer effectiveness of Lamilloy over conventional multipass cooling, thereby providing the leverage to reduce cooling requirement.

In the later stages, spanwise holes which taper from hub to mid-height represent an improvement over the constant diameter holes used in rotor blade cooling. With this technique, increased cooling in the critical mid-height region is obtained by reducing overcooling in the hub region, resulting from the lower coolant temperature as cooling air enters the hub region. Increased hub region flow area obtained by tapering reduces heat transfer in that region, thus reducing temperature rise in the coolant as it flows radially outward.

Another variation in cooling hole geometry is to integrally cast circumferential ribs periodically spaced along the length of each cooling hole. These ribs act as flow turbulators to produce turbulent rather than laminar heat transfer for the cooling air. Field tests have been run on a 501 engine comparing smooth and turbulated holes. These tests verified that the heat transfer coefficient was doubled by the use of the turbulators.

A combination of turbulators and tapered holes could provide a very significant improvement in the cooling effectiveness in the ATS.

Cooling flow could also be reduced if higher temperature material/coating systems could be incorporated. Higher creep strength vane and blade alloys, which when processed to form directionally solidified (DS) or single crystal (SC) structures, should offer temperature advantages of 75° to 200°F over conventionally cast alloys as

illustrated in Figure 7. Hot corrosion/oxidation protection of these blades at the higher operating temperatures will be provided by advances in existing MCrAlY coatings. Development of these systems to allow implementation into the ATS is required.

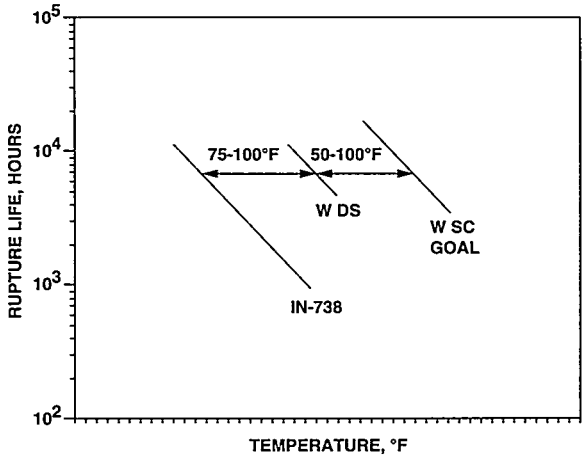


**Figure 7. Temperature Advantage of Westinghouse DS and SC Alloys**

Uncooled blade path components would obviously greatly increase advanced turbine system efficiency. Ceramics and ceramic composites will be considered during the ATS program for application in stationary components (baskets, transitions, row 1 vane).

Another area that has potential for cooling air reduction is the reduction in the severity of the combustor hot spot that must be accounted for during design. In the case of the stage 1 vane, some vanes in the row will be directly impacted by the hot spot. This hot spot will also be carried downstream, but will be attenuated by the averaging out process due to blade rotation. Even so, the hot spot temperature may also have a special effect on the rotating blade due to rotational effects. Reduced peak temperatures will allow less cooling of both stage 1 vanes and blades.

Better utilization of the cooling flow is another potentially beneficial area. In the 501F engine, some 60% of the cooling air is used for aerofoil cooling. Most of the remainder leaks into the turbine hot gas path through clearances in the parts which bound the coolant flow path as it proceeds through the engine. These clearances are required to permit differential expansion of parts during temperature transients in order to avoid low cycle fatigue damage. Improved design techniques will be brought to bear in the ATS program to minimize cooling system leakage.

Cooling air flowing through inner and outer shroud cavities prevents hot gas ingress, and maintains the casing and rotor at required temperatures. Cascading some of this flow downstream to the following stages within the cooled shroud regions as illustrated in Figure 8, before finally allowing it to escape to gas path (instead of exhausting immediately into the gas path), will reduce considerably the total quantity of air used for cooling.

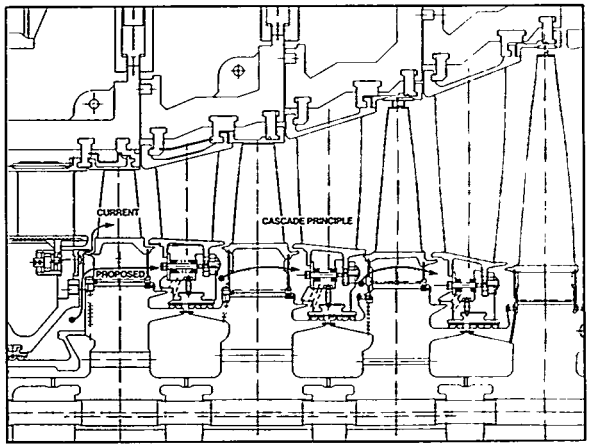


**Figure 8. 501F Engine Cascade Cooling Principle**

For example, a large portion of the torque tube seal leakage, which on the 501F enters the blade path through the stage 1 blade platform seal, could be cascaded into the stage 2 disk cavity through holes added to the stage 1 blade side plates. This flow would then be available to supply a portion of the stage 2 interstage seal leakage, thus reducing the stage 2 cooling air supply. Changes in design philosophy in combination with tightly controlled seals would be required, but the potential 0.2 percentage point increase in ATS cycle efficiency makes it worth the effort.

Another concept to consider that could raise plant cycle efficienty is pressure gain, pulse combustion. This is a process by which periodic reignition and combustion of a combustible mixture causes a time averaged steady inflow of fresh air and fuel, and outflow of products of combustion. In essence, the combustor, in addition to combusting the fuel, pumps its own air. The advantage of this phenomena is that in the ATS environment the combustor can act as an additional compression device instead of a pressure loss component.

With a potential 5% pressure gain in the ATS from a pulse combustor (vs. 3 to 4% loss with conventional combustors) it is estimated that ATS efficiency should increase at least 1.2 percentage points by incorporation of a pulse combustor.

NOx production from pulse combustors is inherently low because of the very short duration of the pulse (approximately 6 milliseconds at 80 Hz frequency), and the fact that thermal NOx is generated both as a function of temperature and time. With the requirement for dry, ultra-low NOx, CO and UHC emissions driving combustor development, the possible use of pulse combustion will be explored to estabish emission levels for a larger scale combustor.

Within the ICRCC configuration, improving the aerodynamic efficiencies of the compressors to reduce compression work, and the turbine to increase expansion work will enhance overall efficiency. The 501F compressor with an average polytropic of 92% is very efficient, and was designed based on Westinghouse's 20 years of accumulated 501AA to D5 design experience. However, it has not yet reached the limit of aerodynamic efficiency. Aero technology, now available to Westinghouse through a 15-year technology agreement with Rolls-Royce, will enable the ATS compressors to be designed to optimize loading with minimum loss for each row of aerofoils.

Likewise the 501F's highly efficient 4-stage turbine which already incorporates the results of 3-Dimensional, viscous, aerodynamic computations will be further refined using sophisticated aero engine procedures integrating through flow, blade-to-blade, boundary layer and 3-D viscous calculations.

Configurations of all diffusers in the engine will be carefully designed to maximize efficiency and all pressure losses through ducting, piping, manifolding, and components such as inter (and after) coolers and recuperators, will be minimized to reduce compression work and maximize expansion potential.

ATS efficiency will be improved even further by reducing all clearances between stationary and rotating parts. Leakage has always been of concern in gas turbines and is even more important as the potential of the cycle is pushed to the limit. Blade tip clearances will be maintained as small as possible by careful control of casing circularity and temperature. Reactive clearance control to avoid transient rubs would be needed to hold these tight clearances.

Diaphragm/vane segment seal clearances will be minimized and leakage further reduced through the extensive use of abradable material or filled honeycomb structures in combination with knife edge seals. Innovative seals such as #brush" seals, which have had aero application, will be investigated.

## EMISSIONS

The requirement for single digit NOx (15% $O_2$) with CO and UHC less than 20 ppmvd each, to be achieved without any post-combustion emissions control devices, is a serious challenge which will require significant R&D effort. Currently, premix, lean burn combustion systems are receiving the focus of attention, and it is predicted that these will eventually reach the required emissions levels. An alternative which is gaining attractiveness is the use of a catalytic metal or a ceramic matrix reactor within the combustor.

Both of these systems will benefit from the higher (when compared to compressor delivery temperature in the 501F) air temperature entering from the recuperator of the ATS. For catalytic combustion, the higher temperature air will enhance the reactivity threshold of the catalyst for natural gas fuel. In the case of the lean premixed combustor, the flammability range should be broadened, thus reducing pilot burner fuel. In both cases, no additional temperature rise will be needed across the combustor (compared to the base cycle) since both combustor outlet and combustor inlet temperatures increase in the ATS.

If large concentrations of moisture become part of the ATS, then combustor stability and CO production will have to be further developed, as these quantities of water vapor will far exceed past experience with steam injection.

## ADAPTABILITY TO COAL-DERIVED FUELS

A key feature of the ICRCC chosen as the reference natural gas fired ATS is the combustor shell design. The shell will not be structural, but will contain only pressurized compressor delivery and recuperator return air. The structural connection between HP compressor and turbine cylinders will be through radial-axial struts. This leaves the shell free to be reconfigured for compressor air take-off to the coal fuel processing system, and return from the recuperator.

The coal-fired system is an integrated system bleeding air from the compressor and returning low Btu fuel. The increase in volume flow to the turbine when compared to a natural gas fired (dry) system is small, and can usually be accommodated without turbine modifications. However, if large amounts of moisture are evaporated into the air stream in the gas fired ATS, then by comparison, turbine flow would be much reduced in the coal-fired case. To match compressor and turbine flows, compressor flow may be increased by the addition of inlet stages to the LP compressor, and/or by the use of variable compressor geometry.

## CONCLUSIONS

The feasibility of achieving 60% (LHV) efficiency in a natural gas fired cycle within a 8-year time frame was established. Cycle innovations, increased firing, reduced cooling air usage, improved component efficiencies and improved material/coating systems will all be needed to accomplish this ambitious goal. The resulting advanced turbine system will be environmentally superior, as well as adaptable to coal-derived fuel systems.

Lessons learned from the Westinghouse/ Rolls-Royce WR21 ICR project for the U.S. Navy and a Rolls-Royce project under the Collaborative Advanced Gas Turbine Program to establish power plant cycle efficiency when using aero-derived gas turbines will be incorporated into the ATS program, as applicable.


## ACKNOWLEDGEMENTS

The ATS concepts discussed in this paper were documented under DOE Contract No. DE-AC21-86MC23167. The program is admistered for DOE by the Morgantown Energy Technology Center under the guidance of Mr. Doanld W. Geiling.

## 1.2 GE Power Generation Technology Challenges for Advanced Gas Turbines

### CONTRACT INFORMATION

| | |
|---|---|
| **Contract Number** | DE-AC21-87MC23170 |
| **Contractor** | GE Environmental Services, Inc.<br>200 N. Seventh St.<br>Lebanon, PA 17042<br>(717) 274–7000 |
| **Contractor Project Manager** | Dr. Charles S. Cook |
| **Principal Investigators** | John G. Nourse<br>GE Power Generation |
| **METC Project Manager** | Justin L. Beeson |
| **Period of Performance** | September 30, 1987 to September 30, 1993 |

### GENERAL ELECTRIC ADVANCED TURBINE SYSTEMS PROGRAM SUMMARY

GE has achieved a leadership position in the worldwide gas turbine industry in both industrial/utility markets and in aircraft engines. This design and manufacturing base plus our close contact with the users provides the technology for creation of the next generation advanced power generation systems for both the industrial and utility industries. GE has been active in the definition of advanced turbine systems for several years. These systems will leverage the technology from the latest developments in the entire GE gas turbine product line.

Achieving the advanced turbine system goals of 60% efficiency, 8 ppmvd NOx and 10% electric power cost reduction imposes competing characteristics on the gas turbine system. Two basic technical issues arise from this. The turbine inlet temperature of the gas turbine must increase to achieve both efficiency and cost goals. However, higher temperatures move in the direction of increased NOx emission. Improved coating and materials technologies along with creative combustor design can result in solutions to achieve the ultimate goal.

GE's view of the market, in conjunction with the industrial and utility objectives requires the development of Advanced Gas Turbine Systems which encompasses two potential

products: a new aeroderivative combined cycle system for the industrial market and a combined cycle system for the utility sector that is based on an advanced frame machine.

The GE Advanced Gas Turbine Development program is focused on two specific products.

1. A 70 MW class industrial gas turbine based on the GE90 core technology utilizing an innovative air cooling methodology.

2. A 200 MW class utility gas turbine based on an advanced GE heavy duty machines utilizing advanced cooling and enhancement in component efficiency.

Both of these activities require the identification and resolution of technical issues critical to achieving Advanced Turbine System (ATS) goals. The emphasis for the industrial ATS will be placed upon innovative cycle design and low emission combustion. The emphasis for the utility ATS will be placed on developing a technology base for advanced turbine cooling while utilizing demonstrated and planned improvements in low emissions combustion. Significant overlap in the development programs will allow common technologies to be applied to both products. GE's Industrial and Power Systems is solely responsible for offering GE products for the industrial and utility markets. The GE ATS program will be managed fully by this organization with core engine technology being supplied by GE Aircraft Engines (GEAE) and fundamental studies supporting both product developments being conducted by GE Corporate Research and Development (CRD). GE's worldwide experience in commercialization of these products will ensure that the ATS program can proceed to the marketplace.

## BACKGROUND INFORMATION

GE has introduced three major power generation gas turbine technologies. The initial machines produced in the 1950-1968 era pushed firing temperatures from 1450 to 1650°F. The second generation, the first with internally air cooled buckets, permitted temperatures from 1840 to 2055°F. The third, or "F" class, raised the temperature to 2350°F. This was accomplished largely by incorporating GE Aircraft Engine cooling and material technologies to the turbine components in the "F" Class machines (see Fig. 1 and 2). Since introduction in 1987, commitments for over 80 "F" units have been made. Included are approximately 30 commitments from the international market, a tribute to their technical success and GE's worldwide capability to market its products.

GE's product line direction is aimed at improving performance, controlling combustion emissions and providing fuel flexibility. GE products include gas turbines from 42 MW to large frame combined cycle units at 343 MW with up to 54% net efficiency (see Fig. 3).

## THE GE INDUSTRIAL ADVANCED TURBINE SYSTEM

A GE90 aeroderivative gas turbine that incorporates a new cooling system and advanced materials has the potential to achieve the ATS objectives. The new cooling system which will be referred to as Turbo-Cooling, will allow the GE90 aeroderivative to achieve a rotor inlet temperature in excess of 2600°F with today's engine materials and more advanced thermal barrier coatings (TBC's).

The Turbo-Cooling cycle provides low temperature high pressure cooling air to the gas turbine's hot gas path components (from HP compressor discharge to LP turbine inlet). This makes the high firing temperatures of the Turbo-Cooled GE90 possible. Aeroderivative gas turbines currently use high temperature compressor discharge air for turbine cooling. This cooling air is at high temperature,

particularly with high pressure ratio compressors and this has limited the firing temperature capabilities of today's aeroderivative gas turbines.

Very high combined cycle efficiencies are possible in this engine configuration due to the high firing temperatures made possible by the Turbo-Cooled cycle. A 59% net power plant efficiency along with less than 10 ppm NOx should be attainable with today's engine materials, advanced TBC's and GEAE's first generation Dry Low Emissions (DLE) system. A net power plant efficiency in excess of 60% and still less than 10 ppm NOx is anticipated as the result of further study and modest improvement to a second generation DLE system.

## THE GE UTILITY ADVANCED TURBINE SYSTEM

The GE Utility ATS is a large gas turbine, derived from proven GEPG designs and integrated GEAE technology, that utilizes a new turbine cooling system and incorporates advanced materials. This system has the potential to achieve ATS objectives for a utility sized machine. Combined with use of advanced Thermal Barrier Coatings (TBC's), the new cooling system will allow higher firing temperatures and improved cycle efficiency that represents a significant improvement over currently available machines.

Developing advances in gas turbine efficiency and emissions is an ongoing process at GEPG. The third generation, "F" class, of utility gas turbines offers net combined cycle efficiencies in the 55% range, with NOx programs in place to reduce emissions to less than 10 ppm. The gas turbines have firing temperatures of 2350°F, and pressure ratios of 15 to 1. The turbine components are cooled by air extracted from the cycle at various stages of the compressor. The heat recovery cycle is a three pressure steam system, with reheat. Throttle conditions are nominally 1400 psi and 1000°F reheat.

As part of GEPG's ongoing advanced power generation system development program, it is expected that a gas fired advanced turbine system providing 300 MW power output greater than 58% net efficiency and < 10 ppm NOx will be defined. The new turbine cooling system developed with technology support from the ATS program will achieve system net efficiency levels in excess of 60%. Advanced cooling system will be utilized to cool static hot gas path components as well as rotating hot gas path components. Experimental validation of the concepts which are required to address the advanced cooling system are critical to achieving the ATS goals.

## TECHNOLOGY ALTERNATIVES FOR ATS

In order to achieve the ATS goals of 60% net thermal efficiency and 8 PPM of NOx, a number of technology alternatives need to be considered. These alternatives include:

Cycle Configurations
- Intercooling
- Cool Hot Gas Path Component Cooling Air

New Cooling Concepts
- Advanced Air Cooling
- Closed Cycle Cooling

Materials Developments
- New Alloys
- New Coatings
- Non Metallic Materials/Ceramics

In all of these alternatives the requirement for improvement in performance and combustion emissions are linked.

## INTERCOOLING &TURBO-COOLING

Inter-cooling entails the introduction of a heat exchanger between the low pressure and high pressure compressor sections of the gas turbine. This reduces the temperature of the air entering the high pressure compressor and significantly increases the power density of the machine. Intercooling also lowers the temperature of the hot gas path component cooling air and allows higher firing temperatures and increased power and efficiency (see Fig. 4). Turbo-cooling, similar to intercooling, leads to a cooler source of hot gas path cooling air via the use of a heat exchanger which cools the air exiting the high pressure compressor. The gas turbine fuel can be used as the heat sink. This cycle configuration can lead to higher firing temperatures and increased efficiency. (See Fig. 5).

## NOx CONTROL STRATEGIES

The existing low emissions development programs in both GE Power Generation (GEPG) and GE Aircraft Engines (GEAE) has allowed natural gas fired turbines to substantially reduce NOx emissions without the need for water or steam diluent or selective catalytic reduction (SCR) equipment. GE utility gas turbines with dry low NOx combustion systems (see Figs. 6 & 7) planned for production in 1993 will provide capability for 25 ppmvd NOx, 15 ppmvd CO and 7 ppmvd UHC at a firing temperature of 2350°F with future advances driving these values to lower levels. Advances from these emissions activities will be leveraged into the ATS Program.

Today's gas turbines exhibit several hundred degrees of temperature difference between the flame reaction temperature and turbine inlet temperature due to cooling flows and leakage. In order to capitalize on the performance improvements achievable with higher firing temperatures (turbine rotational stage inlet temperature) without raising flame temperature beyond levels acceptable for low NOx production, innovative improvements will be necessary in hot gas path component cooling (see Fig. 8). The ATS firing temperature goal of 2600°F requires a maximum temperature drop of 250°F between flame and the turbine inlet temperatures in order to keep NOx production low. To achieve a 250°F temperature difference, cooling air for the combustor must be minimized and first stage nozzles must be cooled using advanced concepts with allowance for little or no cooling air dilution, and leakage paths must be reduced. Water, steam and air have been evaluated as heat transfer media in several alternative gas turbine cycles to reduce gas path cooling flows. Substantial improvement in gas turbine efficiency can be obtained if these advanced cooling concepts are successfully employed.

## IMPROVED COOLING CONCEPTS

Two areas requiring major technology developments are improved cooling of the rotor stages of turbine airfoils for efficiency and improved cooling of the first stator turbine airfoils for improved emission control. Advanced air cooling and closed cycle cooling concepts need to be explored for the rotor blades so that parasitic cooling flow can be reduced and thus its negative impact on cycle efficiency can be minimized. Up to 2% improvement in efficiency is possible for this component alone.

Nozzle airfoil cooling flow needs to be minimized as previously mentioned for improved emission performance (see Fig. 9). Even if some material improvements are realized, current F technology type cooling is not capable of meeting the 2600°F DOE target. Advanced GE90 type cooling comes closer to the target. Only with a new novel cooling concept with no air diluent injection can the 2600°F target be reached.

## SUMMARY

GE's view of market needs, in conjunction with the industrial and utility objectives specified for the ATS, have produced a two-pronged approach. This will permit product development in two combined cycle power plant output power ranges, 80-100 MW and 250-350 MW and will be accomplished by 1) development of an Industrial Advanced Turbine System and 2) development of a Utility Advanced Turbine System. Both programs require the identification and resolution of critical technical issues. The emphasis for the Industrial ATS will be placed on innovative cycle design, high temperature materials and low emission combustion. The emphasis for the Utility ATS will be placed on innovative cycle design and the technology advances which will permit a new turbine cooling design while utilizing demonstrated and planned improvements in low emissions combustion.

# Aircraft Engine Technology to Utility Gas Turbines

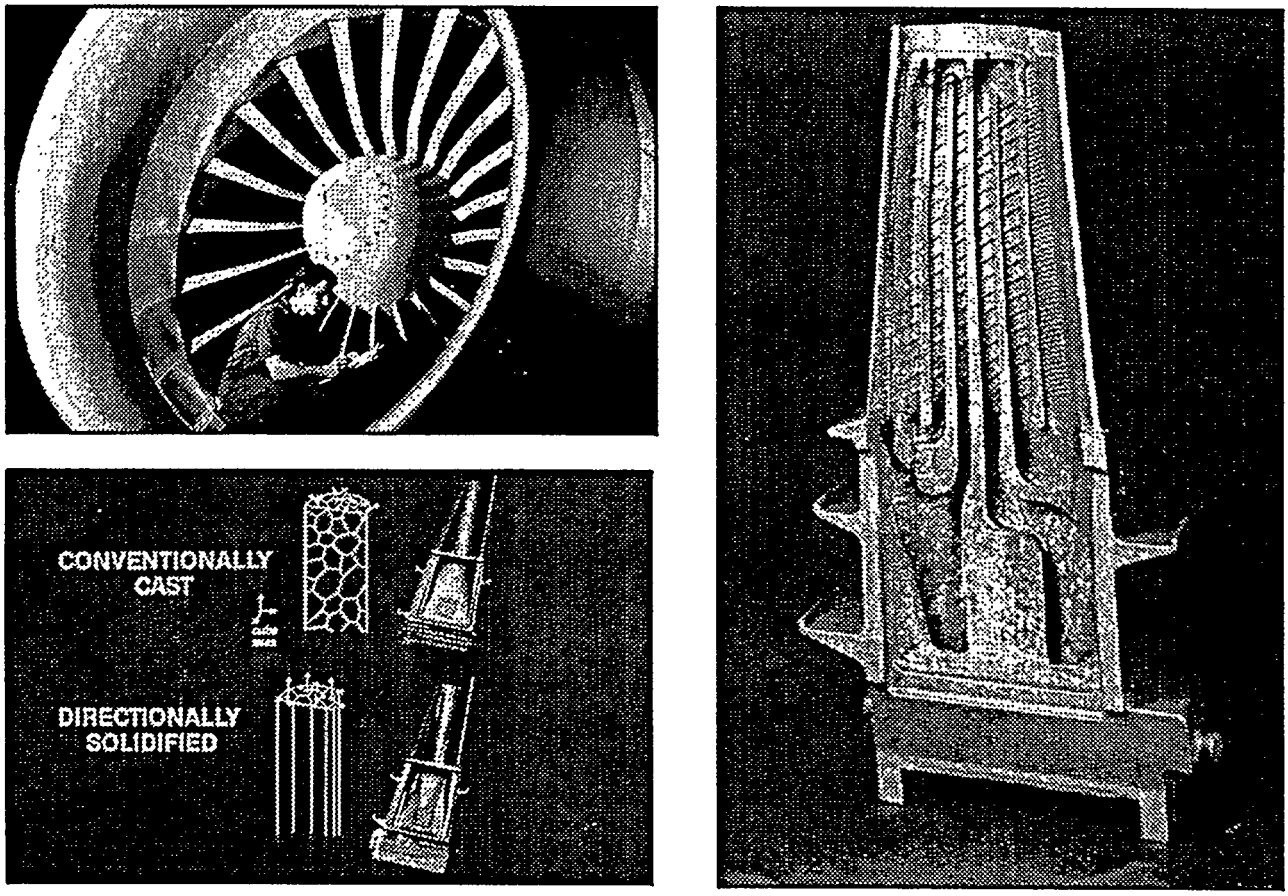


**Figure 1.**

# GE F-Technology Gas Turbines

## Firing Temperature >2350°F/1288°C - 54% CC Efficiency

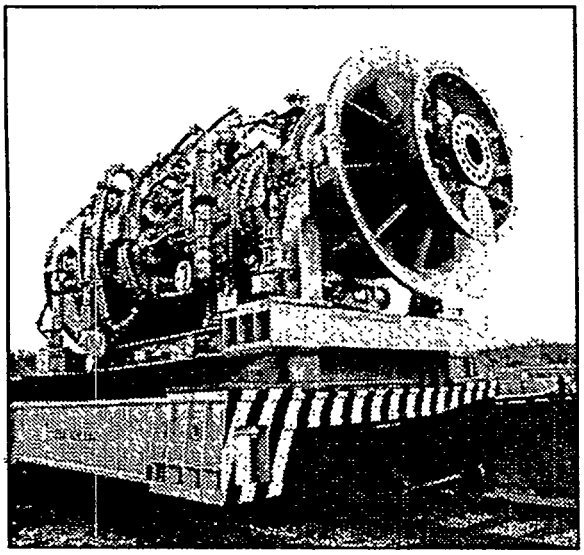

7F-A
60-Hertz
159 MW

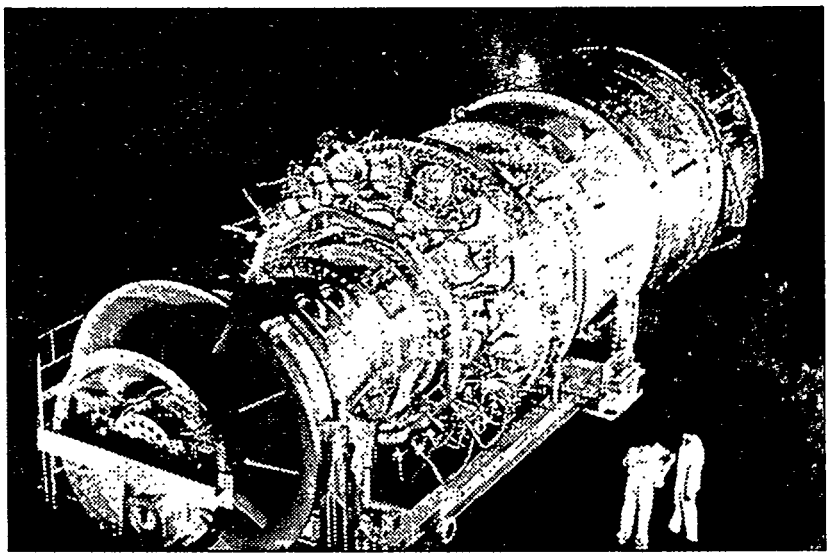

9F-A
50-Hertz
226 MW

**Figure 2.**

## Gas Turbine Product Line Direction

Performance

F ⟶ FA 2350°F

| | 7FA | 9FA |
|---|---|---|
| SC | 158 MW 36% | 216 MW 36% |
| CC | 234 MW 54% | 343 MW 54% |

LM5000 ⟶ LM6000 2300°F

| | |
|---|---|
| SC | 42 MW 41% |
| CC | 52 MW 52% |

Combustion Emissions

| | |
|---|---|
| DLN | 25 ppm ⟶ 9 ppm |
| Fuel Flexibility | < 150 Btu/SCF |
| Low Btu Coal Gas | |

Figure 3.

## Combined Cycle Efficiency

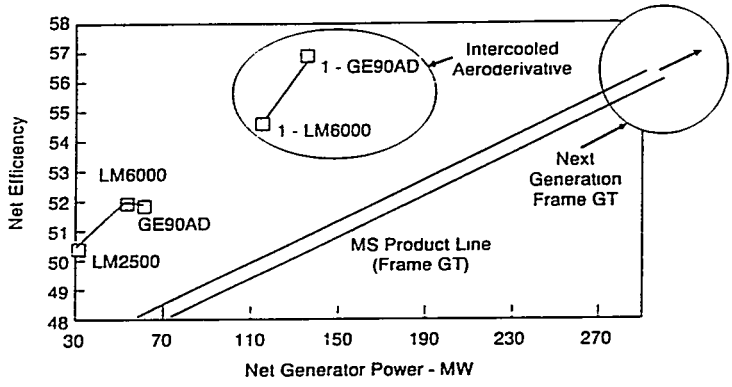


Figure 4.

## New External Cooler System

- With External Cooler It Is Possible To
  - Cool the Combustor
  - Cool the 1st Stage HPT Nozzle
  - Improve Blade Cooling

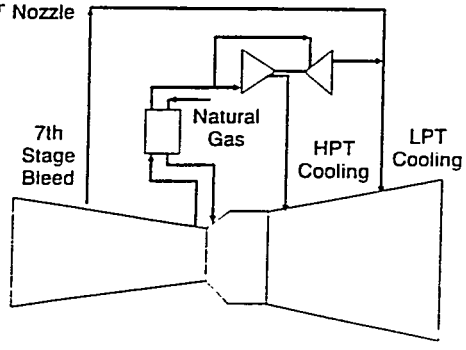


Figure 5.

## $NO_X$ Control Strategies

### Control Strategies

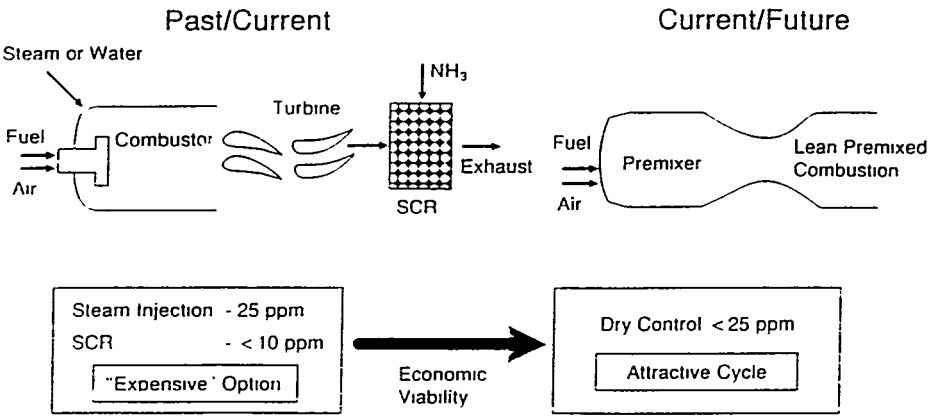


**Figure 6.**

## Staged Combustion Premix-Lean

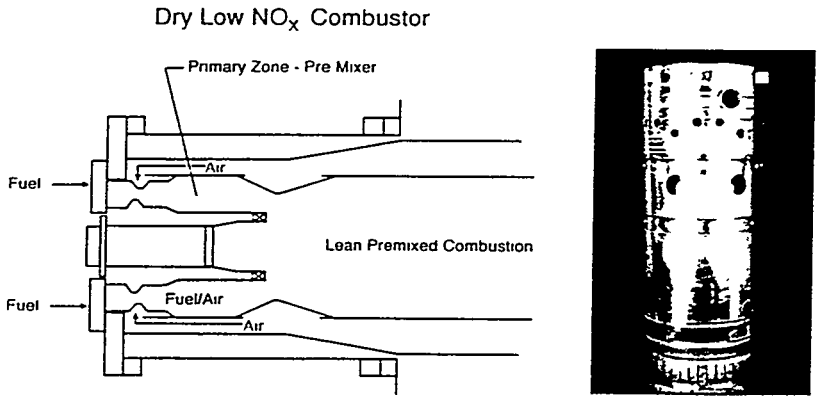


**Figure 7.**

## Advanced Gas Turbine - Performance vs. Emission Control

## Sets Maximum Combustion Exit Temperature

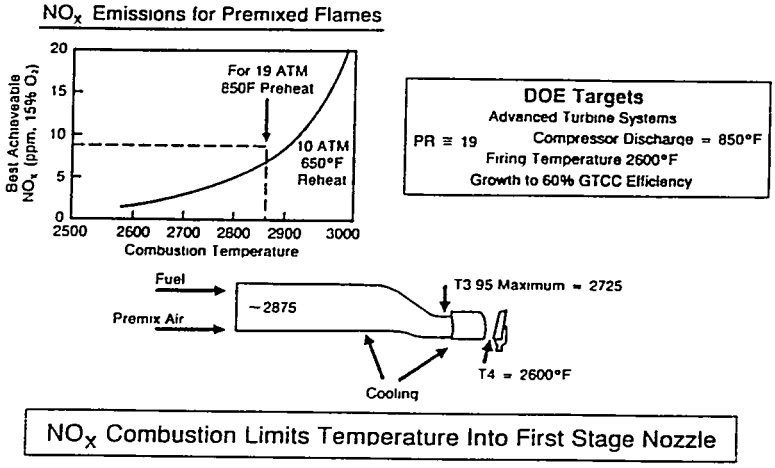


**Figure 8.**

## Maximum Firing Temperature

## Function of Nozzle Cooling Technology

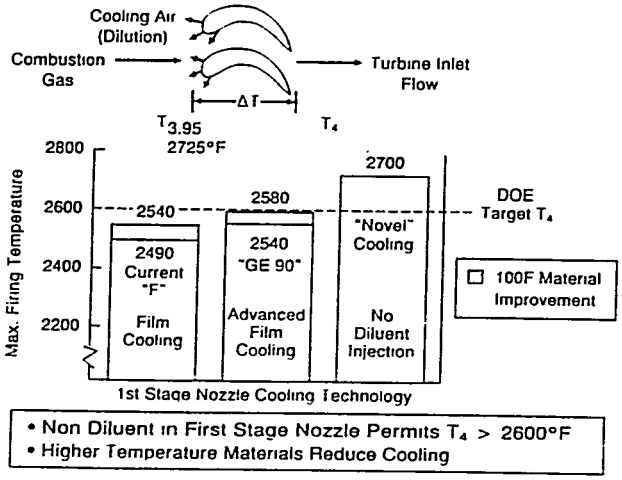


**Figure 9.**

## 1.3 Gas Fired Advanced Turbine System

Phase 1 - System Scoping and Feasibility Studies

### CONTRACT INFORMATION

| | |
|---|---|
| **Contract Number** | DE-AC22-86MC23166 |
| **Contractor** | Solar Turbines Incorporated<br>P.O. Box 85376<br>San Diego CA 92185-5376<br>(619) 544-5000 |
| **Contract Project Manager** | Mr. Richard T. LeCren |
| **Principal Investigators** | Mr. David J. White |
| **METC Project Manager** | Mr. Paul Micheli |

### OBJECTIVES

The objective of the first phase of the Advanced Gas Turbine System (ATS) program was the concept definition of an advanced engine system that could meet the program's exacting efficiency and emission goals. The thermal efficiency goal for this advanced industrial engine was set at 50%, some 15 percentage points higher than current equipment levels. Exhaust emissions goals for oxides of nitrogen ($NO_x$), carbon monoxide (CO), and unburned hydrocarbons (UH) were fixed at 8 parts per million by volume (ppmv), 20 ppmv, and 20 ppmv respectively, corrected to 15% oxygen ($O_2$) levels. Other goals also had to be addressed; these involved reducing the cost of power produced by 10% and improving the reliability, availability, and maintainability (RAM) over current levels. Although this advanced gas turbine was to be fueled with natural gas, it also had to embody features that allowed easy modification to burn coal or coal derived fuels.

### BACKGROUND INFORMATION

Solar Turbines Incorporated is the world's leading supplier of industrial gas turbine power generation and mechanical drive systems in the 1,000 to 25,000-horsepower (hp) size range. Because of its substantial market base Solar is very much aware of the future needs of the customers who buy equipment in this size range.

#### Marketplace Demands

Internal studies conducted with existing customers show that engine emissions and efficiency are rising rapidly in importance in the list of requirements demanded by the customer. It is believed that these two requirements will

displace "first cost" from its second place on the list by the year 2000. These "key buying criteria" for industrial gas turbine customers are shown in Figure 1 for different time periods. Reliability, availability, and maintainability (RAM) are generally considered together to be the most important of all factors in buying gas turbines. This is not likely to change in the future.

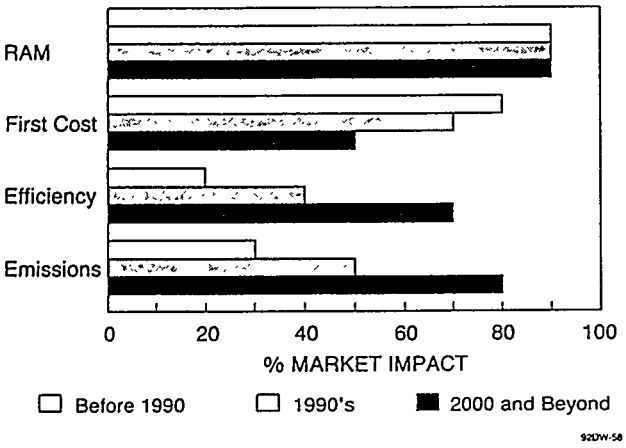


**Figure 1. Key Buying Criteria**

### Advanced Technology Development

Solar intends to work with the U.S. Department of Energy (DOE) on all aspects of advanced technologies for energy conversion systems under 25,000 hp. These joint efforts will enable Solar and the U.S. industrial gas turbine community to maintain its leadership position and expand world market share, while creating new jobs in the process. As an example, Solar is working with the DOE on two ceramic programs: (1) to develop hot-end parts for existing gas turbines and (2) to develop the technologies to support the design of high temperature ceramic heat exchangers.

These two programs will provide invaluable technology support to the ATS program. The ceramic turbine program is considered critical to the success of ATS, and it is Solar's intent to use the technologies generated on the two programs and to forge synergistic relationships from them.

## PROJECT DESCRIPTION

Information generated on previous Solar gas turbine development programs was used as a starting point for the first phase of the ATS program. For example, Solar has had considerable experience with combined-cycle and cogeneration systems that have demonstrated high efficiencies. The data available on these systems were used as a baseline to evaluate the various advanced engine options generated during the study. The simple-cycle gas turbine is the main type of machine offered in the market plac,e and is today the dominant design concept (Figure 2). Early in the system scoping, it became apparent that the traditional simple cycle machine would not be a practical approach to achieve the 50% thermal efficiency goal without some additional bottoming cycle.

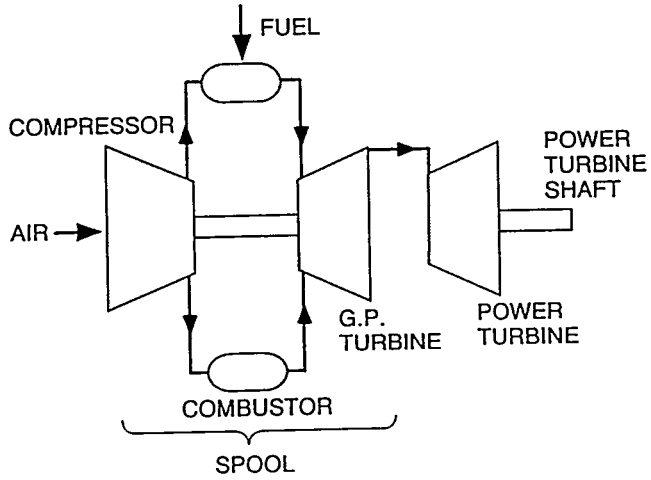


**Figure 2. Simple-Cycle Gas Turbine System**

### Technical Challenges

Although the simple cycle gas turbine is today the dominant product sold by most industrial gas turbine manufacturers, the realities of tomorrow will force a change to other cycles. One of the reasons for this change is the difficulty

in meeting the ATS efficiency goal with a simple cycle machine. From a practical point of view, it is impossible to achieve a 50% thermal efficiency with a simple cycle machine without resorting to some bottoming or topping cycles. Even accepting a lower efficiency would lead to significant problems. The high pressure ratios required for high simple cycle efficiencies (46%) are not practical in small size machines. Blade sizes on the last rows of an axial compressor providing pressure ratios on the order of 50:1 for a 16,000 hp machine will have to be extremely small. These blades would be expensive to produce and would have a limited efficiency life due to rapid erosion of the knife-like leading edges. This rapid loss in compressor efficiency would affect the overall thermal efficiency dramatically. Additionally, the small size of the blades in the first stage of the turbine section would make it difficult to employ some of the sophisticated cooling techniques needed to allow operation at temperatures on the order of 3000°F needed for the 46% efficiency.

### Cycle Selection

As a consequence of the problems faced by the simple-cycle machine, Solar was forced to look at a number of more complex cycles. The theoretical Ericsson Cycle, as applied to the gas turbine, appeared to be one of the most attractive options. This cycle is shown as a temperature-entropy diagram in comparison with the Brayton Cycle in Figure 3. The area enclosed by the Ericsson Cycle is considerably greater than the corresponding area of the Brayton Cycle. This area is a measure of the work available and the greater the area, the more efficient the cycle.

### Cycle Selection

Although impractical in its fundamental form, the Ericsson Cycle can be simplified to provide a system with high efficiency and high reliability. the impractical part of the Ericsson

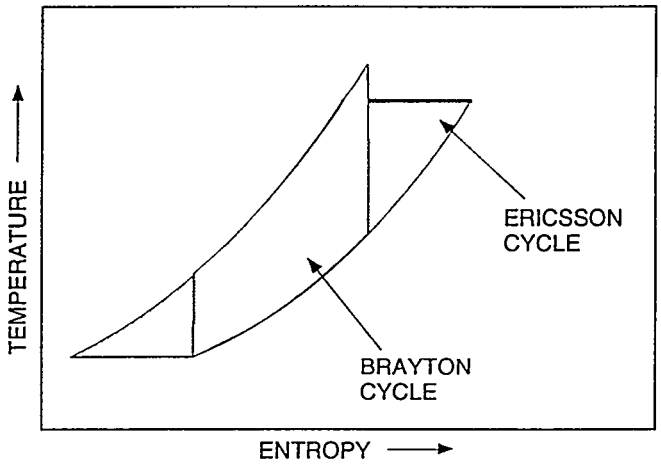


**Figure 3. Simple-Cycle Gas Turbine System**

cycle is the isothermal compression and the isothermal expansion, which are represented by the horizontal lines at the top and bottom of the closed curve. Isothermal compression uses much less energy to compress air to a given pressure ratio than the normal (adiabatic) methods used in compressing air. Similarly more energy can be extracted from an isothermal expansion process than an adiabatic one. True isothermal compression systems such as hydraulic systems are difficult to integrate into an engine and, to be practical, approximations have to be used. Typically, intercooling between compressor stages is used to approximate isothermal compression. Similarly, isothermal expansion is usually approximated by the use of reheat between turbine stages. Reheat usually involves the addition of a combustion system between the gas producer turbines and the power turbine. Fuel is burned ahead of the power turbine to provide temperatures on the order of the main combustor outlet temperatures. These high power turbine temperatures lead to high efficiencies and high power density levels.

## RESULTS

The basic concept thus derived from the Ericsson cycle is an intercooled, recuperated, and

reheated gas turbine. Theoretical performance analyses, however, showed that reheat at high turbine rotor inlet temperatures (TRIT) did not provide significant efficiency gains and that the 50 percent efficiency goal could be met without reheat. Based upon these findings, the engine concept adopted as a starting point for the gas-fired advanced turbine system is an intercooled, recuperated (ICR) gas turbine (Figure 4).

## Turbine Cooling

It was found that, at inlet temperatures greater than 2450°F, the thermal efficiency could be maintained above 50%, provided that the turbine cooling flows could be reduced to 7% of the main air flow or lower. This dual and conflicting requirement of increased temperatures and reduced cooling will probably force the abandonment of tranditional air cooled turbine parts. Thus, the use of either ceramic materials or non-air cooling fluids has to be considered for the turbine nozzle guide vanes and turbine blades.

## Turbine Section Materials

The use of ceramic components for the proposed engine system is generally preferred because of the potential growth to higher temperatures that is available with such materials. Figure 5 shows comparatively the performance of an ICR cycle using metallic components in one case and ceramics in the other. Similarly, Figure 6 depicts an ICR with reheat which, in one case, uses ceramic hot-end parts and, in the other, a metal-based turbine system. These two figures demonstrate the potentially significant improvements in efficiency that can be obtained by utilizing ceramic parts. In addition, by comparing the two figures, the differences between the reheated and non-reheated versions can be seen. These differences are not great at the

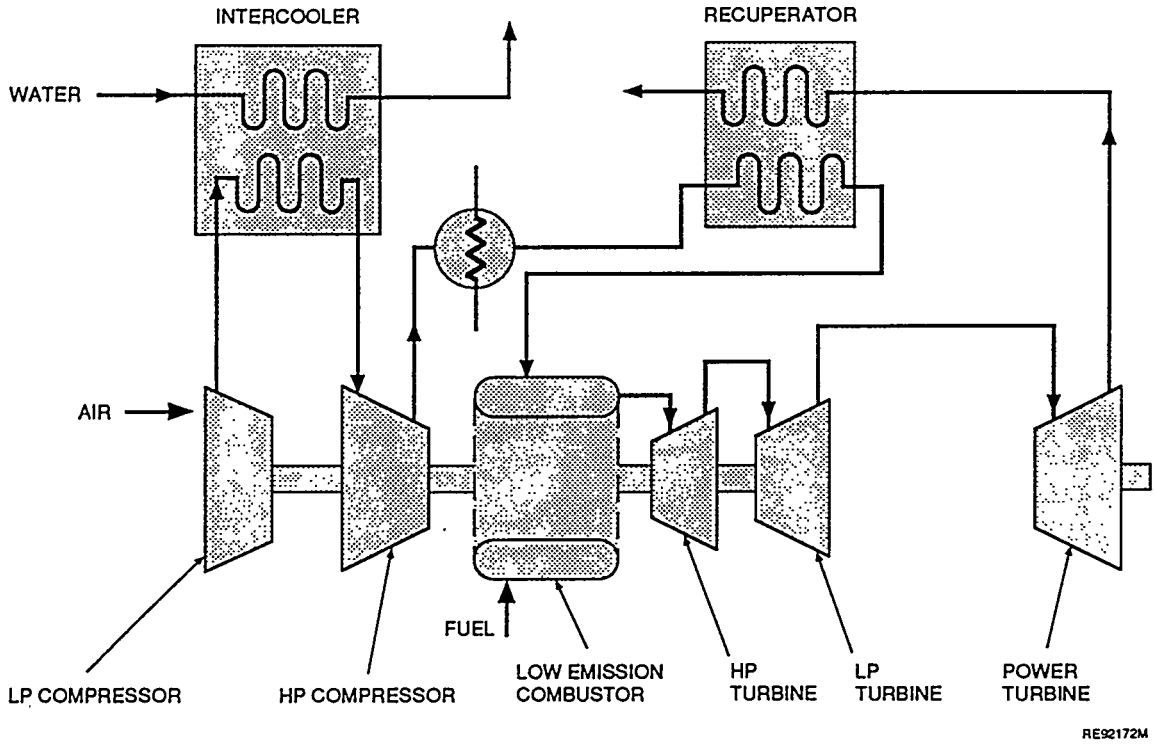


**Figure 4. ICR Gas Turbine**

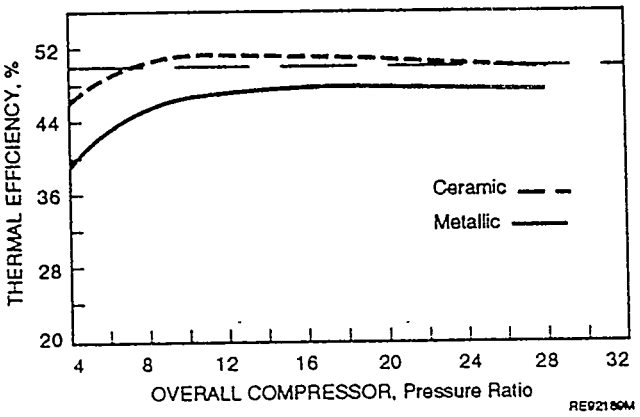


**Figure 5. Intercooled Recuperated (ICR) Engine Performance**

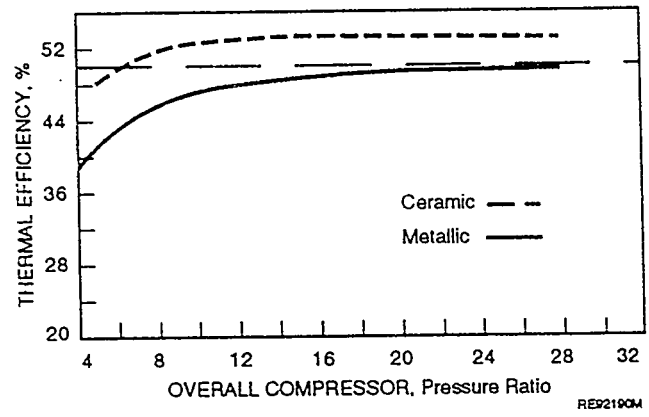


**Figure 6. Solar Intercooled Recuperated and Reheat Cycle**

lower pressure ratios where operation is more desirable. Generally, low pressure operation is preferred with natural gas-fired machines because of the energy penalties paid in compressing the fuel to pressures high enough to allow injection into the combustor. As the pressure ratio increases, the difference between the efficiencies increases due to a more rapid decrease in the efficiency of the ICR system.

The turbine and the hot-end parts in general will have to be fabricated from ceramic materials that have better performance than those materials available today. Fortunately, there are a number of programs world-wide that are developing these higher performance ceramic materials, and these should be available for the production ATS. Ceramic composites, perhaps silicon carbide fibers in a matrix of silicon carbide or silicon nitride may provide the primary structure for the turbine disks and related static parts. These composites will probably employ protective surface coatings such as alumina, silicon nitride, or boron nitride. The first-stage vanes and blades will probably be monolithic structures fabricated from advanced ceramics. These blades will utilize some form of air (or other fluid) cooling when operating at TRITs of 2450°F and above.

Other materials that will be considered include the intermetallics such as nickel aluminide and molybdenum disilicide. These materials may also be used as coatings on more conventional metal hot-end parts to minimize oxidation and thus allow operation at higher temperatures. Intermetallics when combined with thermal barrier coatings (TBC) may provide competition to the ceramic composites, and trade studies will have to be conducted to determine the better material set. Some of the newer formulations of yttria stabilized zirconia that utilize "bond coats" of platinum aluminide have demonstrated exceptional reliability at high temperatures. These bond coats are also compatible with the intermetallics, and thus this could lead to a new class of turbine materials.

### Cycle Flexibility

If difficulties in meeting the efficiency goals are encountered, it is anticipated that reheat would be added to the basic ICR system proposed as a baseline. This adds complexity and cost; however, it also provides some benefits. It is possible with a reheat system, for example, to provide all of the load following from minimum to maximum load by modulating the reheat fuel flow. By using this approach, a flat but high-

efficiency characteristic can be obtained. The response time of an engine using reheat is also much faster than other two-shaft gas turbine designs.

Solar will also consider the use of autothermal reforming of the natural gas fuel as an external add-on device. This type of approach would be adopted if difficulties in meeting the extremely low $NO_x$ emissions required were encountered. When natural gas is reacted catalytically with steam in an autothermal reactor a high hydrogen content gaseous secondary fuel is produced. This secondary fuel has a lower heating value (LHV) that is greater (per unit weight) than the parent natural gas and can burn stably at much lower reaction temperatures. This ability to burn at very lean mixture ratios or low flame temperatures provides extremely low $NO_x$ levels. In operation, the steam needed would be raised in the intercooler and boosted in temperature by a heat exchanger in the exhaust. Because thermal energy which normally goes to waste is being utilized in the autothermal reformer, very high system efficiencies can be obtained typically on the order of 60%.

An advanced engine system employing ICR, reheat, and autothermal reforming is shown schematically in Figure 7. The autothermal reformer, if used, would be integrated into the low emission combustor as shown in Figure 8. In practice, autothermal reforming could be used in those cogeneration applications where a periodic demand for steam is found. The steam raising, as described above, could be diverted for industrial use and, when not needed, passed to the auto-thermal reformer to maximize efficiency and minimize emissions. This would require a dual-fuel combustor. Such a system is entirely possible.

With the above options available to add on to the basic ICR concept, Solar is confident that all of the program goals will be met successfully.

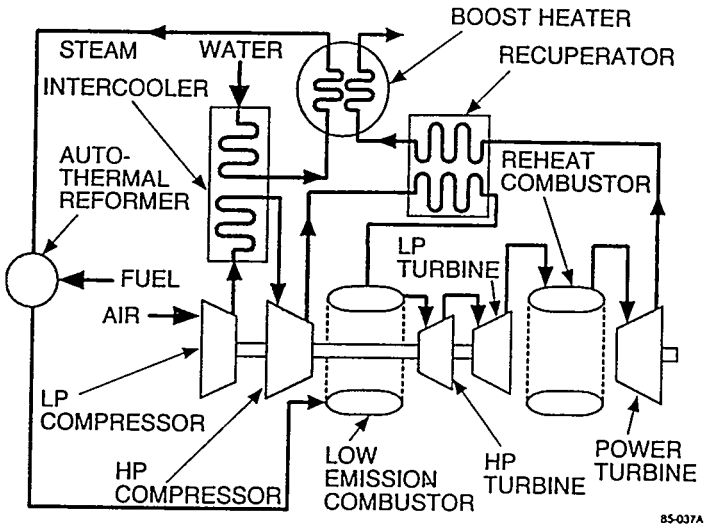


**Figure 7. Advanced Turbine System (ATS)**

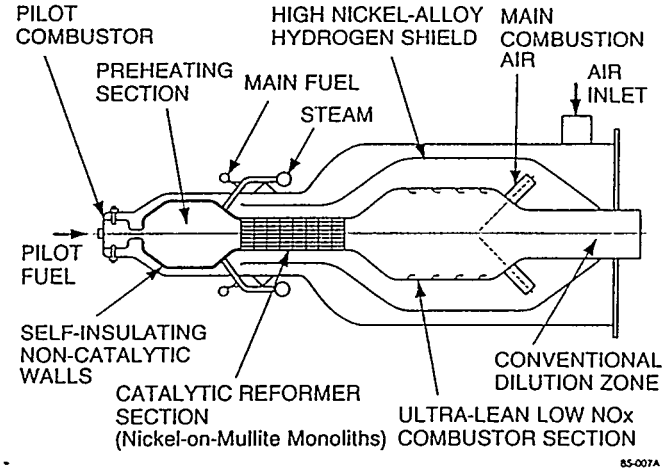


**Figure 8. Integrated Autothermal Reformer and Combustor**

## FUTURE WORK

This paper summarizes the work performed by Solar in the first phase of a multi-phase program that culminates in the demonstration of two prototypical engine systems in 2002. Solar is certain that these gas turbine engines will meet the above-described goals and would be competitive in terms of price with all likely contemporary systems. Solar possesses the personnel, equipment, and the special interest to perform the

aggressively paced developments required in the future phases of the ATS program. Solar welcomes the opportunity to participate in this challenging program, and is confident that the concept described herein will evolve into a highly successful product.

## 1.4 Advanced Turbine Systems Program

### CONTRACT INFORMATION

| | |
|---|---|
| **Contract Number** | DE-AC21-86MC23165 |
| **Contractor** | Allison Gas Turbine Division<br>General Motors Corporation<br>P.O. Box 420<br>Indianapolis, Indiana 46206<br>(317) 230-2548 |
| **Contractor Project Manager** | Colin Wilkes |
| **Principal Investigators** | Dale W. Mukavetz<br>T. K. Knickerbocker<br>Dr. Sy A. Ali |
| **METC Project Manager** | Leland E. Paulson |
| **Period of Performance** | July 1986 - October 1993 |

### OBJECTIVES

The objectives of Phase I of the Advanced Turbine Systems (ATS) program are the following:

- efficiency, on a lower heating value (LHV), greater than 60% for utility-scale, natural-gas-fired, combined-cycle systems; LHV efficiency for industrial-scale systems 15% greater than 1991 vintage efficiency
- base-load emissions consistent with the following:
  - no post-combustion emissions control devices
  - 1991 state-of-the-art system efficiencies
  - nitrogen oxides (NOx), 10 parts per million by volume dry (ppmvd) at 15% oxygen
  - carbon monoxide (CO) and unburned hydrocarbon (UHC), 20 ppmvd
- cost of electricity (COE) 10% below COE of 1991-vintage power generation systems in the same market class and size range, and meeting the same emissions requirements
- amenable to change for use in a coal-based system
- reliability, availability, and maintainability (RAM) comparable to today's advanced power generation systems

## BACKGROUND INFORMATION

Phase I of the ATS program was initiated in the spring of 1992 as System Scoping and Feasibility Studies—a contract modification to the existing contract noted previously entitled *Advanced Coal-Fired Gas Turbine Systems*. The period of performance was approximately six months.

## PROJECT DESCRIPTION

In accordance with the goals of the DOE program, improvements in the gas turbine are the primary focus of Allison activity during Phase I. To this end, Allison conducted a survey of potentially applicable gas turbine cycles and selected the advanced combined cycle as reference system. Extensive analysis of two versions of the advanced combined cycle was performed against the requirement for a 60% thermal efficiency (LHV) utility-sized, natural gas fired system.

Allison's October 1992 report to this forum concentrated on the turbine technology required to achieve the ATS system. Regardless of cycle type chosen, the hot section, including combustor, was determined at that time to be the key to success.

This 1993 report deals with some of our preliminary screening work done to determine the industrial engine configurations we will want to study under Phase II of ATS Task 6.

## PROCEDURE

This preliminary screening effort proceeded in five steps:

1. The basic industrial engine thermodynamic cycles to be studied were chosen
2. The major industrial engine market sectors were determined
3. Applicability of each thermodynamic cycle to each market sector was determined on a global basis
4. Engine thermodynamic cycles applicable to a given market sector were rated against each other on a global basis for that particular market sector
5. Desirable cycle types were determined for several market sectors. These configurations will be studied in detail during ATS Phase II (especially tasks 3, 5, and 6)

The reader is reminded that this is a preliminary screening activity and the real work is to be accomplished under the Phase II ATS effort. These results provide direction to the Phase II work when this effort comes under contract.

## THERMODYNAMIC CYCLES

Allison investigated the four basic cycles commonly known and used in our industry. These are:

1. Humid air turbine
2. Intercooled-recuperated systems
3. Simple cycle (with cogen)
4. Chemically recuperated cycle

Initial performance analysis indicates that all have the potential of reaching stated ATS performance objectives. We also concluded in the Phase I study that engine hot section technology would be the critical engine technology regardless of which cycle is chosen for any given market sector. As noted previously, this work was

reported on in detail in the October 1992 Contractor Review Meeting.

Figures 1 through 4 present thermal efficiency capability as a function of turbine inlet temperature for various compressor pressure ratios for cycle types 1, 2, and 3 above. The charts assume use of each of the thermodynamic cycles in the electrical power generating mode. These Figures lead to four conclusions:

1. The ATS advanced technology hot section at 2600°F firing temperature provides significant improvement in thermal efficiency regardless of cycle type chosen. Specific power increases with turbine temperature should result in significant reduction of COE.
2. The combined cycle and the simple cycle optimize at a pressure ratio of approximately 25.

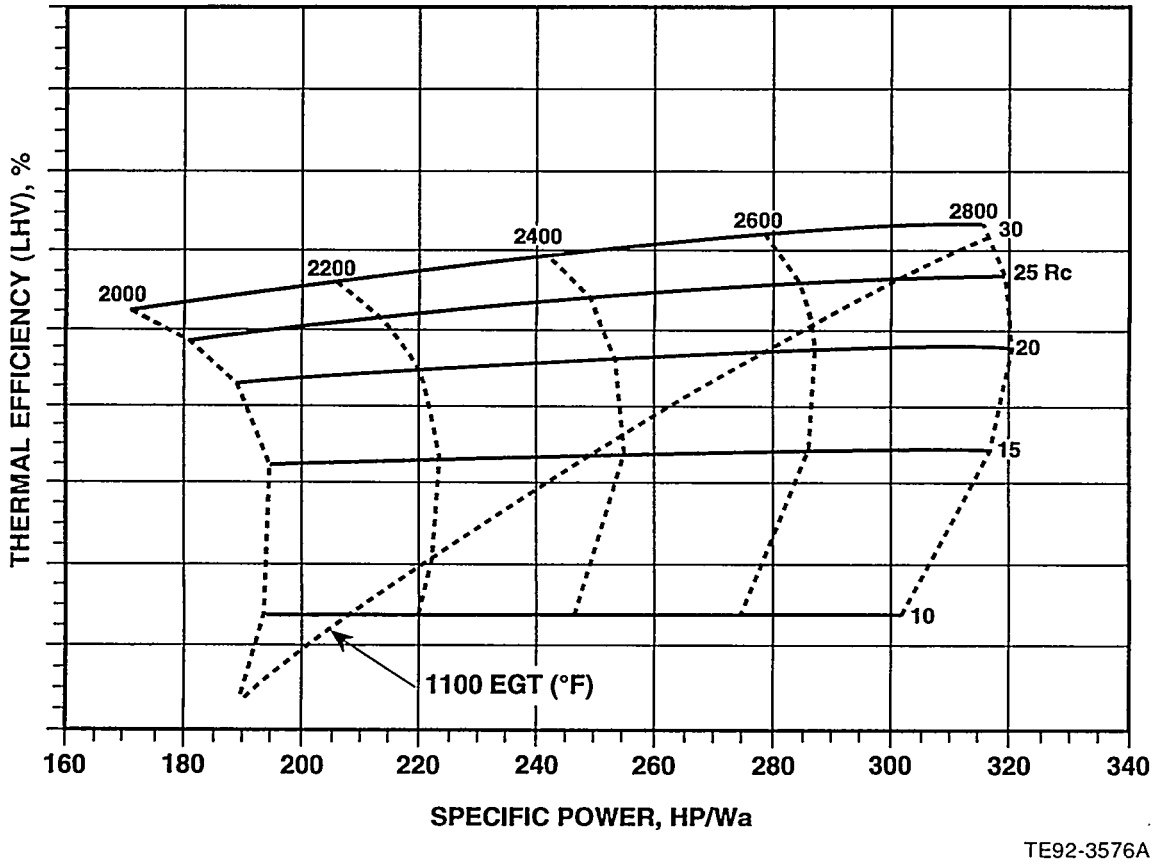


**Figure 1. Simple cycle thermal efficiency versus turbine temperature and pressure ratio.**

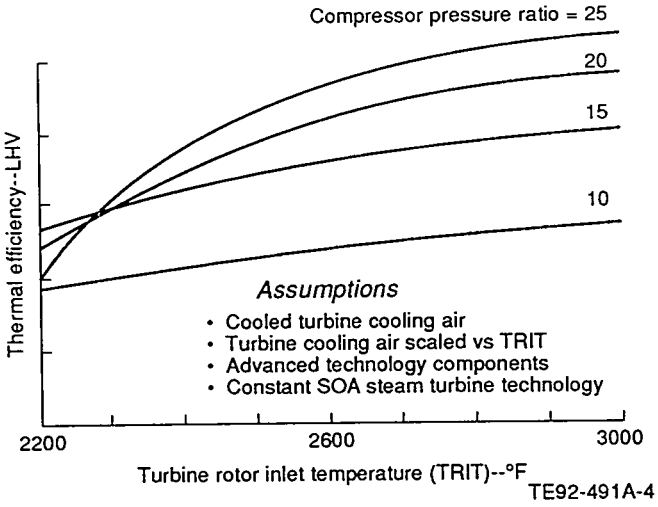


**Figure 2. Combined cycle thermal efficiency—no intercooling.**

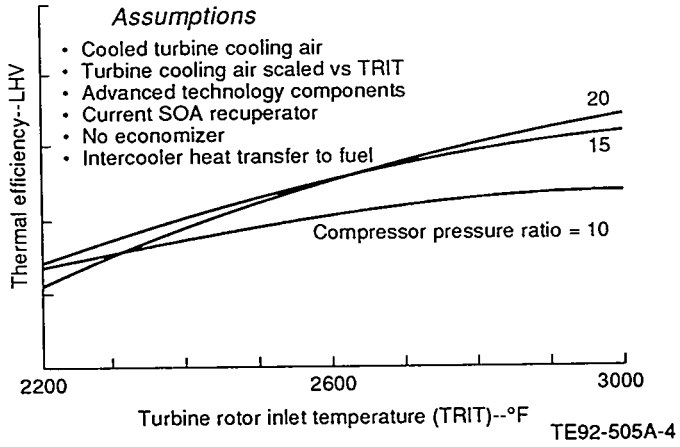


**Figure 3. Intercooled/recuperated cycle thermal efficiency.**

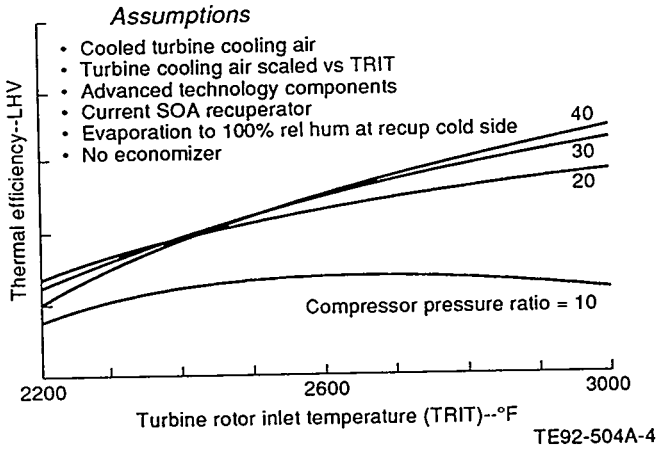


**Figure 4. Intercooled/recuperated/humid air turbine cycle thermal efficiency.**

3. The intercooled-recuperated cycle optimizes at approximately a pressure ratio of approximately 15.
4. The HAT cycle optimizes at a pressure ratio similar to that of the simple and combined cycles; approximately 25.

This type of carpet plot could not be done for the chemical recuperation cycle because of our lack of a recuperator model which could be integrated with Allison's cycle matching modeling system. Several cycles were studied using external iteration. It was concluded that the chemical recuperator and standard recuperation were thermodynamically similar cycles requiring relatively low pressure ratios in order to have high exhaust gas temperatures. Our study resulted in a 2800°F requirement for turbine inlet temperature, 200°F higher than the Allison selected ATS reference cycle, in order to supply the reformer with appropriate gas temperature. A logical but probably less efficient alternative is an auxiliary

combustion system at turbine exhaust to provide adequate reformer inlet temperatures without the high (2800°F) turbine inlet temperature. This cycle has high specific power (output power per unit airflow) similar to the HAT cycle due to the level of steam production in the reformer. Detailed study of this cycle will be accomplished as part of ATS Phase II.

Table 1 presents a summary of performance levels for the various cycles. Thermal efficiency is presented twice; once for the base system and once for the base system with economizer. Site requirements will determine whether an economizer is useful or not. Data in this table are used to rate the engine cycles in terms of fuel efficiency and, secondarily, in terms of specific power which might bear some relation to purchase price.

## MARKET SECTORS

Cogeneration is a major market segment. The gas turbine is utilized for production of electrical power along with steam and/or hot water. The steam/hot water are often the primary outputs with electricity of secondary importance. Examples are found in heat intensive industries such as food processing, chemical, and paper plants.

Pumping of gas in pipelines and compression systems in general is a significant market. The output of the engine is mechanical power. Bottoming cycles are generally not used due to a lack of water at the site, although this can be site dependent.

Generator sets supply prime power without heat recovery. Examples are shipboard power and offshore platform power.

Prime power for marine propulsion is a small but growing market in both commercial and military applications.

Emergency or standby power generation systems such as those used by hospitals are an important market.

## APPLICABILITY TO MARKET SECTORS

Table 2 presents a summary of the various engine cycles and their applicability to the major industrial engine market segments. Both the simple cycle and the ICR enjoy wide application capability. Note that in cogeneration-steam Allison sees no substitute for the simple cycle. This same

Table 1.
Fuel efficiency and power density comparison—10-20 MW.

| | Cycle | | | | | |
|---|---|---|---|---|---|---|
| Parameter | Simple cycle | Cogen steam turb | Cogen hybrid | ICR | HAT | Chem recup |
| TRIT (°F) | 2600 | 2600 | 2600 | 2600 | 2600 | 2800 |
| Turbine technology | Metallic/ ceramic | Metallic/ ceramic | Metallic/ ceramic | Metallic/ ceramic | Metallic/ ceramic | Metallic/ ceramic |
| Thermal eff (LHV) | 0.41 | 0.544 | 0.48 | 0.504 | 0.528 | 0.541 |
| Specific power | 202 | 267 | 235 | 217 | 312 | 348 |
| Overall press ratio | 25 | 25 | 25 | 15 | 30 | 15 |
| Thermal effic with economizer | N/A | 0.544 | N/A | 0.565 | 0.554 | 0.554 |

Table 2.
Industrial ATS application matrix.

| Markets | Simple cycle | ICR | HAT | Intercooled chem recuperator |
|---|---|---|---|---|
| Cogeneration-steam | X + steam generator | O | O | O |
| Cogeneration-electric | X + steam turbine/hybrid | X | X | X |
| Compression/pumping | X | X | O | X |
| Generator sets | X | X | O | O |
| Marine propulsion | X | X | O | O |
| Emergency electrical | X | O | O | O |

X = applicable
O = not applicable

simple cycle when properly designed can be used in the hybrid mode (steam generation and re-injection) or with a steam turbine for electric power generation.

The HAT and chemical recuperation cycles have only narrow applicability. The HAT cycle, due to its complexity and high water usage, is probably only applicable to electrical generation. The chemically recuperated cycle is limited to those applications where natural gas is readily available as a fuel; i.e. electric cogeneration and gas pumping.

## COMPARATIVE UTILITY IN KEY MARKET SECTORS

Table 3 presents the basic purchase decision drivers. Units which do not meet emissions standards (NOx, CO, HC) will not be sited making this factor a go-no-go gate. There are, however, basic differences such as combustor inlet pressure and temperature and water vapor content. These parameters affect each cycle's inherent ability to meet emission goals and the magnitude of development effort required to do so. First cost (purchase price) or initial investment has been and is expected to continue as a strong driver in the industrial market. Fuel usage is separated out from the remainder of economics (service, overhaul, cost of money, etc) because it is a major proportion of expenses in any non-standby application.

Table 4 shows the result of rating the various engine cycles in electric cogeneration. Note that fuel usage was weighted

Table 3.
Purchase decision drivers—year 2000.

| Application | Driver |
|---|---|
| Cogen-steam generator | Economics |
| Cogen-steam turbine | Economics |
| Cogen-hybrid | Economics |
| Compression/pumping | First cost/ economics |
| Generator sets | First cost/ economics |
| Marine propulsion | Economics/ first cost/site |
| Emergency electrical | First cost |

Table 4.
Comparative utility in electric power cogeneration.

| Assessment parameters | Cycle type: Simple cycle steam turbine | Simple cycle hybrid | ICR | HAT | Chem recup |
|---|---|---|---|---|---|
| Emissions | 7 | 9 | 8 | 9 | 10 |
| First cost | 7 | 10 | 8 | 6 | 5 |
| Fuel efficiency (4.0 weight factor with econom) | 36 | 38 | 40 | 36 | 36 |
| Economics | 8 | 10 | 6 | 5 | 4 |
| Totals | 58 | 67 | 62 | 56 | 55 |

Rating scale: 10 = best, 0 = worst

heavily in this application. Also note that performance is compared as though all systems were equipped with an economizer; an optimistic assumption for the ICR cycle. Results show that the hybrid simple cycle is the favorite although the ICR and steam turbine versions are very competitive. The hybrid simple cycle requires a high pressure ratio compressor with excellent operating range to surge; a design challenge.

Table 5 shows the result of rating the various applicable cycles in compression/ pumping. The outcome is not clear-cut at all. No economizer was assumed and first cost and fuel efficiency were weighted by a factor of 2.0 over other parameters. All three configurations will have to be studied in ATS Phase II. The ideal solution might be to offer standard and chemical recuperation as options off the same engine core. This may be a turbine design challenge due to the additional steam mass flow in the chemical recuperated version. Site conditions may dictate an air-to-air intercooler which can be a disadvantage with the ICR and chemical recuperator cycles. The

Table 5.
Comparative utility in compression/ pumping.

| Assessment parameters | Cycle type: Simple cycle | ICR | Chem recup |
|---|---|---|---|
| Emissions | 7 | 8 | 10 |
| First cost (2.0 weight factor | 20 | 16 | 12 |
| Fuel efficiency (2.0 weight factor) (no economizer) | 14 | 18 | 20 |
| Economics | 10 | 8 | 6 |
| Totals | 51 | 50 | 48 |

Rating scale: 10 = best, 0 = worst

chemical recuperator may have an additional site disadvantage if make-up water is required.

Table 6 shows the result of rating the various applicable cycles in generator sets. The outcome is again not clear-cut but favors the ICR cycle because of fuel efficiency. In particular applications space claim (not rated here) might be a factor.

It is the opinion of the author that ATS technology will not be favored at all in standby or emergency power units. First cost is essentially the only driver. Emissions should not be a factor in the occasional use scenario.

The ICR is currently favored in marine propulsion. A recent Navy competition selected this cycle over others. The ICR in this application has several advantages including water availability for the intercooler and specific fuel consumption. Recuperator fouling is a problem which can be alleviated through proper design.

Table 6.
Comparative utility in generator sets.

| Assessment parameters | Cycle type: Simple cycle | ICR |
|---|---|---|
| Emissions | 7 | 8 |
| First cost | 10 | 8 |
| Fuel efficiency (4.0 weight factor) (No economizer) | 30 | 40 |
| Economics | 10 | 8 |
| Totals | 57 | 64 |

Rating scale: 10 = best, 0 = worst

There appears to be no substitute for the simple cycle with steam generation in the cogen-steam market since steam is, by definition, a valuable product of the cycle.

## CONCLUSIONS

Allison draws the following preliminary conclusions from this preliminary design effort:

1. All cycles investigated require a high temperature turbine capability to be developed under ATS.
2. The HAT and intercooled chemical recuperation cycles compete in only a narrow sector of the industrial engine market. This is the result of the complexity and water usage of the HAT cycle and the limitation of the chemical recuperation cycle to applications where natural gas is readily available.
3. From a cycle point of view, the ICR and chemical recuperation cycles are similar. Both optimize at fairly low compressor pressure ratios (~15) because both want high temperature in the exhaust to optimize the recuperation process. Excess steam production with the chemical recuperation process makes it somewhat doubtful that the two recuperation processes are interchangeable from a hardware point of view. Allison intends to perform a global optimization on this cycle during Phase II of ATS.
4. There appears to be no substitute for the simple cycle with steam generation in the cogen-steam market since steam is, by definition, a valuable product of the cycle.

5. Both the ICR and the simple cycle in the hybrid mode or bottoming unit are competitive in electric cogeneration
   - ICR requires a moderate compression ratio ~10-15
   - Bottomed simple cycle:
     - Requires higher optimum pressure ratio ~20-25
     - Offers moderately high exhaust gas temperature for advanced steam turbines where desired
     - Can be used in the hybrid mode as electrical power requirements vary
6. Simple cycle and ICR are favored in compression/pumping.
7. ICR is currently favored in marine propulsion.
8. ATS systems in general will not be favored in standby/emergency power applications for purchase price reasons.

## FUTURE WORK

ATS Phase II will allow detailed study of the various industrial markets. The preliminary results of this paper will be used as a starting point. In the final analysis, the product picked for development must pay off. For the manufacturer, projected revenue stream must exceed development costs; and for the customer-revenue stream must return a profit on purchase price.

## REFERENCES

Mukavetz, Dale w. et al. *Proceedings of the Ninth Annual Coal-Fueled Heat Engines Contractors Review Meeting,* Morgantown Energy Technology Center, Oct. 1992

## 1.5 Advanced Turbine Systems - Studies and Conceptual Design

**CONTRACT INFORMATION**

| | |
|---|---|
| **Contract Number** | DE-AC21-92MC29234 |
| **Contractor** | ABB Power Generation Inc.<br>Turbine Power Division<br>1460 Livingston Avenue<br>North Brunswick, NJ 08902<br>(908) 932-6319 |
| **Contractor Project Manager** | Septimus van der Linden |
| **Principal Investigators** | Gregor Gnaedig<br>Franz Kreitmeier |
| **METC Project Manager** | Charles T. Alsup |
| **Period of Performance** | June 24, 1992 to February 24, 1993 |

### 1. INTRODUCTION

Present gas turbine based systems are available to achieve thermal efficiencies of 52%-54%. The need for even higher efficiencies in the future, along with low emissions and low operating costs, is apparent and has resulted in programs which are categorized as Advanced Turbine Systems (ATS).

The prime objective of this project task is to select a natural gas fired ATS capable of reaching 60% cycle efficiency. Several cycles were compared and evaluated under all different kind of aspects, to determine the one with the highest potential and, at the same time, the best overall fit within an experience base to guarantee project goals.

The goals and objectives set for the Advanced Turbine Systems can only be achieved with the introduction of new technology features. Based on ABB's experience over the last 50 years with combustion turbine technology, it was decided that the multi-step development potential of an advanced gas turbine in a combined cycle would offer a great opportunity to achieve major improvements over the current technology.

ABB concluded that a careful investigation of the current technology in combination with the potential of advanced features will result in an advanced combustion turbine plant which could achieve the efficiency and emissions target, as well as fulfilling the RAM requirements and the cost requirements. The results of this investigation will be discussed in this report. The combined cycle plant, with a state-of-the-art HRSG and steam turbine built around an advanced combustion gas turbine with a firing temperature of approximately 2600°F (1430°C), can achieve all of the set goals.

Major improvements aim at increasing the turbine inlet temperature to levels above 2600°F (1430°C) and at improving the cooling of the turbine section. Innovative cooling technology for turbine blades and vanes will be the answer to the high hot gas temperature. This was investigated by ABB in the early '80s and resulted in a steam cooling of the complete turbine in a closed loop system (U.S. Patent 4,424,668-1984). During this investigation, it was determined that several development steps would be needed for a closed loop steam cooling design for the rotor. After investigating the different options, closed cycle steam cooling was chosen for the cooling of turbine vanes and the vane carrier, whereas the rotor and the turbine blades will be cooled by air. Major development areas have been identified in both areas which will result insignificant changes in turbine design.

The technical basis for this project phase will be an already existing gas turbine with all development steps clearly outlined in the context of this machine. This approach will make it easier to define new development areas, as well as making it possible to evaluate the individual steps for achieving the overall goal of thermal efficiencies of 60% or greater.

Advanced turbine systems with firing temperatures above 2600°F (1430°C) will require new materials and the associated development needs have to be clearly defined. This goal will be closely connected to the cooling technology for turbine rotor and stator.

Lean premix combustion technology was identified for reaching low emissions and substantial in-house experience is available to define a development plan for reaching this goal. The challenge will be to increase the turbine inlet temperature and at the same time, to keep the emissions at levels associated with much lower firing temperatures.

The combination of all of the items mentioned above will determine operating and capital cost, as well as items like reliability, availability and maintainability (RAM). Since this study is based on an existing turbine system with multi-step improvements, the level of confidence in defining the necessary outlines is rather high and well founded, which makes the target date for the overall ATS program more easily achievable.

**Figure 1** shows the goals, as well as the trends for emissions, cycle efficiency and RAM combined in one graph. It is apparent that only the thermal efficiency goal coincides with the behavior of a gas turbine based plant, when the turbine inlet temperature is increased. The emissions and the RAM issues tend to increase with higher temperatures. This conflict was analyzed at any early point in a way that made using a well known equipment basis for this project more than an asset, but a necessity to reach all three goals to the same extent.

A further purpose of the study is to look at how such an ATS cycle would be commercialized, as well as examine the market potential for the specific system size that would be scoped.

A variety of different water/steam cycles are available for optimizing the thermal efficiency of a gas turbine based power plant. **Figure 2** shows the most important cycles, divided into two main categories with the gas and steam either separated or mixed. Any configuration in which water or steam is mixed with the hot gases from the turbine have the potential for high thermal efficiencies. However, the combined cycle, with hot gases and steam separated, has several advantages:

1. High efficiencies of more than 54% have been already reached (based on GT 13E2) with rather low firing temperatures of 2160°F (1180°C) (ANSI).

2. Proven components can be used for further development at higher firing temperatures.

3. High multi-step development potential.

4. Optimum expansion possibilities in future including integration of coal-firing.

5. Minimum water consumption with potential of dry combustion.

**Figure 3** shows a qualitative presentation of how to reach the goal of 60% thermal efficiency. The reference curve at the bottom is based on already existing ABB technology. Two points, at 52% and 54% efficiency have been determined in two projects, PEGUS12 in the Netherlands and DEESIDE in the U.K. The multi-step development curves utilize improvements of the different components in a combined cycle, such as turbine cooling technology, compressor inter-cooling and state-of-the-art heat recovery steam generator and steam turbine. The performance projections will determine which of these improvements will be incorporated in the cycle configuration.

## 2. RESULTS AND DISCUSSIONS REFERENCE CYCLE

### GAS TURBINE

Reducing the cooling air requirements for the hot gas components in the turbine section has been an ongoing process, since the turbine inlet temperatures have been increasing steadily. The two main reasons are the loss in gas turbine efficiency and the loss of air otherwise available for lean-premix combustion technology. Any air used for cooling the rotating and stationary parts in the turbine section, will not be expanded to its optimum and will therefore be associated with a decrease in efficiency.

Hence, ABB is proposing the steam cooling of the stator, vanes, stator casing, combustor, etc., i.e. all stationary parts, where it is easy to seal and the steam (after cooling the GT components) can be introduced in the steam turbine.

**Turbine Cooling Technology.** Using today's cooling technology, the increase of the turbine inlet temperature up to 2600°F (1430°C), would result in a very high air mass flow for cooling and, subsequently, in a high penalty on the efficiency rating. After looking at the different options, it was decided to use closed cycle steam cooling (CCSC) for the stationary part of

the turbine **Figure 4** and advanced air cooling technology for the rotating components in the turbine section. CCSC has been recognized as an attractive option for quite some time and ABB has contributed to the technology with their own research and some new development features which resulted in a patent on blade cooling.

The amount of cooling air required is significantly lower, since only the rotor and the turbine blades are air cooled. The advantage is manifold: In an air-cooled turbine the cooling air is compressed in the compressor and cools the vanes/blades, rotor, combustor, etc. and picks up considerable heat. The expansion of this air in the turbine is, however, poor. The difference between work received due to expansion and work needed to compress the air is usually negative, as the cooling air expands at significantly lower pressure. This loss is called throttle loss which is approximately 2% of the turbine efficiency, resulting in around 5% gain in thermal efficiency (multiplicative). Besides, the introduction of closed cycle steam cooling of the stator vanes avoids the mixing losses of coolant and the hot flow from the film cooling in the flow passages and in the trailing edge area of the cooled vanes. There is also an increase in polytropic efficiency of the vanes/blades, as the expansion is taking place as non-adiabatic. In total, these effects should result in approximately 8% (multiplicative) improvement in thermal efficiency of the gas turbine.

Another improvement can be seen in the steam cycle, as the steam temperature is increased during cooling of the gas turbine, resulting in a reheat effect. The total heat introduced in the steam leads to an increase in steam turbine output and hence, the efficiency of the total cycle. For a combined cycle plant, this improvement should result in an improvement of 10% (multiplicative) or more for the combined cycle efficiency.

**Lean-Premix Combustion.** One of the main goals of the ATS project is the limitation of emissions from the gas turbine without the use of post-combustion emissions control devices. The requirements for advanced turbine systems include high gas turbine firing temperatures and low emissions, with both items strongly affecting the combustor technology. ABB has extensive experience in a wide range of different combustor designs and combustion processes. State-of-the-art EV premix burners in various arrangements are available with a proven record of low emissions and high reliability. **Figure 5.**

This technology results in a flame which is much colder than the traditional diffusion flame. Since the production of thermal NOx is mainly influenced by flame temperature, it has been shown that NOx levels of less than 10 ppm can be reached at current turbine inlet temperatures. The flame temperature of the lean-premix system is approximately 2800°F (1540°C) and is typically reduced down to 2100°F to 2300°F (1150°C to 1260°C) at the turbine inlet by mixing it with cooler compressor discharge air. By reducing the cooling air requirements of all the hot gas components, the flame temperature will further decrease and the turbine inlet temperature will approach this new flame temperature. Therefore, it is expected to reach turbine inlet temperatures as high as 2,640°F (1,450°C) without increasing the emissions. However, one other factor for NOx production is the pressure at which combustion is taking place, and we will have to investigate how compressor pressure ratios of 16 to 17 will influence the emissions.

## HEAT RECOVERY STEAM GENERATOR (HRSG)

Recent trends in the application of combustion turbines for power generation indicate that large-frame machines in the size range from 80 MW to 250 MW will be used for utility combined cycle applications. A growth of combined cycle technology is also taking place with utilization of steam cycles with higher steam pressure and temperatures, reheat cycles and steam induction for power augmentation in the steam turbine at intermediate and low pressure levels. These steam cycle

characteristics promote the maximum utilization of gas turbine exhaust heat energy, using proven boiler and turbine technologies. The components supplied by the boiler manufacturer for a Heat Recovery Steam Generator (HRSG) are typically supplied as prefabricated subassemblies. The most advanced combined cycle configuration of today is based on a three-pressure, reheat heat recovery steam generator (HRSG). **Figure 6** shows a typical example of such a configuration.

The arrangement of heat exchanger sections for multiple pressure levels are arranged to take maximum advantage of temperature differences between exhaust gas and tube side temperatures. The HRSG can be arranged for horizontal gas flow across vertical tubes or vertical gas flow across horizontal tubes. Pressure parts are enclosed in an internally insulated casing and are completely free to expand independently of the outer casing structure. The major changes for the ATS program will be on the material side, which is typically designed for gas turbine exhaust gas temperatures of less than 1076°F (580°C). For advanced turbine systems these temperatures will be as high as 1220°F (660° C) and will result in steam temperature of up to 1148°F (620°C). It is apparent that the choice of materials will concentrate on austenetic steels.

The two critical temperature differences that influence the amount of heat-transfer surface and the overall steam generated at each pressure level are the:

- Pinch points: The difference between the gas temperature leaving an evaporating section and the temperature at which boiling is occurring (saturated water temperature).

- Approach temperature: The difference between the saturated water temperature in an evaporating section and the in-coming feedwater temperature.

The pinch point strongly influences the amounts of heat transfer surface in the evaporating section. Current HRSG designs use pinch points in the 15 to 25°F (8 to 14°C) range. In general, these boilers have 50% more surface in the evaporating section than boilers with pinch points of 40 to 50°F (22°C to 28°C).

The approach temperature also influences the amount of surface required for an economizer section, with exponentially increasing amounts required for very low approach temperatures. Current HRSG economizers have approach temperatures in the 15°F to 25°F (8°C to 14°C) range at the design point. Many other operating conditions can occur at off-design points, including start-up. Some conditions will result in steaming at the exit of the economizer, such that it acts as an evaporative surface.

Specific provisions to accommodate steaming at levels up to 5% of total flow in an economizer include: 1) careful control of water distribution in the last downflow passes of the economizer to cause that portion of the economizer to behave as a force-circulation evaporator, or 2) configuring the last few passes of the economizer as entirely up-flow with relief by natural circulation into the steam drum.

Fuel preheating will be part of the cycle configuration. Low pressure steam will be taken to a fuel/steam heat exchanger. **Figure 7** shows a typical example of a process flow diagram for a three pressure, re-heat boiler, including fuel preheating and CCSC for the gas turbine.

## STEAM TURBINE (ST)

A reheat steam turbine, divided in high, intermediate and low pressure section was chosen for this project. The isotropic efficiencies of the different sections are approximately 91 to 92%. **Figure 8** shows a typical cross section of such a steam turbine. This machine is from ABB's compact MT series and has the following design features:

- HP and IP-LP turbines in separate casings for a double casing reheat turbine
- Orientation of turbine that torque is balanced
- LP turbine with axial exhaust for optimum flow conditions with minimum losses
- Designed for fast start-up and fast load changes
- No pre-heater for minimum losses in stack
- The three pressure levels result in corresponding pressure for Closed Cycle Steam Cooling (CCSC) system
- Integration expansion sleeve coupling
- Reaction type blading 8000 according with optimized aerodynamic design for high polytropic efficiencies
- The integration of the reheat steam from the gas turbine in the steam turbine design

Recently, ABB has designed and developed new blading for the high pressure part of the steam turbine. This blading includes 3D features such as compound lean of the trailing edge region to reduce secondary flows and boost efficiency. Scale model tests on a five stage machine indicate that this blading has an aerodynamic efficiency gain of more than one percent. The blading is currently introduced into the ABB compact steam turbines and will be made available to the ATS program. Since all components of the ST are proven, there is no requirements for R&D.

## 3. CONCEPTUAL DESIGN

Within the framework of the DOE-ATS Feasibility Study, ABB has decided to utilize a combined cycle based on the multi-step development potential and the existing experience level. However, it is important to integrate this advanced gas turbine (AGT), together with a heat recovery steam generator (HRSG) and a steam turbine (ST) for maximum efficiency.

In a closed steam cycle available energies are transferred from one component to the next component in the cycle except at the energy rejecting point across the system boundary. Inside the cycle, the available energy degrades it's efficiency due to the various heat losses, pressure losses, mechanical losses, differences in the gas and steam temperature in the HRSG, and limitations in steam expansion due to condenser pressure. The rejected energy includes: energy losses from the HRSG exhaust stack, the energy from steam dumping to condenser, and leakage of energy to the surroundings.

**Reference Case.** The basis for this section of the investigation is the ABB gas turbine GT 13E2, with annular dry low NOx combustor **Figure 9**. The GT 13E2 has a compressor which is both axially and radially split for easy machining and maintenance. The rotor follows traditional ABB design with a welded rotor. The GT 13E2 is designed for the 50 Hz market, but its technology can be scaled down for a 60 Hz machine with a similar efficiency by applying a factor of $1.2^2$ for power output and mass flows. ABB has developed axial compressor technology over the last 50 years. These compressors now have polytropic efficiencies of about 91%. Currently, the computer codes used in the design process have been extensively validated by test rig results and from results in the open literature, and ABB has good confidence in the design methodology used for compressor design.

The main work done here was to establish that the compressor operating conditions will allow for the extra mass flow availability by the reduction of cooling air requirement for the turbine. Besides, the operating point due to lower turbine mass flow leading to reduced pressure ratio needs to be defined in the compressor map.

Due to the reduction in cooling air requirement from the turbine, achieved by steam cooling and advanced air cooling, there will be more mass flow through the compressor and less mass flow through the turbine. This is because intermediate pressure cooling air for the low pressure turbine cooling (drawn from the 5-7th stage of a 15 stage compressor) will be significantly reduced.

Advanced Turbine Technology

ABB has been developing turbines over the last 50 years and are now poised to make significant improvements to the overall turbine efficiencies. Current turbines operate at around 84-85% in-engine cooled polytropic efficiency, including all throttle and mixing losses. ABB is already developing advanced turbine components which will increase this by around two points in efficiency. These turbines will be evolved around the GT 13E2, GT 11N2 type of "family" turbines and do not take into account any significant reductions in cooling air mass flow.

It is considered that within the time frame for the present ATS program, these new turbines will be available well before the engine-in-service date of year 2002. The development of the ATS is therefore considered to be a low risk item in terms of meeting the overall GT cycle efficiency.

The turbine used for the ATS will be that of the GT 13E2 gas turbine or an upgrade thereof. This turbine is well proven and requires little change to meet the performance requirement for the ATS. However, as stated above, ABB is committed to improving turbine aerodynamic performance as part of another internal program of work alongside the present DOE/ATS program. such a change will ensure that any new turbine will be able to comfortably meet or exceed the present performance of the GT 13E2 turbine module with superior RAM features.

Cooling Effectiveness

Preliminary calculations indicate that the cooling effectiveness will be increased by approximately 25% when using steam instead of air at the same conditions. This indicates the relative merit of using steam cooling. Further work will have to be carried out in this area where the steam is introduced at the optimized HRSG delivery conditions which will be at higher pressure and lower temperature. These conditions will be beneficial for the cooling design because the Reynolds number of the cooling steam will be higher and makes for higher cooling efficiency. The actual cooling effectiveness and the cooling efficiency for the steam cooled part will have to be established and fixed on the cooling technology charts, **Figure 10.**

Air Cooled Rotor Blade Components

The technology difference between utility and aircraft engine cooling system effectiveness and efficiency is shown on **Figure 11**. The goal for the air cooled parts for the ATS program lies between the two technologies and therefore it is clear that there needs to be a migration upwards for the utility machines to meet the requirements of the ATS program. This is considered to be a low risk development because the aircraft engine technology can already comfortably exceed the cooling targets. However, work will need to be done in transferring the highly complex aircraft cooling systems into the utility size components.

ABB has already introduced an aggressive program of work (1990) to improve the cooling performance of air cooled vanes and blades. This is done by a two step approach whereby the cooling system efficiency is improved while, at the same time, advanced materials technology is introduced. ABB and AGT (Allison Gas Turbines) will apply their experience to progress very high efficiency air cooling technology for the ATS rotor blading. It is expected that one approach would be for AGT to utilize Lamilloy/Cast Cool® technology to achieve efficiencies higher than available with conventional casting techniques. It is expected that this will result in turbines operating at 2750°F (1510°C) by the end of the century. It is considered that this is a realistic goal, because modern aircraft engine designs can already operate with increased firing.

As previously reported based on GT 13E2 technology, ATS in CC operation can reach the overall goal of 60% thermal efficiency. With steam cooling technology fixed at present operational levels, but incorporating improved GT component efficiencies, the cycle efficiency can be extended to 61%. Steam turbine

improvement programs for the HP section could be incorporated in the future for additional gains in efficiency.

## 4. INTERMEDIATE DEVELOPMENT NEEDS

The multi-step development project proposal of ABB requires, amongst others, the introduction of advanced high temperature materials and advanced steam cooling concepts. The high temperature materials will be needed to raise the turbine inlet temperature (TIT) and to reduce the requirements for cooling air in the combustor. A future dramatic increase of TIT will be possible by the use of steam cooling.

ABB has significant experience in optimizing the materials technologies for steam and combustion turbine systems, to meet market needs. ABB has developed proprietary alloy and coating compositions to meet the unique demands of the power generation systems. An integrated program of research and development continues at ABB's international facilities in the USA, Germany, Sweden and Switzerland. In general support of this program. independently funded activities are underway in the following research topics:

- Corrosion-resistant, high-castability, directionally-solidified and single-crystal alloys.
- Casting process science for directionally-solidified and single-crystal blading.
- Optimization of blading design for high casting-yield by process simulation modeling.
- Improved reliability, high temperature oxidation/corrosion protection coatings.
- Improved bond coatings for thermal barrier coatings.
- Ceramic systems for lightly loaded combustor components.
- Power metallurgical manufacture of large steam turbine blades.
- Lightweight blading for intermediate temperatures.

The output from these programs, in terms of developed materials and processes, will be used in further development of the ATS program.

The unique material solutions required to meet the innovative power-generation cycles will require demonstration/validation. Thus, while improved temperature capability combustor and turbine materials will be made available from the ABB generic research and development activities, the specific needs associated with steam cooled turbine vane will need to be validated within the program.

In developing systems for the next family of power generation turbines, the increased gas turbine entry temperatures necessary for improved cycle efficiency, coupled with the need to maintain or reduce environmentally degrading emissions, results in a lower availability of cooling air for the turbine components. Thus, improved temperature capability components are required. These can be realized by a combination of improved material capability and high cooling-efficiency design. From the materials technology perspective, these changes require an integrated approach for improved materials and manufacturing processing. The high efficiency cooling designs place a premium on manufacturability. For blading, **Figure 12** illustrates the increasing complexity relative to castability of aero-engine turbine blade cross sections.

Through a combination of new materials and advanced cooling technologies, it is planned to raise the current turbine inlet temperature by 100°C. The application of steam cooling to the blades and vanes of the turbine will give a further increase of TIT of 300°F (160°C), bringing the total TIT increase to 480°F (260°C).

Traditionally, the land based power generation gas turbines have utilized conventionally cast blading alloys with oxidation/corrosion protection coating. ABB has traditionally used high chromium containing alloys such as IN738LC (16% Cr as compared with 6 - 9% in

typical aero-engine alloys), and chromia forming vacuum plasma sprayed coating such as the ABB proprietary SV20. These systems, combined with relatively conservative cooling efficiency designs have performed well relative to competing systems. **Figure 13** illustrates the family of corrosion coatings available, and the surface temperature limits for 24,000 hours life.

As firing temperatures have increased, an increase in blade cooling efficiency has been necessary. Highly cooled blades tend to suffer from material damage accumulation during temperature transients. Thus the trend has been away from blade life limitation due to creep damage accumulation, towards limitations because of thermo-mechanical fatigue damage. (Also known as LCF damage.)

Without taking into account the concurrent improvements in blade cooling technology, advances by DS and SC technology will give increases of T.I.T. 100°F and 180°F (55° C and 100°C), respectively. An important feature of our program involves the introduction of steam-cooling to blades.

## STEAM COOLED COMPONENTS DEVELOPMENT AND TESTING PROGRAM

The design of a steam cooled blade would follow normal design procedures employing knowledge gained from past cooling designs with care being taken that the change of the solubility of the steam does not lead to deposits in the cooling passages. The cooling of the trailing edge portion of the vane represents the most technically challenging part of the design due to the constrained geometrical space here which must house the cooling system.

Following the scale model verification and material tests, testing of steam cooled vane prototypes are planned in guide vane cascades and/or actual engine application in collaboration with a utility customer under real design conditions of ATS. The prototype tests will demonstrate the feasibility of using steam cooling confirming the cooling efficiency and higher effectiveness predictions, vane mean metal temperature and expected life time.

A further development need is to conduct a 16,000 hour testing of various superalloys, including single crystal materials exposed to the cooling steam environment at two temperatures up to 2000°F (1090°C) (at ambient pressures). Specimens will be examined at several times during the test exposure visually and metallographically. Testing can be done in existing facilities at ABB. The data will indicate the cycle behavior of these materials under a high temperature steam environment and can be utilized for materials selection for the steam cooled parts.

## PLANT LAYOUT

With the proposed conceptual design, plant layout will not differ from current compact combined cycle plants developed and built by ABB worldwide, the improvement being higher power density and increased MWs, i.e. one unit vs. two 1991- vintage machines **Figure 14.**

## 5. CONVERSION TO COAL-FUELED REFERENCE CASE

ABB has made many conceptual designs for coal-fueled systems incorporating today's gas turbines. There are several advanced coal fueled systems being developed which may have advantages such as better efficiency and lower emissions. These systems include:

Coal Gasification Combined Cycle - both integrated with the power plant (called IGCC, Integrated Gasification Combined Cycle) and non-integrated with gasifier and power plant at separate locations.

Pressurized Fluidized Bed Combustion - both the current generation with modest turbine firing temperatures of about 1600°F

(871°C) and the advanced concepts with higher firing temperatures.

Externally Fired Cycles - in various configurations, with high temperature heat exchanges.

Integrated Gasification Humid Air Turbine - where the steam cycle is eliminated and the gas turbine provides all the power.

Even before this current study, ABB has investigated most of these concepts and is very active in IGCC and PFBC.

For the purpose of this study, ABB has identified IGCC as the coal-fueled system to which we would like to adapt the advanced gas turbine. Some of the factors in this selection include:

The combined cycle is a proven cycle with high efficiency. As we chose the combined cycle for our natural gas-fired reference system, we believe the same advantages apply to the coal-fueled system.

There are many parties developing gasification and IGCC systems and there are many configurations being considered for gasification systems: gasification for chemical feedstock production, IGCC, cogeneration applications, IGCC with off-peak chemical production, etc. Thus it appears that gasification and IGCC have great potential to be commercialized in the near future.

Given that IGCC is the selected coal-fueled system, there are still many variations which impact the gas turbine design. One issue is in the source of the oxygen for gasification. In most oxygen-blown gasification systems, an independent air separation unit (ASU) supplies oxygen to the gasifier. No air is extracted from the gas turbine compressor for the gasification process, and the fuel to the gas turbine is all extra mass. Since the coal gas has a lower energy density than natural gas, there is more extra mass flow, which has implications for balancing the compressor and expander.

Most air-blown IGCC concepts and oxygen-blown IGCC with an integrated ASU extract the air for gasification from the gas turbine compressor. This requires a design change for the extraction, which in turn means less extra mass flows through the turbine expander.

The following three sections which discuss the gas turbine design impacts consider all of these factors. For performance and emission estimates, we have used an oxygen-blown gasification system with no air extraction for the purpose of the illustrative calculations.

**Implications for Gas Turbine Design**

Integration of the advanced gas turbine into an IGCC system will require some changes in the gas turbine design:

A. Extraction of Compressor Air - Some IGCC configurations require extraction of air from the compressor for the gasifier. As the turbine firing temperatures rise, however, more of the compressor air is required for cooling, leaving less available for extraction. The steam cooling provides a significant advantage in this regard for oxygen-blown gasification as extraction is not needed, as the GT will have sufficient margins.

B. Environmental Factors - $NO_x$, CO, and unburned hydrocarbon (UHC) emission will be influenced by the fuel fired in the gas turbine combustor. Modifications to the combustion system may be required. Other pollutant such as $SO_2$ and some air oxics will be less dependent on the turbine combustion system, but depend more on the gasification process.

C. Materials Implications of Fuel Quality - In an IGCC system, products of coal combustion pass through the turbine section. This gas will contain some level of sulfur, alkalis, metals, and particulate which can harm the turbine materials and

degrade the performance. Possible impacts include selection of materials, allowable temperatures, and tolerances.

D. Compressor/Turbine Balancing - In today's natural gas combined cycles, the added fuel is about 2% (wt) of the compressor air flow. With the higher firing temperature of the advanced turbine system, it could be about 2.5%. In an IGCC system, a higher percentage of added mass will flow through the turbine, which has implications for balancing the compressor and turbine sections.

Note that some of these factors can be addressed in the gasification system as well as in the gas turbine.

- An IGCC system can be designed with air extraction from the compressor or with a separate source of air.
- The gas turbine materials can be protected by more stringent cleanup of particulate and alkali if necessary from gasifiers.
- Ammonia removal from fuel gas has been considered to reduce the levels of $NO_x$ from the turbine combustor.

**Performance of the IGCC System**

The steam bottoming cycle used in the coal-fueled combined cycle system for these calculations is similar to that in the natural-gas-fired reference system - three pressure levels with reheat and steam cooling of the gas turbine. There are two differences between the two steam cycles:

In natural gas fired combined cycles, the exhaust gas has a very low sulfur content so the stack temperature can be very low without concern for acid dewpoint. To achieve a low stack temperature, the feedwater coming into the economizers should be cool. Feedwater heaters raise the temperature of this feedwater, so in the natural gas reference case we had no feedwater heater other than the deaerator. The feedwater enters the HRSG at the deaerator temperature of about 55°C (130°F) and cools the stack temperature to about 80°C (175°F). In the coal fueled case, the exhaust gas contains more sulfur, so the stack gas cannot be cooled to the same extent. With one additional feedwater heater, the feedwater enters the HRSG at about 100°C (212°F) and cools the stack gas to about 120°C (250°F). (Figure 15)

In the IGCC system, the gasification process gives up heat which is used in the steam cycle. In the present calculation, 16% of the coal's lower heating value is used to generate high pressure superheated steam. Feedwater is taken from the HRSG after the second high pressure economizer and taken to the gasifier island. The superheated steam is mixed with that from the HRSG just before the high pressure turbine. This affects the distribution of heat duties in the HRSG somewhat, since the first two economizers in the HRSG handle the full high pressure flow but the third economizer, evaporator, and superheater in the HRSG handle just a portion of the full flow. **Figure 16**

The oxygen-blown gasifier in the calculation is assumed to have a cold-gas efficiency of 80.3%, i.e. 80.3% of the coal's LHV shows up as fuel gas LHV. In addition, some sensible energy is in the fuel gas. The estimated overall efficiency of the cycle is 52.17% (LHV basis). An air-blown gasifier would be expected to have a performance improvement because of the auxiliary power requirement of the ASU in $O_2$ gasifiers. This will require further investigation with developments taking place in Air Blown Systems.

In a recent development program, slightly modified version low $NO_x$ EV-burner successfully completed a series of tests with a simulated MBTU gas under real high pressure engine conditions. The EV-burner works in a pre-mix mode without flashback and $NO_x$ emission levels measured at 25 vppm @ 15% $O_2$.

Gas Turbines with this EV-burner concept can now use an independent ASU, which will be superior to all integrated ASU concepts with respect to electrical efficiency.

**Gasification Process Description**

The ABB CE gasification process uses an entrained-flow, slagging bottom gasifier. **Figure 17** shows the main components of the gasifier island. Coal is pulverized to 70% through a 200 mesh screen and pressurized in a lock hopper system for feeding to the gasifier. The coal and the recycle char are fed to the gasifier. The coal and char are mixed with oxygen from an independent air separation unit, and the fuel-rich mixture is burned creating the high temperature necessary to gasify the coal and to melt the mineral matter in the coal. The slag flows through a slag tap at the bottom of the gasifier into a water-filled slag tank where it is quenched and transformed into an inert, glassy, granular material. This vitrified slag is non-leaching making it easy to dispose of in an environmentally-acceptable manner.

Gasification occurs along the height of the gasifier until the temperature falls to a point where the gasification kinetics become too slow. Once the gas temperature reaches this level, essentially no further gasification takes place and the gases subsequently are cooled with convective surface to a temperature low enough to enter the cleanup system. Thus, nearly all of the liberated energy from the coal that does not go into producing fuel gas is collected and recovered with steam generating surface either in the walls of the vessel or by conventional boiler convective surfaces in the backpass of the gasifier. This boiler style design provides for recovery of coal energy as either fuel gas or steam (for use in the steam turbine to generate electricity).

A mixture of unburned carbon and ash (called char) is carried out of the gasifier with the product gas stream. The char is collected and recycled back to the gasifier where it is completely consumed. Thus, there is no net production of char, which results in negligible carbon loss.

The produce gas then enters a desulfurization system where it is cleaned of any sulfur compounds present in the fuel gas. The clean fuel gas is now available for use in the gas turbine combustor for the combined cycle application.

There are many factors that affect the quality of the product gas derived from IGCC or PFBC, such as the contamination of the gas, the heating value, the flammability, and the composition of the gas. In view of the potential existence of the corrosive substances (sulfur, alkalis, and metals in ash/gas), a near free-of-contamination particulate removal system and gas cleanup system is critical to the success of the conversion from the gas turbine to the coal-fueled gas turbine. Special concerns shall address the more stringent cleanup of particulate and corrosive substances proper material selections for the critical elements, heat tracing of fuel lines, proper gas pressure in design, adequate inlet air filtration system, and proper safety consideration for the high hydrogen contents, etc.

## 8. COMMERCIALIZATION - NATURAL GAS-FIRED REFERENCE SYSTEM

The ABB team is convinced that the advanced gas turbine system (ATS) technology power plant fits a variety of market requirements. The team believes that a substantial market exists and will further develop for installation rated

between 100 and 250 MW modularized construction that is easily transportable and suitable for fast installation. However, one of the major issues for any new technology is customer acceptance. From the customer point of view, the question is whether the potential advantages of new technology offset the risks involved; what cost, reliability, maintainability, and size criteria must be met for an electric utility to buy an advanced gas turbine system? The Task 1 (Phase I) study is a first important step in that direction. The results of this study and subsequent work should greatly help in answering these questions. Further R&D work, however, is required and demonstration plants and first commercial deployment plants would have to be built before a satisfactory answer becomes available.

**Demonstration Plant**

The primary technology issue for commercialization is to achieve successful performance demonstration of the selected system. The logical step is to build a demonstration plant. To reduce cost, it is recommended to build a retrofit demonstration plant in the size range of current engine size. These are several power stations which have small generating units and are to some extent inactive. The units which have been shut down for various reasons would still have the available steam turbine generators and balance of plants support systems suitable for continued operation. Furthermore, an interest in reactivating these units exits, if they can be made to operate economically and reliably, which is one of the objectives of this program. It must be recognized that the demonstration plant, although very attractive to the host utility, involves risks, and these should be substantially sponsored by DOE and possibly EPRI and other institutions.

**First Commercial Plant**

The major objective of the first commercial plant is to demonstrate reliability, economic competitiveness, and to evaluate performance of the commercial marketable unit. The design, fabrication, start-up, and operating schedule has to be judicially drawn up to ensure proper timing of a market breakthrough. It will require monitoring the market needs and demands on a regional basis and throughout North America and, for that matter, on a worldwide basis. This will be supported by further market studies.

Preliminary cycle studies indicate the objective of high efficiency Reference Cycle is achievable. Furthermore, many of the components utilized in the cycle evaluations are state-of-the-art. This feasibility assessment would indicate that the commercial deployment of high efficiency systems could be accelerated to late 1990s. The team's objective is to be a participant in the commercialization of a selected Reference Cycle configuration of GT Combined Cycle with CCSC.

Lower electricity costs are in the economic interest of the USA and the manufacturing industry. With substantial investment in 50 facilities, as well as the growing importance of ABB's Turbine Manufacturing Division in Richmond, Virginia, commercialization of the ATS program will be a primary factor.

**Business Factors In Support Of Commercialization**

- Evolutionary technologies in Company's Strategic Plan, Phase I selection
- Availability of engineering capabilities to support the Plan
- Market interests and needs
- Marketing expertise
- Manufacturing facilities to support the plan
- Financing alternatives to implement the Plan
- Host utilities - consortia and joint ventures

**Market Development**

It is considered very important to acquaint the utilities with the advanced power plant concepts with emphasis on their economics and advantages to develop a market for this technology. It is recommended that EPRI, and GRI, with DOE's leadership, take various steps to promote the technology with potential clients.

Active steps under ABB's guidance will be initiated, which would provide more definitive data on performance optimization and system selection. This effort should be focused especially toward those utilities who would be making power plant additions and would be the likely candidates for the proposed advanced technology gas turbines.

Keeping utilities informed of the progress made by the proposed technology throughout the various phases of this program is a necessity. The utility response would finally decide the market potential, expected market share, and commercial plant size; only then can the return on investment be evaluated. The on-going market development activities, which should be started at or during Phase 2 by the team members, will end only after the technology becomes fully commercial.

## 7. CONCLUSION

The ABB selection for the Advanced Turbine System (ATS) includes advanced developments especially in the hot gas path of the combustion turbine and new state-of-the-art units such as the steam turbine and the HRSG. The increase in efficiency by more than 10% multiplicative compared to current designs will be based on:

- Turbine Inlet Temperature Increase
- New Cooling Techniques for Stationary and Rotating Parts
- New Materials

Present, projected component improvements that will be introduced with the above mentioned issues will yield improved CCSC turbine performance, which will drive the ATS selected gas-fired reference CC power plant to 61% LHV or better.

The decrease in emission levels requests a careful optimization of the cycle design, where cooling air consumption has to be minimized. All interfaces of the individual systems in the complete CC Plant need careful checks, especially to avoid unnecessary margins in the individual designs.

Coal conversion with $O_2$ blown gasifiers with cold efficiency of 80.3% will provide estimated overall performance in excess of 52% LHV.

This study is an important step pointing out the feasibility of the ATS program with realistic goals set by DOE, which, however, will present challenges for Phase II time schedule of 18 months. With the approach outlined in this study and close cooperation with DOE, ATS program success can be achieved to deliver low emissions and low cost of electricity by the year 2002. The ABB conceptual design and step approach will lead to early component demonstration which will help accelerate the overall program objectives.

*ACKOWLEDGEMENT*

*Acknowledgment is made to the ABB GT Engineering department in Richmond as key participants and investigators throughout the program: Axel von Rappard and Gregor Gnaedig; ABB/GT Development department in Baden: Franz Kreitmeier, Hans Frutschi, and Dr. Prith Harasgama who provided cycle concepts and technical direction regarding turbine development. ABB/PPL R&T department in Windsor: Dr. Gernot Gessinger, Dave Turek, John Chiu and Mike Hargrove who provided cycle calculations, materials consideration as well as coal conversion concepts.*

**REFERENCE LIST**


1. Frutschi, H. and Plancherel, A.
   Comparison of Combined Cycle with Steam Injection and Evaporization Cycles
   ASME COGEN-TURBO 1988, Montreux

2. Ziegler, D. et al.
   PEGUS 12, The World's Most Efficient Power Station
   ASME 90-JPGC/GT-3

3. Viereck, D. et al.
   GT 13E2, The Cleanest Gas Turbine for Combined Cycle and Cogeneration Application
   ASME COGEN TURBO 1992, Houston

4. California Energy Commission Hearings Proceedings
   April, 1992; Sacramento

5. Advanced Combustion Turbine Conference
   Sponsored by ENERGY DAILY
   June, 1992; Washington, D.C.

6. W. Jury, P. Muller, K. Reyser
   Gas Turbine (GT) Air Separation Unit (ASU)
   Integration for IGCC A Study Based on ABB-EV Burner Technology for Gas Turbines
   EPRI - Utility Gasification Conference
   October, 1992; San Francisco, CA

7. Novem
   System Study High Temperature Gas Cleaning at IGCC Systems
   1992

8. Thibeault, Paul R.
   Internal Report
   Hot Gas Cleanup Systems Status Report
   May 1990

9. Twelfth Annual Gasification and Gas Stream Cleanup Systems Contractors Review Meeting
   Abstracts
   September, 1992

10. Eleventh Annual Gasification and Gas Stream Cleanup Systems Contractors Review Meeting
    Proceedings
    August 1991

11. ATS Design Program - Ninth Annual Coal Fueled Heat Engine Conference
    October 26/27, 1992

12. Final Technical Report - work performed under Contract No. DE-AC21-92MC 29234
    February 24, 1993

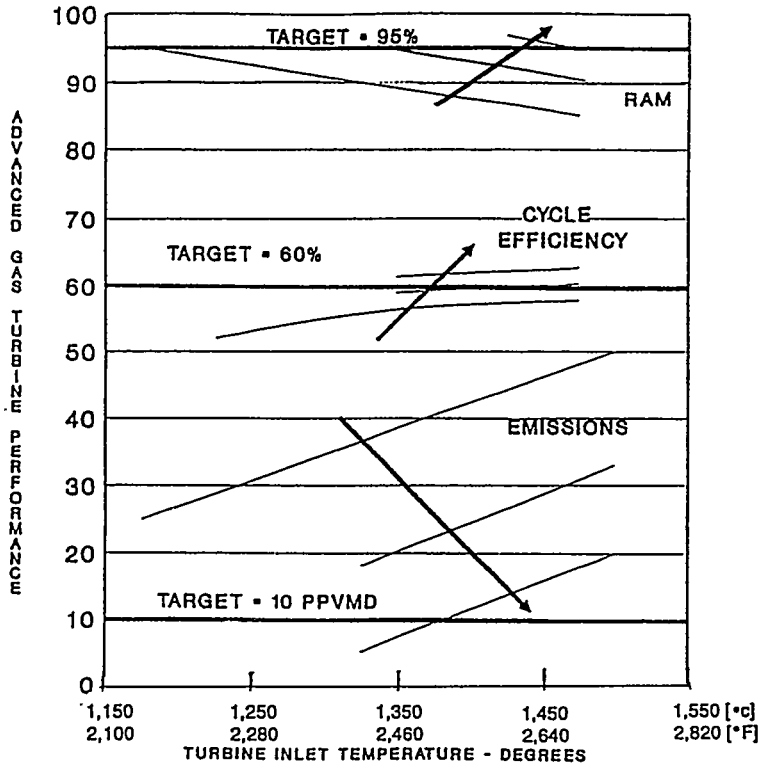


## Issues:

- High RAM
- High Efficiency
- Low Emissions

**Figure 1** Goals - Predicted Trends for ATS Program

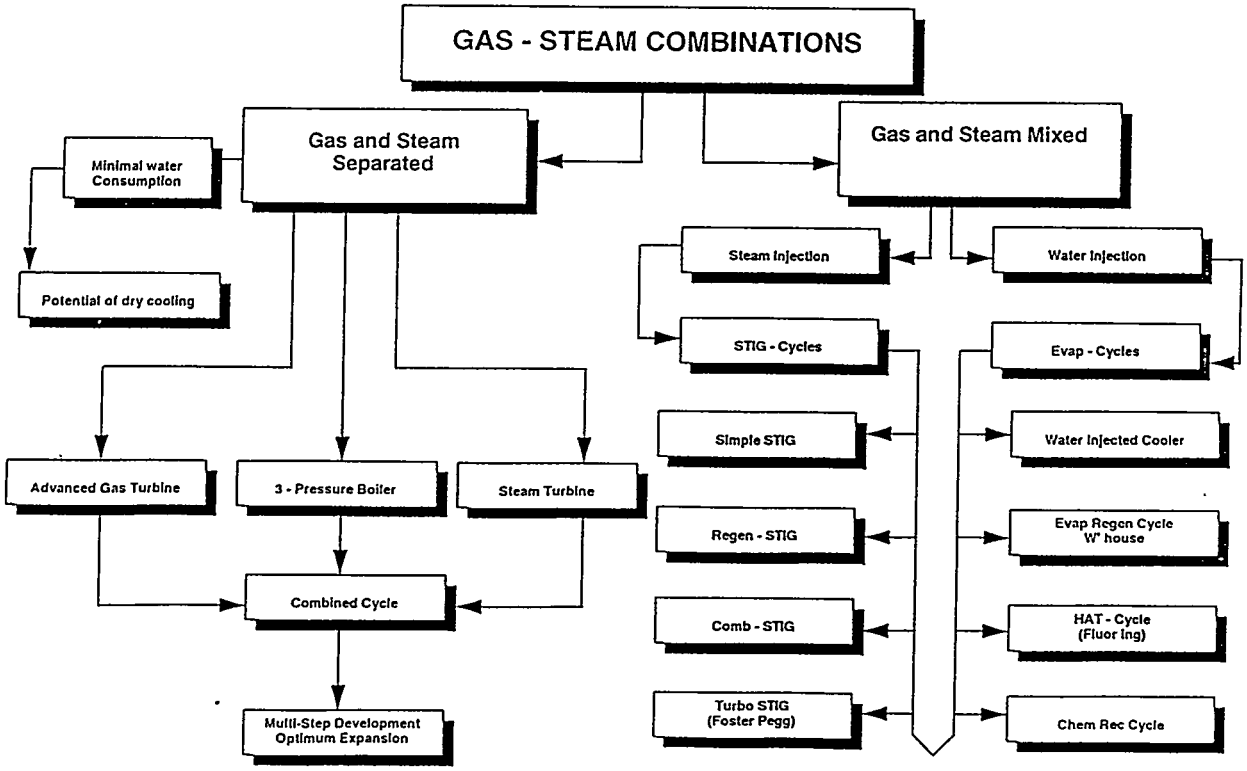


**Figure 2. Water/Steam Cycles for Optimizing GT Cycles**

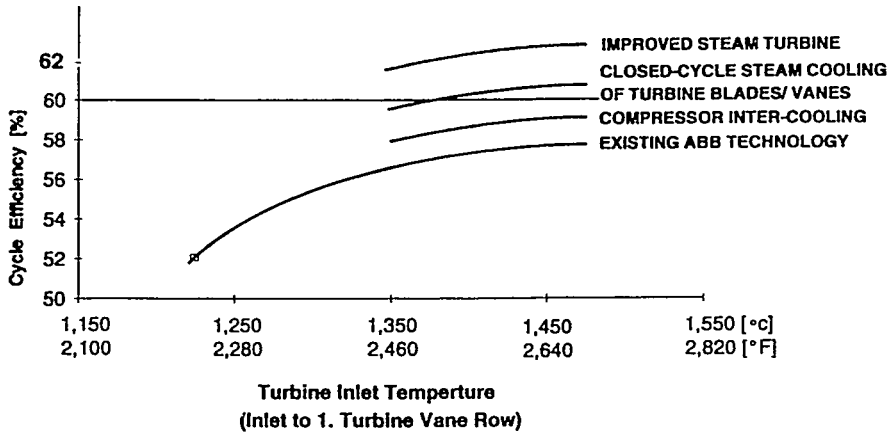


**Figure 3** ATS Multi-step Development Potential of Combined Cycle

# U.S. Patent, D. Mukherjee

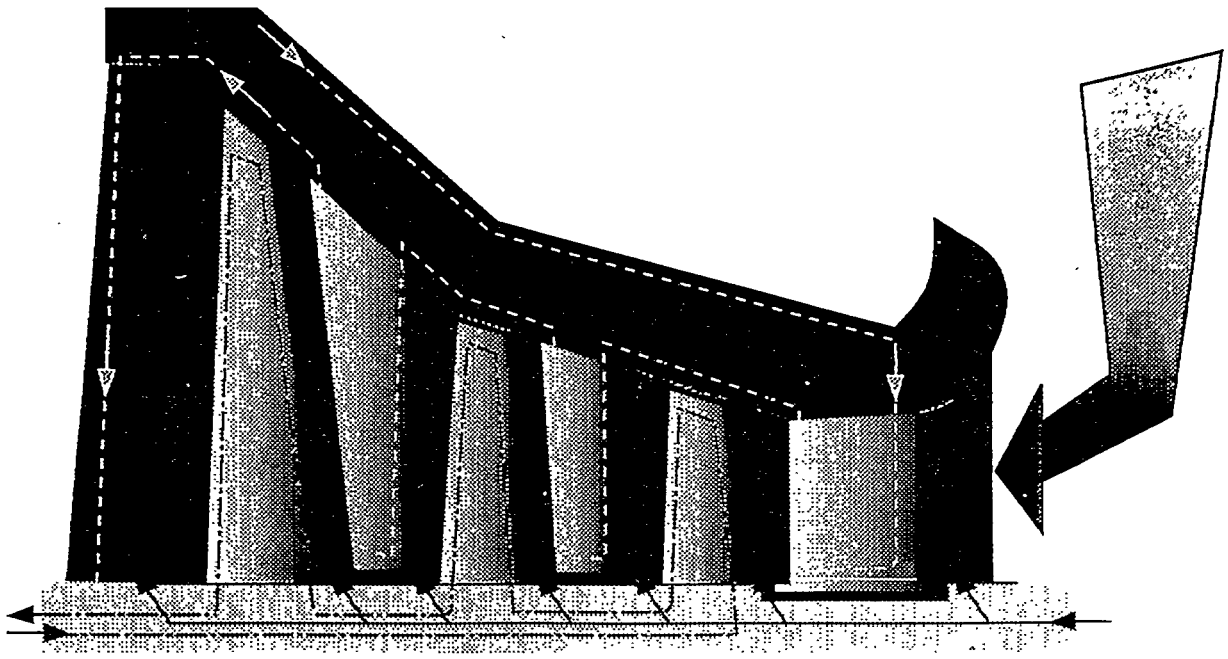

FIGURE 4. GT STEAM COOLED VANE AND VANE CARRIER

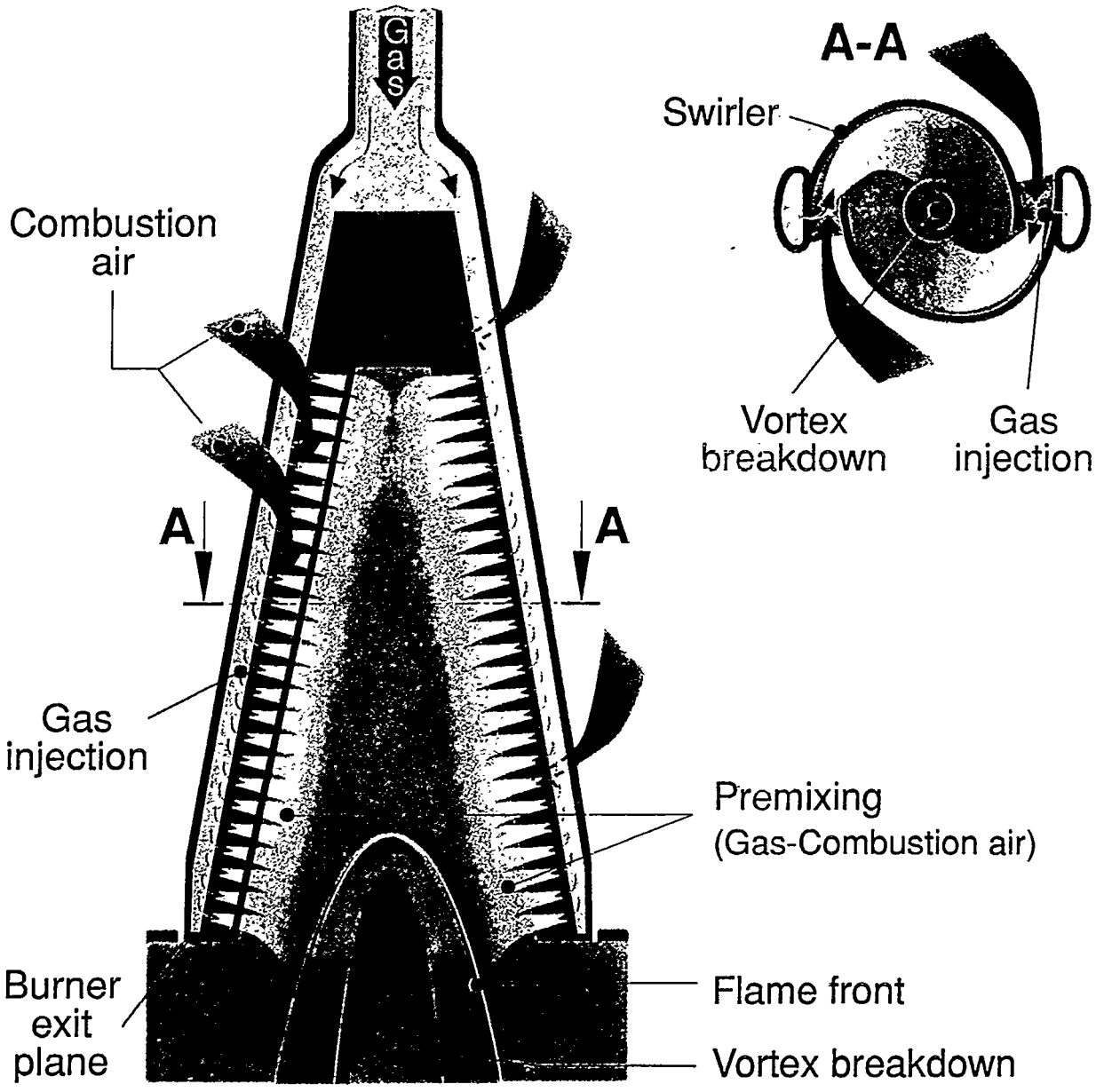


FIGURE 5. EV LEAN PRE-MIX BURNER

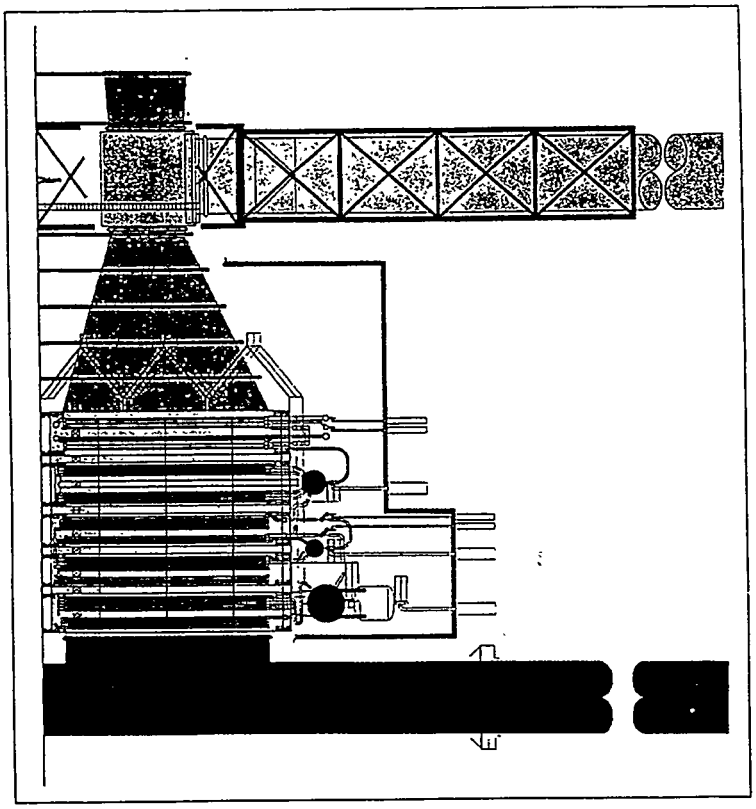

**Figure 6. Three Pressure HRSG With Optional Bypass**

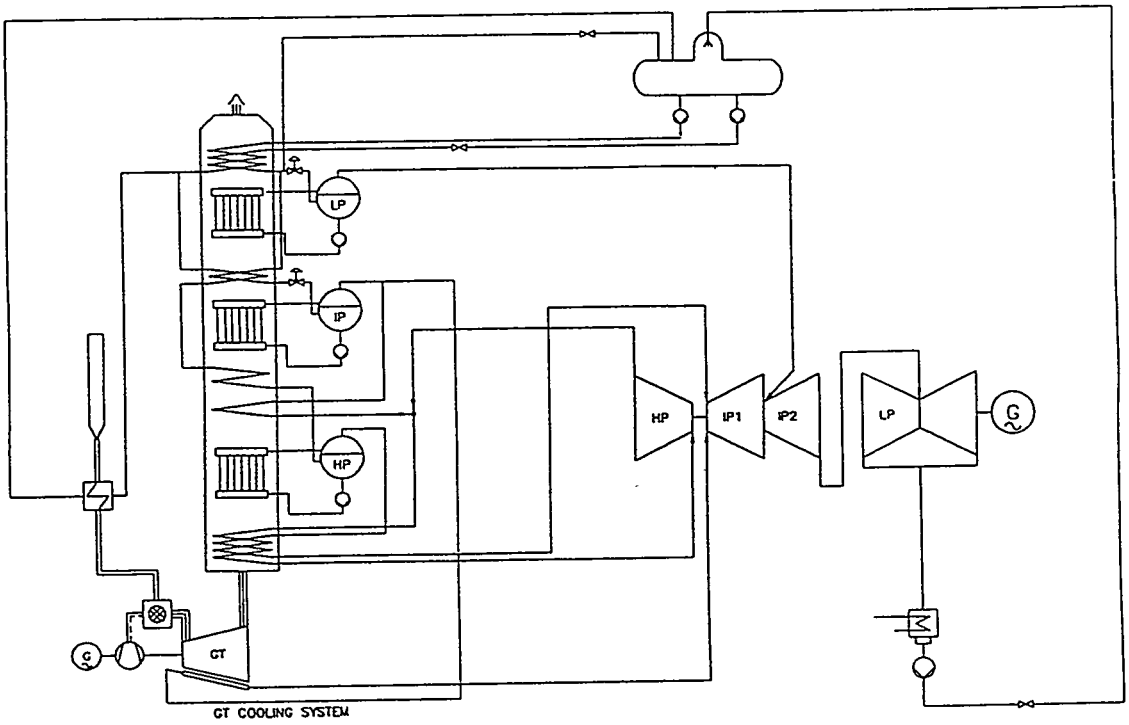


**Figure 7. ATS CCSC Process Flow Diagram**

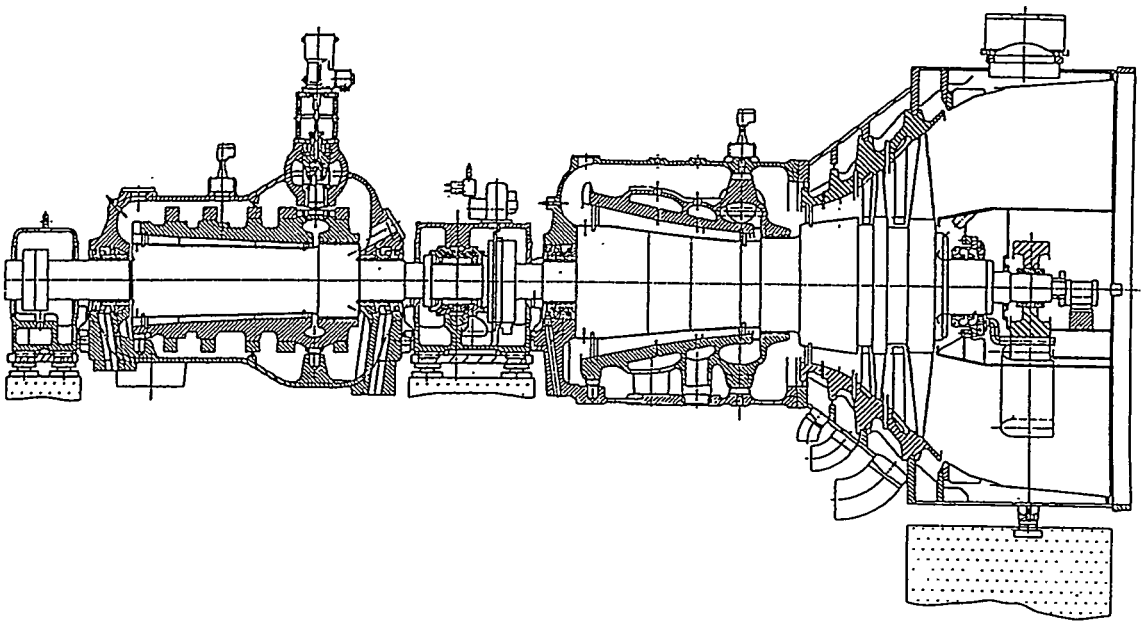

**Figure 8. Compact MT Reheat Steam Turbine With Axial Exhaust (KA-13E2-1)**

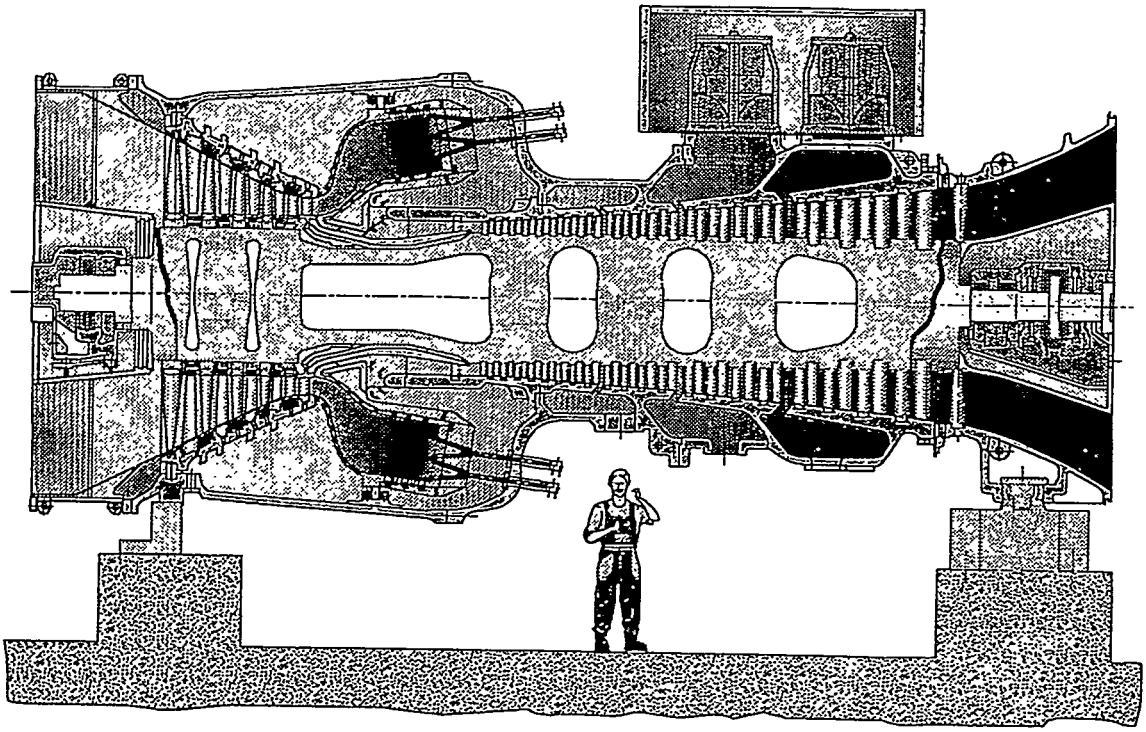

**Figure 9. GT 13E2 With Annular Dry Low $NO_x$ Combustor**

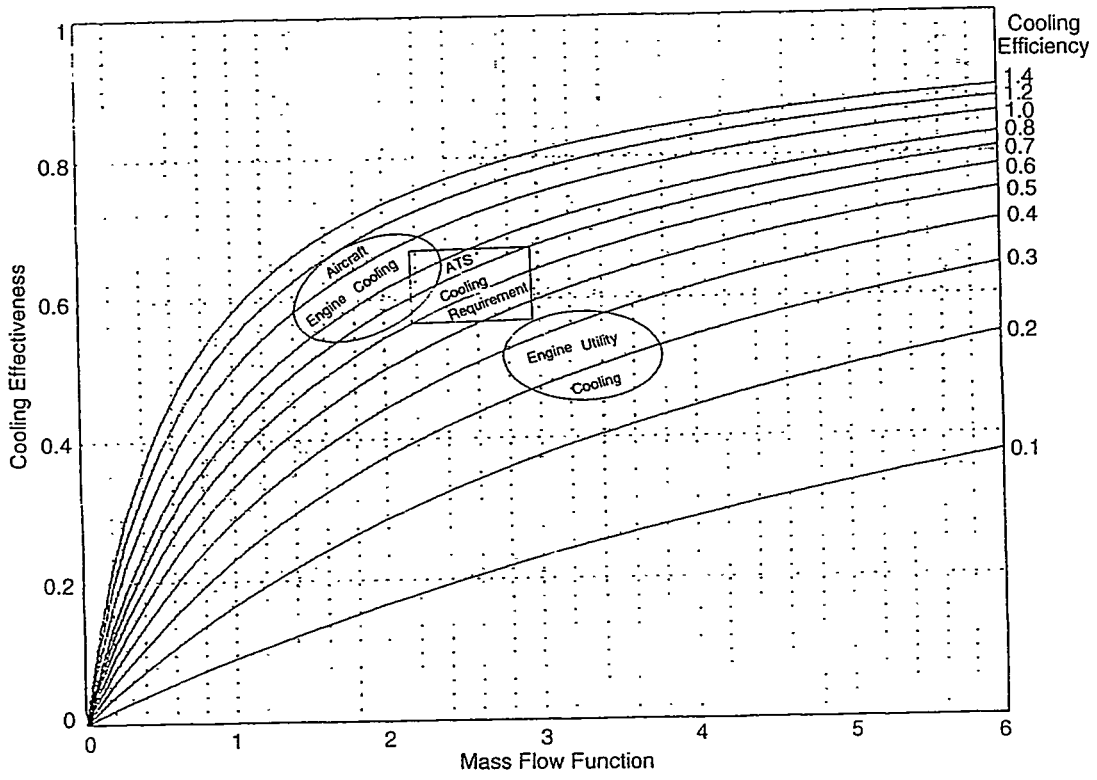


**Figure 10** Non-Dimensional Cooling Performance for Stator Vanes

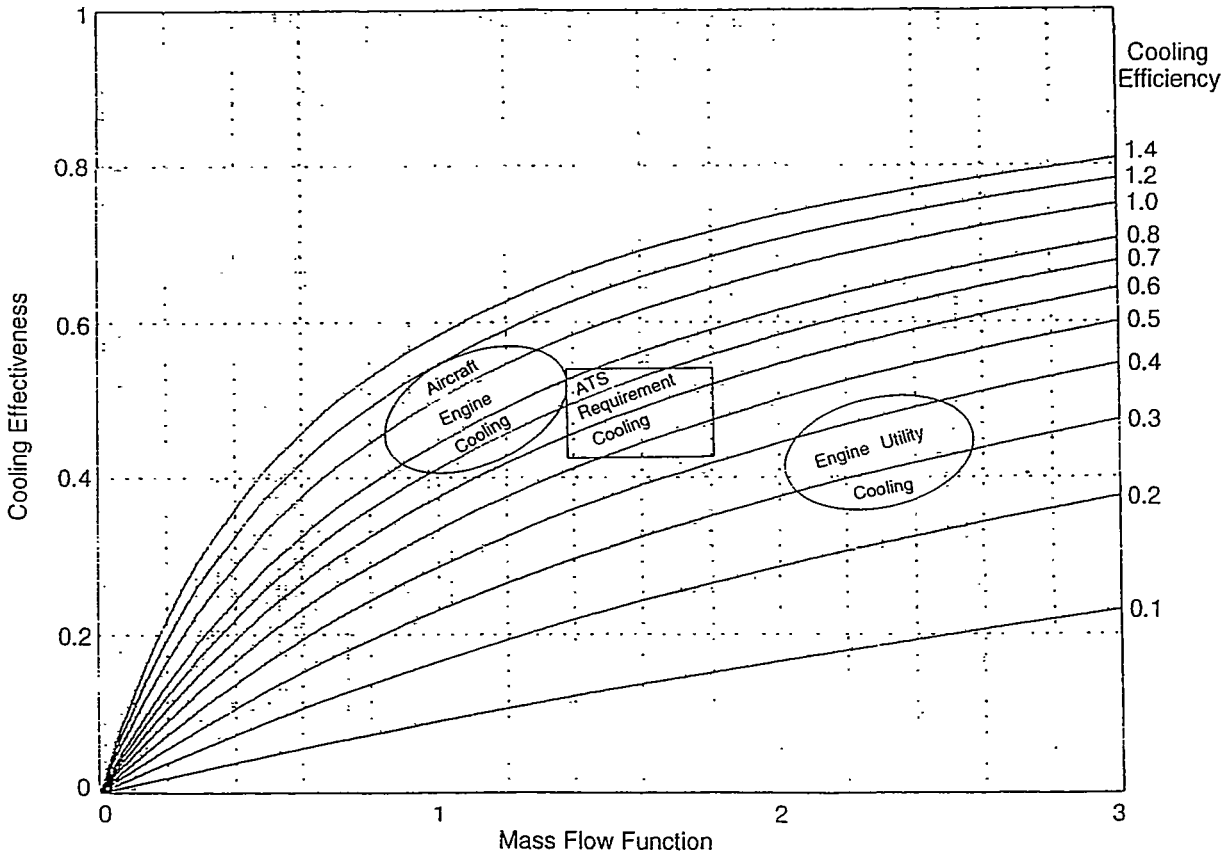


**Figure 11** Non-Dimensional Cooling Performance for Rotor Blades

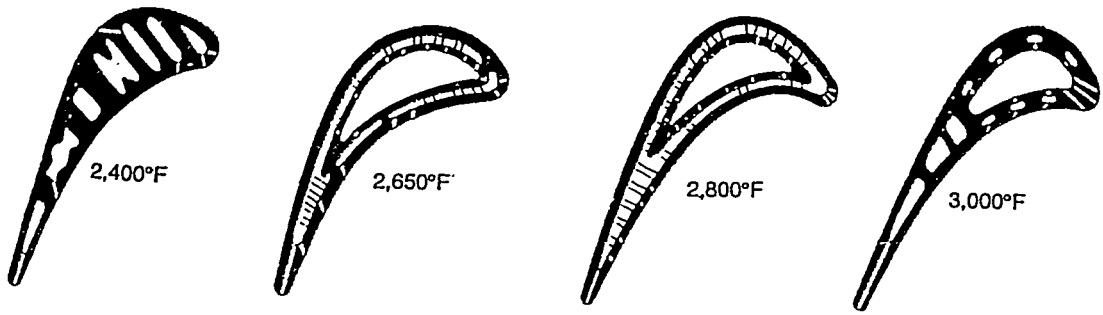


*As Blade Geometry Increases in Complexity;*

- Improved Core Technology Needed for Dimensional Stability
- Casting Process - Design Interaction Optimization Required.

**Figure 12. Improved Cooling Effectiveness - Increases Complexity Relative to Castability**

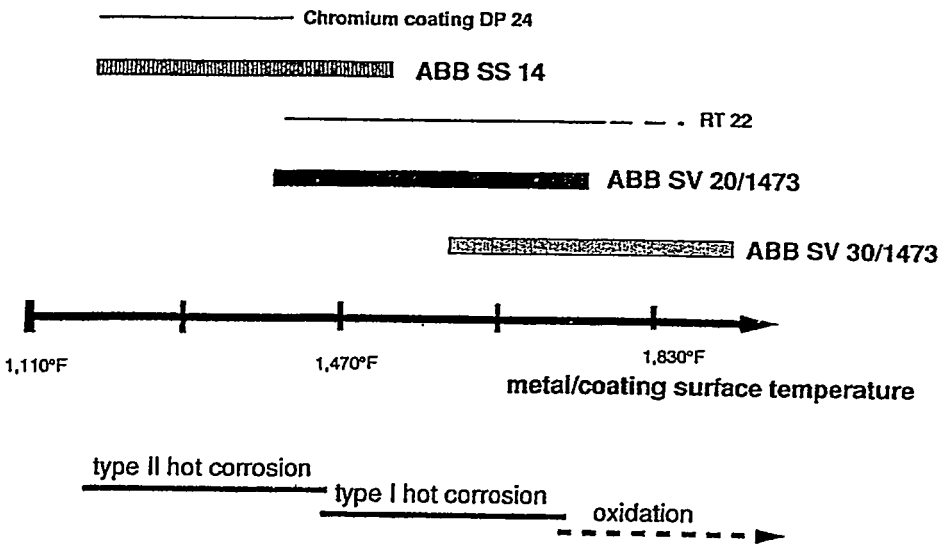


**Figure 13** Comparison of Blading Coating Temperature Capabilities

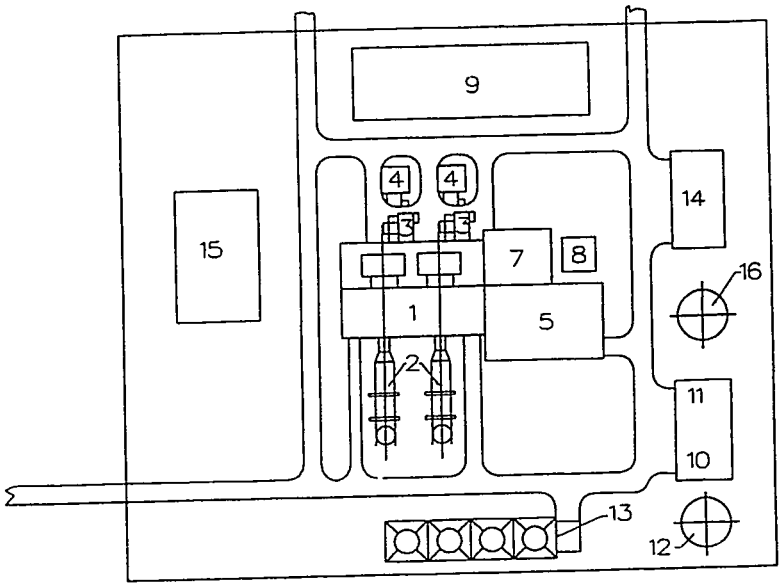


LEGEND

1 GAS TURBINE BUILDING
2 HEAT RECOVERY STEAM GENERATOR
3 ELECTRICAL MODULES GAS TURBINE
4 TRANSFORMERS – GAS TURBINE
5 STEAM TURBINE BUILDING
7 ELECTRICAL BUILDING
8 TRANSFORMER – STEAM TURBINE
9 HV SWITCHYARD
10 WATER TREATMENT PLANT
11 CHEMICAL STORAGE TANKS & UNLOADING
12 DEMI WATER TANK
13 COOLING TOWER & COOLING WATER PUMP STATION
14 WORKSHOP
15 FUEL GAS METERING/REDUCING STATION
16 RAW WATER STORAGE TANK (OPTION)

2 Unit 1991 Vintage (240MW Power Plant)
Single Unit ATS (280 MW Power Plant)

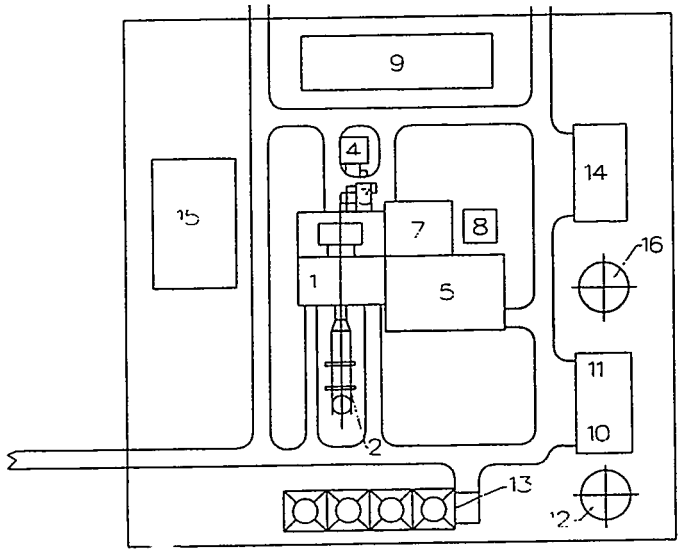


FIGURE 14. PLANT LAYOUT

FOR SINGLE ATS UNIT (280 MW)

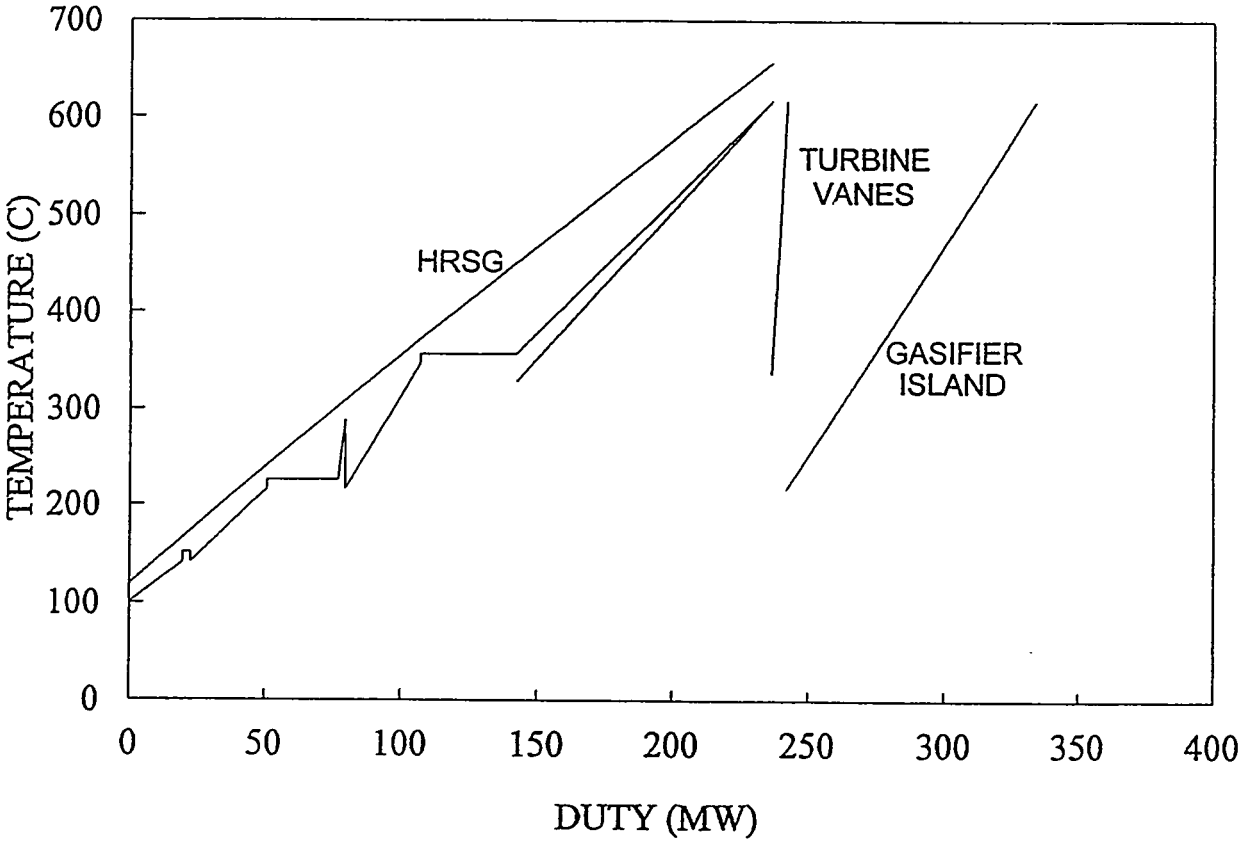


**Figure 15. IGCC - HRSG Diagram**

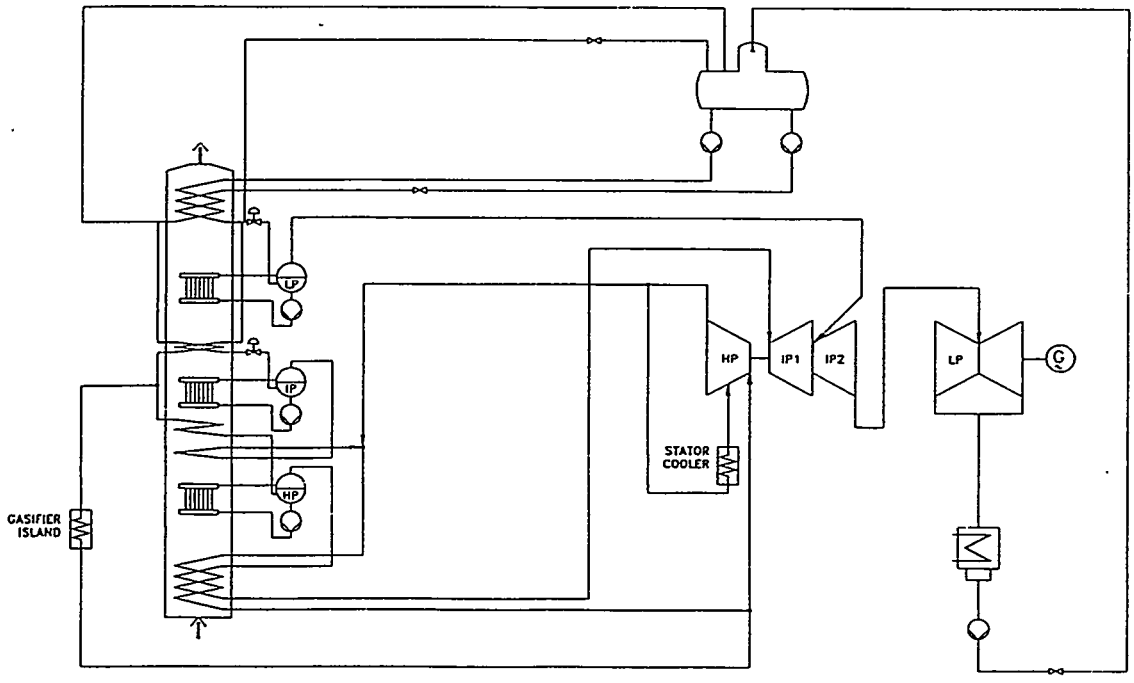


**Figure 16. ATS Cycle With Gasifier Island**

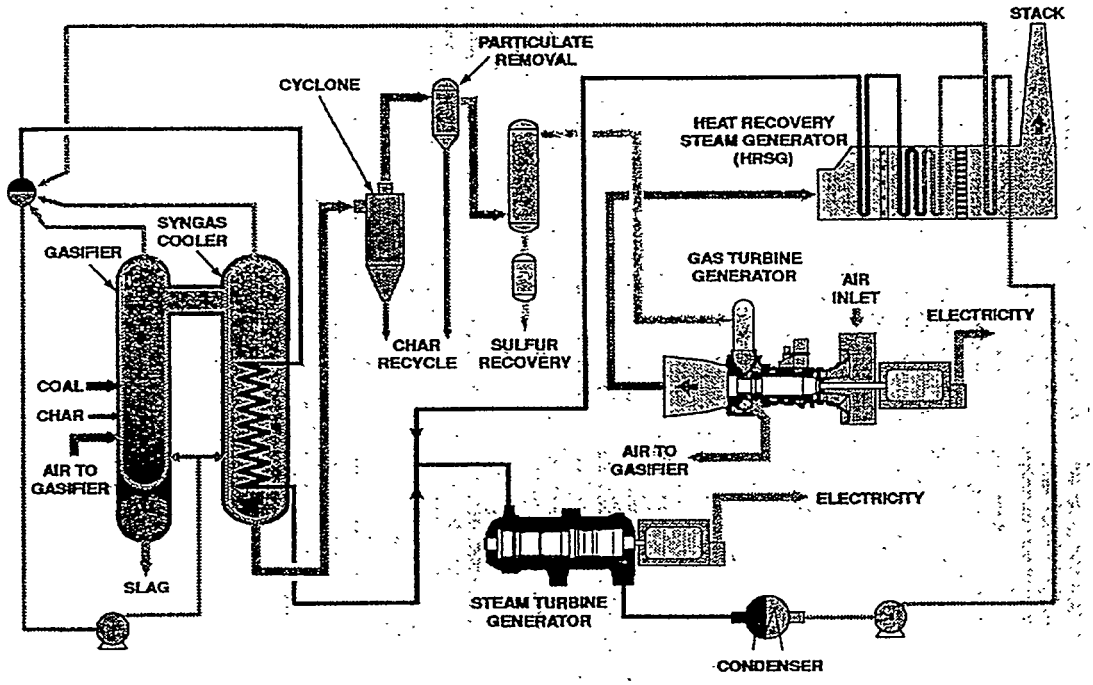


**Figure 17. ABB C-E IGCC Flow Diagram**

# 1.6 METC Combustion Research Facility

John S. Halow
Daniel J. Maloney
George A. Richards
Morgantown Energy Technology Center

## OBJECTIVES

The objective of the Morgantown Energy Technology Center (METC) high pressure combustion facility is to provide a mid-scale facility for combustion and cleanup research to support DOE's advanced gas turbine, pressurized, fluidized-bed combustion, and hot gas cleanup programs. The facility is intended to fill a gap between lab scale facilities typical of universities and large scale combustion/turbine test facilities typical of turbine manufacturers. The facility is now available to industry and university partners through cooperative programs with METC.

## BACKGROUND

Consistent with the national energy strategy, a major DOE program, the Advanced Turbine Systems (ATS) Program has been initiated to develop more efficient gas turbine systems for both utility and industrial electric power generation (U.S. Department of Energy 1992). The program targets base load power systems for commercial offering in the 2000 to 2002 time frame. The program will target a 15 percent improvement in efficiency, reductions in $NO_x$, $CO_2$, CO, and unburnt hydrocarbon, and provide for a 10 percent lower cost of electricity than current technology.

The basic strategy of the program is to fund teams led by U.S. turbine manufacturers to develop ATS while in parallel to develop a technology base to address key technical issues. A university/industry consortium administered by the South Carolina Energy Research and Development Center will provide cross-cutting technical support for the ATS program. Under this consortium, the first round of research proposals was selected through a competitive process. Other activities including projects in the METC combustion facility will contribute to this technology base development.

High pressure combustion research is also important to other DOE programs. Integrated gasification combined cycle (IGCC) systems and second-generation, pressurized, fluidized-bed combustion (PFBC) systems use gas turbines/electric generators as primary power generators. The turbine combustors play an important role in achieving high efficiency and low emissions in these novel systems. These systems use a coal-derived fuel gas as fuel for the turbine combustor. The METC facility is designed to support coal fuel gas-fired combustors as well as the natural gas fired combustor used in the advanced turbine program.

## PROJECT DESCRIPTION

In 1990, an existing METC building, Building 6 or B-6, that had been used to dry and prepare coal for the METC gasifier and other projects was decommissioned. The need for a modern, high-pressure combustion facility was recognized and the decision was made to modernize and upgrade B-6 to meet this need.

The primary considerations that dictated the renovations included safety in the event of an accident, the ability to remotely operate the test rigs, availability of substantial volumes of high pressure preheated combustion air, availability of high pressure methane and other fuels, and a modern high speed data acquisition system. The

renovations required to meet these needs were extensive. These included addition of blast walls to create isolated test cells, a separate control room, installation of a large ventilation system capable of reducing the risks from accidental release of gaseous fuels and dissipating the heat released by the combustors, installation of the needed high pressure utilities to the test cells, addition of a modern data acquisition system, and numerous smaller changes to the building.

The renovations were completed in January of 1993. A pressurized pulsed combustor began operating in July and several others are expected to be in operation by the end of 1993.

## BUILDING LAYOUT

Figure 1 shows the physical layout of the facility which consists of two primary test cells, areas 103 and 105, a staging area, fuel handling room, control room, and a clean area. The test cell 105 is a high bay area with a ceiling height of 30 feet. It is capable of holding at least two test units. Test cell 103 has a ceiling height of 20 feet on the north side and a height of 10 feet on the south half. The staging area is used to assemble combustors for tests and to do minor repair and fabrication tasks. It is also used as a test area for cold flow visualization models and other small ambient pressure and temperature rigs. The distributed control system in the

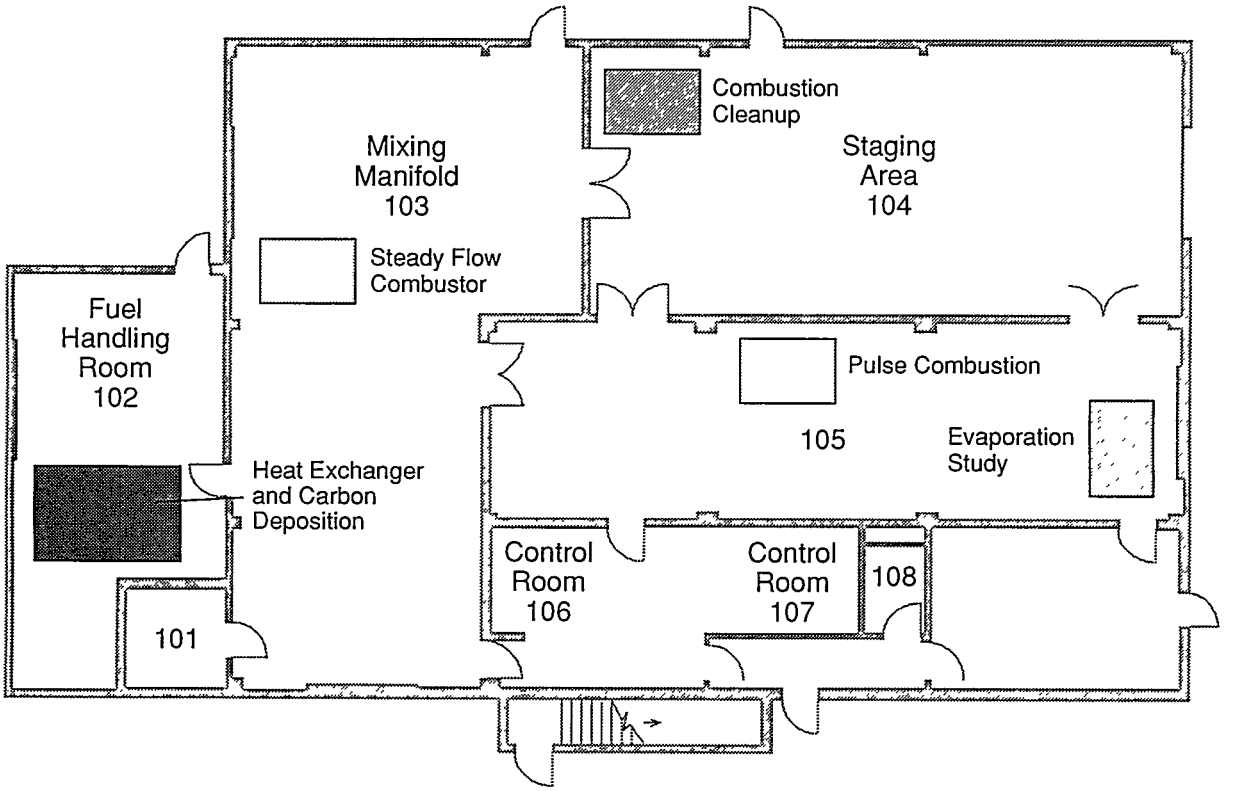


**Figure 1. B-6 Combustion Facility**

control room will be used to remotely operate rigs that are in either the 103 or 105 test cells. The common computer system is readily configured to control the various rigs. The fuel handling room was originally intended for use with coal water slurries and liquid fuels but currently it houses a methane compressor and some auxiliary equipment.

## UTILITIES

Table 1 summarizes the utilities and services available in the main test cells in the facility. Basically the facility was sized to support a 10,000,000 Btu/h combustion process. One such process or a combination of smaller processes could be serviced at one time. Up to 180,000 scf/h of air is available for combustion, atomization and other needs. High pressure water is available as city, deionized or process cooling water.

High pressure air entering the building passes through a manifold where a portion or all of the air can be diverted to preheaters. The preheaters can deliver up to 156,000 scf/h at 1,050 °F. Preheated air is metered and then can be delivered to either of the two high pressure cells.

## CURRENT PROJECTS

Currently one combustion rig is operating in B-6 and two additional projects are under construction for the facility. Space is available in the test cells for at least one additional test rig.

A pressurized pulsed combustor began operating in July of 1993 in the 105 test cell. The combustor will carry out pulsed combustion of natural gas at pressures up to 10 atmospheres. Figure 2 illustrates the components in this combustor. The objective of the test program is to test various pulsed combustor geometries to determine pressure gain performance, high pressure operating characteristics, evaluate formation of pollutants, and obtain information on scaling laws for this class of combustors. The information obtained will be used to evaluate the potential of pulsed combustors for achieving pressure gain in gas turbine systems.

A high pressure steady flow rig is currently in procurement and fabrication. The objective of this rig is to test novel, steady-flow, pressurized combustors that produce very low $NO_x$ and other emissions. Figure 3 is a schematic of the steady flow rig. The rig will be able to test burners in the range of 1 to 10 million Btu/h. It has a modular design that allows alternate burners to be installed in the rig.

An evaporation rig is also being fabricated and will be installed in area 105 of B-6. Figure 4 illustrates the basic components of this rig. This rig will test the concept of water injection in an externally fired cycle. The specific technical issue that the unit will address is evaporation rates of water droplets in high pressure flows.

Several cold flow visualization models are planned for installation in a section of the staging area in B-6. This model will support the cleanup program, gasification and combustion programs.

## FUTURE WORK

The METC B-6 combustion facility is a modern equipment laboratory with sufficient ancillary equipment and utilities to simultaneously support at least four major combustion projects. Currently one project is beginning operation and two others are in the procurement/fabrication stage. One of these, the high-pressure, steady-flow rig, will be capable of testing alternate burners. METC plans to work cooperatively with industrial and university partners on these projects.

**Table 1. Building B-6 Services**

| | |
|---|---|
| Air Supply -- Total of 180,000 scf/h | |
| • 700 psig combustion air @ up to 1,050 °F | 156,000 scf/h |
| • 1,000 psig atomization air | 5,700 scf/h |
| • 700 psig purge air | |
| • 125 psig plant air | |
| Water Systems | |
| • 500 psig city water | 12 gal/min |
| • 500 psig deionized water | 5 gal/min |
| • Process cooling water (closed loop) | 250 gal/min |
| ◦ Low pressure steam | 1,000 lb/h |
| • 90 psig city water | |
| Fuels -- Up to 10,000,000 Btu/h | |
| • 700 psig natural gas | 2,100 scf/h |
| • 600 psig synthesis gas @ 1,500 °F | 150,000 scf/h |
| • Provisions for solid and slurry feeding | |
| Gas Analyzers | |
| • Mass spectrometer | |
| • $O_2$/CO analyzers | |
| • CSI gas analyzer (SO, $CO_2$, $NO_x$, HC, $H_2$) | |
| • $N_2O$ analyzer | |
| • $H_2O$ analyzer | |
| Control and Data Acquisition | |
| • Low speed: 100 channels @ 0.5 Hertz | |
| • High speed: 8 channels @ 100,000 Hertz | |
| Safety Features | |
| • Ventilated test cells | 135,700 scf/min max |
| • High pressure nitrogen | 50 scf/min |
| • Low pressure nitrogen | 30 scf/min |
| • Video monitoring systems in test cells | |
| • Remote control and operation of rigs | |
| • Blow out panels room 105 | |
| • Toxic gas monitors and alarms | |
| • Combustible mixture monitor and alarm | |

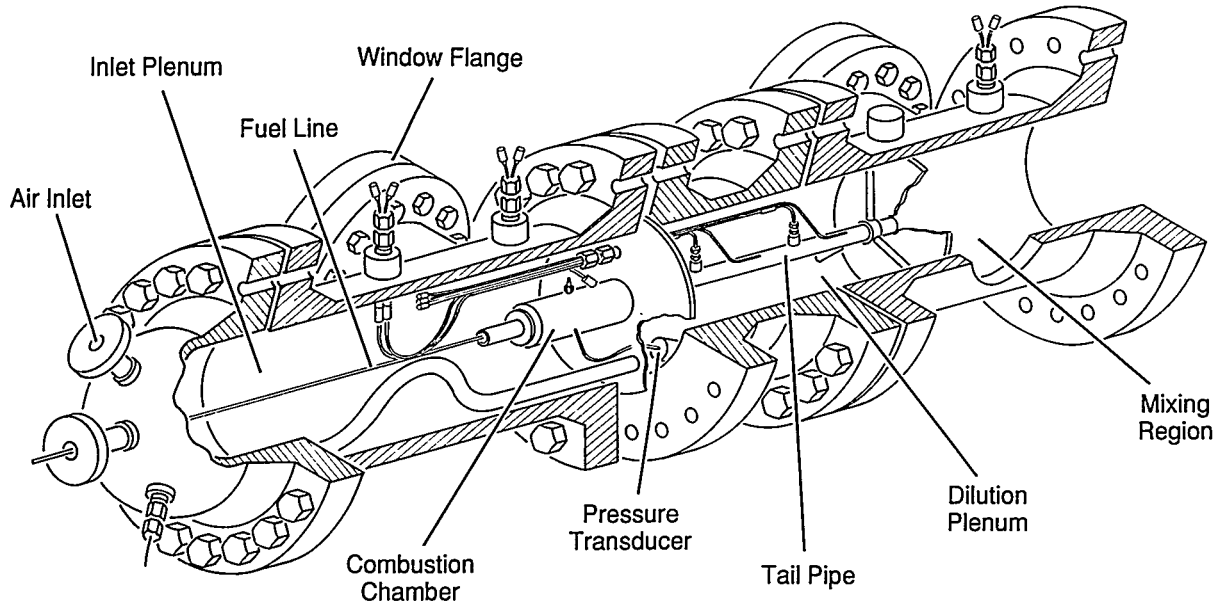


**Figure 2. Pressurized Pulse Combustor**

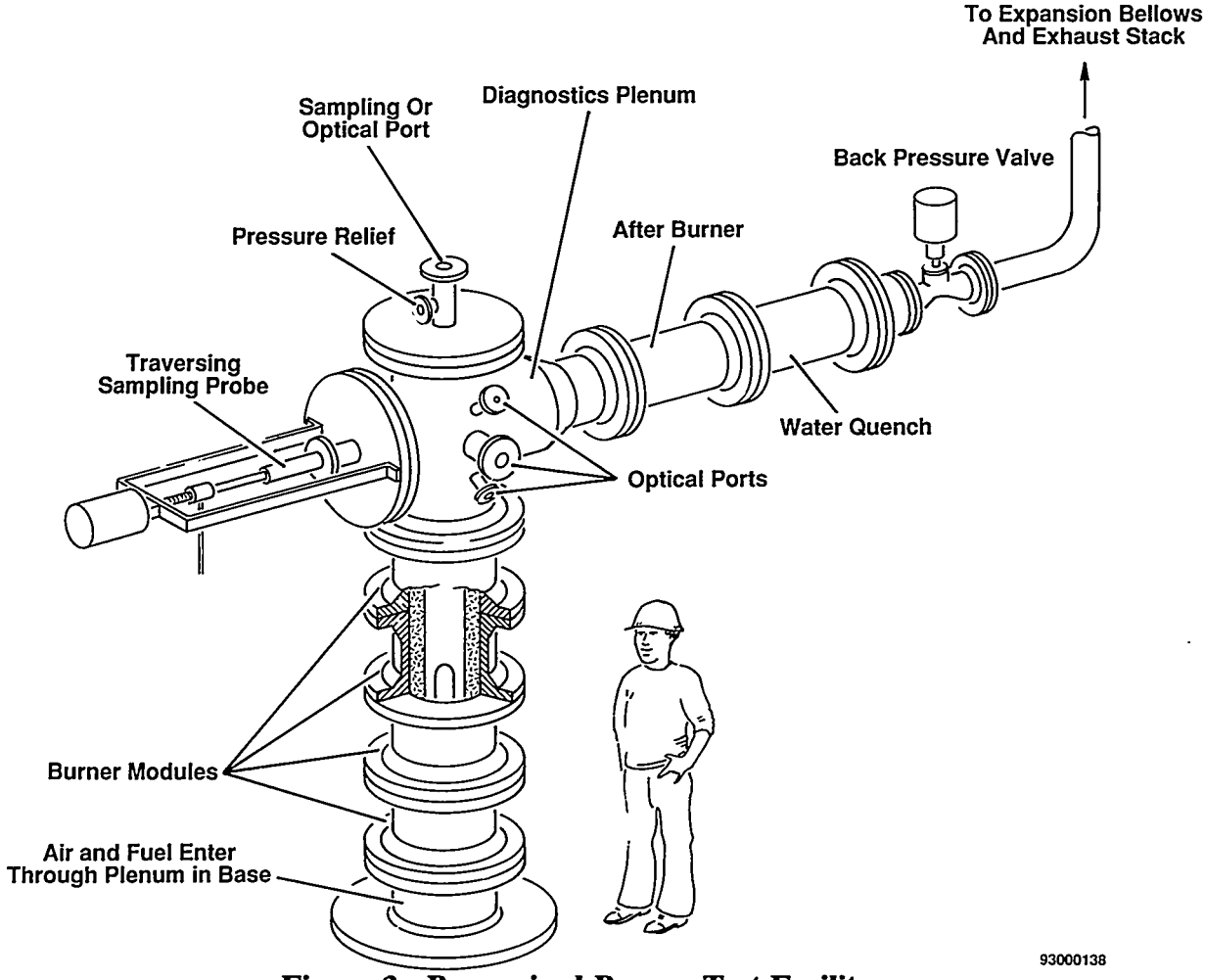


**Figure 3. Pressurized Burner Test Facility**

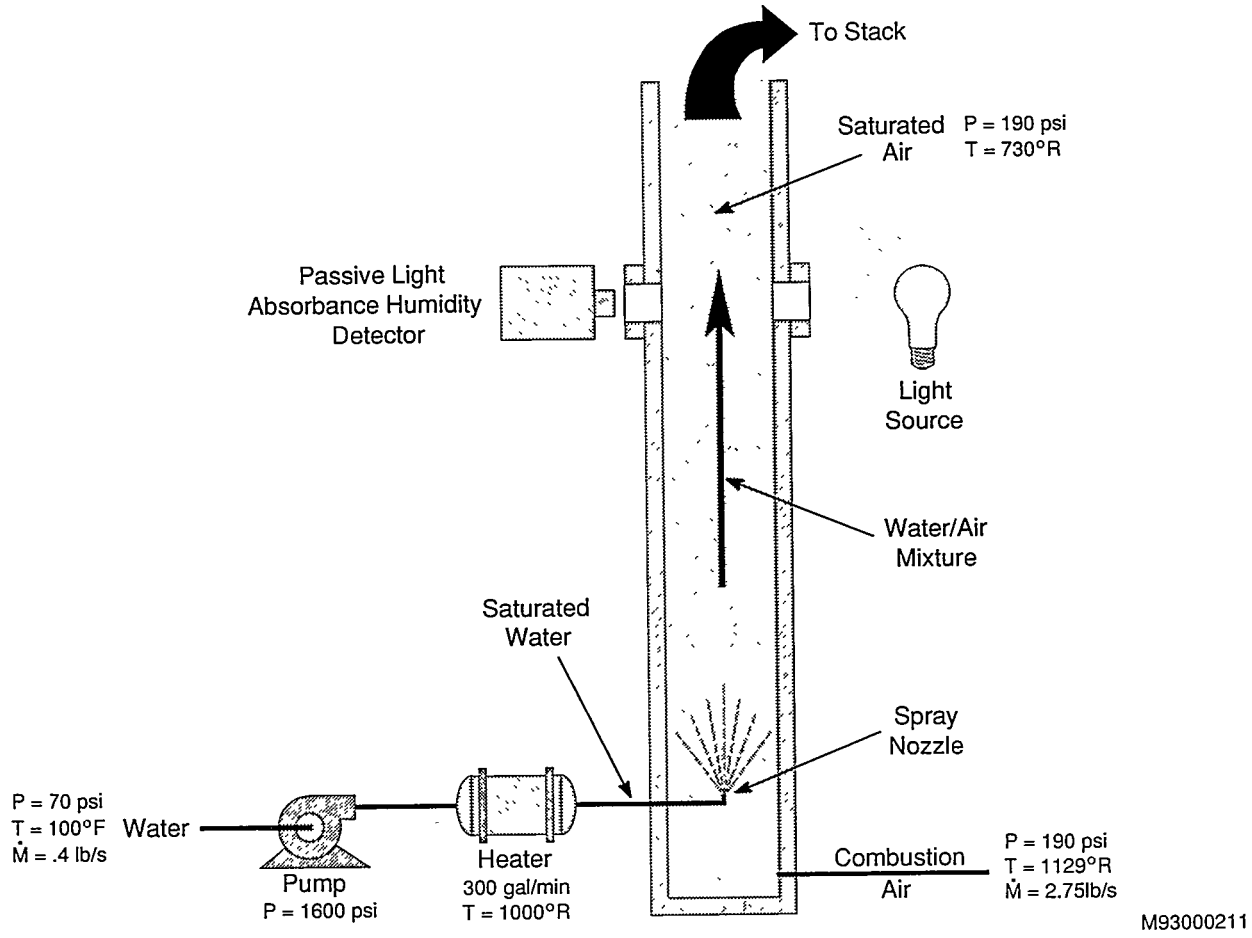


**Figure 4. Evaporation Unit**

One method for a cooperative program is through Cooperative Research and Development Agreements (CRADAs). CRADAs were authorized by several Congressional actions that encourage Federal laboratories to work with industry. The general goal of the CRADAs is to improve U.S. competitiveness. Under a CRADA, data generated in the project can be kept confidential to the parties for up to five years and the industrial party can be given an exclusive license to inventions made under the CRADA or prior inventions owned by the government. CRADAs are not contracts and do not fall under the government acquisition regulations. CRADAs must be cost shared between the government and the industrial party. No government money may go to the partner under the CRADA, although money may be received by the government in the form of royalties and direct payments from the partner.

A CRADA is a fairly simple document that can be negotiated and implemented in a relatively short time. METC has put into place approximately 10 CRADAs covering various areas over the past two years. None of these, however, involve B-6.

Another means of joint work in the combustion facility is through the South Carolina

Energy R&D Center's (SCERDC) advanced turbine program for R&D solicitations. Acting for DOE the center will conduct competitive solicitations and award contracts to develop the technology base needed for the advance turbine program. If agreed to by METC, bidders may propose utilizing the B-6 facility as part of their project. METC will participate with Vanderbilt University on one such project.

Other avenues are available for participation in projects in the facility. Education programs including the ORISE (formerly ORAU) program and the DOE COOP programs are two such programs. Other arrangements for both academic and industrial parties are possible. METC would like to encourage industry and universities to consider a cooperative project using the METC facility when planning high pressure combustion R&D.

## REFERENCES

"Report to Congress, Program Plan, Advanced Turbine Systems," U.S. Department of Energy, 1992.

JHALOW\1:931684

# FE/EE Advanced Turbine Systems Conference

## Session 2

## *Industrial Systems*

## 2.1 Ceramic Retrofit Program

**CONTRACT INFORMATION**

| | |
|---|---|
| **Contract Number** | DE-AC02-92CE40960 |
| **Contractor** | Solar Turbines Incorporated<br>2200 Pacific Highway<br>San Diego, CA 92101<br>(619) 544-5000 |
| **Contractor Project Manager** | Mark van Roode |
| **Principal Investigators** | Paul F. Norton<br>William D. Brentnall |
| **DOE Technical Manager** | Stephen Waslo |
| **Period of Performance** | September 25, 1992 to April 30, 1998 |

**FY93 Program Schedule**

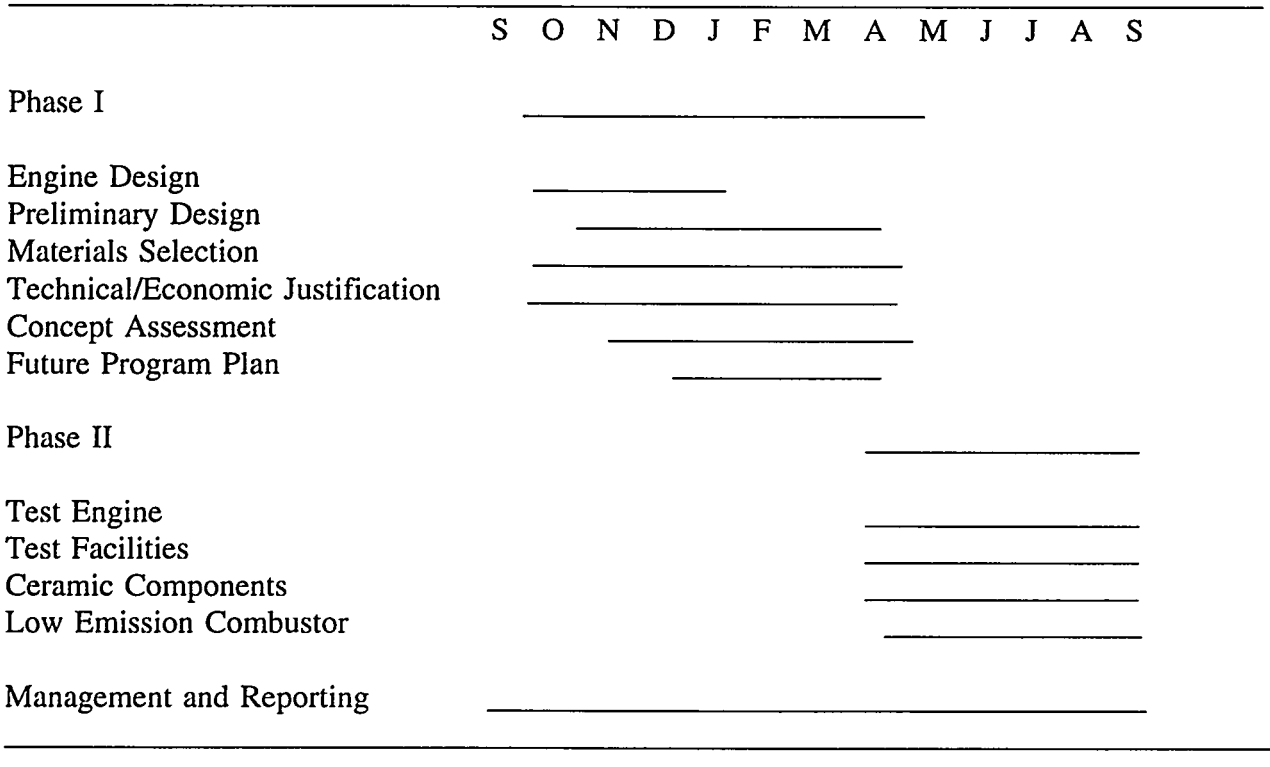

## OBJECTIVES

The overall objective of the DOE Ceramic Retrofit Program (Stationary Gas Turbine (CSGT) Development Program) is to improve the performance of retrofit stationary gas turbines in cogeneration through the selective replacement of metallic hot section parts with uncooled ceramic components. The successful demonstration of ceramic gas turbine technology, and the systematic incorporation of ceramics in existing and future gas turbines will enable more efficient engine operation, resulting in significant fuel savings, increased output power, and reduced emissions.

## BACKGROUND

The performance of current industrial gas turbines is limited by the temperature and strength capabilities of the metallic structural materials in the engine hot section. Because of their superior high temperature strength and durability ceramics can be used as structural materials for hot section components (blades, nozzles, combustor liners) in innovative designs at increased turbine firing temperatures. The benefits include the ability to increase the turbine inlet temperature (TIT) to about 2200°F or more with uncooled ceramics. Once the basic ceramic turbine technolgy has been demonstrated the potential to optimize the flow path and aerodynamics at these higher TIT's may result in further performance improvements.

It has been projected that fully optimized ceramic stationary gas turbines would have a ≈20% gain in efficiency and ≈40% gain in output power compared to all-metal engines with air-cooled components[1]. Annual fuel savings in the U.S. alone would be on the order of 0.2 Quad by 2010. Emissions reductions to to < 10 ppmv $NO_x$ are also forecast[2].

Against this background the Department of Energy, Office of Industrial Technology, initiated in September of 1992 a program to achieve energy savings and environmental emissions reduction in cogeneration by selectively replacing metallic blades, nozzles, and the combustor liner in an existing industrial gas turbine engine with ceramic components. The technology base for this program is provided by the significant advances in ceramic design and fabrication know how developed under past ceramic turbine programs for transportation and military applications.

Solar Turbines Incorporated is the prime contractor under a five year three phase program. The Solar led team also includes major suppliers of ceramic turbine components, nationally recognized test laboratories, and a cogeneration enduser.

The engine selected for the program, the Solar Centaur 'H' will be retrofitted with first stage ceramic blades, first stage ceramic nozzles, and a ceramic combustor liner. The engine hot section is being redesigned to adapt the ceramic parts to the existing metallic support structure. The ceramic turbine technology to be developed under this program is a key enabling technology to realize the performance and environmental goals of the Advanced Turbine Systems program. The overall program approach, design strategy, and materials selection has been presented previously[3].

## PROJECT DESCRIPTION

### Program Strategy

The program strategy selected by the Solar led team provides a strong focus on near term ceramic turbine technology demonstration and lowering barriers for the acceptance of ceramic components by the market place. The risk for the end users is minimized by:

- limiting the number of ceramic components to a single stage of blades, nozzles, and the combustor liner;

- introduction of programmed start-up and shut-down procedures that are consistent with industrial usage but minimize transient stresses;

- achieving early demonstration of components in a gasifier rig which will exactly duplicate engine conditions;

- performing sufficient design iterations to reduce sources of stress in the components to a minimum;

- using flaw-tolerant designs which ensure that stresses and temperatures are below slow crack growth and the creep-dominated regime;

- adopting step-wise increases in firing temeperature;

- favoring materials, designs, and manufacturing procedures that are well-characterized and have high potential for scale-up to cost-effective product applications.

**Project Team**

The Solar team and the responsibilities of the team members is shown in Table 1. Suppliers were selected with a proven track record in the fabrication of ceramic turbine components from past programs. Since eventual commercialization is the program focus, the ability to scale up to cost effective volume fabrication of parts was a major supplier selection criterion. Multiple suppliers were selected for each part to maximize the potential of establishing a reliable component supplier base.

Historically, most of the development work on ceramic turbines has been for relatively short engine life applications, and as a result long term property data (1000+ hrs) is limited. Industrial turbine users expect continuous operation of their equipment for service of 30,000+ hrs between overhauls. Expert test laboratories responsible for the generation of long term materials property data, and for the development of non-destructive, and life prediction methodologies have therefore been included in the program.

The inclusion of a cogeneration end user on the team ensures that the market acceptance by the end user community is given proper emphasis on the program.

**Program Activities**

The program is structured in three phases. Phase I focuses on preliminary engine design, Phase II involves final engine design, material testing, component development, and rig testing. Phase III includes a 4,000 hour engine test to evaluate the performance and durability of the ceramic components.

Phase I of the program which was performed from September, 1992, through April, 1993, had six major tasks which focused on ceramic component conceptual design, component preliminary design, materials selection, technical and economic evaluation, concept assessment, and future program planning.

Phase II which started in April, 1993, and will be performed through April, 1996, addresses the detailed design of the program engine, its ceramic components, metallic support structures; set-up and modification of test rigs; fabrication and testing of ceramic components and test specimens; development and testing of a low-emissions combustor, and planning of the field test for Phase III.

Phase III, to be performed from April 1996 through April 1998, will include the manufacturing and instrumented testing of the field engine, the actual 4,000 hr field test at the cogeneration

**Table 1. Program Team**

| CERAMIC COMPONENT SUPPLIERS | |
|---|---|
| Garrett Ceramic Components | Blade |
| Carborundum | Nozzle, Combustor Liner |
| Norton Advanced Ceramics | Blade, Nozzle |
| Kyocera Ind. Ceramics Corp. | Blade |
| DuPont Composites | Combustor Liner |
| Babcock & Wilcox | Combustor Liner |
| NGK Insulators | Nozzle |

| TEST LABORATORIES | |
|---|---|
| Caterpillar Technical Center | Non-Destructive Evaluation |
| Argonne National Laboratory | |
| University of Dayton Research Institute | Long Term Testing of Ceramics |

| SOLAR TURBINES INC. |
|---|
| *Program Management<br>*Engine Design<br>*Materials Evaluation<br>*Component Testing<br>*Engine Testing<br>*Market Evaluation<br><br>*Technology Integration<br>*Commercialization |
| **SUNDSTRAND POWER SYSTEMS** |
| *Life Prediction<br>*Design Support<br>*Materials Evaluation Support |

| ARCO OIL & GAS |
|---|
| *Enduser Representation<br>*Commercial Application<br>*Cogeneration Field Test Site |

test site, and pre- and post-testing component evaluation/characterization.

Management and reporting is an integral task for all phases of the program.

## RESULTS

This paper summarizes the Phase I results. A detailed account will be provided in the Phase I Technical Progress Report[4].

### Task 1: Turbine Design

### Performance

The objective of Task 1 was to define performance goals for the ceramic stationary gas turbine (CSGT), the Solar Centaur 'H', selected for the program (CSGT-'H'), develop conceptual designs for the ceramic components, and perform preliminary stress analyses.

Figure 1 shows a schematic of the engine selected for ceramic insertion, the Solar Centaur 'H'. This engine has an inlet airflow of 40 lbs/s, with an axial geometry. The gas producer turbine has two stages, the first one of which has 62 cooled MAR-M247 blades and 15 cooled two-vane FS-414 nozzles. Both first stage blades and nozzles are coated with precious metal aluminide diffusion coatings for oxidation protection.

Table 2 provides a comparison of key engine parameters for the current all-metal Centaur 'H' and the CSGT-'H' engine. The data for the Centaur 'H' is based on average performance data for the first 21 engines installed.

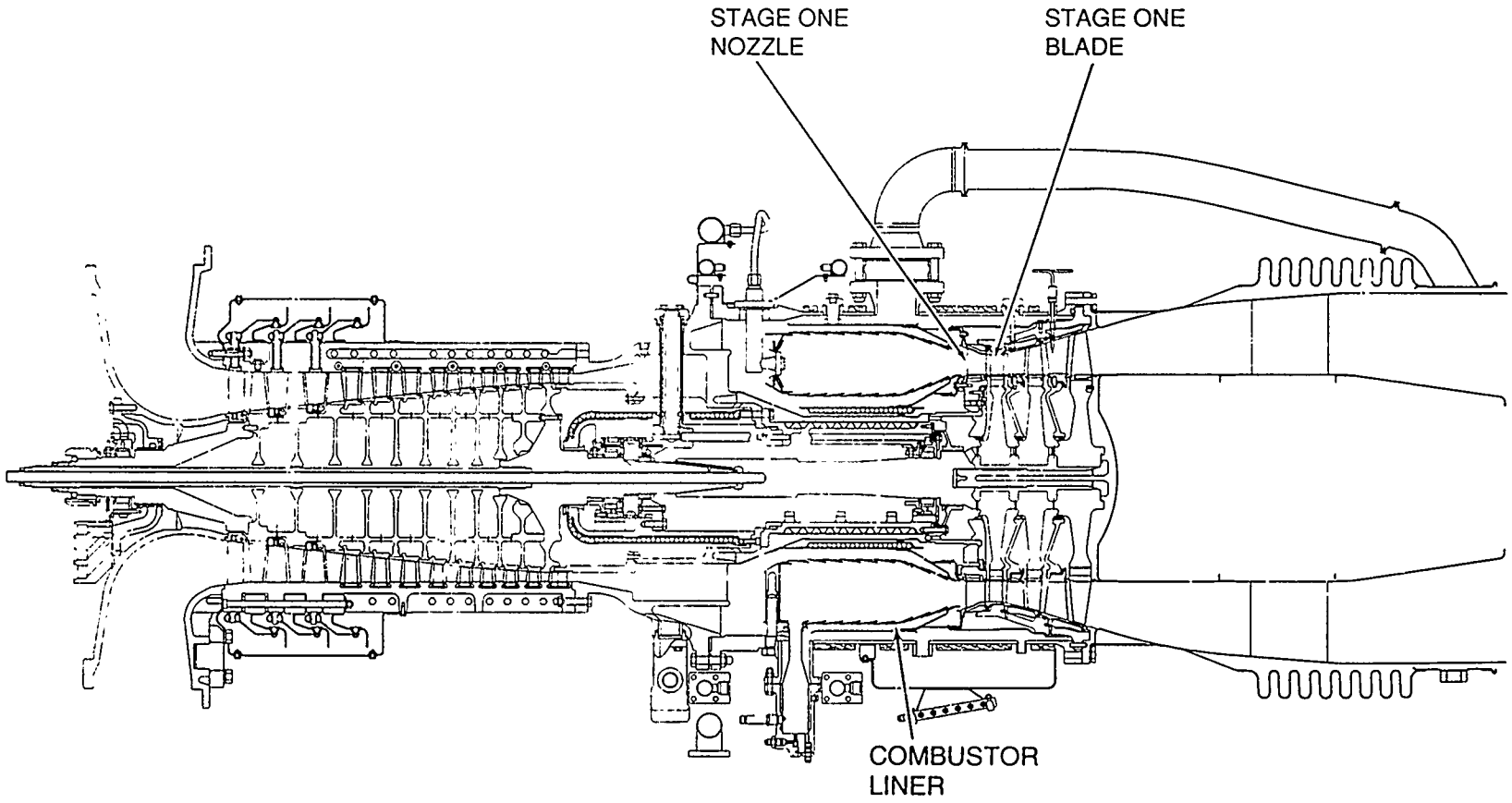


**Figure 1. Centaur 'H' Gas Turbine. Components for Ceramic Substitution Have Been Indicated**

**Table 2. Centaur 'H' Generator Set Compared With CSGT-'H' Generator Set**

| ENGINE PARAMETERS | CENTAUR - 'H' | CSGT -'H' |
|---|---|---|
| **In Simple Cycle Mode:** | | |
| TRIT* | 1850°F | 2050°F |
| Shaft Output | 5880 SHP | 7402 HP |
| Shaft Thermal Efficiency | 29.63% | 31.29% |
| Electrical Output | 4144 kW | 5217 kW |
| Electrical Thermal Efficiency | 28.01% | 29.58% |
| **In cogeneration mode:** | | |
| Electrical Output | 4051 kW | 5088 kW |
| Electrical Thermal Efficiency | 27.38% | 28.84% |
| Overall Thermal Efficiency | 75.39% | 80.33% |

The CSGT-'H' data were generated from aerothermal predictions for the engine modified with a first stage of ceramic blades and nozzles, and an uncooled ceramic combustor liner in the concentric outer and inner wall sections of the combustor.

### Ceramic Blade Design

Several conceptual designs were evaluated for each of the three components targeted for ceramic substitution. Figure 2 shows sketches representing the current Centaur 'H' blade and one of the conceptual blade designs in which the current firtree root has been replaced with a 60° dovetail attachment. The dovetail attachment is used in conjunction with a thin metallic compliant layer which minimizes and/or redistributes contact stresses at the centrifugally loaded interface with the disk.

The dovetail and alternative attachment configurations which were investigated incorporate

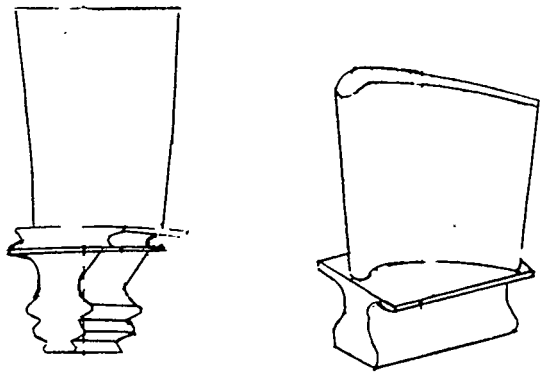


**Figure 2. Metallic and Ceramic Blades**

criteria essential for high reliability, such as minizing the deleterious sliding at the disk/blade contact area, and of course, simplicity. Other usual blade design issues have been addressed as well such as dynamic response, avoidance of engine order interferences, blade damping and tip rub.

## Ceramic Nozzle Design

Conceptual nozzle design was initiated through a thorough eveluation of prior axial flow ceramic nozzle designs in the area of mechanical load path, the need for isothermal operation for low component stresses, and vibration response due to mounting schemes. Figure 3 shows sketches of the current cooled two-vane nozzle design and a ceramic single-vane conceptual design. The tip shoe integral with the nozzle in the current Centaur 'H', has been decoupled from the nozzle in the CSGT-'H'.

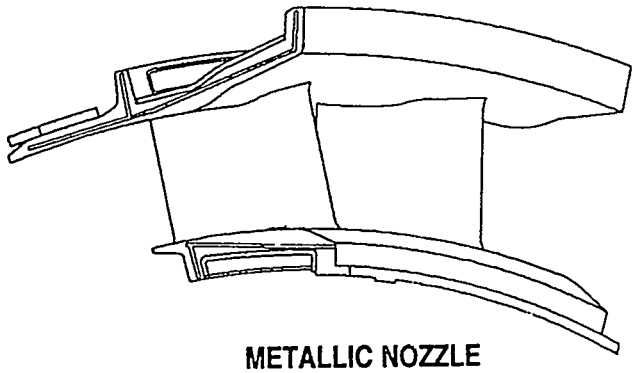

METALLIC NOZZLE

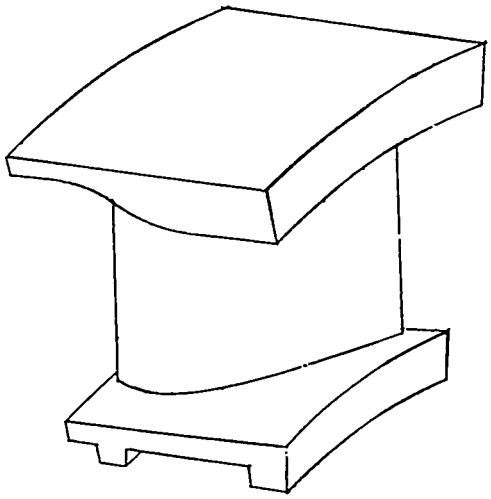

CERAMIC NOZZLE

**Figure 3. Metallic and Ceramic Nozzle**

Minimizing the stresses in the critical trailing edge region of the nozzle airfoil, interfacing the ceramic nozzle with the metallic support structure in a manner that minimizes the effects of the expansion mismatch with the nozzle case, and minimizing blade tipshoe clearance are major design challenges that are being addressed.

## Ceramic Combustor Liner Design

The program goal is to demonstrate a $NO_x$ emission level of 25 ppmv and to show the potential for 10 ppmv or better. These goals are important steps on the way to achieving the Advanced Turbine Systems target of 8 ppmv $NO_x$. The improved oxidation life of ceramic materials enables increased wall temperature, coupled with reduced film cooling. This in turn will increase the dilution air and reduce emissions of $NO_x$ and CO.

The ceramic combustor conceptual design envisions ceramic liners in the concentric sections of the current $SoLoNO_x$ combustor. In Phase I three different concepts have been explored: axial monolithic tiles, concentric monolithic ring segments, and integral continuous fiber-reinforced ceramic matrix composite (CFCC) cylindrical liners. Figure 4 shows the conceptual design common to all these designs. Design factors include minimizing stresses, and attaching the ceramic liner to the metallic support structure.

## Task 2: Preliminary Design of Key Components

The work in Task 2 focused on the preliminary design of the key components for which design solutions were developed under Task 1. Critical materials properties were defined and stress temperature profiles were run for selected ceramic components and the metallic support structures using 3-D finite element analysis.

## Ceramic Rotor Blade

Figures 5 and 6 show ANSYS finite element temperature and stress maps, respectively,

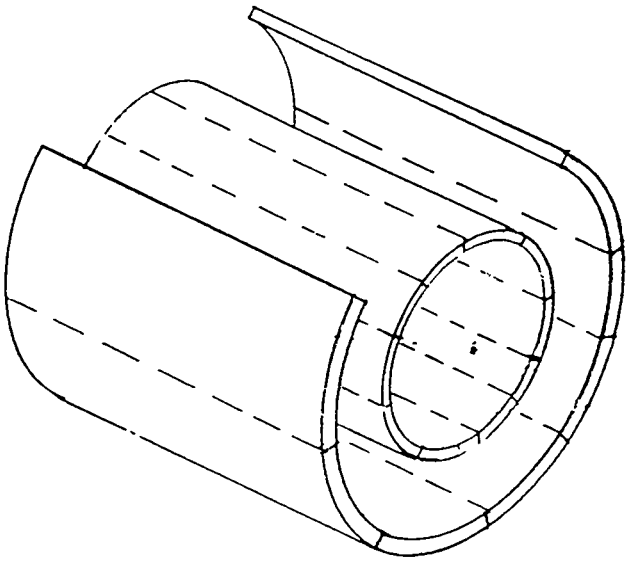

**Figure 4. Ceramic Combustor Liners**

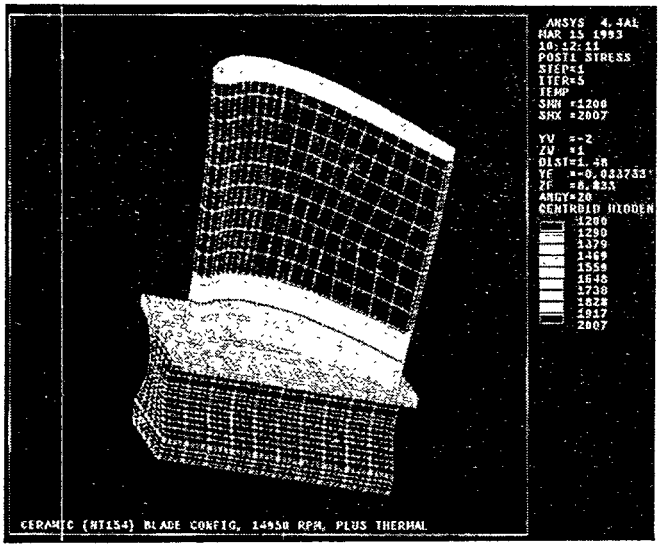


**Figure 5. Analytically Predicted Temperature Distribution in "Dovetail" Blade**

for the ceramic dovetail blade design which was illustrated in Figure 1. The ceramic material selected for the analysis was NT154 silicon nitride from Norton Advanced Ceramics. Through iterative design and mechanical analysis, centrifugally induced stresses were minimized to about 26 ksi in the critical necked down portion of the blade root area. An additional temperature

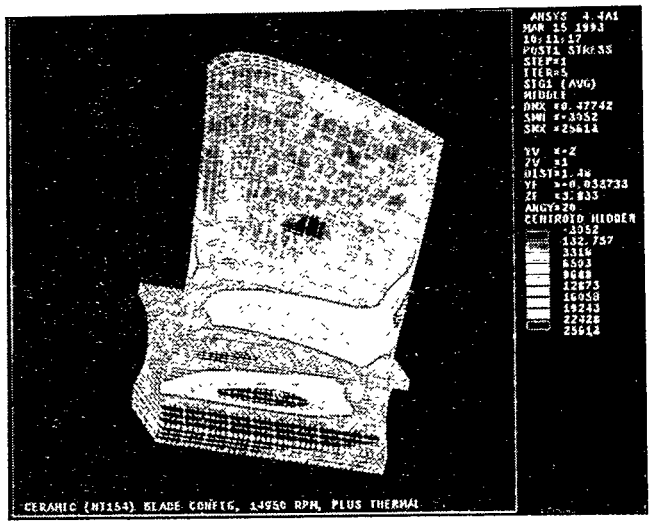


**Figure 6. Analytically Predicated Aerodynamic, Thermal, and Centrifugally Induced stresses in the "Dovetail" Blade**

induced tensile stress of about 25 ksi is present in the airfoil trailing edge at a radial position of approximately 20% of airfoil chord from the blade shroud platform.

Reliability analysis using NASA CARES and SPSLIFE life assessment computer routines indicated about 98% probability of survival (POS) for an as-processed blade with a machined attachment section. Slow crack growth was identified as the life limiting failure mode. The POS improved to 99.99% for a fully machined blade airfoil. This suggests that localized surface treatment through abrasive flow machining could be used to improve the POS for this blade design to achieve high POS values.

## Ceramic Nozzle

Finite element analyses were also performed to generate temperature and stress maps for the nozzle designs for the CSGT-'H'. ANSYS analyses gave maximum steady state stresses at "hot spot" trailing edge areas of ≈38 ksi for NT154 $Si_3N_4$ ($T_{max}$ = 2356°F) and ≈40 ksi for

Hexaloy® SiC ($T_{max}$ = 2314°F). It is planned to reduce these stresses to values of ≈20 ksi through modification of the combustor radial temperature profile, trailing edge cutbacks, and other unique design methods to obtain POS values consistent with the service life goals for the program.

## Ceramic Combustor Liner

ANSYS 3D finite element analyses were completed for two monolithic combustor liner designs. Figures 7 through 10 show temperature and stress maps for an axial tile and for an integral ring design, respectively. Tensile stress concentrations approaching 28 ksi ($T_{max}$ = 2490°F) and about 11 ksi ($T_{max}$ = 2490°F) were predicted for an axial monolithic tile and for a continuous monolithic inner ring design, respectively. While the lower stress favors the ring design at this point other factors such as component reliability based on actual stressed volume and fabrication feasibility will be taken into account when establishing the preferred design.

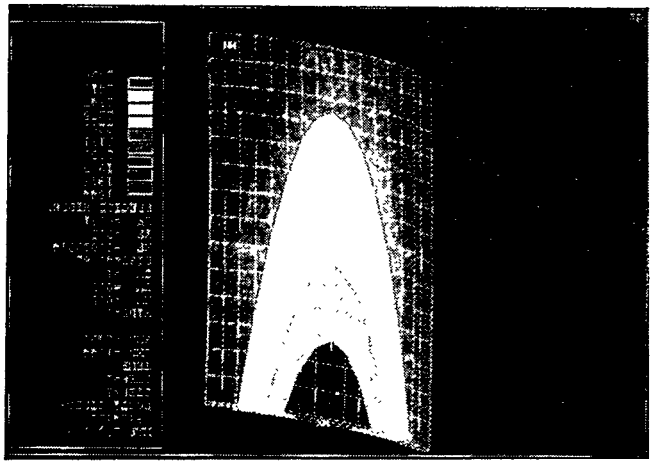

**Figure 7. SiC Tile - Analytically Predicted Steady State Temperature Profile**

Finite element temperature and stress analyses are also being performed for the CFCC liner materials for the program. Initial data for an oxide/oxide CFCC liner shows acceptable levels of in-plane stress in the fiber direction but excessive

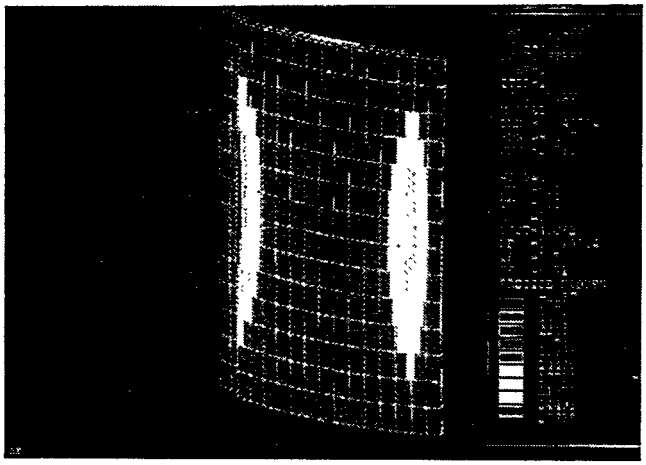

**Figure 8. SiC Tile Analytically Predicted Steady State Tile Stress Profile**

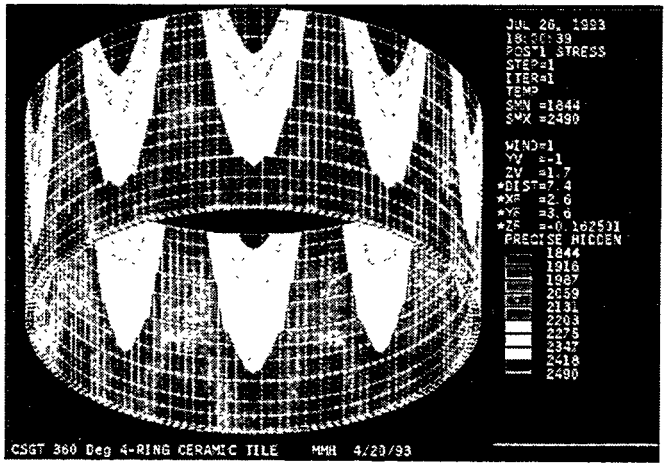


**Figure 9. SiC Ring - Analytically Predicted Liner Temperature Profile**

stress in the in-plane transverse direction. Efforts are under way to modify the fiber preform structure to obtain acceptable stresses in the latter direction.

As part of the Task 2 effort the suppliers that will be fabricating the ceramic components in Phase II provided comments on the fabrication ease and cost impact of each of the preliminary designs.

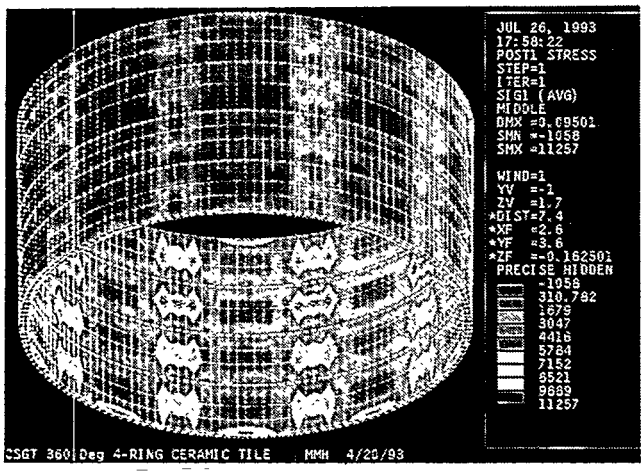


**Figure 10. SiC Ring - Analytically Predicted Liner Stress Profile**

## Task 3: Material Selection

The primary objectives of Task 3 were to assess the ability of each supplier to fabricate their assigned component(s) to the designs supplied by Solar. This assessment included a thorough evaluation of the existing data base for the materials selected in view of the component design requirements, and the preparation of preliminary fabrication plans for each component. Gaps in the data base were identified, and testing requirements for Phase II were established.

### Materials Selection

- Assessment in selecting the materials and their suppliers was based on the following criteria:

  - High POS of the material under engine conditions defined by preliminary design

  - Credibility based on prior experience to deliver in a timely fashion similar component configurations

  - Credibility to later establish volume manufacturing.

The assessment was conducted through a combination of activities including subtask letter reports, weekly telephone discussions, visits, and a comprehensive quality survey.

Table 3 summarizes the critical steady state temperatures and stresses established in the preliminary design. The components should be able to withstand these stresses over the long (≈30,000 hrs) service life between engine overhauls.

**Table 3. Critical Steady State Component Temperatures and Stresses**

| Component | Peak Temp. | Peak Stress |
|---|---|---|
| Blade | 2000°F | 27 ksi |
| Nozzle | 2360°F | 35-40 ksi |
| Combustor Tile | 2500°F | 28 ksi |
| Combustor Ring | 2500°F | 11 ksi |
| Combustor CFCC (Fiber) | 2100°F | 10-15 ksi |

The initial approach has been to extrapolate the existing data for slow crack growth and creep for the candidate materials to the design service life and to select the materials that showed sufficient margin to meet the desired life. Properties of the selected ceramics were then used for ANSYS finite element temperature/stress analyses and SPSLIFE assessment of the program components. The results from these evaluations are being used to further iterate the component design to achieve temperature/stress levels consistent with acceptable component life. Table 4 lists the ceramic materials after the Phase I assessment for each component and the suppliers who will be fabricating them in Phase II.

### Long Term Materials Property Testing

It should be noted that the existing long term materials data base required for gas turbine component design is currently limited. For example, creep data are only available for a few

**Table 4. Candidate Ceramic Materials and Suppliers for Each Component**

| Component | Supplier | Ceramic | Designation |
|---|---|---|---|
| Blade | Allied Signal Ceramic Components | $Si_3N_4$ | GN-10 |
| | Kyocera Industrial Ceramics Corp. | $Si_3N_4$ | SN-253 |
| | Norton Advanced Ceramics | $Si_3N_4$ | NT164 |
| Nozzle | Norton Advanced Ceramics | $Si_3N_4$ | NT164 |
| | NGK Insulators, Inc. | $Si_3N_4$ | SN-88 |
| | Carborundum | SiC | Hexoloy® SA |
| Combustor | Carborundum | SiC | Hexoloy® SA |
| | Norton Advanced Ceramics | SiC | NT230 |
| | DuPont Composites | SiC/SiC | |
| | Babcock & Wilcox | Oxide/Oxide | |

thousand hours while engine oepration between overhaul will require component life on 30,000+ hrs. The gathering of a long term materials property data base for creep, slow crack growth, and oxidation is therefore an integral part of the program. A substantial portion of this work will be conducted by the University of Dayton Research Institute (UDRI) under a subcontract. In addition, data will also be generated under a larger complementary separately funded effort coordinated by Oak Ridge National Laboratory. It is anticipated that during Phase II materials property data representative of 10,000 hrs of exposures under typical component temperature and stress conditions will become available. Table 5 summarizes the UDRI long term material test plan. Additional data will be gathered from testing at Solar and at the supplier subcontractors.

## Non-Destructive Evaluation

Development of appropriate non-destructive evaluation (NDE) methodology is an integral aspect of the program. This work is performed in a collaborative effort by the Caterpillar Technical Center (CAT TC) and Argonne National Laboratory (ANL). The initial methodology development work and component evaluations are the responsibility of ANL while CAT TC has responsibility for the coordination of the NDE effort and for technology transfer to Solar.

The Phase I NDE activities focused on a review of techiques currently used by the ceramic suppliers. The methods are principally visual inspection, density measurements, microfocus radiography, and fluorescant penetrant inspection (FPI). Microfocus radiography is used to examine internal defects (inclusions, voids, cracks) at both the powder compact and final part stages. FPI is used for final part inspection for surface defects (cracks, porous regions). Since the vast majority of rig and engine testing performance to-date was of short duration (<200 hrs) all that can be concluded at this stage is that NDE has been a useful technique in eliminating parts that would have had a high likelihood of failure in fast fracture. The application of NDE techniques to the evaluation of test specimens and components that have been exposed for significanly longer exposures is the main objective of the NDE effort under the program.

Of the techniques that were recommended for further evaluation in Phase II by ANL and CAT TC included: microfocus radiography using non-photographic data gathering and image

**Table 5. Long Term Materials Test Plan at UDRI**

| Test Type | Test Description | No. of Test Specimens |
|---|---|---|
| TESTING ON FOUR CANDIDATE SILICON BASED CERAMIC MATERIALS NT-154 (NAC), Hexoloy SA (Carborundum), SN-252 (Kyocera), SN-88 (NGK) | | |
| Fast Fracture Tensile Strength | Temperature = Airfoil $T_{max}$<br>Crosshead Speed = 0.004 cm/s | 10 Tensile Specimens per Supplier |
| Slow Fracture Tensile Strength | Temperature = Airfoil $T_{max}$<br>Crosshead Speed - 0.00004 cm/s | 10 Tensile Specimens per Supplier |
| Cycle Fatigue | Temperature = Airfoil $T_{max}$<br>Cycle From 35-172 MPa (5-25 ksi)<br>5000 Cycles | 3 Tensile Specimens per Supplier |
| Constant Stress Varying Temperature | Constant Stress 172 MPa (25 ksi)<br>Temperature Step 1 1177°C (2150°F) 100 hrs<br>Temperature Step 2 1232°C (2250°F) 100 hrs<br>Temperature Step 3 1288°C (2350°F) 100 hrs<br>Temperature Step 4 1343°C (2450°F) 100 hrs | 3 Tensile Specimen per Supplier |
| Creep Tests | Stress Level 35-172 MPa (5-25 ksi)<br>Temperature = Airfoil $T_{max}$<br>Time 500 Hours | 3 Tensile Specimens per Supplier |
| SHORT LIST OF TWO MATERIALS BASED ON THE ABOVE TESTS | | |
| Creep Tests | Stress Level 35-172 MPa (5-25 ksi)<br>Temperature = Airfoil $T_{max}$<br>Time 1000 Hours | 6 Tensile Specimens per Supplier |
| Creep Tests | Stress Level 35-172 MPa (5-25 ksi)<br>Temperature = Airfoil $T_{max}$<br>Time 5000 Hours | 6 Tensile Specimens per Supplier |

enhancement, selected area x-ray computed tomography, laser scattering, infrared imaging, positron annihilation, and high resolution FPI. Phase II work will involve characterization of test specimens and components in the as-received condition as well as after fracturing to correlate the position and size of defects with the NDE diagnosis, examination by various NDE techniques of test specimens after long term exposure by oxidation and creep, and correlation of NDE with life assessment data.

### Task 4: Technical and Economic Justification and Market Potential

The Task 4 work examined the market potential of the CSGT-'H' engine and that of future engines that will incorporate the ceramic gas turbine technologies to be developed under the program. The economic analysis valuation methodology was based on a comparison of the net present value (NPV) of the ceramic stationary gas turbine with the net present value of the

metallic engine baseline. The value of a commercial gas turbine over its operating life can be expressed as:

Value = Revenue - {Equipment Cost + Operating Cost}

Revenue consists of the value of electricity and steam generated, and the availability of the equipment. Equipment cost includes engineering, land, equipment, permits, legal, construction, financing, and start up. Operating cost includes fuel, waste disposal, maintenance, operators, down time, taxes, and insurance.

In the analysis the ceramic gas turbine technology contributes to revenue because an economic value can be attached to the additional electricity and steam generated by the ceramic engine compared to its metal baseline. The net present value methodology incorporates the risk inherent in the novel ceramic technology by discounting the cash flow generated by the equipment over its useful operating life. Since the technology is considered high risk a high discount rate (30% before taxes) rate was used in the analysis.

Table 6 presents a summary of the added value of the CSGT-'H' engine examined in Task 4. Performance data for the CSGT-'H' and Centaur 'H' baseline are those listed in Table 2.

The data in Table 6 indicate that substantial increases can be achieved from ceramic conversions of existing engines. For the Centaur 'H' the modifications to the current metallic engine are relatively minor. Only those design modifications required to adapt the current all-metal engine to the ceramic hot section parts are being considered. Additionally, scenarios were also considered for future engine models. The performance improvements for these engines and predicted added values are significantly in excess of those predicted for the CSGT-'H'. The Delta NPV estimates in Table 6 do not include an adjustment for the cost of ceramic components and the cost increase associated with modifications to the metallic engine components to enable operation at the higher firing temperatures of the ceramic uprates. For the CSGT-'H' the cost increase is estimated to be minor compared to the very large Delta NPV's predicted.

The supplier-subcontractors have estimated the cost of ceramic components for the CSGT-'H' engine assuming these parts would be fabricated in quantities typical for industrial gas turbine manufacturers. The estimates from various suppliers are within a narrow price band and indicate that blades and nozzles can be fabricated at costs below those of current state-of-the-art cooled metallic components using advanced alloys (single crystal, etc.) required for the TRIT's in excess of 2000°F. Combustor liner costs tend to be comparable (monolithics) or higher than those of current metallic combustor liners.

Given that the economic analysis for the ceramic stationary gas turbine was favorable an assessment was made of the time frame for production release and market penetration of the CSGT-'H'. The results of this analysis are summarized in Figure 11. Three scenarios were examined. The optimisitic scenario assumes that equipment economics will strongly favor fuel efficiency, i.e. a high cost of energy will apply at the time of product introduction. Ceramic material costs are assumed to be within current estimates. It is also assumed that the Phase III field test has been successful, and that a production version of the CSGT-'H' has been designed and successfully tested for 8000 hrs. Given these conditions full ceramic replacement of the Centaur 'H' will require 4 years from production release. In the expected scenario all the aforementioned prerequisites are still assumed to apply, but full ceramic replacement is forecast to require 5 years from the date of production release. This is based on Solar's experience with

**Table 6. Delta Value (Ceramic - All Metal) for the Program Engine**

| Engine | Scenario* | NPV Delta Minimum ($) | Electricity Rate (kWh) | Natural Gas Price ($) | NPV Delta Maximum ($) | Electricity Rate (kWh) | Natural Gas Price ($) |
|---|---|---|---|---|---|---|---|
| Centaur 'H' | Base Load | 424,848 | 0.06 | 2/MMBtu | 988,495 | 0.08 | 2/MMBtu |
| | Cogen | 642,289 | 0.06 | 3/MMBtu | 1,432,477 | 0.08 | 2/MMBtu |
| | Cogen-Supp | 53,817 | 0.06 | 2/MMBtu | 815,775 | 0.08 | 2/MMBtu |

* Base Load: Simple cycle
Cogen: Cogeneration: credit is taken for the steam produced at a rate of $6/1000 lbs of steam
Cogen-Sup: Cogeneration with suppplemental firing in the exhaust

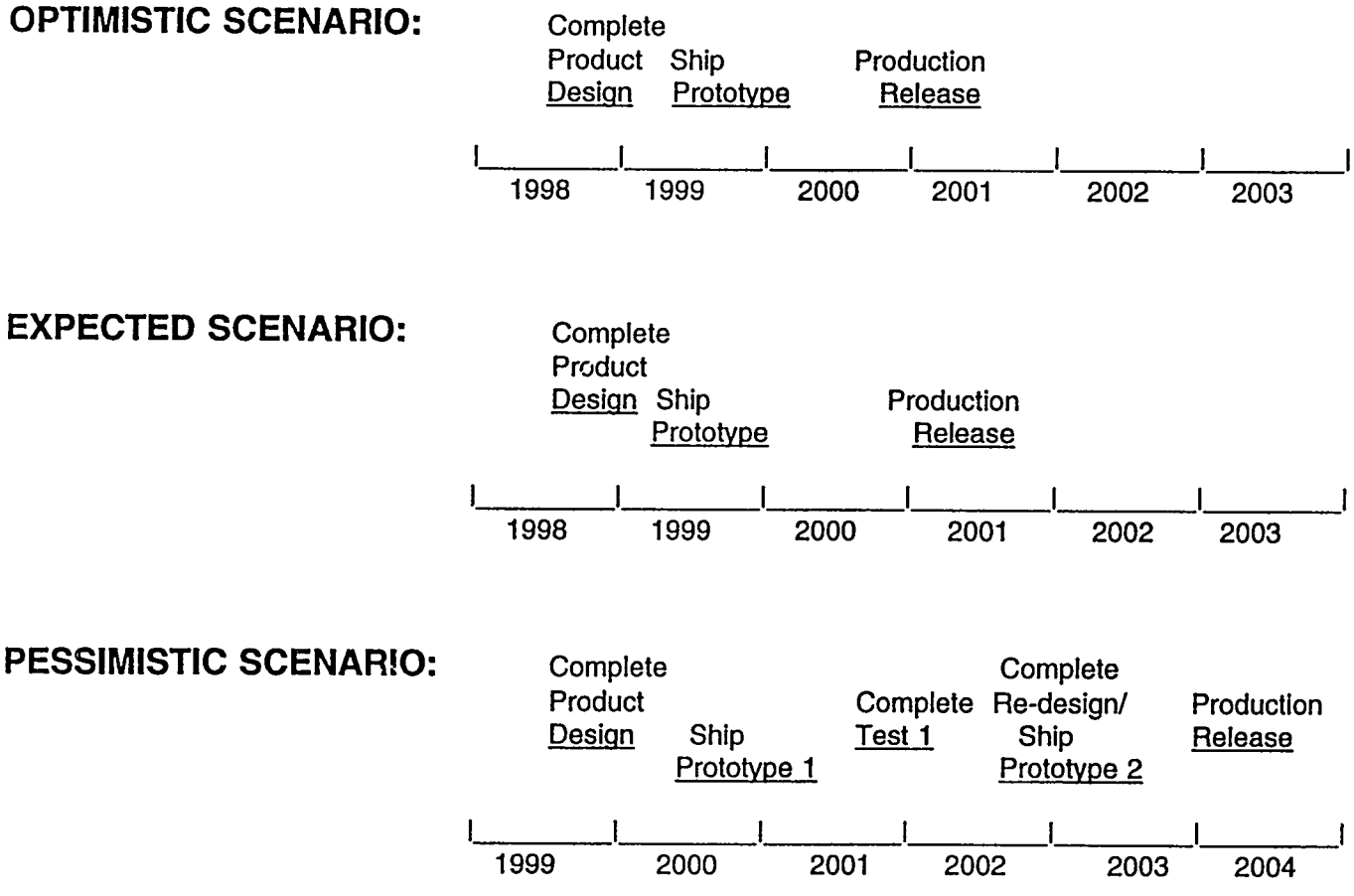


**Figure 11. Three CSGT Market Penetration Scenarios**

new product introduction where an existing product is already well established. In the pessimistic scenario equipment costs are still favoring ceramics, but some delays in the design and successful field testing of the engine will require redesign and another 4000 hr field test. Total development time is now expected to add another 3 years to the time frame for production release compared to the optimistic scenario.

**Task 5: Concept Assessment**

The results of Tasks 1-5 were used for an overall evaluation of the ceramic stationary gas turbine technology, to assess its benefits and detriments/risks, and to identify the critical activities required for the success fuel commercialization of the technology.

The approach taken was to assess the benefits and detriments of the ceramic stationary gas turbine technology from the perspective of the nation (DOE), the end user, and the gas turbine equipment manufacturer. From the perspective of the nation, the major benefits are the national energy savings resulting from improved thermal effiency and output power, lessening the burden on the environment through reduced emissions of $NO_x$ and CO, and improved gas turbine product competitiveness in the international market place. The benefits to the enduser parallel the benefits to the nation. Higher output and reduced fuel costs reduce life cycle costs and cost of generating electricity, and improve return on investment, while reduced emissions lowers the cost of compliance with environmental regulations. Performance improvements also afford significant benefits to the gas turbine equipment manufacturer. Product competitiveness is increased, potentially over a wide range of products. This translates into more favorable market share, and improved competitiveness versus alternate energy generation technologies.

Detriments are derived from failure to achieve the performance improvements that result in the above benefits. The risks stem primarily from potential design inadequacies, customer acceptance in the market place, investment required to develop the ceramic technologies, and an inadequate supplier base. The risk remains that competitors may develop the technology first.

There are activities that are critical for the success of the program. In the area of design these activities include the need to obtain adequate resistance to failure modes by selecting superior materials, and achieving designs with low stresses and favorable interfacial properties. Clearance control in the hot section is important to optimize efficiency gains.

The ceramic technology must demonstrate <25 ppmv $NO_x$, and have the potential to achieve levels of $NO_x$ of 10 ppmv $NO_x$ or better. The latter level, significantly below the level obtainable with existing state-of-the-art low-emissions techniques for metallic combustors, is an important milestone on the way to meeting the emissions goal of the ATS program. A critical activity will be to demonstrate early on in Phase II to what extent the current Solar lean premix low-emissions approach modified for ceramic lined combustors can reduce $NO_x$ levels. Alternative approaches that have the potential to achieve levels of 10 ppmv or better are being considered together with the lean premix approach.

The establishment of a data base for long term materials properties is especially critical if the ceramic gas turbine technology is to be fully accepted by the design community. Likewise, a comprehensive life prediction strategy covering all major failure modes and NDE techniques to enable parts evaluation during inspection and overhauls are important elements for the success of the program.

## FUTURE WORK

### Task 6: Future Plans

Figure 12 summarizes the Phase II component design/development approach of the program in which design analysis is iterated with life prediction and testing. The testing in Phase II involves essentially three stages. In the first stage simulated components will be tested in test rigs to prove out key design concepts such as blade root configuration and compliant layers for the blade, attachment to the case for the nozzle, and fixturing to the metallic support structure for the combustor liner. The testing will be performed using various attachment rigs, blade spin rigs, and subscale combustor component rigs. In the second stage the findings from these tests will be fed back into the design of the first component prototypes which will be tested in a gasifier rig, a Solar Centaur 'H' engine modified to accept ceramic parts. The results of the first generation prototype testing will be used to modify the component designs. In the third stage second generation parts will be manufactured, which will also be tested in the gasifier rig. Second generation parts with superior performance will be used for the 4,000 hr engine field test in Phase III of the program. The testing sequence for each of the three components targeted for ceramic conversion is shown in Figure 13.

## REFERENCES


1. Anson, D., Sheppard, W.J., Norland, L.D., and DeCorso, M., "Application of Ceramics to Industrial Gas Turbines; Tasks 2, 3, and 4, Economics, Market Analysis and


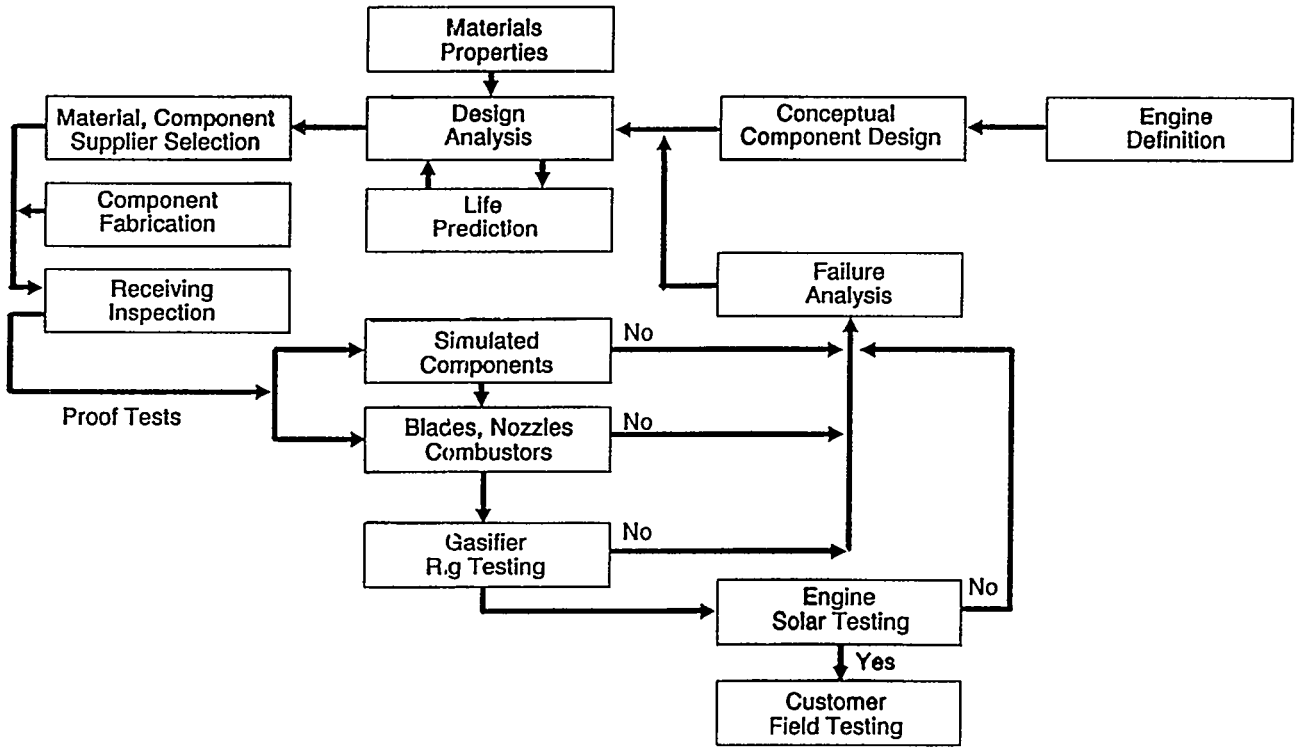


**Figure 12. Iterative Ceramic Component Design/Development Approach**

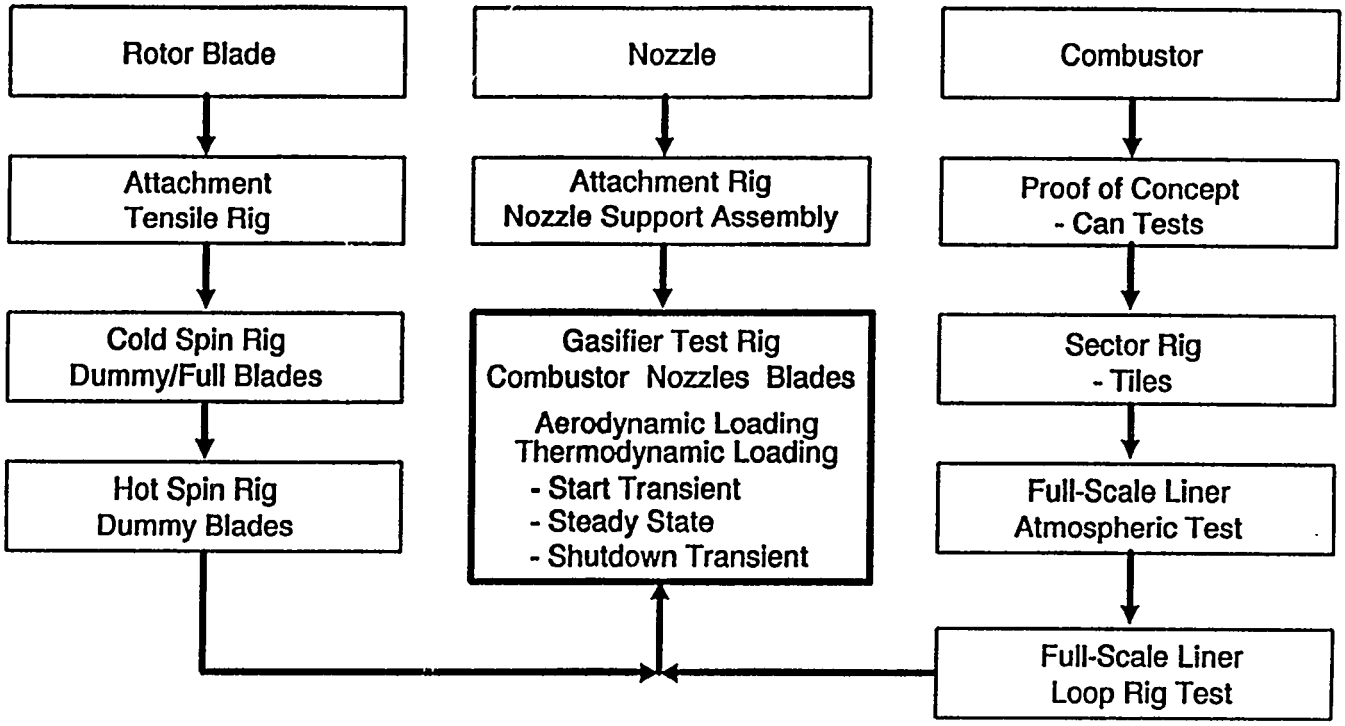


**Figure 13. Proof/Screening Testing for Low-Risk Development Approach**

R&D Plan", Tasks 2, 3,and 4 Final Report, Battelle Memorial Institute, DOE Contract No. DE-AC02-89CE40878, 1991.

2. Anson, D., Sheppard, W.J., and Parks, Jr., W.P., "Impact of Ceramic Components in Gas Turbines for Industrial Cogeneration", Paper 92-GT-393, presented at the Intenational Gas Turbine and Aeroengine Congress and Exposition, Cologne, Germany, June 1-4, 1992.

3. van Roode, M., Brentnall, W.D., Norton, P.F., and Pytanowski, G.P., "Ceramic Stationary Gas Turbine Development", Paper presented at the International Gas Turbine and Aeroengine Congress and Exposition, Cincinnati, Ohio, May 24-27, 1993. Paper ASME 93-GT-309.

4. "Ceramic Stationary Gas Turbine Development", Phase I Technical Progress Report, DOE Contract No. DE-AC02-92CE40960, Solar Turbines Incorporated, SR93-R-5921-09. May, 1993. Under review.

## 2.2 Materials/Manufacturing Element of the Advanced Turbine System Program

CONTRACT INFORMATION

| | |
|---|---|
| **Contract Number** | ED 32 01 00 0<br>Field Work Proposal |
| **Contractor** | Oak Ridge National Laboratory<br>P.O. Box 2008<br>Oak Ridge, TN 37831-6065<br>(615) 574-5150 |
| **Contractor Project Manager** | Michael A. Karnitz |
| **Principal Investigators** | Michael A. Karnitz<br>Jack H. De Van<br>Robert S. Holcomb<br>Arvid E. Pasto |
| **DOE Project Manager** | Eugene Edward Hoffman |
| **Period of Performance** | July 1992 to September 2000 |

ABSTRACT

One of the supporting elements of the Advanced Turbine Systems (ATS) Program is the materials/manufacturing technologies task. The objective of this element is to address critical materials issues for both industrial and utility gas turbines. DOE Oak Ridge Operations Office (ORO) will manage this element of the program, and a team from DOE-ORO and Oak Ridge National Laboratory is coordinating the planning for the materials/manufacturing effort. This paper describes that planning activity which is in the early stages.

## INTRODUCTION

A new DOE Program to develop advanced gas turbines for power generation in the utility and industrial section has been initiated. The objective of the program is to develop advanced gas turbines for utility and industrial power generation. The goals of the program are to increase the efficiencies to greater than 60% in utility combined-cycle systems and a 15% improvement in industrial turbines. Additional goals include a 10% reduction in power costs and reduction in acid gas emissions. ATS is a joint program that is managed by both DOE Fossil Energy (FE) and DOE Energy Efficiency and Renewable Energy (EE). The primary focus of the program is on natural gas turbines with program supporting elements on adaption to coal-derived fuels and biomass fuels. ATS is an eight year program which involves turbine manufacturers, utilities, industrial users, national laboratories, and universities. A work breakdown structure is given in Figure 1. The main element of the program is the system design and systemdemonstrations conducted by the turbine manufacturers.

## BACKGROUND/RELEVANCE OF MATERIALS/ MANUFACTURING ELEMENT

Six screening studies have been completed by the turbine manufacturers and several approaches have been defined to achieve the higher efficiencies. One main approach has been higher turbine inlet temperatures greater than 2600° F. To achieve these temperatures for extended operation periods there is a need for materials development and new blade and nozzle cooling concepts. At the two Clemson ATS planning meetings the gas turbine industry stated a clear need for a materials element in the ATS Program. They also indicated a need for effective interaction between the gas turbine manufacturers, materials suppliers, national laboratories, and others. Therefore, one element of the program is a materials/ manufacturing activity, as shown in Figure 1. This element will address critical materials/manufacturing issues for the whole program, including both industrial and utility turbines.

## OBJECTIVES OF THE MATERIALS/ MANUFACTURING ELEMENT

The primary objective of the materials/ manufacturing element is to provide support to the ATS contractors. Direct support is intended to help supplement the ATS team efforts and provide expertise not available to a single company. Another objective is to develop materials/manufacturing technologies for the various ATS teams and the gas turbine industry at large. The technology development will focus on high risk materials, components, and manufacturing processes with emphasis on generic development. Another objective is to provide a technology transfer mechanism between the various NASA, DoD, and DOE

programs to the ATS Program. Many of these materials efforts will have a direct impact on the ATS Program, and a coordination effort is necessary.

## PLANNING STRATEGY

DOE-Oak Ridge Operations Office (ORO) will manage the materials/manufacturing task, and a team of DOE-ORO and Oak Ridge National Laboratory (ORNL) is coordinating the planning for this element of the program. ORNL's Metals & Ceramics Division is involved in various national DOE materials programs including: (1) Ceramic Technology for Advanced Heat Engines, (2) Fossils Materials Program, (3) Continuous Fiber Ceramic Composite Program, (4) Advanced Industrial Concepts Materials Program, and (5) Basic Energy Science Welding Program. ORNL also has the High Temperature Materials Laboratory (HTML) which is a modern facility that serves as a focal point for high temperature materials research. It is a major user facility providing members of industry and the university research communities access to an extensive array of special research equipment needed to characterize the micro-structure and micro-chemistry of materials and to investigate the effects of these parameters on the physical and mechanical properties of materials. The gas turbine industry is already using this facility, and it will most likely be heavily utilized in the materials element of the ATS Program.

The planning for the materials/manufacturing element of the ATS Program is in the early stages. A portion of the Clemson planning meetings that were held in 1992 was on materials issues. In addition, ORNL has made some preliminary contacts with the gas turbine manufacturers, materials producers, gas turbine consultants, and contacts with DoD and NASA. In addition,three strategy papers have been developed, and the results of these papers were presented at a workshop in Cincinnati on May 28, 1993.

The intent is to develop a materials/ manufacturing plan in FY 1994 and start implementing that plan in FY 1995. This schedule will allow sufficient time to obtain the necessary input from the ATS prime contractors, materials suppliers, DoD, EPRI, NASA, and other gas turbine manufacturers. Using this input, a draft plan will be assembled, and the industry will be allowed time to comment on the draft. The last step is the finalization of the plan using industry feedback. A Small Advanced Materials and Turbine Technology (AM&TT) team will be used to develop the plan. The intent is to develop a strong plan using this blend of capabilities. In FY 1995, the AM&TT team will be expanded and used to provide recommendations to DOE on the materials/ manufacturing element.

The projects in the materials/manufacturing element will be performed at national laboratories, private industry sites, and universities. A major segment of the effort will be conducted by materials suppliers. DOE-ORO and ORNL will utilize solicitations and a variety of contractual mechanisms. Work under this sub-element will be performed mainly in existing facilities. Only when absolutely necessary will new facilities be constructed. There are a number of existing facilities available for materials research and these will be utilized prior to any consideration of developing new facilities. However, it is likely that modification of existing facilities will be necessary.

Several possible project areas were identified in the strategy papers that were reviewed at the workshop in Cincinnati on May 28, 1993. The developmental needs generally fall into two categories: evolutionary and revolutionary. Evolutionary materials carry forward the design capability of existing

turbine materials. Revolutionary materials would leap-frog current materials limitations, but their feasibility still must be proven. One of the critical evolutionary technologies is improved thermal barrier coatings (TBCs). TBCs build on current technology to achieve the turbine inlet temperature and life requirements set for the ATS Program and are therefore a key to near-term ATS deployment. They can provide a 100°-200°F benefit which is equivalent to 2-3 generations of super alloy development. However, significant advances in thermal barrier coating technology will be required to meet the ATS development goals. Additional evolutionary materials needs include: (1) turbine/disk alloy development, (2) large air-foil directional solidification casting, (3) metallic coating technology, (4) seal technology/closed circuit steam cooling, (5) modeling of large casting for disks, and (6) manufacturing processes. The key objective to the revolutionary materials development is to reduce or eliminate the need for air-cooling of hot section components. The potential use of steam for blade cooling introduces questions concerning hydrogen embrittlement, oxidation, and fouling. Revolutionary materials needs include: (1) ceramics, (2) intermetallics, (3) refractory metals, and (4) composite materials. One strategy being proposed for revolutionary materials development is to tie in with on-going programs within NASA, DOE, and other DOE programs.

## CURRENT MATERIALS SUPPORT PROJECT

The Ceramics for Stationary Gas Turbines Project is one of the main elements of the ATS Program. This project is being conducted by the Solar Turbines, Inc. and was started in September 1992. The goal of this project is to improve the performance of stationary gas turbines in industrial applications through the selective replacement of metallic hot section parts with uncooled ceramic components. The materials/manufacturing element is providing support to Solar Turbines, and this project is a good example of possible future tasks under the materials/manufacturing element.

The primary goal of the Ceramics for Stationary Gas Turbines project is to determine the long-term survivability of ceramic materials for industrial gas turbine applications. Because existing data for many candidate structural ceramics are limited to testing times less than 2,000 h, this project will focus on extending these data times on the order of 10,000 h, which represents the lower limit of operating time anticipated for ceramic blades and vanes. This long-term test effort will be done in coordination with Solar Turbines and University of Dayton Research Institute (UDRI) as shown in Figure 2.

The specific of the research project includes evaluating the static tensile creep and stress rupture (SR) behavior of three commercially available structural ceramics that have been identified by Solar Turbine as leading candidates for use in industrial gas turbines. Tensile creep data will be generated in air by measuring creep strain as a function of time, applied stress, and temperature. The SR resistance will be evaluated by continuing each creep test until the specimen fails. For each material investigated, a minimum of three temperatures and four stresses will be used to establish the stress and temperature sensitivities of the creep and SR behavior. The test matrix utilized in this program is intended to extend the test conditions investigated by the engine component manufacturers. These conditions focus primarily upon the evaluation of the creep and SR behavior of two candidate materials at one temperature only. Consequently, the temperatures chosen for the ORNL/UDRI

effort will bracket that used by the engine component manufacturers.

For each material investigated, the associated creep and SR data will be used to generate a mechanical reliability diagram describing the time-to-failure and failure mode (creep damage versus slow crack growth) as functions of stress and temperature. The applicability of various creep and SR models (Monkman-Grant, Sherby-Dorn, Larson-Miller, etc.) to the description of the experimental data will also be investigated. The final material selection will be based upon the comparison of these diagrams.

## SUMMARY

The materials/manufacturing element of the ATS Program is needed to attain the goals of the overall program. One of the main approaches to achieving the higher efficiency goals is to obtain higher turbine inlet temperatures of greater than 2600° F for extended operation periods. To achieve these temperatures, there is a need for materials development.

The specific objectives of the materials/ manufacturing element include: (1) providing support on materials/ manufacturing activities to the ATS prime contractors, (2) develop materials/ manufacturing technologies for the various ATS teams and gas turbine industry at-large, and (3) provide a technology transfer service between the various programs at NASA, DoD, DOE, and the ATS Program. The schedule calls for the development of several projects in FY 1995. The plan will be developed in several stages with input from the gas turbine manufacturers, materials suppliers, and various other organizations. An Advanced Materials and Turbine Technology team will be used to develop the plan. In future years this team will also be used to guide this element. The detailed plan will be the foundation for a strong start in FY 1995.

ORNL-DWG 93M-8560

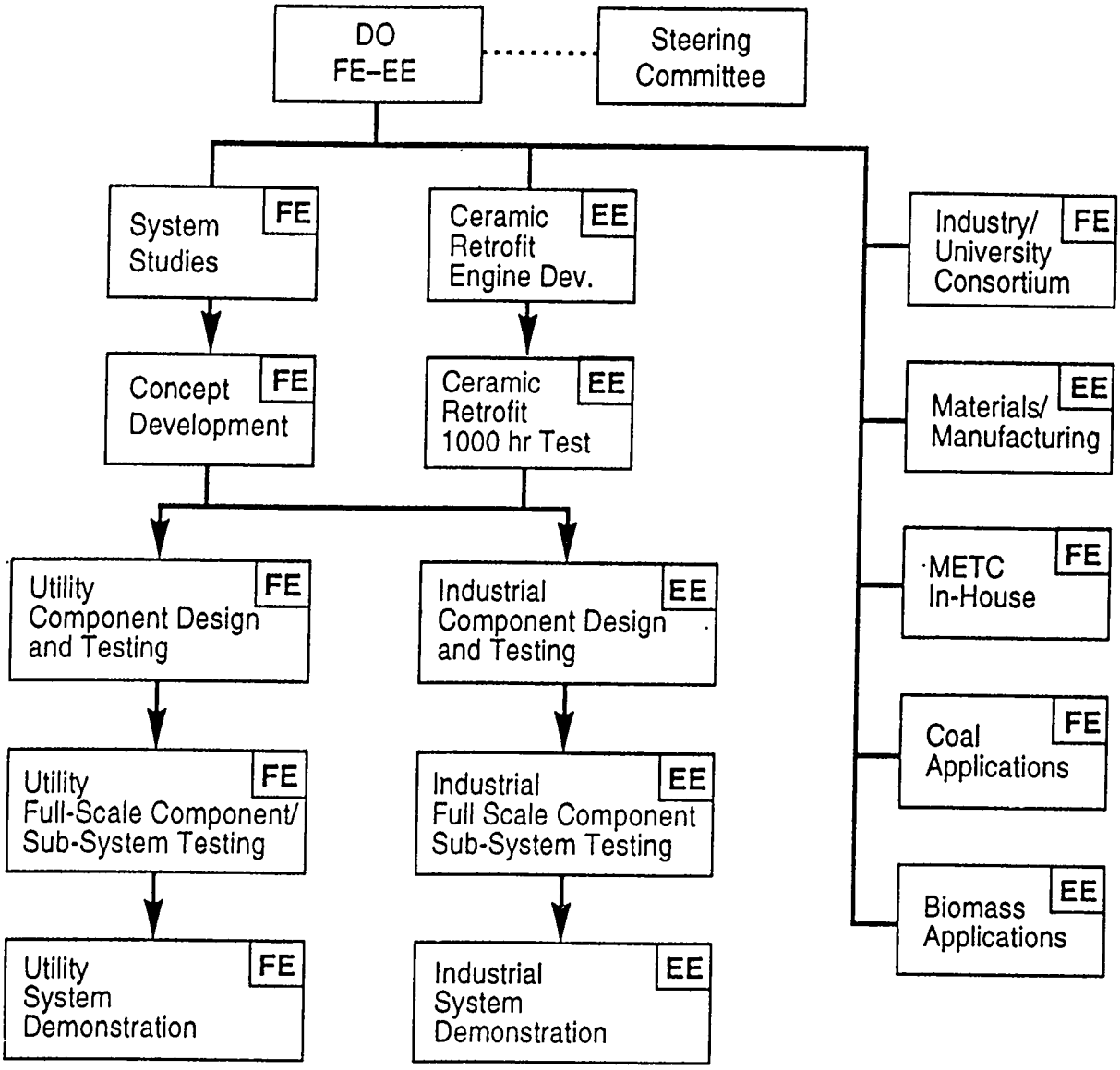


Figure 1. Advanced Turbine System Program

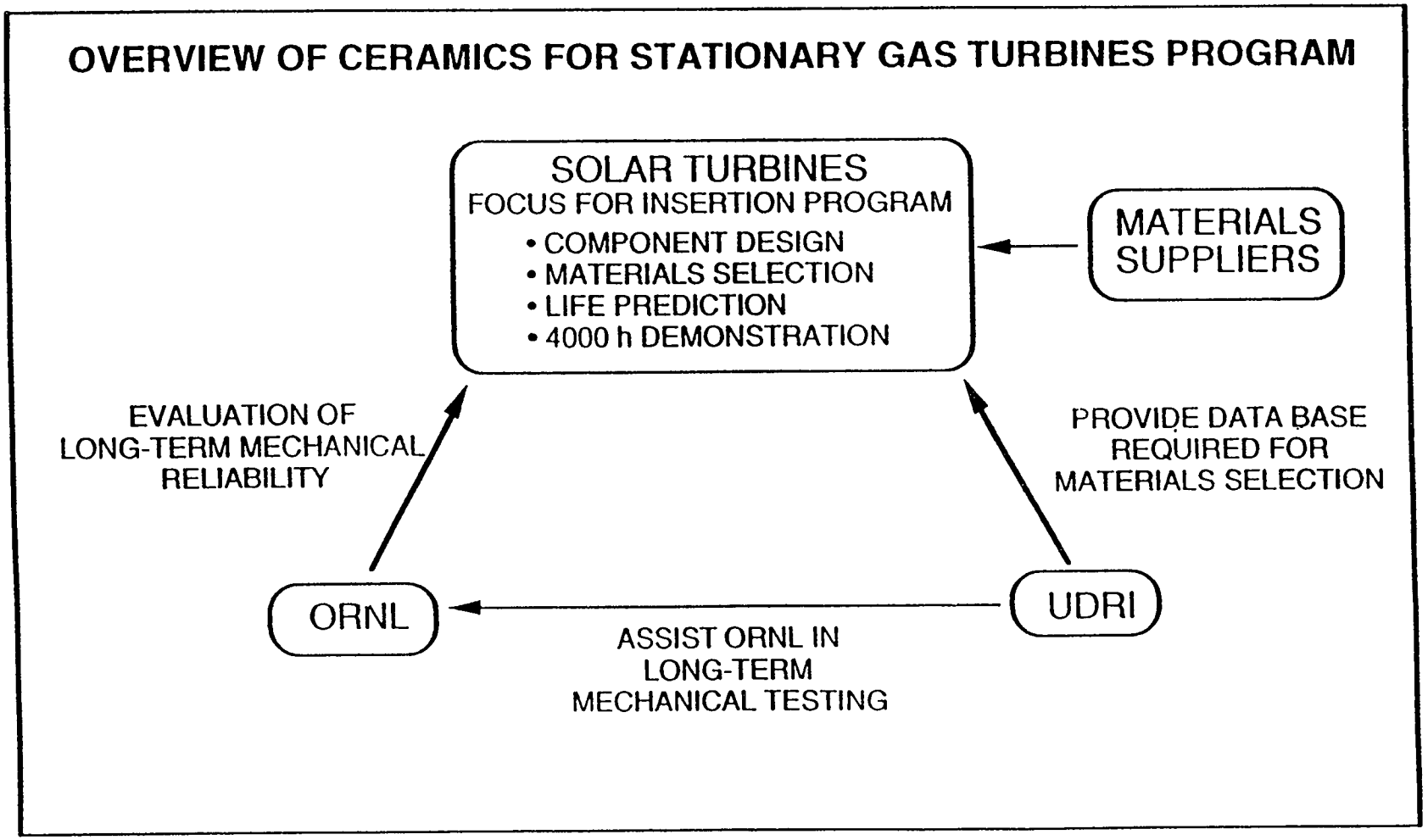


Figure 2. Current Project with Solar Turbines

# FE/EE Advanced Turbine Systems Conference

## Session 3

*Related Programs*

# 3.1 Collaborative Advanced Gas Turbine Program

Arthur Cohn
Generation and Storage Division
Electric Power Research Institute
Palo Alto, California, USA

The Electric Power Research Institute (EPRI), on behalf of its member utility organizations as well as the broader community of users of combustion turbines for power generation, has assumed primary management responsibilities for a new consortium involving elements of both the electric and gas utility industries as well as aircraft engine and gas turbine manufacturers. The objective of the program is to accelerate the commercial availability, to within the turn of the century, of advanced, high-efficiency gas-fired turbines for utility repowering, capacity expansion, and other applications.

The consortium—called the Collaborative Advanced Gas Turbine (CAGT) Program—represents a unique combination of gas producers and sellers, electric power generators, and equipment manufacturers aimed at creating the optimum mix of market-pull and technology-push necessary to realize the technical potential for rapidly incorporating the latest aircraft fan-jet engine technology into high-efficiency, low-emission, compact, and modular power plant packages. These advanced gas turbine plants offer a broad range of possible applications for high-efficiency power generation with the lowest inherent (and even lower achievable) emissions of any fossil fuel based system.

## Broad Coalition

The CAGT represents a broad—and, significantly, international—coalition of industries and organizations spanning both the private and public sector that are motivated by the substantial opportunity in advanced gas turbines to join forces and collaborate in a coordinated effort that seeks to minimize overall and individual development costs through an accelerated program. Organized in 1991 by Pacific Gas and Electric Co., which remains a principal sponsor, other CAGT members, in addition to EPRI, include Southern California Edison Co., San Diego Gas & Electric Co., British Gas, the Canadian Electrical Association, Elkraft Power Company, Ltd., of Denmark, Electricité de France, the Gas Research Institute, National Power Plc of Britain, Sacramento Municipal Utility District, So. Cal. Gas and TransAlta Utilities Corp. of Alberta, Canada.

The U.S. Department of Energy (DOE) and the California Energy Commission interact with the CAGT on both technical and executive levels as observers and the source of funds in support of the CAGT Phase I effort. Phase I is the only currently funded element of a planned three-phase CAGT program that could extend into the 21st century. CAGT members are coordinating their evolving collaborative program with the DOE's Advanced Turbine Systems (ATS) Program for opportunities both to pursue common objectives as well as to stimulate the much larger DOE program and the equipment vendors participating in it to demonstrate advanced turbine concepts and systems of greatest interest to utilities and to the international power community.

The vision is that, by close and cooperative collaboration, the community of stakeholders in the growing market for electric power generation, primarily utilizing natural gas as fuel, may collectively provide the right combination of

market-pull and technology-push that will enable a substantial leap forward to lower-cost, yet high-efficiency and highly reliable primarily gas-fired power plants and advanced power cycles that will make the new turbines even more flexible for application as both dispersed and central-station power plants.

**Widening Potential**

As originally conceived by PG&E, the CAGT was aimed at exploiting the significant opportunity represented by the latest high-efficiency fan-jet engines that are entering service in commercial aircraft—which can enable a jumbo jetliner to make nonstop flights of more than 8500 miles. Based on information from the aircraft engine manufacturers themselves—General Electric, the Pratt & Whitney Division of United Technologies, and Britain's Rolls-Royce are the leading makers of large fanjets—it was believed these machines could be incorporated without major design modifications of the core engines into packages as compact, lightweight aeroderivative combustion turbines.

Featuring multiple compressor spools that can be configured for efficiency-boosting intercooling, along with much higher pressure ratios than heavy-frame combustion turbines, aeroderivatives have been more expensive per unit of generating capacity than heavy-frame machines for many years, despite the aeroderivatives' already largely recovered higher development costs. Yet partly because these aeroengines are so extensively engineered for compactness, low weight-to-power ratio, and very high reliability, even simple design modifications to make a ground-based aeroderivative require considerable reengineering and will usually result in a still relatively expensive power plant compared with an industrial turbine.

But because of the advantages they offer, PG&E determined it could use advanced aeroderivative gas turbines to repower much of its aging 7000 MW of fossil-fuel steam generating capacity, which is typically natural gas-fired. PG&E anticipated the need to replace much of its fossil-fired capacity beginning around 2000 but, like many utilities, faced low load growth and limited access to new power plant sites near load centers. Modular, high-efficiency and compact aeroderivative-turbine-based power plants incorporating current state-of-the-art superfan jet engines appeared to offer significant potential for both repowering gas-fired steam generating capacity at existing plant sites and as small, distributed generating units for siting near substations or load centers.

In the program definition for CAGT, PG&E utilized the body of EPRI research over the past 15 years on advanced power cycles and power systems that had identified and analyzed a variety of advanced cycles with potentially very attractive efficiencies—some approaching 60%—and very low emissions. Some of these advanced cycles promise comparable capacity ratings and efficiencies about or above those for a combined-cycle plant using, heavy-frame, combustion turbines, but without that configuration's requirement for a bottoming-cycle steam turbine. Incorporated into a series of advanced gas turbines that did not each require full-scale development and demonstration, such advanced systems—which would be likely, but not necessarily, based on aeroderivative turbines—could help make gas-fired combustion turbines more broadly appealing to utilities beyond the machines' traditional role (stand-alone without bottoming cycle) as peaking generators.

The expected high performance and reliability of such turbines, coupled with inherently modular, phased construction, make them valuable in capacity planning for baseload and intermediate duty cycles in addition to peaking, for complete or partial station repowering as well as for greenfield plant sites, or as generating units that can be built in stages and

dispatched as both small and large capacity increments. Because these power plants would be modular, lightweight packaged generating units with a relatively small overall footprint, they could potentially be used as portable power plants for temporary siting at dispersed load centers or transmission substations, in addition to the more conventional distributed generation application originally envisioned.

**CAGT's Three-Phase Development Program**

The CAGT effort is presently focused in Phase I on conceptual design studies by three teams of fan-jet engine manufacturers and power plant engineering firms. Contract awards of $2.5 million total have been made to the teams of General Electric and Stewart & Stevenson with Bechtel; Rolls-Royce with Bechtel; and United Technologies' Turbo Power & Marine Division with Fluor. Each of the aircraft engine makers presently offer top-of-the-line turbo-fan machines providing thrust of from 50,000 pounds up to 80,000 or 90,000 pounds in models that are used in virtually all wide-body, long-haul jetliners in service today or planned to enter service soon, such as the Boeing 777 (set to fly commercially in 1995). GE recently began testing an even more-advanced fan-jet, designated the GE-90, that is expected to be capable of delivering up to 100,000 pounds of thrust.

Engineering and economic evaluations by the vendor teams of various gas-turbine power plant designs and configurations that would incorporate these advanced aero engines are expected to be completed by the second quarter of 1994. The vendor teams are to identify preferred conceptual designs from a comprehensive screening of options for those that could be readily commercialized. Also as part of Phase I, the vendor teams are to develop proposals that will detail the technical, business, and financial requirements necessary for demonstrating a preferred-concept machine that could become commercially available by 1998. Such early commercial plant designs may be anywhere from 50 MW to 200 MW in capacity. During the first phase, the CAGT's members will attempt to catalyze early market interest in each team's preferred design in order to establish an initial level of market pull represented by potential customer orders.

Based on feedback from CAGT members to the vendor proposals from Phase I, the next phase envisions the early commercialization of the leading designs for advanced aeroderivative turbine-based generating systems. The details of Phase II are yet to be finalized but they most likely will include the placement in service of demonstration units with risk-sharing, pioneer owner-operators such as utilities and other generating entities. CAGT members would share this risk and could have priority on orders of new machines and royalties on those sold to other power producers. During this second phase, which would run from 1994 through about 1998, substantial user feedback to the manufacturers and interaction among the CAGT members on the new machines' initial operating experience will help confirm and validate the development strategy.

The process is also expected to lead to the collaborative identification of a path for development and application of advanced, innovative power cycles to the preferred turbine designs during the project's third phase. The eventual incorporation of such advanced cycles into commercial designs sometime after 2000 may represent the ultimate technical realization of an advanced, high-efficiency gas-turbine power plant.

Specific areas of current technical focus within the program include studies of various applications of intercooling as a means of increasing turbine efficiency and power output, both as a short-term enhancement to existing high-thrust aeroderivative designs and as part

of longer-term advances in combined and more-complex power cycle applications, including the use of intercooling in combination with fuel reforming and with reheat combined cycles. There is also interest in high-efficiency combustion turbine designs that would combine components of both aeroderivative turbines and heavy-frame machines. The implications of intercooling for redesigning or replacing the first compressor spool of an aeroderivative machine with a lower-cost compressor designed to industrial turbine standards is an example.

In addition to the potential for intercooling, critical investigation is being made into such other advanced cycle concepts as chemical recuperation (fuel reforming) with intercooling and steam injection, and a humid air turbine—an intercooled, regenerated cycle with a saturator that adds moisture to the compressor discharge air.

An interim report on the most promising of these advanced cycles in the context of the CAGT's accelerated development effort is expected to be available by the second quarter 1994. The most immediate emphasis will be on those cycles or combinations of cycles that are the best candidates for commercial introduction in gas-turbine power plant designs by 1998.

The overall aim of the accelerated program is the development of actual power plant designs that provide the best combination of capital cost, development cost, performance, and low emissions (particularly those of nitrogen oxides).

Minimizing the consumption of water, whether for boosting power and efficiency or for limiting $NO_x$ emissions, is also a criteria for some of the advanced cycles. Some tradeoffs may be necessary between the capital cost and technical performance of advanced designs and the costs and risks of certain development paths.

## Product Positioning Relative to Industrial Turbines

Figures 1 and 2 integrate the initial CAGT comparative analyses of the efficiency and capacity potentials for advanced aeroderivative-based gas turbine power plants relative to the evolution of current heavy-frame industrial gas turbines to their expected next generation. The figures suggest that near-term advancements such as intercooling and the longer-term incorporation of advanced cycles could propel high-thrust aeroderivative turbines into a new dimension of power and performance that would make them extremely advantageous for intermediate load operation and competitive with existing and future heavy frame turbines for base load operation.

Intercooling could make aeroderivative-based gas turbines competitive in cost and power rating with today's industrial machines operating in simple cycle, but the aeroderivative would be substantially more efficient. The potential is clear for intercooling to boost the simple-cycle efficiency of an aeroderivative turbine by about 5 absolute percentage points—or 15-20% better than the best current heavy-frame machines—while more than doubling the power output, for a possibly substantial capital cost reduction per kilowatt of generating capacity. Meanwhile, advanced cycles incorporating high-thrust aeroderivative turbines could achieve efficiencies as high or possibly even higher than those anticipated with the next generation of industrial turbines in combined-cycle, but in smaller capacity increments.

## Summary

A rare convergence of near-term economic, political, and regulatory forces and technological development with longer-term environmental choices and capacity-planning decisions is

Product Positioning—Advanced Cycles Relative to Competing Simple Cycle Gas Turbines

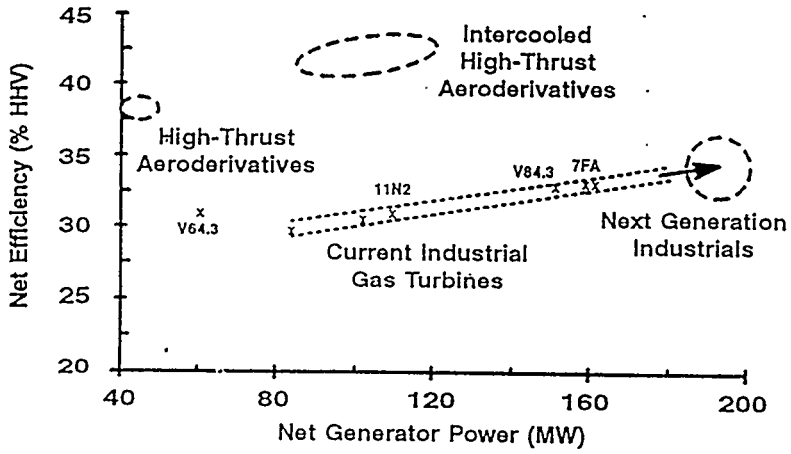


**Figure 1. Product Positioning—Advanced Cycles Relative to Competing Simple Cycle Gas Turbines**

Product Positioning—Advanced Cycles Relative to Competing Gas Turbine Combined Cycles

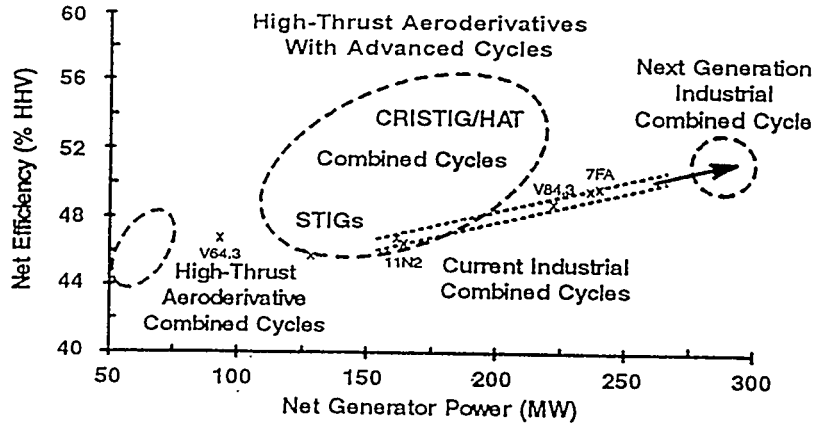


**Figure 2. Product Positioning—Advanced Cycles Relative to Competing Gas Turbine Combined Cycles**

making the power generation market both here and abroad eager for higher-efficiency conversion technologies that will permit more economical use of natural gas as a fuel for power generation. Advanced aeroderivative gas turbine power plants prepresent an opportunity for potentially very high payoff from a coordinated, collaborative research, development, and demonstration effort aimed at achieving this larger goal.

The CAGT Program provides a framework for overcoming the technical and institutional barriers to higher efficiency gas turbines, while reflecting the preference of its members for a collaborative approach to development. With broad industry support to ensure a successful completion of the program, modular advanced gas turbine-based electric generating plants with unparalleled efficiency and performance will be operating by 2000, and a clear path will be illuminated for the inclusion by early next century of innovative power cycles for even greater efficiency and lower emissions.

# 3.2 U.S. Navy Intercooled Recuperated (ICR) Engine

Thomas L. Bowen
Naval Surface Warfare Center
Annapolis Detachment, Carderock Division
Annapolis, Maryland

## ABSTRACT

The U.S. Navy is developing an Intercooled Recuperated (ICR) gas turbine engine for propulsion of future surface ships. The objectives of this development program are to reduce propulsion fuel consumption by 30 percent, increase maintenance flexibility, improve supportability, enable meeting future emissions standards, and enhance ship mobility.

The advanced development phase of this program began in December 1991 with the competitive award of the prime contract to Westinghouse Marine Division in Sunnyvale, California. During the 48-month advanced development phase, the contractor will design, develop, fabricate and test the complete system which is designated the WR-21. This engine is based on the Rolls Royce RB211 family of commercial airline engines. The parent aero engine components are modified to incorporate an intercooler and recuperator into the existing simple cycle engine configuration. The intercooler and recuperator are being developed by Allied Signal Aerospace Systems and Equipment in Torrance, California. Since the majority of ship operating time is spent at low power and low speed, variable area nozzles are incorporated into the RB211 power turbine to maintain high thermal efficiency at off-design conditions. The development of a digital control system for the WR-21 is subcontracted to CAE in Montreal, Canada.

This paper presents an overview of the WR-21 design and performance characteristics, and the operational advantages gained with this new engine. The program schedule and status of the development effort are summarized.

## INTRODUCTION

The operational requirements of naval surface combatants are quite different from most commercial vessels. Commercial vessels operate at their most efficient speed as much as possible. However, the various missions which the surface combatant must perform requires it to operate over a wide range of speeds. The distribution of operating time as a function of ship speed is referred to as the ship's mission profile. Figure 1 is the assumed peace-time mission profile for the U.S. Navy's newest destroyer, i.e, the DDG-51 Arleigh Burke Class. This chart indicates that the ship should spend two-thirds of the underway operating hours at speeds of 20 knots or less, and very few underway operating hours spent at maximum speed. Since propulsion power is roughly proportional to the cube of ship speed, the

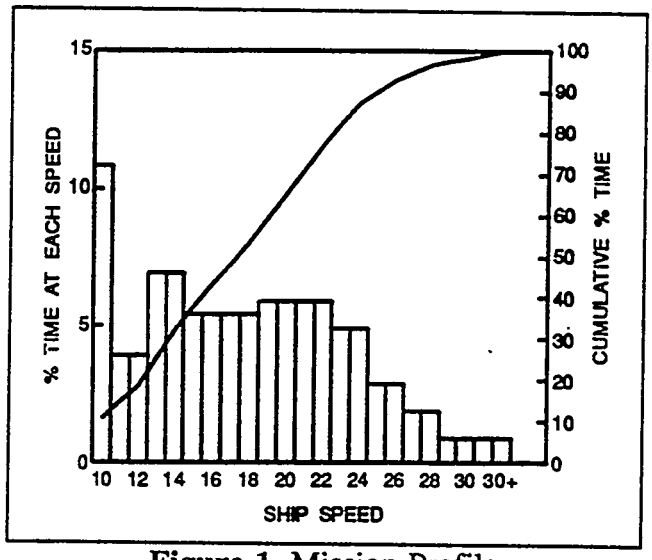


**Figure 1.** Mission Profile

power required to cruise at 20 knots is approximately one-third of the total installed propulsion power.

This unique requirement for very different levels of propulsion power at low speed and high speed operations has led to a variety of naval power plants. Many ships of foreign navies use two different types of propulsion engines, a small diesel or gas turbine engine for cruising and a large gas turbine for high speed operation, connected to the same gearbox. In some ships these engines may be operated independently of each other, while in other ships the two different engines may be operated together at ship speeds above the capability of the smaller engine. The U.S. Navy has used multiples of the same propulsion engine in order to simplify logistic support requirements.

The U.S. Navy began using gas turbine engines for propulsion of surface combatants in 1975 with the introduction of the DD-963 Spruance Class destroyer. This ship has four simple-cycle gas turbine engines with two in each engine room connected to a reduction gear which is connected by shafting to a propeller. This propulsion plant configuration has become the standard for subsequent classes of cruisers and destroyers. The smaller FFG-7 Perry Class frigate uses half of the standard configuration, i.e., a single-shaft, two-engine propulsion plant. The U.S. Navy fleet presently includes nearly 100 surface combatants powered by over 300 gas turbine engines. The current propulsion gas turbine is a derivative of a dual-use military/commercial aircraft engine developed during the 1960's. This high power density engine has proven to be a compact, lightweight, and maintainable naval prime mover. After nearly two decades of service, this engine has logged more than 3 million hours of operation. A Component Improvement Program has been continuously funded by the U.S. Navy since the introduction of this engine. Through research under this CIP program and by incorporating design upgrades from later aircraft engine variants, the current engine matured into a highly reliable marine gas turbine. This engine is used widely in other navies and industrial applications.

Despite the past success experienced with the current propulsion gas turbine, the U.S Navy has sought to significantly reduce the fuel consumption of its surface combatants. The typical ship will consume 100,000 barrels of fuel each year of which 60% is burned by the propulsion engines. The specific fuel consumption of the simple-cycle gas turbine inherently increases as the output power of the engine is decreased. A propulsion engine with the attributes of the gas turbine cited above, but with a specific fuel consumption characteristic approaching that of a diesel engine was the vision for the next generation naval propulsion gas turbine. Limitations on the state-of-the-art of simple-cycle gas turbines required that waste heat recuperation and perhaps compressor intercooling be considered to achieve significant improvement in efficiency at the design point. Use of variable area nozzles in the power turbine would be essential if high efficiency is to be maintained at part load operating conditions.

The Navy-funded research during the past decade resulted in the transition of the advanced-cycle marine gas turbine concept from feasibility study phase to preliminary design phase to advanced development phase. The results of this research have been documented in several open literature publications [1 - 6]. Based on this collective body of work, the U.S. Navy chose to invest research and development resources towards the intercooled recuperated gas turbine engine identified as the WR-21. This paper will present the WR-21 design and performance characteristics, operational advantages, program schedule, and development status.

## DESIGN OVERVIEW

The principle of operation of the WR-21 is illustrated in the cycle schematic shown as Figure 2. Combustion air enters the engine via the ship's intake air ducting and is compressed in the Intermediate Pressure Compressor (IPC). The IPC discharge air enters an on-engine intercooler where a mixture of freshwater and ethylene glycol is used to cool the combustion air with a minimum of pressure loss. The work required by the High Pressure Compressor (HPC) to compress this high density, low temperature air is reduced as a result of the intercooling process. The HPC discharge air is routed to a recuperator for preheating by heat recovery from the exhaust gas stream. The return air from the recuperator enters the combustor where it is mixed with fuel and

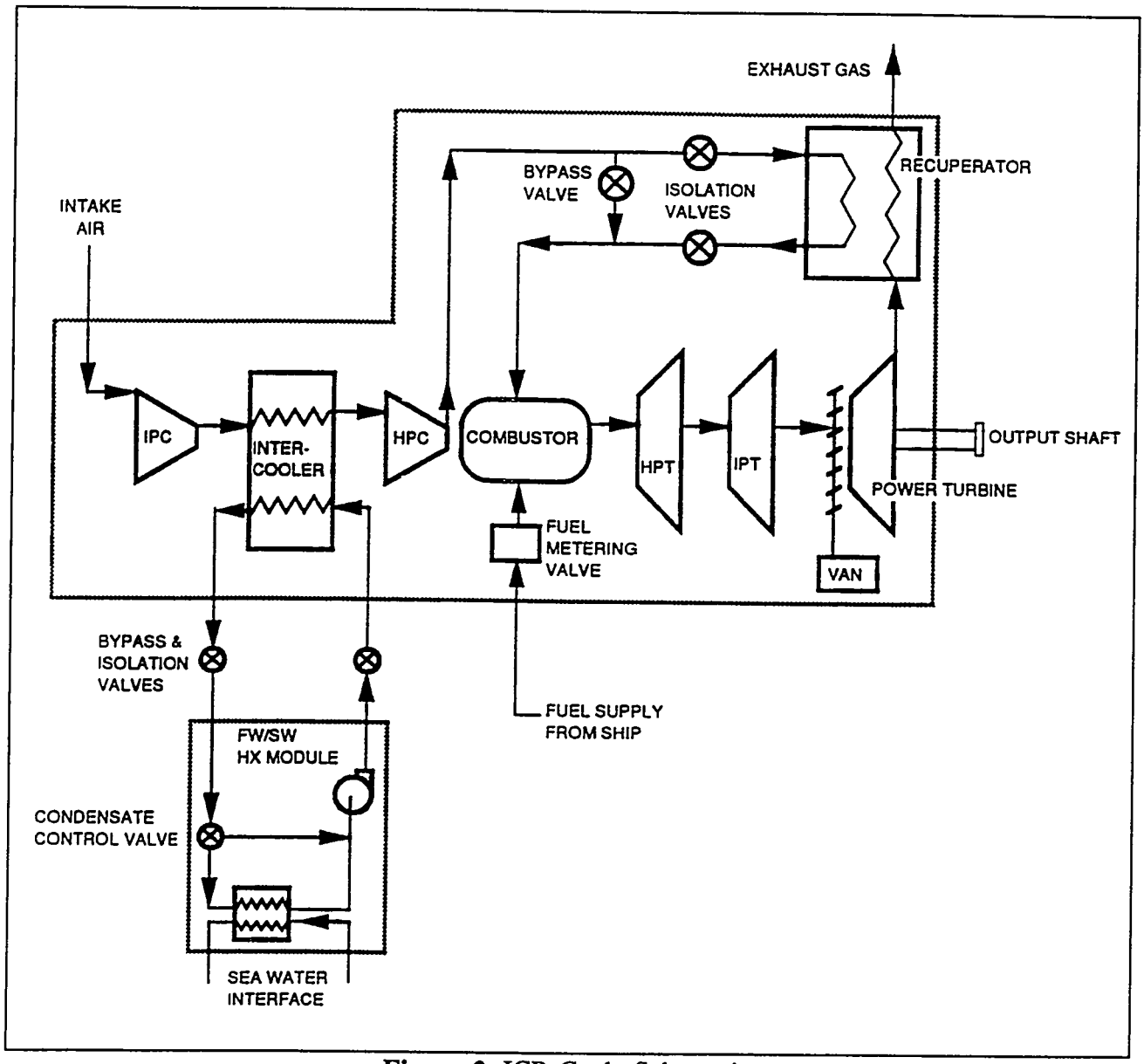


**Figure 2.** ICR Cycle Schematic

burned to increase the temperature of the working fluid to its maximum level. Work is extracted from the fluid as it passes through the High Pressure Turbine (HPT) and Intermediate Pressure Turbine (IPT) to drive the HPC and IPC, respectively. The gas generator section of the engine includes both compressors, the combustor, and the turbines which drive these compressors. Gas exiting the IPT enters the variable area nozzle (VAN) and power turbine assembly where work is extracted to propel the ship. Exhaust gas from the power turbine is cooled as it passes through the recuperator as a result of heat being transferred to the HPC discharge air. The ship's uptake ducting carries the recuperator gas-side discharge back to the ambient atmosphere. The combination of compressor intercooling lowering HPC exit air temperature and the VAN maintaining high recuperator gas inlet temperature maximizes the heat recovery in the recuperator and minimizes fuel consumption at part load conditions.

The ICR hardware under development by Westinghouse and its associate contractors is illustrated in Figure 3. The total dry weight of the ICR hardware is contractually limited to 120,000 lbs. The largest item is the gas turbine engine module which consists of the gas generator and power turbine mounted on a structural subbase and surrounded by an environmental enclosure. The

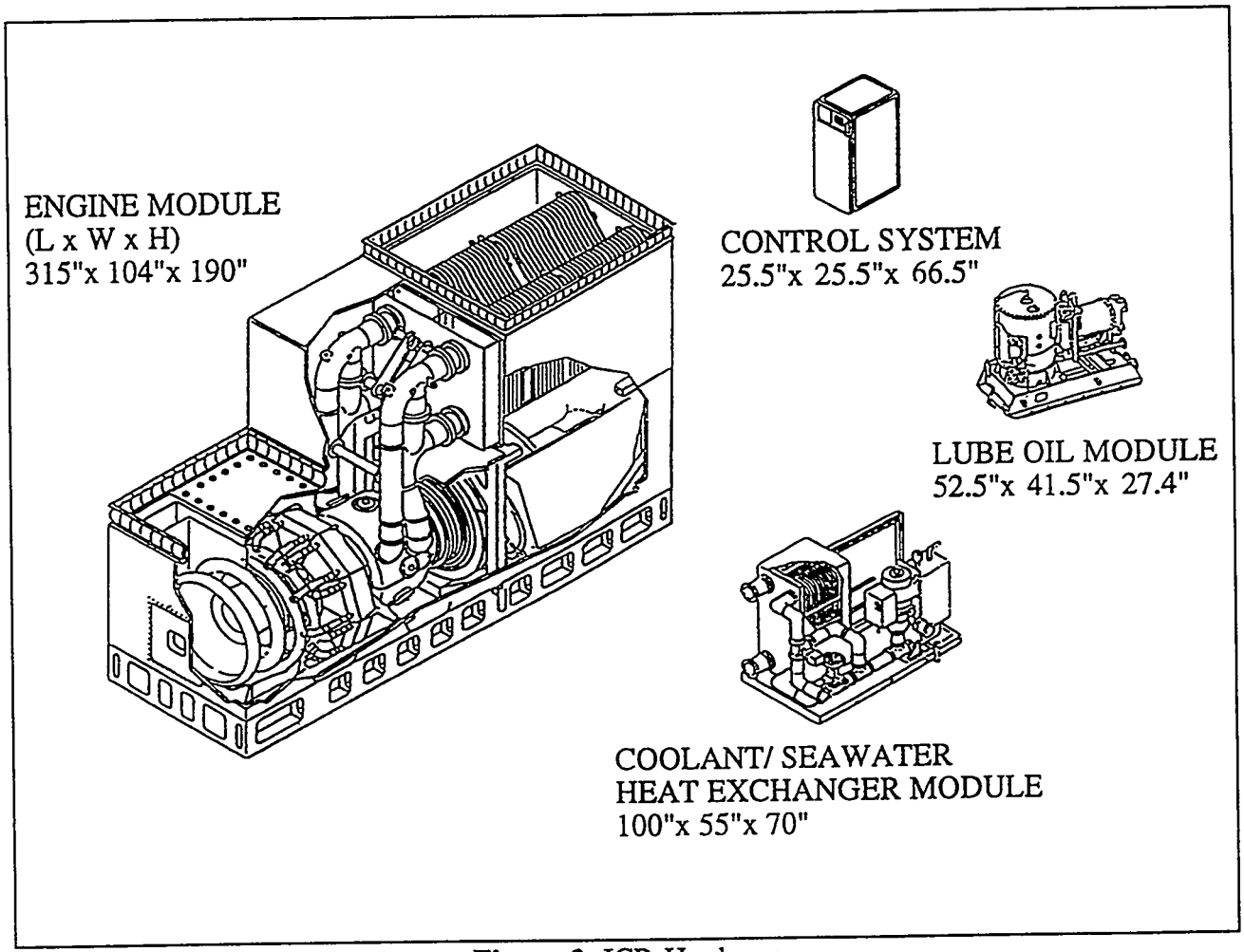


**Figure 3.** ICR Hardware

on-engine intercooler and the recuperator are mounted integrally with the gas turbine engine inside the enclosure. The overall width and length of this module are the same as the current propulsion gas turbine. The overall height is greater due to the recuperator, but this hardware will occupy some of the space currently allocated to the ship's uptake ducting. The next largest module is the off-engine intercooler module which consists of a plate-frame freshwater-to-seawater heat exchanger, freshwater pump and piping, and coolant storage tank. This module is the one unique or additional piece of equipment relative to the current propulsion gas turbine and requires about 300 cubic feet of volume in the ship's engine room. Additional design information on these modules can be found in a recent paper published by Crissali and Parker [7]. The remaining items are the lube oil module to cool the engine lubricating oil and the digital electronic control system with a man-machine interface console. The digital control system has been described in a technical paper by Carlson, West, and Azouz [8].

## PERFORMANCE CHARACTERISTICS

The U.S. Navy bases its gas turbine engine ratings and other performance characteristics on stricter (i.e., more conservative) operating conditions than the commercial users. This is done to ensure that the surface combatant can meet its speed and endurance requirements even at the extremes of the environmental envelope. Most notable is the difference in assumed ambient air temperature which the U.S. Navy specifies as 100°F while other users normally specify as 59°F. The Navy specifies standard installation losses for the ship's intake and uptake ducts. Ambient seawater temperature and relative humidity are important factors in defining the performance characteristics of the ICR, but previously were not a factor or have negligible effect on performance of the simple-cycle gas turbine. The standard operating conditions specified by the U.S. Navy for ICR performance predictions are as follows:

- 100°F ambient air temperature
- 14.696 psia ambient air pressure
- 4 inches of water intake loss
- 6 inches of water uptake loss
- 85°F ambient seawater temperature
- 40% relative humidity
- fuel lower heating value of 18,300 Btu/lb

At part-load operation, the duct losses are assumed to vary proportionally with the ratio of the square of corrected flow.

Although rated at 26,400 brake horsepower, the ICR is being designed as a 29,000 brake horsepower gas turbine engine. Figure 4 shows the variation in output power capability as a function of ambient air temperature, ambient seawater temperature, and relative humidity. The

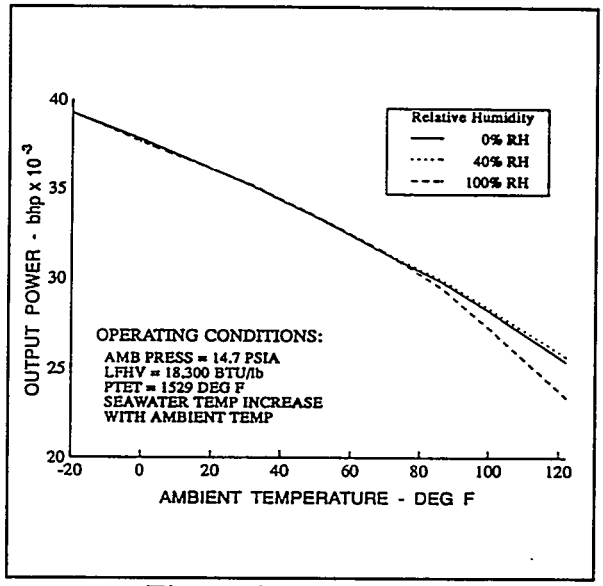


**Figure 4.** Rated Power

U.S. Navy specification requires that the ICR be capable of operating with the recuperator and/or intercooler bypassed. In the recuperator bypass mode full output power capability is available, albeit at the higher fuel consumption level of a

simple-cycle gas turbine. In the intercooler bypass mode, or with both intercooler and recuperator bypassed, the ICR power capability is degraded due to the mismatch between rotating components with the intercooler inoperative. Output power from the ICR in the intercooler bypass mode varies between a low of about 8,000 brake horsepower to a high of about 15,000 brake horsepower depending on the engine's output speed. Operation in the intercooler bypass mode is considered an emergency condition. The bypass and isolation valves required to accomplish the recuperator and intercooler bypass functions were illustrated previously in Figure 2.

Figure 5 shows the specific fuel consumption of the ICR compared to the current propulsion gas turbine along a cubic (i.e., typical propeller) load line. The improvement in fuel consumption is shown to increase as power level is reduced. At rated power the reduction in fuel consumption is 17.2%, and increases to 43.6% at 10% power. The medium speed diesel curve is shown for reference.

## OPERATIONAL ADVANTAGES

The primary benefit of the ICR engine is fuel savings. The typical mission profile for the surface combatant, as discussed above, has the majority of operating time at the lower ship speeds. When applied across the mission profile, the lower fuel consumption of the ICR engine relative to the current simple cycle propulsion gas turbine translates into a 30% reduction in annual

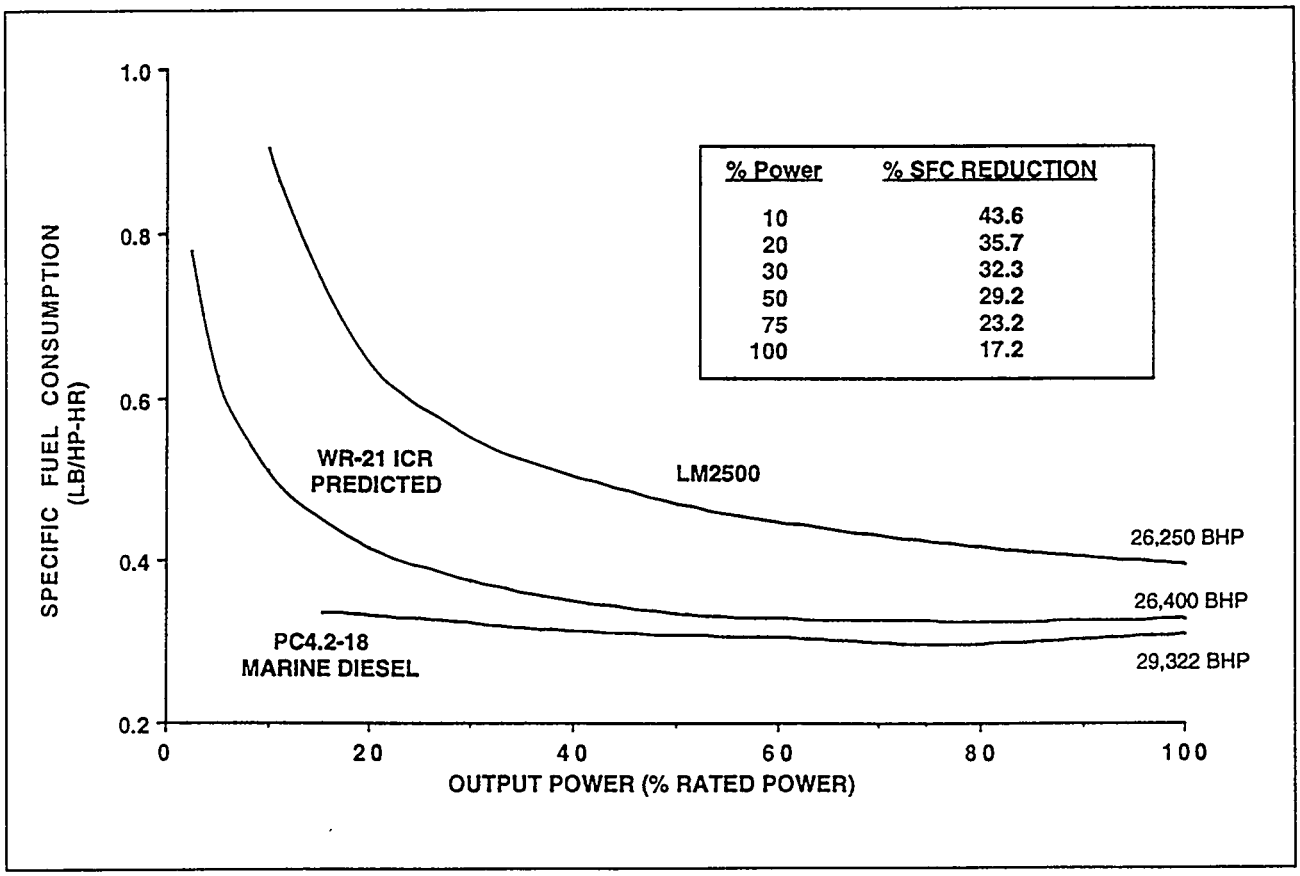


**Figure 5.** ICR Fuel Consumption Characteristics

propulsion fuel consumption. Based on the cost to the Navy to purchase, handle, store and deliver fuel to the fleet, this represents over a million dollars per ship per year lower operating costs. The lower fuel burn rate of the ICR engine results in a ship with greater range given the same fuel load as ships with the current simple cycle gas turbine. Crisalli and Parker [7] report that the DDG-51 range would increase by 35% at a ship speed of 15 knots and by 27% at 20 knots. Given a mission to transit a distance from point "A" to point "B" which is less than the ship's range, the ship with ICR engines will have a greater quantity of fuel remaining to conduct operations upon arrival and hence be capable of spending more time on station before refueling. Alternatively, the ship propelled with ICR engines could transit to a destination at a speed of 22 knots burning the same quantity of fuel that the current ship would consume at a much slower speed of 17 knots.

Current ships with four simple-cycle gas turbines are sometimes operated with only one of the four engines on line. This mode of operation is referred to as "trail shafting" because the shaftline and propeller which is unpowered is declutched from the engines and allowed to trail or windmill through the water. This allows the one simple-cycle gas turbine to operate nearer its more efficient design point, but the total propulsion power required at a given speed is increased due to the drag added by the windmilling propeller. Trail shafting is not necessary on a ship with ICR engines due to the nearly flat fuel consumption characteristic of this engine.

Another operational benefit could result from the much lower exhaust gas temperature of the ICR engine. Under conditions where the engine exhaust plume is the dominant source of infrared radiation, the ship with ICR engines would be less detectable by infrared seeking missiles. Finally, the ICR engine design enables the current combustor cans to be replaced in the future with a dry low emissions version of the combustor can which could substantially reduce the level of pollutants released into the atmosphere. Dry low emissions combustor technology is being aggressively pursued by Rolls Royce for the RB211 industrial gas turbine engines in order to comply with the more stringent future environmental regulations.

## PROGRAM SCHEDULE

The U.S. Navy issued a Request for Proposals in June 1991 for the design, development, fabrication and qualification of the ICR engine and proposals were received in October 1991. In December 1991, a contract for the Advanced Development (AD) phase was awarded to Westinghouse Marine Division located in Sunnyvale, California. Major subcontractors involved in the development include Rolls Royce the supplier of the gas turbine engine, Allied Signal the supplier of the intercooler and recuperator, and CAE Electronics supplier of the digital control system. The program schedule, illustrated in Figure 6, shows the AD phase period of performance is 54 months. The detailed design and development effort during the beginning of the AD phase includes an extensive number of model and component rig tests to verify the predicted performance of the various engine components. The start of AD phase system testing at 30 months into the program is a key milestone. These system tests must demonstrate that the critical design and performance requirements of the ICR engine have been meet in order to proceed to the 42-month Full Scale Development (FSD) phase which involves finalizing the design and conducting qualification testing. The AD and FSD phases are bridged by a Long Lead Time Material (LLTM) phase which begins concurrently with AD system testing. Exercise of this LLTM option in the contract allows the long lead time hardware items to be procured for the FSD engines thereby enabling

FSD phase engine build and testing to begin very early in the FSD phase.

The major program milestones are indicated in Figure 6 including numerous Design Reviews (DR1 through DR6) for the overall system. Separate reviews for the control system development include a System Requirements Review (SRR), Preliminary Design Review (PDR) and Critical Design Review (CDR). During the AD phase, sufficient hardware is fabricated to allow two engines (i.e., ICR-A and ICR-B) to be alternately tested in a single test cell. During the FSD phase, a total of five Engineering Development Model (EDM) engines are fabricated and subjected to various developmental and qualification tests. One of these engines, EDM-F, is shipped to the Navy for technical and operational evaluation at a Land Based Engineering Site (LBES). A Production Readiness Review (PRR) is scheduled near the end of qualification testing. A Functional Configuration Audit (FCA) is performed as part of the final design review (DR6). The final FSD engine, EDM-G, is used to conduct the Physical Configuration Audit (PCA).

## DEVELOPMENT STATUS

More than 18 months of the AD phase has passed and the program has progressed according to plan. The WR-21 design meets or exceeds the U.S. Navy's requirements. Initial tradeoff studies planned for the first six months of the AD phase were completed well ahead of schedule. These tradeoffs considered: (1) alternative intercooler and recuperator suppliers, (2) reduced recuperator volume, (3) use of composite versus steel enclosure panels, (4) lower seawater and

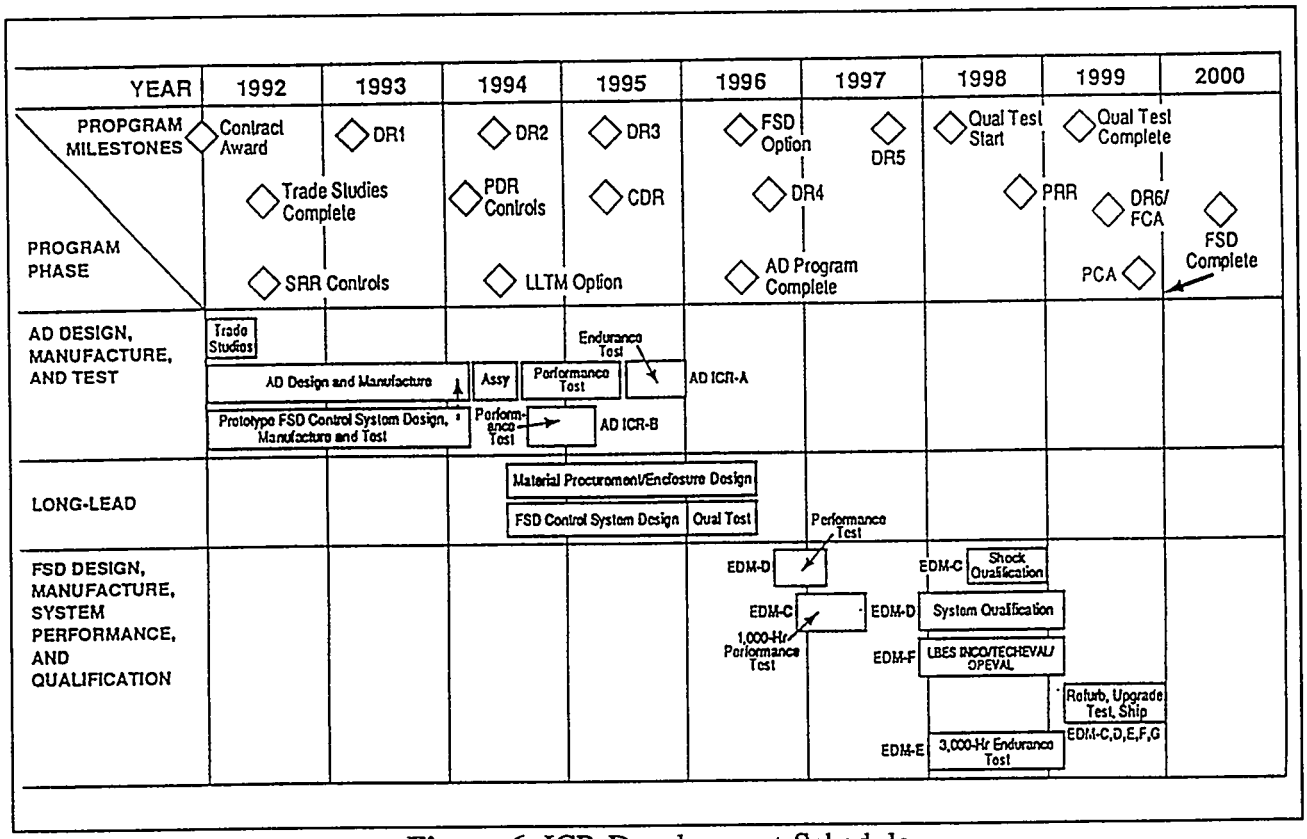


**Figure 6.** ICR Development Schedule

freshwater flow rates, and other technical requirements which tended to drive up the engine acquisition cost. Detail design of the WR-21 is near completion now. The AD phase includes a total of 31 model and component rig tests to verify the predicted performance of various parts of the WR-21 prior to the first engine test. Some examples of the tests include a reduced -scale air intake and bellmouth model test, a full scale test of the on-engine intercooler airflow path, water analogy tests of the combustor section, hot gas tests of the combustor can and water analogy test of the flowpath between the power turbine and recuperator. To date a total of eight rig tests have been completed and five are currently in progress. Most of the remaining rig tests will be completed during the next 12 months prior to the start of system testing. Hardware for the AD phase engine is currently being procured and fabricated to support the buildup process which begins in early 1994. Hardware modules for the first engine are expected to arrive at the AD test site between March and June 1994. Test facility design and data acquisition system definition has progresses as well to support the start of system testing in July 1994.

The U.S. Navy and Westinghouse have recently agreed to rephase the ICR development program to accelerate the fleet introduction. Two major steps taken have been to design and fabricate a tactical enclosure for the first engine to test, and to construct two test facilities for concurrent testing of the AD phase engines. This approach requires additional hardware earlier in the program. Out-year funding must be moved forward to accomplish the rephased program. The advantages of rephasing the program include lower overall development cost and faster return-on-investment by earlier fleet introduction. As a result of the rephasing, the WR-21 development program will be completed 21 months earlier, allowing commitment to a ship as early as fiscal year 1996 instead of fiscal year 1999. Greater opportunities exist for the WR-21 to be used by other navies also.

## SUMMARY

The U.S. Navy's ICR engine development program is the continuation of more than a decade of research aimed at reducing the fuel consumption of surface combatants. The AD phase contract with Westinghouse Marine Division will result in the start of system testing of full scale ICR hardware in mid-1994. The WR-21 design meets all U.S. Navy's requirements and the development program is being rephased to allow fleet introduction three years earlier. The WR-21 will significantly reduce the fuel consumption of surface combatants, resulting in operational advantages and lower operating costs.

## REFERENCES

1. Bowen, T. L., and J. C. Ness; "Regenerated Marine Gas Turbines, Part I: Cycle Estimation," ASME 82-GT-306, Presented in London, England; Apr 1982.

2. Watts, J. W., and T. L. Bowen; "Regenerated Marine Gas Turbines, Part II: Regenerator Technology and Heat Exchanger Sizing," ASME 82-GT-314, Presented in London, England; Apr 1982.

3. Bowen, Thomas L., and Daniel A. Groghan; "Advanced-Cycle Gas Turbines for Naval Ship Propulsion," Naval Engineers Journal, Vol. 96, No. 3, pp. 262-271, May 1984. Reviewers comments and author's reply in Naval Engineers Journal, Vol. 96, No. 4, pp. 120-124, Jul 1984.

4. Thomas, W. J. R., and A. J. Higson; "An Intercooled Regenerative Rolls-Royce Spey

Gas Turbine," ASME 85-IGT-59, Presented in Bejing, People's Republic of China; Sep 1985.

5. Fogg, H. E., C. E. Neilson and A. F. Pyatt; "The Marine Gas Turbine for the 1990's and Beyond," SAE 871378, Presented in Washington, D. C.; Jun 1987.

6. Thomson, G. A., D. J. Pratley and D. A. Owen; "Intercooling and Regenerating the Modern Marine Gas Turbine Propulsion System," SAE 871379, Presented in Washington, D. C.; Jun 1987.

7. Crisalli, A. J., and M. L. Parker; "Overview of the WR-21 Intercooled Recuperated Gas Turbine Engine System - A Modern Engine for a Modern Fleet", ASME 93-GT-231, Presented in Cincinnati, Ohio, May 1993.

8. Carlson, R. J., P. M. West and D. E. Azouz; "Digital Control System Development for an Intercooled Recuperated Gas Turbine", ASME 93-GT-326, Presented in Cincinnati, Ohio, May 1993.

## 3.4 Industry/University Consortium for ATS Research

### CONTRACT INFORMATION

| | |
|---|---|
| **Cooperative Agreement** | DE-FC21-92MC29061 |
| **Contractor** | S.C. Energy Research & Development Center<br>386-2 College Avenue<br>Clemson, SC 29634<br>(803) 656-2267 |
| **Contractor Project Manager** | R.P. Allen |
| **Principal Investigator** | L.P. Golan |
| **METC Project Manager** | Dr. Paul L. Micheli |
| **Period of Performance** | 9/30/92 - 3/30/97 |

### OBJECTIVES

The objective of the overall ATS Program is to develop ultra-high efficiency, environmentally superior, and cost competitive gas turbine systems for base-load application in utility, independent power producer and industrial markets. The overall ATS program has four elements one of Technology Base Development which is designed to support the overall program. The Industry/ University research consortium is part of the ATS Technology Base Development element and is designed to provide the technology research support required by the program. The research is to be industrial driven, non-proprietary, useful to all, and conducted by the University performing members.

### BACKGROUND INFORMATION

The Industry/University ATS research program is the result of two planning workshops. Workshop I was held April 8-10, 1991 and had the goal of identifying research needs for advanced gas turbine cycles that would permit rapid commercialization of cycles with significant improvements over the machines currently under development, in terms of the cost of electricity produced and the environmental burdens resulting from their use in power producing.

Workshop I was attended by key decision-makers in the gas turbine industry, relevant academic, and involved government technology sponsors. The Workshop was initiated with general overview presentations covering important background areas such as the users desires, manufacturers perspective, Federal government R&D policy and interested industry/technical groups. The attendees then broke into three technical "focus" groups for discussion sessions. The results from the discussions were summarized into two general categories: programmatic and technical. Several significant programmatic conclusions were reached. The attendees unanimously believed the philosophy/goals of the Workshop were nationally very relevant and timely. The attendees agreed that better coordination of industry, university, and government activities would be very helpful in accelerating the development of advanced gas turbines. One approach suggested to meet this end would be an industry driven university-led Gas Turbine Research Program. Such a program could execute research activities of joint industry/university/ government interest, result in more relevant academic programs, and increase the future supply of graduates with skills needed by the gas turbine industry.

Workshop II was held in January 1992 and continued the identification of the research needs to develop advanced gas turbine systems. The goals established for the ATS systems were

- efficiency exceeding 60% for large utility turbine system and 15% improvement in heat rate for industrial systems
- busbar energy costs 10% less than current state of the art and
- fuel flexible designs.

In addition Workshop II participants agreed that an industry driven research consortium was an acceptable mechanism to achieve base technology development needs.

In September 1992 a cooperative agreement was signed between DOE/METC and the South Carolina Energy Research and Development Center for an industry/university consortium to conduct the R&D needed to support the overall ATS program. Fifty-six universities from 30 states have joined the ATS research activity as performing members (see Table I). Five turbine manufacturers (Allison Gas Turbine Division of General Motors, General Electric Power Generation Department, Solar Turbines United Technologies Turbo Power and Marine Inc., and Westinghouse Electric Power Generation Unit) along with Fluor Daniel, an engineering/construction firm, have agreed to be co-sponsors.

**Table 1. Performing University Members**

University of Alabama - Huntsville
University of Arkansas
Auburn University
Brigham Young University
University of California - Berkeley
University of California - Davis
University of California - Irvine
California Institute of Technology
Carnegie Mellon University
Clarkson University
Clemson University
Cleveland State University
Cornell University
University of Dayton
University of Delaware
University of Denver
Drexel University
Florida Atlantic University
Florida Institute of Technology
Georgia Institute of Technology
University of Hawaii - Manoa
University of Houston
Iowa State University
University of Iowa
University of Kansas
Lehigh University
Louisiana State University
University of Maryland - College Park
Mercer University
Michigan State University
Michigan Technological University
University of Michigan
University of Minnesota
University of Missouri - Rolla
University of Notre Dame
University of Oklahoma
Penn State University
University of Pittsburgh
Princeton University
Purdue University
University of South Alabama
University of South Carolina
Southern University
Syracuse University
University of Tennessee
Tennessee Technological University
Texas A&M
University of Texas - Arlington
University of Utah
Vanderbilt University
Virginia Polytechnic Institute
Washington University
West Virginia University
University of Wisconsin-Milwaukee
Worcester Polytechnic Institute
University of Wyoming

The research program is managed by the South Carolina Energy Research and Development Center, however, the Industrial co-sponsors along with representatives from EPRI and GRI form an Industrial Review Board which identified ATS issues needed by industry and suitable for university research.

The SCERDC issues competitive solicitations reflecting the guidance from the IRB. The proposals are evaluated by the IRB which recommends which programs are to be funded based on the available financial resources. The research performed by the universities is to be performed in existing facilities so that research dollars are spent on people power rather than development of new facilities. University membership remains open.

## PROJECT DESCRIPTION/RESULTS

The SCERDC released the first RFP solicitation in the spring of 93. Fifty-one proposals from 43 schools distributed in 26 states were received. The total funding requested by the schools was 29M$. The technology splits of the research are shown on Table II.

**Table 2. Technology Splits, %**

| | |
|---|---|
| Heat Transfer | 23 |
| Combustion | 21 |
| Materials | 18 |
| Aero | 13 |
| Dynamics | 11 |
| Cycles | 5 |
| Controls | 3 |
| Other | 6 |
| | 100 |

The Industrial Review Board met at the SCERDC over a three day period in early June and recommended the following:

The proposals were selected by the program's Industrial Review Board from 51 submitted by 43 universities. Award recipients and research subjects include:

- Brigham Young University, combustion modeling for advanced gas turbines;
- University of California - Berkeley, porous combustion material investigation;
- Clarkson University, ice formation design method for loss reduction;
- Lehigh University, functionally gradient materials for thermal barrier coatings;
- Louisiana State University, vortex generator induced heat transfer;
- Pennsylvania State University, life prediction of advanced materials;
- Purdue University, NOx reduction for advanced gas turbines;
- Texas A&M University, turbine cooling and heat transfer studies;
- Vanderbilt University, NOx and CO models for lean premixed combustors; and
- Virginia Polytechnic Institute and State University, ceramic actuators for combustion control.

## FUTURE

Assuming that the 1994 budget request before Congress is approved, the SCERDC expects to issue another RFP in late 1993. At that time, additional research awards could be made dependent on the proposals and university capabilities.

As part of the plan to broaden the gas turbine technology base among American engineering schools a seminar series is being planned and requests have been released to the Industrial Review Board members to provide problems suitable for senior project design are to be used by the university. Via the involvement of the undergraduate engineers in this program, we will benefit the industry by providing an experienced crop of potential employees. The senior-design project activity will be of no cost to the research program. These areas will be developed slowly and evaluated to assure the success.

## REFERENCES


1. *Proceedings of Workshop to Define Gas Turbine System Research Needs,* April 8-10, 1991, Greenville, South Carolina.

2. *Proceedings of Workshop to Define Gas Turbine System Research Needs - II,* January 7-8, 1992, Greenville, South Carolina.

3. Bajura, R.A., H.A. Webb, and E.L. Parsons, "A Proposed Plan for an Advanced Turbine Systems Program," In *Proceedings of Workshop to Define Gas Turbine System Research Needs - II.*

4. Webb, H.A., and R.A. Bajura, "Development of Advanced Turbine Systems -- Meeting Tomorrow's Needs," presented at the *Energy Daily Conference: Advanced Combustion Turbines: Looking Past the 90's,* June 25-26, 1992, Washington, DC.

5. Golan, L.P., Center for Advanced Gas Turbine Systems Research, In *Proceedings of the Ninth Annual Coal Fueled Heat Engines, Advanced Pressurized Fluidized Bed Combustion and Gas Stream Cleanup Systems Contractor's Meetings,* 259-265, DOE/METC - 93/6/29. NTIS/DE9300233.

# ATS University Workshop

## Opening Session

# Welcome - ATS University Workshop

## CONTRACT INFORMATION

| | |
|---|---|
| **Cooperative Agreement** | DE-FC21-92MC29061 |
| **Contractor** | S.C. Energy Research & Development Center<br>386-2 College Avenue<br>Clemson, SC 29634<br>(803) 656-2267 |
| **Contractor Project Manager** | R.P. Allen |
| **Principal Investigator** | L.P. Golan |
| **METC Project Manager** | Dr. Paul L. Micheli |
| **Period of Performance** | 9/30/92 - 3/30/97 |

---

## WELCOME ADDRESS

Welcome to the Advanced Turbine System Workshop for University members. This meeting is the first of what I hope are many opportunities for the U.S. universities to gather as a single focused body contributing to the national effort to develop advanced electrical power generating systems.

Our work began nearly two years ago with two Workshops which provided input to DOE on the overall ATS program. These Workshops were attended by over 150 representatives of gas turbine manufacturers, funding organizations, universities and utilities. Workshop I identified ATS R&D needs and the need for R&D coordination. Workshop II further refined the R&D needs, reviewed the concept of R&D coordination and set stringent goals for the ATS program next generation systems:

- ultra high efficiency
- environmental superiority
- cost competitive, and
- fuel flexibility

We're now well beyond the planning stage. A cooperative agreement has been signed by METC and the South Carolina Energy Research and Development Center for the management of a university/industry R&D consortium. This industry driven group via the performing university membership will conduct the base R&D required for the ATS program. Fifty-six universities have agreed to be the performing member base, five U.S. turbine manufacturers and an engineering/ construction company have agreed to be the industrial co-sponsors of the program. The industrial team along with EPRI and GRI form our Advisory Board.

We've come a long way as the group by-laws, contract format, numerous site visits and the first RFP solicitation with proposal reviews and awards made for our first round. The response was impressive as the Universities showed their wide acceptance and submitted 29M$ in research requests. Considering the research results are not for facilities, but strictly for people performance, the idea base was excellent.

The Universities have accepted the challenge to contribute to the nation's needs with respect to new electrical power systems. Within the U.S. alone the need is estimated at 15GW per year of new and replacement capacity after the year 2000. Now we must perform in a timely, cost effective and technically responsive way. While at this meeting I urge you to attend as many sessions

as possible, engage in as many different discussions possible so that we collectively understand the problems and meet all the players.

For those not already aware Roy P. Allen, a former G. E. employee, is managing the ATS effort for the South Carolina Energy Research & Development Center. Roy will present more details of our program status next. Again - Welcome, we look forward to working with you during the course of this program. We welcome your suggestions and input.

## REFERENCES


1. *Proceedings of Workshop to Define Gas Turbine System Research Needs*, April 8-10, 1991, Greenville, South Carolina.

2. *Proceedings of Workshop to Define Gas Turbine System Research Needs - II*, January 7-8, 1992, Greenville, South Carolina.

3. Bajura, R.A., H.A. Webb, and E.L. Parsons, "A Proposed Plan for an Advanced Turbine Systems Program," In *Proceedings of Workshop to Define Gas Turbine System Research Needs - II.*

4. Webb, H.A., and R.A. Bajura, "Development of Advanced Turbine Systems -- Meeting Tomorrow's Needs," presented at the Energy Daily Conference: *Advanced Combustion Turbines: Looking Past the 90's*, June 25-26, 1992, Washington, DC.

5. Golan, L.P., Center for Advanced Gas Turbine Systems Research, In *Proceedings of the Ninth Annual Coal Fueled Heat Engines, Advanced Pressurized Fluidized Bed Combustion and Gas Stream Cleanup Systems Contractor's Meetings*, 259-265, DOE/METC - 93/6/29. NTIS/DE9300233.

# University Participation in the ATS Program

## CONTRACT INFORMATION

**Cooperative Agreement** FC21-92MC29061

**Contractor** Clemson University Research Foundation
110 Daniel Drive
Clemson, SC 29634-5602

**Contractor Project Manager** Roy P. Allen

**Principal Investigator** Lawrence P. Golan

**METC Project Manager** Paul L. Micheli

**Period of Performance** September 30, 1992 to March 31, 1994

**Schedule and Milestones**

**FY93 - FY94 Schedule**

| | 4Q92 | 1Q93 | 2Q93 | 3Q93 | 4Q93 | 1Q94 |
|---|---|---|---|---|---|---|
| Organization Tasks | xx | xxx | | | | |
| 93 RFP Issued | | xx | xx | | | |
| Evaluation | | | xx | | | |
| Contract Work | | | | x | xxxx | xxxx |
| Issue 94 RFP | | | | | xx | xx |
| Evaluation | | | | | | xx |

## OBJECTIVES

The Advanced Gas Turbine Systems Research Program was included in DOE's Advanced Turbine Systems initiative to conduct basic research in support of the overall ATS program, and to strengthen the university gas turbine technology base in the USA. The results of the research will be transferred to the industrial members to enhance and/or facilitate their designs of advanced gas turbine powerplants. Concurrently, the involvement of many students, both graduate and undergraduate, will provide a better qualified group of engineers for hire by the industry.

## BACKGROUND INFORMATION

The AGTSR was formed to represent the "Industry/University" consortium shown on the overall ATS plan (Figure 1). A Cooperative Agreement was awarded to the South Carolina Energy Research and Development Center to administer this program. SCERDC, formed by the South Carolina legislature in 1981, deals with energy matters at the state and national level, and is located at Clemson University.

Every American university with an accredited engineering college was invited to participate in the AGTSR program. Requirements to become a Performing Member are minimal; the schools need to have some experience and expertise in the turbomachinery or power generation fields, and the department head or dean must authorize the faculty members' participation.

Presently, this solicitation has resulted in 56 universities qualifying as Performing Members. They are located in 30 states; 17 are private and 39 are public institutions. Figure 2 shows the geographic distribution, and the members are listed in Appendix A.

To provide technical guidance and to evaluate technical progress, an Industrial Review Board was formed. This board consists of American gas turbine industry leaders, both manufacturers and user representatives. For 1993, the members are:

Allison Gas Turbine Division, General Motors
Fluor Daniel
General Electric Power Generation
Solar Turbines, Inc., Caterpillar
TurboPower & Marine Systems, United Technologies
Westinghouse Electric Power Generation
Electric Power Research Institute
Gas Research Institute

Voting members of the board (all except the two Institutes) pay an annual fee of $25,000, which is added to the research subcontract funds.

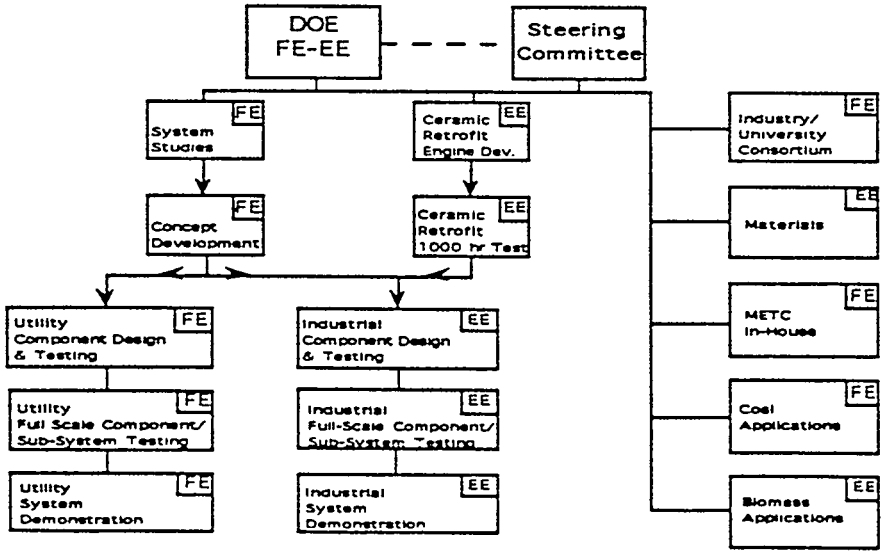


**Figure 1. Advanced Turbine Systems Program Structure**

A set of By-Laws was prepared by AGTSR, and approved by the IRB in February 1993. These provide the basic ground rules for the operation of the board and of the program.

## PROPOSAL DESCRIPTION

The first Request for Proposals was issued in March 1993. To provide as must latitude as possible for the proposers, the technology areas were general rather than specific. Essentially, they were the areas of interest identified in the two workshops that led to the formation of the ATS program. The areas are listed in Table 1.

A set of evaluation criteria were included in the RFP to assist the universities in proposal preparation. Table 2 lists these criteria and their relative weighting. Technology transfer is, of course, the most important. Equally weighted are the results vs. cost, timeliness of completion, and quality of the team put together to do the work.

The review process was structured to be as thorough and fair as possible. Because of the expected large volume of proposals, diversity of proposed research, and the need for rapid review of the proposals, each IRB member was assigned two tasks:

1. Review approximately six of the proposals in depth, and be prepared to discuss them and respond to questions from other board members. This was called an "Expert Review."

2. Review all of the other proposals briefly, and rate them on a scale of 0-100 based on the evaluation criteria of Table 2. These were the "Executive Reviews."

The scores for both were tabulated and added, and a list made in order of total score. This list was then discussed in detail, with some changes made based on the expert's opinions, number in each technology area, and board consensus. The awardees were then selected, with the number of awards based on the available funding vs. the projected contract expense profile for the next three years.

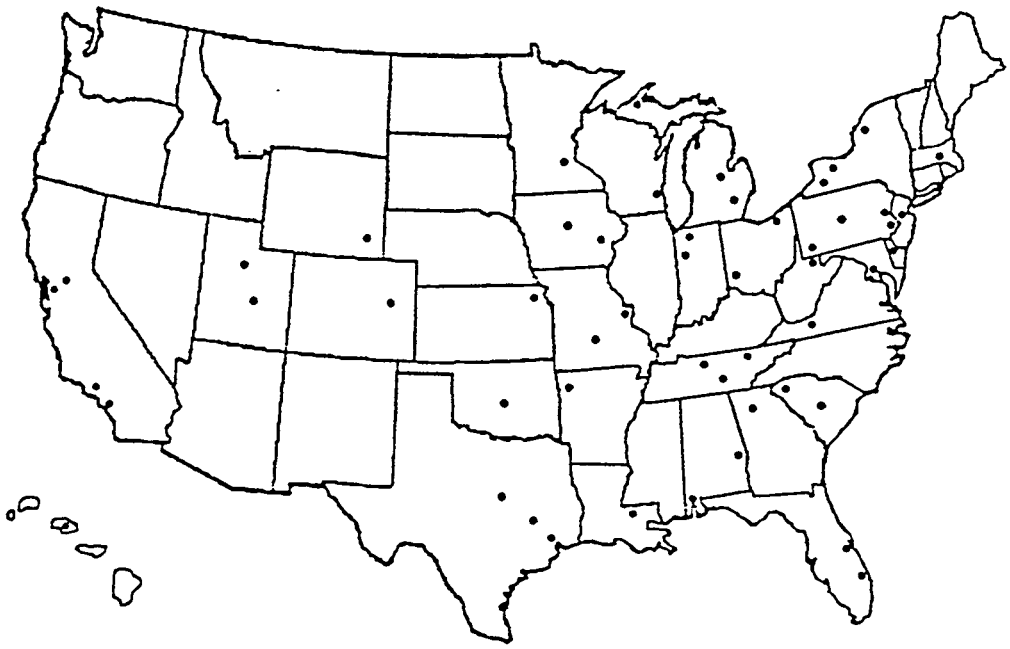

**Figure 2. Locations of University Performing Members**

**Table 1. Technology Priority Areas for RFP 93-01**

| |
|---|
| High temperature materials--metallic, ceramic, coatings |
| Advanced cooling and heat transfer |
| Combustion modeling, including emissions |
| Vibration and noise control |
| Performance improvements--seals, aerodynamics |
| Multivariable control systems |
| System performance and economics |
| Applicability to coal and alternate fuels |
| Concurrent engineering |

## RESULTS

The IRB spent three days at SCERDC in June evaluating the 51 proposals received in response to the RFP. Forty-three of the 56 Performing Members submitted proposals, seven sent in more than one. In Figure 3, the percentage splits by basic technology contained in the proposals are presented. All of the areas identified in Table 1 were represented.

Ten awards were made based on the assumption that the FY93 funding level of $2 million would continue for three years; the total value of the contracts will be about $6 million. The award technology splits are shown in Figure 4, and reflect the Board's initial priorities for expanding the research work.

Prior to announcing the award winners, the recommendations developed by the IRB were presented to DOE at Morgantown. DOE approved the awards as submitted.

The universities receiving awards and the title of their proposed work effort are presented in Table 3. Some 35 faculty members and a like number of students will be participating. Most of the programs are set for completion in three years, with BYU's at four and Clarkson offering an option for two. It is expected that contracts can be negotiated and signed during the summer so that work can commence by September 1.

**Table 2. Proposal Evaluation Criteria**

| | |
|---|---|
| TECHNICAL significance | 40% |
| Support of ATS goals | |
| Ease of technology transfer | |
| VALUE | 20% |
| Scope, results vs. cost | |
| Educational value | |
| Effective use of facilities | |
| TIMELINESS OF RESULTS | 20% |
| Availability of useful data | |
| QUALIFICATIONS and experience | 20% |
| Relative gas turbine work | |
| Strength of team | |

| | No. | % |
|---|---|---|
| Heat Transfer | 15 | 22 |
| Combustion | 13 | 19 |
| Materials | 13 | 19 |
| Aerodynamics | 10 | 15 |
| Vibration, acoustics | 8 | 12 |
| Cycles and evaluation | 3 | 5 |
| Coal applications | 3 | 5 |
| Multivariable controls | 2 | 3 |
| Concurrent engineering | 1 | - |
| TOTAL | 68 | 100 |

Note: Total exceeds 51 since several proposals covered multiple disciplines.

**Figure 3. Technology Distribution Among RFP 93-01 Submittals**

| | No. of Awards | Awards as % of Submitted |
|---|---|---|
| Combustion | 5 | 38 |
| Heat transfer | 3 | 20 |
| Materials | 2 | 15 |
| Aerodynamics | 2 | 20 |

Note: Number exceeds ten due to multiple disciplines.

**Figure 4. Technology Distribution for Awards Made for RFP 93-01 Submittals**

## FUTURE WORK

The funding request sent to Congress for the ATS program includes an increase for the AGTSR to $4 million in FY94, and to $5 million for the remainder of the program (through the year 2000). Should that be approved, RFP's can be issued each year to supplement the work in progress. Without an increase in funds, the $6 million in contracts recently awarded will use up the FY94 and FY95 authorizations, assuming they continue at the $2 million level. Hence, no additional RFP's could be issued until 1996.

It is likely that future RFP's may be more specific, or limit the fields for research. The Board wishes to broaden the entire technology base if possible, while keeping the most critical technologies at the top of the list. Available funding will obviously affect the strategy here.

To provide additional communication and integration, SCERDC will coordinate two other activities. Board members agreed to provide appropriate gas turbine related problem statements or design challenges to schools that offer a senior level project course. This would essentially be a no cost program; the industry sponsors would have a small time commitment, and they may incur some travel expense for final report presentations.

Secondly, DOE has agreed to provide some modest funding for travel and administrative costs associated with holding seminars throughout the academic year. SCERDC envisions that university and industry speakers will present gas turbine related sessions at member schools, to promote technology transfer, improve communications, and offer opportunities for future collaboration.

**Table 3. Awardees and Proposal Titles**

| UNIVERSITY | PROPOSAL TITLE |
|---|---|
| Brigham Young | Combustion Modeling in Advanced Gas Turbines |
| California/Berkeley | Ultra Low Gas Turbine Emissions Using Catalytic & non Catalytic Porous Combustors |
| Clarkson | Reduction of Turbine Endwall Total Pressure Loss and Heat Transfer Using the Iceformation Design Method |
| Lehigh | Functionally Gradient Materials for Thermal Barrier Coatings in Advanced Gas Turbine Systems |
| Louisiana State | Vortex-generator Induced Enhanced Heat Transfer in Gas Turbine Blade Coolant Channels with Rotation |
| Penn State | Life Prediction of Advanced Materials for Gas Turbine Applications |
| Purdue | NOx Reduction in Advanced Gas Turbines |
| Texas A&M | Advanced Turbine Cooling, Heat Transfer, and Aerodynamic Studies |
| Vanderbilt | NOx & CO Emissions Models for Gas Fired, Lean Premixed Combustion Turbines |
| Virginia Polytechnic | Advanced Combustion Technologies for Gas Turbine Power Plants |

## APPENDIX A

## UNIVERSITIES REPRESENTED IN AGTSR PROGRAM

Through June 30, 1993 (56)

*University of Alabama-Huntsville
University of Arkansas
*Auburn University
Brigham Young University
University of California-Berkeley
University of California-Davis
University of California-Irvine
California Institute of Technology
*Carnegie Mellon
Clarkson University
*Clemson University
Cleveland State University
Cornell University
University of Dayton
*University of Delaware
University of Denver
*Drexel University
Florida Atlantic University
Florida Institute of Technology
Georgia Institute of Technology
University of Hawaii
*University of Houston
*Iowa State University
*University of Iowa
University of Kansas
*Lehigh University
Louisiana State University
*University of Maryland-College Park
*Mercer University
Michigan State University
Michigan Technological University
*University of Michigan
University of Minnesota
*University of Missouri-Rolla
*University of Notre Dame
University of Oklahoma
Penn State University
University of Pittsburgh
Princeton University
*Purdue University
University of South Alabama
*University of South Carolina
Southern University
Syracuse University
*University of Tenn., Space Institute
*Tennessee Technological University
*Texas A&M
*University of Texas-Arlington
University of Utah
*Vanderbilt University
*Virginia Polytechnic Institute
*Washington University
*West Virginia University
University of Wisconsin-Milwaukee
Worcester Polytechnic Institute
University of Wyoming

*Visits made through June 30

# ATS University Workshop

# University Presentations

# W2 Ultra-Low Gas Turbine Emissions Using Catalytic and Noncatalytic Porous Combustors

## CONTRACT INFORMATION

| | |
|---|---|
| **Contract Number** | **DE-FC21-92MC29061** |
| **Contractor** | **The Regents of the University of California**<br>**c/o Sponsored Projects Office**<br>**University of California**<br>**Berkeley, California 94720** |
| **Contract Project Manager** | **Roy P. Allen, Director**<br>**Advanced Gas Turbine Systems Research**<br>**South Carolina Energy R&D Center** |
| **Principal Investigators** | **Professor Robert W. Dibble**<br>**Professor Juh-Yuan Chen**<br>**Professor Robert F. Sawyer** |
| **METC Project Manager** | **Paul L. Micheli** |
| **Period of Performance** | **9/1/93 - 8/31/96** |

## ABSTRACT

The goal of our work is to explore ultra-low (one ppm $NO_x$) emission gas turbine concepts which sustain the high efficiency of the combustion process already achieved by the gas turbine industry. We propose to focus on one promising but poorly understood concept, combustors with catalytic or noncatalytic surfaces. Our research will employ experiment and computational modeling to develop an improved understanding of combustion with strong surface interactions under conditions appropriate to gas turbines. Models will guide experimental design and data interpretation; experimental results will guide model development. We anticipate that the model will provide a tool for extrapolation from laboratory to design thereby providing gas turbine manufacturers with a means to make intelligent decisions on the applicability of catalytic and noncatalytic combustion.

The concept of catalytic combustors which employ catalytic surfaces in high porosity matrices has been demonstrated; the use of noncatalytic porous materials to stabilize flames has received less attention. Such concepts allow the combustion of low calorific value fuels, or very lean mixtures, or low temperature combustion through radiant heat transfer and can result in very low $NO_x$. The stabilization of combustion at conditions ordinarily beyond the lean (or dilute) flammability limit is promoted by catalytic and/or preheating processes. The possibilities are new and under-explored. The mechanisms are poorly understood and describing models not well-developed.

Our initial experimental work will be in an atmospheric pressure combustion tunnel upon both catalytic and non-catalytic combustors with interior access for optical monitoring of combustion progress and intermediates. Evolving surface combustion models which are an extension of the Sandia CHEMKIN programs will be further developed and applied to catalytic and non-catalytic combustion. We will explore experimentally and numerically the effect of fuel types including natural gas, a low calorific value fuel (to model gasified coal), methanol and/or ethanol (representative of biomass derived fuels), and fuels reformed with water. These fuels represent a broad range of current and future, potential energy sources. Later work will extend combustor inlet temperatures and pressures to conditions typical of stationary gas turbines.

# W3 Reduction of Turbine Endwall Total Pressure Loss and Heat Transfer Using the Iceformation Design Method

## CONTRACT INFORMATION

| | |
|---|---|
| **Contract Number** | DE-FC21-92MC29061 |
| **Contractor** | Clarkson University<br>Box 5725<br>Potsdam, NY 13699-5725<br>(315) 268-3823 |
| **Contract Program Manager** | Roy P. Allen<br>Advanced Gas Turbine Systems Research<br>South Carolina Energy R&D Center |
| **Principal Investigator** | Dr. Ronald S. LaFleur, Assistant Professor<br>Department of Mechanical and Aeronautical Engineering<br>Clarkson University |
| **METC Project Manager** | Paul L. Micheli |
| **Period of Performance** | September 1, 1993 to August 31, 1995 |

## ABSTRACT

This presentation outlines a project to study the iceformation method design of turbine endwall shapes as contoured hubs or shrouds. The controlled phase change process of iceformation allows the flow to directly shape the surface while proceeding toward lowered energy dissipation. The goal of the work is to demonstrate a method for altering near endwall pressure gradients and beneficially affect the complex juncture flow such that total pressure losses and heat transfer from the gas flow are reduced and/or minimized. This will greatly enhance the performance of gas turbines by reducing a primary source of available energy losses. The focus is on a high pressure inlet guide vane (two endwalls) turbine geometry where off-design flow has a great impact on overall gas turbine performance. The proposed study uses a linear cascade model to demonstrate the design methodology, resulting geometries and performance improvements. The research will be conducted by a team of Clarkson University and General Electric engineers with an emphasis on obtaining new designs and educating the next generation of turbine designers.

# W4 Functionally Gradient Materials For Thermal Barrier Coatings In Advanced Gas Turbine Systems

## CONTRACT INFORMATION

| | |
|---|---|
| **Cooperative Agreement Number** | FC21-92MC29061 |
| **Contractor** | Office of Research and Sponsored Programs<br>Lehigh University<br>526 Brodhead Avenue<br>Bethlehem, PA 18015<br>(215) 758-3021 |
| **Contract Project Manager** | Roy P. Allen |
| **Principal Investigator** | Dr. Arnold R. Marder |
| **METC Project Manager** | Paul Micheli |
| **Period of Performance** | September 1, 1993 to August 31, 1996 |

## ABSTRACT

New designs for the advanced gas turbine engine for power production will require Thermal Barrier Coatings (TBC) to protect some turbine components. TBC's represent a potential major operational improvement in turbine engine performance by allowing an increase in the maximum inlet temperature for an operating engine. Higher operating inlet air temperature produces a more efficient turbine engine and provides better fuel economy. It has been estimated that TBC application to all high turbine airfoils could save 10 million gallons of fuel annually for a 250 aircraft fleet. Furthermore, the TBC can increase the service lifetime of its coated component providing an added cost benefit. Extending engine maintenance intervals and reducing unscheduled downtime are included in the benefits of thermal barrier coating application.

Although thermal barrier technology is over thirty years old, the principal failure mechanism is still the spallation of the coating. Thermal barrier coating systems have traditionally been comprised of a ceramic outer layer, which provides the thermal barrier, and a metallic bond coat, that protects the substrate alloy from the corrosive combustion gases in the turbine engine. Thermal fatigue damage, in the form of microcracks, accumulates at the TBC/bond coat interface. This damages results from the mismatch in thermal expansion coefficient between the metal bond coat and the ceramic thermal barrier layer. The solution to this problem is to develop a coating that combines the thermal barrier qualitites of the ceramic layer and the corrosion protection provided by the metallic bond coat. A ceramic/metal hybrid

material that is being developed for just such properties and has been called a Functionally Gradient Material (FGM).

Functionally Gradient Materials are specifically designed and manufactured ceramic/metal composites that combine a heat-resistant ceramic outer skin with a higher toughness metallic inner layer. In a FGM, there is a continuous, gradual change in composition from 100% ceramic at the surface to 100% metal at the interior. The center of the material is a ceramic/metal mixture that represents a smooth transition in material composition and mechanical properties. As a result, coating spallation based on a thermal fatigue microcrack accumulation mechanism would be eliminated because there is no interface separating two dissimilar materials. In addition, novel compositions that will resist higher temperatures than existing TBC systems without coating degradation can be developed.

It is the objective of this research program to investigate novel compositions and unique processes to utilize Functionally Gradient Materials as thermal barrier coatings in advanced gas turbine engines. The technical approach to this research program consists of three tasks:

- Task A: LITERATURE REVIEW- Determine potential novel FGM compositions and unique processing techniques based upon a literature review.

- Task B: PROCESSING/STRUCTURE CHARACTERIZATION OF FGMs- Produce FGM coatings by novel processing techniques and develop proper characterization techniques.

- Task C: ENVIRONMENTAL TESTING OF FGMs- Evaluate the thermal fatigue properties, corrosion resistance, and optimum coating thickness of potential FGM systems.

It is expected that the results of this research program will lead to the selection, production, and implementation of particular FGM coating systems in advanced gas turbine engines.

# W5 Vortex-Generator Induced Enhanced Heat Transfer in Gas Turbine Blade Coolant Channels With Rotation

## CONTRACT INFORMATION

| | |
|---|---|
| **Contract Number** | DE-FC21-92MC29061 |
| **Contractor** | Louisiana State University<br>Mechanical Engineering Department<br>Baton Rouge, LA 70803<br>(504) 388-5809 |
| **Contract Project Manager** | Roy P. Allen, Director<br>Advanced Gas Turbine Systems Research<br>South Carolina Energy R & D Center |
| **Principal Investigators** | Sumanta Acharya<br>Tod A. Myrum<br>Dimitris Nikitopoulos<br>Joel Tohline |
| **METC Project Manager** | Paul L. Micheli |
| **Period of Performance** | October 1, 1993 to September 30, 1996 |

## ABSTRACT

A three-year, combined experimental and computational research program will be conducted with the intent of developing a novel technique for augmenting the heat transfer in ribbed gas turbine blade cooling channels. This technique involves placing vortex generators (circular cylinders) in the vicinity of key rib elements so that the vortex street that forms behind the generator excites the shear layers behind the ribs at subharmonics of their most amplified frequency and thereby enhances mixing and heat transfer. At the end of the three-year period, experimentally based design data for a number of effective generator placements and a general-purpose, experimentally validated computer code will be made available to the gas turbine industry.

The experimental portion of work will involve obtaining local and average Nusselt number results for radially inward and outward flows through a square, rotating ribbed duct, with and without vortex generators. Local and average Nusselt number results will be deduced from mass transfer measurements, using the napthalene-sublimation technique, and the subsequent application of the heat/mass transfer analogy. Hot-wire-based flow spectra measurements behind ribs and generator-rib pairs in a rotating duct will also be performed. These measurements will identify the geometrical parameter values leading to the desired subharmonic forcing of the rib shear layers.

The computational work will (1) lead to the development of an experimentally validated predictive computer code for the design of gas turbine blade coolant channels with and without vortex generators, (2) aid the experimental study by identifying optimal generator-rib configurations, (3) provide detailed velocity, temperature, and heat/mass transfer distributions that will supplement the experimental data, and (4) extend the experimental parameter range. In this portion of the work, the time-dependent Navier-Stokes, energy, and mass concentration equations

will be solved using the direct numerical simulation (DNS) technique, which does away with time averaging and conventional modeling approximations.

During the first year, the experimental facility will be designed, fabricated, and tested. After completing the testing phase, local and average mass transfer measurements will be performed in a rotating ribbed duct. Baseline measurements, performed in a duct without generators, will be obtained first. This will be followed by mass transfer measurements in rotating ribbed ducts using the preliminary vortex-generator configurations from earlier stationary duct measurements. The computational work during the first year will be largely devoted to developing and validating the computational procedure for rotating smooth ducts.

During the second year, the computational code will be extended to include flows through rotating ribbed channels, with and without vortex generators. The computational code will be validated through comparisons with the mass transfer measurements of the first year and the flow spectra measurements. Then, numerical experiments will be performed to preliminarily identify the optimal generator-rib configurations. These will be augmented by flow spectra measurements that will definitively determine the optimal generator-rib configurations.

Mass transfer measurements will be performed to test and fine-tune the optimal generator-rib configurations identified during the second year. In addition, a computational parametric study will be conducted to include the effects of buoyancy, rotation, and other parameters.

# W6 Life Prediction of Advanced Materials for Gas Turbine Applications

## CONTRACT INFORMATION

| | |
|---|---|
| **Contract Number** | DE-FC21-92MC29061 |
| **Contractor** | The Pennsylvania State University<br>Engineering Science & Mechanics<br>227 Hammond Building<br>University Park, PA 16802<br>(814) 865-4523 |
| **Contract Program Manager** | Roy P. Allen<br>Advanced Gas Turbine Systems Research<br>South Carolina Energy R&D Center |
| **Principal Investigators** | Sam Y. Zamrik<br>Asok Ray<br>Donald A. Koss |
| **METC Project Manager** | Paul L. Micheli |
| **Period of Performance** | September 01, 1993 to August 31, 1995 |

## ABSTRACT

The long-term performance and reliability of advanced gas turbine systems is critically dependent on damage evolution within the materials operating in the hot sections of the turbine. The accumulation of damage is driven by the temperature-load cycling that a component experiences while its service life depends on the inherent sensitivity of the material to the level of induced damage. A life prediction methodology thus demands not only an accurate assessment of damage evolution on a real-time basis during exposure to service conditions but also a quantitative framework for predicting the component life as a function of damage accumulation. This research proposal focuses on life prediction and long-term performance and reliability of advanced materials for gas turbines. To this effect, experimental and analytical research will be conducted in the following areas:

- The thermal-mechanical fatigue (TMF) and creep-fatigue behavior of superalloys in coated and uncoated conditions.

The above issues are critical to the efficient utilization of high temperature materials in advanced gas turbines for base-load applications. An underlying characteristic of the proposed research is the coordination of the microscale events, namely, damage evolution with the macroscale properties, namely, TMF life and creep life.

The major thrust will be directed to life prediction of Ni-base superalloys when subjected to thermal-mechanical fatigue (TMF) and creep-fatigue, and their behavior will be examined primarily in the coated conditions. The research efforts in life prediction under TMF cycling and

creep-fatigue will be coordinated with the following two industrial partners; namely, Westinghouse Power Generation Technology Division, Orlando, Florida and Garrett Engine Division, Allied Aerospace Co., Phoenix, Arizona.

Both the macromechanical and the microstructural responses of selected specimens (to be provided by the industrial partners) will be determined under a range of TMF conditions in the laboratory environment. Particular attention will be paid to the influence of coatings on the evolution of damage in the form of populations of short cracks which initiate and grow into long cracks. Quantitative descriptions of damage will be used to develop an analytical model for creep-oxidation-fatigue interactions for a coated alloy system subjected to operations under TMF conditions.

## W7 NOx Abatement in Advanced Gas Turbines

CONTRACT INFORMATION

| | |
|---|---|
| **Contract Number** | DE-FC21-92MC29061 |
| **Contractor** | Purdue University<br>School of Mechanical Engineering<br>Thermal Sciences and Propulsion Center |
| **Contract Program Manager** | Roy P. Allen<br>Advanced Gas Turbine Systems Research<br>South Carolina Energy R&D Center |
| **Principal Investigators** | P.E. Sojka<br>J.P. Gore<br>N.M. Laurendeau |
| **METC Project Manager** | Paul L. Micheli |
| **Period of Performance** | 9/1/93 - 8/31/95 |


## ABSTRACT

The thrust of this proposal is the development of an experimentally verified, computationally efficient, high pressure $NO_X$ submodel for use in designing future generations of gas turbine engines. This submodel (1) will include chemical kinetics capable of predicting $NO_X$ levels at operating pressures and inlet temperatures up to 15 atmospheres and 800 K, (2) will describe turbulence-chemistry interactions by developing and calibrating a new computationally efficient approach that will reduce CPU time, and (3) will be verified by comparing its predictions to data obtained from a high pressure, preheated, natural gas fired gas turbine-analog combustor. The primary deliverable will be a $NO_X$ model including high pressure chemistry and turbulence-chemistry interaction submodels ready for incorporation into all manufacturers' combustor design codes. Secondary deliverables will be the chemical kinetic description of high pressure $NO_X$ formation and the computationally efficient approach for describing turbulence-chemistry interactions.

The development of this model will proceed through three inter-related tasks. The first task is to gain a thorough understanding of the

chemical kinetics involved in the production of NO in high-pressure natural gas fired systems. The second task is to develop a fundamental understanding, and an accurate *and computationally efficient* as well as experimentally verified description of the turbulence-chemistry interactions that influence $NO_X$ formation. The third task is to combine the chemical kinetic and turbulence-chemistry interaction submodels and *verify their combined performance* by comparing their predictions to data taken from carefully controlled experiments performed on an analog gas-turbine combustor.

The primary deliverable is a model describing $NO_X$ formation in high-pressure, preheated, natural gas-fired gas turbine systems. The model will be provided as FORTRAN source code, with complete documentation and instructions as to how it should be incorporated into a manufacturer's combustor design code.

There are also two secondary deliverables: the chemical kinetic submodel and the turbulence-chemistry interaction submodel. The chemical kinetic submodel will be provided as a tabular listing of appropriate forward rate coefficients (in modified Arrhenius form). The turbulence-chemistry submodel will be provided as FORTRAN source code, again with complete documentation as to how it should be incorporated into a manufacturers design code.

We believe that gas turbine manufacturers will be most interested in the complete $NO_X$ model, i.e. the experimentally verified description of the chemistry and turbulence-chemistry interactions, because it will be easiest to incorporate the results of our work into their existing combustor design codes in one single step. Since this is the ultimate goal of this program, it will be available at the end of year three.

While the complete model is clearly most beneficial, some (or all) manufacturers may wish to take advantage of several intermediate results that will accrue from the secondary deliverables. These intermediate results include: (1) a submodel describing high pressure (non-preheated) $NO_X$ kinetics, available at the end of year one, (2) a submodel of high temperature (ambient pressure) $NO_X$ kinetics, available midway through year two, (3) the low pressure turbulence-chemistry interaction approach, available at the end of year one, (4) the high pressure turbulence chemistry interaction approach available at the end of year two, and (5) a submodel of high temperature-high pressure $NO_X$ kinetics, available midway through year three. These submodels can be incorporated singly, or in sequence depending on how a particular manufacturer wishes to proceed.

# FE Coal-Fired Heat Engines Conference

## Session 1

## *Coal-Fueled Turbines*

# 1.1 Interface Between a Gas Turbine and PFBC

## CONTRACT INFORMATION

| | |
|---|---|
| **Contract Number** | DE-AC21-86MC23167 |
| **Contractor** | Westinghouse Electric Corporation<br>4400 Alafaya Trail<br>Orlando, Florida 32326-2399<br>(407) 281-2000 |
| **Contractor Project Manager** | Ronald L. Bannister |
| **Principal Investigators** | Arthur W. McGuigan<br>James A. Christenson<br>Ivan L. Howell<br>Ezio Marson<br>Michael V. Post<br>Thomas P. Risley<br>Terry L. Vota |
| **METC Project Manager** | Donald W. Geiling |
| **Period of Performance** | July 24, 1986, to August 15, 1993 |

## OBJECTIVES

First-generation pressurized fluidized bed combustion (PFBC) technology has potential advantages that include lower capital cost, improved environmental performance, shorter lead times, higher efficiency, and enhanced fuel flexibility.

Many advances have been made in this technology as it moves toward commercial demonstration. The objective of this program is to ensure that combustion turbine designs stay current with PFBC technology, specifically to ensure that the Westinghouse 251B12 combustion turbine is suitable for demonstration phases of this technology as it progresses toward commercial deployment.

This paper presents the preliminary design of system interfaces that permit combining a PFBC and a Westinghouse 251B12 combustion turbine.

## BACKGROUND INFORMATION

The combustion turbine is an integral part of the clean coal PFBC power plant. For the first-generation plant (to be demonstrated under a Clean Coal Technology III initiative), the combustion turbine has to be modified to provide compressed air to the bed and to receive

hot gas (1600°F) from the bed. For second-generation plants (to be demonstrated under a Clean Coal Technology V Program), a topping combustor will be placed upstream of the hot-gas entrance into the combustion turbine. The topping combustor augments the hot vitiated air from the PFBC to provide a higher temperature gas to the inlet of the combustion turbine.

For either program, casing modifications are required to connect the combustion turbine to the PFBC. Demonstration projects such as Tidd and Grimethorpe have shown that these plants can be operated, but not without giving special consideration to the design of complex, high-temperature, hot-gas piping systems and a common control system for two units that normally operate independently. Both first- and second-generation PFBC applications place additional requirements on the gas turbine and its control system to ensure proper interface with the PFBC system.

Special piping systems are required to route compressed air from the combustion turbine to the PFBC bed and from the PFBC hot-gas cleanup filter system to the combustion turbine inlet. These piping interfaces for first- and second-generation PFBC applications must be designed to meet unique requirements. These include

- Gas turbine shell outlet and inlet modifications
- Bypass/isolation lines for separate startup piping
- Hot-gas and compressed-air valves
- Corrosive hot-gas environment

The control system needs to incorporate the operation of each unit into a common control for the overall system. The PFBC plant control requires the two major components, the PFBC bed and the combustion turbine, to operate as a single power-producing plant. Because of interdependencies, the startup and shutdown processes are somewhat more complex than for either operating independently. Some applications may further require the capability to operate the gas turbine independently.

## PROJECT DESCRIPTION

This project was organized into the Work Breakdown Structure illustrated in Figure 1. The tasks were completed using the requirements of the Clean Coal program's first-generation PFBC demonstration at Des Moines Energy Center (DMEC-1), Pleasant Hill, Iowa as the baseline. A brief description of each task follows:

- Task 1. Analysis of Turbine and Plant Performance - evaluated W251B12 engine performance for baseline requirements.
- Task 2. Analysis of Optimum Blading and Cooling - defined the 251B12 engine modifications required for the reduced airflow of the baseline application.
- Task 3. Analysis of Casing Arrangements for Interface of PFBC and Off-Base Combustor - designed a casing interface for the compressed-air outlet and hot-gas inlet piping.
- Task 4. Analysis of Turbine System Modifications - determined requirements for the control system, startup fuel system, and combustion turbine inlet and exhaust systems.
- Task 5. Design of Startup Combustor - developed a conceptual design for the

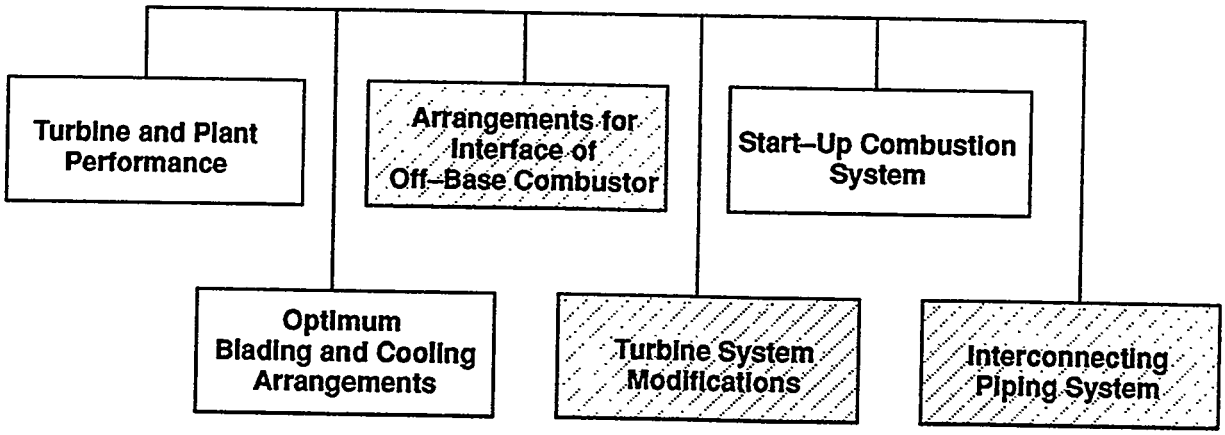


**Figure 1. Work Breakdown Structure**

combustion turbine startup combustor, including pressure vessel and combustor configuration.

- Task 6. Design of Interconnecting Piping - detailed the piping configuration necessary to connect the combustion turbine and the PFBC.

This paper discusses the results of tasks 3, 4, and 6. The remaining results are discussed in the final report on this program.

## RESULTS

### Casing Arrangements for Interface of PFBC and Off-Base Combustor

The production W251B12 combustion turbine, as shown in Figure 2, has a center section in which air from the compressor is heated in eight combustor baskets and is ducted by transition liners into a uniform annual flow. The baseline plant configuration required less compressed-air mass flow than the W251B12 can provide, so the compressor section was modified to reduce the flow. For this reduced flow, the center section of the gas turbine was modified, as shown in Figure 3, by using a configuration having one inlet and one outlet. For higher flow requirements two inlets and two outlets would be necessary.

The production W251B12 is manufactured on a bedplate for ease of handling and to prepackage much of the bleed air, control system, and auxiliary piping and wiring. For the reduced airflow requirements of the baseline application, a single inlet/outlet design with the piping on the lower right-hand side of the casing was developed to reduce the impact on the bedplate. An internal manifold was designed to route "clean" hot gas from the PFBC to the transitions and into the turbine. The combustors were removed for this application, but the internal manifold design is flexible enough to accommodate the insertion of the combustor baskets in case they are needed as startup or topping combustors. A computational fluid dynamic (CFD) analysis of the internal manifold was performed to ensure adequate distribution of the inlet hot gas.

During the design process, other casing concepts were developed including a concentric inlet/outlet and a dual-inlet, single-outlet design. The concentric design, shown in Figure 4, uses an internal hot-gas pipe surrounded by the cooler compressed air that exits through the outlet pipe. The airflow requirements will

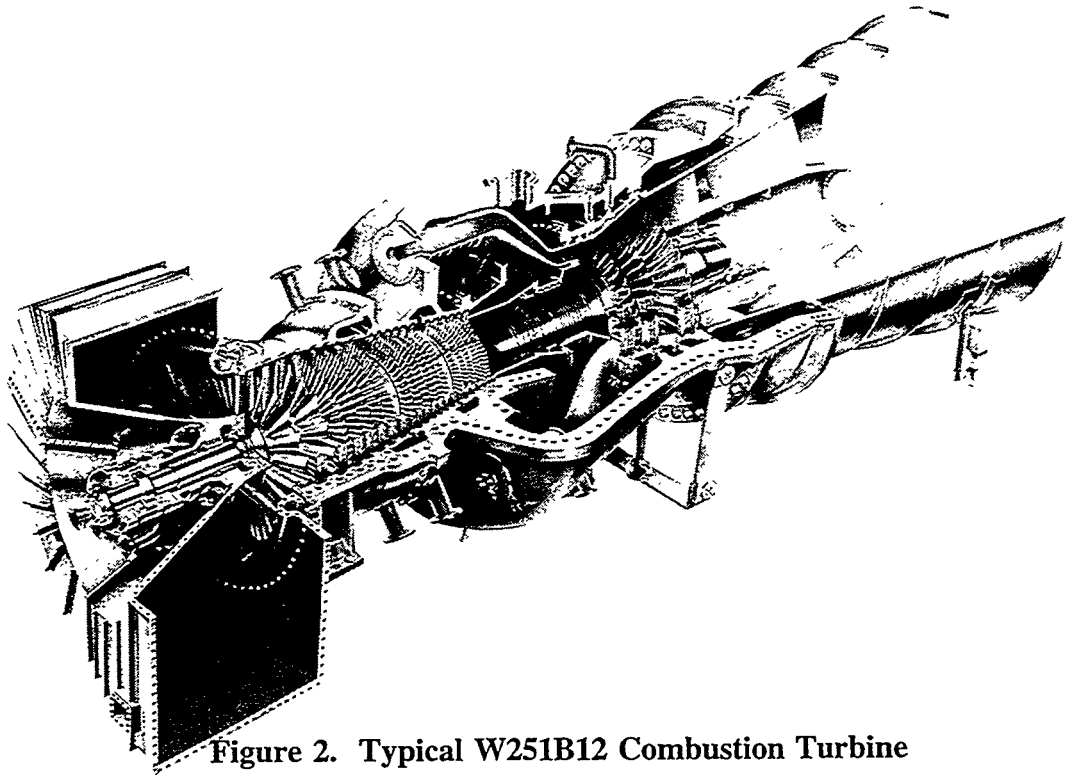

Figure 2. Typical W251B12 Combustion Turbine

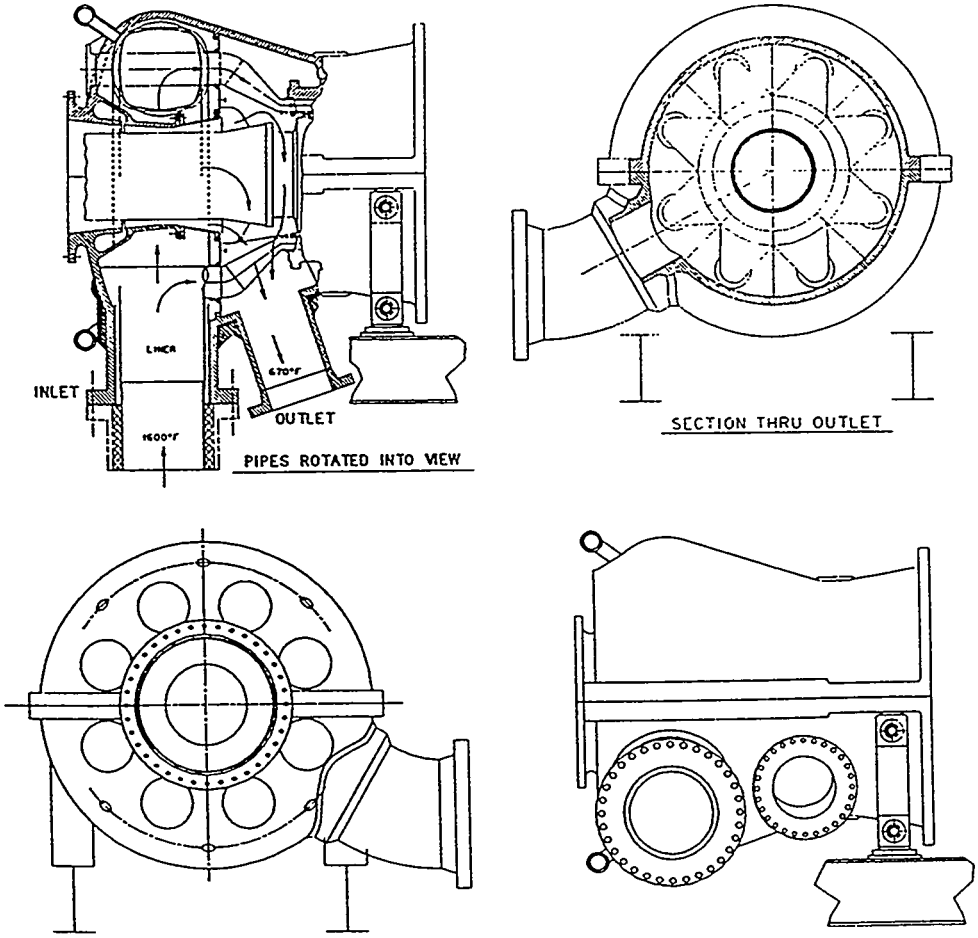


Figure 3. Modified Combustion Turbine Center Section for the Baseline PFBC Application

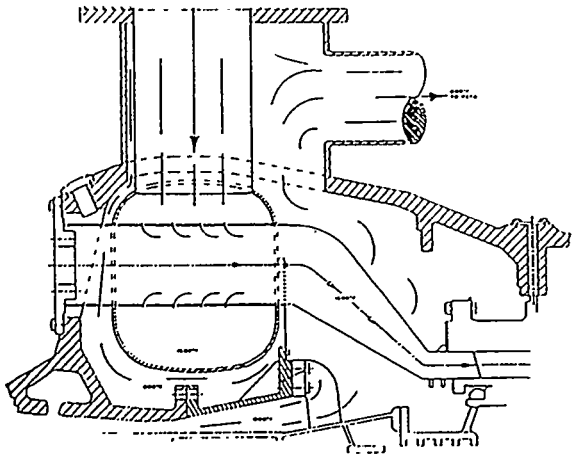

**Figure 4. Concentric Inlet and Outlet Piping**

dictate the number and size of the casing penetrations. The dual-inlet, single-outlet concept, shown in Figure 5, uses two inlet pipes at the top and bottom of the casing. Two inlets provide uniform flow distribution and lower inlet velocities. Either concept may be used, depending on the airflow and combustion turbine configuration requirements.

## Interconnecting Piping System

The baseline plant layout was used as a reference for an interconnecting piping system, including piping connections to and from the PFBC. Concepts applicable to the design of the interconnecting piping scheme and control strategy were developed previously for a similar application in cooperation with Foster Wheeler Corporation [1]. Figure 6 is a simple schematic of the combustion turbine piping system. The compressed-air discharge line (location 3) carries compressed air from the center section of the combustion turbine, as shown in Figure 2, and routes it through various piping systems such as aftercoolers and intercoolers (not shown) to the PFBC bed. An inlet valve in the compressed-air piping (location 5) isolates the combustion turbine from the PFBC. The filtered hot gas (locations 6 and 7) is then piped back to the

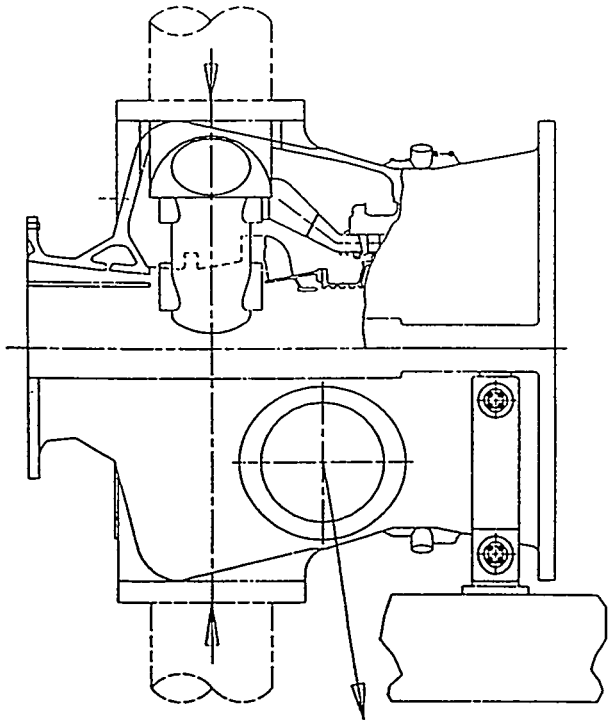

**Figure 5. Dual Inlet Concept**

inlet pipe of the center section of the casing. The hot gas then enters the internal manifold and passes through the transitions to the turbine inlet. An outlet valve isolates the PFBC from the combustion turbine and rapidly shuts off the PFBC hot gas to the turbine; a vent valve is provided for the PFBC. A bypass line (location 4) connects the compressed-air piping and the hot-gas piping so that the combustion turbine can be started with the turbine startup combustor.

The piping system and plant arrangement is shown in Figures 7a and 7b. The arrangement satisfies baseline plant layout requirements and addresses the following design considerations:

- Isolating the turbine casing from pipe forces due to thermal expansion
- Minimizing air volume in the startup combustor circuit

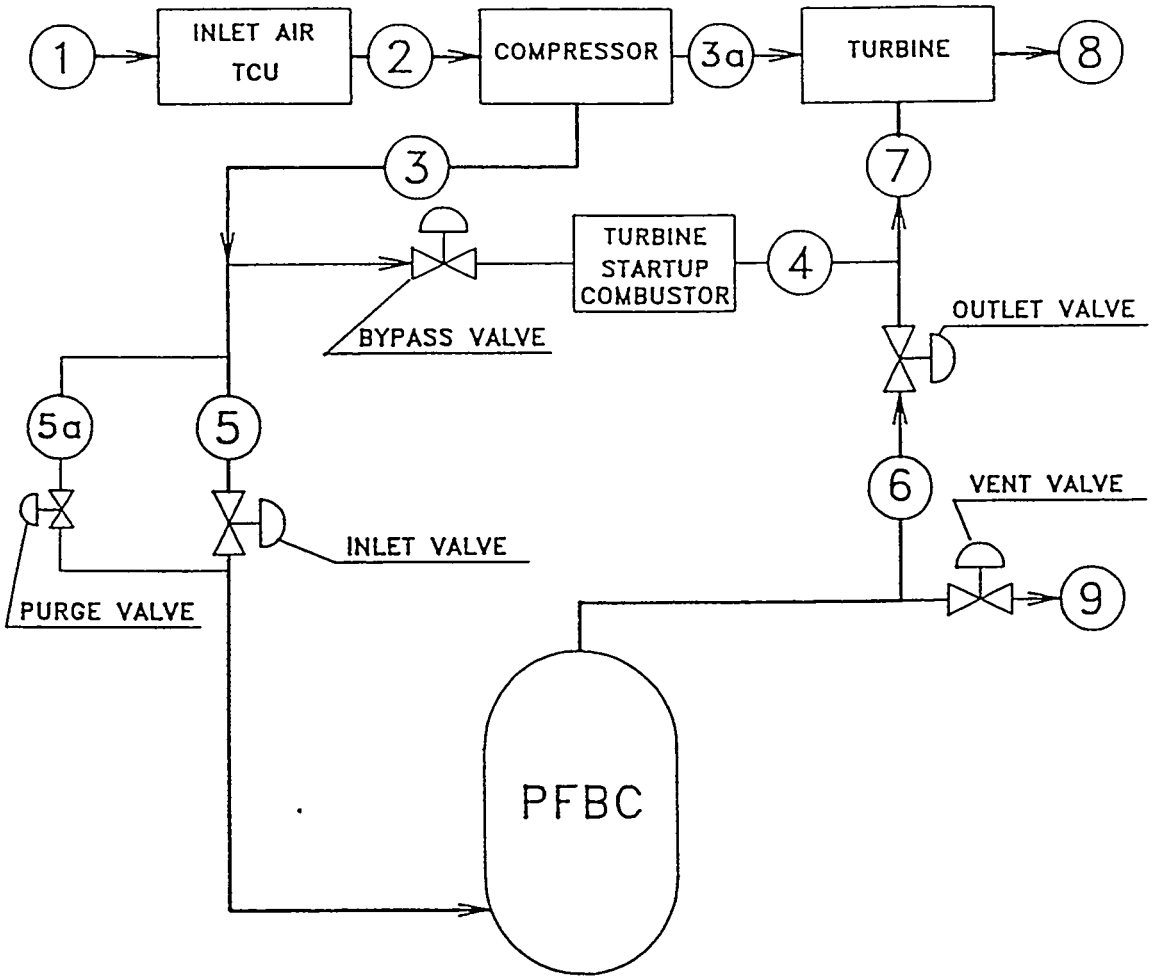


**Figure 6. Interconnecting Piping Simplified Schematic**

- Minimizing cost consistent with reasonable pressure drop
- Satisfying startup and shutdown airflow and turbine control requirements
- Incorporating manufacturing requirements for insulated pipe

Figure 8 details the compressed-air, startup combustor/bypass, and clean hot-gas piping around the combustion turbine. In arranging the piping and components, the hot return pipe was considered first. The pressure-balanced expansion elbow was placed as close as possible to the casing flange and connected by a reducing section to mate the pipe insulation liner diameter with the casing liner diameter. The expansion joint provides an anchor point for the main run of hot pipe to isolate its motion from the casing.

On top of the expansion joint is a flanged tee that connects to the PFBC system outlet valve and to the discharge of the turbine startup combustor. Above the system outlet valve the PFBC outlet pipe expands to 60 inches in diameter. The turbine startup combustor line contains a throttle valve and an expansion joint. The combined lengths of the components in this crossover pipe determined the location of the compressor discharge pipe.

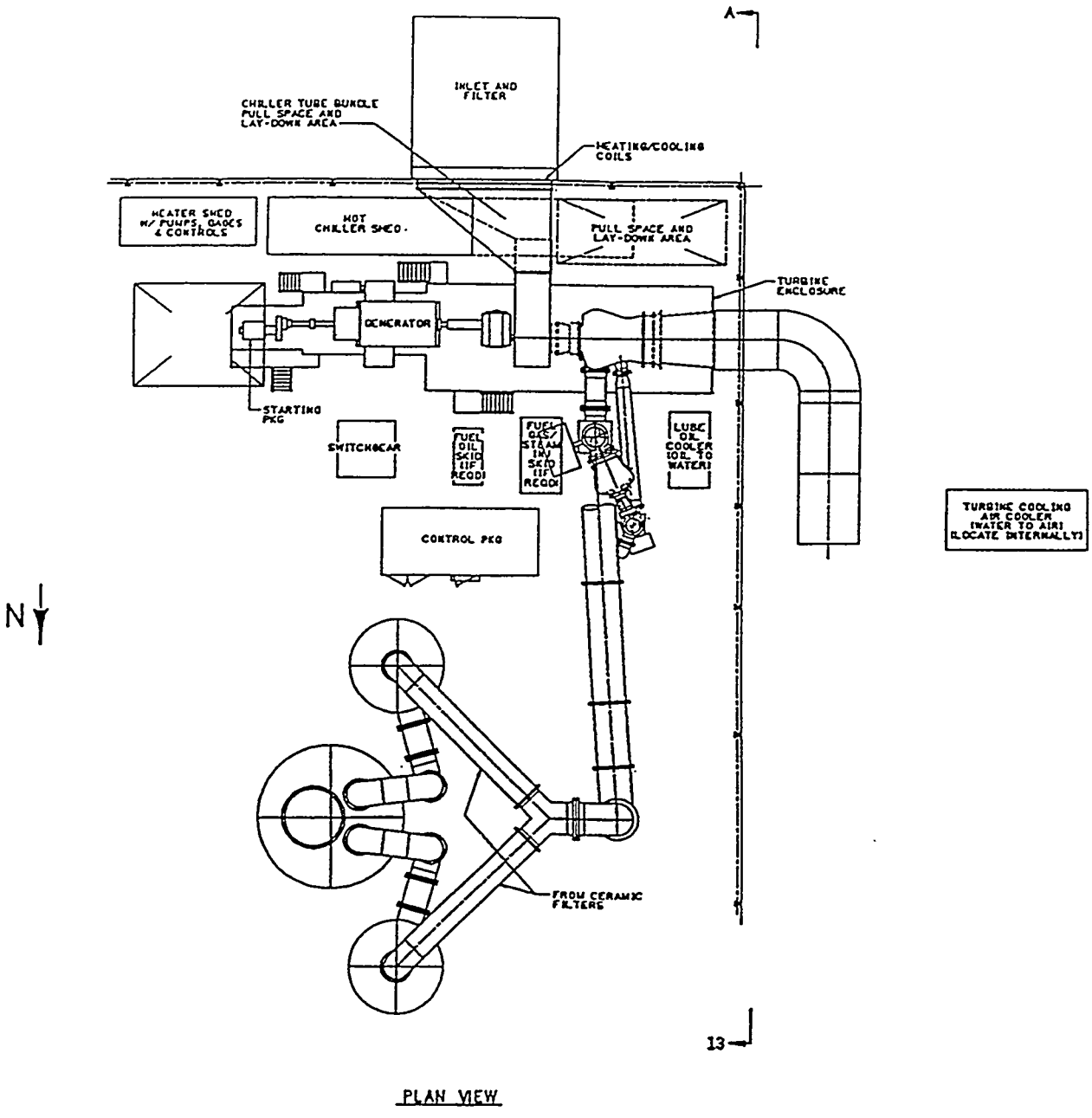


PLAN VIEW

**Figure 7a. Plant Arrangement - Plan View**

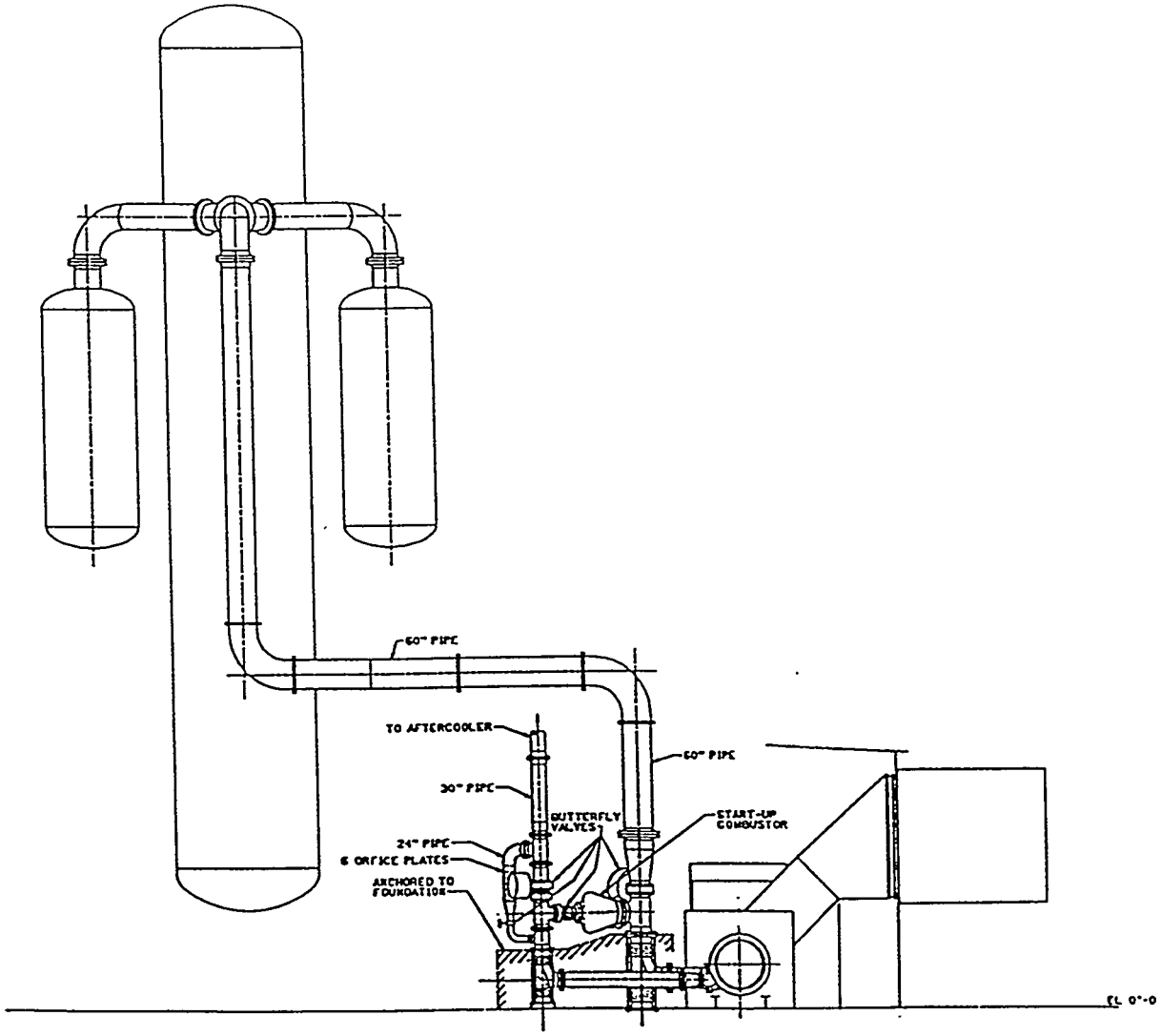


**Figure 7b. Plant Arrangement - Elevation View**

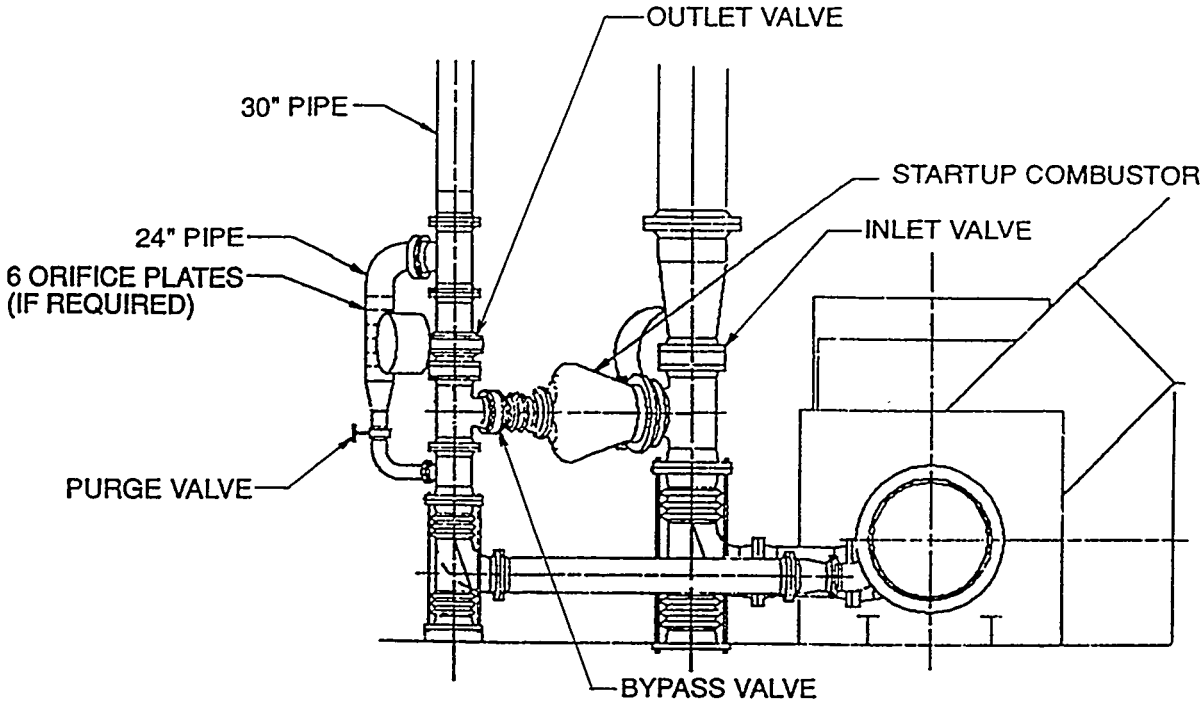


**Figure 8. Interconnecting piping - Detailed View**

A reducer connects the 24-inch casing flange to the 30-inch compressor discharge pipe diameter. A 22-foot pipe section connects the reducer with a pressure-balanced expansion elbow. The outlet of the elbow connects to an 8-foot long vertical pipe section flanged to a tee leading to the turbine startup combustor. Straight through the tee is the PFBC system inlet valve, which may be bypassed by the PFBC system purge valve.

**Compressed-Air Piping Design.** The piping system for the compressed-air discharge lines is designed for a compressor discharge temperature of 700°F and a pressure of 170 psia. The compressor discharge piping is insulated externally and can be made of carbon steel pipe.

**Startup Combustor/Bypass Line Piping Design.** The startup combustor/bypass line performs three functions. During plant startup the combustion turbine is isolated from the PFBC and is externally fired by the startup combustor. The startup combustor/bypass line is also used to regulate the bypass air between the combustion turbine and the PFBC during startup and normal shutdown of the PFBC. It also enables the system to bypass air from the combustion turbine compressor to the turbine for emergency shutdown. The compressor side of the bypass line will handle only compressed air; the startup combustor outlet side must be designed as a hot-gas pipe.

The startup combustor is a natural gas-fired combustion system. It comprises a pressure vessel, five W251B12 combustor baskets, and fuel nozzle piping systems similar to those typically supplied with the W251B12 combustion turbine.

**Clean Hot-Gas Piping Design.** The clean hot-gas piping is the most complex part of the combustion turbine/PFBC interface. The high-temperature (1600°F) gas supplied by the PFBC has passed through a ceramic candle filter that removes particulates harmful to the combustion turbine. The combination of high temperature, moderate pressures, and potential corrosiveness of the gases (if cooled) necessitates that the piping be specially designed.

Previous experience at similar plants has provided a variety of hot gas piping designs capable of meeting the PFBC hot-gas piping design requirements. In the early 1980s Westinghouse conducted work on coal gasifiers [2]. This work led to the development of a design standard for high-temperature gas piping systems [3]. The piping was built as a system with one or two layers of cast refractory anchored on the inside of a carbon steel liner.

The recent Tidd PFBC demonstration plant hot-gas cleanup test facility report discussed experience with hot-gas piping and certain design deficiencies such as hot spots, elevated expansion joint temperatures, corrosion of stainless steel (type 321) expansion joint bellows, and corrosion of uncoated areas of the carbon steel pipe that makes up the pressure boundary for the hot-gas pipe [4]. The revised hot-gas piping system design included a stainless steel liner (310), Cer-Wool Fiber layer, Cer-lite 50 insulating refractory, Hastelloy C22 Liner, and A53 carbon steel pipe.

In a paper summarizing the test program conducted at Grimethorpe [5], the hot-gas piping system was operated for 1108 hours and 25 starts without incident. The temperature of the surface of the piping ranged from 122°F to 194°F. The hot-gas piping system from inside to outside consisted of a stainless steel liner (310), ceramic paper, layer of abrasion refractory, layer of insulating refractory, and carbon steel pipe.

Figure 9 shows the hot-gas pipe design selected for the 48-inch and 60-inch hot-gas pipe. The piping system includes a stainless steel liner (310), castable refractory thermal insulation, and a carbon steel pipe as the outside pressure boundary. The thermal insulation selected was Harbison-Walker Lightweight Castable 20. This insulation is designed to be cast in place and anchored at the pipe. Its maximum service temperature is 2000°F, with a thermal conductivity of 1.5 Btu/hr-ft$^2$-°F/in at the design temperature of 1600°F. The inner surface of the insulation is separated from the hot gas by a 1/16-inch-thick stainless steel liner to protect the insulation from erosion.

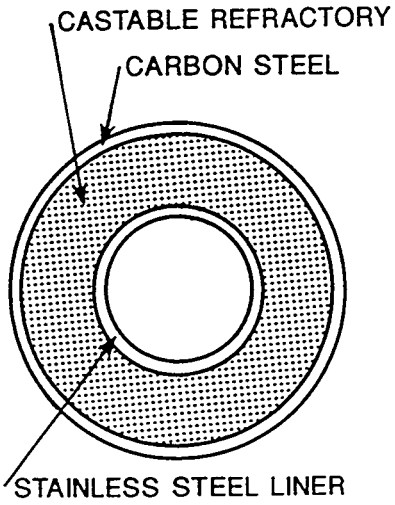


**Figure 9. Hot-Gas Piping - Sectional View**

The surface temperature of the 60-inch pipe with 7.5-inch insulation is approximately 200°F; the temperature of the 48-inch pipe with 5.5-inch insulation is approximately 225°F. To reduce the pipe temperature to 140°F would require an additional 9 inches of insulation inside the pipe or 2 inches outside the pipe. The outside insulation was rejected because the resulting pipe wall temperature is 650°F.

The final piping design must meet several additional mechanical design requirements because of the cast-in-place refractory insulation. These include:

- Maximum pipe section length for cast insulation of 10 feet
- Insulated pipe that can be welded together with proper joint design
- Flanged joints every 20 to 30 feet to provide access for inspection and repair
- No insulation of the pipe liner except at one support location to permit axial thermal expansion. Slip joints must also be provided between liner sections.
- Gap between the liner and the insulation to permit radial thermal expansion. Flexible standoffs support the liner from the insulation.
- Careful use of external insulation. A thin layer (1/4 inch) of low-conductivity material could be used to protect personnel against contact burns.

The paper presented by Gilbert/ Commonwealth, Inc., at the recent IGCC and PFBC meeting at Morgantown shows various pipe configurations that appear to meet the challenge of hot-gas piping systems [6]. The piping design shown in Figure 9 closely resembles Case 9 (separate carbon steel and alloy pipes with expansion joints; alloy pipe Hastelloy lined) cited in reference 5 except that insulation on the outside wall of the carbon steel piping is minimal, and stainless steel (310) replaces the Hastelloy. The final study by Gilbert/Commonwealth should help the hot-gas piping designer in selecting the piping system.

Hot valves were another consideration in hot-gas pipe system design. The requirements for valves in the turbine/compressor system of the PFBC plant are, in part, determined by the startup and shutdown sequences and operating modes the various plant systems require. The final valve requirements will be developed by dynamic flow analysis of the systems during the final design phase. The three major hot valves required for the combustion turbine interface to a PFBC plant are shown in Figure 8 and include the PFBC System Bypass, PFBC System Inlet, and PFBC System Outlet. The preliminary characteristics for these valves are shown in Table 1.

The PFBC system bypass valve supplies compressor discharge flow to the turbine inlet during turbine and PFBC startup. During turbine startup, this valve will be wide open to provide 100-percent compressor flow to the turbine. During PFBC bed startup and shutdown, this valve will throttle the bed bypass flow. Depending on the control strategy, this valve may also be used to provide a controlled bypass to modulate the inlet temperature, thereby controlling the power output of the combustion turbine. During emergency shutdown this valve will also open to cool the turbine inlet air, quickly reducing the power.

The PFBC system inlet valve isolates the PFBC system from the compressor discharge during combustion turbine startup, PFBC bed startup, and plant shutdown. During power operation this valve is open.

**Table 1. PFBC Interface Valves**

| | Bypass Valve | Inlet Valve | Outlet Valve |
|---|---|---|---|
| Type | Butterfly | Butterfly | Butterfly |
| Size, inches | 24 | 36 | 44 id flange |
| Connections | Flanged | Flanged | Flanged (60 inch) |
| Temperature, °F | 700 (max), 20 (min) | 700 (max), (20 min) | 1600 (max), 20 (min) |
| Pressure, psig | 200 | 200 | 200 |
| Shutoff | 1% of design flow at design pressure | 1% of design flow at design pressure | 1% of design flow at design pressure |
| Throttle Range, % | 20-80 @ rated flow | 20-30 @ rated flow | 20-80 @ rated flow |

The PFBC system outlet valve isolates the turbine inlet from the PFBC during PFBC bed startup and plant shutdown. During power operation the valve is open. Throttling may be required during the changeover from startup to power operation and during shutdown.

The final overspeed protection requirements will be determined during the detailed design phase of a PFBC plant. It is likely that a vent line and valve may need to be installed on the hot-gas leg as near as possible to the turbine inlet. The valve would be used to vent off the hot-gas trapped in the line after the system trips off line, working in conjunction with the bypass circuit and providing additional overspeed protection.

## Combustion Turbine Control System

Westinghouse combustion turbines currently use the Westinghouse Distributed Processing Family (WDPF) control system. The typical combustion turbine has on-engine combustors with options for natural gas, distillate fuel, or dual fuel capability. The system must also control the steam and water injection systems that are typically supplied to reduce exhaust emissions. Combustion turbine control is achieved by controlling fuel to the combustors.

In addition to the normal control system pressure, temperature, speed, and power indicators, the PFBC combustion turbine will need a control panel dedicated to monitoring the airflow through the system. Figure 10 shows a typical airflow control panel that would be supplied with a PFBC-fired WDPF combustion turbine control system. The system control logic would be modified to match the actual plant configuration.

The WDPF system will meet the control requirements of this PFBC-fired combustion turbine application. Certain control system changes will be required to convert the current combustion turbine WDPF system to a PFBC application. These changes include:

- Combustion control
- PFBC interface
- Emergency shutdown and overspeed protection

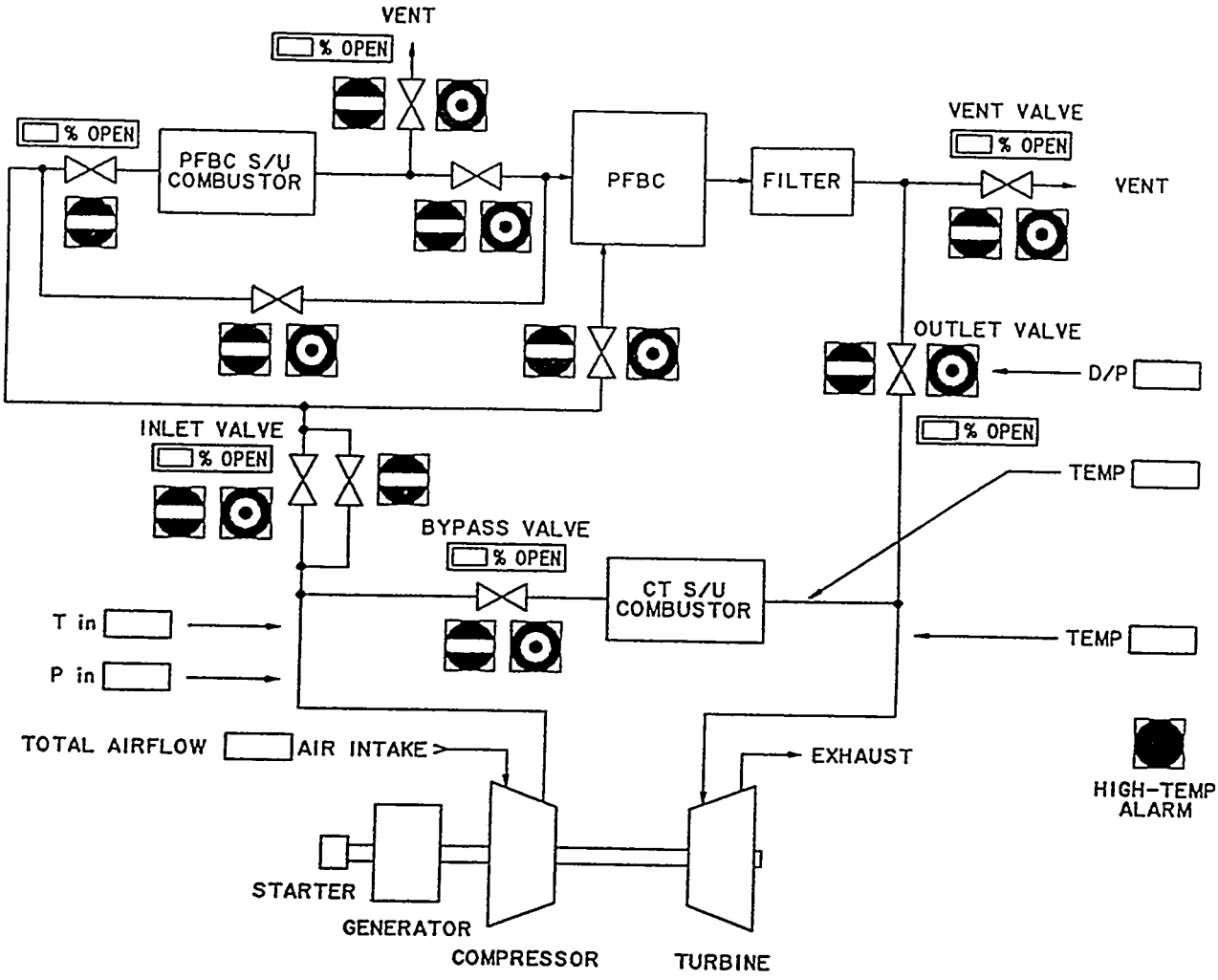


**Figure 10. CT and PFBC Airflow Control Panel**

The controls for the fuel nozzles and combustors need to be moved to control the off-engine startup combustor and modified so that they can initiate an appropriate sequence for PFBC startup. The combustion control system is flexible enough to enable the combustion turbine to operate separately, if required, independent of the PFBC.

The control system must also work with the PFBC controls to enable it to operate in conjunction with the bed during startup, purge, normal operation, shutdown, and emergency shutdown. The startup and purge sequences will depend on the PFBC requirements. During operation in a PFBC system, gas turbine power output at synchronous speed is controlled buy modulating the temperature of the hot gases entering the turbine.

The emergency shutdown and overspeed protection scheme is very important to the PFBC combustion turbine application. Load control is

maintained by modulating the temperature of the hot gas entering the combustion turbine. In the event of a loss in load, combustion turbine overspeed is a concern. On a normal combustion turbine, fuel to the combustors is immediately shut down, slowing down the combustion turbine. On a PFBC, however, the hot gases from the bed must be shut off to the combustion turbine using an isolation valve located in the hot gas leg as near as possible to the combustion turbine. To protect the combustion turbine from the remaining volume of hot gas in the pipe, the bypass valve in the startup combustor/bypass line will open to bypass compressor air into the hot gas line. This will provide immediate mixing of lower temperature air with the remaining hot gases and will cause the combustion turbine to slow down. The PFBC bed will have its own protection scheme that uses vent valves and bypass lines.

## REFERENCES


1. Robertson, A., et al. "Second Generation Pressurized Fluidized Bed Combustion Plant: Conceptual Design and Optimization of a Second-Generation PFB Combustion Plant," Phase 1 Task 1 Report, Volume 1, Foster Wheeler Development Corporation, Livingston, N.J., September 1989.

2. Arthurs, M. J. "The Westinghouse Fluidized Bed Coal Gasification Process," *CHEMSA,* 85-91, July 1982.

3. "Design Standard for Monolithic Refractory Concrete Linings for Vessels and Piping," KRW Energy Systems, Inc., Madison, Pa., MSD-82-001, 1982.

4. Hoffman, J. D. "Initial Operation of the Tidd PFBC HGCU Test Facility." In *Proceedings of the Ninth Annual Coal-Fueled Heat Engines, Advanced Pressurized Fluidized-Bed Combustion (PFBC), and Gas Stream Cleanup Systems Contractors Review Meeting,* October 1992.

5. Wright, S. J., R. Andrews, and B. Booth. "The Designs Required for the Installation and Operation of a Gas Turbine on the Flue Gas from the Grimethorpe Pressurized Fluidized Bed Combustor." In *Proceedings of the 12th International Conference on Fluidized Bed Combustion,* Volume 11, p 1061, San Diego, Calif., 1993.

6. Harvey, L. E., J. T. Zalewski, and M. R. DeLallo, Jr. "Alternative High Temperature Gas Piping Systems for PFBC." Paper presented at the Coal Fired Power Systems 93 - IGCC and PFBC Review Meeting, Morgantown, W. Va., June 28-30, 1993.

# 1.2 Full-Scale and Bench-Scale Testing of a Coal-Fueled Gas Turbine System

## CONTRACT INFORMATION


| | |
|---|---|
| **Contract Number** | DE-AC21-86MC23166 |
| **Contractor:** | Solar Turbines Incorporated<br>P.O.Box 85376<br>San Diego, CA 92186-5376<br>(619) 544-5079 |
| **Contract Project Manager** | Peter B. Roberts |
| **Principal Investigators** | Richard T. LeCren<br>Luke H. Cowell<br>Marlene A. Galica<br>Michael D. Stephenson<br>Chaur S. Wen |
| **METC Projector Managers** | Donald W. Geiling<br>Paul L. Micheli |
| **Period of Performance** | June 2, 1986 to December 23, 1993 |


## ABSTRACT


Work since the last Heat Engine Conference has been concentrated on completing the following supporting tasks since the main effort was curtailed:

- Analysis of the candles from the xx hour rig test by Acurex as part of their program
- Evaluation of the Two Stage Slagging Combustor (TSSC) burning crude oil
- Continued study of the effervescent fuel injector at Purdue
- Phase I of the Advanced Turbine Systems program
- Computational Fluid Dynamic Modelling

Initial testing of the TSSC burning crude oil from the San Joaquin valley in California was accomplished with some preliminary results along with some refractory difficulties. The combustor refractory has been recast and is ready for additional testing. A combined test using crude oil and CWM with the effervescent injectors is envisaged.

The studies at Purdue of the effervescent fuel injector have yielded some results which are contradictory to initial hypotheses and development of holographic techniques to evaluate the

near nozzle breakup process.

Phase I of the Advanced Turbine Systems program was added to this contract. The study was completed and has been reported in another paper at this conference.

It was realized that a better understanding of the TSSC operation would be useful for future use. The use of CFD modelling was proposed and two contracts were let. One was to Advanced Fuel Research in conjunction with Brigham Young University to use PCGC-2 to analyze the Solar TSSC. This work was completed and draft of the final report submitted. Another contract was let to CFD Research Corporation to examine how to obtain low $NO_x$ while burning liquids (crudes and residuals and CWM). This work is intended to complete the study of the TSSC and to support subsequent phases of the ATS programs.

## 1.3 High Pressure Ceramic Air Heater for Indirectly-Fired Gas Turbine Applications

| | |
|---|---|
| **Contract Number** | DE–FC21–90MC26008 |
| **Contractor** | Hague International<br>3 Adams Street<br>South Portland, Maine 04106<br>(207) 799–7346 |
| **Contract Project Manager** | Paul G. LaHaye |
| **Program Manager** | Gwynne F. Briggs |
| **Principal Investigators** | Nelson J. Orozco<br>John L. Seger |
| **METC Project Manager** | Diane T. Hooie |
| **Period of Performance** | February 7, 1990 to November 11, 1993 |

FY 92–93 EFCC PROGRAM SCHEDULE

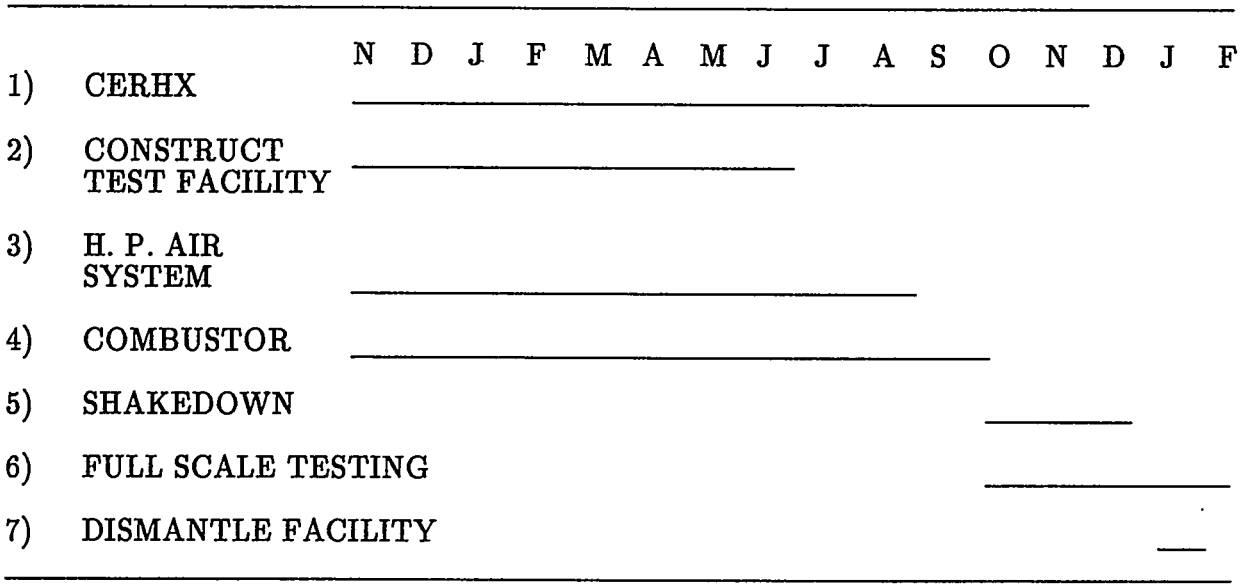

## OBJECTIVES

The Externally–Fired Combined Cycle (EFCC) is an attractive emerging technology for powering high efficiency combined gas and steam turbine cycles with coal or other ash bearing fuels. In the EFCC, the heat input to the gas turbine is supplied indirectly through a ceramic heat exchanger. The heat exchanger, coupled with an atmospheric coal combustor and auxiliary components, replaces the conventional gas turbine combustor. Addition of a steam bottoming plant and exhaust cleanup system completes the combined cycle.

Numerous programs have attempted to fire gas turbines directly with coal by using filters, cyclone separators, or other means of removing ash from the hot combustion gases. These have generally met with limited success; fouling of the turbine blades occurred within a few hours of operation. Corrosion of the direct coal–fired gas turbine nozzles and blades also occurred as a result of the aggressive chemical nature of the products of coal combustion, particularly the trace alkali metal or sulfur compounds in the gas stream. Previous experience has shown that ceramic heat exchangers are significantly less susceptible to ash deposition or corrosion than the gas turbine materials in the gas path.

The EFCC, though conceptually simple, requires the development of a high temperature, high pressure ceramic heat exchanger (CerHX). Ceramic materials allow pressurized air to be heated to turbine inlet temperatures required of present generation engines. However, their use in this application requires technology development. Concerns include fouling, sealing of high temperature joints, alkali corrosion, and the possibility of rapid sequential failure of an array of ceramic tubes.

The purpose of the EFCC Development Program is to demonstrate that the EFCC is a viable technology for powering high efficiency combined gas and steam turbine cycles with coal or other ash bearing fuels. This program is expected to provide all of the data essential to the commercialization of the EFCC concept. The scale of the Kennebunk test facility is adequate to lead into the first, small scale industrial or utility application. This, in turn, is expected to lead into the first large scale industrial or utility application during the last half of this decade.

Phase II of the EFCC Development Program, currently in progress, focuses on "proof of concept" testing of the CerHX and slag screen and integrated system testing. As part of Phase II, a coal–fired test facility, rated at 25 x $10^6$ Btu/hr is in the final stages of construction in Kennebunk, Maine. The Kennebunk Test Facility (KTF) will be utilized to test a prototype of the under gas turbine operating conditions. The primary objectives are to 1) demonstrate that the ceramic air heater can contain gas turbine operating pressures, 2) show that the ceramic air heater can withstand exposure to coal combustion products and remain functionally viable for extended periods, and 3) obtain basic performance data.

## BACKGROUND INFORMATION

### Introduction

In the past, the conversion of the chemical energy in coal to electric power was restricted to conventional steam cycles due to the ash content of this fuel. External firing would permit the use of coal in a combined gas and steam turbine cycle. In some cases, pre–existing steam plants could be upgraded to become an EFCC through addition of the gas turbine topping cycle, resulting in a reduction in heat rate of approximately 25 percent, narrowing the heat rate advantage enjoyed by natural gas and distillate oils. Higher efficiency means reduced fuel consumption for a given electric power output, resulting in inherently lower emissions.

The EFCC cycle, shown in Figure 1, is conceptually simple. Air enters the compressor where it is pressurized and becomes the tube–side flow of the ceramic air

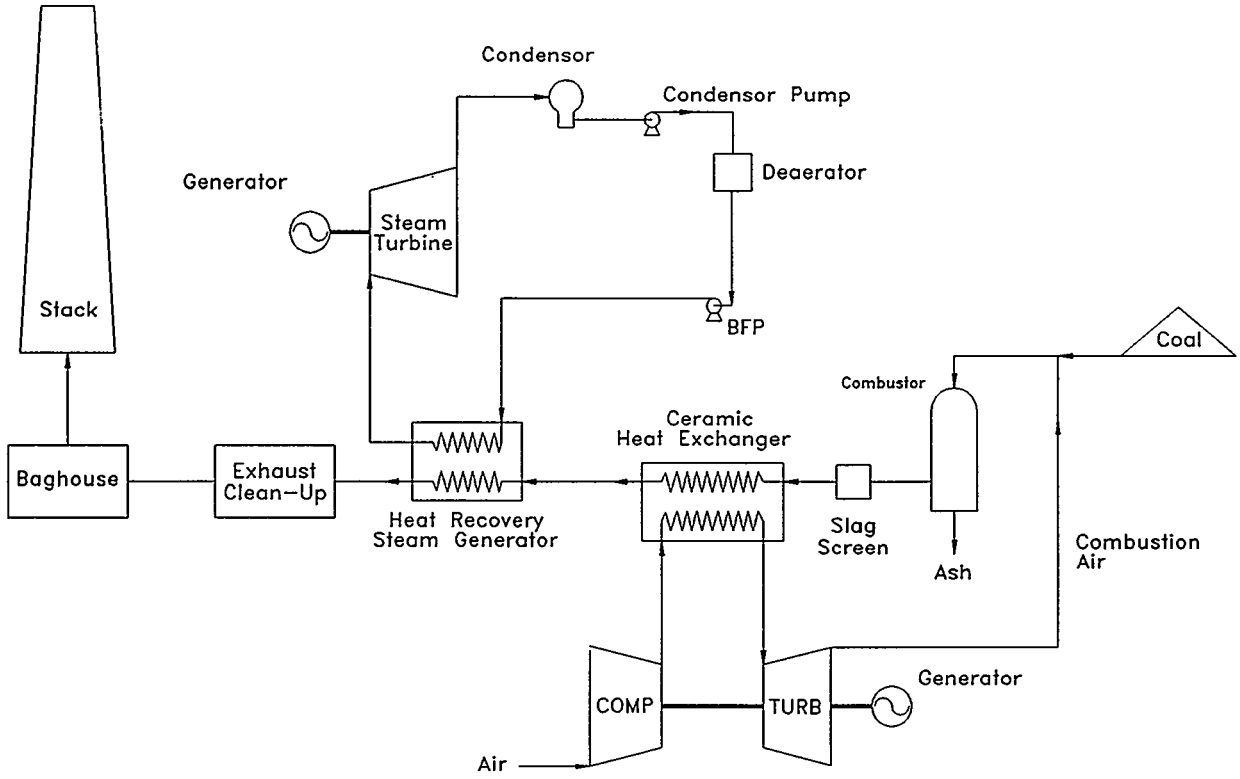


**Figure 1. The Externally Fired Combined Cycle (EFCC) Concept**

heater. Heat transferred from the hot combustion gases flowing through the shell–side raises the air temperature to the desired turbine inlet temperature. Internally insulated high pressure piping returns the heated compressor air to the turbine, where it is expanded providing power to drive the electric generator and gas turbine compressor. Exhaust air from the turbine is used as the combustion air for the coal combustor.

The EFCC cycle burns pulverized coal in an atmospheric combustion chamber similar to the combustion system in a conventional steam generator. The combustion gas exits the combustor and enters a slag screen, or impact separator, where the larger ash particles are collected to prevent fouling of the heat exchanger. After the slag screen, the combustion gas enters the shell–side of the CerHX where its thermal energy is transferred to the tube side air flow. Shell–side exit temperatures are sufficiently high to provide thermal energy for the bottoming Rankine Cycle through a heat recovery steam generator. Exhaust gas exiting the steam generator passes through a flue gas desulfurization system and a particulate removal system.

## Historical Background

The EFCC is not a new concept, indirect–fired gas turbine power plants have been studied since the 1930's, summarized by Keller [1] in 1945. Applications of low–rank coal and peat–fired air heaters were reported by Keller and Gaehler [2]. The first closed–cycle gas turbine (500 kW) with a peat–fired, metallic air heater was built and operated, leading to installation of several cogeneration facilities that performed reliably. Simultaneously, experimental studies conducted by Mordell [3] showed promising results for an open–cycle, indirect–fired gas turbine, the predecessor to the EFCC. Unfortunately, metallic heat exchangers used

in these earlier versions of the cycle did not allow sufficiently high turbine inlet temperatures for economic power production. Use of a ceramic air heater eliminates this obstacle.

Through the 1960's work on EFCC concept consisted of paper studies, summarized by LaHaye [4]. In 1971, HI began a series of experiments with ceramic materials that culminated in the construction of the first ceramic heat exchanger. Most of the work during this period was on heat recovery equipment (recuperators) for the secondary metals industry. By the early 1980's, HI had about fifty low pressure units in operation, which to date have accumulated over two million hours of successful operation in corrosive, high temperature industrial environments.

In the early 1980's, HI initiated work to increase the pressure capability of the CerHX. In 1987, the U.S. Department of Energy and a Consortium of electric utilities and industrial organizations was formed to further pursue the concept. Work was initiated on Phase I of the EFCC development program, and subsequently summarized by LaHaye and Zabolotny [5]. A low pressure recuperator was exposed to the products of combustion of a coal/water slurry over time intervals of up to 40 hours. Ash build–up occurred on the heat exchanger tubes indicating the need for an upstream ash collection system. However, the ceramic tubes exhibited good mechanical durability and corrosion resistance under all test conditions.

## PROJECT DESCRIPTION AND RESULTS

The primary focus of the EFCC Development Program, as described below, has been to find solutions to the technical challenges for the effective and safe operation of the CerHX and EFCC cycle. Phase II of the EFCC development program began in 1990. This ongoing program includes material development for the CerHX and the design, construction, and operation of the KTF, discussed by Vandervort et al. [6] and updated in this report. The CerHX development effort has stressed increased performance, extended lifetime, and reduced production costs.

Construction of the Kennebunk Test Facility is to be completed in late 1993. The design of the major EFCC components is complete, and fabrication is in progress. It is anticipated that "proof testing" of the EFCC components will start during the latter part of FY 1993. The status and development effort of 1) the CerHX which is the principal technical focus of this program, 2) the low $NO_x$ combustor, and 3) the integration of a 500 kW gas turbine into the test facility, to provide a complete indirect–fired gas turbine demonstration facility (pilot plant) are summarized below.

### CerHX Development and Optimization

The ceramic air heater for the Kennebunk Test Facility is a multi–pass shell and tube heat exchanger with a heat exchanger effectiveness of 0.85. The compressor discharge air from the gas turbine flows through the tubes, while the ash–laden combustion gas flow across the tubes. Most of the heat exchanger components are made of ceramics to accommodate material temperatures well in excess of 1900$^0$F and to resist corrosion from the combustion gas. Metal alloys can be utilized in the low temperature end of the heat exchanger which operates in the range of 600$^0$F to 1400$^0$F. The multi–pass shell–and–tube design is the most cost effective and efficient for application to the EFCC, of the various types of heat exchangers considered (e.g. bayonet tubes, Solar Turbines, HIPHES project).

Figure 2 shows a schematic of the three–pass heat exchanger and tube string assembly. Each tube string consists of two ceramic internally enhanced tubes (CIET), a metallic internally enhanced tube (MIET), adapter hex sleeves, and the spring pack assembly. The tubes are held vertically in compression, with the compressive forces developed by the spring pack and bellows

assembly. The spring pack assembly is located on the cold end of the tube–string, outside of the gas patch, so that its components are never exposed to temperatures above 400âF.

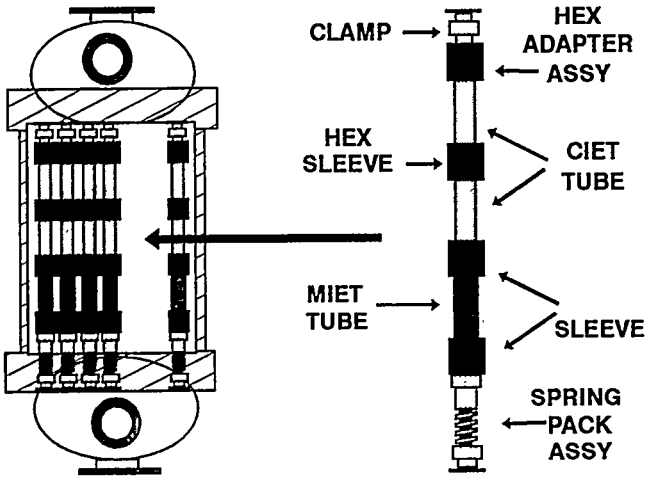


**Figure 2. Ceramic Heat Exchanger**

The hexagonal ("hex") adapter assembly, at the hot end of the heat exchanger joins the tube string assembly to the heat exchanger frame. The center hex sleeves function as the interface between two tubes in series. They are hex shaped so they can interlock with neighboring hex pieces forming a "honeycomb" tube sheet or wall. This wall isolates the shell side flow of one pass from an adjoining pass. The hex sleeves are fabricated from a reinforced ceramic composite. Hex sleeve fabrication procedures have been defined as a result of component testing described below. Efforts continue to find more cost effective materials or design, since each tube string contains four hex sleeves and a large scale commercial size CerHX may contain 3000 tubes.

The CIET and MIET tubes provide the heat transfer surface and containment of the high pressure air. They are internally enhanced, resulting in an overall heat transfer coefficient of approximately 10 Btu/hr–ft"–âF. The maximum shell side temperature is currently held below 2750âF because of material considerations. The end of each tube is machined to closely match the inner surface of the hex sleeves. This interface surface is spherically shaped to produce a ball and socket joint. This allows each tube to move independently of one another as needed to accommodate thermal distortion of the assembly.

A key issue in the development of ceramic tube materials for high pressure air heaters is the possibility of high velocity fragments from a failed tube, initiating a chain reaction tube failure. HI has developed a proprietary tube design which has resulted in a "graceful failure"; that is, tube failure occurs in a non–explosive manner without damaging adjacent tubes. The CIET tube material has to be non–gas permeable, a good thermal conductor and resistant to corrosion by the chemically aggressive products of coal combustion.

High temperature gaskets are used at each hex to tube joint to prevent leakage from the tube side to the shell side. A key concern with the gasket design is the effect of tube leakage on cycle efficiency. Cycle studies indicate that for a 3% air leakage rate there is a resulting 1.5% loss in cycle efficiency for the 300 MW plant. HI has developed a gasket design to meet of all these requirements. Fabrication of the gaskets for the Test Facility is in process. As with the other tube string components, continued efforts to reduce costs, enhance fabricability, and improve performance are necessary.

**Tube String Assembly Tests.** From 1988 through the present, tube strings have undergone over 2,700 hours of high temperature, pressurized testing in the Component Pressure Integrity (CPI) test facility under conditions similar to those experienced in EFCC applications. Testing has included severe thermal cycles simulating operational transients for an EFCC plant, including startup and shutdown. The CPI test apparatus, shown in Figure 3, exposes a single tube string assembly to temperatures of

2000âF, and pressures of 165 psia. Electric clam shell heaters radiatively heat the tube string components. A hydraulic actuator at the top adjusts the amount of spring pack compression to simulate the same compressive loads as in the CerHX. Effect of tube string misalignment due to the number of joints in the assembly can be also simulated in CPI testing. During exposure to these conditions, the leakage of high pressure air through the tube/hex joints or porous components is measured. The durability and mechanical integrity of tube string components can be assessed after long term exposure.

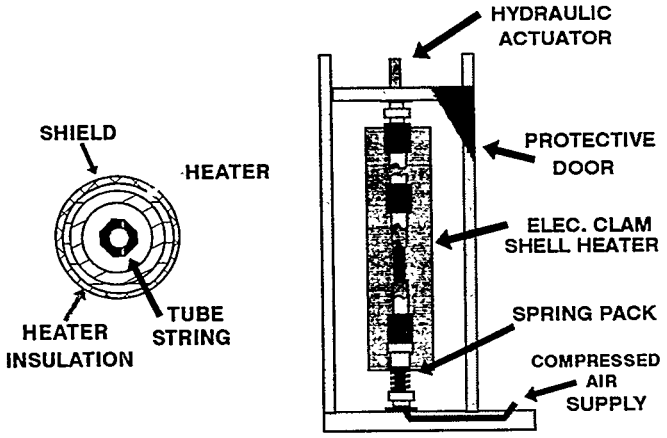


**Figure 3. Schematic of CPI Test Apparatus**

Results of CPI tests have exceeded expectations. Initial tests with prototype components demonstrated less than 3% leakage. Tests with production components have shown leakage rates of 1% and in some cases as low as 0.5%. Thermal cycling tests have also been encouraging, demonstrating leakage rates below 2%. CPI testing is a continuing effort to optimize tube string components.

## Ash Deposition Studies

In addition to the leakage concern, fouling of the heat exchanger from the build up of ash particles, suspended in the products of coal combustion, is also addressed. As the CerHX replaces the gas turbine combustor, the EFCC shows promise because it is easier to prevent ash buildup on tubes of a shell and tube heat exchanger than on the blades of a gas turbine. CerHX components can also be chosen which exhibit excellent resistance to chemical attack when exposed to the products of coal combustion.

Ash deposition for the EFCC is controlled through the use of a slag screen, discussed in detail by Vandervort [7]. This device is a staggered array of refractory tubes, acting as an impact separator. Particle inertia tends to counteract the fluid drag forces which act to "sweep" the particles past the separator tubes. Impact separators are quite effective for removing particles above a certain diameter, ranging from 5 to 50 microns. If these particles are not removed by the slag screen, these same inertial forces can cause impaction upon the ceramic air heater tubes. Resulting ash buildup can hinder heat transfer and, eventually, bridge the gaps between tubes and clog the device.

A slag screen/ceramic air heater system can be designed where all particles of sufficient inertia to impact the heat exchanger tubes are removed upstream by the slag screen. Slag screen tubes also represent a flow obstruction and, accordingly, a source of pressure loss. For optimal efficiency of the EFCC, pressure loss between the combustor and the heat exchanger must be maintained as low as possible. Optimal cycle efficiency requires that pressure drop across the slag screen is maintained at less than 10 in. w.g. A clear tradeoff exists between separator performance and pressure drop.

Ash size distribution is important, as impact separator efficiency is a strong function of particle diameter, particle density, gas stream velocity and impact target size. Particle density is similarly affected by the chemical composition of the fuel. As stated, chemical composition influences the fusion temperature, which impacts the "stickiness" of the coal ash particles. Thus, ash fusion temperature and combustor exit temperature combine to affect collection efficiency and subsequent reentrainment rates. Success of the slag screen/heat exchanger system for ash

deposition control strongly depends upon the performance of the combustor. It is necessary to minimize the average ash particle size exiting the combustor. Ash particle size is also a strong function of the coal chemical composition and size distribution; maximum ash particles sizes may exceed 15 microns for certain coal types. An average particle size of 10 microns can be assumed. At this size, the majority of ash particles will pass directly through the slag screen and the air heater to be collected in a baghouse.

Design of the slag screen is shown as Figure 4. The slag screen rods are supported by a hexagonal lattice of refractory blocks. Products of combustion exit the combustor with a relatively high velocity; smaller particles will be carried by the hot gas stream into the slag screen where all particles larger than about 12 microns impact upon the slag screen tubes. At the exit of the slag screen, the gas stream is directed into an ash collection area. Following this bend, the gas flow is decelerated into the air heater. Within the air heater, the lower gas velocity and larger tube diameters significantly lower the particle collection efficiency; particles over 30 microns will impact the heat exchanger tubes.

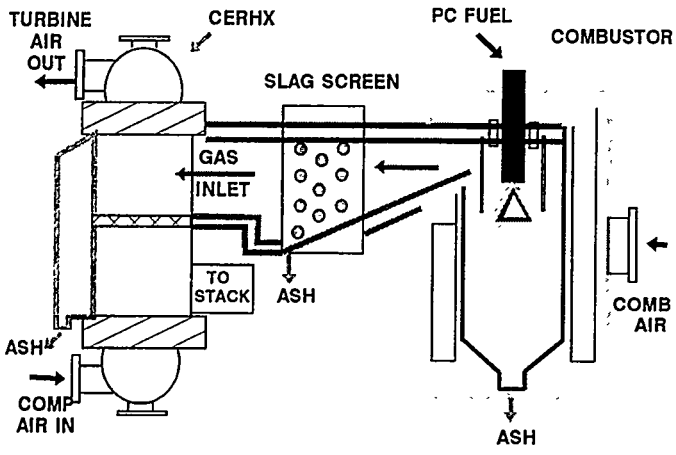


**Figure 4. Slag Screen Design**

Performance of this system is summarized in Figure 5. Particles less than 12 microns can be collected in a baghouse; the region between 12 microns and 30 microns can be considered the "safety factor". These are particles which impact the slag screen but are swept around the heat exchanger tubes.

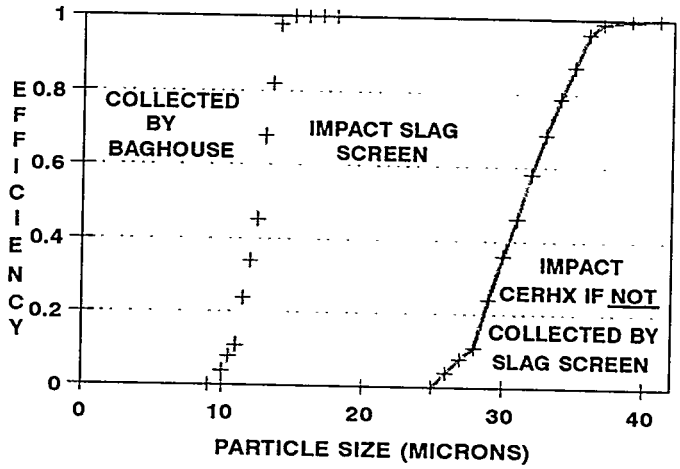


**Figure 5. Slag Screen Performance**

## Coal Combustion System

The coal combustion system provides combustion gases for the "proof of concept", or pilot tests, of the Hague International high pressure ceramic air heater (CerHX). As the CerHX Test Facility has evolved, the significance of the combustion system has increased. Successful heat exchanger operation strongly depends on the performance of the combustion system in maximizing carbon burnout and slag or ash capture.

The latest federal environmental legislation specifies, the New Source Performance Standards (NSPS), for $NO_x$ emissions to be held below 165 ppm dry corrected to 15 percent $0_2$. This corresponds to 0.6 lb of $NO_x$ per million Btu. However, the principal competition for the EFCC are stationary gas turbines in natural gas and distillate fueled combined cycles. When fueled by natural gas, these systems can achieve $NO_x$ emissions below 30 ppm. The objective of this program is to limit $NO_x$ from coal combustion to values below 30 ppm. This is to be accomplished by staging of the combustion process.

Sources of $NO_x$ from pulverized coal burning boilers can be grouped into three categories. First, thermal $NO_x$ is generated at high flame temperatures by thermal fixation of atmospheric nitrogen ($N_2$). Here, high temperature refers to levels above $2300^0$F. Second, conversion of fuel–bound or organic nitrogen in the volatile fraction of the coal, and third, conversion of fuel–bound nitrogen in the coal char fraction. The latter mechanisms depend on the fuel nitrogen content and its distribution between the volatile and char fractions. The result is that $NO_x$ emission levels for different types of coals in the same combustion system can vary by a factor of two, according to Makansi [8].

Staging the combustor has been shown to effectively reduce $NO_x$ emission levels to below 30 ppm (0.1 lb/$10^6$ Btu). The first stage operates fuel–rich, with a fuel–air equivalence ratio from 1.67 to 1.0, the remaining combustion air is added in the second stage, where combustion is completed. The advantage of operating fuel–rich in the first stage is in reduction of conversion of fuel–bound nitrogen to $NO_x$. Oxygen in the combustion air reacts more readily with the hydro–carbon fuel than with nitrogen, so that the nitrogen can recombine as molecular $N_2$. It is also possible that $NO_x$ formed as thermal $NO_x$ can dissociate and the resulting nitrogen species react to form $N_2$.

Staged combustion studies have been performed by numerous researchers, including Hague International in the early 1970's. Recent examples of the ability to reduce $NO_x$ emissions through staging are the work of Diehl et al. [9] and Pillsbury et al. [10]. Figure 6 represents the measured $NO_x$ emissions for both pulverized coal and coal–water mixture as a function of the primary zone fuel–air equivalence ratio. The trends of reduced $NO_x$ as a function of first stage equivalence ratio are clearly indicated, with a minimum level below 30 ppm at 15 percent $0_2$ (0.1 lb/$10^6$ Btu). It is important that these results are for a pressurized (6 atm) combustor, designed for direct–fired gas turbine application. However, pressure has been shown to be a second order effect, and the direction of impact remains a topic of discussion. Similar results were reported by Cowell et al. [11], under approximately the same conditions.

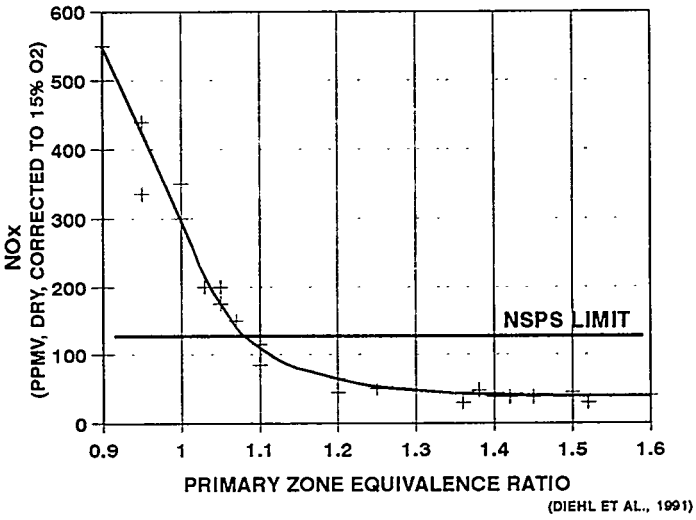


**Figure 6. Potential $NO_x$ Reduction by Staged Operation**

The KTF coal combustor is down–fired into two cylindrical combustion chambers with the primary stage directly atop the second stage. The total height of the combustor, including the burner, is approximately 40 feet, and the outer diameter of the cylindrical casing is nominally 13 feet. Approximately 2/3 of the total volume is provided for the first stage, with the remaining 1/3 for the second stage. A collar divides the first zone from the second, and also provides convenient access ports for the second stage combustor air.

A slag tap is located at the base of the combustor. Slag is expected to be released in both the primary and secondary chambers. A portion of the slag formed in the primary chambers will flow down the walls and exit through the collar. The primary region was sized to provide several seconds of residence time for maximum carbon burnout. The molten slag will fall into the secondary region where the remaining combustion air is mixed and combustion completed. Through proper

control of the trim air, the second stage temperature can be controlled for optimized slag capture.

The coal pulverizer and feed system is the Williams Model DF–25. This system has the capacity of supplying a feed rate of 1800 lb/hr. The coal feed size is to be 95 percent minus 0.75 inch, and the product is to be 70 percent minus 200 mesh. The ambient primary air referred to in the above paragraph is delivered through the pulverizing system and carries the pulverized coal. The dilution air from the gas turbine exhaust is used to raise the mixture temperature to 271°F.

## EFCC Cycle Integration

An important aspect of the EFCC Development Program is the integration of a 500 kW gas turbine into the KTF. Technical and economic justification exists for installation of an actual gas turbine and auxiliary components in the test facility. Once assembled, these components represent a complete, integrated system that is representative of the final EFCC configuration for electric utility or industrial applications. This complete system, following successful operation, will provide the information needed to design an electric utility sized demonstration plant (60 MW or larger) leading to commercialization of the system. This includes the control system development required for performance of these tests, that can also be directly extended to commercial applications.

The gas turbine selected is the Garret IM–831. The Garret gas turbine engine is a single shaft, open cycle gas turbine engine rated at 735 SHP for ISO continuous duty. Output shaft speed is limited to 12,000 rpm. Electric generators are coupled to the gear box and controlled at 1800 rpm for 60 Hz power. This machine uses a two–stage centrifugal compressor and three–stage axial turbine. Mass flow through the engine varies from 7 to 8 pounds/second. The package will be leased for the planned test period, and includes the gear box, control system, silencers, starter, lubrications system, fuel pump, and an electric generator.

The key control of turbine output power is by a turbine control valve (TCV) system. This system allows a portion of the compressor discharge air to bypass the ceramic heat exchanger and mix with the hot discharge air to control the turbine inlet temperatures. In this way, the ceramic heat exchanger can be maintained as a constant temperature heat reservoir and gas turbine load variations are accommodated by control of the bypass flow. The TCV serves the additional function of preventing an over speed of the gas turbine in the event of a generator trip. In this case, the TCV acts quickly enough to bypass sufficient compressor discharge air to reduce the turbine inlet temperature to below the self–sustaining temperature. Under this casualty, coal feed to the combustor will also be interrupted and the ceramic air heater can be cooled.

The gas turbine controls supplied with the Garrett gas turbine will be adapted to account for the replacement of the fuel control valve with the turbine control valve. The turbine control valve assumes a fully open "dump" position on an over–speed signal from the protection system. Due to the high thermal inertia of the ceramic air heater and combustor, changes in coal input lag a turbine load change. Turbine load changes are initially satisfied by a change in the turbine control valve position, followed by a change in the fuel flow rate, with a corresponding change in the combustion air flow. The system protects the ceramic air heater by maintaining a constant temperature in the ceramic air heater and accommodating load changes by altering the air flow through the by–pass valve, followed by a change in the combustion rate that would gradually return the turbine control valve to a steady–state position.

Testing of the turbine control valve and development of the associated control system represents an important step in the commercialization of the EFCC. Note that the gas turbine system also requires use of

double wall piping between the turbine control valve and the combustor flanges. As with the turbine control valve, this represents a system that is needed in the final utility or industrial application.

## FUTURE WORK

Upon completion of the Kennebunk Test Facility, testing should be initiated in the fall of 1993. The goals of the test plan are to conduct proof of concept tests of the CerHX, slag screen and a fully integrated EFCC facility. Since the gas turbine is the source of compressed air for the these tests, baseline tests of the gas turbine will be performed to verify its proper operation. Testing of the CerHX is performed in three distinct stages with extensive sub–tests in each stage.

In the first stage, the CerHX will be assembled using metal tubes and fired on natural gas. The purpose of the metal tube–string tests will be to experiment with various methods for assembling the CerHX. Use of three tube passes is an extension of Hague's previous experience and it is expected that several attempts may be necessary. Following assembly, the multiple tube–strings will be pressurized and heated to approximately 1200°F, where air leakage measurements will be taken. Heat input will be supplied by natural gas at a minimum level of $2 \times 10^6$ Btu/hr by the FWC burner.

In the second stage, ceramic tubes will replace the metal tubes. The goal of this series of tests will be to demonstrate that the entire ceramic air heater can 1) contain pressures up to 175 psia, 2) endure at least 100 hours of operation under static and dynamic loadings, and 3) meet thermal performance requirements. During the these tests the combustor will be fired with natural gas. The use of natural gas facilitates testing whereas coal requires use of coal feed and handling equipment, adequate slag and ash removal upstream of the CerHX, and the possibility of ash deposition on the CerHX tubes complicates evaluation of heat transfer performance. The maximum heat input value will be approximately $25 \times 10^6$ Btu/hr.

In the third stage, the combustor will be coal–fired to verify the ability of the slag screen to protect the ceramic air heater from coal ash and to test the "self–cleaning" feature. In parallel with the first two test sequences, the apparatus required for the coal–fired tests will be installed. This will include the coal handling/pulverizing steam, the Foster–Wheeler coal burner, the burner control and safety system, the ash collection system, soot blowers for the ceramic heat exchanger, and the combustor itself.

The goals of this series of tests will be to achieve 300 hours of cumulative run time and a 100 hour continuous test. Material durability of the air heater tubes, slag screen tubes, and refractory walls will be assessed throughout these tests; following their completion the tubes will be removed for careful measurement of surface erosion or to seek evidence of slag buildup. This may require surface examination of the tubes prior to use in these tests.

Completion of the 100 hour continuous run will demonstrate the functionality of the ceramic air heater/slag screen island and the feasibility of the EFCC.

This amount of operating time described above is not sufficient to prove the concept as commercially viable, so that additional operation of the facility is anticipated during 1994 and 1995. In parallel with this program, conceptual designs have been initiated for Phase III, a retrofit application of an existing coal–fired steam plant. A ceramic air heater, slag screen, combustor and gas turbine of approximately 20 MW would be retrofitted to an existing power plant. Steam produced by a new heat recovery steam generator would be used for steam injection and power production using the existing steam turbines. This system is expected to produce electricity by the late 1990's at a cost competitive with other emerging technologies.

Experience gained through design and operation at the retrofit facility will be applied to Phase IV, the construction of large, utility–scale EFCC plants. For production of

100 MW of electrical energy with conventional gas and steam turbine technology, heat rates are predicted to range from 7000 to 8000 Btu/kW–hr. There are no other means of achieving performance at this level with coal in an economically viable fashion.

## REFERENCES


1. Keller, C., "The Escher Wyss–AK Closed Cycle Turbine, Its Actual Development and Future Prospects", Trans. ASME, Vol. 68, pp. 791–882, 1946.

2. Keller, C. and Gaehler, W., "Coal–Burning Gas Turbine", ASME Paper No. 61–GTP–2, Presented at the Gas Turbine Power Conference, Washington, DC, March 5–9, 1961.

3. Mordell, D.L., "The Exhaust–Heated Gas Turbine Cycle", Trans. ASME, Vol. 72, pp. 323–329, 1950.

4. LaHaye, P.G., "High Temperature Heat Exchanger for Closed–Cycle, Coal–Fired Gas Turbines", Presented at National Coal Association Technical Sales Conference and Bituminous Coal Research Annual Meeting, Pittsburgh, PA, September 14, 1966.

5. LaHaye, P.G. and Zabolotny, E., "Externally–Fired Combined Cycle (EFCC)", Presented at the ASME Cogen–Turbo Meeting August 30 – September 2, 1989.

6. Vandervort, C.L., LaHaye, P.G., Briggs, G.F., and Seger, J.L, "High–Pressure Ceramic Air Heater for Indirectly Fired Gas Turbine Application", Proceedings of the Ninth Annual Coal–Fueled Heat Engines, Advanced Pressurized Fluidized–Bed Combustion (PFBC), and Gas Stream Cleanup Systems Contractors Review Meeting, DOE/METC–93/6129, pp. 89–96, October 1992.

7. Vandervort, C.L., "Factors Influencing Ash Particle Deposition in an Impact Separator at High Velocities and Temperatures", Proceedings of the Engineering Foundation Conference on Inorganic Transformations and Ash Deposition During Combustion, pp. 815–827, March 1991.

8. Makansi, J., "How Fuel Quality Affects $NO_x$ Formation – and CAA Compliance", Power, July 1991.

9. Diehl, R.C. Loftus, P.J., Bannister, R.L., and Pillsbury, P.W., "A Slagging Combustor for Direct Coal–Fired Gas Turbines", Presented at the Sixth Annual Pittsburgh Coal Conference, Pittsburgh, PA, September 25–29, 1989.

10. Pillsbury, P.W., Bannister, R.L., Diehl, R.C., and Loftus, P.J., "Development of a 220–MW Coal–fired Combustion Turbine Combined Cycle: Current Status", Presented at the International Gas Turbine and Aeroengine Congress and Exposition, ASME Paper No. 91–GT–184, Orlando, FL, June 3–6, 1991.

11. Cowell, L.H., LeCren, R.T., and Tenbrook, C.E., "Two–Stage Slagging Combustor Design for a Coal–Fueled Industrial Gas Turbine", Presented at the International Gas Turbine and Aeroengine Congress and Exposition, ASME Paper No. 91–GT–212, Orlando, FL, June 3–6, 1991.


## ACKNOWLEDGEMENTS


Support for Phase II of the EFCC program is provided by the United States Department of Energy – Morgantown Energy Technology Center under contract number DE–FC21–90MC26008 and the EFCC Consortium of government agencies, electric utilities, and both foreign and domestic industrial organizations. Their contributions are gratefully acknowledged.

## 1.4 Direct Coal-Fired Gas Turbines for Combined Cycle Plants

### CONTRACT INFORMATION

| | |
|---|---|
| Contract Number | DE-AC21-86MC23165 |
| Contractor | Allison Gas Turbine Division<br>General Motors Corporation<br>P. O. Box 420<br>Indianapolis, IN 46206<br>(317) 230-3057 |
| Contractor Project Manager | John Rothrock |
| Principal Investigators | Richard Wenglarz, Peter Hart,<br>Hukam Mongia |
| METC Project Manager | Leland Paulson |
| Period of Performance | July 1986 to July 1993 |

### OBJECTIVES

The overall goal of this program is to develop and demonstrate the technological bases for economically attractive, commercial, coal-fueled gas turbine systems. Objectives to accomplish this goal include:

- identify candidate technical approaches to meet the challenges of using coal as a turbine fuel.
- screen the candidate technical approaches by testing their relative performance and evaluating their effects on the economic attractiveness of commercial coal-fueled systems.
- demonstrate the most promising technologies and associated components in proof-of-concept system tests leading up to commercialization.

### BACKGROUND INFORMATION

Coal is an abundant domestic fuel source and has been evaluated as a turbine fuel in two major programs that started in the late 1940s in the U.S. (Smith et al., 1966) and later in Australia (Interdepartment Gas Turbine Steering Committee, 1973). Although these projects were only partially successful, later advancements in coal technologies stimulated a renewed interest (Pitrolo, 1983; Stettler et al., 1983) in coal as a potential source of fuel for commercial gas turbines.

The Allison Gas Turbine Division of General Motors Corporation tested a rich-quench-lean (RQL), low nitrogen oxide (NOx) combustor in a NASA program which started in the late 1970s. The U.S. Department of Energy (DOE) continued

this program with coal-derived fuels (including coal water fuels [CWF]) in tests that extended into the early 1980s. A DOE/ Allison Component Screening Program was initiated in 1984. The RQL combustor was modified for improved combustion efficiency using CWF, and deposition, erosion, corrosion (DEC) tests were conducted with specimens exposed at turbine flow-path conditions. Allison and other turbine manufacturers were awarded Advanced Coal-Fueled Gas Turbine Systems Programs in mid-1986. This report describes efforts in the Allison program.

## PROJECT DESCRIPTION

### Coal-Fuel Turbine Technology Development

The Allison RQL combustor tested in the earlier programs was of metallic construction and used air quench. In this program, the combustion approach was changed to a refractory lined design with water quench to improve NOx performance and increase the combustor durability. This bench-scale combustor (about 1/10 flow rate of a combustor sized for the Allison 501K turbine) was tested for combustion and emissions (NOx and CO) performance with several CWF.

Based on experience from the bench-scale combustor, a full 501K turbine scale combustor facility was developed. This combustor was also tested with CWF for combustion and emissions performance. An Allison 501K turbine was then operated for about four hours using the full-scale combustor and a subbituminous CWF. Ash from the products from the combustor rich zone was removed upstream of the turbine using two parallel cyclone separators.

During most of the program, a number of organizations had been developing CWF; however, in recent years most suppliers have terminated their CWF efforts. Low cost commercial CWF for turbines are no longer expected to be available in the foreseeable future. Consequently, efforts were directed to preparing the two Allison facilities (bench-scale and full-scale) for operation with fine powder coal.

Subscale dry coal feed tests have started. A bench-scale (25 candle) hot gas filter vessel has been installed for the purpose of tests following combustion/emissions verification with powder coal. Two DEC test sections have been installed downstream of the combustor for the purpose of exposing specimens at conditions of two turbine rows. Improved combustor refractories have been installed along with a slipstream to evaluate Zn titanate sulfur control.

Work has started to install in the full-scale facility the refurbished 501K turbine, a dry coal feed system, and the combustor with improved refractories. A preliminary design effort has been initiated for a hot gas filter for the engine facility.

### Commercial System Definition and Assessments

Two types of commercial direct coal-fired plants have been defined and analyzed:

- cogeneration plants based on the Allison 501K turbine
- combined cycle plants based on large utility turbines

Performance, costs and economics have been assessed for several variations of these systems.

A reference cogeneration system that has been evaluated uses a hot gas filter to control particulate emission and protect the turbine flow path from particulate effects (deposition and erosion). Alternate cogeneration systems have also been evaluated. These alternate systems use cyclone separators and various other measures to protect the environment and turbine from particulate. Systems and cost analyses have also been conducted for several direct coal-fueled turbine combined cycle (CFTCC) plants based on turbines ranging in size from about 50MW to over 100MW.

## RESULTS

Results of program technical evaluations have been reported previously (Santanam, et al., 1990; Wilkes, et al., 1992) along with systems analyses results for the baseline cogeneration system (Merrion, 1991; Wenglarz, 1992) and alternate cogeneration systems (Wenglarz, 1991). This paper summarizes results of systems evaluations for CFTCC plants.

### CFTCC Power Plants

**CFTCC Schematic.** The CFTCC system is illustrated by the simplified schematic diagram shown in Figure 1. The system consists of two major blocks, the coal combustion/emissions control block and the power generation block. The power generation block is a combined cycle (gas turbine and steam turbine cycle) system and uses equipment designed to operate with conventional turbine fuels (e.g., natural gas). The coal combustion and emissions control block converts the conventionally-fueled combined cycle plant to operation with coal. As will be discussed later, the coal combustion equipment uses gas turbine technology rather than process plant technology and provides compactness and cost advantages over other coal utilization systems.

Referring to Figure 1, a portion of the gas turbine compressor discharge air is directed to the combustion/emissions control block where it is reacted with coal. Coal contaminants (e.g., sulfur and ash particulate) are removed from the combustion product stream before final combustion and expansion in the turbine. Quench water and heat extraction are used in the combustion/emissions control block to lower the temperature of the combustion products to a suitable level (1340°F) for removal of coal contaminants and emissions control. The heat extracted in the combustion/emissions control block is used in the steam equipment of the combined cycle power generation block to produce power.

**Combustion/Emissions Control Block.** NOx is controlled in the combustion/emissions block by RQL combustion of coal. The rich zone of the combustor operates under fuel rich conditions, which inhibits the formation of NOx from fuel bound nitrogen found in the coal. The quench and final lean combustion zones involve relatively low reaction temperatures that minimize the formation of thermal NOx from dissociation of molecular nitrogen found in air. Tests with the RQL coal combustor sized to the Allison Model 501K industrial gas turbine have demonstrated simultaneous control of NOx and CO emissions to less than 25 ppmv (at 15% $O_2$)

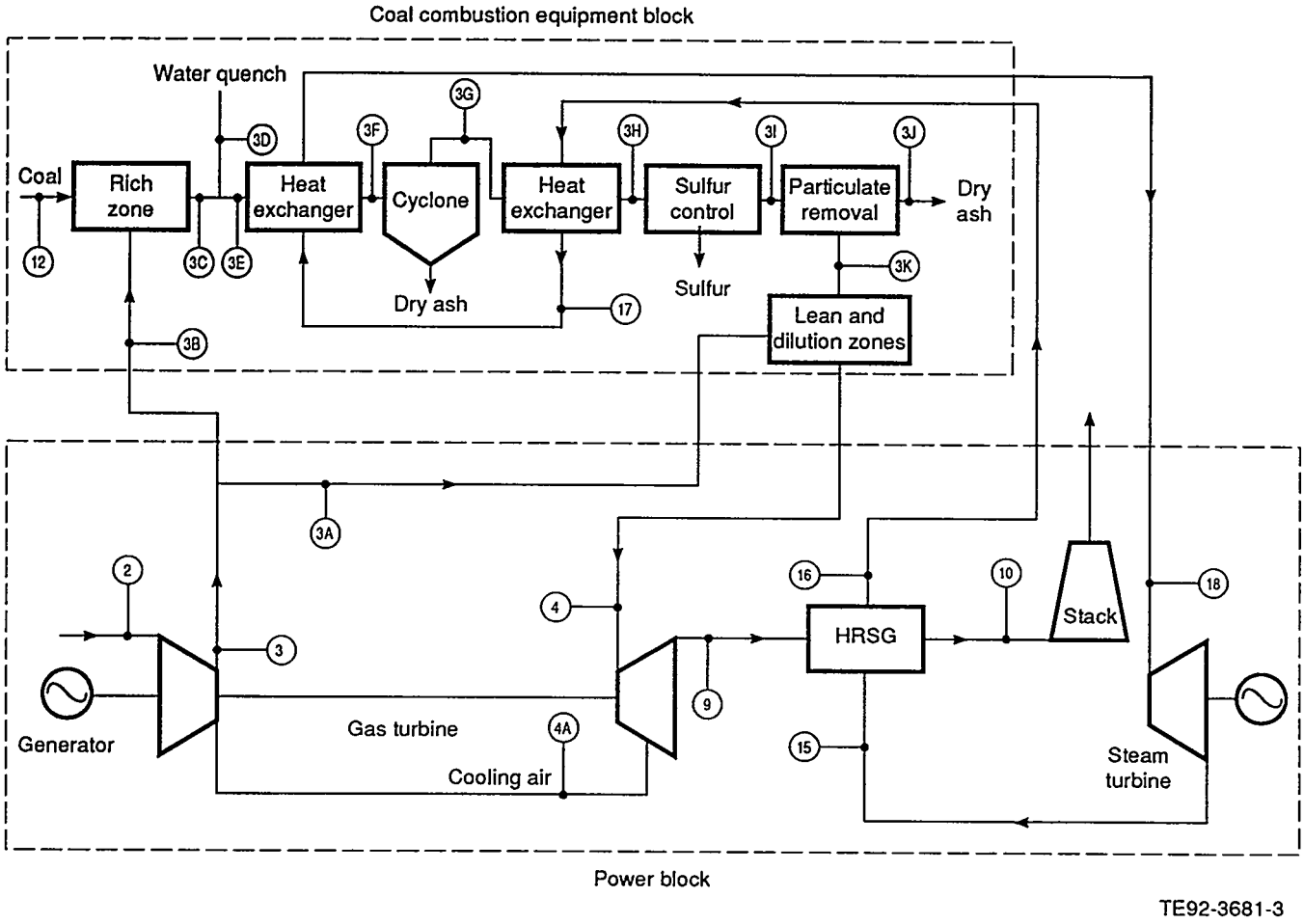


**Figure 1. Simplified Block Diagram of CST Demonstration Project**

with prospects for lower levels with further optimization of the local stoichiometry.

Sulfur oxide (SOx) is controlled in the combustion/emission block by a zinc titanate sulfur scrubber. Tests indicate that this control method should ultimately be capable of reducing SOx emissions by over 99%.

Particulates are controlled in two stages by a cyclone separator followed by a hot gas ceramic barrier filter. A number of high temperature filter tests have reduced gas stream particle carryover to under 10 ppmw.

## Applications

The CFTCC technology can be utilized for new power plants or for re-powering of existing natural gas-fired, combined cycle power plants. Depending on the gas tur-

bine used, this technology can provide coal-fueled power blocks with electrical outputs from about 85 MWe (e.g., for the GE MS6000 turbine) to over 350 MWe (e.g., for the Westinghouse 501F turbine) and even higher outputs for future advanced turbines. Figure 2 illustrates the layout for a 100 MWe plant based on the Westinghouse 251 turbine.

## CFTCC Advantages

The combustion/emissions control island of the CFTCC plant produces cleaned coal combustion gases for expansion in the gas turbine. The gases are cleaned to protect the turbine from flow-path degeneration due to coal contaminants and to reduce environmental emissions to comparable or lower levels than alternate clean coal power plant technologies.

Most of these alternate clean coal technologies have been developed by organizations that design process plants. As a result, incorporation of these coal technologies with a combined cycle power generation system requires integration of turbine equipment with a process plant. An advantage of the CFTCC system over other clean coal technologies using gas turbines results from the CFTCC system having been designed as an adaptation to coal of a natural gas-fired combined cycle plant. Gas turbines are built for compactness and simplicity. The RQL combustor is designed using gas turbine combustion technology rather than process plant reactor technology used in other pressurized coal systems. The result is simpler and more compact combustion equipment than for alternate technologies. The natural effect is lower cost and improved reliability.

To illustrate the difference in technology, the residence time in the rich zone of the RQL system is typically only about 20% to 30% of that for many entrained coal gasifiers that have the shortest residence times of the alternate coal technologies. This results in a more compact system. Combustion in the RQL system is achieved with air, thereby not requiring the complexity and the high cost of the oxygen plant needed for many coal gasification systems. No equipment is necessary in the RQL combustion system to capture and recycle combustion product fines while such equipment is usually need for efficient coal consumption in advanced pressurized systems.

In addition to new power generation plants, CFTCC technology will provide relatively compact and gas turbine compatible coal combustion/emissions control islands that can adapt existing natural gas-fired combined cycle plants to coal when gas prices rise to the point where conversion is economically attractive. Because of the simplicity, compactness, and compatibility of the RQL combustion/emission control island compared to other coal technologies, it could be a primary candidate for such conversions.

## 351 MWe CFTCC Plant

**Plant Description.** The following describes the performance of a 351 MWe CFTCC plant that utilizes the Westinghouse 501F turbine and a 2400 psig/1000°F/1000°F/2.5 in. Hg steam cycle. The plant produces 351 MWe output using 112.9 tons/hour of an eastern bituminous coal containing 2.5% sulfur and 16.4% ash. A salable by-product of the plant is elemental sulfur. About 2.7 tons/hour of sulfur is

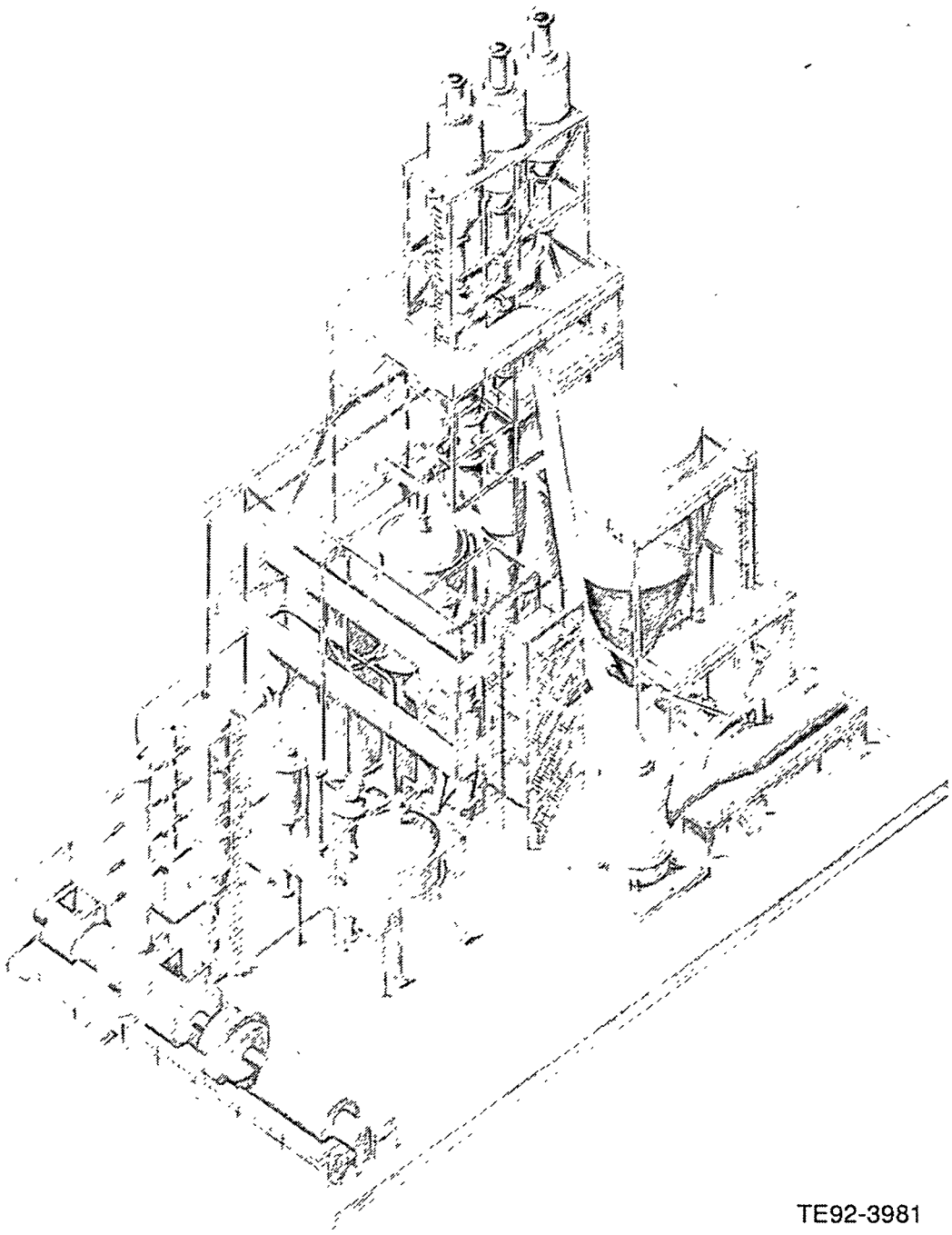


**Figure 2. 100 MWe Demonstration Plant Layout**

extracted from the coal combustion stream using the zinc titanate sulfur capture system.

**Emissions.** Table I shows lower NOx and $SO_2$ and particulate emissions for the CFTCC system than for an existing 300 MWe coal boiler plant without provisions for SOx and NOx control. The CFTCC emissions are also substantially lower than the Federal New Source Performance Standards (NSPS) shown in Table I.

**Efficiency.** Table II shows the efficiency of the 351MWe CFTCC plant and the efficiency of the 300 MWe pulverized coal boiler plant. The CFTCC plant efficiency is over seven percentage points higher than that for the existing conventional power plant.

**Costs.** As discussed earlier, the CFTCC system design approach adapts a conventional combined cycle plant design to operation with coal by using the RQL combustion/emissions control island. The distinction of equipment between combined cycle equipment and coal combustion/emissions control equipment allows identification of the incremental capital costs per kilowatt for the CFTCC plant compared to a combined cycle plant that uses conventional fuels. Cost evaluations have indicated an incremental cost of about $480/kW for the coal combustion/emissions control equipment.

**Table I. Comparison of Air Emissions of 300 MWe Coal Boiler Plant with the CFTCC Plant**

| Emission specie (HHV basis) | PC boiler plant | CFTCC plant | NSPS |
|---|---|---|---|
| $NO_2$, lb/MMBtu | 1.24 | 0.113 | 0.5 |
| $SO_2$, lb/MMBtu | 3.96 | 0.101 | 1.20 |
| Particulates, lb/MMBtu | 0.10 | 0.013 | 0.03 |

**Table II. Power Plant Efficiencies**

| System | Heat rate Btu/kW-hr HHV basis | HHV efficiency--% |
|---|---|---|
| 351 MWe CFTCC plant | 7785 | 43.8 |
| 300 MWe PC boiler plant | 9493 | 36.0 |

## REFERENCES


Australian Government Publishing Service, 1973, *The Coal-Burning Gas Turbine Project,* Report of the Interdepartment Gas Turbine Steering Committee, Canberra.

Merrion, R. F., and Wenglarz, R. A., 1991, *Commercialization of Coal-Fueled Gas Turbines,* Proceedings of the Eighth Annual Coal-Fueled Heat Engines and Gas Stream Cleanup Systems Contractors Review Meeting, 29-34. DOE/METC - 91/6122. NTIS DE 91002091

Pitrolo, A. A., 1983, *Coal-Fired Gas Turbines: An Old Dream Revisited,,* Keynote Address for the 1983 International Gas Turbine Conference, Phoenix, Arizona.

Santanam, C., Wilkes, C., Caraker, K., Rothrock, J., and Bourke, R. C., 1990, *Coal-Fueled Gas Turbine Program - An Overview,* Proceedings of the Seventh Annual Coal-Fueled Heat Engine and Gas Stream Cleanup Systems Contractors Review Meeting, 31-41, DOE/METC 90/6110. NTIS DE 90000480.

Smith, J., Strimbeck, D. C., Coates, N. H., and McGee, J. P., 1966, *Bureau of Mines Progress in Developing Open and Closed Coal-Burning Gas Turbine Plants,* ASME Paper No. 66-GT/CLC International Gas Turbine Conference, Zurich, Switzerland.

Stettler, R. J., Bell, A. H., Shows, E. W., 1983, *Initial Evaluation of a Coal Burning Turbine Powered Vehicle System,* ASME Paper 83-GT-183, International Gas Turbine Conference, Phoenix, Arizona.

Wengarz, R. A., and Wilkes, C., 1991, *Emissions Control for a Coal-Fuel Industrial Cogeneration Gas Turbine System,* Proceedings of the Eighth Annual Coal-Fueled Heat Engines and Gas Stream Cleanup Systems Contractors Review Meeting, 433-437, DOE/METC - 91/6122. NTIS DE91002091.

Wenglarz, R. A., and Wilkes, C., 1992, *Commercialization of Coal-Fueled Gas Turbine Systems,* Proceeding of the Ninth Annual Coal Fueled Heat Engine, Advanced Pressurized Fluidized-Bed Combustion (PFBC), and Gas Stream Cleanup systems Contractors Review Meeting, 11-18, DOE/METC - 93/6129, NTIS DE93000232.

Wilkes, C., et al., 1992, *Development of a Coal-Fired Gas Turbine Cogeneration System - Status Report,* Proceedings of the Ninth Annual Coal-Fueled Heat Engines, Advanced Pressurized Fluidized-Bed Combustion (PFBC), and Gas Stream Cleanup Systems Contractors Review Meeting, 121-132, DOE/METC - 93/6129, NTIS DE93000232.

# 1.5 Heavy Duty Gas Turbine Combustion Tests With Simulated Low BTU Coal Gas

## CONTRACT INFORMATION

**Cooperative Agreement No.** DE-FC21-90MC27221

**Contractor:** GE Power Systems
1 River Road
Schenectady, N.Y. 12345

**Contractor Project Manager:** Thomas E. Ekstrom

**Principal Investigators:** Robert A. Battista
Frank H. Belisle
Gregory P. Maxwell

**METC Project Manager:** Leland E. Paulson

**Period of Performance:** August 1991 to September 1993

**Schedule and Milestones:**

**Program Schedule**

| | FY92 | | | | | | | | | | | | FY93 | | | | | | | | | | | | |
|---|---|---|---|---|---|---|---|---|---|---|---|---|---|---|---|---|---|---|---|---|---|---|---|---|---|
| | J | J | A | S | O | N | D | J | F | M | A | M | J | J | A | S | O | N | D | J | F | M | A | M | J | J | A | S | O |
| Test Plan | ***** | | | | | | | | | ** | | | | | | ** | | | | | | | ** | | ** | | | | |
| Hardware Preparation | *** | | | ** | | | | | | | | | | | | | ** | | | | | | | | | | | | |
| Facility Preparation | *** | | * | | | | | | | * | * | | | | | | | | | | | | | | | | | | |
| Fuel Procurement | ** | | ** | | | | | | | ** | | **** | | | | | ******** | | | | *** | | | *** | | | | | |
| Testing | | | | | | | | | | | * | | | | | | * | * | * | | * | | * | | | * | | | |
| Analysis | | | | | | | | | | | ** | | | | | | ** | **** | | | ** | ** | | | | *** | | | |
| Final Report | | | | | | | | | | | | | | | | | | | | | | | | | | **** | | | |

## OBJECTIVES

This program has the objectives to:

A. Parametrically determine the effects of moisture, nitrogen and carbon dioxide as diluents so that the combustion characteristics of many varieties of gasification product gases can be reasonably predicted without physically testing each specific gas composition

B. Determine emissions characteristics including NO, NOx, CO, levels etc. associated with each of the diluents

C. Operate with at least two syngas compositions; DOE chosen air-blown and integrated oxygen-blown, to confirm that the combustion characteristics are in line with predictions

D. Determine if "logical" refinements to the fuel nozzle will yield improved performance for LBTU fuels

E. Determine the conversion rate of ammonia to NOx

F. Determine the effects of methane inclusion in the fuel

G. Determine the effects of head-end nitrogen injection

H. Determine the effect of fuel gas temperature on combustion stability

## BACKGROUND INFORMATION

There is an increasing industry interest in integrated gas turbine combined cycle plants in which coal gasifiers provide the fuel for the gas turbines. Some gasifier plant designs, including the air-blown processes, some integrated oxygen-blown processes and some oxygen-blown processes followed by heavy moisturization, produce fuel gases which have lower heating values ranging from 150 to below 100 BTU/scf for which there is little gas turbine combustion experience. This program will provide a set of "screening" tests of the advanced (high temperature) MS7001F combustion system to determine its combustion characteristics with fuels of the nature described above.

During 1990 a joint EPRI-Shell-GE program began the combustion "screening" test process with simulated coal gas fuels. Steam was used as a diluent and fuel gas compositions with heating values down to the 110 to 120 BTU/scf region were tested. This DOE-EPRI-GE program links those 1990 results, considers other diluents, considers the $H_2/CO/CO_2$ ratios and drives towards heating values below 100BTU/scf.

## PROJECT DESCRIPTION

At this point in August, 1993, all seven planned tests have been completed and the preliminary analyses have been performed for six of those tests. A great deal has been learned (as will be discussed in the results). To describe the project, the facility will be described, the fuel gases described and then scope, objectives and conduct of each of the seven tests will be discussed.

### A. Facilities Description

The combustion testing was performed in the GE Gas Turbine Development Laboratory (Fig. 1) in Schenectady, NY. In the combustion test bay (Fig. 2) are a number of combustion test stands that will each accommodate a single GE heavy frame combustor and simulate actual combustion conditions at rated temperature, pressure and airflow conditions. Fig. 3 is a picture of the 7F test stand during LBTU testing. Multiple fuel lines are needed to carry the high volume flow of LBTU fuel gas at elevated (500 deg.F) fuel gas temperatures.

The combustion test stand simulates the combustion section of the advanced (7F) gas turbine (Fig. 4). Facility air compressors, collectively rated at 18,000 HP, furnish the 50 pps at 210 psi needed to simulate full rated conditions. The fuel gas principal combustibles ($H_2$ and CO) are premixed by a gas supplier and trailered to the site. Each test used six trailers (Fig. 5) which were manifolded together and collectively provided about 600,000 standard cubic feet of gas storage at 2,000 psi. The balance of the fuel gas constituents, including $N_2$, $CO_2$, $CH_4$, steam and ammonia, are blended on line. This method provides both high mixing flexibility and the maximum amount of testing for the available trailer gas capacity.

The majority of testing was performed at half-flow, half-pressure, combustor design conditions which preserve normal velocities and residence times while significantly conserving fuel consumption.

A standard 7F combustion liner (Fig. 6) was used for all tests. Its nominal dimensions are 14" diameter by 30" long. Fig. 7 shows the combustion liner mounted in the test stand and Fig. 8 shows the end cover plate with the six fuel nozzles. In the first tests the standard 7F fuel nozzle configuration was used with the gas fuel orifices significantly enlarged to

| Constituent | EPRI SHELL PROGRAM | DOE Generic Mixture Dry | DOE Generic Mixture Wet | TECO GAS | TEST No. 7 |
|---|---|---|---|---|---|
| $H_2$ | 31.3 | 23 | 16.7 | 34.0 | 57 |
| CO | 62.7 | 7 | 4.8 | 49.0 | 43 |
| $CO_2$ | 1.5 | 20 | 14.3 | 9.7 | |
| $N_2$ | 4.5 | 47 | 34.2 | 6.1 | |
| $H_2O$ | (dry) | 0 | 26.7 | (dry) | (dry) |
| $CH_4$ | | 3 | 3.1 | 0.2 | |
| $NH_3$ | | | 0.1 | | |
| Other | | | 0.1 | 1.0 | |
| LHV (BTU/scf) | 287 | 113 | 89.0 | 251 | 295 |
| $H_2$/CO Ratio | 0.5 | 3.3 | 3.5 | 0.69 | 1.33 |

Table 1 Fuel Gases Tested

accommodate the extremely high volume flow of the LBTU fuel gas. In later tests an alternate nozzle design was used. Both nozzles are shown in Fig. 9.

B. Fuel Gases

For the purposes of these screening tests it was most appropriate to utilize data from the four 7F LBTU tests performed under the 1990 EPRI-SHELL-GE program. The characteristics of the Shell gas mixture are shown and the $H_2$/CO ratio of 0.5 is significant.

The majority of testing done in the DOE program segment was with fuel gas mixtures related to a generic air-blown process and dubbed "DOE generic" gas. The $H_2$/CO ratio for this gas is 3.3 to 1.

After the basic diluent screening tests it was appropriate to validate hypotheses with other gas mixtures so one test was run with the TECO project gas mixture at a $H_2$/CO ratio of 0.69. And finally, in Test No.7, an $H_2$/CO ratio of 1.33 to 1.

C. Test Plan

Test No.1 was set up to study the effects of $CO_2$ as diluent on the DOE basis fuel gas mixture. With a non-diluted fuel gas mixture the fuel lower heating value is about 285 Btu/scf. The addition of varying amounts of $CO_2$ lowered the fuel heating values to several different levels reaching as low as 114 Btu/scf. In addition to $CO_2$, a couple of steam diluent points were made for cross reference to the EPRI-SHELL tests.

Test No.2 was similar to Test No. 1 except that $N_2$ was used as the primary diluent. There were also several steam diluent points taken. Fuel heating values as low as 110 Btu/scf were reached with $N_2$ and as low as 104Btu/scf with a combination of $N_2$ and steam as diluents.

Test No.3 demonstrated the capability of the 7F combustor to burn a simulated air-blown LBTU fuel gas with all normal constituents. Five gas streams were blended simultaneously to obtain the correct mixtures of $H_2$/CO, $CO_2$, $N_2$, steam and $CH_4$. Fuel heating values down to 88 Btu/scf were run.

Test No.4 continued to use the $H_2$/CO ratio of the DOE generic gas. Its first purpose was to compare the combustion performance characteristics of a head-end nitrogen injection system with the results of Test No.2 where the nitrogen was blended with the fuel. More data points with nitrogen as diluent were also taken.

Test No.5 changed fuel gas to the TECO gas mixture with an $H_2$/CO ratio of 0.69 and collected a set of data with this different fuel together with both head-end nitrogen injection and nitrogen blending. $N_2$ and $CO_2$ were blended on line and fuel heating values in the 130 to 170 Btu/scf area were targeted.

Test No.6 reverted back to the DOE generic gas mixture to which trace amounts of ammonia and low levels of $CH_4$ were added. The objectives were to determine the conversion rates of fuel bound ammonia to NOx emission and observe the influence of small amounts of methane.

Test No.7 had been left open expecting that results from the earlier tests would provide direction. They did. The $H_2$/CO ratio was now considered to be influental on combustion stability limits so a midpoint fuel mixture with $H_2$/CO ratio of 1.33 to 1 was selected. Fuel gas inlet temperature was also varied over the range of 380 deg.F. to 650 deg.F. Fuel heating values as low as 88 Btu/scf were run.

## RESULTS TO DATE

The results of each of the tests, taken together with the 1990 EPRI-Shell-GE program data, have provided us an ever-developing picture of trends and relationships about LBTU fuel gas combustion.

Fig. 10 reflects data from the 1990 EPRI-Shell-GE combustion test program and traces the level of CO emission from an MS7001F combustor as the fuel heating value is varied by blending different amounts of steam with the fuel gas. The upper curve at 1100 deg.F. combustor temperature corresponds to the no-load, turbine idle, conditions while the 2550 deg.F. lower curve relates to full load, rated operating conditions. CO emission levels are an indicator of combustion efficiency and stability. At the full-load conditions, CO levels below 25 ppm are indicative of satisfactory combustion. The sharp turn-up of CO levels below 120 BTU/scf indicate a limit of satisfactory combustion for this combination of fuel gas and specific hardware.

As each of the tests of this program were run, new data points were added. Fig. 11 shows the results of the EPRI-Shell tests plus the first six tests of this program under the full firing temperature conditions. The first findings were that the CO turn-up d not occur as readily with the DOE generic gas mixtures; and we believe that this is due to the increased amount of hydrogen in fuel. Second, the slightly higher levels of CO associated with $CO_2$ as diluent are probably due to the very high percentage of $CO_2$ present its time-rate impact upon the equilibrium reactions. An earlier hypothesis may not be true. It had earlier been suggested that Shell gas (with steam diluent) achieved lower CO levels because of the presence of OH radicals in a high moisture environment which facilitate the conversion of CO to $CO_2$ leaving lower CO levels.

Fig. 12 shows the levels of NOx emissions as a function of fuel heating value for moisturized fuel gas in the EPRI-Shell test series. As the diluent (steam) is increased, the fuel heating value decreases, the primary zone flame temperature decreases, and less NOx is produced. At fuel heating values below 150 Btu/scf, the projected NOx emissions levels moved into the very favorable region below 25 ppm. The lower curve represents the majority of test points which were taken at half flow, half pressure conditions. The upper curve shows that emissions data projected to full flow full temperature conditions. Only one full pressure verification point was done in the EPRI-Shell tests.

When the NOx emission levels of DOE Test No.1 were compared to those of the EPRI-Shell test the first impression was that the use of $CO_2$ as a diluent yielded lower NOx levels. However, should the baseline heating value scale was changed to a mass basis (BTU/lbm), instead of the volumetric basis (BTU/scf), the impression reversed. The curve for $CO_2$ as diluent appeared to

indicate higher levels of NOx emissions for the "same" heating value fuel gas. This is because the mole weights of the two fuels were different. And because of the different mole weights and specific heats, the stoichiometric flame temperatures, and consequently the NOx emission levels, are therefore different for the "same" fuel heating value. We realized we needed a better and more common baseline than the fuel heating value. Stoichiometric flame temperature was the better base line!

In Fig. 13, the calculated stoichiometric flame temperature is used as a baseline for NOx emission and a wide collection of data points with both Shell gas and DOE test gas are plotted. We also found that the NOx scale could be normalized to percent NOx and thereby automatically correct for pressure levels and other operating variables. The results indicate that for the diffusion type flame combustion process in the 7F combustor, the generation of thermal NOx is not significantly influenced by the $H_2$/CO ratio or by whether the diluent is moisture, nitrogen or $CO_2$. The generation of thermal NOx is most directly related to the stoichiometric flame temperature.

As a matter of general interest, the measurement of NOx in our combustion test laboratory is done by use of a single, high volume flow, bleed-off line taking exhaust gases from the aft side of the simulated first stage turbine nozzle. The bleed-off line carries the sample exhaust gas to an emissions instrument panel where the levels of CO, $CO_2$, NO, NOx, $O_2$ and unburned hydocarbons (UHC) are measured with separate instruments. NO and NOx are both measured by the chemiluminescent method with Rosemont Model 955 instruments. A converter ahead of one instrument converts the $NO_2$ to NO enabling that instrument to effectively measure NOx. The split between NO and $NO_2$ varies with combustion conditions.

Tests 4 & 5 especially considered the effectiveness of head-end nitrogen injection versus fuel blended nitrogen as a means of reducing NOx emission levels. The results are shown in Fig.14 and indicate that when nitrogen is introduced into the head end of the combustor (through the same center port used for steam injection) the NOx reduction is nearly as effective as when the equivalent amount of nitrogen is premixed (blended) with the fuel gas. As expected, there was also no reduction in combustion stability with the head end nitrogen injection.

In Test No.6, the conversion rate of fuel-bound ammonia was explored by injecting increasing amounts of a 33% solution of ammonium hydroxide into the fuel gas and measuring the resulting levels of NOx in the exhaust gas. Fig.15 depicts the preliminary indicated results. The upper curves at two firing temperatures show the NOx emission levels while the two lower curves reflect the calculated conversion ratio. The appearance of lower NOx levels at higher operating temperatures is the result of application of the regulatory 15% $O_2$ correction formula. The lower-than-expected conversion ratios are to be considered as very preliminary laboratory findings. It is not certain that all the ammonia injected into the 500 deg.F. fuel gas line thirty feet before the test combustor was still entering the combustion chamber as ammonia. More work must still be done in this area.

## PRELIMINARY CONCLUSIONS

This program is a three-party joint effort of the DOE, EPRI and GE that has forged significant progress for understanding the LBTU syngas capabilities of an advanced gas turbine combustor. As a result of this program:

1. GE Engineering is now confident that the syngas fuels produced by all currently- viable coal gasifiers can be accommodated by the GE advanced ("F" Technology) combustion system.

2. For proposed syngas fuels with varying amounts of steam, nitrogen or $CO_2$ diluent, the combustion and emissions characteristics can be reasonably estimated without undertaking expensive new screening tests for each different fuel.

GE is appreciative of the DOE and EPRI encouragement and support for this program.

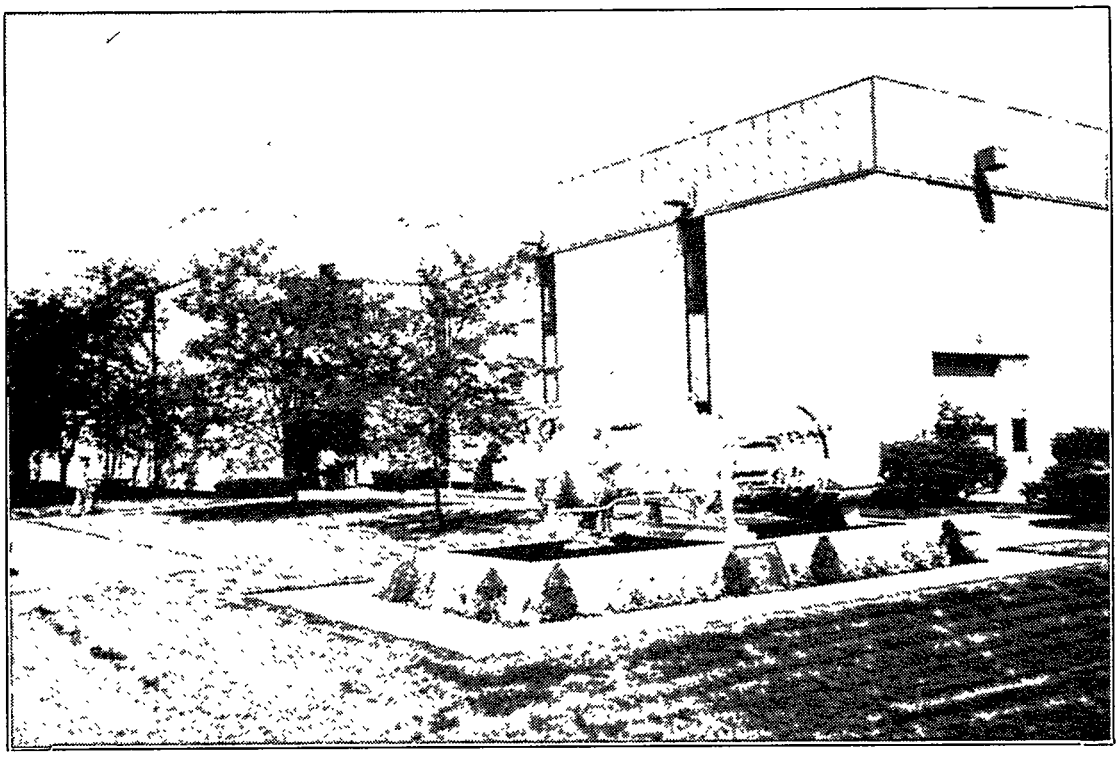

Figure 1, GE Gas Turbine Development Laboratory, Schenectady, NY

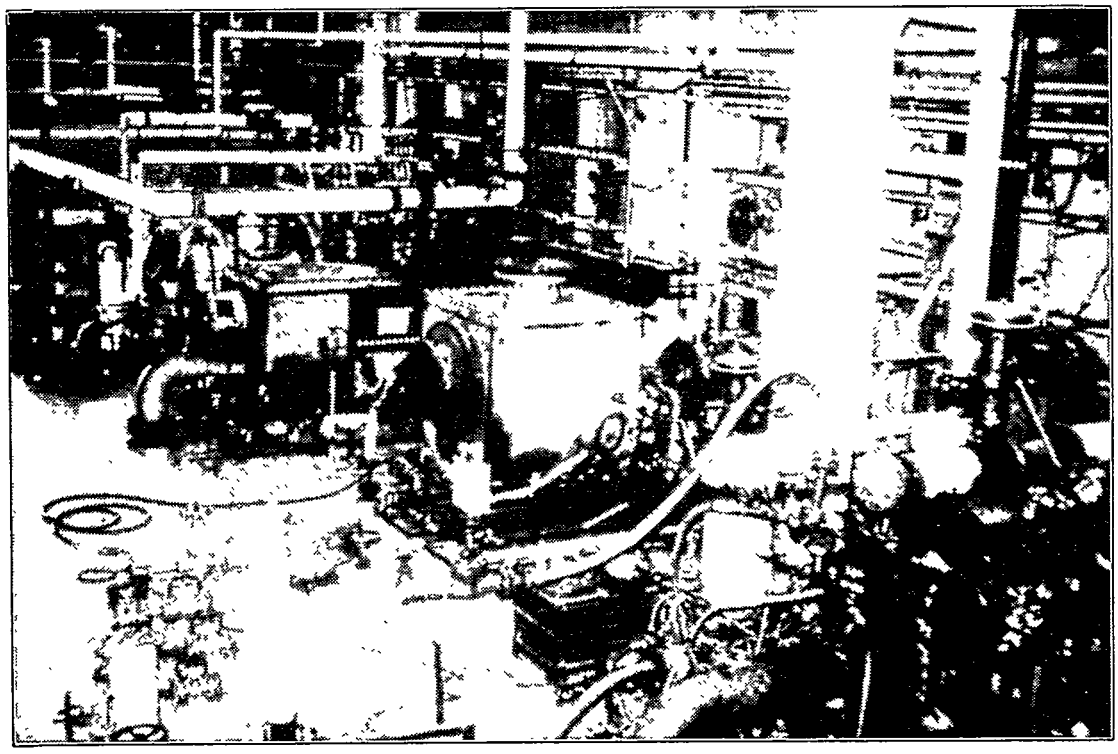

Figure 2. Combustion Test High Bay

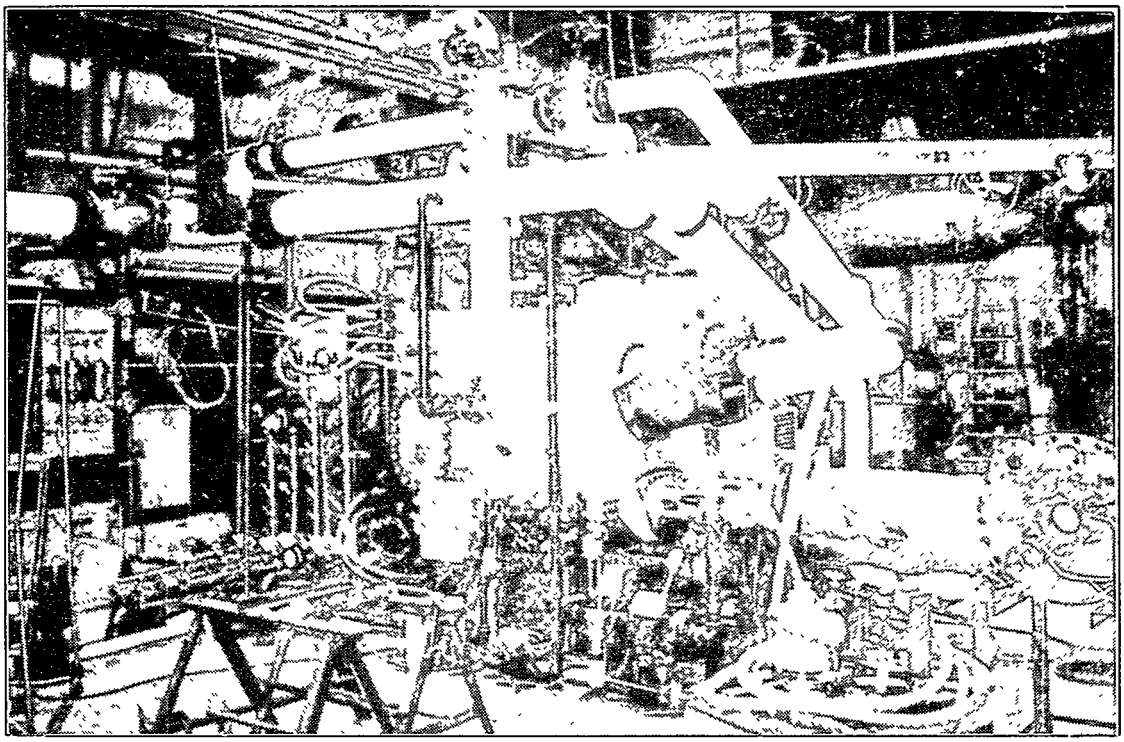

Figure 3. "7F" Combustion Test Stand with LBTU Fuel Gas Piping

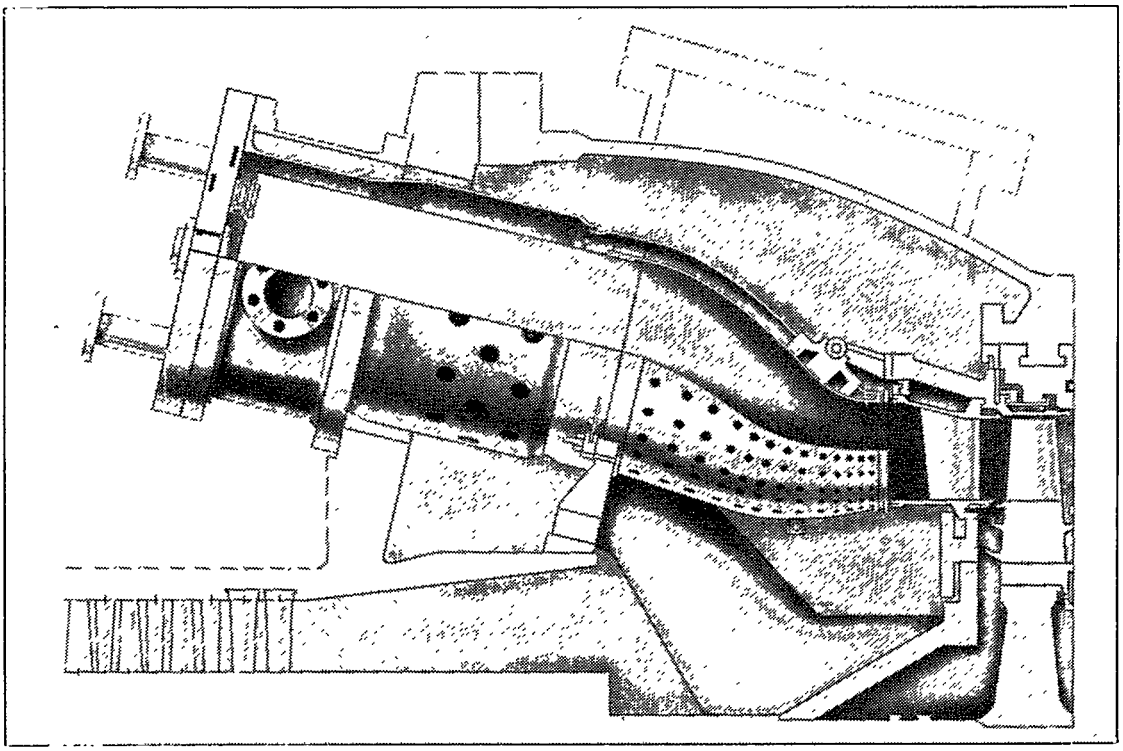

Figure 4. GE Reverse Flow "F" Technology Combustion System

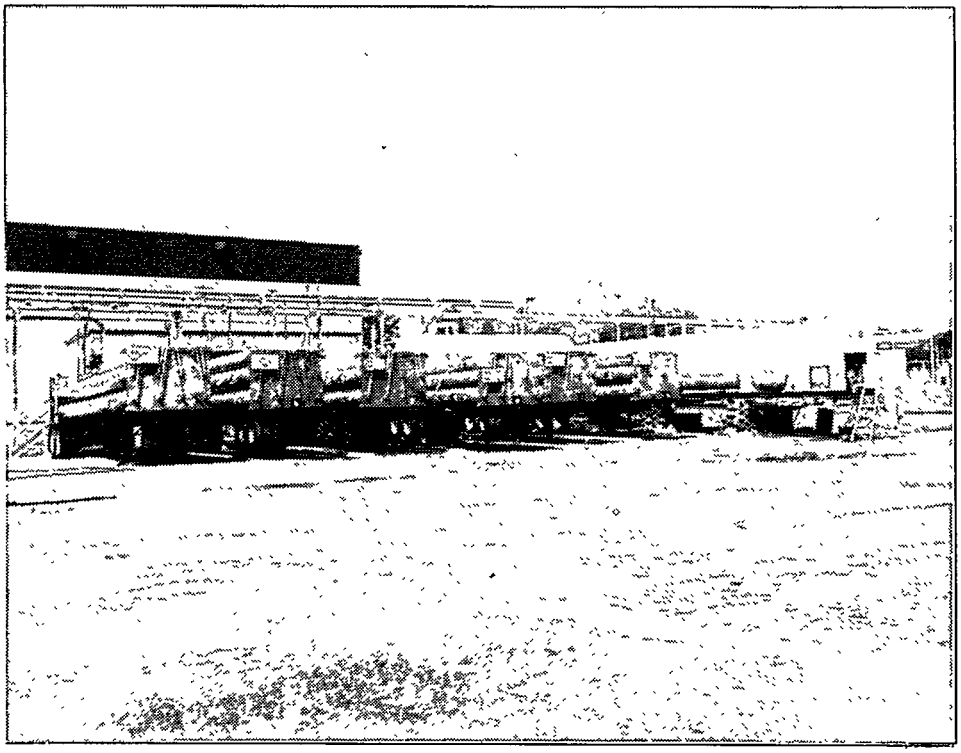

Figure 5. Fuel Gas Trailers at Trailer Dock

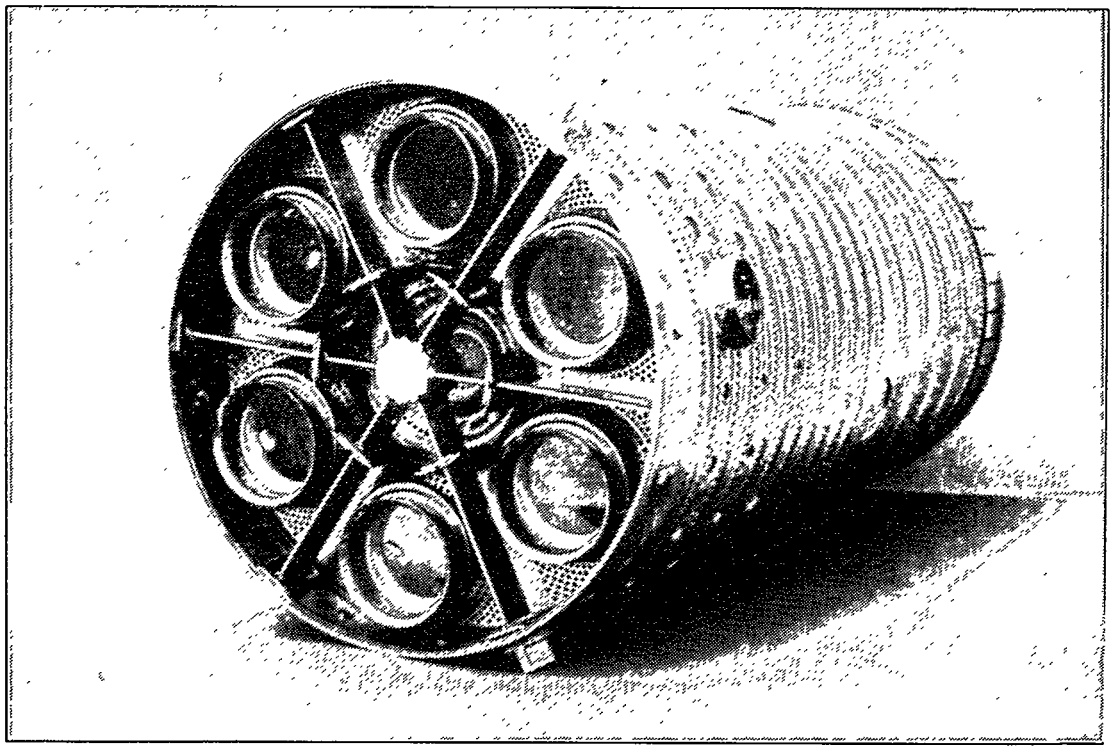

Figure 6. Standard "7F" Combustion Liner

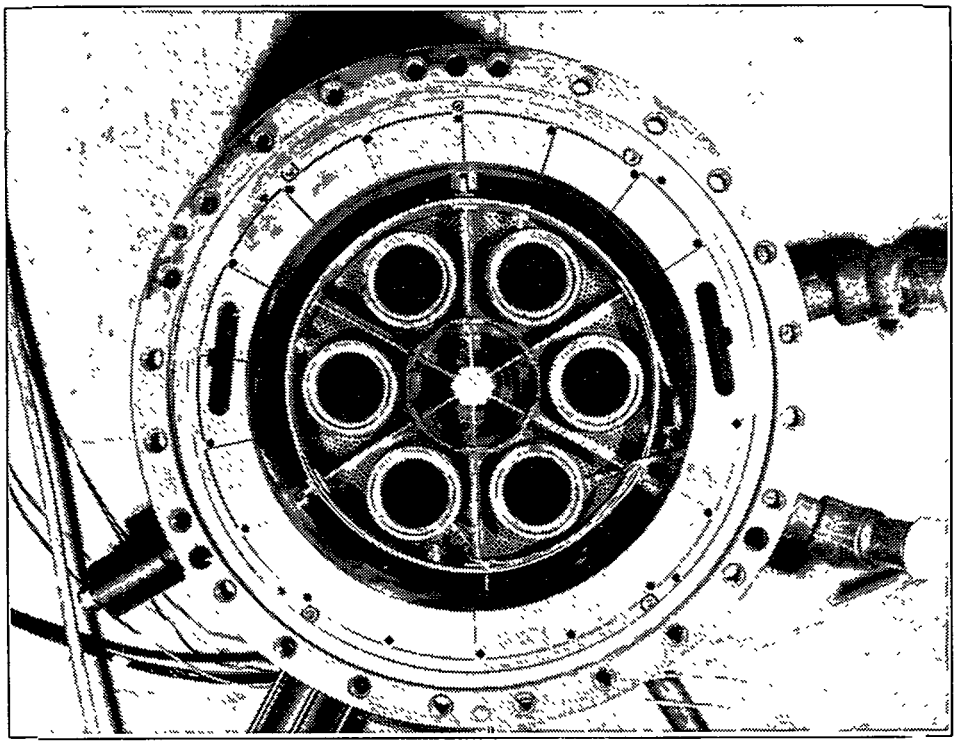

Figure 7. Combustion Liner Mounted in Combustion Test Stand

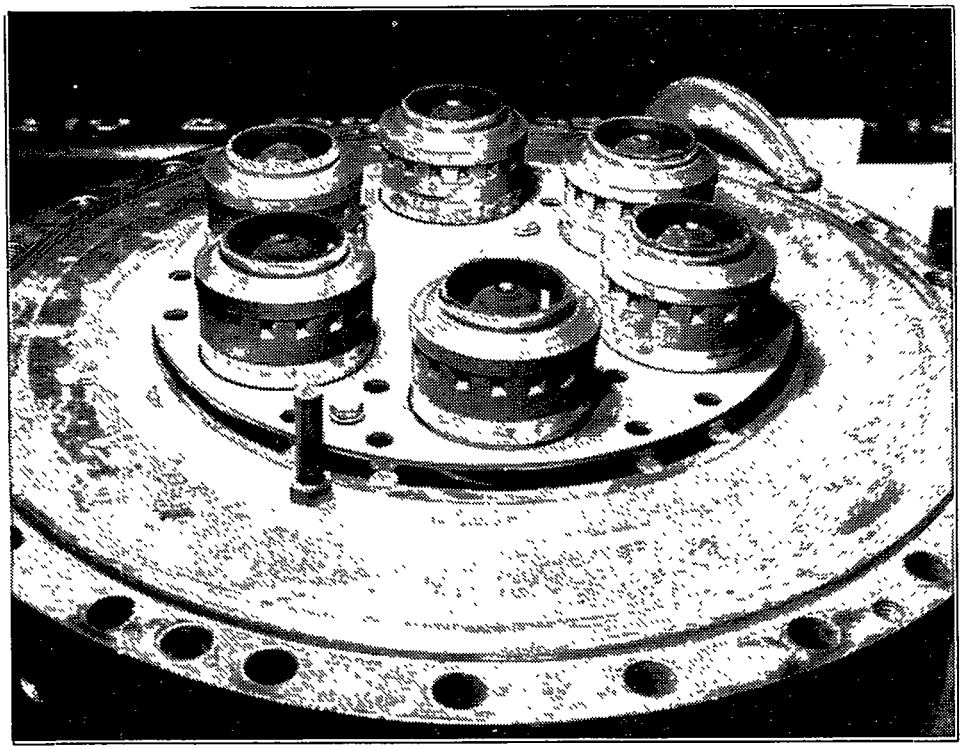

Figure 8. Fuel Nozzles Mounted on End Cover

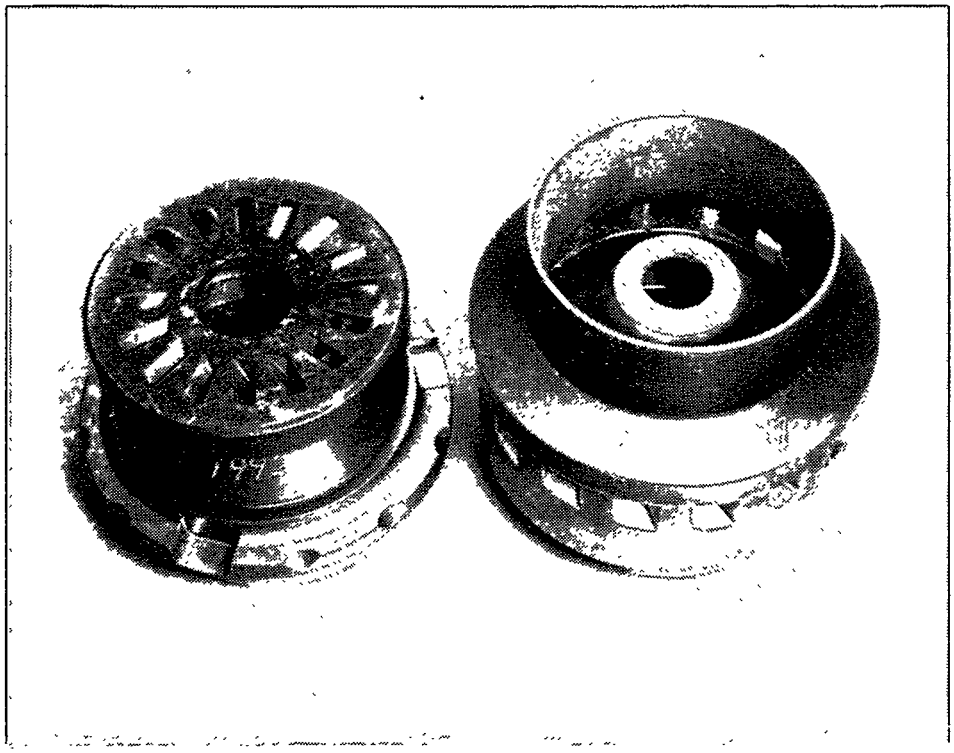

Figure 9. Standard Fuel Nozzle (Left) and Modified Nozzle (Right)

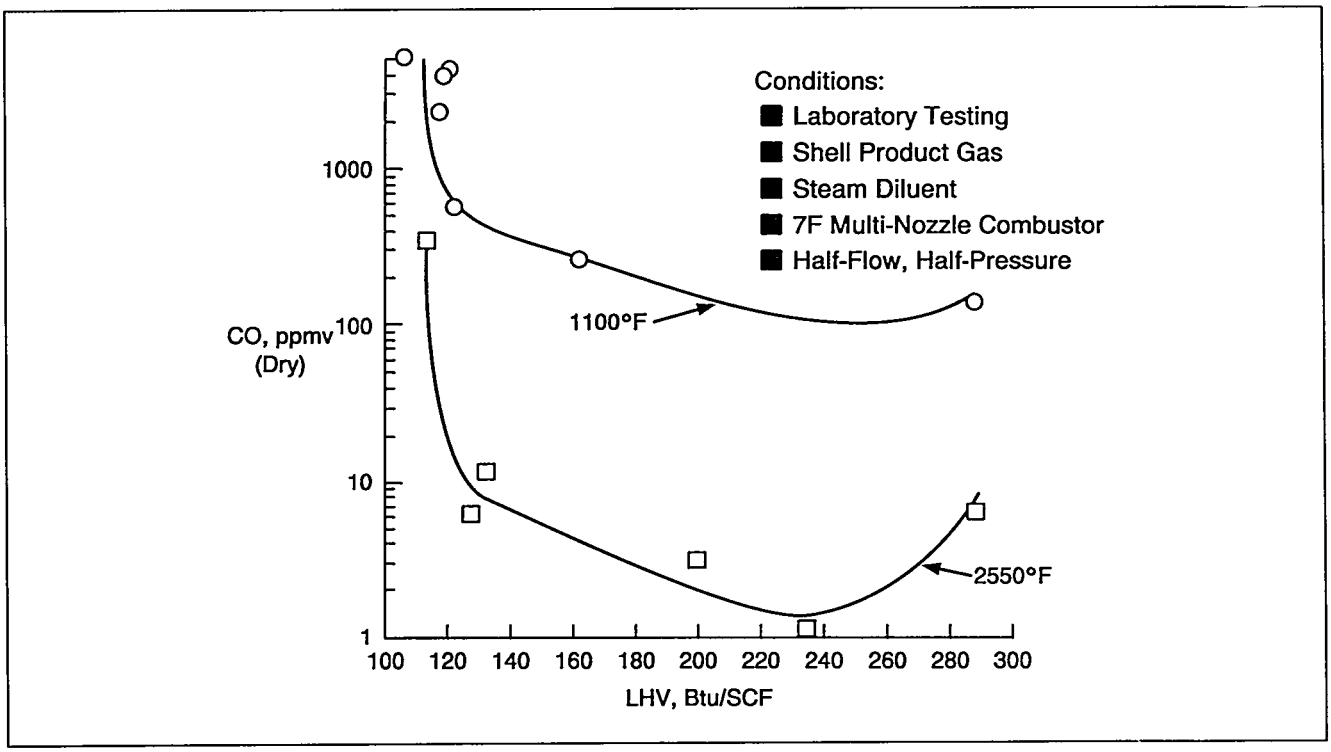


Figure 10. CO Emission vs. Heating Value with Steam Diluent

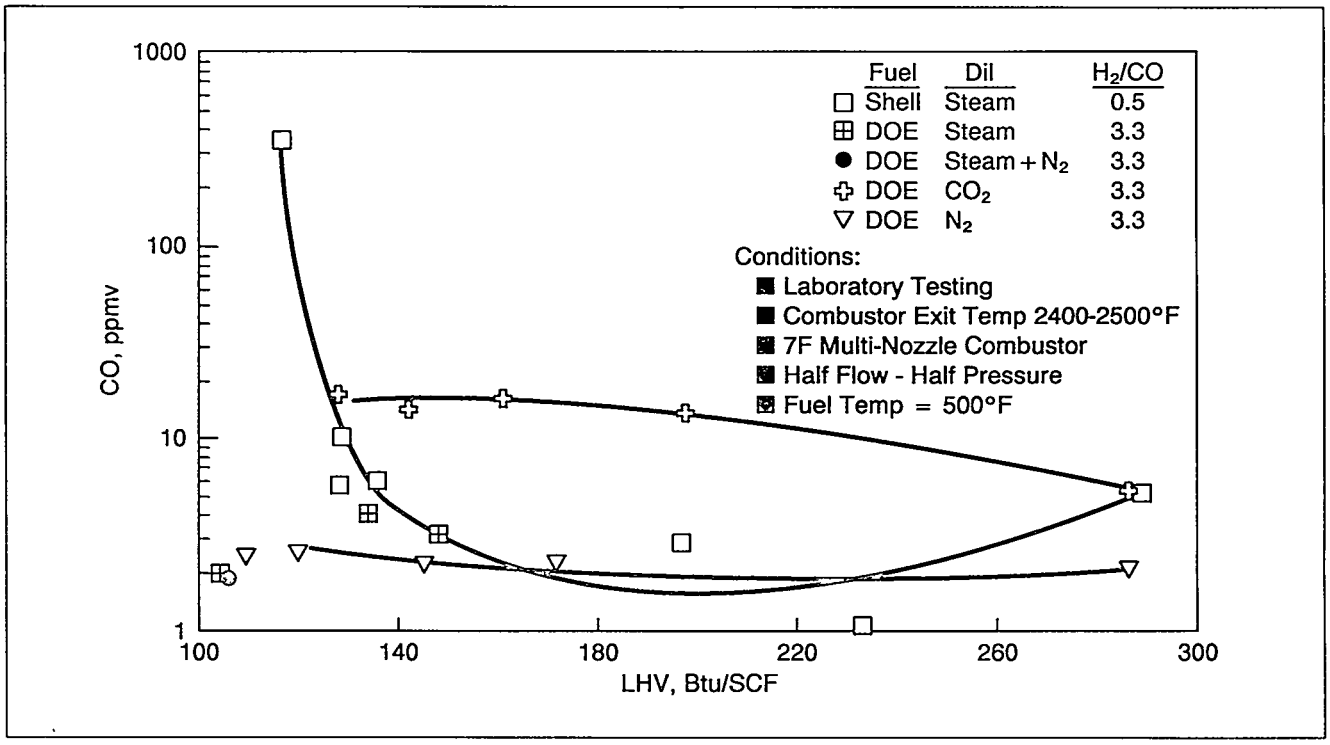


Figure 11. CO Emissions as a Function of Volumetric LHV and Diluent Type

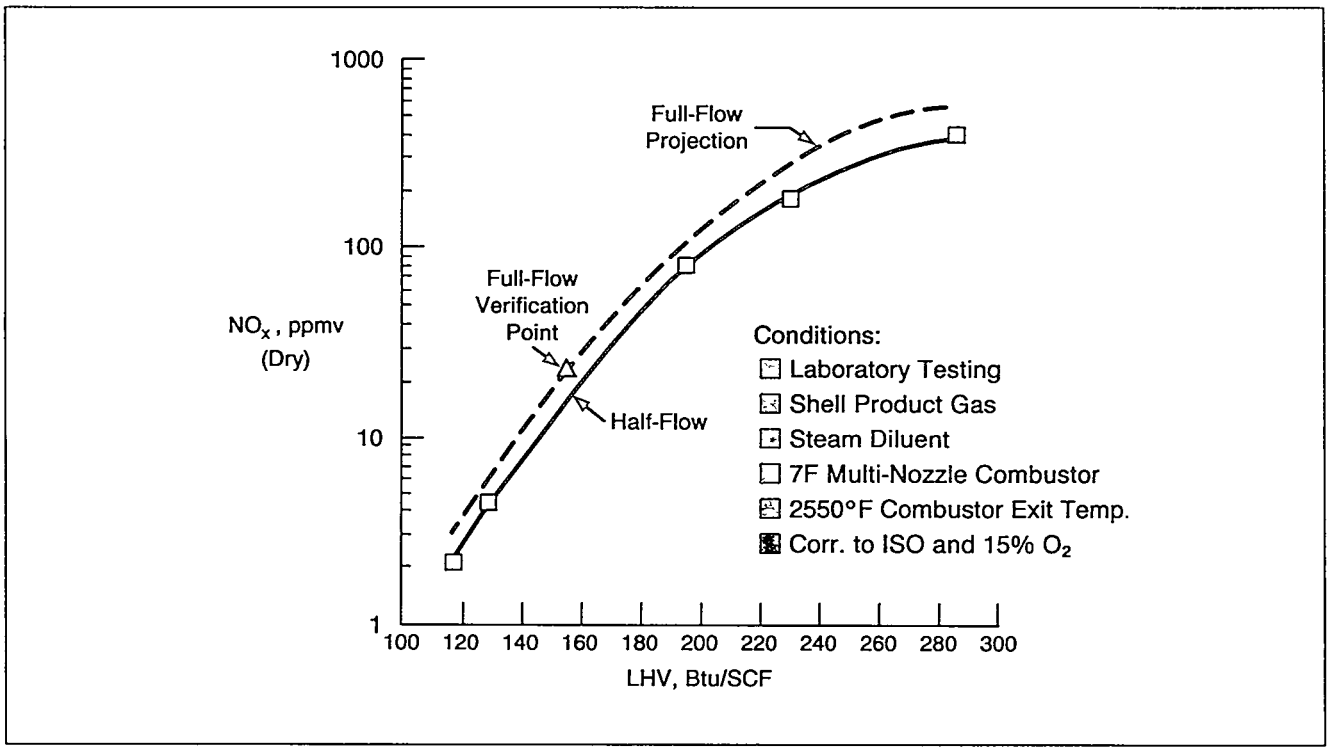


Figure 12. NOx Emissions vs. Heating Value from EPRI/Shell Tests

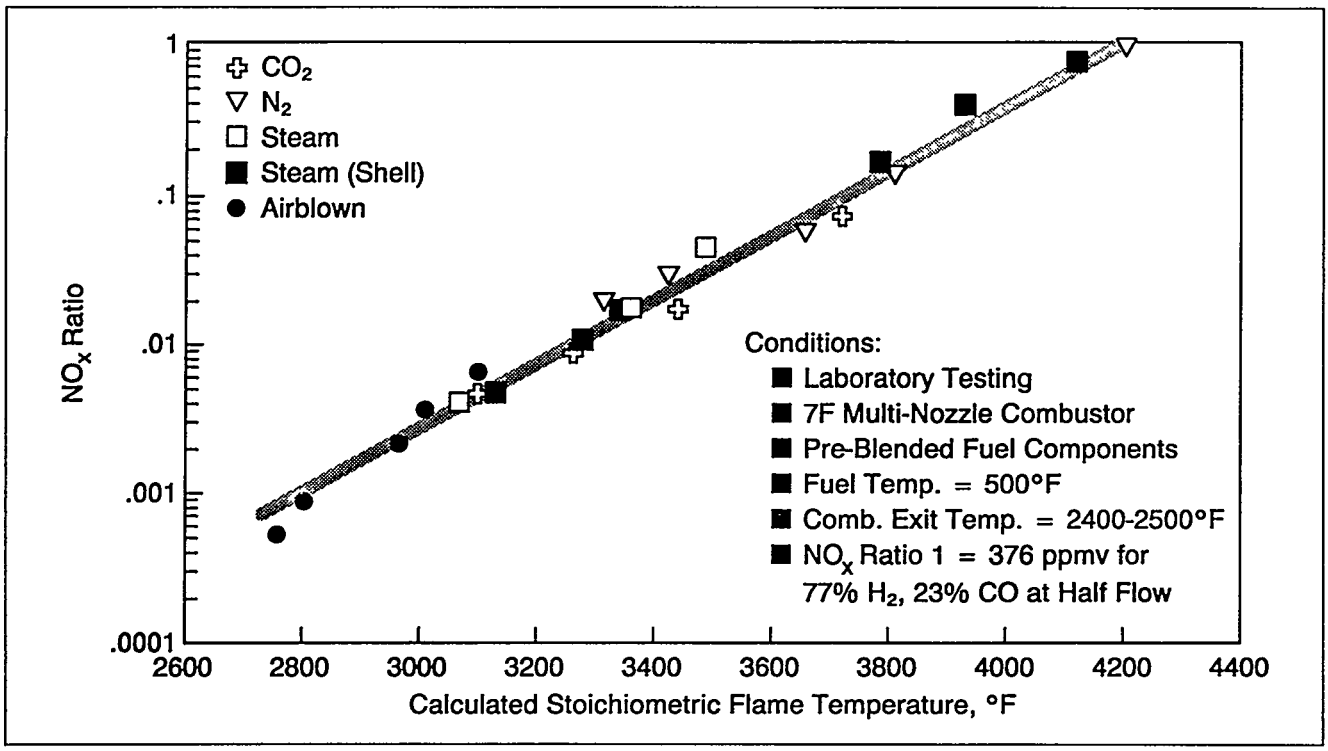


**Figure 13. NOx Reduction as a Function of Stoichmetric Flame Temperature**

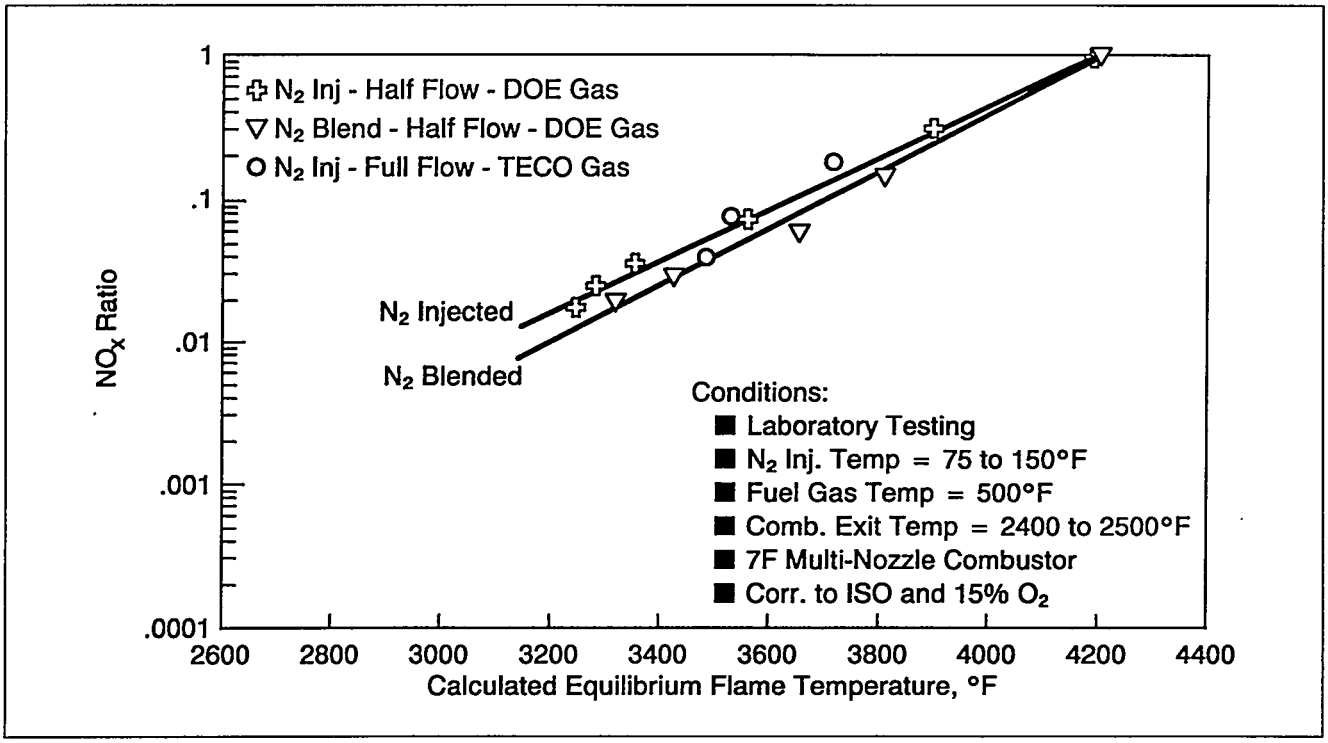


**Figure 14. NOx Emissions for Head-End Nitrogen Injection vs. Nitrogen Blended with the Fuel**

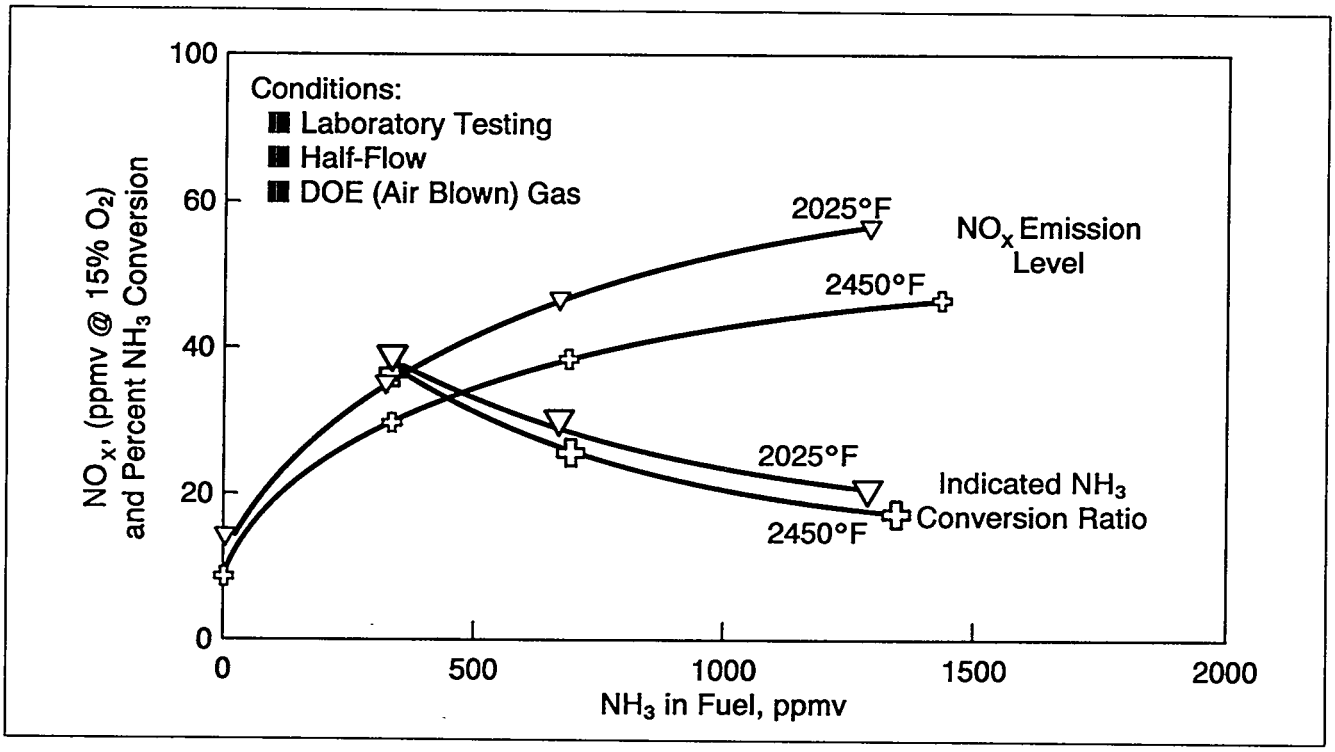


**Figure 15. Ammonia Conversion Rate - (Preliminary Findings)**

## 1.6 Combustion Tests of a Turbine Simulator Burning Low Btu Fuel From a Fixed Bed Gasifier

### CONTRACT INFORMATION

**Contract Number** DE-AC21-87MC23170

**Contractor** GE Environmental Services, Inc.
200 N. Seventh St.
Lebanon, PA 17042
(717) 274–7000

**Contractor Project Manager** Charles S. Cook

**Principal Investigators** Nesim Abuaf, GE Corporate Research and Development
Alan S. Feitelberg
Stephen L. Hung
David J. Najewicz
Martin S. Samuels

**METC Project Manager** Justin L. Beeson

**Period of Performance** September 30, 1987 to September 30, 1993

**Schedule and Milestones**

**Program Schedule**

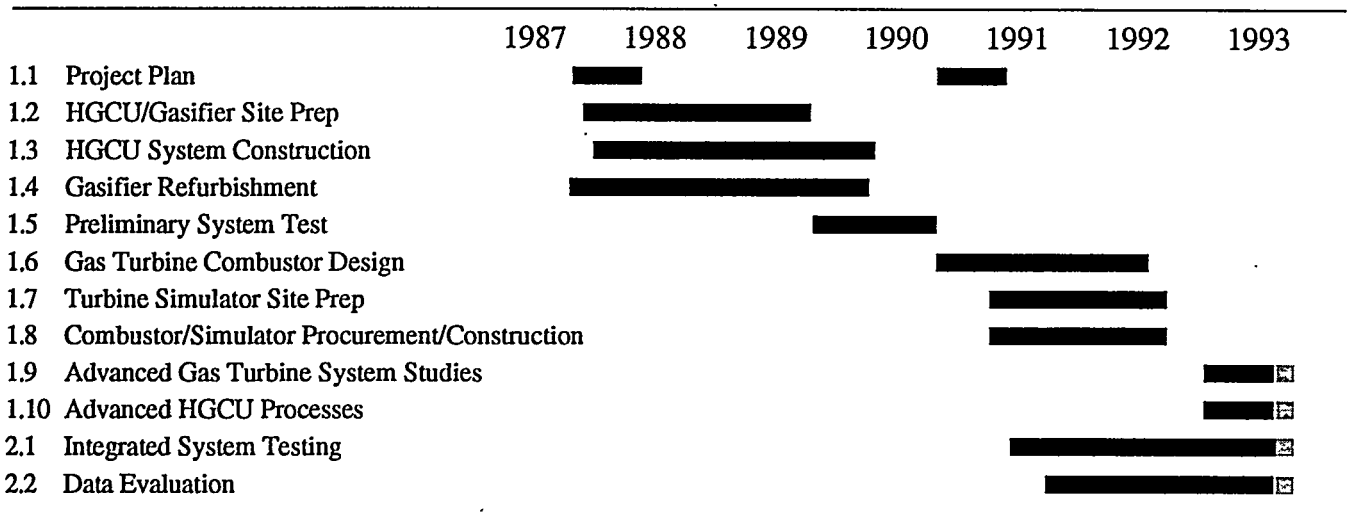

## OBJECTIVES

One of the most efficient and environmentally compatible coal fueled power generation technologies is the integrated gasification combined cycle (IGCC) concept. When IGCC is coupled with high temperature desulfurization, or hot gas cleanup (HGCU), the efficiency and cost advantage of IGCC is further improved with respect to systems based on conventional low temperature gas desulfurization. Commercialization of the IGCC/HGCU concept requires successful development of combustion systems for high temperature low Btu fuel in gas turbines. Toward this goal, a turbine combustion system simulator has been designed, constructed, and fired with high temperature low Btu fuel. Fuel is supplied by a pilot scale fixed bed gasifier and hot gas desulfurization system. The primary objectives of this project are: (1) demonstration of long term operability of the turbine simulator with high temperature low Btu fuel; (2) measurement of $NO_x$, CO, and particulate emissions; and (3) characterization of particulates in the fuel as well as deposits in the fuel nozzle, combustor, and first stage nozzle.

In a related project, a reduced scale rich-quench-lean (RQL) gas turbine combustor has been designed, constructed, and fired with simulated low Btu fuel. The overall objective of this project is to develop an RQL combustor with lower conversion of fuel bound nitrogen (FBN) to $NO_x$ than a conventional combustor.

## BACKGROUND INFORMATION

Combustion of the high temperature (~1000°F) low Btu fuel produced from an IGCC/HGCU system is significantly different from the combustion of typical gas turbine fuels, such as natural gas and fuel oils. Differences in the air/fuel ratio, fuel composition, and fuel temperature affect many of the combustor operating parameters including the lean blowout limit, flame stability, and emissions. These differences require modification of the fuel nozzle and combustor liner. In addition, gas turbines used in IGCC/HGCU applications will require fuel control valves that are capable of operating with high temperature low Btu fuel. Other concerns include the possibility that particles and vapor phase contaminants in the fuel may form deposits on and/or cause the corrosion of the fuel nozzle, combustor liner, and turbine blades.

Rich-quench-lean (RQL) combustion is a well known method for reducing $NO_x$ emissions from the combustion of fuels that contain bound nitrogen. The low Btu fuel produced in an IGCC/HGCU system will contain hundreds to thousands of parts per million of FBN, depending upon the coal composition and the process conditions. In this context FBN refers to all nitrogen-containing compounds other than $N_2$. The most abundant bound nitrogen species in low Btu fuel is typically $NH_3$.

A large fraction of the bound nitrogen in the fuel will form $NO_x$ in a conventional combustor. RQL combustion can achieve lower $NO_x$ emissions from fuels containing bound nitrogen because a large fraction of the FBN is converted into non-reactive $N_2$ on the fuel rich stage. Additional air is introduced on the quench stage, and the lean stage provides the residence time needed to achieve complete combustion.

Although the basic principles of RQL combustion are well known, there are several research issues associated with the development of a practical RQL gas turbine combustor. For example, the optimal air split between the rich and lean stages depends upon many factors, including the fuel composition. The required rich stage residence time is linked to the degree of fuel/air premixing on the rich stage. Increasing the degree of

premixing can reduce the rich stage residence time required for low $NO_x$ emissions. The burned gas exiting the rich stage must be quenched rapidly to prevent thermal $NO_x$ formation. For this reason rapid quench methods need to be developed.

## PROJECT DESCRIPTION

### Turbine Simulator

Figure 1 shows the low Btu gas turbine simulator that has been constructed and integrated with the coal gasification/hot gas cleanup facility at GE Corporate Research and Development in Schenectady NY. The pilot scale gasification/hot gas cleanup system consists of a fixed bed gasifier, a primary cyclone for particulate removal, a moving bed high temperature desulfurization system, and a polishing cyclone. The turbine simulator is designed to operate at the full capacity of the gasifier, 8000 lb./hr of fuel gas from the gasification of 1800 lb./hr of coal. The low Btu fuel is supplied at a pressure of 20 atm and a temperature of 1000°F. A typical fuel composition (after $H_2S$ removal) is given in Table 1. Details of the gasifier and the hot gas cleanup system can be found in Cook *et al.* (1992, 1991).

The turbine simulator includes: a low Btu fuel nozzle; a modified GE MS6000 combustor liner; a film cooled, first stage LM6000 nozzle

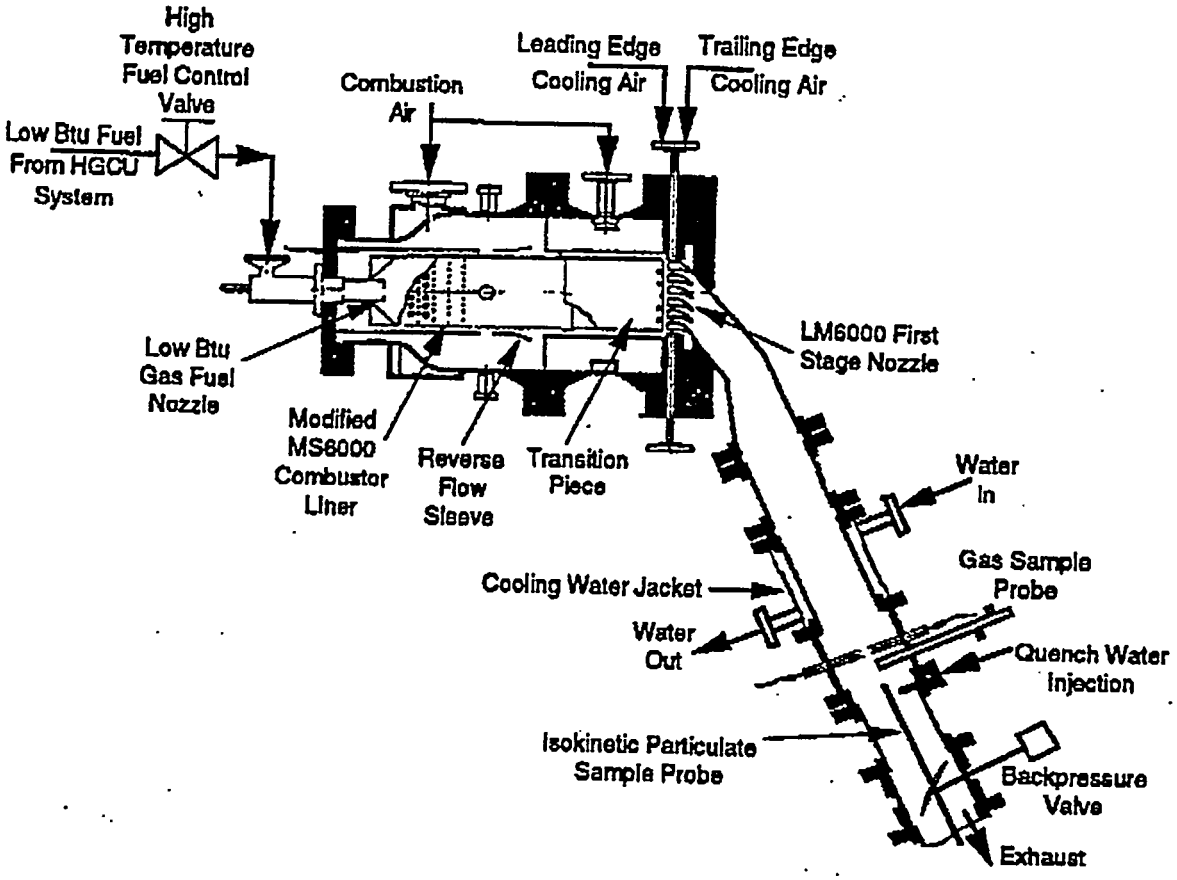


**Figure 1. The Turbine Simulator Test Stand**

assembly, and an impingement cooled transition piece. A GE MS6000 combustor liner was chosen because its fuel requirements match the capacity of the gasifier/HGCU system. The liner was modified to meet the air requirements of low Btu fuel combustion, while the reverse flow sleeve is standard hardware. The fuel nozzle was designed specifically for low Btu gas combustion (Lawson, 1985). A film cooled LM6000 first stage nozzle was chosen to simulate the film cooled nozzles found in advanced gas turbines with high firing temperatures.

Design of the turbine simulator was initiated in April 1991. Fabrication and assembly were completed in August 1992. The current test plan includes five fired tests with coal gas from the pilot scale gasifier/HGCU system, designated as Runs 3, 3A, 4, 5, and 6. Run 3 was completed in September 1992; Run 3A was completed in February 1993; and Run 4 was conducted in June 1993. Runs 5 and 6 will be completed in the third and fourth quarters of 1993.

**Table 1. Typical Pilot Plant Low Btu Fuel Composition**

| Species | Mole Percent |
|---|---|
| CO | 8.6 |
| $H_2$ | 17.3 |
| $CH_4$ | 2.7 |
| $N_2$ | 30.1 |
| $CO_2$ | 12.6 |
| $H_2O$ | 28.0 |
| Ar | 0.3 |
| $NH_3$ | 0.4 |
| TOTAL | 100.0 |

### Rich-Quench-Lean (RQL) Combustor

The reduced scale RQL combustor that has been designed and tested with simulated low BTU fuel is shown in Figure 2. Nominal design conditions are 0.75 lb./s total flow, 650°F inlet air temperature, and combustor exit temperatures up to 2500°F. The RQL combustor has a modular design, which allows for rapid evaluation of different hardware configurations. The rich and lean stages are separate components, and the air flow to each stage can be independently varied. Both stages are cooled by reverse flow sleeves. To improve cooling, the rich and lean stage liners have been coated with a ceramic thermal barrier coating on the combustion side. A surface roughness coating and a boundary layer trip wire have also been applied to the backside of each stage.

Design of the RQL combustor began in December 1991. Following construction and assembly, the first fired tests of the RQL combustor with natural gas/nitrogen/ammonia blends began in January 1992. Room temperature natural gas/$N_2$/$NH_3$ blends were chosen for these tests because they simulate some of the characteristics of high temperature low Btu fuel (see Figure 3). A test with high temperature low Btu fuel from the pilot plant gasifier/HGCU system is scheduled for 1993.

## RESULTS

### Turbine Simulator

The turbine simulator was fired with coal gas for a total of 10 hours during Run 3 and 47 hours during Run 3A. Due to operating problems with the gasifier and HGCU system, the turbine simulator was fired for only 14 hours during Run 4. The gasifier was fueled with Illinois #6 coal for Run 3, while an anthracite coal was used for Run 3A. The use of anthracite for Run 3A was dictated by HGCU system related issues. For Run 4, the gasifier was fueled with Illinois #6 and Crown II coal.

Figure 4 shows the measured combustor exit temperature over a typical time period during run 3A. The initial time in Figure 4 corresponds to 1 AM on the morning of February 10, 1993. Overall, the combustion of low Btu fuel in the turbine simulator was stable and the turbine simulator was easy to control.

The oscillations in temperature shown in Figure 4 ($\pm 90°F = \pm 1\sigma$) correlate well with the heating value of the low Btu fuel, which in turn correlates with the position of the stirrer in the fixed bed gasifier. To reduce the temperature fluctuations, the manual fuel control used for Runs 3 and 3A was replaced with an automatic fuel control system for Run 4. Figure 5 shows the measured combustor exit temperature over a typical time period during Run 4. Comparison with Figure 4 shows that the automatic fuel control system substantially reduced the temperature oscillations.

The combustor liner, transition piece, and cascade metal temperatures were all within design limits at full flow conditions. There were periods of low fuel flow during Run 3A, and during these periods the air flow was reduced to maintain high combustor exit temperatures. Combustor liner and transition piece temperatures increased to allowable limits during these transient periods. After Run 3A a small (1 inch diameter) hole was found in the head end of the combustor, and the hole is believed to have been formed during one of the transient periods of low air flow. To solve this problem the combustor liner was modified to increase the air flow through the head end of the combustor. No problems with the modified liner were encountered during Run 4.

Figure 6 shows typical $NO_x$ emissions measured during Run 3A, over the same time period as shown in Figure 4. Over the entire run, $NO_x$ emissions averaged about $180 \pm 20$ ppmv on a dry, 15% $O_2$ basis. CO emissions were generally below the detection limit of 1 ppmv. $NO_x$ emissions were not correlated with firing temperature, suggesting that the majority of the $NO_x$ formed came from the $NH_3$ and other FBN species in the fuel. The average measured ammonia concentration in the fuel was approximately 2700 ppmv, indicating that the conversion of $NH_3$ to $NO_x$ was about 39%.

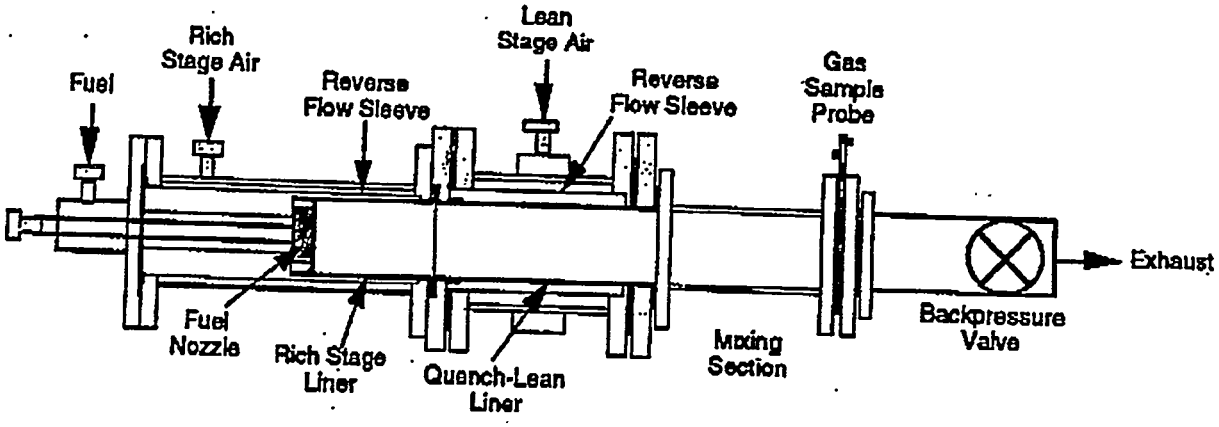


**Figure 2. Reduced Scale Rich-Quench-Lean (RQL) Combustor**

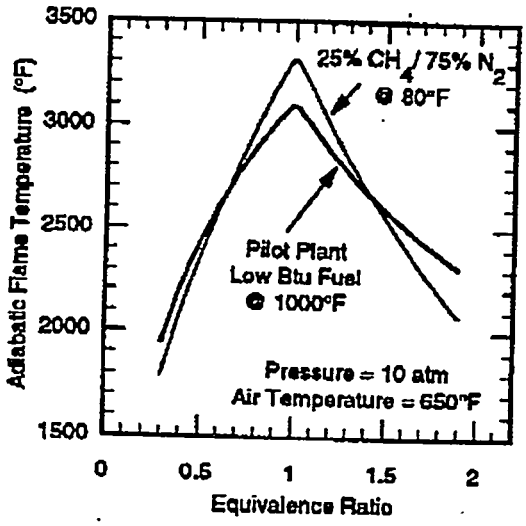


**Figure 3. Comparison of Pilot Plant Fuel and Natural Gas/$N_2$ Blend.**

The anthracite coal used in Run 3A resulted in abnormally high particulate loadings in the low Btu fuel. When gasifying Illinois #6 coal, particulate loadings of 30 to 40 ppmw are typically found in the low Btu fuel leaving the HGCU system, versus the 200 ppmw found during Run 3A. The high particulate loadings in the fuel resulted in reddish-brown deposits on the combustor liner, transition piece, and cascade. Elemental analysis revealed that the composition of the deposits was similar to the composition of the coal ash. The relatively high deposition rate seen in Run 3A is not representative of the deposition rate expected in a commercial IGCC/HGCU power plant equipped with a barrier filter just upstream of the combustor.

Although a barrier filter can remove particulates in the fuel with high efficiency, it may have little effect on the concentrations of vapor-phase contaminants. Vapor-phase levels of alkali metal species are of particular interest, since alkali metals are the principal agents of hot corrosion. To address this issue we have used thermodynamic equilibrium to calculate maximum expected vapor-phase alkali metal levels in hot coal gas. The calculations were performed with a slightly modified version of the NASA chemical equilibrium program (Gordon and McBride, 1976; McBride, 1989). The coal gas composition listed in Table 1 was used for the calculations, with the addition of 200 ppmv HCl, 50 ppmv of $H_2S$, and sufficient amounts of sodium and potassium to insure the existence of condensed sodium and potassium species in the equilibrium mix.

The two principal sources of thermodynamic data were the JANAF Thermochemical Tables (Chase *et al.*, 1985) and the extensive compilation of Barin (1989). In addition to all of the major carbon-, hydrogen-, oxygen-, nitrogen-, and sulfur-containing species, some 60 solid, liquid, and vapor sodium and potassium species were considered. In particular, the alkali cyanides, chlorides, hydrides, carbonates, oxides, hydroxides, sulfides, and sulfates were included in the calculations. Solid carbon (coke) was excluded from the equilibrium composition, based upon kinetic constraints.

Table 2 lists the calculated vapor-phase alkali metal concentrations at coal gas temperatures of 1000°F and 1200°F. Only the most abundant alkali metal species are listed in Table 2; all other alkali metal species were present in the vapor phase at concentrations below 0.1 ppb by weight as Na or K. At 1000°F, the total vapor-phase alkali species levels are well within gas turbine limits. At this temperature, the bulk of the sodium is predicted to exist in the solid phase as sodium carbonate ($Na_2CO_3$), and the bulk of the potassium is predicted to exist in the solid phase as potassium cyanide (KCN). As the temperature increases, vapor phase sodium and potassium chloride concentrations increase dramatically. Note that both NaCl and KCl dimerize in the vapor phase, and that the contributions of $(NaCl)_2$ and $(KCl)_2$ are significant.

Sodium and potassium silicates and aluminates were not included in the thermodynamic calculations. If these species were included, the predicted vapor phase concentrations of sodium and potassium species would be significantly reduced. For this reason, the values listed in Table 2 probably overestimate the actual vapor phase concentrations of alkali species.

**Rich-Quench-Lean (RQL) Combustor**

Typical $NO_x$ and CO emissions from the RQL combustor are shown in Figure 7. For this test the fuel was a blend of natural gas and nitrogen (25.0 volume percent natural gas, 75.0 volume percent nitrogen), and contained no ammonia. The rich stage air temperature was not identical to the lean stage air temperature because the two stages are fed by two separate air lines with different diameters and different heat losses. The rich stage and lean stage air flow rates were held constant as the total fuel flow rate was varied. In this manner the ratio of the rich stage equivalence ratio ($\varphi_{rich}$) to the lean stage equivalence ratio ($\varphi_{lean}$) was held constant. A practical RQL gas turbine combustor will probably have to operate at a fixed air split, that is, a fixed $\varphi_{lean}/\varphi_{rich}$.

Complete combustion (CO less than 1 ppmv) was achieved under almost all conditions, as long as the lean stage temperature was greater than 1800°F. As the lean stage temperature decreased below about 1750°F, CO increased sharply. A sharp increase in CO emissions as burned gas temperature decreases is commonly observed near blowout. In this case the lean stage was approaching blowout, even though the rich stage was still lit and far from blowout.

Figure 7 shows that $NO_x$ emissions are very sensitive to the air split between the rich and lean stages, or $\varphi_{lean}/\varphi_{rich}$. This result was expected from previous experimental work and chemical kinetic modeling (Goebel and Feitelberg, 1992). Figure 7 also shows that $NO_x$ emissions decrease monotonically as the combustor exit temperature decreases. Previous work suggested that there should be a minimum in $NO_x$ emissions in Figure 7, that is, an optimum $\varphi_{rich}$. The most probable reason for the difference between these results and the previous work is the structure of the rich stage flame. In the previous work, and in the chemical kinetic models, the rich stage flame was premixed. The scaled down low Btu fuel nozzle used in these tests creates a diffusion flame. While a diffusion flame is advantageous from a

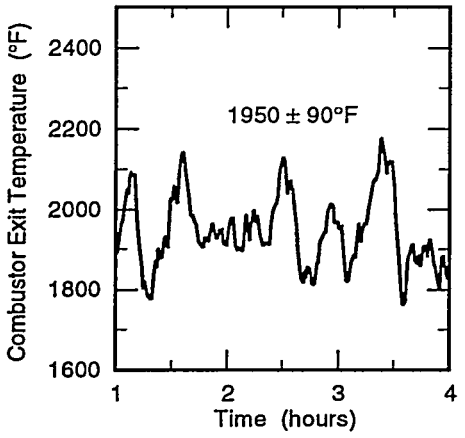


**Figure 4. Typical Turbine Simulator Temperatures From Run 3A**

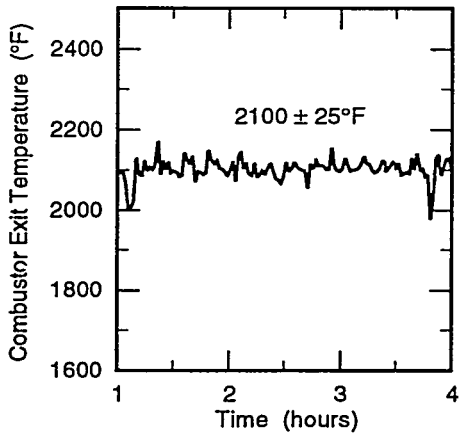


**Figure 5. Typical Turbine Simulator Temperatures From Run 4**

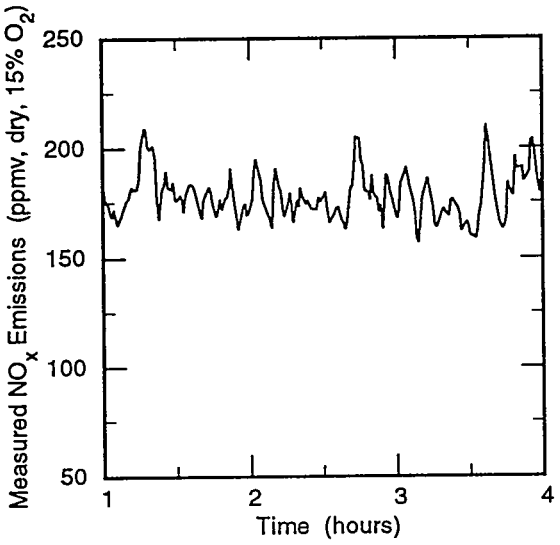


**Figure 6. Typical Turbine Simulator $NO_x$ Emissions From Run 3A**

flame stability and flame dynamics point of view, a premixed flame is advantageous from a low $NO_x$ emissions point of view. A premixing rich stage fuel nozzle should significantly reduce $NO_x$ emissions.

With no ammonia in the fuel, the best performance achieved to date is less than 10 ppmv $NO_x$ (on a dry, 15% $O_2$ basis) at a combustor exit temperature of 2350°F, using the long rich stage liner. Increasing the rich stage residence time significantly reduces $NO_x$ emissions. Given sufficient rich stage residence time, $NO_x$ emissions are relatively insensitive to the flow split between the rich and lean stages (that is, $\varphi_{lean}/\varphi_{rich}$). Increasing the rich stage residence time had little effect on CO emissions.

Measurements of $NO_x$ emissions without ammonia in the fuel establish a baseline of performance for the RQL combustor. These measurements are also an indication of the effectiveness of the quench section design. Rapid quenching will result in low $NO_x$ emissions, while slow quenching will result in high $NO_x$ emissions. Note that the stoichiometric flame temperature of this natural gas/nitrogen blend is more than 200°F higher than the stoichiometric flame temperature of a typical low Btu fuel (see Figure 3). These results demonstrate the effectiveness of the quench stage design.

Similar tests were conducted with ammonia added to the natural gas/$N_2$ fuel blend. $NO_x$ emissions and the conversion of $NH_3$ to $NO_x$ have been higher than expected. With 2800 to 3500 ppmv $NH_3$ in the fuel, the conversion of

**Table 2. Calculated Equilibrium Levels of Alkali Species in Low Btu Fuel**

| | Gas Phase Concentration (ppb by weight as Na or K) | |
|---|---|---|
| Gas Phase Species | $T = 1000$°F | $T = 1200$°F |
| Na | < 0.1 | < 0.1 |
| NaCl | 4.3 | 225 |
| NaOH | < 0.1 | 0.5 |
| $(NaCl)_2$ | 1.9 | 145 |
| K | < 0.1 | < 0.1 |
| KCl | < 0.1 | 920 |
| KOH | < 0.1 | 22 |
| $(KCl)_2$ | < 0.1 | 580 |

ammonia to $NO_x$ ranged from 35% at low firing temperatures to 55% at high firing temperatures. These tests were conducted over a range of flow splits ($0.21 < \varphi_{lean}/\varphi_{rich} < 0.30$). Doubling the rich stage residence time had little effect on $NO_x$ emissions with ammonia in the fuel. The expected minimum in the conversion of ammonia to $NO_x$ was not observed. In a series of tests conducted with low ammonia concentrations in the fuel (125 to 165 ppmv $NH_3$), the conversion of $NH_3$ to $NO_x$ was about 90%. The addition of ammonia to the fuel had little effect on measured CO emissions.

The use of a diffusion flame fuel nozzle is believed to be the reason for the relatively high conversion of $NH_3$ to $NO_x$. With a rich stage diffusion flame, $NH_3$ can convert to $NO_x$ at the stoichiometric fuel/air interface. Although $NO_x$ is destroyed in the rich stage, a very long rich stage residence time is required for low $NO_x$ emissions, because $NO_x$ destruction rates are slower than $NH_3$ destruction rates. A premixed rich stage flame should avoid this problem. Rich stage residence times on the order of 1 second may be required if the rich stage flame is a diffusion flame, versus 0.1 seconds if the rich stage flame is premixed. A premixing rich stage fuel nozzle, suitable for low Btu fuel applications, is currently being developed.

## FUTURE WORK

Two additional long duration tests of the turbine simulator are scheduled for 1993. Deposits on the fuel nozzle, combustor liner, and cascade will be characterized, along with particulates in the fuel and the burned gas. Future tests will also be conducted at higher turbine inlet temperatures

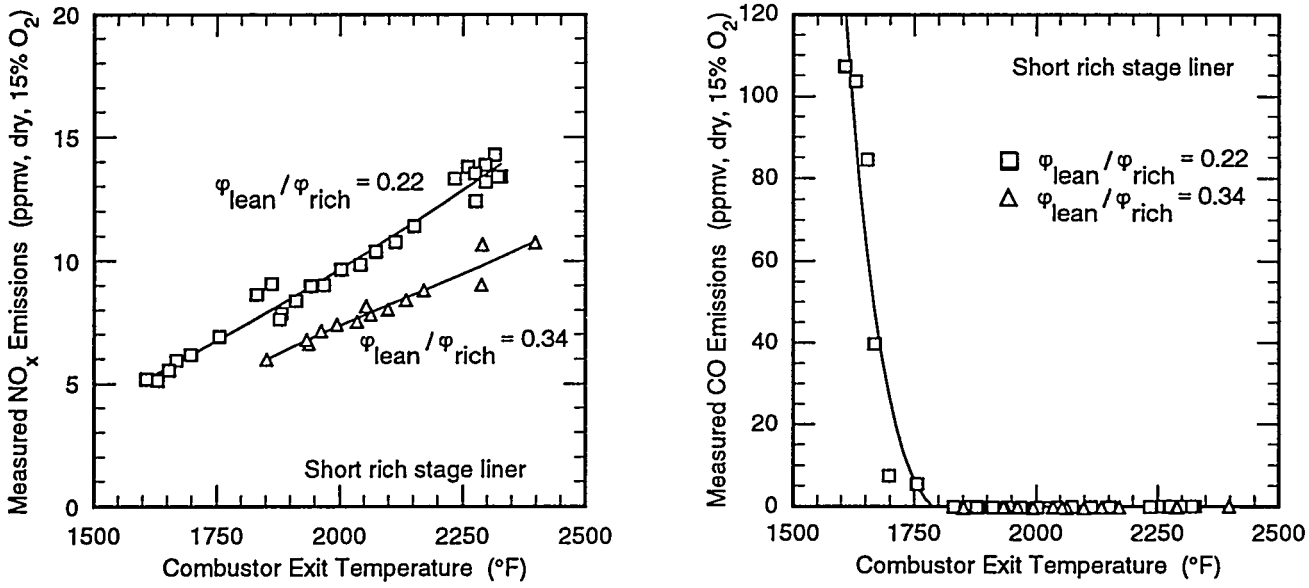


Pressure: 10 atm
Fuel: 25% NG / 75% $N_2$, 80°F, no $NH_3$

Lean stage air: 0.37 lb./s, 645°F
Rich stage air: 0.10 lb./s, 525°F (□)
*or* 0.19 lb./s, 610°F (△)

**Figure 7. Typical Emissions From the RQL Combustor With no FBN in the Fuel Left: $NO_x$ Emissions. Right: CO Emissions.**

than Run 3A. The objective of these tests will be to simulate "F" machine conditions (turbine inlet temperature = 2350°F).

RQL combustor tests with natural gas/nitrogen/ammonia blends are nearing complete. Remaining tests include evaluation of a premixing fuel nozzle and tests of an improved quench section design.

An RQL combustion test with a slip stream of high temperature low Btu fuel from the pilot plant gasifier/HGCU system is scheduled for 1993. The information gathered from these tests will be used to design a larger scale (turbine simulator scale) RQL combustor.

## REFERENCES


Barin, I. 1989. Thermochemical Data of Pure Substances. New York: VCH.

Chase, M. W., C. A. Davies, J. R. Downey, Jr., D. J. Frurip, R. A. McDonald, and A. N. Syverud. 1985. JANAF Thermochemical Tables, Third Edition. Journal of Physical and Chemical Reference Data, 14, Supplement 1.

Cook, C. S., E. Gal, A. H. Furman, and R. Ayala. 1992. Integrated Operation of a Pressurized Fixed Bed Gasifier and Hot Gas Desulfurization System. In *Proceedings of the Twelfth Annual Gasification and Gas Stream Cleanup Systems Contractors Review Meeting*, 84-94. DOE/METC-92/6128. NTIS/DE93000228. Springfield, Va.: National Technical Information Service.

Cook, C. S., E. Gal, A. H. Furman, and R. Ayala. 1991. Integrated Operation of a Pressurized Fixed Bed Gasifier and Hot Gas Desulfurization System. In *Proceedings of the Eleventh Annual Gasification and Gas Stream Cleanup Systems Contractors Review Meeting*, 45-55. DOE/METC-91/6123. NTIS/DE92001101. Springfield, Va.: National Technical Information Service.

Cutrone, M. B. 1982. Low $NO_x$ Heavy Fuel Combustor Concept Program Phase 1A Gas Tests. DOE/NASA/0147-2. NASA CR-167877.

Goebel, S. G. and A. S. Feitelberg. 1992. Experimental and Theoretical Study of Low Emissions Rich-Quench-Lean Combustion. Presented at the $24^{th}$ Symposium (International) on Combustion, University of Sydney, Australia, July 5-10, 1992.

Gordon, S. and B. J. McBride. 1976. Computer Program for Calculation of Complex Chemical Equilibrium Compositions, Rocket Performance, Incident and Reflected Shocks, and Chapman-Jouget Detonations. NASA SP-273, Interim Revision, March 1976.

Lawson, C. C. 1985. Water-Cooled Components Test Program, Final Report. DOE/MC/20192-1953. Contract DE-AC21-83MC20192.

McBride, B. J. 1989. CET89 - Chemical Equilibrium With Transport Properties. University of Georgia: Computer Software Management and Information Center.

# FE Coal-Fired Heat Engines Conference

## Session 2

## *Coal-Fueled Diesels*

## 2.1 Commercialization of Coal Diesel Engines for Non-Utility and Export Power Markets

### CONTRACT INFORMATION

**Contract Number:** DE-AC21-88MC-25124

**Contractor:** Arthur D. Little, Inc.
20 Acorn Park
Cambridge, MA 02140

**Contract Project Manager:** Robert P. Wilson

**Principal Investigators:** Kam Rao (Cooper-Bessemer)
Eric N. Balles (Arthur D. Little)
Karen R. Benedek (Arthur D. Little)
Charles E. Benson (Arthur D. Little)
Ronald A. Mayville (Arthur D. Little)
Daniel Itse (PSIT)
Jack Kimberley (AMBAC)
James Parkinson (CQ, Inc.)

**METC Project Manager:** W. Cary Smith

**Period Of Performance:** March 1, 1988 to September 30, 1993

**Schedule and Milestones**

**FY93 Program Schedule**

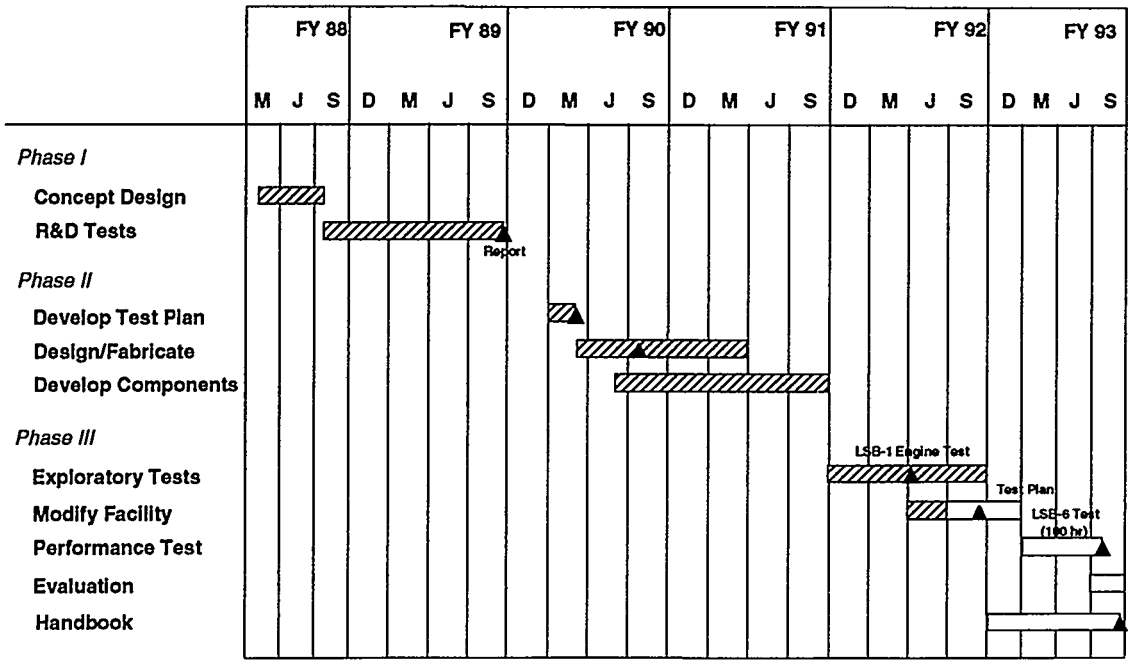

## OBJECTIVES

The primary objective of this METC project is to established practical, durable components compatible with clean coal slurry fuel and capable of low emissions. The components will be integrated into a coal power system for a 100-hr proof-of-concept test. The goal of this program is to advance the stationary coal-fueled diesel engine to the next plateau of technological readiness, and thus provide the springboard to commercialization.

## BACKGROUND INFORMATION

The basic motivation behind this project is to develop coal-burning heat engine technology primarily for 10-100 MW modular stationary power applications in the late 1990's and beyond, when oil and gas prices may return to the $5-7/MMBtu range. The fuel is a low-cost, coal-based liquid with the consistency of black paint, composed of 12-micron mean size premium 2% ash coal dust mixed 50/50 with water.

The Clean Coal Diesel Plant of the future is targeted for the 10-100 MW non-utility generation (NUG) and small utility markets, including independent power producers (IPP) and cogeneration. A family of plant designs will be offered using the Cooper-Bessemer 3.8, 5.0, and 6.3 MW Model LS engines as building blocks. In addition, larger plants will be configured with an engine in the 10-25 MW class (Cooper will license the technology to other large bore stationary engine manufacturers).

Although somewhat rare in the U.S., it is quite common worldwide to install larger diesel plants configured with engines in the 10-25 MW capacity range; in fact, the 10-25 MW class diesel engines offer a heat rate efficiency of 45% vs. 40% simple cycle for the smaller engines. While a plant can be built as small as 2 MW (based on the Cooper-Bessemer Model LS-6 engine), our cost projections indicate that an 8 MW plant is likely to be at the lower end of what is economically attractive. It should also be noted that the coal diesel plant also can be configured for cogeneration applications. Figure 1 shows a typical plant layout for a 14 MW diesel plant with SCR and heat recovery boiler.

The reciprocating engine offers a remarkable degree of flexibility in selecting plant capacity. This flexibility exists because the engines are modular in every sense (fuel cell stacks have similar modularity). Scale-up is accomplished simply by adding cylinders (e.g., 20 vs. 16) or by adding engines (4 vs. 3). There is no scale-up of the basic cylinder size. Thus, there is essentially no technical development needed to scale-up the Cooper-Bessemer Clean Coal Diesel Technology all the way from 2 MW (one 6-cylinder engine) to 50 MW (eight 20-cylinder engines), other than engineering adaptation of the turbocharger to match the engine.

The emissions control system for the coal diesel plant includes the following:

- Cyclone separators remove large particulate upstream of the turbocharger.
- $NO_x$ control is achieved by combustion optimization, selective catalytic reduction (SCR) and by reduction across the duct injection system.
- $SO_2$ control is achieved by duct injection of sodium bicarbonate followed by sorbent separation in a fabric filter.
- Final particulate control is achieved by use of a fabric filter.

Use of advanced diesel engines which operate at high brake mean effective pressures, suitably converted for coal-water slurry firing, in future commercial coal diesel plant can lead to combined cycle generating efficiencies of up to 50 percent.

### Key Performance Characteristics of the Clean Coal Diesel

The Clean Coal Diesel will offer the following performance characteristics beginning in the 2005-2010 timeframe:

- Installed cost $1300/kW (1992 dollars)
- Efficiency 48.2% (LHV) (demonstrated: 41% - LHV)
- $NO_x$ emissions 0.11 lb/MMBtu (demonstrated: 0.18 lb/MMBtu)
- $SO_x$ emissions 0.37 lb/MMBtu (equivalent to emissions from 0.3% sulfur diesel fuel oil)
- Particulate emissions 0.01 lb/MMBtu

**Basis of Competition - Other Clean Coal Powerplant Technologies**

The advantage of this 10-100 MW clean coal diesel technology is that it is targeted for NUG and small utility capacities, whereas all other clean coal technologies have been designed for the central station utility market (generally 200-500 MW).

| | |
|---|---|
| • IGCC | 200-500 MW |
| • PFBC | 100-300 MW |
| • Fuel Cell with Integrated Gasification | 200-500 MW |

Fuel cell technology is under rapid development and, although initially more costly, fuel cell power plants using natural gas reformers will eventually compete in the 100kW-10MW range. Figure 2 illustrates the unique market position of the clean coal diesel with respect to its competitors.

In the early market introduction (2000-2010), the clean coal diesel will compete against both natural gas technologies and small coal plants (10-100MW) of the PC, AFB, and stoker variety. The more favorable the price difference between coal and gas (or oil), the more competitive the coal diesel will be.

## PROJECT DESCRIPTION

Arthur D. Little, Inc., is leading a five-year, three-phase component development program with Cooper-Bessemer as the principal subcontractor responsible for development testing. Cooper-Bessemer is the premier manufacturer of 300-450 rpm engines in the United States, and is the only U.S. manufacturer of 300-450 rpm engines which has successfully operated a test engine on coal water slurry. (This engine speed range is significant because the feasibility of burning coal directly in an engine becomes increasingly difficult above the 500 rpm range.)

Phase I, the R&D effort, which is complete, explored candidate alternative solutions to the most pressing design issues. Laboratory, bench-top and engine experiments were conducted as appropriate. Phase II, Component Development, is also complete (see schedule). The program is now in the final stages of Phase III, Performance Testing.

## RESULTS

In 1993, the Cooper-Bessemer prototype engine has been demonstrated with technology advances in all critical areas, including over 100 hours of proof-of-concept testing.

Significant subsystem advances have been made to develop the 6-cylinder, 1.8 MW Cooper-Bessemer coal engine components in preparation for the 100-hour proof-of-concept testing of the integrated system. The key achievements in 1992-1993 were as follows:

- The full-scale (six cylinders--1800 kW) Cooper-Bessemer Model LS engine - coal configuration - was assembled and demonstrated on clean coal slurry. This engine burns 15 times the amount of coal as the previous JS-1 engine (2.5 x per cylinder). This same engine can be built in 6.3 MW configuration without any scale-up of cylinder size--just by increasing the number of cylinders from 6 to 20.
- An improved lower-cost slurry preparation approach was developed by CQ Inc. Integration of the "engine grade" coal cleaning module with conventional mine mouth cleaning lowers cost. Now, with this revised approach, the clean coal can be shipped dry (by rail or barge)

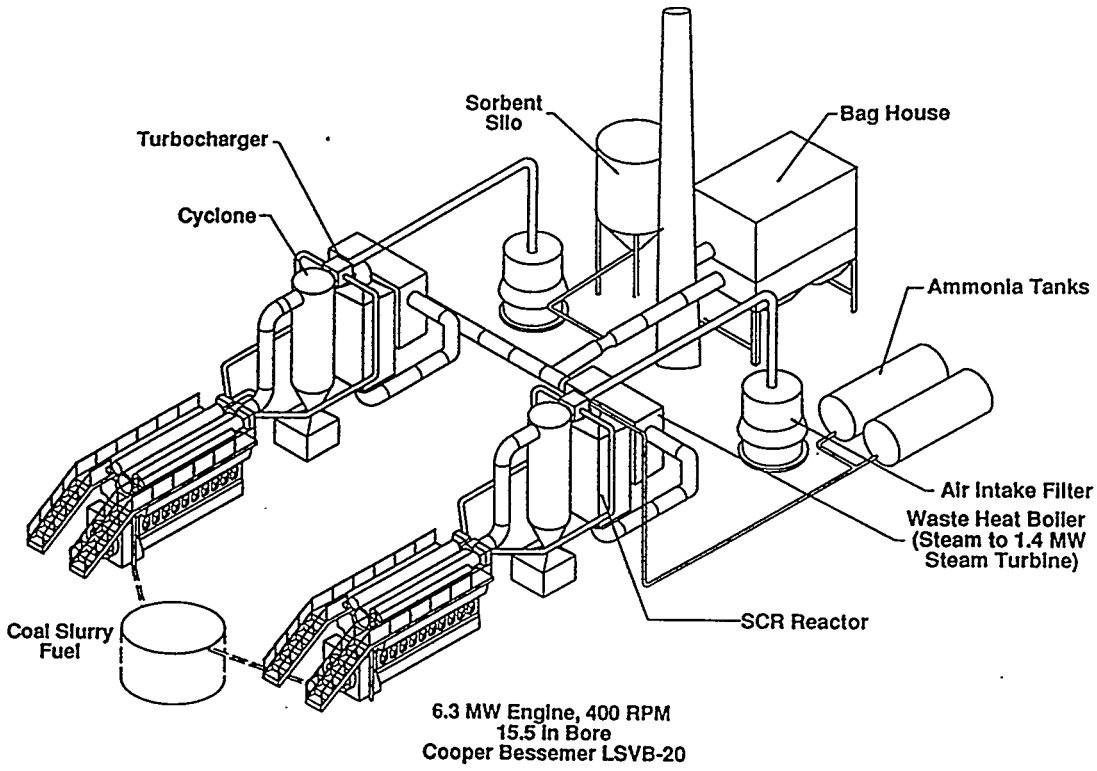


**Figure 1. 14 MW Coal-Fueled Diesel Powerplant with Steam Turbine Bottoming Cycle**

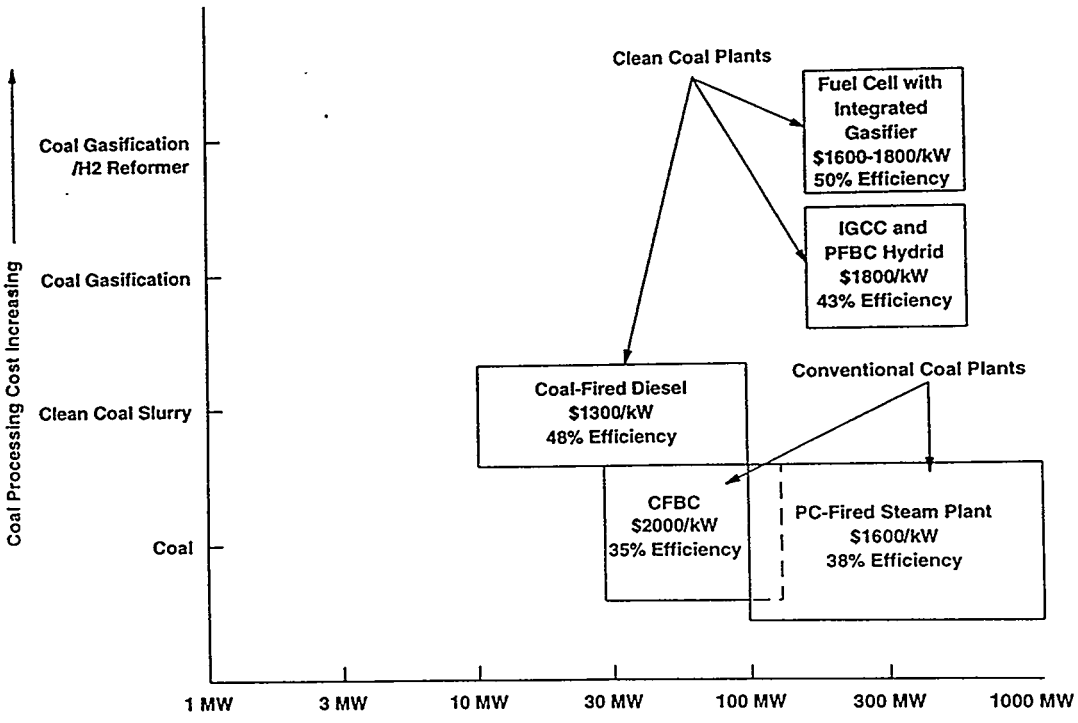


**Figure 2. Coal-Fueled Diesel is an Attractive Option for a 10-100 MW Powerplant**

economically over longer distances, and simple modular on-site slurry plants are economical (5-20 ton/hr typical size).

- A full scale, 6500 gallon slurry storage and handling system was fabricated and demonstrated at the test facility.

- The full scale 1.8 MW emissions control system was demonstrated; $NO_x$ emission data indicated that the coal diesel is competitive with gas turbine $NO_x$ emissions (0.13 lb/MMBtu).

- Another 200 hours of engine testing was achieved on coal water slurry, bringing the total to 760 hours (see Figure 3). The engine tests have provided valuable insights related to component design.

## Energy Efficiency (Heat Rate) of the Coal Diesel Powerplant

The current prototype coal-diesel being used in the technology development is the Cooper-Bessemer LS Series engine. This engine series is nominally rated at 315 kW per cylinder and can be built either as an in-line engine or as a vee- form engine (up to 6300 kW). The brake mean effective pressure (bmep) for this engine is 208 psi, which is relatively conservative. This engine has a simple cycle efficiency of approximately 40 percent and a combined cycle efficiency of approximately 45 percent. However, in its mature configuration, the commercial coal diesel plant will be based around high-bmep, larger diesel engines which will have a simple cycle efficiency of 45 percent and a combined cycle efficiency of approximately 49 percent.

The commercial coal diesel plant is illustrated schematically in Figure 4, which illustrates a 45 MW plant. The commercial coal diesel plant is expected to range from 14 MW (two 6 MW engines plus steam turbine) to 160 MW (six 25 MW engines plus steam turbine), with a typical size being 45 MW (three 14 MW engines plus steam turbine), as illustrated. Key performance parameters for the commercial coal diesel plant are given below:

| | |
|---|---|
| Coal heat input: | 318.5 MMBtu/hr |
| Diesel engine electrical output: | 42.0 MW |
| Diesel engine heat rate (LHV): | 7582 Btu/kWh |
| Steam turbine electrical output: | 3.0 MW |
| Total plant electrical output: | 45.0 MW |
| Plant heat rate (LHV): | 7078 Btu/kWh |
| Overall generating efficiency (LHV): | 48.2% |

This plant is based on modern diesel engines which operate at 45 percent simple-cycle efficiency. Such engines are currently in commercial production for liquid and gaseous fuel operation and can be converted (with Cooper-Bessemer designs) for coal-water slurry operation. Table 1 lists examples of high efficiency diesel manufacturers and engine models. All of these engines are rated in the range of 280-320 bmep.

**Table 1. Proven High Efficiency For Selected Diesel Engine Models (Over 10 MW Output)**

| Manufacturer | Model | kW/Cyl | Rating (MW) | Simple Cycle Efficiency (% LHV) |
|---|---|---|---|---|
| MAN B&W | K 80 MC-C | 3410 | 40.9 | 49.2 |
| Pielstick (Coltec - Fairbanks Morse Div.) | PC 4.2 | 1210 | 21.8 | 43.4 |
| Mitsubishi | UEC 85 LSII | 5250 | 42.0 | 53.0 |
| New Sulzer | RTA 84C | 3820 | 30.6 | 50.8 |

One example of a high efficiency diesel engine is the MAN-B&W 9K80MC-S two- stroke engine. This engine operates at 100 rpm, generates 24.5 MW, and has a simple cycle efficiency of 50.2 percent (LHV) on fuel oil. A 50 MW combined cycle power plant at Coloane in Macau, based on two such engines, has an overall generation efficiency of 52.5 percent (LHV). Future diesel engines are expected to achieve simple cycle efficiencies of up to 53 percent and combined cycle efficiencies of up to 55 percent. The fact that actual existing diesel plants operate at 52.5% (LHV) supports the projection that the

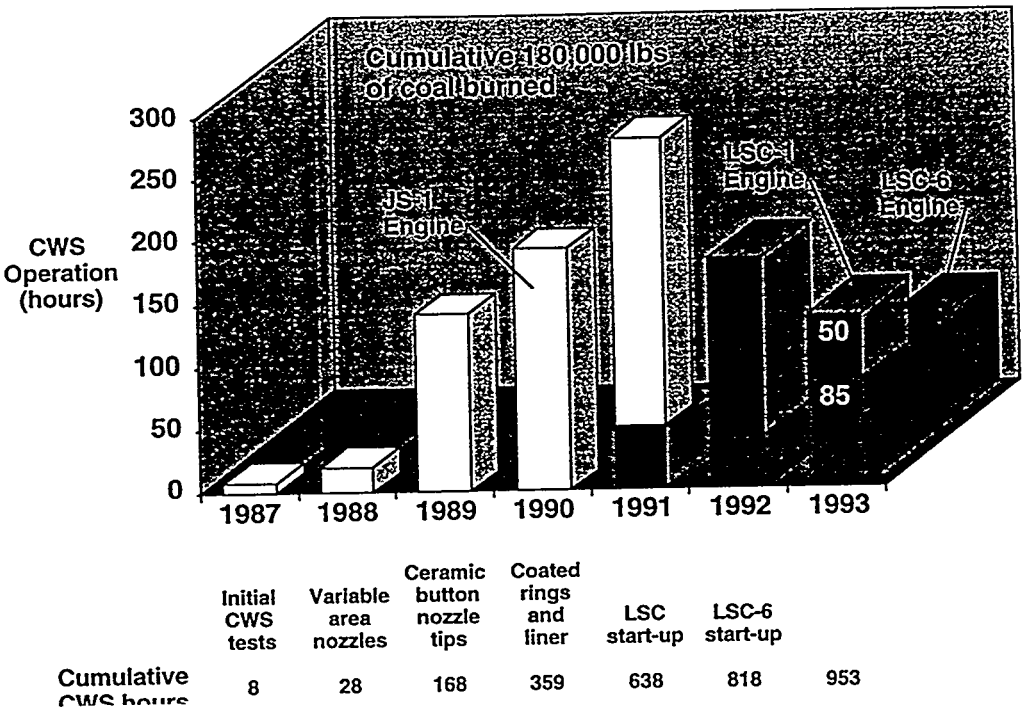


**Figure 3. History of Engine Test Experience**

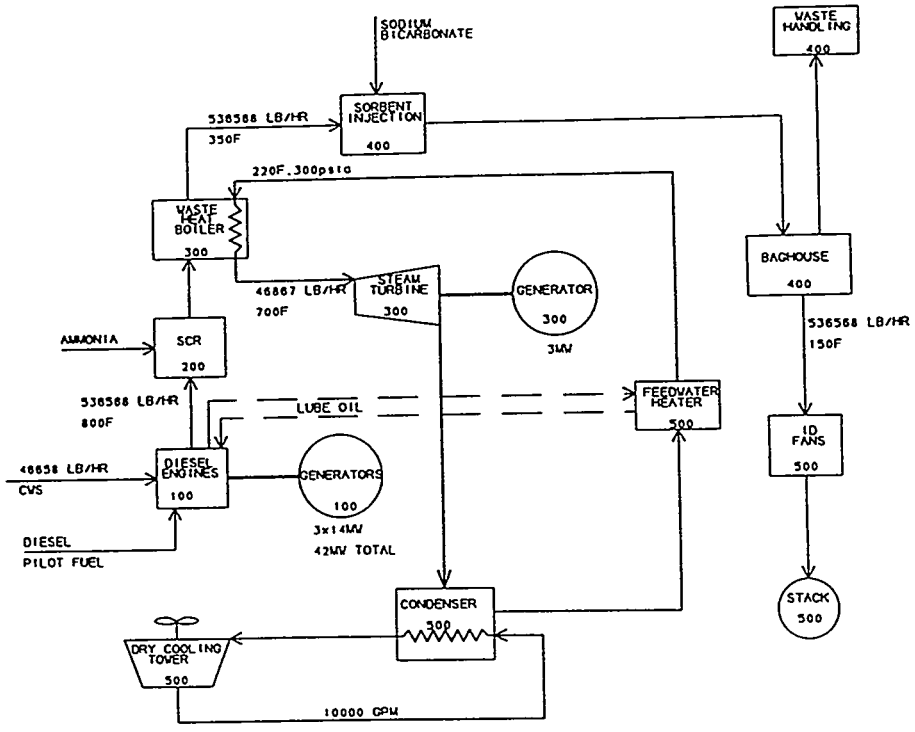


**Figure 4. Flow Diagram for Commercial, 45 MW Coal-Fueled Diesel Combined Cycle Plant**

coal diesel will readily reach these performance levels when offered to the NUG and small utility market.

## Cost of Electricity Estimates For Coal Diesel Plants

The mature clean coal diesel technology is estimated to achieve a levelized cost of electricity as low as 6¢/kWh for installations in the 2000 - 2010 time period, as shown in Table 2 (estimates are in 1992 dollars). This estimate is based on capital and operating cost estimates for a 45 MW commercial Coal Diesel Combined Cycle plant operating at an 80% percent capacity factor, with capital cost of $1300/kW. The economics of the coal-fueled diesel plant has been continually re-evaluated as new information on coal fuels, emission control technologies, engine component performance and other factors has been developed.

The cost estimates for the commercial Coal Diesel Combined Cycle (CDCC) plant are summarized and compared to those for conventional IC engines in Figure 5. Our conclusions, as explained in detail below, are that:

- The projected levelized cost of coal diesel power is 6¢/kWh for installations in the 2000 - 2010 period.
- Coal diesel technology will be competitive with gas and oil technologies when gas and oil prices reach approximately $4.50/MMBtu (the National Energy Strategy expects this to occur in 2000 - 2005). At that time, the price of coal is estimated to be $1.64-1.73/MMBtu (in 1992 dollars).
- Economic viability hinges on the cost of CWS production (the engine-grade CWS price must be kept below approximately $3/MM Btu).

**Table 2. Comparison of Projected Cost of Power For 45 Mw Coal Diesel Plant and Oil/Gas Diesel Plant**

| Cost Element | Coal Plant ¢/kWh | Oil/Gas Plant ¢/kWh | Notes |
|---|---|---|---|
| Capital (installed) | | | |
| Engines + gen sets | 1.46 | 1.22 | |
| Emissions control | 0.29 | 0.13 | Oil/gas plant has SCR |
| Bottoming cycle | 0.25 | 0.25 | |
| Balance of plant | 0.25 | 0.25 | |
| Subtotal | 2.25 | 1.85 | |
| Variable Operating | | | Fuel |
| Fuel | 2.40 | 3.67 | CWS $2.95/MBtu, |
| Non-fuel variable | 0.58 | 0.10 | Oil/Gas: $4.50/MBtu |
| | | | Non-Fuel |
| | | | Coal: sorbent + waste + $NH_3$ + catalyst |
| | | | Oil/Gas: $NH_3$ + catalyst |
| Subtotal | 2.98 | 3.77 | |
| Fixed O&M | 0.88 | 0.63 | |
| **Total Cost of Power** | 6.11 | 6.25 | |

Assumptions:
45 MW combined cycle plant
Plant heat rate: 7078 Btu/kWh
Plant capacity factor: 80%
Future oil/gas: $4.50/MMBtu
All costs are in 1992 dollars

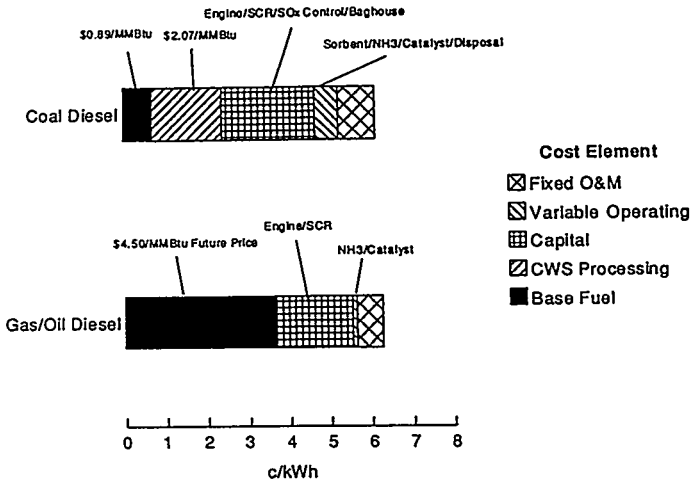


**Figure 5. Cost of Power for Coal-Fueled Diesel Combined Cycle Plant Is Competitive With Oil- Or Gas-Fueled Plant**

## Engine Component Cost Premiums Associated with Coal

The use of beneficiated coal-water slurry necessitates certain modifications to the standard large diesel engine, both in terms of special components and special maintenance practices. Modified coal-tolerant engine components include larger fuel pumps for CWS; larger hardened injectors; modified fuel cams; larger camshafts; a modified engine block; AMBAC-designed CWS injection system; ceramic coated piston rings and liners; and a ceramic coated turbocharger.

Present maintenance practices for Cooper-Bessemer oil or gas diesel engines are compared to those for the coal diesel in Table 3.

The cost associated with the increased level of maintenance and overhaul is projected to be $22.8 million over a 20 year period versus $9.8 million for the standard diesels. This corresponds to 0.36 ¢/kWh for the coal engine versus 0.16 ¢/kWh for the standard diesel. Thus the engine purchase and maintenance cost premiums associated with the use of coal for the 45 MW commercial coal diesel plant is approximately 0.44 ¢/kWh.

**Table 3. Impact of Coal Fuel on Maintenance and Overhaul Practices**

| Item | Standard Diesel | Coal Diesel Projections | 20-Year Overhaul Cost[1] |
|---|---|---|---|
| Injectors | 2,000 hr | 1,000 hr | $5.93M |
| Minor maintenance checks | 8,000 hr | 4,000 hr | $2.28M |
| Top-end overhaul | 25,000 hr | 12,000 hr | $4.56M |
| Major overhaul | 100,000 hr | 25,000 hr | $10.03M |
| Total | | | $22.8M |

[1]Coal Diesel Combined Cycle plant, engine overhaul costs only (45MW)

## Cost to Produce Engine-Grade Coal Fuels

An essential ingredient in the future of coal-fueled diesels is the eventual emergence of a price advantage of the engine-grade coal fuel over gas or oil. Our CWS costing is based on detailed inputs from CQ Inc., AMAX, and Otisca.

Our approach to a low cost clean coal is based on premium coal (0.5-2.0% ash) as a by-product. Coal sources that have some premium coal content are selected and the premium coal is extracted as a by-product of the existing coal cleaning operations using conventional coal cleaning technology such as heavy media cyclones. The overall process is as follows:

- Coal is physically cleaned at the mine in a 250 tph addition to an existing cleaning plant. Premium coal is extracted for transport to the slurrying plant and middlings are extracted for sale as utility steam coal.
- Premium coal is transported to a 100 tph slurrying plant located in the supply region.
- The engine-grade CWS is transported by tanker truck (or rail if economical) a mean distance of 25 miles to the coal diesel power plant.

The CWS cost for fuel delivered to the coal diesel plant based on these assumptions is projected at $2.97/MMBtu (see Table 4). The economics are based on $14.59/ton for operating the coal cleaning plant and $42.8 million for capital cost of a 100 tph slurry plant and associated cost cleaning equipment.

**Table 4. Projected CWS Price For Regional Production**

| Cost Component | Cost ($/MMBtu) | % of Total CWS Cost |
|---|---|---|
| Feed coal[1] | 0.888 | 29.9 |
| Coal Cleaning | | |
| O&M | 0.188 | 6.3 |
| Capital recovery[2] | 0.112 | 3.8 |
| Subtotal | 0.301 | 10.1 |
| Coal transportation | 0.264 | 8.9 |
| Coal slurrying | | |
| O&M | 0.513 | 17.3 |
| Capital recovery[2] | 0.542 | 18.3 |
| Subtotal | 1.055 | 35.6 |
| CWS transportation | 0.461 | 15.5 |
| Total | 2.979 | 100.0 |

[1]Pre-cleaned feed coal is $24/ton. It is re-cleaned producing middlings that are sold for $22.98/ton and premium coal with a feed cost equivalent to $25.25/ton.

[2]Capital recovery includes 12.5% cost of money.

## Market Analysis of Modular Powerplants, 2005-2030

The basic motivation behind this development effort is to provide coal-burning heat engine technology primarily for 10-100 MW modular stationary power applications in the next decade and beyond, when oil and gas prices may return to the $5-7/MMBtu range. There are three major target markets for the clean coal diesel technology:

- Non-utility (NUG) new capacity (an estimated 98,000 MW between 2005 and 2030).
- Small utility repowering (an estimated 28,000 MW between 2005 and 2030).
- Exports to the developing countries of coal technology below 100 MW plant size (an estimated 57,000 MW in U.S. exports between 2000 and 2030).

The NUG market, which is the largest, is discussed further below. These new capacity applications typically involve multiple engines at a single plant where requirements are favorable for coal firing: high annual utilization, existing infrastructure, space for coal handling and emission controls, and relatively constant load operation. The coal diesel, once demonstrated, potentially can capture a significant share of new capacity in these three markets from 2005-2030. The NUG market appears to be the primary target.

## Trends in New Capacity Installations

The 1990's is expected to be the decade of natural-gas for new power capacity, and much of this capacity will be in the 10-50 MW "modular" size range, powered by prime movers rather than the traditional Rankine cycle. For plants built with smaller prime movers (below 15 MW unit size), reciprocating engines will continue to take the lion's share of this modular power market (recips outsell turbines by nearly 3 to 1 for this size class, both in the U.S. and worldwide). There are good reasons that reciprocating engines outsell turbines in smaller sizes: higher efficiency, better part load performance, excellent availability, and ability to burn much heavier fuels. However, gas turbines will be the preferred prime mover for, say, 40-100 MW modular power plants, because of lower capital cost, excellent baseload performance (as typified by the GE LM 6000 (40 MW)), and low emissions.

Developments in the power generation industry over the last year have strengthened the market prospects for the Coal-Fueled Diesel Power Plant, beginning in the 2000-2010 timeframe when natural gas prices are expected to rise. The following developments are relevant:

- Many utilities and non-utilities have demonstrated reluctance to commit to natural gas for major power needs, despite its current low price. Recent projections show that coal will be the preferred fuel for 57,000 MW out of the total 148,000 MW of new capacity and repowering expected to be installed by utilities and NUGs between 1995 and 2010 (Source: EIA, 1993).

- Faced with the Clean Air Act, a large fraction of utilities have elected clean coal, coal slurry, and coal switching, rather than $SO_2$ scrubbers. This will help build the infrastructure for engine-grade coal slurry.

- The non-utility power generation sector has continued to thrive. Currently, there are 184 coal-fired NUG units installed, totalling 7000 MW of capacity. Coal consumption by NUGs is projected to increase more than 300% from 6.1 million tons in 1991 to 21.2 million tons in 2000. The size of plants and other factors make this an excellent future market for coal diesel plants.

- Certain large public utility companies are champions of the "dispersed power" approach whereby 2-50 MW modular low emissions powerplants are installed at existing transmission/distribution substations. This avoids the need for new T&D, among other advantages. The coal diesel promises to capture part of this market sector on the basis of high-efficiency and low emissions.

## NUG Market

The Non-Utility Generation (NUG) phenomenon has grown rapidly over the last five years, and the clean coal technology "industry" until now has not responded with suitable 10-100 MW products for NUG applications. The average coal NUG plant is 38 MW in capacity - only small PC boilers and small CFBs are being installed in these coal applications and these are not advanced clean coal technologies in the same class as the coal diesel. The NUG industry is expected to add 30,000 to 40,000 MW in each ten-year period in the U.S., or between 40%-50% of all new capacity installed. Recent EIA and NES projections confirm that 71,000 MW of new non-utility capacity is projected in the period 1991-2010, of which we conclude the dominant share will be for gas turbine and reciprocating engines. Figure 6 shows that coal-fueled heat engines will compete for 3160 MW/year after the year 2005 in the non-utility power sector. This level of engine production activity would revitalize the U.S. large engine industry. The number of large stationary engines produced per year would increase from about 20-40 (current) to 200-400.

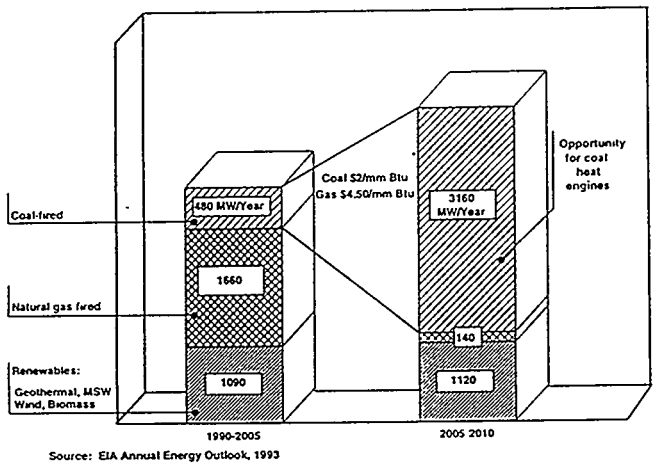


**FIGURE 6. Coal NUG Plants Will Be Favored After 2005**

Trends in U.S. power requirements over the next 40 years appear to be highly favorable for the adoption of these coal-fired diesel applications. The coal diesel stationary power plant is being demonstrated at a time when there is an ongoing upheaval in the stationary power industry. This upheaval is in large part driven by the steady growth in U.S. power requirement, which continues to grow at 2.2 to 2.6% per year nationwide, and up to 6% per year in certain regions. For perspective, each extra 0.2% of growth nationwide represents 10,000 MW of new capacity on-line. Another driving force has been the major changes to the infrastructure such as PURPA and the rise of independent power plants (IPPs) and other NUGs. Traditional procedures whereby utilities added stationary power capacity in the form of large central station generators, in increments of 250 to 1300 MW, are gradually giving way to new procedures whereby modular plants are installed in the 10 to 200 MW size range, and many of these are non-utility owned generators (NUGs). At the present time, the fuels of choice for these modular plants are natural gas and oil, due to two factors:

- Gas and oil are currently priced at attractive levels ($2 to $4 million Btu).

- There is no competitive coal-fueled modular power technology available with low emissions yet, particularly in the 10 to 50 MW range.

The coal diesel is positioned as a new technology option for this emerging NUG market starting in the 2005-2010 timeframe when gas and oil prices increase.

## REFERENCES


Benedek, K.R., Menzies, K.T., Johnson, S.A., Wilson, R.P., Rao, A.K., Schaub, F.S., "Emission Characteristics and Control Technology for Stationary Coal-Fueled Diesel Engines," ASME Engine Emission Technology Conference, San Antonio, October 1988.

Mayville, R.A., "Abrasive Concentration Effects on Wear Under Reciprocating Conditions, International Conference on Wear of Materials, Denver, Colorado, April 1989.

Rao, A.K., Melcher, C.H., Schaub, F.S., Wilson, R.P., Balles, E.N., And Kimberley, J.A., "Operating Results of the Cooper-Bessemer JS-1 Engine on Coal Water Slurry," ASME Paper, Session ICE-12, Energy Sources and Technology Conference Exhibition, New Orleans, LA, January 1988.

Wilson, R.P., "Coal-Fueled Diesel Systems for Stationary Power Applications," Task 1 topical Report, Contract MC-22182-2242, U.S. Department of Energy, September 1986.

Rao, A.K., Wilson, R.P., Balles, E.N., Mayville, R.A., McMillian, M.H., Kimberley, J.A., "Cooper-Bessemer Coal-Fueled Engine System - Progress Report," ASME ICE - Vol. 7, p. 9, January 1989.

Johnson, S.A., Senior C.L., Katz, C.K., Wilson, R.P., "Development of $NO_x$ Control Technologies for Coal-fueled Stationary Diesel Power Plants," Stationary Sources $NO_x$ Symposium, San Francisco, March 1989.

Balles, E.N., Benedek, K.R., Wilson, R.P., and Rao, A.K., "Analysis of Cylinder Pressure and Combustion Products from an Experimental Coal-Fueled Diesel Engine," presented at the Internal Combustion Engine Division Technical Conference, Kansas City, MO, ICE Vol. 2, p. 75, ASME, October 1987.

Benedek, K.R., Menzies, K.T., Johnson, S.A., Wilson, R.P., Rao, A.K., Schaub, F.S., "Emission Characteristics and Control Technology for Stationary Coal-Fueled Diesel Engines", ASME, Journal of Engineering for Gas Turbines and Power, Vol. 111, pg. 507, July 1989.

Balles, E.N., Wilson, R.P., Rao, A.K., And Melcher, C.H., "Coal-Fueled Diesel Engine for Power Generation," ASME, Presented at the Joint Power Generation conference and Exhibition, Dallas, Texas, October 1989.

Mayville, R.A., Wilson, R.P., Rao, A.K., "Cooper-Bessemer Coal-Fueled Engine System: Recent Developments in Durable Components," ASME/ETCE Meeting, New Orleans, January 1990.

Wilson, R.P., Rao, A.K., Balles, E.N., Kimberley, J., "Cooper-Bessemer Coal-Fueled Six-Cylinder LSB Engine--A Performance Update," ASME/ETCE Meeting, Houston, January 1993.

Rao, A.K., Wilson, R.P., "Cooper-Bessemer Coal-Fueled LSC-6 Engine," CIMAC, 20th International Congress on Combustion Engines, London, 1993.

## 2.2 Coal-Fueled Diesel Engines for Locomotive Applications

### CONTRACT INFORMATION

| | |
|---|---|
| **Contract Number:** | DE-AC21-88MC23174 |
| **Contractor** | GE Transportation Systems<br>Erie, PA, 16531.<br>814-875-2110 |
| **GE Program Manager:** | Bertrand D. Hsu, GE Transportation Systems |
| **Principal Investigators:** | Bertrand D. Hsu, GE Transportation Systems<br>David J. Najewicz, GE Corporate Research<br>Charles S. Cook, GE Environmental Systems |
| **METC Project Manager:** | William C. Smith |
| **Period of Performance:** | March 3, 1988 to January 31, 1994 |

**Schedule and Milestones**

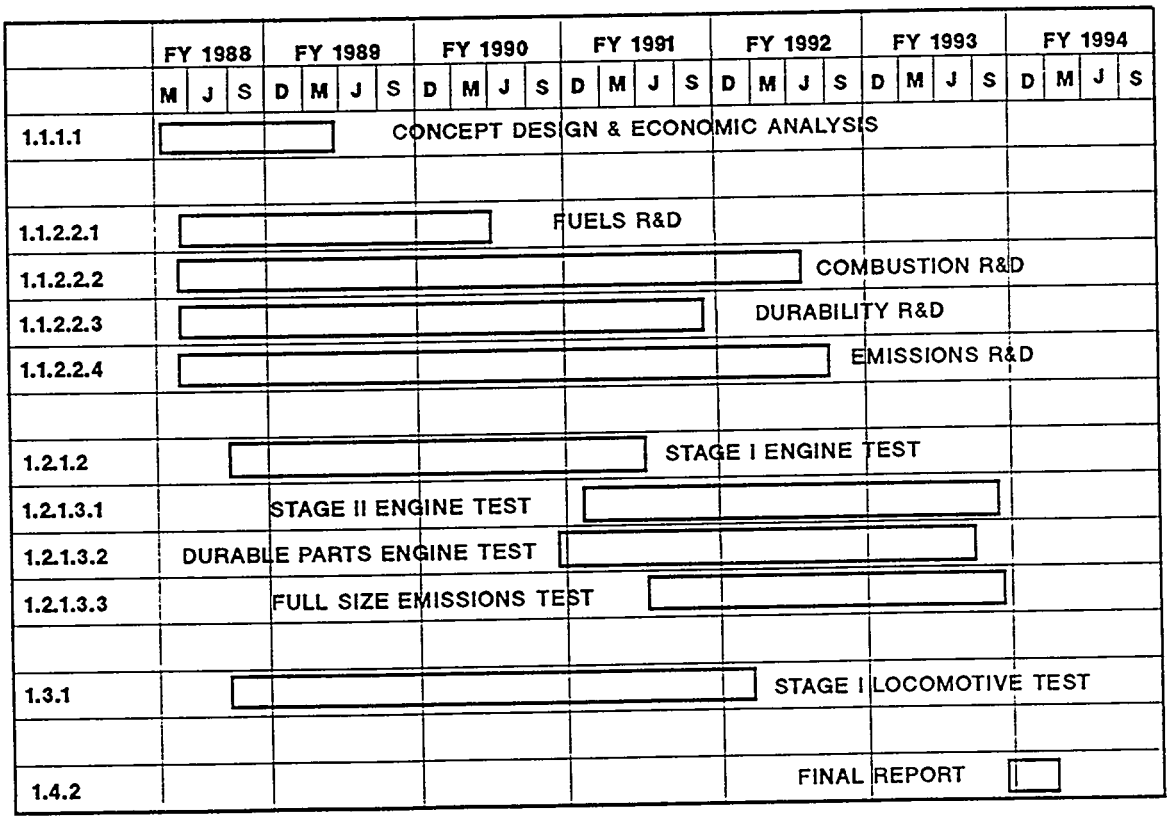

## OBJECTIVES

The objective of this program is to develop the technology necessary for future commercialization of a coal-fueled diesel locomotive. The engine under development is a medium speed diesel (1050 rpm) that operates at 250 hp per cylinder in locomotive applications.

## BACKGROUND INFORMATION

The General Electric Company has been active in coal burning technology programs for the past 40 years. About nine years ago, under the partial sponsorship of the Burlington Northern and Norfolk Southern Railroads, GE Transportation Systems (GE/TS) completed a two and one half year study into the economic viability of a coal fueled locomotive. The coal fueled diesel engine was deemed to be one of the most attractive options.

Building on the BN-NS study, a proposal was submitted to DOE to continue researching economic and technical feasibility of a coal fueled diesel engine for locomotives. The contract DE-AC21-85MC22181 was awarded to GE Corporate Research and Development (GE/CRD) for a three year program that began in March 1985. This program included an economic assessment and a technical feasibility study.

The economic assessment study examined seven areas and their economic impact on the use of coal fueled diesels. These areas included impact on railroad infrastructure, expected maintenance cost, environmental considerations, impact of higher capital costs, railroad training and crew costs, beneficiated coal costs for viable economics, and future cost of money. The results of the study indicated the merits for development of a coal-water slurry (CWS) fueled diesel engine.

The technical feasibility study examined the combustion of CWS through lab and bench scale experiments. The major accomplishments from this study have been the development of CWS injection hardware, the successful testing of CWS fuel in a full size, single cylinder, medium speed diesel engine, evaluation of full scale engine wear rates with metal and ceramic components, and the characterization of gaseous and particulate emissions.

## PROJECT DESCRIPTION

The project is planned to operate in four parallel phases. They are: Concept Design and Analysis, Technology Research and Development, Engine Component Development, and Locomotive System Test.

The first phase conducts a conceptual design and economic analysis of a coal fueled diesel locomotive.

The Technology Research and Development phase is to perform bench scale and single cylinder engine tests on fuel injection equipment (FIE), combustion system, CWS fuels, materials, and emission control systems.

The Engine Component Development phase is to design, build and operate two consecutive phased 12 cylinder engines to develop the combustion and operating characteristics. A full scale emission control system will be tested on the second phase 12 cylinder engine. Two cylinders of another eight cylinder engine will be operated on CWS fuel to evaluate the durability of engine components.

The Locomotive System Test phase was to be conducted in two stages. The first stage locomotive will only be conducted on the GE/TS test track for a short time. The engine used in the first stage test does not have durable engine parts or emissions cleaning setup. This test is a system checkout of design concept.

The original second stage locomotive test was to be conducted on commercial railroad with all the latest developed technologies. However, in 1991, due to the persistency of low oil prices in recent years, the market interest of the coal fueled systems did not realize. The U.S. buget deficit called for the winding down of all federal funded alternate fuels program that does not see any short term commercialization prospect. The GE program scope was reduced. It was decided to eliminated the second phase of locomotive test. Details of the original project are in [2] and [27].

## RESULTS

### Conceptual Locomotive Design and Economic Analysis

A concept locomotive was designed for economic study and eventual production. It is envisioned as a modified GE Dash 8 4000 hp, 6 axle, microprocessor controlled locomotive. As shown in Fig. 1, the primary modifications involve the engine, fuel tank, and emissions control system. The additional equipment to inject the slurry, resist wear, and control exhaust $SO_2$ and particulates significantly increases the cost of building the coal-fueled locomotive. An itemized cost roll-up indicates that a coal-fueled locomotive will require a price premium of about $280,000 over the price of an oil-fueled locomotive. A topical report, Integrated System Design Report was issued to DOE in July, 1989.

An economic analysis was performed on the investment in coal-fueled locomotives by calculating the fuel cost savings for three duty cycles and deducting the additional maintenance and operation costs. Production CWS costs were estimated by Otisca and Amax Research to be about $3.10/MBtu. The net savings were used to pay off the investment in locomotive and infrastructure at 15 and 20 percent depreciated rates of return (DCRR). The heavier duty cycles with more savings allow the investment to be justified at lower diesel fuel prices. An average duty cycle for eastern railroads could be justified at $0.91/gallon diesel fuel compared to the average

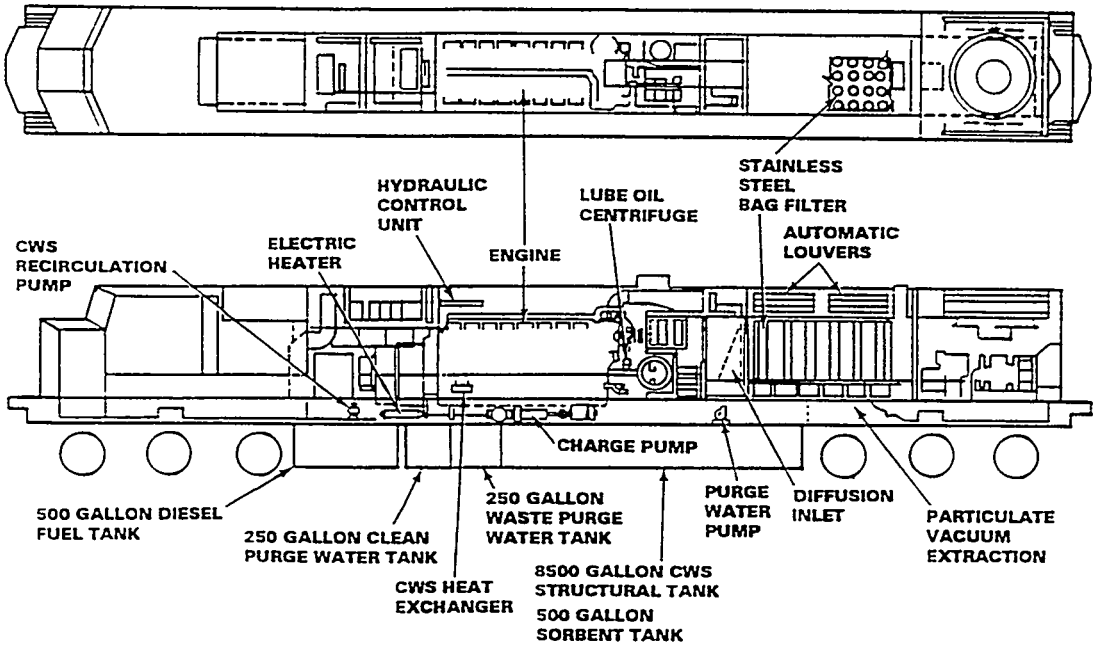


Fig. 1 Concept Coal-Fueled Diesel Locomotive

western duty cycle, which could pay off the investment at $0.81/gallon. The most attractive scenario was a unit coal train operating in Wyoming's Powder River Basin. This application had a heavy-duty cycle and a low-cost, readily available coal source, which combined to generate a very high level of fuel cost savings. The economic analysis showed that this "Best Case" application could be justified with diesel fuel as low as $0.47/gallon. A topical report, Coal Fueled Diesel Locomotive Conceptual System Economic Analysis, was issued to DOE in September, 1989. They are also described in [11] and [31].

## Technology Research and Development

**Fuels R&D.** One of the tasks of the project is to investigate the combustion tolerance of injection hardware due to CWS fuel variations. The CWS fuel comparison tests were completed during 1990. Fuels were procured from Otisca of Syracuse, NY, AMAX of Golden, CO, and UNDERC of Grand Forks, ND. Source coals included bituminous coal from Kentucky and Pennsylvania and subbituminous coal from Wyoming. Cleaning methods ranged from heavy media cyclone to oil agglomeration and chemical cleaning. Ash levels ranged from 0.7% to 2.8%. Mean particle sizes ranged from 3 microns to 15 microns. The GE diesel engine, using the accumulator fuel injection system, was able to burn all the CWS fuels at relatively high burnout levels (over 98%) at engine full load. However, the engine required different combustion parameters and some possible hardware modifications for optimum performance with each fuel (ex. injector hole configurations etc.). A thorough description of the CWS fuel test results are in the topical report, Priliminary Investigation of the Effects of Coal-water Slurry Fuels on the Combustion in GE Coal Fueled Diesel Engine, released in June, 1990. They are also in [7] and [35].

**Combustion R&D - Mechanical FIE Combustion Optimization.** The first task of the combustion R&D is to develop a mechanical CWS FIE with a mechanical pilot/starting diesel fuel system based on the technology developed during the previous DOE contract. This system is to be built onto the first phase 12 cylinder engine and complete full scale engine test. This system does not have durable parts and could only run for a short period of time. It is intended to help identify some of the coal engine and locomotive system problems for better focus on R&D needs.

This task was completed in 1989. The mechanical FIE combustion system enabled CWS fuel to be successfully used from N8 (locomotive throttle position) full load down to N5 part load with over 90% burnout. Diesel fuel was used as pilot from N5 to N8 loads and all diesel fuel was used for the lower loads. The pilot fuel injector was also used to start the engine. Calculated for a tylical locomotive duty cycle, it used 66% CWS and 34% diesel fuel. A topical report, System II Positive Displacement Fuel Injection Equipment First Phase R&D Report, was issued in December, 1988. The results are also in [2] and [29].

**Combustion R&D - Electronic Fuel Injection Hardware Development.** All electronic controlled FIE systems, both for coal and diesel fuels, were developed under this part of the program. The main CWS system employs the previously (earlier DOE contract) developed accumulator injector with the capability of providing over 80 MPa injection pressure. Piston isolation pump replaced the diaphragm type to increase the pumping efficiency and the system reliability. The durability of the check valve used in the system was greatly improved by carefully designing the pressure decade characteristics created by the charge pump element.

The pilot injection system is an electronically controlled common rail

type fuel injection system with a pressure intensifier built into each injector. It was developed by BKM, Inc. of Sandiego, CA for this project. The pilot system enables the engine to be started and idle with diesel fuel only. It can also provide the small amount of pilot fuel for partial and full load operation.

For both systems, the injection timing and duration are controlled by electrical pulses. The appropriate individual control signals are determined for best engine combustion during the single cylinder research engine test. They can later be programmed and executed by a master controller when used on the second phase coal fueled diesel engine. These are described in [11].

**Combustion R&D - Pressure Chamber CWS Fuel Spray Investigation.** Experiments were conducted at Texas A&M University (TAMU) to characterize coal-water slurry fuel sprays from diesel engine injectors. Since the combustion event is a strong function of the fuel spray, full characterization of the spray is a necessity for successful engine design and for modeling of the combustion process. Two experimental facilities were used at TAMU to study the injection of coal slurry fuels. The first experimental facility incorporates GE mechanical fuel injection system (injection pump, fuel line, and nozzle) and a specially designed diaphragm to separate the abrasive coal slurry fuel from the moving parts of the pump. The second experimental facility is based on the electronically controlled accumulator injector from GE. A pressurized visualization chamber was used to provide a spray environment which simulated the engine gas density and permitted the use of spray diagnostic techniques.

The study included high speed movies and direct photography of CWS sprays. Specific characteristics such as spray growth, penetration, shape, and cone angles were determined as functions of operating conditions and nozzle design. In addition to this overall characterization of the spray, this study also characterized the details of the atomization quality. A laser diffraction imaging technique was used to examine the atomization quality by measuring the droplet size and droplet size distribution in the spray. Both spatial and temporal droplet size variations were investigated in detail as a function of fuel injection pressure, nozzle orifice dimensions and background air condition. The drop-size measurement study in conjunction with the spray visualization provides a good knowledge base of isothermal CWS diesel sprays and insures a sound foundation for the study of CWS diesel engine combustion. A topical Report, Characterization of Coal-Water Slurry Fuel Sprays From Diesel Engine Injectors, was issued in June, 1993. Results are also reported in [10], [13], [17], [18], [23], [24], [25], [26], and [37].

**Combustion R&D - Engine Combustion Computer Simulation.** A combustion model has been developed for a direct injected diesel engine fueled with CWS and assisted by diesel pilot injection by Ricardo, North America. The model combines the unique heat and mass transport and chemical kinetic processes of CWS combustion with the normal in-cylinder processes of a diesel engine. It includes a two stage evaporation submodel for the drying of the CWS droplet, a global kinetic submodel for devolatilization, and a char combustion submodel describing surface gasification by oxygen, carbon-dioxide and water vapor. The combustion volume is discretized into multiple zones, each of whose individual thermochemistry is determined by in-situ equilibrium calculations. This provides an accurate determination of the boundary conditions for the CWS droplet combustion submodels and the gas phase heat release. A CWS fuel jet development, entrainment and mixing submodel is used to calculate the mass of unburned air in each of the burned

zones. A separate submodel of diesel pilot fuel combustion is incorporated into the overall mode, as it has been found that pilot fuel is required to achieve satisfactory combustion under many operating conditions.

The combustion model is integrated with an advanced engine design analysis code, IRIS, which is also developed by Ricardo. Simulations have been performed from generating maps of fuel consumption rate and peak pressure at each notch (locomotive throttle load and speed) setting, thus allowing selection of the best combination of CWS and pilot injection timing under the constraint of maximum firing pressure. In addition, the model has been used as a tool to explore the tradeoffs between different operating options. Detail description of this task and results are in the topical report, Development and Application of a Comprehensive Model for Pilot-Ignited Coal/Water Mixture Combustion in a Direct Injection Diesel Engine, Sept., 1991, and references [3] and [8].

**Combustion R&D - Single Cylinder Engine Combustion Optimization.** Extensive CWS combustion optimization study was completed on the single cylinder engine. The goal is to provide the highest combustion efficiency (burnout rate) while not exceeding the firing pressure limit and having reasonable fuel consumption rates. It is also a goal to use the least practical amount of pilot diesel fuel. Among the parameters studied, included CWS injection pressure, CWS and pilot injection timings, CWS injector hole size, number, shape and spray included angles, as well as engine inlet air conditions. Many interesting phenomena were noticed. For instance, for all practical purpose, CWS fuel ignites after its spray impinges on the combustion chamber walls. Impingement does not necessarily hamper combustion as long as it is not overly attached to the walls or hit the cooler cylinder liner surface.

Another interesting point that has been observed lies in the fact that, for optimum combustion, at the lower loads, the pilot diesel fuel is injected early in the cycle to serve as an igniter. However, at full load, pilot fuel should only be introduced late in the cycle to become a combustion enhancer after allowing a long delay time for the water in CWS fuel to evaporate before ignition ("Delayed Ignition"). As a result of optimization, the combustion efficiency at full engine load reached 99.5%. Details of all the findings are documented in a topical report, Coal Slurry Combustion Optimization on Single Cylinder Engine, September, 1992, and references [12] and [15].

**Combustion R&D - In-Cylinder Combustion Photography Study.** The high speed in-cylinder combustion photography study is conducted to better understand and improve the engine performance. In the photographs, distinct flames of pilot and CWS combustion were noticed. It was proven that the coal fuel burns after piston impingement and secondary atomization. Agglomerated particles will develop when combustion conditions are not favorable. Cylinder pressure data were simultaneously recorded for each film frame. Heat release data can thus be produced for each photo study. Most of the findings of earlier combustion studies on engine performances were confirmed. Detail findings are summarized in a technical paper [21].

**Emissions R&D.** The goal for emissions control was to reduce the pollutant levels of the coal engine to the levels of a conventional diesel engine. Achieving the minimum goal requires a reduction of approximately 50% in $SO_2$ emissions and a 90 to 95% reduction in particulate emissions, the actual percentages varying with the fuel. NOx emissions from the coal diesel are approximately 50% of the conventional diesel level.

The space limitations on board the locomotive present the greatest obstacle to the design of an emissions control system. The cleanup system must be compact as well as multifunctional. The development of a particulate collection device was undertaken by GE Environmental Services, Inc. (GEESI). Among the options evaluated were high-temperature metal filters, cyclones, and a granular bed. The development of a cleanup method for $SO_2$ and possibly NOx was undertaken at GE/CRD. A process was sought which could incorporate one of the particulate removal devices under consideration.

At GE Corporate Research & Development, bench scale tests were conducted to investigate the effectiveness of using both the copper oxide (CuO) supported pellets and the $CuO/Al_2O_3$ powder to remove sulfur in the emissions. Later, a small size Yanmar engine was set up with the exhaust gas passing through candle type stainless steel filters. The filters were equipped with reverse pulse air cleaning. The engine fuel was doped with carbon disulfide ($CS_2$) to increase the engine exhaust $SO_2$ concentration. Promising results were obtained using copper oxide (CuO) sorbent coupled with ammonia injection to simultaneously greatly reduce $SO_2$ and NOx emissions. This effort is described in [39].

Early in the program, an emissions sampling system was constructed to extract a small portion of the exhaust of the single cylinder engine. The system can test a sub-scale cyclone, fabric filter or granular bed, singly or in combination. Calcium sorbents were also tested on engine to capture $SO_2$ from the exhaust. Lime was either mixed into the CWS fuel or injected into the exhaust manifold. Details of the findings have been reported in the topical report, Characterization and Control of Exhaust Gas from Diesel Engine Firing Coal-Water Mixture, March, 1990, as well as [4] and [32].

Based on findings of the above investigation, cyclone was rejected for its inability to remove particulate with the required efficiency. Lime based $SO_2$ sorbent was found to be insufficient. The granular bed option is potentially promising. However, in order to develop it into a locomotive engine system, the cost and time will be much more than the presently selected system. The final selected methods are:

- Regenerative CuO sorbent and ammonia injection downstream of turbo charger;
- High temperature barrier filter downstream of sorbent injection;
- Off line regeneration of sorbent.

The expected individual emission removal efficiencies of the system are:

- Particulate 99%
- $SO_2$ 90%
- NOx 85%

A cold flow facility of the envelop type barrier filter has been built and successfully flow tested. It was designed into a partial hot flow single cylinder engine test system of 500 acfm capacity. Test on actual engine of this system confirmed the effectiveness of the selected cleanup methods chosen. Details of this part of the program has been presented in the technical papers [22] and [41].

**Durability R&D.** The abrasive and erosive nature of coal water slurry and its combustion products impaired previous development of the coal fuel engine. Earlier tests demonstrated that the primary wear componenets in a coal-fueled diesel engine were injector nozzle tips, piston rings, and cylinder liners. The development of suitable materials and processes for these parts were undertaken at GE/CRD.

The development of an erosion resistant nozzle for the coal-fueled locomotive was given the highest priority.

Extensive dry erosion and orifice flow erosion tests were conducted. Results demonstrated that nozzles built of synthetic diamond would withstand the erosive nature of the high-velocity slurry. Nozzles with diamond orifices were designed, fabricated, and sucessfully tested in an actual engine.

The development of piston rings and cylinder liners that could withstand the abrasive nature of the coal-ash deposited on the combustion liner was also a high-priority activity. Pin-on-disc and ring segment bench scale tests were used to select optimized materials and processing conditions for plasma-deposited coatings. Tungsten carbide/cobalt was the material of choice for both the ring and liner. Small-scale engine components were built and tested. The materials performed very well. Large engine components were built and tested in the durability engine at GE/TS engine lab. Finally, tests were conducted to identify the optimum plasma spray processing conditions for deposits of tungsten carbide/cobalt mixtures.

Details of the studies have been summarized in the topical report, Improved Materials for Durable Rings, Liners, and Injector Nozzles, R&D Final Report: Durability, December, 1991, as well as [9], [19], [30] and [33].

## Engine Systems Verification

**Mechanical FIE 12 Cylinder Engine System.** The mechanical FIE 12-cylinder coal-fueled engine was modified from a General Electric model 7FDL diesel engine by having dual positive-displacement fuel injection systems. A cross section of one of the 12 cylinder layout is shown in Fig. 2. The fuel injection system for CWS is used exclusively at higher loads. The CWS main injector is centrally mounted in the combustion chamber, with a nozzle having ten holes of 0.55mm diameter. The pilot injector is mounted off-center in the cylinder head and sprays into the combustion chamber from the side through four unequal holes (two 0.50mm, two 0.30mm). The diesel fuel injection system provides both a small amount of pilot to enhance coal combustion and large amounts of diesel fuel for starting and low loads. The pilot diesel fuel pump is mounted on the side of the engine. A unique mechanical fuel-rack linkage controls the amount of both CWS and diesel fuel injected into the cylinders on the 12-cylinder coal fueled diesel engine. The linkage synchronizes both CWS main and diesel fuel pilot injection pumps on all twelve cylinders during start up, acceleration on diesel fuel, transition to coal combustion, and high power running on CWS. This engine was operated for 10 hours at up to 1880 kW at 1050 rpm. Details of the design and testing of this engine are in [14], [34] and [38].

**Stage II Electronic Controlled FIE 12 Cylinder Engine.** The Phase II coal fueled diesel engine was also constructed by modifying a production GE 7FDL12 engine. The cylinder liner and

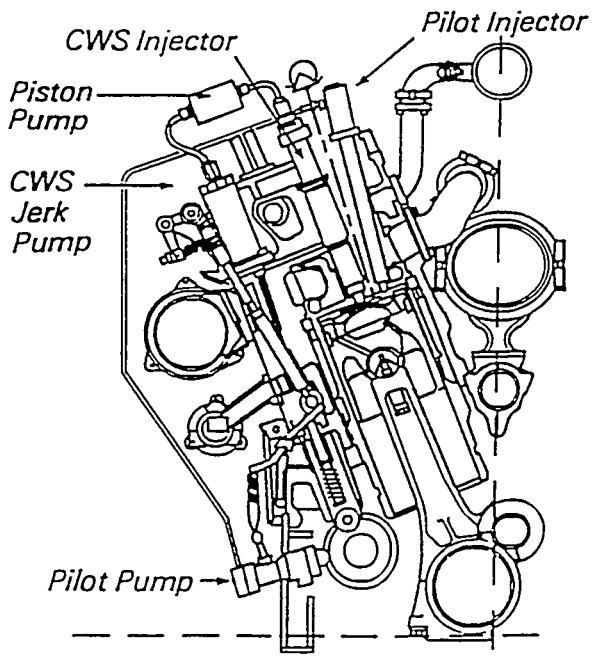


Fig. 2 Mechanical FIE Engine

the piston rings of this engine were Tungsten Carbide coated for wear resistance. It also has the full size emission control system to cleanup the exhaust gas. The cross section of one of the 12 cylinders is shown in Fig. 3. This engine has a dual accumulator type fuel injection system with electronic control. One system, the main system, is used to inject CWS into the combustion chamber when the engine is under load. The second system, the pilot injection system, is used to idle the engine, to provide a source for ignition in the low horsepower notches, and to enhance combustion under full load. Both systems are electronically controlled and independent of one another. A master controller was developed by Woodward Governor Co. of Ft. Collins, CO. Each injector subsystem, pilot or coal, is watched over by the master controller which governs engine speed and engine safety parameters such as oil pressure and water temperature. The master controller also determines injection timing and injection duration for each load and speed

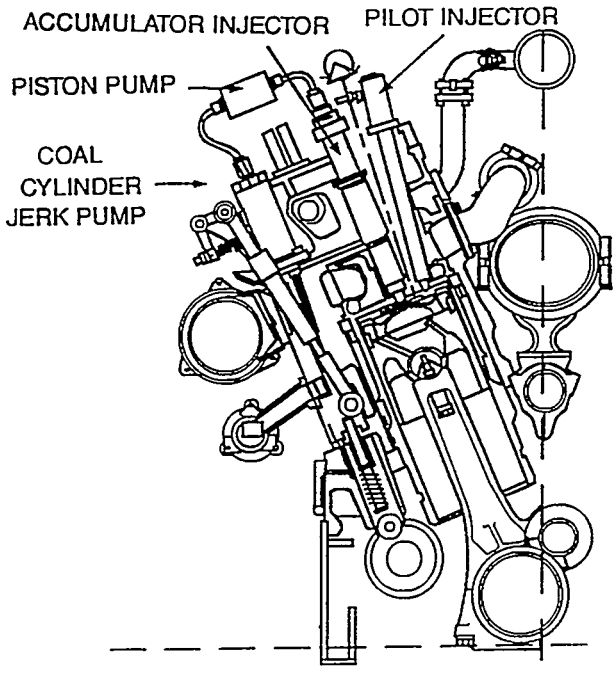


Fig. 3 Electronic FIE Engine

combination (Notch) and provides an interface for Notch selection from the operator. This engine is presently under test at GE/TS engine laboratory.

**12 Cylinder Engine Emission test.** A simplified flow diagram of the emissions control system is illustrated in Fig. 4. This system was designed by GEESI and installed at GETS engine laboratory. It is presently being tested.

Gas enters the system by passing through a two-way bypass/isolation damper. The ductwork system upstream of the envelope filter casing is compact and encloses a sorbent storage hopper. Sorbent particulate is metered into the gas stream by a rotary feed valve. The sorbent may be a regenerative type, copper oxide coated on alumina particles, or a throwaway type, Nahcolite/sodium bicarbonate. Process stoichiometry using copper oxide sorbent removes exhaust gas $SO_2$ by the formation of copper sulfate. Ammonia gas injected into the exhaust gas, in the presence of copper sulfate, produces a reduction of NOx. However, when throwaway Nahcolite/sodium bicarbonate sorbent is used, there is no reduction of NOx accomplished.

Exhaust gas, including the sorbent/precoat and CWS ash particulates, enters the filter through a plenum at the top of the casing. The barrier filter elements, made of a compaction of Inconel metal fibers, consist of 28 two sided envelopes approximately 6 ft. high by 6 ft. wide and produce approximately 2000 sq. ft. of filtration area and a filtration velocity (air/cloth ratio) of 10 ft./min. Entry of the gas into the top inlet plenum results in gas flow in a general downward direction to approach the filter media. The combination of downward gas flow and the baffles creates a favorable situation for direction of collected particulates downward into the filter hopper.

Particulate is collected on the out-

side of the envelope filters. Cleaned gas exits from the envelopes to one side into a cleaned gas plenum and exits the filter system in an upward direction. The design of the entire envelope filter system is consistent with the size and space constraints required for installation on a CWS fuel diesel engine locomotive. Cleaning of the envelope filters is accomplished by a high pressure air directed into the interior of the envelopes. It creates a short duration reverse flow through the filter media to remove collected particulates. Cleaning control may be automatic, controlled by filter pressure drop, or manual activation at any time for any desired duration. It is expected that maximum filter pressure drop will be controlled to a range of 10-15 in. $H_2O$ pressure drop.

**Engine Test of Durable Parts.** Components specifically designed for running in a medium speed coal fueled diesel engine were durability tested. The test bed was a slightly modified General Electric model 7FDL V-8 diesel engine, with the left bank provided with two durability cylinders to run on coal water slurry fuel using #2 diesel fuel as pilot and the right bank standard. The other two cylinders on the left bank provided the pilot to the coal fueled cylinders and produced no power. A standard four-pipe exhaust manifold allowed both the two coal fueled cylinders and the two dummy cylinders to be isolated in the exhaust up-stream of the turbocharger turbine. The engine is started on the right bank; the coal fueled durability cylinders are then brought on line at full speed, half load. Components tested include: tunsten carbide coated cylinder liners and piston rings, and fuel injection nozzles for CWS fuel operation. 200 cylinder hours have been run on the above various parts. Results are presently being evaluated.

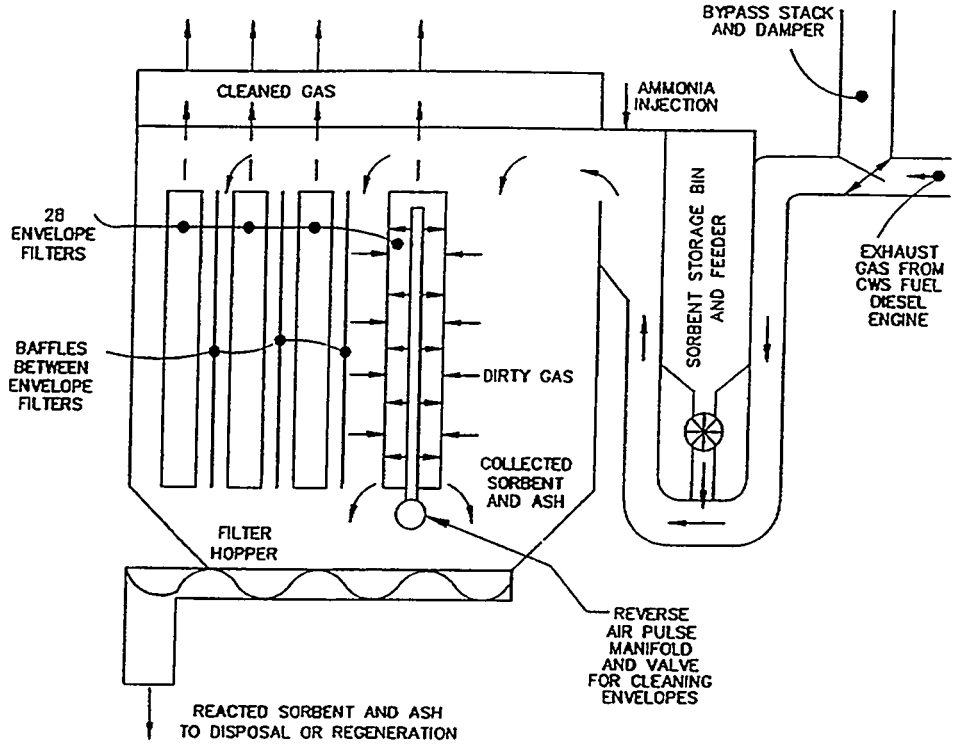


Fig. 4 Emissions Cleanup System Schematic

## Locomotive System Test.

The main thrust of the first stage coal-fueled diesel locomotive testing was to verify that the various engine support and control systems functioned as required, gaining operational experience and identifying problems. A test locomotive, GE 609, was modified for this test. It is a model C39-8, a microprocessor controlled, six-axle locomotive, having motor-driven blowers, radiator fans, and air compressor. The first stage 12-cylinder coal-fueled diesel engine was installed in this locomotive after completion of testing in the GE diesel engine laboratory.

The first stage coal-fueled diesel locomotive testing included a fuel tender car coupled to its rear, see Fig. 5. The fuel tender uses a railroad flatcar to carry the tanks, pumps, valves, and associated controls for the first stage locomotive CWS fuel system. CWS is supplied to the locomotive from the tender, along with purge water. Having a separate fuel tender car facilitated testing to study problems related to CWS mixing, long-term storage, freezing, and variations in coal loading within a large tank.

Locomotive testing included both stationary testing and running on the GE/TS Erie test track. During the stationary test, the locomotive runs in self-load mode. After some system debugging, self-load test of the locomotive was successful. It made the transitions from starting with diesel fuel both into and out of coal combustion and purging the CWS fuel injectors prior to shutdown. The test track at GE/TS is about 4 miles long. For the track run, two diesel-electric locomotives, operating in dynamic braking mode, were used as load units for the coal-fueled diesel locomotive (GE 609) to simulate a trailing train. After the completion of the stationary test, successful track test runs were made in November of 1991.

Many locomotive systems operation requirements on engine were learned. They included the sudden load change needed on the engine during "wheel slip" and the requirement on the engine during "tunnel operation" mode. The first locomotive system did not have provisions to accommodate these. However, for future railroad test, they have to be designed into the control system of the engine. A video tape was made of the actual test run and presented to the DOE Contractors' Review Conference and the ASME coal-fueled diesel meeting in 1992. A technical paper [40] was written describing the details of the test.

## Conclusions

Important achievements in technology have been made in bringing a coal fueled diesel engine for locomotive application into reality. Approximately 500 hours of engine operation has been accumulated

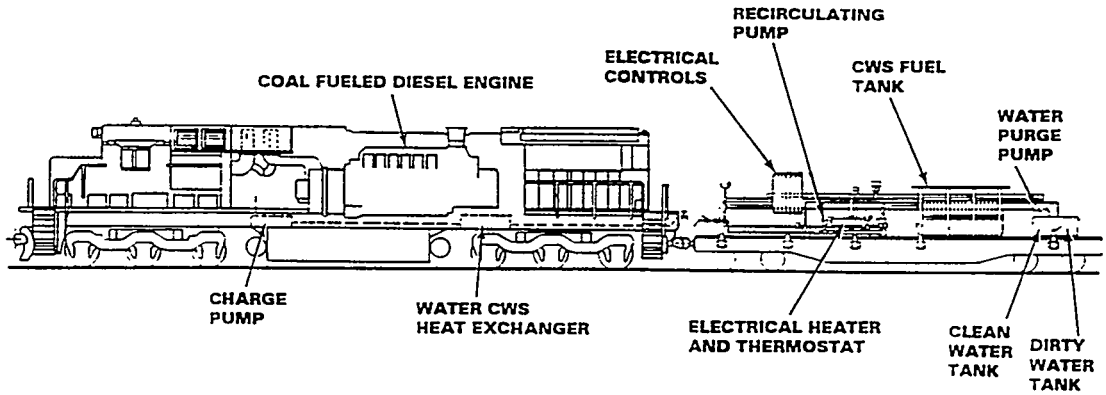


Fig. 5 Stage I Locmotive Test Configuration

with coal fuel. Due to the persistent low oil prices and the federal budget deficit, the present program scope was reduced. However, the critical technologies developed are retained and summarized in the completion of the second phase electronic controlled FIE engine with its emissions cleanup system. When market environment becomes favorable in the future, the technologies can be further improved and packaged into a commercial system very quickly.

## REFERENCES

### Publications in Technical Society Literatures


[1] Flynn, P.L., "Coal Fueled Locomotives: Energy Independence and Economic Sense," National Coal Association publication Landmarc, 1989.

[2] Flynn, P.L., Hsu, B.D. and Leonard, G.L., "Coal Fueled Diesel Engine Progress at GE Transportation Systems," ASME Transactions, Journal of Engineering for Gas Turbines and Power, Vol. 112, No. 3, July 1990, pp. 369-375.

[3] Wahiduzzaman, S., Blumberg, P.N., Keribar, R. and Rackmil, C.I., "A Comprehensive Model for Pilot Ignited, Coal Water Mixture Combustion in a Direct Injection Diesel Engine," ASME Transactions, Journal of Engineering for Gas Turbines and Power, Vol. 112, No. 3, July, 1990, pp. 384-390.

[4] Slaughter, D., Cohen, M., Samuel, E., Mengel, M., and Gal, E., "Control of Emissions in the Coal Fueled Diesel Locomotive," ASME Publication, Coal Fueled Diesel Engines, ICE Vol. 12, 1990, pp. 11-16.

[5] Hapeman, M.J., "Review and Update of the Coal Fired Diesel Engine," University of North Dakota Energy and Environmental Research Center, Preprints of the Opportunuties in the Synfuels Industry Proceedings, August 27-29, 1990.

[6] Rairden, J.R., Mehan, R.L. and Giammarise, A.W., "The Effects of Processing Conditions on the Wear Resistance of Plasma Sprayed WC-Co Coatings," Proceedings of the DOE Conference on Coatings for Heat Engines, Meeting held in Castine, Maine, August, 1990

[7] Hsu, B.D. and Confer, G.L., "Progress on the Investigation of Coal-Water Slurry Fuel Combustion in a Medium Speed Diesel Engine: Part 4 - Fuels Effect," ASME Publication, Coal Fueled Diesel Engines, ICE Vol. 14, 1991.

[8] Wahiduzzaman, S., Blumberg, P.N. and Hsu, B.D., "Simulation of Significant Design and Operating Characteristics of a Coal Fueled Locomotive Diesel Engine," ASME Publication, Coal Fueled Diesel Engines, ICE Vol. 14, 1991.

[9] Mehan, R.L., Flynn, P.L. and Giammarise, A.W., "Evaluation of Piston Ring Materials in Oil Containing Abrasive Using a Ring-On-Block Test Machine," Wear (Elsevier Sequoia S.A., Lausanne), No. 147, 1991, pp. 41-57.

[10] Caton, J.A., Kihm, K.D., Seshadri, A.K. and Zicterman, G., "Micronized Coal Water Slurry Sprays from a Diesel Engine Positive Displacement Fuel Injection System," Proceedings of the Central States Section /Combustion Institute Spring Technical Meeting, April, 1991, pp. 361-366.

[11] Hsu, B.D., "Coal Fueled Diesel Engine Development Update at GE Transportation Systems," ASME Transactions, Journal of Engineering for Gas Turbines and Power, Vol. 114, No. 3, July, 1992, pp. 502-508.

[12] Hsu, B.D., Confer, G.L. and Shen, Z.J., "Progress on the Investigation of Coal-Water Slurry Fuel Combustion in a Medium Speed Diesel Engine: Part 5 - Combustion Studies," ASME Transactions, Journal of Engineering for Gas Turbines

and Power, Vol. 114, No. 3, July, 1992, pp. 515-521.

[13] Seshadri, A.K., Caton, J.A., and Kihm, K.D., "Coal Water Slurry Spray Characteristics of a Positive Displacement Fuel Injection System," ASME Publication, ASME Transactions, Journal of Engineering for Gas Turbines and Power, Vol. 114, No. 3, July, 1992, pp. 528-533.

[14] McDowell, R.E., Basic, S.L. and Confer, G.L., "Design and Operation of a Medium Speed 12-Cylinder Coal-Fueled Diesel Engine," ASME Publication, Coal Fueled Diesel Engines, ICE Vol. 16, 1992, pp. 33-38.

[15] Hsu, B.D., Shen, Z.J. and Caton, J.A., "Combustion Characteristics of Coal-Water Slurry Fuel in a Medium Speed Diesel Engine," Proceedings of the Ninth Annual International Pittsburgh Coal Conference, Pitts., PA, October, 1992, pp. 335-340.

[16] Hsu, B.D., Johnson, R.N. and Jones, A.G., "Fuel Injection Equipment for a Coal-Water Slurry Fuelled Medium Speed Diesel Engine," I. Mech. E. Publication (UK), Diesel Fuel Injection Systems, 1992, pp. 45-52.

[17] Kihm, K.D. and Caton, J.A., "Synchronization of a Laser Fraunhofer Diffraction Sizing Technique with Intermittent Spray Systems," Journal of Applied Optics, Vol. 31, No. 23, 1992, pp.1914-1916

[18] Caton, J.A., Seshadri, A.K., and Kihm, K.D., "Spray Tip Penetration and Cone Angles for Coal Water Slurry Using a Modified Medium-Speed Diesel Engine Injection System," Proceedings of the Central States Section /Combustion Institute Spring Technical Meeting, April, 1992, pp. 234-239.

[19] Gray, D.M., Rairden, J.R. and Giammarise, A.W., "A Parametric Study of the Effects of Processing Conditions on the Wear Resistance of Plasma Sprayed WC-Co Coatings," Presented to the International Conference on Metallurgical Coatings and Thin Films, Sandiego, CA, April 4-10, 1992.

[20] Hapeman, M.J. "The Coal Fired Locomotive Development," Presented to the 15th Annual Seminar on Transportation Polies and Coal Distribution (National Coal Association), Sarasota, FL, January 29-31, 1992.

[21] Hsu, B.D. and Branyon, D.P., "Progress on the Investigation of Coal-Water Slurry Fuel Combustion in a Medium Speed Diesel Engine: Part 6 - In-Cylinder Combustion Photography Studies," ASME Publication, Coal Fueled Diesel Engines, ICE Vol. 19, 1993, pp. 15-24.

[22] Cook, C., Gal, E., Mengel, M., and Van Kleunen, W., "Coal-Fuel Diesel Emissions Control Technology Development," ASME Publication, Coal Fueled Diesel Engines, ICE Vol. 19, 1993, pp. 9-14.

[23] Caton, J.A., Payne, S.E., Terracine, D.P., and Kihm, K.D., "Coal Water Slurry Atomization Characteristics of an Electronically Controlled Accumulator Fuel Injection System," ASME Publication, Coal Fueled Diesel Engines, ICE Vol. 19, 1993, pp. 25-32.

[24] Kihm, K.D., Terracine, D.P., Payne, S.E., and Caton, J.A., "Synchronized Droplet Size Measurements For Coal-Water Slurry Diesel Sprays of an Electronically-Controlled Accumulator Fuel Injection System," ASME Publication, Coal Fueled Diesel Engines, ICE Vol. 19, 1993, pp. 33-42.

[25] Kihm, K.D., Terracine, D.P., Payne, S.E., and Caton, J.A., "Properly Synchronized Measurements of Droplet Size For High Pressure Intermittent Coal-Water Slurry Diesel Sprays," Proceedings of the 1993 Joint Central and Eastern States Section /Combustion Institute Spring Technical Meeting, Paper No. 50, pp. 271-275, March, 1993.

[26] Caton, J.A., Payne, S.E., Terracine, D.P., and Kihm, K.D., "Coal Water Slurry from an Electronically Controlled Accumulator Fuel Injection System: Break-up Distances and Times," Proceedings of the 1993 Joint Central and Eastern States Section /Combustion Institute Spring Technical Meeting, Paper No. 76, pp. 404-409, March, 1993.

**Publications in DOE Annual Heat Engine Conference Proceedings**

[27] Flynn, P.L., B.D. Hsu, G.L. Leonard, and C.S. Cook. 1988. Coal-Fueled Diesels "Proof of Concept" Program. Fifth Annual Conference Proceedings, 11-19. DOE/METC-88/6094.

[28] Flynn, P.L., B.D. Hsu, G.L. Leonard, and C.S. Cook. 1989. Coal-Fueled Diesels for Locomotives. Sixth Annual Conference Proceedings, 79-90. DOE/METC-89/6101.

[29] Hsu, B.D. 1989. Coal-Fueled Diesel Technology Development GE Single Cylinder Diesel Engine Results. Sixth Annual Conference Proceedings, 169-175. DOE/METC-89/6101.

[30] Mehan, R.L., G.L. Leonard, and R.N. Johnson. 1989. Hardened Materials in Coal-Fueled Diesels. Sixth Annual Conference Proceedings, 211-225. DOE/METC-89/6101.

[31] Flynn, P.L., B.D. Hsu, G.L. Leonard, and C.S. Cook. 1990. Coal-Fueled Diesel Locomotives Overview. Seventh Annual Conference Proceedings, 11-22. DOE/METC-90/6110.

[32] Gal, E., E.A. Samuel, and M. Cohen. 1990. Coal-Fueled Diesel Technology Development Emissions: A Status Report. Seventh Annual Conference Proceedings, 206-215. DOE/METC-90/6110.

[33] Mehan, R.L., J.R. Rairden, and A.W. Giammarise. 1990. Wear Resistant Materials and Processes for the 7FDL Diesel Engine. Seventh Annual Conference Proceedings, 328. DOE/METC-90/6110.

[34] McDowell, R.E., G.L. Confer and S.L. Basic. 1990. 12-Cylinder Coal-Fired Engine Design. Seventh Annual Conference Proceedings, 440. DOE/METC-90/6110.

[35] Hsu, B.D., and G.L. Confer. 1990. Coal-Fueled Diesel Engine Performance - Fuels Effect. Seventh Annual Conference Proceedings, 262-271. DOE/METC-90/6110.

[36] Hsu, B.D., A.K. Kalafala, and C.S. Cook. 1991. Coal-Fueled Diesel Locomotives Overview. Eighth Annual Conference Proceedings, 72-80. DOE/METC-91/6122.

[37] Caton, J.A., and K.D. 1991. Coal-Water Slurry Atomization Characteristics. Eighth Annual Conference Proceedings, 273-282. DOE/METC-91/6122.

[38] McDowell, R.E., G.L. Confer and S.L. Basic. 1991. Design and Operation of a Coal-Fueled 12-Cylinder Medium Speed Diesel Engine. Eighth Annual Conference Proceedings, 283-292. DOE/METC-91/6122.

[39] Gal, E., W. Van Kleunen, R.W. Hamilton, and M. Cohen. 1991. Coal-Fueled Diesel Emissions Control Technology Development: A Status Report. Eighth Annual Conference Proceedings, 459-466. DOE/METC-91/6122.

[40] McDowell, R.E., G.L. Confer and S.L. Basic. 1992. Coal Fueled Diesel Locomotive Test. Ninth Annual Conference Proceedings, 39-50. DOE/METC-93/6129.

[41] Gal, E., M. Mengel, and W. Van Kleunen. 1992. Coal-Fueled Diesel Emissions Control Technology Development: A Status Report. Ninth Annual Conference Proceedings, 190-197. DOE/METC-93/6129.

# FE Fuel Cells Conference

## Session 1

## *Molten Carbonate Fuel Cells*

## 1.1 Overview of ERC's Carbonate Fuel Cell Development Program

Bernard S. Baker, Christopher R. Bentley and Donald R. Glenn
Energy Research Corporation
3 Great Pasture Road
Danbury, CT 06813

The near-term elements of ERC's Direct Carbonate Fuel Cell commercialization program are embodied in the following areas:

1. Product Development
2. Manufacturing
3. Demonstration Power Plants
4. Early Production Units
5. Customer Relations
6. Market Analysis
7. Organization

### PRODUCT DEVELOPMENT

Product development is being described in this seminar in another ERC paper[1] and will not be discussed here.

### MANUFACTURING

Fuel Cell Manufacturing Corporation (FCMC), is a privately funded carbonate fuel cell stack production facility. Located in Torrington, CT, the facility is capable of 2 MW/per year of stack production on a single shift basis. The plant occupies approximately 50,000 sq.ft. and employees 35 people.

Process trials began in the summer of 1991 with component production based on ERC labscale processes. Some growing pains were incurred in the transfer of process technology to new, different and substantially larger machines. Additionally, a number of batch processes were converted to semi-continuous or continuous production. The size of parts being produced went from 4,000 to 6,000 sq.cm. Limited production of full sized components was achieved and shipments began in July of 1992.

A number of major production operations take place at FCMC, including:

1. Power blending
2. Drying
3. Tape Casting
4. Sintering
5. Heat treating
6. Electrolyte filling
7. Metal fabrication
8. Stacking
9. Manifolding
10. Instrumentation
11. Insulating
12. Shipping

In some cases, FCMC starts with raw materials from vendors and in other cases, fully manufactured components are purchased. Make-buy decisions are constantly being evaluated.

There has been a steady improvement in yields; in certain cases yields have gone from an initial 35% in 1992 to over 90% at the present time. In selected areas, existing equipment has shown the ability to produce up to 52 MW/year as shown in Table 1. Scale up to six square fee components has been achieved.

TABLE 1

FUEL CELL MANUFACTURING CORPORATION
PROCESS OPTIMIZATION

| ANNUALIZED CONTINUOUS TAPE CASTING RATES FOR ONE MACHINE OPERATING ON A SINGLE SHEET | | | |
|---|---|---|---|
| | FACTORY DESIGN BASIS | PRESENT PRODUCTION CAPABILITY | DEMONSTRATED FEASIBILITY |
| Matrix | 2 MW | 7 MW | 52 MW |
| Electrodes (2) | 2 MW | 12 MW | 24 MW |

Technology transfer from ERC has been successfully proven in 2, 8 and 20 kW stacks. Currently, stacks with 246 series connected bipolar cells have been built and tested.

Quality control and automated inventory procedures are in place.

Focus is on both producing demonstration hardware and establishing the baseline for full commercial manufacturing.

## DEMONSTRATION POWER PLANTS

The 2 MW Santa Clara Demonstration Project (SCDP) power plant project is being described in another paper[2] by FCE and SCDP in this seminar and will not be discussed here.

FCE is also beginning design related activities for the multimegawatt Clean Coal V program wherein a fuel cell for the first time was selected as part of a Clean Coal award. This project, based on coal gas from a British Gas Lurgi gasifier, has been the subject of several earlier design studies[3,4] with ERC's carbonate fuel cell.

## EARLY PRODUCTION UNITS (EPU)

The ERC commercialization plan calls for the introduction of EPUs as the first generation of commercial power plants. These will be very close to full commercial units in many respects, but will be somewhat more expensive and have some performance limitations. Their purpose is to help bridge the difficult economic transition from demonstration to commercial units -- the age old chicken-egg situation.

ERC has begun a company-funded EPU design effort building on our own stack and Balance of Plant (BOP) experience, Nth plant design studies[5] and SCDP detailed design experience.

## CUSTOMER RELATIONS

ERC believes it is necessary to interface with customers at the earliest possible stage in the evolution of the product. This is especially true in the utility industry when the customer is inherently conservative and when planning cycles are relatively long. In the late 70's and early 80's when ERC first began its relatively small carbonate fuel cell efforts, its customers

were primarily DOE, EPRI and GRI. Contact with utility customers was via the latter two entities, and only an occasional presentation was made to utility program committees.

By 1986, ERC was working closely with Pacific Gas and Electric Company in certain carbonate fuel cell stack development areas. In 1988, ERC became involved with the municipal utility sector via its response to their Notice of Market Opportunity announcement. By 1990, the Fuel Cell Commercialization Group (FCCG) was formed, a mix of 12 municipal utilities (MU) and investor owned utilities (IOU).

Involvement with FCCG brought ERC directly into contact with a broad base of small and large MUs and IOUs. FCCG established a number of committees, including design, planning, information and model contracts. Interfacing with these utility committees and their utility representatives enabled ERC to exchange information relative to their interests, requirements and product needs, while at the same time allowing ERC to present to the utilities the status of its fuel cell developments and anticipated power plant characteristics.

The dialogues gave rise to a number of activities by the utilities themselves based on the ERC Direct Fuel Cell product. For example, working with and through EPRI[6], the Los Angeles Department of Water and Power (LADWP) analyzed the use of the Company's 2 MW DFC in the LA area, and established that credits in the range of 1.2 to 6 cents/kWh could be derived from the use of this type of fuel in their territory. Similarly, Central and Southwest Services analyzed the ERC fuel cell use in its totally different environment and estimated credits in the 1.6 to 4 cents/kWh range. Studies were also conducted by Oglethorpe Power Corporation in Georgia and yielded comparative results.

ERC direct dialogue with utilities increased with the detailed design and contract negotiation activities with the SCDP utilities and in working with PSE&G and other utilities on model contract activities and with the City of Pasadena and the Lincoln Electric System on system planning.

ERC staff has established a working interface with a broad base of utility representatives on a routine basis and a constructive exchange now exists.

FCCG, meanwhile, has grown to 40 members representing a broad gamut of utility types, locations and sizes which we feel are well representative of the industry as a whole as shown in Figure 1. We continue to seek to learn more about the industry and have initiated a number of other activities described in the next section.

## MARKET ANALYSIS

### Large Systems - Gas & Coal

In 1991, working with Fluor Daniel, ERC initiated a market study to better understand utility requirements relative to natural gas and coal gas fueled power plants.

The market survey was designed to address long-term strategic planning issues for assessing the utilities' acceptance and future implementation of the carbonate fuel cell technology in their power generation mix. The questions in this survey addressed fuel sources, future power generation needs, competing technologies, power plant size, fuel preferences, dispatch factors, site constraints, and capital cost sensitivity. A total of 31 utilities responded (63% response) to the questionnaire. These results are analyzed in the following sections.

The study addressed:

1. Future Energy Sources including fuel mix and coal vs. gas issues.

2. Technology and Carbonate Fuel Cell Power Plant Input - focusing on dispatch factors, emissions, fuel cell characteristics, carbonate fuel cell power plant (CFCPP) competitors, CFCPP type and operating mode, and essential commercialization milestones.

3. Capacity Addition - for example, CFCPP attractiveness, size and early CFCPP adoption and competition.

All these studies focused on larger size powerplants incorporating phased construction concepts based on natural gas and coal.

From a time profile viewpoint, the first three decades of the 21st century were projected.

The availability of fuels is presented in Table 2 below. The numbers shown for total current availability indicate the percentages of the responses stating that a fuel is currently available. The numbers shown for incremental availability indicate the percentages of responses stating that a fuel is expected to be used for future capacity additions.

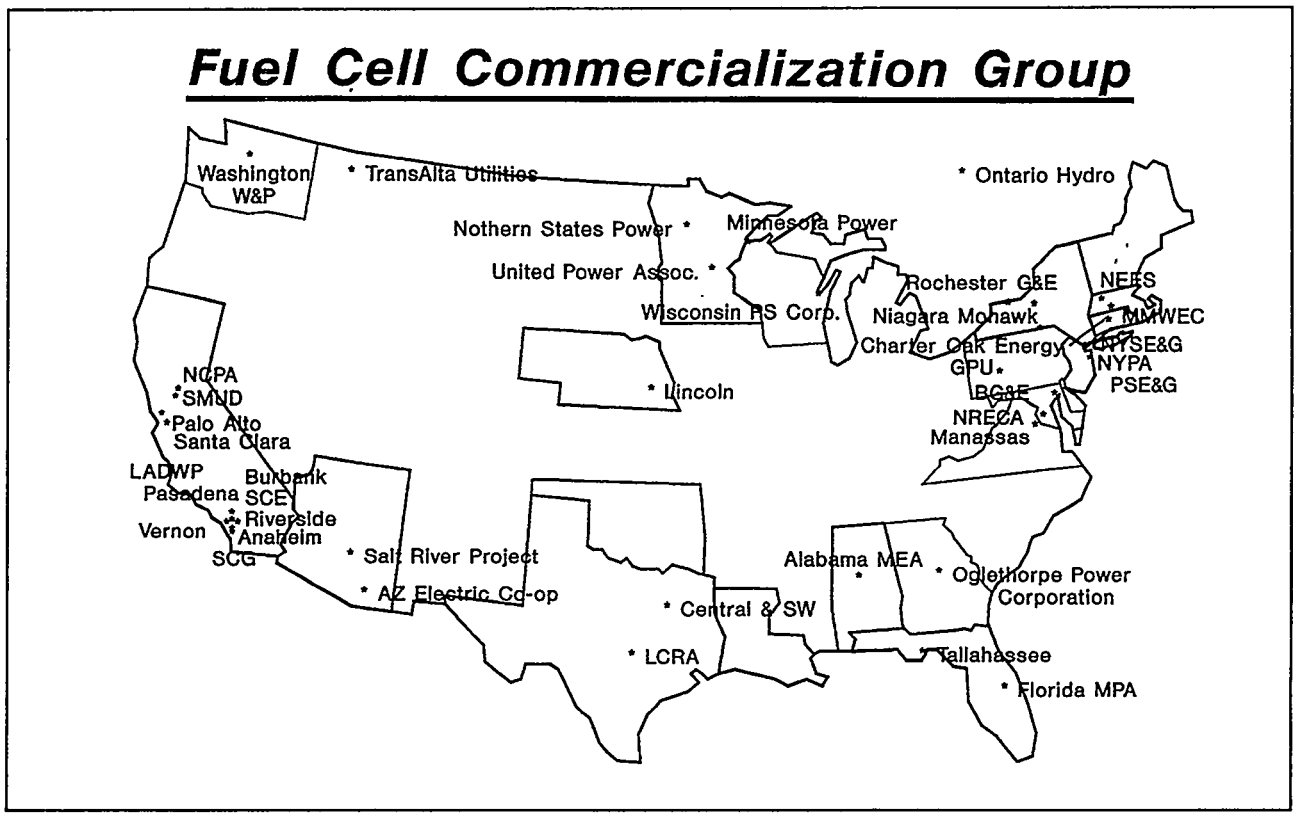


FIGURE 1. CURRENT FCCG MEMBERS

Table 2

FUEL AVAILABILITY

| Energy Source | Total Current % | Incremental in 2000-2009 % | Incremental in 2010-2019 % | Incremental in 2020-2029 % |
|---|---|---|---|---|
| Natural Gas | 97 | 93 | 69 | 65 |
| Coal | 84 | 60 | 85 | 85 |
| Hydroelectric | 74 | 30 | 15 | 20 |
| Nuclear | 65 | 3 | 15 | 18 |
| Fuel Oil | 61 | 20 | 15 | 20 |
| Renewable | 16 | 37 | 31 | 30 |
| Solar | 10 | 20 | 35 | 25 |
| Wind | 6 | 20 | 35 | 30 |
| LNG | 6 | 3 | 0 | 0 |

The current 1992 power generation capacities of the 31 responding utilities are shown in Table 3. We believe these to be representative of the entire U.S. and Canadian power generation capacities. Almost 90% of the respondents expect natural gas to be the preferred fuel for the CFCPP in the 2000-2009 period. In the following decade, coal is expected to be the preferred fuel by a ratio of three to two rising to three to one in the 2020-2029 period.

Almost all utilities indicated they dispatch based on the marginal cost of production of electricity as shown in Figure 2. Twenty-six percent of the utilities indicated that in addition to the COE they dispatch based on other factors such as heat rate, environmental transmission restrictions or reliability. Environmental factors are expected to play a much more important role in the 21st century with $SO_x$, $NO_x$, and $CO_2$ being of roughly equal importance as shown in Figure 3. Survey respondees rated fuel cell characteristics as shown in Figure 4. Again, emphasis was on costs. Again, it should be noted that this study focused on larger plants so that many of the small, i.e., 2 MW plant attributes were not considered in this particular survey.

Competing technologies were assessed and their relative importance is shown in Table 4. Combined cycle and IGCC plants were the major sources of competition.

Finally, the survey indicated that the greatest

Table 3

CURRENT POWER GENERATION

| Fuel | Capacity, MW |
|---|---|
| Natural Gas - Baseload | 24,017 |
| Natural Gas - Peaking | 24,558 |
| LNG + Natural Gas | 2,716 |
| Coal | 127,658 |
| Fuel Oil | 13,023 |
| Nuclear | 51,667 |
| Hydroelectric | 34,439 |
| Renewable Fuels | 210 |
| Solar | 2 |
| Wind | 419 |
| Other (1) | 2,093 |
| TOTAL | **280,802** |

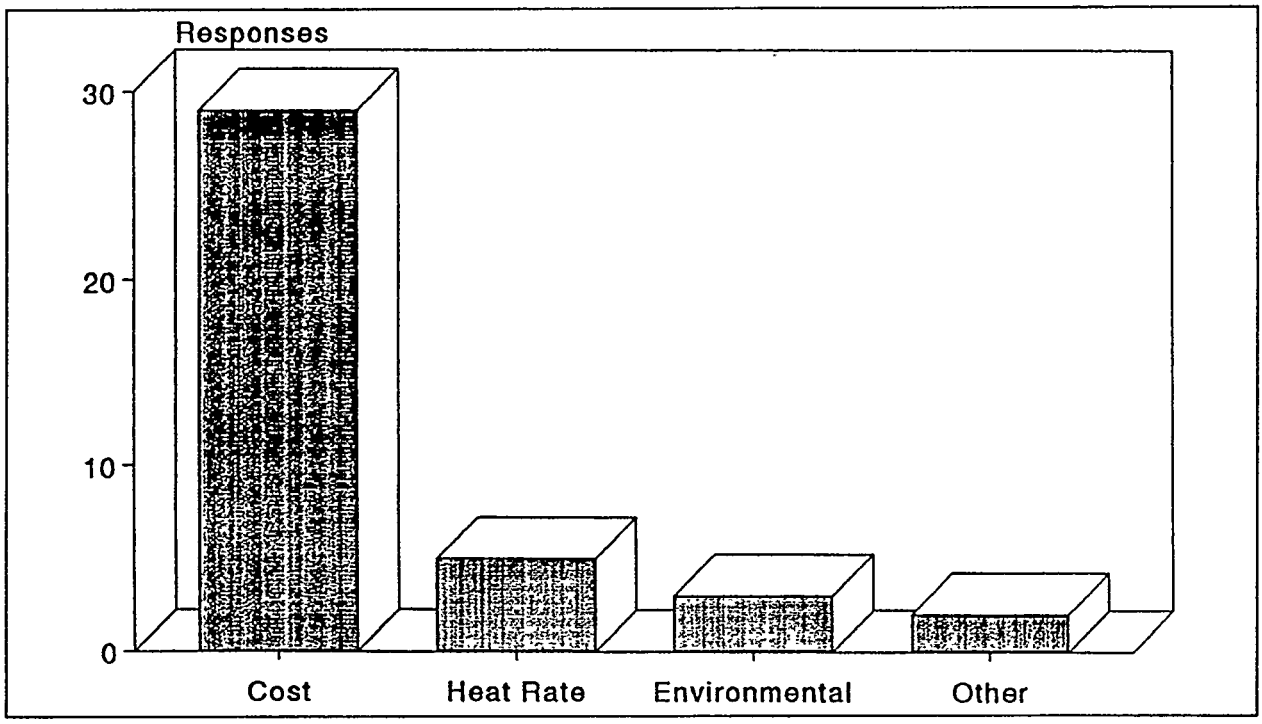


FIGURE 2. BASIS FOR DISPATCHING PLANTS

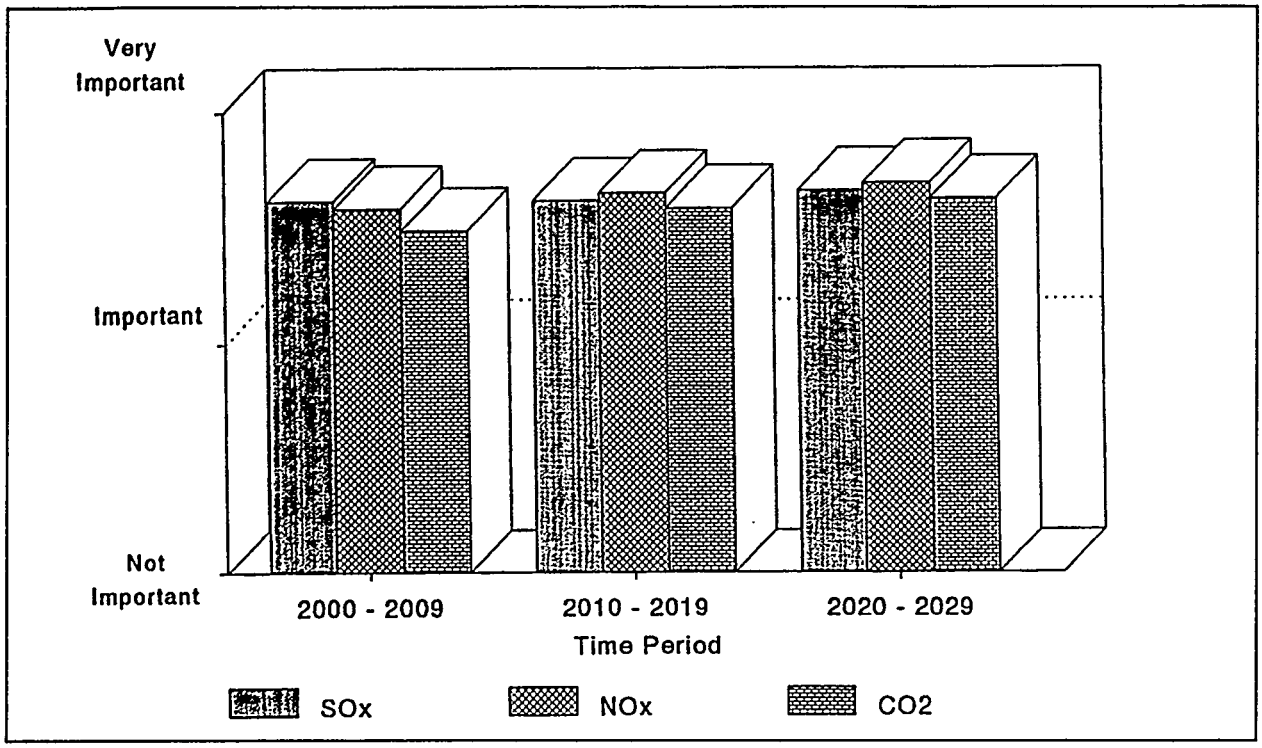


FIGURE 3. IMPORTANCE OF EMISSIONS

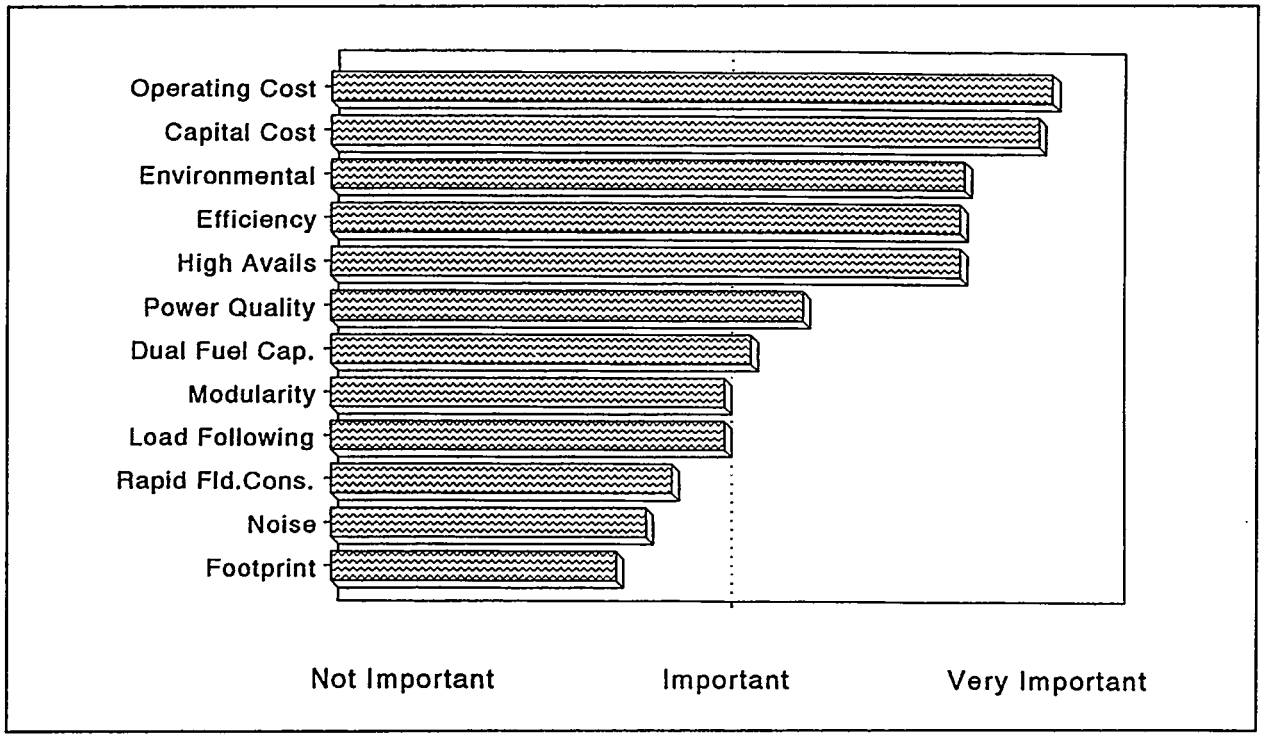


FIGURE 4. IMPORTANCE OF FUEL CELL CHARACTERISTICS

TABLE 4

COMPETING TECHNOLOGIES

| High | Medium to High | Medium | Low |
|---|---|---|---|
| Combined Cycle | IGCC | Pulverized Coal | Nuclear |
| | Humid Air Turbine | Fluidized Bed Coal | |
| | Gas Turbine | Chemically Recuperative Cycle | |

interest was in smaller plant sizes. Of the positive responses with respect to being one of the first to add a CFCPP, about 64% were interested in a plant size less than 50 MW and for mature technology, most interest was still for plants below 100 MW in size as shown in Figure 5.

2 MW Direct Fuel Cell Power Plant

ERC's initial target market has been directed at small power plants in the 2 MW size range. There are several market opportunities:

- Municipal Utility

Municipal utilities represent 15% of the U.S. market for electricity sales. This amounts to about 90 GW. The average MU is less than 50 MW in size although several such as LADWP and Salt River Project (Phoenix) are quite large.

The small MUs including National Rural Electric Cooperative Association (NRECA) members, are good candidates for the small DFC power plants in the 2 MW size range or in multiples thereof. They can achieve low COEs and clean non-polluting electric generation even with small power plants. No other generation option can compete with the DFC in this arena. This is baseload and intermediate generation on a small scale but very competitive. The MU market is well documented in a report for EPRI[7].

- Dispersed Generation

Larger utilities until recently would normally not even consider a 2 MW generation in their mix. But times are changing, and like the telephone industry a decade ago, the utilities are seeing more competition. Individual utilities will react in different ways to the changes. Some will leave generation to the independent power producers. Others will move on to more aggressive dispersed generation as one option. In this mode, the utility benefits from the low COE and non-polluting characteristics of the fuel cell, while at the same time, may benefit from transmission and distribution credits, VAR control, shorter planning and construction times, cogeneration

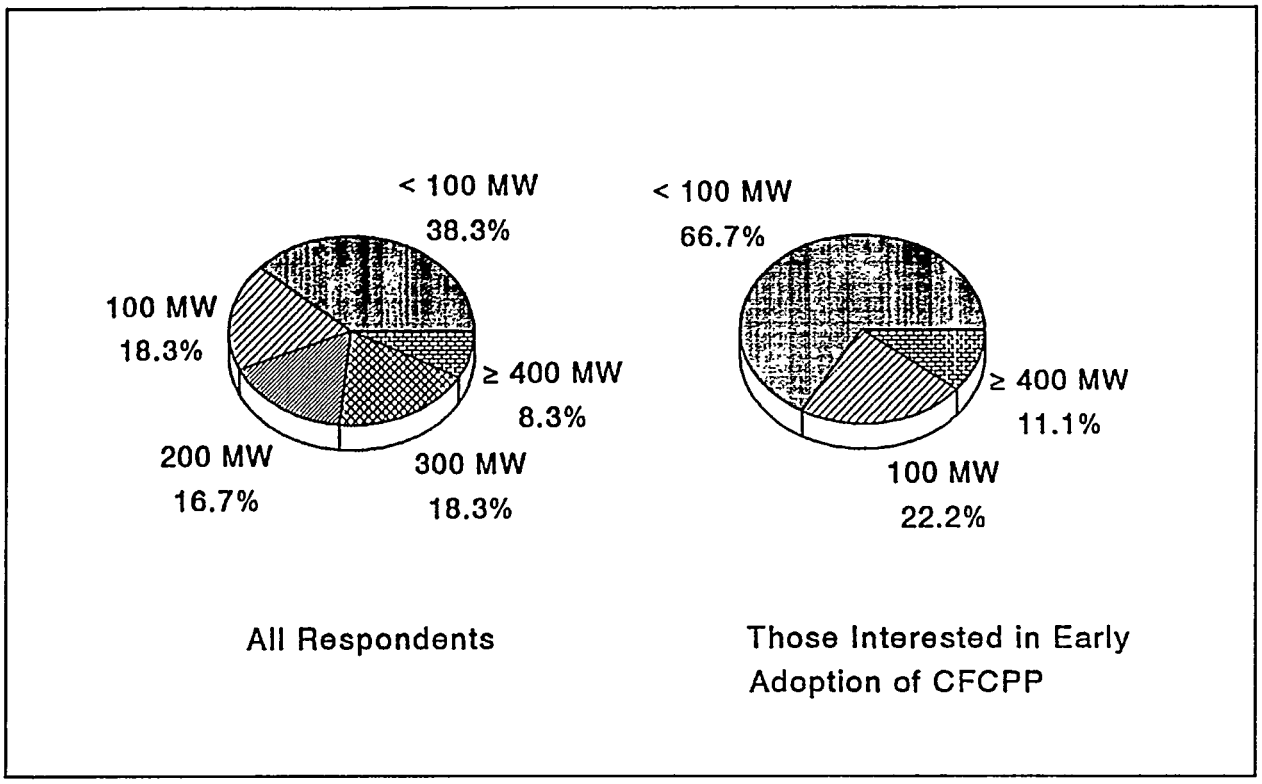


FIGURE 5. MOST ATTRACTIVE CFCPP SIZE

opportunities and ease of siting. These and other benefits lead to real credits described in the previous section which can be used to offset either plant, fuel or operating costs.

- Niche Markets

EPRI has identified at least one major specialty market - landfill gas [8,9]. Over 700 sites in the 2-10 MW size range have been identified. The DFC performance is not greatly impacted by the high carbon dioxide concentrations in landfill gas. While the gas must be cleaned, it represents a low cost fuel source uniquely suited for DFC fuel. The total market in the neighborhood of 5000 MW represents a nice opportunity for early DFC sales.

- Cogeneration

The ability to build 2 MW DFC plants near the user site opens up many possibilities for cogeneration. Because of the high quality of waste heat (~700F) available, a number of options are possible. High and low pressure steam for industrial applications as well as water heating, air conditioning and space heating for both industrial and commercial applications and even district heating are feasible.

In general, the waste heat utilization credit is an order of magnitude lower in economic terms compared to the value of the electricity produced but the energy efficiency is increased to the 75-80% level. For larger plants, except

for some industrial cogeneration applications, the waste heat is better used in a bottoming cycle to produce more electricity.

The quality of waste heat is very important in the wide spread general applicability of cogeneration and the carbonate fuel cell is best positioned for the cogeneration market.

## ORGANIZATION

Energy Research Corporation (ERC) has created two wholly-owned subsidiary companies Fuel Cell Manufacturing Corporation (FCMC) and Fuel Cell Engineering Corporation (FCE). The three companies have three distinct missions. ERC, the parent company, is responsible for research, development, administrative and financial activities relating to fuel cells, batteries and other products. FCMC is responsible for the manufacturing of Direct Fuel Cell Stacks and Modules. FCE has the overall responsibility for power plant design, site construction, marketing, sales and after market servicing with access to FCMC products. ERC and its subsidiaries have been working together with Fluor Daniel Corp. since 1981 on a variety of natural gas and coal gas phosphoric acid and carbonate fuel cell projects. Most recently, Fluor has been working with FCE on the balance of plant design for the 2 MW SCDP project whose design is essentially complete and in the carbonate fuel cell portion of Clean Coal V project.

In addition to the intercompany relationships, ERC and FCE have formal and informal relationships with respect to the carbonate fuel cell on a worldwide basis.

FCE is in the process of completing a supply agreement and license agreement with SCDP. Further, ERC is negotiating a model contract with FCCG. ERC has cooperative agreements with Deutsche Aerospace AG, Mitsubishi Electric Co., and Sanyo Electric Co. ERC/FCMC has production agreements with Deutsche Aerospace AG. Deutsche Aerospace AG in turn, has formed a European Consortium consisting of RWE AG and Ruhrgas AG, large German electric and gas utility companies respectively, and with Haldor Topsoe A/S and Elkraft Power Company Ltd., Danish engineering and electric utility companies, respectively.

The ERC relationships endure in many cases in the engineering and cooperative agreement areas dating back at least a dozen years or more. We believe this reflects a consistency derived from sound technical progress and mutual trust.

## REFERENCES


1. "MCFC Power Plant System Verification," M. Farooque, et al, Joint Contractors Review Meeting, DOE, Aug. 1993

2. "MCFC Product Development Test," A. K. Kush, A. Leo and T. O'Shea, Joint Contractors Review Meeting, DOE, Aug. 1993.

3. "Development of Internal Reforming Carbonate Fuel Cell Stack Technology," M. Farooque, et al, Final Report for DOE Contract No. DE-AC21-87MC23274, 1990.

4. "Advanced Molten Carbonate Fuel Cell Systems Using BGL Gasification," S. J. Meyers, 9th Annual Conference on Gasification Power Plants, EPRI, Oct. 1990.

5. "Cost and Performance of an $N^{th}$ Generation 2 MW Carbonate Fuel Cell Power Plant Based on the Santa Clara

Demonstration Project Design," H. S. Sandler, M. Farooque, Fuel Cell Seminar, Nov./Dec. 1992.

6. "Molten Carbonate Fuel Cells as Distributed-Generation Resources, Case Studies for the Los Angeles Department of Water and Power," M. M. El-Gasseir, Final Report, EPRI, May 1992.

7. "The Market for Fuel Cell Power Plants Within Municipally Owned Utilities," Technology Transition Corporation, Final Report, EPRI, Jan. 1990

8. "Survey of Landfill Gas Generation Potential, 2 MW Molten Carbonate Fuel Cell," Resource Management International, Inc., Interim Report, EPRI, Sept. 1992

9. "Evaluation of a 2 MW Carbonate Fuel Cell Power Plant Fueled by Landfill Gas," Haldor Topsoe, Inc., Final Report, EPRI, Nov. 1991

## 1.2 Overview of M-C Power's MCFC Power Generation System

CONTRACT INFORMATION

| | |
|---|---|
| Contract Number | DE-AC21-90MC27394 |
| Contractor | M-C Power Corporation<br>8040 S. Madison Ave.<br>Burr Ridge, IL 60521-5808<br>(708) 986-8040 |
| Contractor Project Manager | Thomas G. Benjamin |
| Principal Investigator | Richard R. Woods |
| METC Project Manager | Mark Williams |
| Period of Performance | September 13, 1990 to September 14, 1994 |

Schedule and Milestones

IMHEX® Commercialization Program Schedule

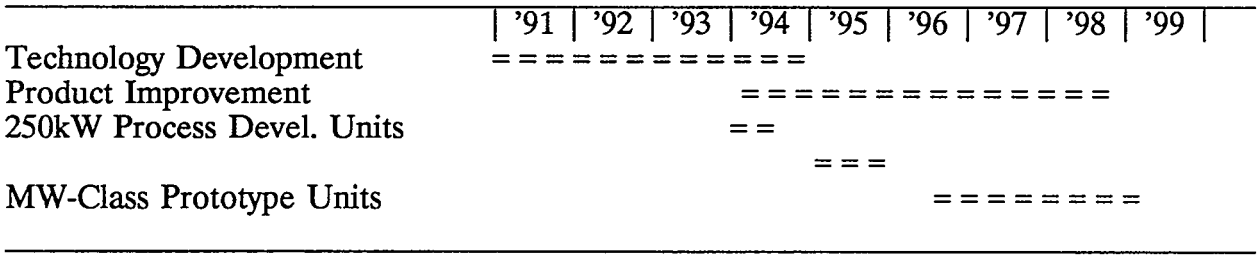


### OBJECTIVE

The objective to the IMHEX® Commercialization Program is to develop market-responsive molten carbonate fuel cell products. The program has four integrated elements: Technology Development, Field Verification, Manufacturing Technologies, and Market Development. The program goal is to achieve initial market entry by the late 1990s. Ongoing product definition activities are focusing on a nominal 1 MW power plant which achieves an electric generation efficiency of 50% HHV.

### BACKGROUND INFORMATION

With the turn of the decade, the power generation industry in the United States is continuing the evolutionary process that began in the 1980s. Increased competition and stronger environmental restrictions are at the center of these changes. The typical electric utility is likely to appear quite different after the year 2000, and this evolution may continue for another twenty years. Competitive bidding within the

power generation industry is responding to the need for new capacity, and as it now appears, transmission system access is on the horizon. Natural gas is becoming the fuel of choice in the near term for most new capacity or repowering projects.

The IMHEX® fuel cell power generation system is a skid mounted power plant which efficiently generates electricity and useful thermal energy. The primary benefits are its high electric generation efficiency (50% or greater), modular capacities (500kW to 3MW per unit) and minimal environmental impacts (less than 1ppm $NO_x$). A cost effective, modular capacity fuel cell power plant provides the industry with an attractive alternative to large central station facilities, and its advantages have the potential to optimize the way electric power is generated and distributed to the users.

Environmental issues are becoming the single most uncertain aspect of the power business. These issues may be manifested in air emissions permits or allowances for $NO_x$ or $SO_2$, energy taxes, $CO_2$ limits, "carbon taxes", etc. and may appear as siting permits for generation, transmission, or distribution facilities. Utilities are "down-sizing" with the goal of becoming the lowest cost supplier of electricity and are beginning to examine the concepts of "energy service" to improve their economic competitiveness. These issues are leading utilities to examine the benefits of distributed generation. Siting small capacity generation near the customer loads or at distribution substations can improve system efficiency and quality while reducing distribution system costs. The advantages that fuel cell power plants have over conventional technologies are critical to the success of these evolving opportunities in the power generation marketplace.

## IMHEX® TEAM

M-C Power Corporation was formed in 1987 with the sole mission (Figure 1) of commercializing molten carbonate fuel

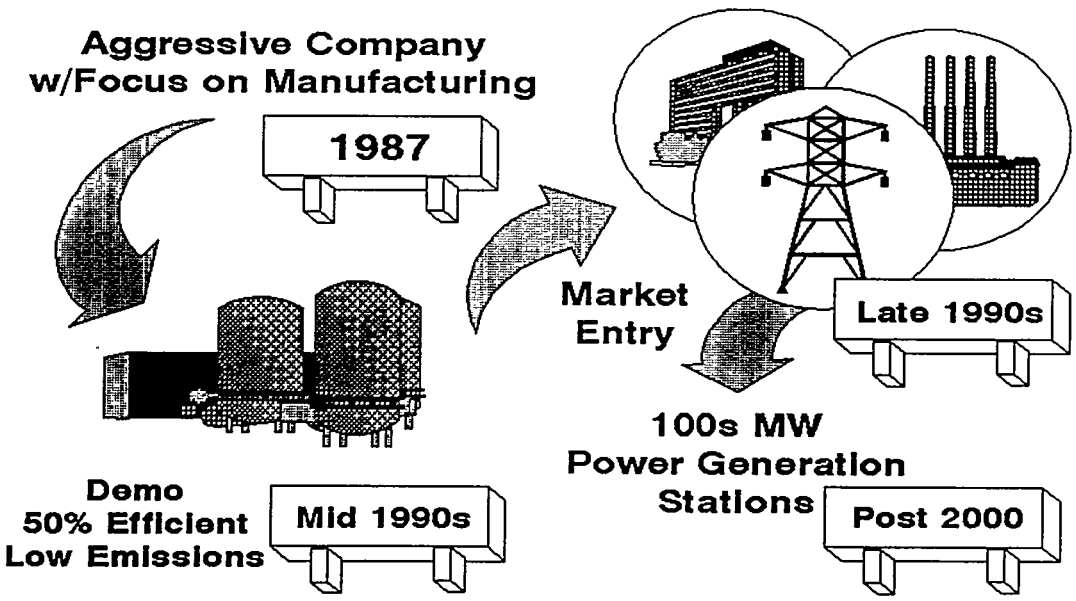


**Figure 1. M-C Power's Mission**

cells (MCFC). Central to this effort is the internally manifolded heat exchanger (IMHEX®) stack design concept which eliminates key engineering issues present in other stack designs.

To achieve this goal, a impressive partnership (Figure 2) has been established. M-C Power's leadership role includes development and manufacturing of commercial scale IMHEX® fuel cell stacks and management of the IMHEX® Team.

optimization efforts required to integrate the fuel cell stack into a complete power plant.

The final member is Stewart and Stevenson Services, which is the world's largest supplier of packaged diesel and aero-derivative gas turbine power generation systems. Their primary business focus is unitized, factory packaged power plants up to 50MW capacity. Stewart and Stevenson will fabricate the balance-of-plant equipment into transportable skid

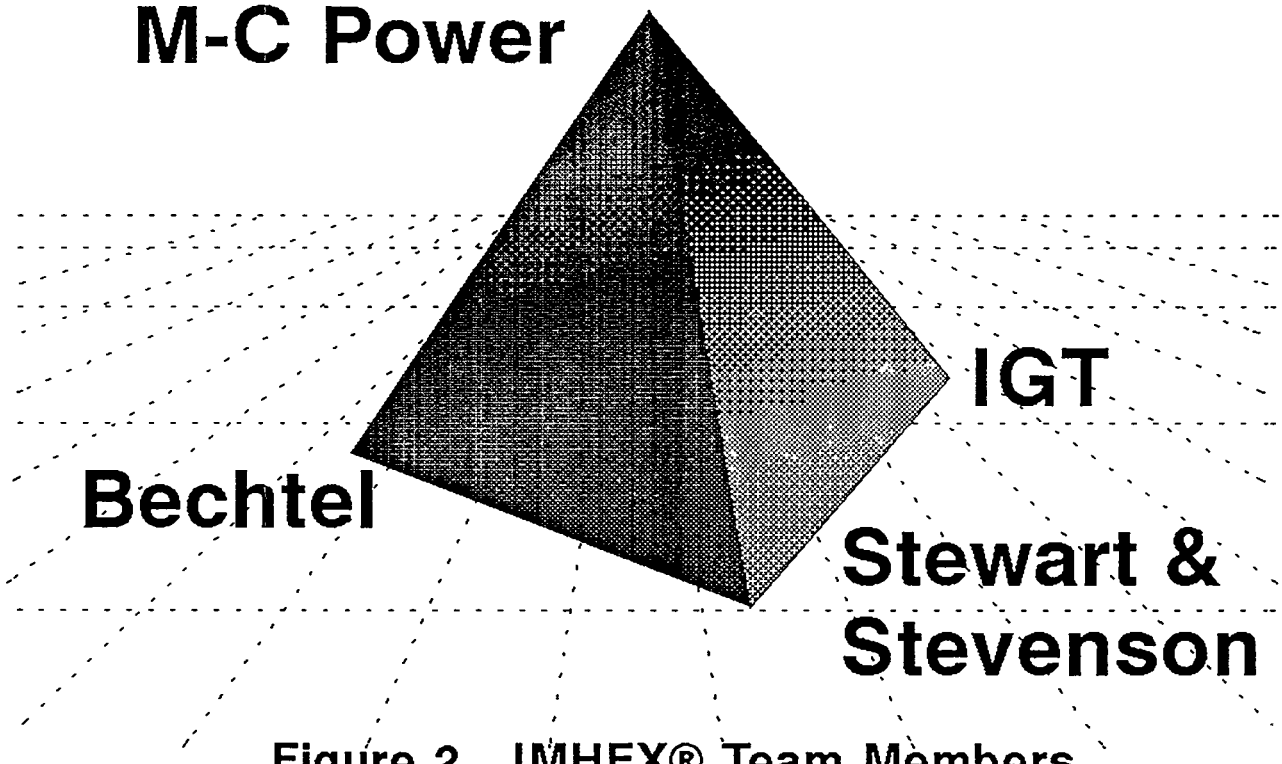


**Figure 2. IMHEX® Team Members**

The Institute of Gas Technology, M-C Power's parent company and inventor of the IMHEX® concept, provided the fundamental MCFC component technology and continue to contribute product improvements.

The Bechtel Group, the premier engineering and construction firm in the U.S.A., is the third team member. Their role is the process engineering and system design assemblies and provide the distribution, service and maintenance infrastructure required by the marketplace.

## MARKETPLACE CRITERIA

In addition to the above team, the Alliance to Commercialize Carbonate Technology (ACCT) was formed in 1991 and consists of representatives from over

sixty companies interested in our developing technology. These members provide an vital link between the marketplace requirements and definition of a market responsive product.

Over the past few years market surveys have been conducted with these representatives to assess their product requirements and decision criteria. The primary results can be summarized in a very few words - durability, performance and cost-effectiveness.

Each individual company has a different view of the how fuel cells will be applied within their resource mix, and as a result, no clear, single application or product definition arises from these generic surveys. All seem to anticipate very large opportunities for the fuel cell's high performance and clean emissions. Some focus on more traditional larger scale facilities, while others on the potential for repowering applications in the 30 to 100 MW range. The broadest segment appears to concentrate on the smaller capacity distributed generation applications, but this segment diverges based on specific site criteria, such as by-product heat utilization and operating strategy.

During 1993 the ACCT members responded to a M-C Power survey which addressed performance and cost issues. Prior discussions indicated that power plants must be cost-competitive even during the introduction phases of commercialization. A series of power plant specification options were identified which traded-off part load performance characteristics against cost and unit capacity. The results indicated that ACCT members preferred the high performance options (from 50 to 100% of rated output) over both lower cost and smaller capacity options.

With the increasing competitive environment in which the utilities find themselves, an advanced product must first meet the customer's expected durability and reliability criteria. Any product, independent of its ultimate promise, must be durable in the intended application. If an introductory product does not meet this go no/go criteria, follow-on orders will not exist. As a result, the IMHEX® team has selected a step-wise power plant development effort which minimizes the risks in preparation for a series of MW-Class verification units.

## COMMERCIALIZATION PROGRAM

The IMHEX® Commercialization Program is a comprehensive research, development and demonstration effort which was defined in 1990 with the single focus of introducing a IMHEX® fuel cell power plant by the late 1990s. Stack technology, scale-up and development have been the focus areas over the past few years including the successful operation of several 20kW units. Current focus is shifting toward the design, installation and operation of two 250kW process development power plants in 1994/1995.

In parallel with these process verifications, application specific product definition activities by selected ACCT members and design optimization and cost-trade-off studies by the IMHEX® Team members will finalize the design, characteristics and features of a MW class power plant for initial market entry. Operation of three to six prototype power plants in the 1996 to 1998 time frame is designed to demonstrate the viability, durability and performance of this market entry product.

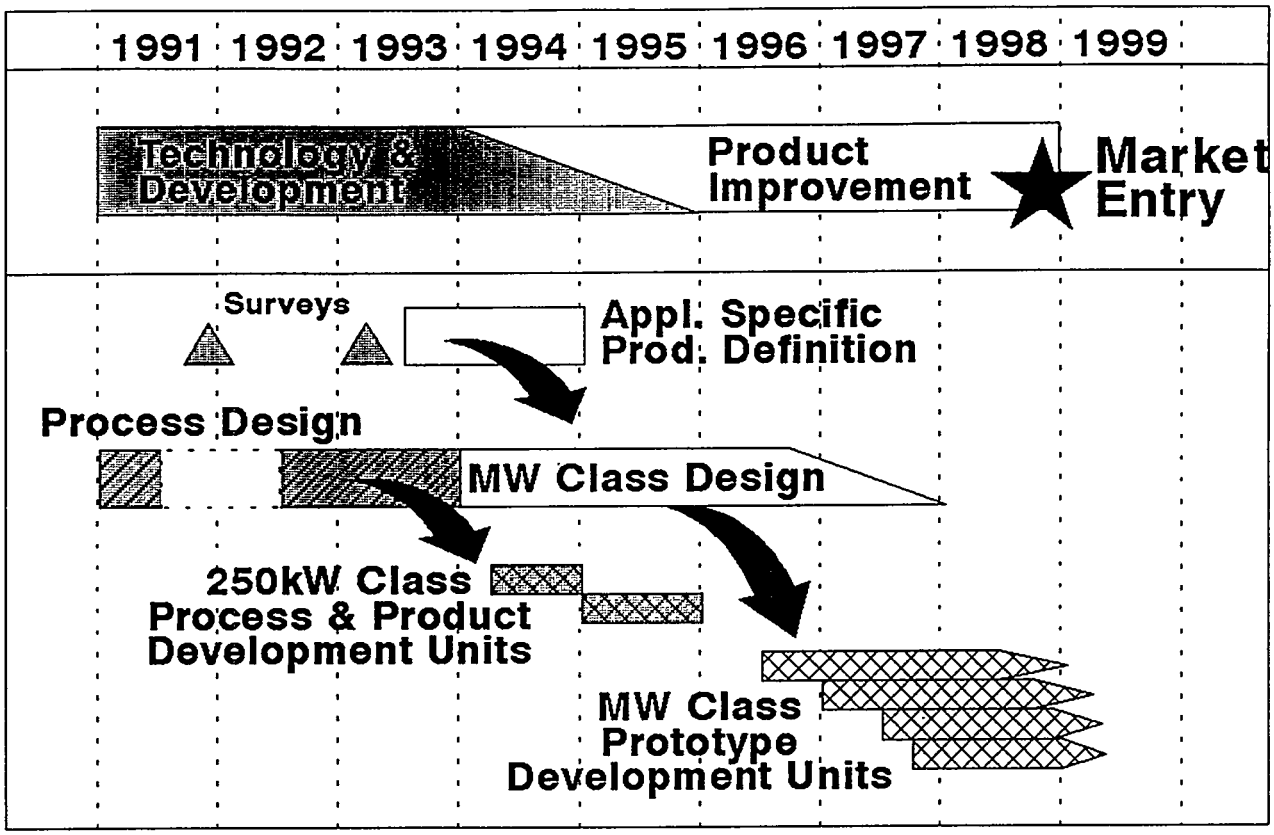


**Figure 3. IMHEX® Commercialization Program**

The IMHEX® Team would like to thank our sponsors:
U.S. Department of Energy, Gas Research Institute, Electric Power Research Institute, San Diego Gas & Electric, Southern California Edison, Union Oil of California, Southern California Gas, South Coast Air Quality Management District, the State of Illinois, PSI Energy and Tenneco Gas.

## 1.3 MCFC Product Development Test

### CONTRACT INFORMATION

| | |
|---|---|
| **Cooperative Agreement Number** | DE-FC21-92MC29237 |
| **Contractor** | Fuel Cell Engineering Corporation<br>3 Great Pasture Road<br>Danbury, CT 06813<br>(203) 790-6922 |
| **Contractor Project Manager** | Ashok K. Kush |
| **Principal Investigators** | Ashok K. Kush (FCE)<br>Anthony J. Leo (FCE)<br>Thomas P. O'Shea (Santa Clara Demonstration Project) |
| **METC Project Manager** | Thomas J. George |
| **Period of Performance** | October 1, 1992 to December 31, 1996 |

**Schedule and Milestones**

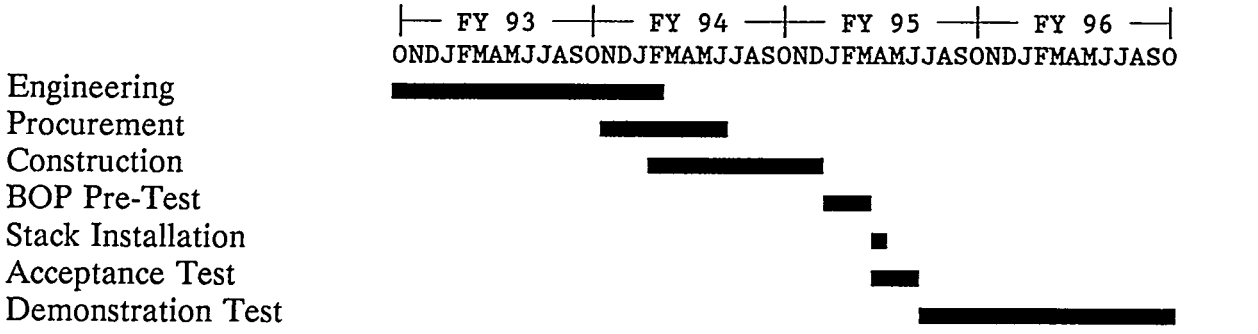


### OBJECTIVES

The objective of the 2MW Santa Clara Demonstration Project is the demonstration of the direct carbonate fuel cell technology at full scale. Specific objectives of the project include the demonstration of advantages of the carbonate fuel cell power plant, such as high efficiency, low emissions, reactive power capability, and high reliability and availability. The project will also provide a design basis for pre-commercial power plants.

## BACKGROUND INFORMATION

The project is an outgrowth of the ongoing direct carbonate technology development work and commercialization efforts at Energy Research Corporation (ERC, parent company to Fuel Cell Engineering Corporation). ERC is working with the Fuel Cell Commercialization Group (FCCG) in a collaboration to commercialize the carbonate fuel cell technology in the late 1990's. The FCCG is a group of 41 utilities who are potential buyers of the pre-commercial Early Production Unit power plants. A commercialization path has been identified which includes the demonstration of the technology in power plants prior to the Early Production Unit phase. The Santa Clara Plant will be the first of these demonstrations, and the project's utility participants also belong to the FCCG membership. The participants in the Santa Clara Demonstration Project (SCDP) are as follows: City of Santa Clara, City of Los Angeles Department of Water and Power, City of Vernon Light and Power Department, Electric Power Research Institute, National Rural Electric Cooperative Association, Sacramento Municipal Utility District, and Southern California Edison Company.

A critical step in ERC's commercialization effort was the formation of two subsidiaries in 1990: The Fuel Cell Manufacturing Corporation (FCMC) and the Fuel Cell Engineering Corporation (FCE). FCMC will manufacture carbonate stacks and multi-stack modules, initially from its pilot manufacturing facility in Torrington, CT and eventually from a commercial manufacturing facility. FCE is responsible for power plant design, integration of all subsystems, sales/marketing, and client services.

FCE began work on the Santa Clara demonstration power plant design in 1990, and submitted a preliminary design to the SCDP in August, 1991. A series of studies were conducted to optimize the design over the next year, and Final Engineering began in September, 1992. The design of the multi-stack modules used in the DC power section of the plant was begun earlier under EPRI and ERC support. The DOE supported portion of the project began in October, 1992 and included the development of environmental information and the development of the final design of the multi-stack module. The DOE cooperative effort will also cover the manufacture of the fuel cell stacks and multi-stack modules for the plant.

## PROJECT DESCRIPTION

The project is being funded by the SCDP, ERC and by the U.S. Department of Energy under the Cooperative Agreement. Fuel Cell Engineering Corporation is providing over all management of the project. The stack design is being developed by ERC based on technology from separate ongoing development programs. The fuel cell stacks and multi-stack modules will be fabricated by FCMC. Fluor Daniel, Inc. is serving as the power plant A&E and is providing engineering support to the design of the multi-stack modules. An organization chart for the project is shown in Figure 1.

The site for the plant is located at 1255 Space Park Drive in the City of Santa Clara. The site is owned by the City's Electric Department and is immediately adjacent to the Scott Receiving Station, a 115/60kV switching station on the City electrical system.

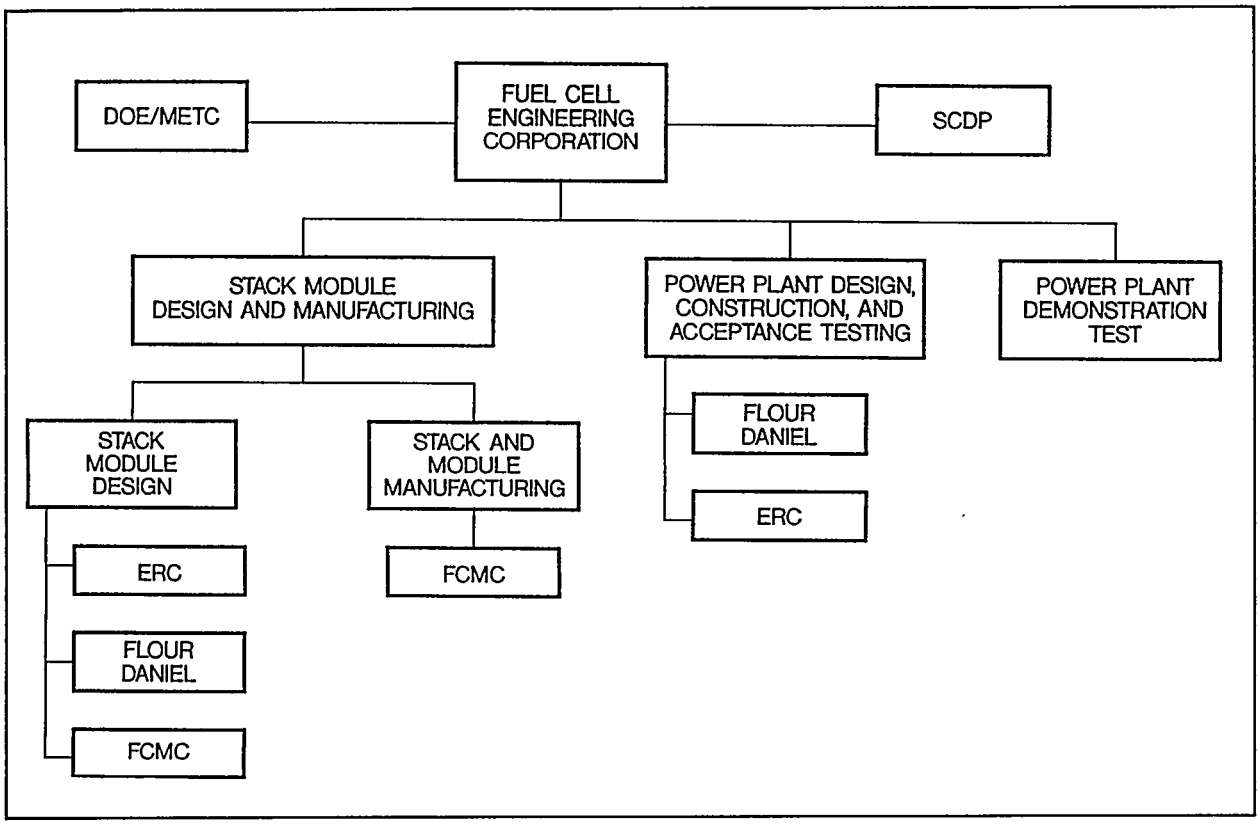


Figure 1. 2 MW Carbonate Fuel Cell Demonstration Program Organization

The power plant will use 16 fuel cell stacks, delivered to the site in truck-shippable 4-stack submodules, which will be installed into the two 1MW modules to comprise the DC power section of the plant. The power plant process is ERC's Simplified Design, as described below.

## RESULTS

### Power Plant Process and Mechanical Design

The process involves treating natural gas to remove impurities, after which it is mixed with steam and sent to the fuel cell stacks. The fuel/steam mixture is reformed within the stacks, providing the hydrogen which is consumed in the fuel cell anodes. The anode reaction also produces $CO_2$, which is required in the fuel cell cathodes. The cathode feed is produced by taking the anode exhaust, oxidizing any residual fuel with air, and sending the flue gas with excess air to the cathodes.

A simplified process flow diagram is shown in Figure 2. The system represents ERC's Simplified Design, with provision for startup, fuel cleanup, recirculation of carbon dioxide to the cathode side and exhaust of spent gases. Natural gas is preheated using the system exhaust gases and treated to remove odorants and impurities before being mixed with steam for use in the fuel cells. The fuel is internally reformed to hydrogen in the fuel cell stacks, and 75% of the hydrogen is

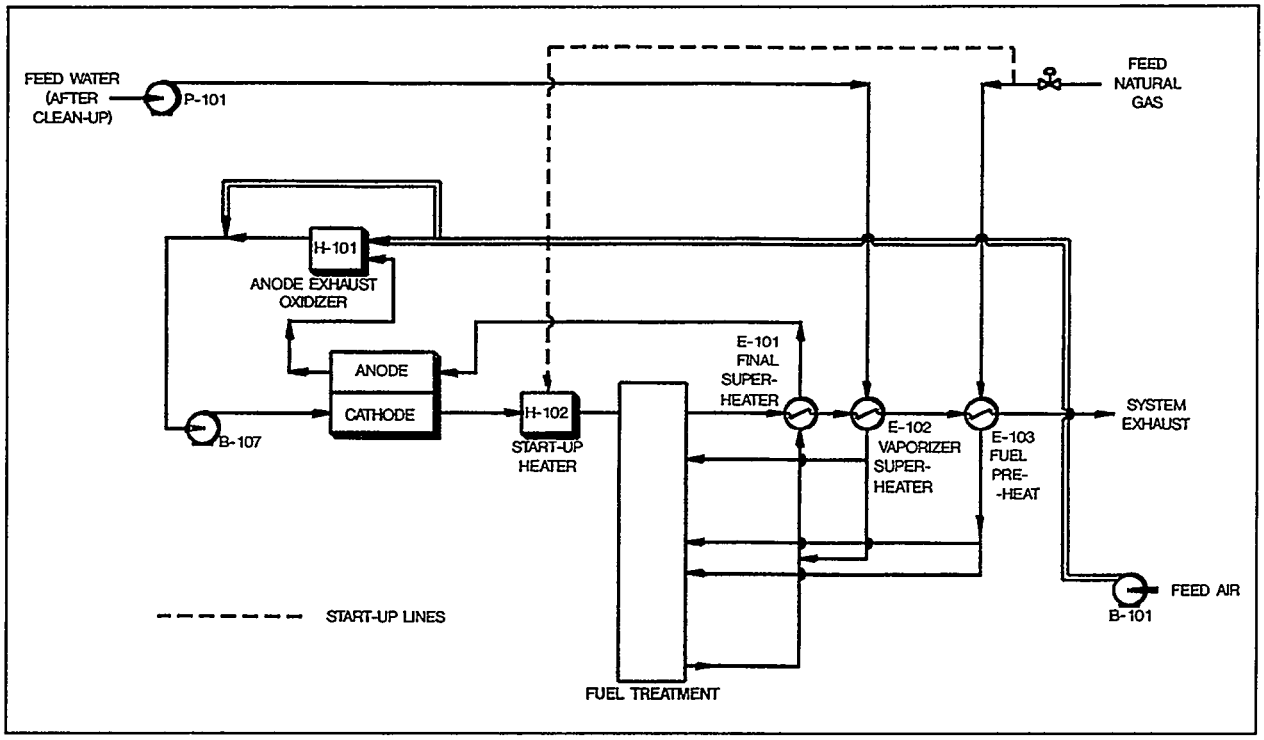


Figure 2. Simplified Process Flow Diagram For 2 MW Santa Clara Carbonate Fuel Cell Demonstration Plant

consumed in the power generation reactions of the fuel cell anodes, producing water and $CO_2$. The anode exit stream consists of steam, $CO_2$, carbon monoxide from the reforming and shift reactions, and 25% of the residual hydrogen. The exit stream is sent to the oxidizer, H-101, where the hydrogen and carbon monoxide react with excess air. This oxidizer produces no measureable $NO_x$.

This quenched flue gas stream contains the oxygen and $CO_2$ required by the fuel cell cathodes, and is sent back to the fuel cells as the cathode feed stream. The quench air used in the anode exit stream oxidizer is adjusted to provide the desired temperature for use in the fuel cell cathodes. After the cathode reactions consume some of the oxygen and $CO_2$, the cathode exit gases are sent to the heat recovery system. The exit gases provide heat to the fuel treatment system, the fuel/steam heater (E-101), water boiler/superheater (E-102) and the fuel preheater. These heat exchangers are configured into a packaged heat recovery unit, which also contains the start-up heater (H-102), the steam generator deaerator, and the system exhaust stack.

In addition to the systems described above, other subsystems in the plant include the water treatment system, instrument air compressor, and backup power generator. The layout of the plant is shown in Figure 3. The plot plan shows the location of the major equipment shown in the process flow diagram, plus additional facilities such as the control room, visitors center, parking area, etc.

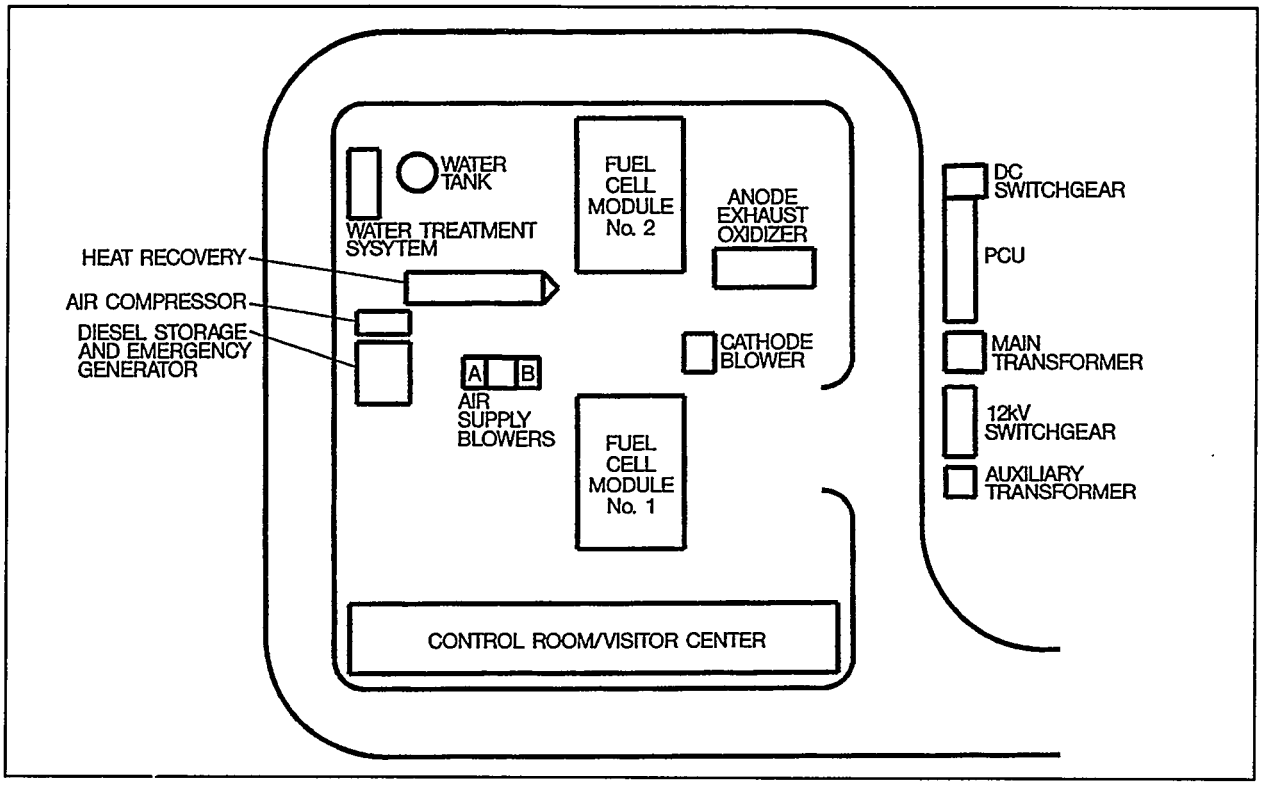


Figure 3. 2 MW Santa Clara Carbonate Fuel Cell Power Plant Plot Plan

The power plant design objectives are listed in Table 1.

**Multi-Stack Module Design**

As can be seen in Figure 3, the DC power section of the plant will consist of two 1MW stack modules. Each of these modules will contain two submodules, which are the truck shippable units which enclose the fuel cell stacks. Each submodule will consist of four stacks and associated piping, instrumentation, and electrical components in a sealed enclosure.

The structural enclosure for the stack submodules will be shop fabricated and shipped to the FCMC facility in Torrington, CT. There the fuel cell stacks will be installed in the enclosure and all piping, electrical, and instrumentation work within the enclosure will be completed. All piping connections will terminate at the enclosure sides with weld connections which will be sealed during shipment to the site. The penetrations of the pipe connections through the enclosure have been specially designed to limit heat loss from the hot pipes to the cool enclosure structure, and to withstand the mechanical stresses caused by the thermal expansion as the process pipes heat from ambient to operating temperature.

All electrical and instrument connections will be brought to terminal boxes on the outside of the enclosure. This design approach provides for installation of the submodules at the Santa Clara site with a minimum of field labor.

Table 1. Power Plant Design Objectives

| | |
|---|---|
| Nominal Capacity (MW) | 2 |
| Power Plant Rating (MW) Net AC | 1.8 |
| Heat Rate (LHV) @ Power Plant Rating (Btu/kWh) | 6850 |
| Maximum Emissions @ Plant Rating (lb/MWh)<br>$SO_x$<br>$NO_x$<br>$CO_2$ | <br>0.003<br>0.0004<br>~845.0 |
| Noise (dB(A) @ 100 ft) | 60 |
| Nominal Output Voltage | 12 kV AC<br>3 Phase, 60 Hz |
| Power Quality | IEEE Std 519 |
| Frequency/Power Droop | 5% |
| Reliability<br>Designed To Meet Utility Standards<br>Availability Factor | <br><br>90% |
| Reactive Power Capability | +/-1.67 MVAR |

An illustration of the module arrangement is shown in Figure 4. Each module will consist of two submodules with associated gas distribution piping, instrumentation connections, and electrical connections. The design of the gas distribution piping is critical to the power plant. Significant variations in flow from stack to stack may lead to reactant utilizations in excess of the design range. A flow modeling effort was conducted during the module design work to insure that the gas distribution system could meet the flow variation specification. To further insure the attainment of good flow uniformity, flow trimming valves have been incorporated in the cathode feed lines. These valves will be set once during the BOP pre-test (before the stacks are installed), using spool pieces which simulate the pressure drop characteristics of the stacks.

**Regulatory and Permit Status**

The project has already addressed many of the regulatory requirements for the power plant. At the beginning of the DOE supported portion of the project, FCE submitted environmental information to DOE to support the submittal of an Environmental Assessment for the National Environmental Policy Act (NEPA) approval. Prior to this, the Bay Area Air Quality Management District had granted the project an exemption from Air Quality permitting requirements. Also, under the California Environmental Quality Act (CEQA) a declaration has been issued, indicating that no significant environmental impact is anticipated, and a Conditional Use Permit has been issued.

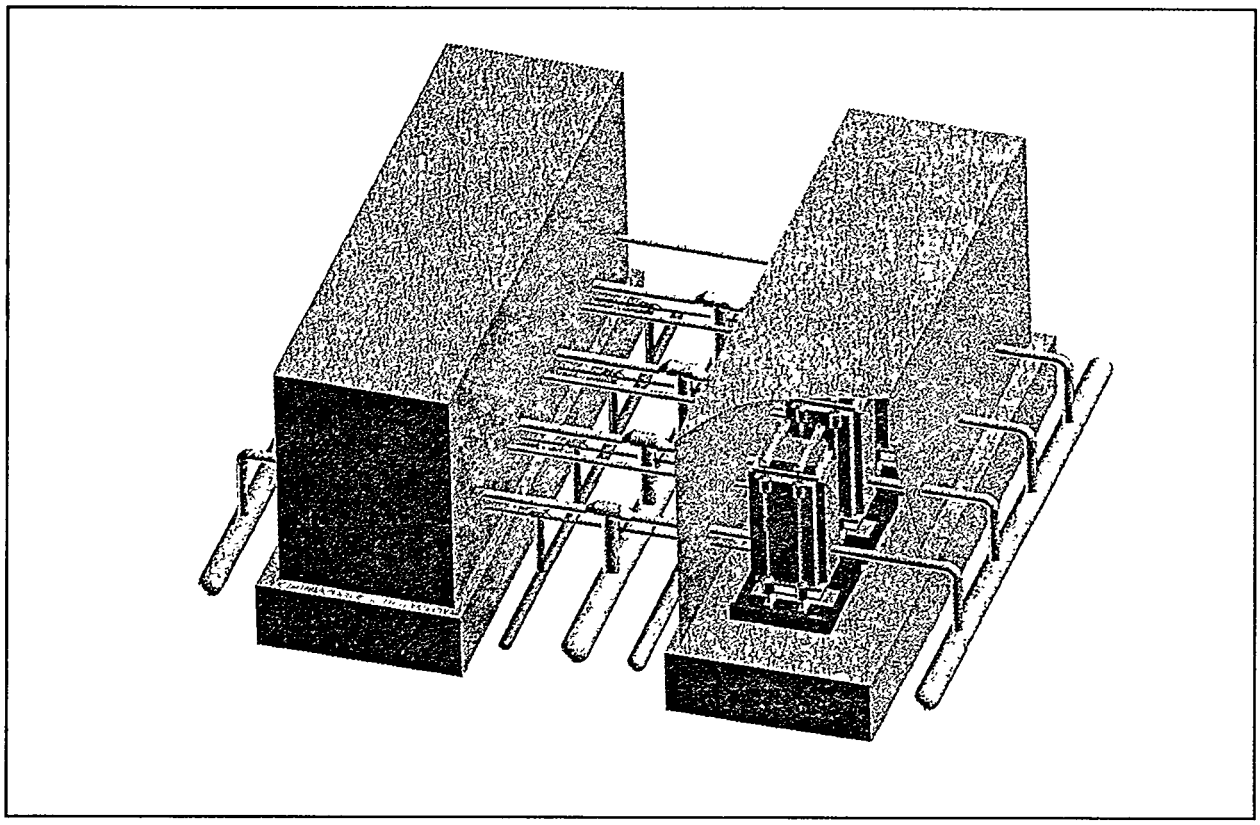

Figure 4. 1MW Carbonate Fuel Cell Module

## FUTURE WORK

The project is currently in the engineering phase, with procurement scheduled to start in late 1993 and construction in early 1994. Upon completion of these activities, the plant start-up phase will begin. This includes BOP testing, stack installation, and power plant initial start-up. Following this, the operational phase of the plant will consist of an acceptance test, followed by the demonstration test period. The acceptance test will be conducted in mid 1995 and the demonstration test is expected to last into late 1996.

## REFERENCES


Eichenberger, P.H., and O'Shea, T.P.;

Update on the World's First 2-MW Carbonate Fuel Cell Demonstration. *1992 Fuel Cell Seminar Program and Abstracts*, p. 183. Nov/Dec 1992.

Serfass, J.A., Glenn, D.R., and Claussen, R.W.; Preparing for Commercialization: The Collaboration Matures. *1992 Fuel Cell Seminar Program and Abstracts*, p. 183. Nov/Dec 1992.

Farooque, M.; An Update of ERC's Carbonate Fuel Cell Development Program. *Proceedings of the Fourth Annual Fuel Cells Contractors Review Meeting*, p. 19. DOE/METC-92/6127. NTIS/DE92001290.

Baker, B.S.; ERC's Carbonate Fuel Cell Power Plant Commercialization Progress. *Proceedings of the Third Annual Fuel Cells Contractors Review Meeting*, p. 74. DOE/METC-91/6120. NTIS/DE91002086.

## 1.4 Molten Carbonate Fuel Cell Product Development Test

### CONTRACT INFORMATION

| | |
|---|---|
| **Contract Number** | DOE Contract No. DE-FC21-92MC28065 |
| **Contractor** | M-C Power Corporation<br>8040 S. Madison Street<br>Burr Ridge, IL 60521<br>(708) 986-8040 |
| **Contractor Project Manager** | Joseph A. Scroppo |
| **Principal Investigators** | Elias H. Cámara<br>Joseph A. Scroppo<br>R. Al Figueroa |
| **METC Project Manager** | Dr. Mark C. Williams |
| **Period of Performance** | September 30, 1992 to March 31, 1996 |

**Product Development Test Schedule**

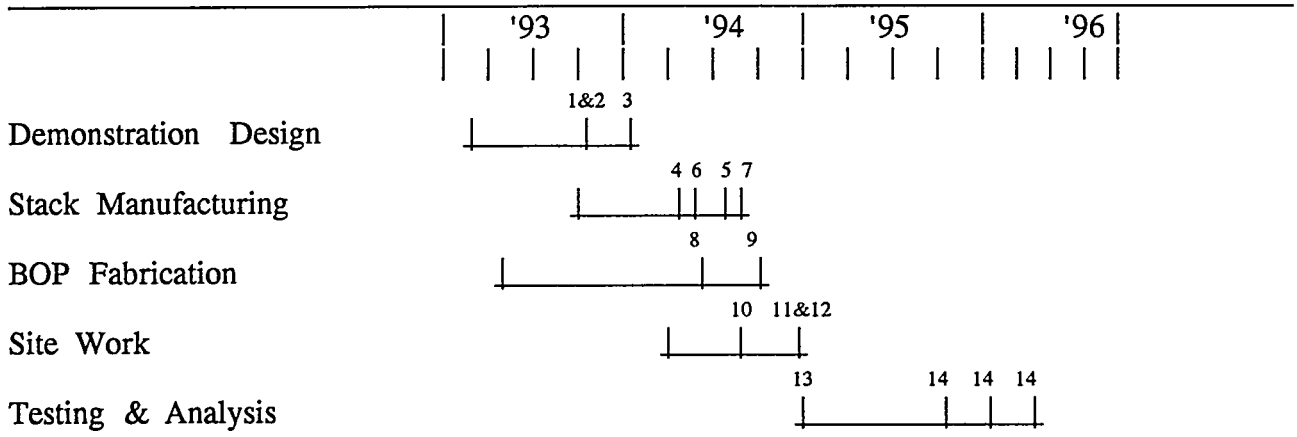


1) Stack Design
2) BOP Design
3) Site Interface Design
4) Stack 1 Assembled
5) Stack 2 Assembled
6) Stack 1 Ship
7) Stack 2 Ship
8) BOP Assembly
9) BOP Ship
10) Site Preparation Complete
11) Plant Installation Complete
12) Plant Commission
13) Ongoing Operation
14) Test Report

## OBJECTIVES

The PDT design objectives will include improved performance at reduced cost compared with the Unocal POC. Other design objectives that will distinguish this demonstration from the Unocal demonstration will be more compact packaging, longer unattended operation, and increased reliability. Additionally, the experience gained during the design and construction of the Unocal power plant will be incorporated. Control system automation will be increased to include start-up. This power plant is being designed for compatibility with the SDG&E electrical distribution grid.

Design goals for this power plant incorporate the results of product definition work and market research performed over the past few years and currently being updated. Design goals for the PDT demonstration unit include:

(1) High electrical and overall efficiency
(2) Cogeneration acceptability
(3) Environmental acceptability (noise and emissions)
(4) Site acceptance (size, aesthetics)
(5) Ease of operation (start-up, shutdown, unattended operation)
(6) Reliability/availability/maintainability/safety
(7) Potential for cost competitiveness

## BACKGROUND INFORMATION

M-C Power Corporation will design, fabricate, install, test, and evaluate a 250 kW Proof-of-Concept MCFC Power Plant. The plant, to be located at Kaiser Permanente's San Diego Medical Center in San Diego, California will be designed and built by Bechtel Corporation, which is responsible for the design, detailed engineering, construction management, and start-up of the proposed MCFC PDT demonstration system. Stewart & Stevenson Services, Inc. will fabricate the BOP equipment on skids. The project defined as "MCFC Product Development Test" (PDT) has been developed in accordance with DOE guidelines under solicitation for cooperative agreement No. De-SC21-91MC28065. DOE will fund design, manufacturing, and fabrication of two IMHEX® stacks for the San Diego power plant. All costs associated with the necessary BOP and the testing of the demonstration power plant are being provided by San Diego Gas and Electric Company (SDG&E), the Gas Research Institute (GRI), the Electric Power Research Institute (EPRI), Bechtel Corporation, and Stewart & Stevenson Services.

Two 250 kW MCFC stacks will be assembled and tested at M-C Power prior to shipment to the field. The Balance-of-Plant, which includes fuel processing, thermal management/heat recovery, controls, and power conditioning systems, will be integrated into a power plant system and shop tested prior to its shipment to Kaiser Medical Center. The 250 kW PDT unit will be operated for a one-year test period. The fuel cell power plant will generate electrical energy and provide by-product heat to the Medical Center's existing steam system. The second stack will be used by M-C Power in its factory to support the San Diego field demonstration effort. Data gathered during power plant operation and maintenance will be analyzed by M-C Power, Bechtel, SDG&E, and Kaiser personnel. Conclusions and recommendations drawn will be used to define future natural gas-fueled MCFC power plants which are fully responsive to the needs of potential customers.

The MCFC PDT demonstration is an integral part of the M-C Power Team's comprehensive commercialization program aimed at bringing on-site MCFC power plants to the commercial market by the late 1990s. A key element of the commercialization effort

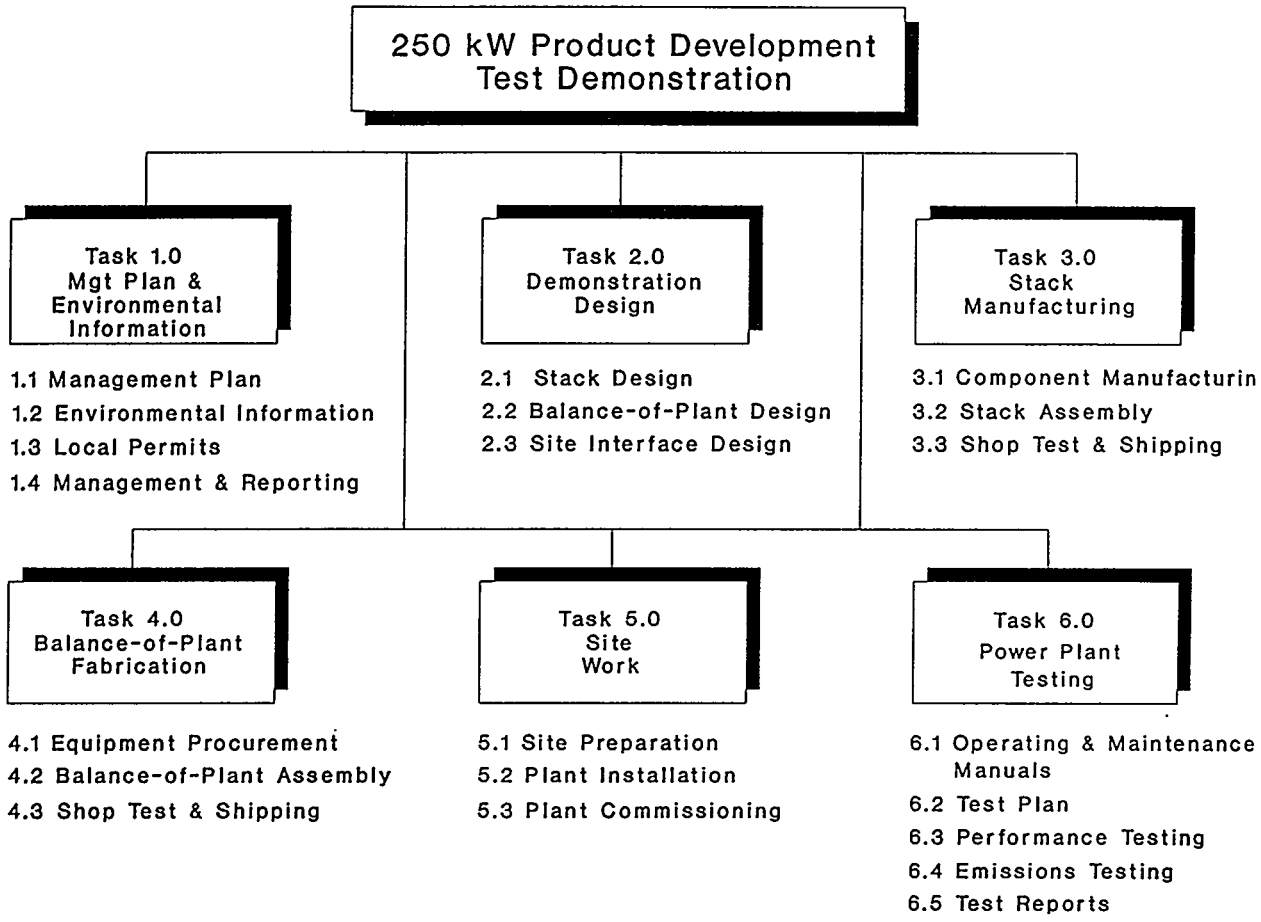


FIGURE 1, WORK BREAKDOWN STRUCTURE

## Figure 2. Work Breakdown Structure Dictionary

**Task 1. Project Management/Permitting**

Objective: Development of project management system for planning, budgeting, executing, and controlling the costs and schedules associated with the work. To obtain permits required for stack and BOP fabrication/testing and site related activities.

| | |
|---|---|
| 1.1 Management Plan | (MCP/Bechtel/SDG&E) |
| 1.2 Environmental Information | (MCP/SDG&E) |
| 1.3 Local Permits | (Bechtel/SDG&E) |
| 1.4 Management and Reporting | (MCP/Bechtel/SDG&E) |

**Task 2. Demonstration Design**

Objective: Prepare designs for the stack, BOP, and site which are integrated and consistent with the 250 kW PDT demonstration plant performance objectives.

| | |
|---|---|
| 2.1 Stack Design | (MCP) |
| 2.2 BOP Design | (Bechtel/MCP/Stewart & Stevenson) |
| 2.3 Site Interface Design | (Bechtel/SDG&E/Stewart & Stevenson) |

**Task 3. Stack Manufacturing**

Objective: Manufacture stack components, for two 250 kW MCFC stacks, assemble components, test completed stacks, and ship one stack for factory testing in an integrated system by Bechtel. The second stack shall be shipped to the field demonstration site in San Diego.

| | |
|---|---|
| 3.1 Component Manufacturing | (MCP) |
| 3.2 Stack Assembly | (MCP) |
| 3.3 Shop Test and Shipping | (MCP) |

**Task 4. BOP Fabrication**

Objective: Purchase major equipment items, shop test equipment, fabricate skids in accordance with design specifications, and ship BOP skids to demonstration site.

| | |
|---|---|
| 4.1 Equipment Procurement | (Bechtel/Stewart & Stevenson) |
| 4.2 BOP Assembly | (Stewart & Stevenson) |
| 4.3 Shop Testing and Shipping | (MCP/Bechtel/Stewart & Stevenson) |

**Task 5. Site Work**

Objective: Prepare site, installation, and commission 250 kW PDT demonstration plant.

| | |
|---|---|
| 5.1 Site Preparation | (Bechtel/SDG&E) |
| 5.2 Plant Installation | (Bechtel/SDG&E/MCP) |
| 5.3 Plant Commissioning | (Bechtel/SDG&E/MCP) |

**Task 6. Testing**

Objective: Prepare manuals/test plans and execute test program which document the PDT demonstration plant's performance.

| | |
|---|---|
| 6.1 Operating and Maintenance Manuals | (Bechtel/MCP) |
| 6.2 Test Plan | (Bechtel/SDG&E/MCP) |
| 6.3 Performance Testing | (Bechtel/SDG&E/MCP) |
| 6.4 Emission Testing | (Bechtel/SDG&E) |
| 6.5 Test Reports | (Bechtel/SDG&E/MCP) |

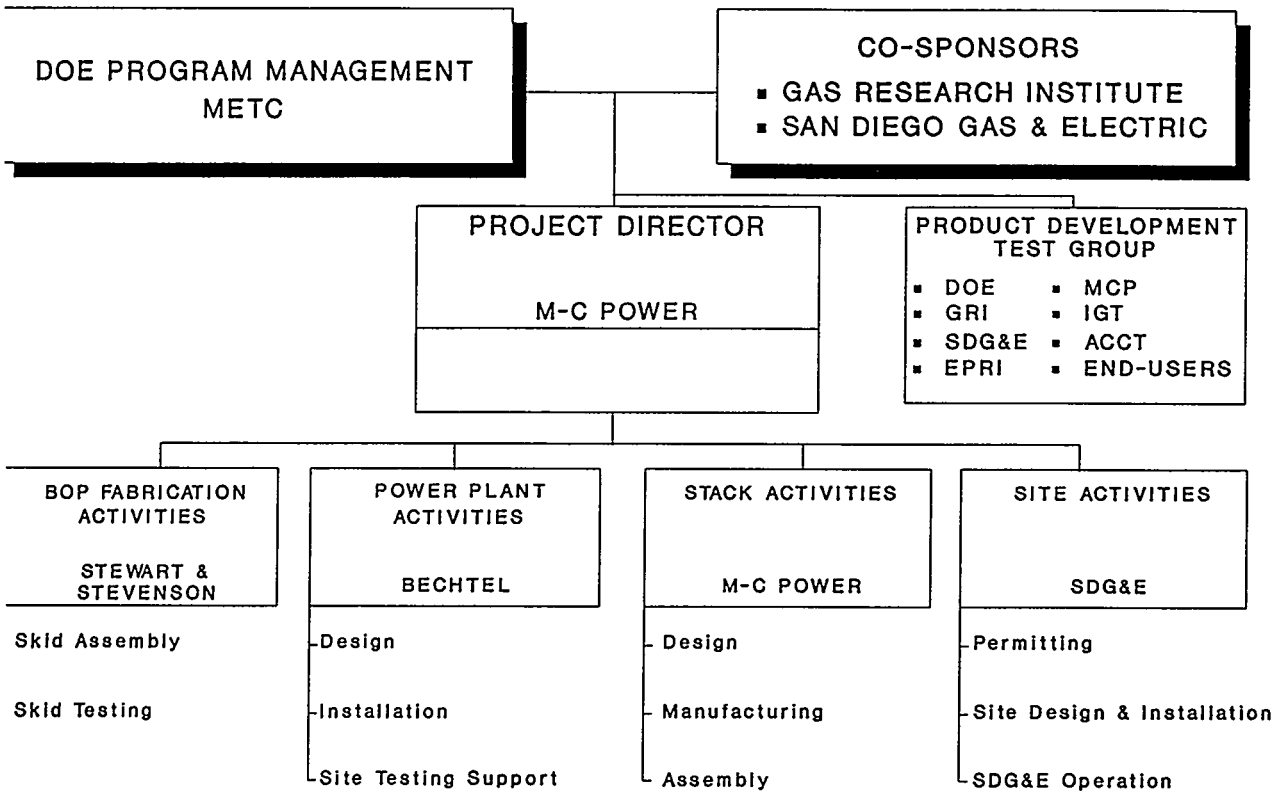


FIGURE 3. 250 kW PRODUCT DEVELOPMENT TEST DEMONSTRATION PROJECT ORGANIZATION

involves design and field verification of on-site power plants. Initially a 250 kW dual-fueled POC unit will be tested beginning in 1993 at the Unocal Science and Technology Center in the Los Angeles basin. The second field verification test in the commercialization program is the PDT demonstration described herein. Subsequent field verification tests are planned.

Market analysis has identified on-site natural gas-fueled energy systems in the 250 kW to 2 MW range as the most promising market for initial commercialization focus, to be followed by larger natural gas-, then coal gas-fueled systems. Hospitals, offices, hotels/motels, nursing homes, stores, and restaurants are the most desirable commercial market segments for on-site MCFC units. The Kaiser Medical Center is an ideal location for the MCFC PDT demonstration.

## PROJECT DESCRIPTION

### Work Breakdown Structure and Dictionary

The Work Breakdown Structure for the project is shown in Figure 1, by task and major subtask heading. The Work Breakdown Structure Dictionary shown in Figure 2 indicates the organizations performing work in each subtask.

## TASK 1. PROJECT MANAGEMENT/ PERMITTING

### Subtask 1.1. Management Plan

The project organization is led by M-C Power Corporation as the prime contractor with DOE and prime contractor with GRI. Major project participating organizations include Bechtel Corporation, which is responsible for system design, procurement, and construction management; Stewart & Stevenson Services which is responsible for skid assembly and shop testing; and SDG&E which is responsible for site-related activities. The Balance-of-Plant components will be assembled and tested by Stewart & Stevenson Services who will perform their work under M-C Power's supervision and in accordance with specifications prepared by Bechtel. The team was formed for the specific purpose of combining the professional, technical, and managerial resources required to successfully complete the PDT demonstration project and to move the IMHEX® MCFC toward commercialization.

The management plan documents project management techniques, control systems, and procedures to be used to control schedule, cost, and quality of all work performed.

### Subtask 1.2. Environmental Information

M-C Power and SDG&E have prepared an environmental assessment which contains the information necessary to allow DOE to prepare documentation to support a request for a categorical exclusion. A categorical exclusion has been received.

### Subtask 1.3. Local Permits

SDG&E, in conjunction with Kaiser Permanente, have identified local permit requirements and to date have obtained permits which are consistent with current project activities.

### Subtask 1.4. Management and Reporting

#### Organization and Management

M-C Power has overall project responsibilities as shown in Figure 3, Project Organization Chart. M-C Power has responsibility for all stack related activities, and Bechtel for the Balance-of-Plant design, installation, and testing. Fabrication of the BOP will be performed by Stewart &

Stevenson. SDG&E is responsible for plant installation, operation, and maintenance activities at the Kaiser Medical Center site.

**Project Management**

M-C Power's Project Manager is responsible for providing overall project direction, including cost control, schedule, and performance. Resources necessary to perform the work are assigned in accordance with the forecasted requirements. Work progress is closely measured relative to materials and labor expenditures. The project schedule shown in Figure 4 is continuously monitored using the flow of documents (correspondence, drawings, transmittals, etc.) and personal reviews to detect trends and potential problem areas. Updated schedules provide the reporting mechanism for the execution of action plans to accelerate positive trends, reverse negative trends, and resolve problem areas.

**Program Reporting**

Periodic reports from project participants are analyzed for completeness and accuracy. Costs and physical progress to date are verified on a monthly basis. Data supplied by M-C Power, Bechtel, Stewart & Stevenson, and SDG&E project personnel are used for updating the monthly schedule.

## TASK 2. DEMONSTRATION DESIGN

This PDT demonstration unit will be fueled by pipeline natural gas from SDG&E and possibly hydrogen from a plasma pyrolysis project being developed by Kaiser.

### Subtask 2.1. Stack Design

The stack design is based on established technical, environmental, and cost goals for the integrated MCFC power plant system. The design takes into consideration manufacturing simplicity, stack cost, reliability, safety, maintenance requirements, and overall performance necessary to achieve MCFC power plant performance goals.

Overcoming cost penalties associated with transitioning product and process requirements from R&D towards commercialization is being addressed. The stack design is continuously upgraded using data from applied research, component development studies, pneumatic and structural analyses, and data analysis from the operation of subscale, short-stack, and full-size stacks.

Detailed thermal, structural, and fluid analyses are being performed to define the cell stack components, for both repeat and non-repeat elements. Component Design Specifications (CDS) and the stack Design Control Document (DCD) are updated and maintained throughout the project's duration.

Thermal stresses imposed during heat-up, cool-down, at steady load conditions and during power transients are being determined to ascertain the structural integrity of all stack components. Fluid flow analyses are performed to define the stack and cell design features necessary to ensure proper reactant flow distribution. In a similar manner, structural analyses will ensure stack tolerance of shock and vibration loads. Specifications applicable to the manufacturing of commercial stacks are being developed. The compressive and tensile moduli, permeability and conductivity of the non-metallic stack components, the sealing load requirements, and similar basic design criteria will be incorporated into the final stack design.

Cell stack preliminary design specifications include:

Cell Area: 1 $m^2$ (nominal)
#Cells/Stack: 250
Design Current Density: 160 Amps/$ft^2$

## FIGURE 4. 250 kW PROOF-OF-CONCEPT DEMONSTRATION SCHEDULE

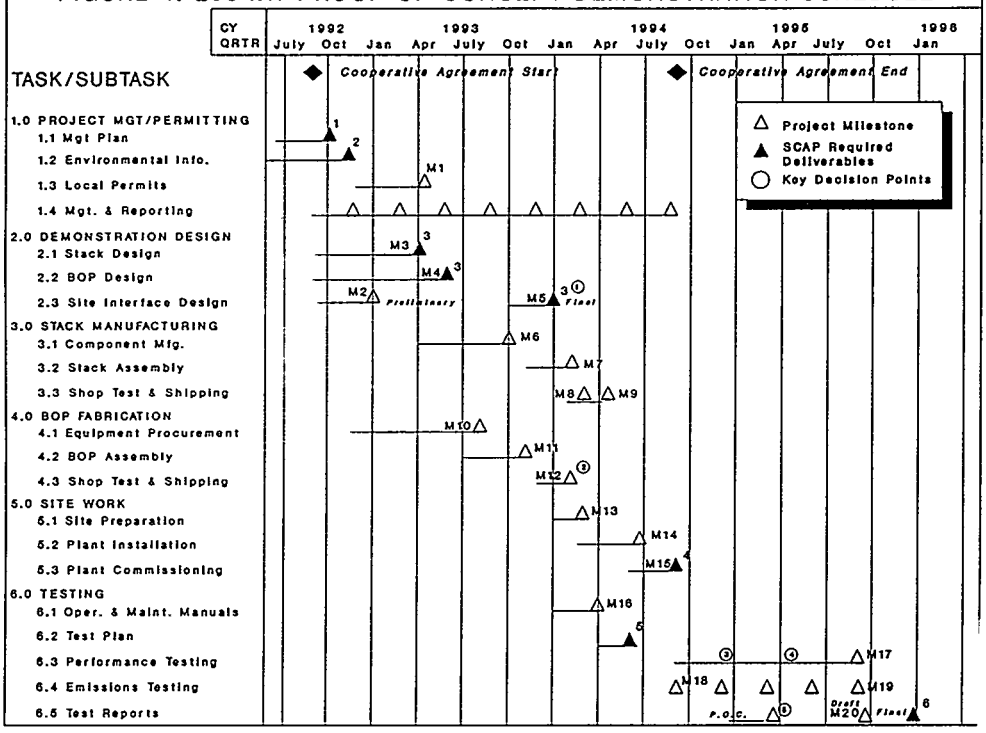


△ Project Milestone

1 Permits Obtained
2 Preliminary Site Design Completed
3 Stack Design Completed
4 BOP Design Completed
5 Final Site Design Completed
6 Stack Component Manufacturing Completed
7 Assembly of Both Stacks Completed
8 Stack POC-1 to ABB C-E Shipped
9 Stack POC-2 to SDG&E Shipped
10 BOP Equipment at ABB C-E Received
11 BOP Assembly at ABB C-E Completed
12 BOP to SDG&E Shipped
13 Site Preparation Completed
14 BOP and Stack Installation Completed
15 Plant Start-Up Completed
16 O&M Manuals Completed
17 Performance Testing Completed
18 Baseline Emissions Measured
19 Emissions Testing Completed
20 Demonstration Evaluation Completed

▲ SCAP Deliverables

1 Management Plan
2 Environmental Information - Topical Report
3 Plant Final Design - Topical Report
4 Plant Start-Up Report
5 Test Plan - Topical Report
6 Final Report

○ Key Decision Points

1 Interface Design Approval
2 Determine Fitness for Shipment
3, 4 } Evaluate Operation/Modify Plant
5 Determine Proof-of-Concept

Cooling Approach: Cathode Recycle
Fuel Utilization: 85% maximum
System Excess Air: 70%

Temperatures
Average: 1200°F
Minimum: 1050°F
Maximum: 1290°F
Operating Pressure: 2.5 - 3 atm

**Subtask 2.2. BOP Design**

The design objective of the PDT demonstration plant is to improve performance and reduce costs with minimal environmental impacts.

The BOP equipment is being designed to integrate with the stack and provide the following power plant characteristics:

**Output:** Electrical - 250 kW AC
Thermal - 430,000 BTU/hr of steam

**Input:** Fuel - Natural Gas or hydrogen rich pyrolysis gas
Process Water - 800-1000 GPD or no requirement, if water recovery option is selected

**Efficiency:** 40-48% Electrical
65-75% Overall

**Emissions:**
- $\leq$ 0.1 ppm CO
- $\leq$ 0.01 ppm non-methane hydrocarbons
- $\leq$ 0.1 ppm $NO_x$
- $\leq$ 0.1 ppm $SO_x$
- $\leq$ 55 dBa noise level at 50 feet from the plant perimeter

**Controls:** Capable of unattended operation, automatic shutdown and start-up

A preliminary schematic of the BOP system is shown in Figure 5. It includes the reformer, recycle blower, DC/AC inverter, heat recovery equipment, and the control system.

In this subtask the following activities are being performed:

- Conduct process design and prepare P&IDs
- Provide detailed engineering for the plant control system, electrical system, foundation, structure, and piping
- Skid design interface
- Site layout
- Prepare cost estimate and budget plan

A complete process design for the integrated 250 kW power plant is being developed. The design includes a process flow diagram, a material and energy balance, and piping and instrumentation diagrams (P&IDs). The process flow diagram shows the major equipment, connecting flow lines, and material streams entering into and discharging from the major equipment.

The P&IDs will define the plant piping and the function of the control and monitoring instrumentation. The control functions will consider plant start-up, normal operation, normal shutdown, warm standby, and emergency shutdown. The monitoring function will consider both local indicators and signals sent to the data acquisition system.

Bechtel is responsible for design and engineering for miscellaneous equipment, for site installation of the skids, and for the overall design coordination. Miscellaneous equipment includes items such as the nitrogen, $CO_2$, and $H_2$ supply, cooling water system, fire protection, electrical system including an uninterruptible power supply (UPS), controls and instrumentation, data acquisition system, flue gas stack, and associated bulk materials. Site installation will include connecting the

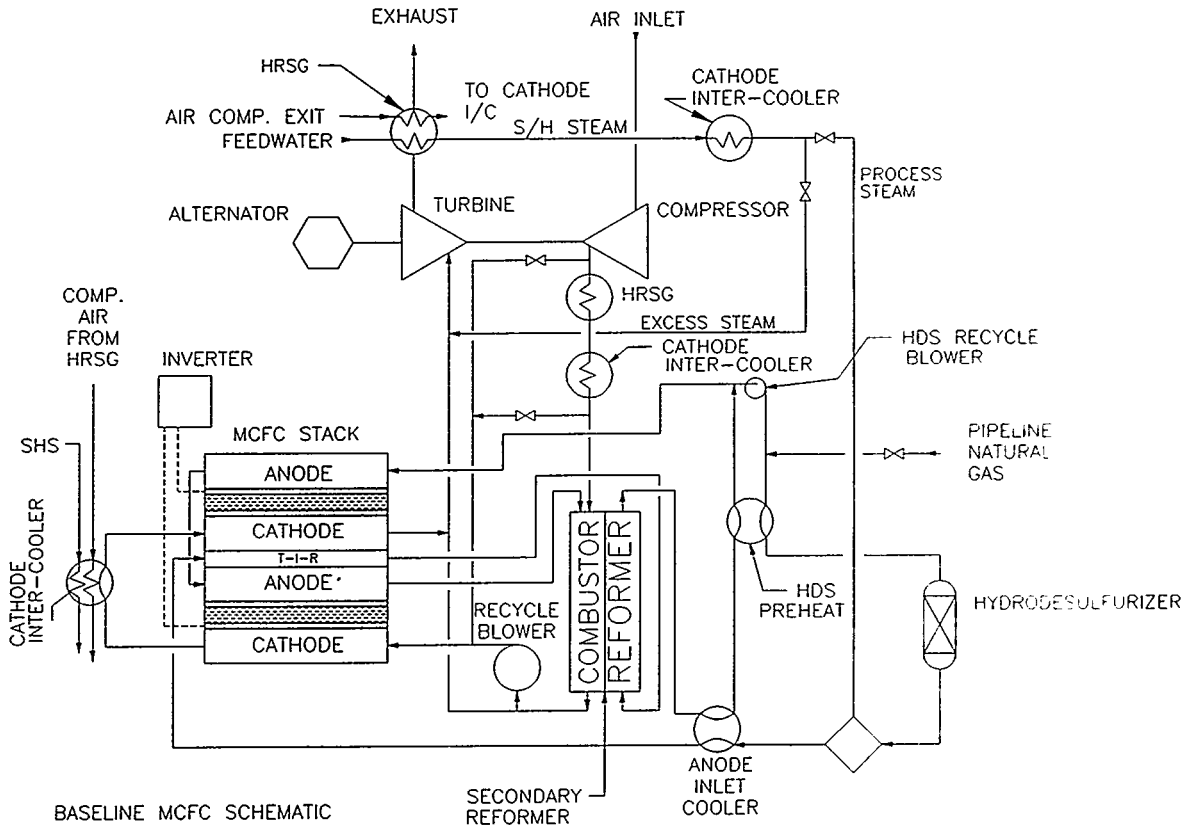


FIGURE 5. PRELIMINARY SCHEMATIC OF THE BOP SYSTEM

flue gas stack, and associated bulk materials. Site installation will include connecting the skids together, foundation design for the connected skids, integration with miscellaneous equipment not contained on the skids, and utility hookup at interface points. The design will be in full compliance with applicable codes such as those for noise, safety, and fire protection.

The control system design will be based on a highly integrated, highly automated plant capable of automatic start-up and maximum unattended operation. The control system will be a combination of microprocessor-based distributed digital control and monitoring system (DCS) and hardwired instrument and control loops. The system will be fully instrumented. The output of the control and instrumentation system will be input to a fully automated, computerized data acquisition system.

A definitive cost estimate for the power plant will be prepared. The estimate will be based on the bids received for the equipment and subcontractor services, and will include estimates provided by the selected fabricators for their portions of the construction activities.

The goals of the PDT demonstration include producing a compact and highly integrated plant. To help achieve this, the construction concept for the plant is to shop fabricate and minimize field erection. This concept will promote efficient packaging and allow for significant pretesting, while improving quality of construction and reducing construction time and costs.

Stewart & Stevenson is responsible for the detailed engineering of the skids including the design, engineering, and procurement of the piping, instrumentation, controls, and structure. They will assemble the equipment in their battery limits into preassemblies or onto skids in their shop and will specify the interface requirements for their equipment.

Bechtel coordinates with Stewart & Stevenson for the necessary design interface between the skids and the rest of the plant. This is an iterative process. As the fabricators find out that the skid configuration demands process changes, the process design and the P&IDs are revised accordingly.

**Subtask 2.3. Site Interface Design**

The Kaiser Permanente San Diego Medical Center, located in the City of San Diego, has been chosen as the PDT demonstration site. The site was selected based upon the Medical Center's history as an industry innovator, its willingness to provide support operating personnel, the large potential market offered by hospitals/medical centers, and its flexibility to accommodate the utility interfaces required by the project. The site's technical qualifications and Kaiser's strong relationship with SDG&E make it an ideal candidate for the demonstration.

A site interface design is prepared to guide plant installation activities. Design criteria dictates the ranges of conditions under which the plant will be designed and operated. Criteria includes location, temperature (elevation and humidity ratio), fuel(s) to be consumed, nominal plant output (electrical and thermal), and seismic design requirements. The preliminary site interface design serves as input for permitting. The first design review meeting has taken place. Site constraints and results from the Unocal dual-fuel demonstration design are used for guidance in development of the design documents. Site requirements are being used to develop layout drawings, foundation drawings, electrical and mechanical interface diagrams, and subcontractor installation/construction packages. All applicable federal, state, local, and industry codes are taken into consideration in the development of design documents.

## TASK 3. STACK MANUFACTURING

The nominal 250-cell stack ($1m^2$ area) is the basic building block for all M-C Power IMHEX® power plant applications.

### Subtask 3.1. Component Manufacturing General Approach

M-C Power has developed a manufacturing plan under GRI sponsorship which is guiding and directing the manufacturing of stack components. installed and qualified commercial scale tape casting and sintering equipment to manufacture anodes, cathodes, matrices, and electrolyte sheets. Separator plates are being stamped by a company that manufactures formed-plate heat exchangers with plan areas up to 15 $ft^2$. Fabrication variables which affect part quality are being defined and incorporated in a comprehensive QA/QC program.

### Subtask 3.2. Stack Assembly

Interchangeable parts and use of automated manufacturing and assembly equipment meeting the cost goals established for commercial MCFC stacks require development. To date, selective hand assembly of parts have been used until designs and component manufacturing techniques have been improved.

One of the major issues in stacking a large number of cells is accommodating the accumulated component manufacturing tolerances that result in non-parallel end plates. The design of an automated stack assembly machine has been completed. Current plans are to use this machine in assembly of the two 250 kW PDT demonstration stacks.

### Subtask 3.3. Shop Test and Shipping

Stack pre-conditioning is followed by an acceptance test. The acceptance test is used to verify that the stack meets performance, leakage, crossover, and electrical isolation specifications. The stack is operated to verify performance and demonstrate mechanical and electrical integrity.

Following acceptance testing at M-C Power, the stacks will be placed into shipping fixtures for transport to the demonstration site. Shock and tilt detection devices are attached to the shipping container to verify that shipping and handling have been completed without exceeding maximum load specifications.

## TASK 4. BOP FABRICATION

### Subtask 4.1. Equipment Procurement

The BOP design documents generated in Subtasks 2.2 and 2.3 are used by Bechtel to prepare materials and equipment specifications in the development of vendor bid packages. Bid packages contain performance requirements which are in accordance with design specifications. A list of qualified vendors has been prepared. Bechtel will issue requests for quotations and will analyze all bids received. All equipment items will be subject to inspection when received by Stewart & Stevenson. For certain major equipment items, Bechtel will witness testing in the vendor's shop. Included in the inspection function is an expediting activity which will ensure that equipment is properly packaged and shipped in accordance with the established schedule.

Stewart & Stevenson will procure bulk materials (piping, insulation, structural steel, etc.) to complete skid fabrication. The bulk material procurement for installation of the plant at the site will be the responsibility of the installation subcontractor under SDG&E supervision with overview by the Bechtel construction manager.

### Subtask 4.2. BOP Assembly

Skid mounted subsystems will be assembled by Stewart & Stevenson based upon Bechtel's design. Stewart & Stevenson has participated in review of Bechtel's design for "constructability, maintenance, and cost." Skids will be configured in accordance with Bechtel specifications. Stewart & Stevenson will prepare skid designs based on Bechtel's process design. The design will allow for routine shipment and easy installation and interconnection at the field site. Stewart & Stevenson will insure that components are integrated into functioning subsystems that will be tested. Design of the electrical panels and cabinets will be performed by Bechtel and assembled by Stewart & Stevenson. There are three major skids. The inverter and control panels are located on the electrical skid. A second skid contains the reformer, desulfurizer, and gas preheat exchangers. The stack containment vessel, recycle blowers, and turbo compressor make up the third skid. Each skid is being designed to be road transportable.

### Subtask 4.3. Shop Testing and Shipping

Shop testing of packaged components will be performed in accordance with clearly defined acceptance testing procedures. The mechanical packages will be tested for pressure integrity. Rotating components, such as blowers, will receive manufacturer shop tests to verify capacity, head and gas seals. A full operating test of the assembled skids will take place at Stewart & Stevenson's fabrication facilities and/or at the demonstration site.

## TASK 5. SITE WORK

### Subtask 5.1. Site Preparation

A site construction plan is being prepared to guide all plant installation activities. Both Kaiser and SDG&E engineers are working closely with Bechtel to identify the existing site conditions, define interface requirements, and develop the site construction plan. SDG&E field engineers and Bechtel are working with Kaiser to identify specific code and site architectural requirements which must be met.

The site construction plan includes layout drawings, foundation drawings, electrical and mechanical interface diagrams, and an installation contractor specification. Using the site design, a local construction contractor will be selected to accomplish all site preparation activities including grading, foundations, and underground piping runs.

### Subtask 5.2. Plant Installation

Bechtel is preparing the installation specification and will work with SDG&E in requesting bids from qualified local construction contractors which have been pre-approved by SDG&E and the Kaiser site representatives. Bids will be evaluated and a contract awarded to install the PDT demonstration unit at the Kaiser Medical Center site. SDG&E and Bechtel personnel will witness power plant off-loading and placement as well as completion of skid interfaces, completion of power plant/building interfaces, mechanical testing of equipment and completion of the final installation check list. All installation activities will be thoroughly documented through photographs and in writing. The Bechtel construction manager will insure that all subcontractors perform their work in accordance with bid documents, the construction plan, and installation specifications. Prior to turnover of the constructed facility to the Bechtel/SDG&E start-up team, pressurized components will be cleaned and leak tested, rotating equipment will be powered and checked for vibration. Continuity checks will verify component interconnections and all

instrumentation and control circuits will be checked against the design specifications.

### Subtask 5.3 Plant Commissioning

The PDT demonstration unit will be commissioned by the SDG&E operating staff with assistance from Bechtel and M-C Power start-up personnel. Bechtel will be responsible for development and implementation of the plant commissioning plan. Bechtel will provide technical direction to the site commissioning team. A training program will be conducted for the operating team to review system/component designs and teach normal and emergency procedures. Lessons learned from start-up and operation of the Unocal POC demonstration will be documented. By incorporating previous operating and start-up experience into an integrated training program, a rapid start-up schedule is anticipated.

## TASK 6. TESTING

### Subtask 6.1. Operating & Maintenance Manuals

Prior to development of the operating and maintenance manuals, Bechtel will assist M-C Power in establishing the test goals and requirements for the PDT demonstration. The operating and maintenance manuals will contain descriptions of the overall power plant, each major subsystem, design values, predicted steady state process values, and operating procedures. These descriptions will be provided for cold and warm start-up, warm hold, transition to automatic control, power escalation, emergency and normal shutdowns, and cool down.

### Subtask 6.2. Test Plan

M-C Power, Bechtel, SDG&E, and Kaiser will establish technical objectives and goals for the plant operating period. These goals will guide preparation of test plans and procedures for both steady-state and transient testing. The test plan will be designed to verify plant operating characteristics at power levels from idle to rated and during start-up and shutdown sequences. Each of the components undergoing Proof-of-Concept testing will be included in the test plan which will identify expected process flow, temperature and pressure data, electrical output and fuel consumption, emissions, and other pertinent data. Special instrumentation/procedures and emission data requirements will be identified prior to start-up. The plan will include methods for acquisition and analysis of plant operating data and will specify post test dismantling and inspection procedures for the stack, reformer, and other equipment.

### Subtask 6.3. Performance Testing

#### Plant Start-up

M-C Power and Bechtel will assist SDG&E with initial plant start-up. The PDT unit subsystems will be started up and their performance will be recorded and compared with start-up tests performed at the Unocal demonstration. All plant subsystems will be retested to confirm that performance is consistent with their factory test results. Changes in operating parameters will be recorded and corrective action will be taken, if required. Stack, reformer, inverter, and ancillary subsystems tests will be conducted. M-C Power, Bechtel, and SDG&E personnel will be on-site during plant start-up to insure that proper procedures are implemented and to modify manuals as required to reflect the necessary changes in procedures.

#### Plant Operation

The plant operating period will be a minimum of one year to obtain normal operating data and to conduct various special tests in accordance with the Test Plan.

However, it is anticipated that sufficient data will be obtained within the first six months of testing to establish successful Proof-of-Concept.

The power plant will be operated in the steady-state mode to establish baseline operating conditions for all subsystems. Once steady-state operation has been established, the testing specified in the Test Plan will be implemented. The data acquisition and analysis system will record operating data and perform initial calculations to verify operating results.

Data gathered during the operating period will be summarized by SDG&E, who will report findings to M-C Power and Bechtel. M-C Power will analyze stack related findings and Bechtel and Stewart & Stevenson will examine data related to the balance of plant.

**Subtask 6.4. Emissions Testing**

One of the key objectives of the 250 kW PDT demonstration is to prove that air, noise, and liquid emissions from the plant are significantly lower than emissions from competitive conventional cogeneration technologies. Therefore, emissions will be thoroughly documented. An independent testing laboratory will be retained to measure emission levels during the test at Kaiser Medical Center; after initial start-up, then quarterly throughout the annual operating period. The San Diego County APCD and other local environmental agencies will be consulted when establishing emission testing procedures to insure that data collected will be useful in evaluating the 250 kW demonstration's environmental impacts.

**Subtask 6.5. Test Reports**

All aspects of the PDT testing activity will be fully documented. A PDT Test Report and Final Test Report on the following subjects will be prepared and issued.

These reports will document the work accomplished and the successes/failures which occurred during each step of the activity. All test activities will be coordinated by SDG&E who will make sure there is proper communication among all demonstration participants. This communication will allow establishment of a common basis for reporting of activities. Communication will be enhanced through quarterly test meetings, monthly progress reports, technical reports, and personal correspondence between participants.

Monthly updates will be issued on the status of the operation and monitoring activities. These updates will include an overview of test activities such as, hours of operation, reasons for downtime, maintenance activities, kWh production, by-product heat delivered to Kaiser, fuel consumption, and special testing activities. Environmental performance will be reported throughout the demonstration period in order to document air emissions, effluent, noise, and other environmental impacts.

**RESULTS**

San Diego Gas & Electric (SDG&E) will host the 250 kW PDT plant to be installed and operated by SDG&E in 1994-1995 timeframe. The overall objective of this demonstration is to design, construct, and operate a MCFC PDT power plant integrating pre-commercial components. The work includes a management plan, gathering of environmental information, design of the PDT power plant, acquisition of MCFC stack and balance-of-plant equipment, construction, and plant testing. All electric and thermal energy produced by the plant is to be utilized on-site.

The PDT consists of the MCFC stack, reformer, desulfurizer, heat exchangers, blowers, expander, compressor, inverter, and

control panel. In the MCFC stack, hydrogen ($H_2$) and carbon monoxide (CO) made from reformed natural gas is utilized as fuel and oxygen inputs for the generation of electricity and heat. Upstream of the fuel cell, a guard bed of manganese dioxide captures any sulfur present in the natural gas fuel streams, thus reducing significantly the potential for $SO_x$ emissions. Downstream, the exhaust gases are used in heat recovery processes to generate steam. The spent gas (principally water vapor, $CO_2$, and nitrogen ($N_2$) is then exhausted to the atmosphere.

To enhance the demonstration's value, the M-C Power team selected an end-use application site for which installation and operation of the PDT plant rather than a SDG&E power plant facility. The selected site is the Kaiser Permanente Medical Center located at 4647 Zion Avenue in San Diego, California. This center is a 300-bed hospital with emergency care, pharmacy, and associated medical office facilities. The electric energy from the PDT plant will provide about 10% of the Medical Center's electric load. The thermal energy generated by the PDT plant will be used for process heat, hot water, and sterilization.

The PDT site is located near an existing cogeneration system in the loading area of the hospital. It is next to an existing two-level parking structure currently landscaped with ivy and an out-of-commission incinerator building. Approximately 30 ft. X 80 ft. of the embankment and the incinerator building will be removed to install a pad for the PDT power plant.

## ENVIRONMENTAL APPROACH

### Site Description

The existing Kaiser Permanente Medical Center (Center) in San Diego is located in a developed section of the city known as Grantville in which residential and commercial land uses dominate the surrounding area. The Center has existing natural-gas fueled engine cogenerators, and steam generators to supply the Center with auxiliary/ emergency power and steam needs.

### Compliance with Environmental Standards

Anticipated air emissions from the demonstration plant are expected to be significantly below the most strict new source emission standards. The demonstration plant will be packaged to insure that noise levels are well below standards and effluents will be insignificant. The demonstration plant has been exempted by the San Diego Air Pollution Control District (SDAPCD), and is expected to comply with the Clean Air Act, Toxic Substance Control Act, and Clean Water Act.

### Emissions Estimates

Although measured data has not yet been obtained, M-C Power has calculated air emission levels from the PDT plant to be: $SO_2$ $<0.0002$ lbs/hr, $NO_x$ $<0.008$ to 0.025 lbs/hr, water vapor - 483 lbs/hr, and $CO_2$ - 240 lbs/hr at full rated conditions. These emission levels are below the most stringent standards and are significantly below conventional natural gas fueled energy systems.

Throughout the approximately 12 months of operation, important emissions such as water, noise, CO, $CO_2$, $NO_x$, $SO_x$, and unburned hydrocarbons (UBHC) will be measured. One of the key objectives of the PDT demonstration is to prove that noise, gaseous, and liquid emissions from the plant are significantly lower than emissions from competitive power generation technologies. The San Diego APCD and other local environmental agencies are being consulted to

establish testing procedures to ensure that data collected will be useful in evaluating the power plant's environmental impact.

## STATUS

The Kaiser Medical Center site has received a negative declaration to the EIR and California Environmental Quality ACT (CEQA). Also, the San Diego Air Pollution Control District (APCD) has exempted the project from environmental permitting.

A Conditional Use Permit (CUP) issued to Kaiser to operate a 400-bed general hospital, related off-street parking, and other accessory uses, as determined by the San Diego Planning Director, will be used to obtain building permits.

A process flow diagram and equipment and control specifications have been completed by Bechtel Engineering.

Active component materials for the MCFC stack have been procured and delivered to M-C Power.

Electric and gas interconnection requirements are under review by SDG&E and Kaiser engineers.

## FUTURE WORK

Successful demonstration of the 250 kW PDT will contribute significantly to the commercialization objectives of SDG&E and the U.S. Department of Energy's Solicitation for Cooperative Agreement Proposal. The participation of Kaiser Permanente with SDG&E in this demonstration, will help ensure that utility and end-user operating issues of MCFC power plant systems are addressed and operating goals are met.

This demonstration is an integral part of the M-C Power IMHEX® commercialization program which is being monitored and supported by a group of potential users called the Alliance for Commercializing Carbonate Technology (ACCT). Successful demonstration of the 250 kW PDT power plant will result in increased confidence from the ACCT members who represent the gas, electric, and combination utility industry as well as other industry users.

# 1.5 MCFC Power Plant System Verification

## CONTRACT INFORMATION

| | |
|---|---|
| **Contract Number** | DE-AC21-90MC27168 |
| **Contractor** | Energy Research Corporation<br>3 Great Pasture Road<br>Danbury, CT 06813<br>(203)792-1460 |
| **Contract Project Manager** | Mohammad Farooque |
| **Principal Investigators** | R. Bernard, J. Doyon, L. Paetsch, P. Patel, A. Skok, and C. Yuh |
| **METC Project Manager** | Thomas J. George |
| **Period of Performance** | September, 1990 to February, 1994 |

## 1.0 SCHEDULE AND MILESTONES

A simplified schedule and the major milestones of the cost-shared program are shown in Figure 1.

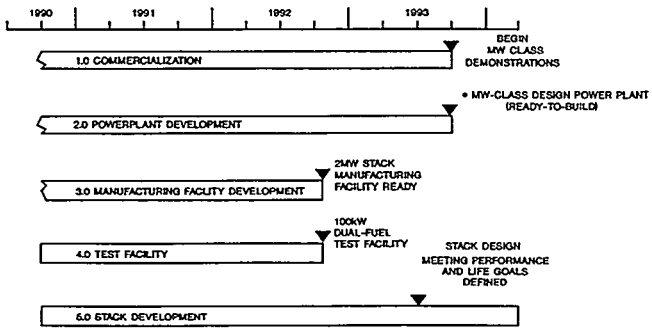


**Figure 1. Overall Schedule and Major Milestones:**
All major milestones of this program has been attained

## 2.0 OBJECTIVES

ERC's carbonate fuel cell goals are commercialization of MW-Class natural gas units in the near-term and 100 MW-Class coal gas/natural gas dual-fuel units later. ERC is ready to demonstrate a 2MW natural gas power plant at the City of Santa Clara, CA in the 1994-1996 time frame, as a major milestone towards achieving this objective. The on-going program effort aggressively prepares this efficient energy conversion technology for the demonstration phase.

## 3.0 BACKGROUND INFORMATION

The carbonate fuel cell promises highly efficient, cost-effective, environmentally superior power generators for pipeline natural gas as well as coal-gas fuels. ERC has been engaged in the development of this unique technology from the very early years, primarily focusing on the development of the direct fuel cell (DFC) technology, pioneered by ERC[1-3]. The DFC design incorporates the unique internal reforming feature which allows utilization of a hydrocarbon fuel directly in the fuel cell without requiring any external reactors and associated heat exchange equipment, allowing direct operation on pipeline natural gas and coal-derived fuels. Overall system efficiency is further improved.

ERC is near the end of the current 3-yr DOE program aimed at preparing the DFC stack and critical components for power plant application. In this program, focused activity has been launched for commercializing this technology by mid- to late-1990's. The stack size has been scaled from 4,000-$cm^2$ to 6,000-$cm^2$ under this program. The stack

height has been increased from 54-cell stack to 246-cell stack. Both 70kW and 120kW stacks have been demonstrated with operating parameters of commercial power plant systems, showing attainment of performance consistent with demonstration goals.

## 4.0 PROJECT DESCRIPTION

The specific program objectives identified to bring the carbonate fuel cell technology to the demonstration stage are:

- Define the requirements for market-responsive power plants and prepare a commercialization strategy for natural gas-fueled MW-Class dispersed and coal gas/natural gas-fueled 100MW-Class baseload carbonate fuel cell power plants.
- Prepare the full-height, dual-fuel stack (100MW-Class) and critical balance-of-plant equipment for power plant demonstration.
- Develop a manufacturing facility and gain manufacturing experience for ERC's dual-fuel, full-height stacks.
- Provide facilities to support testing of full-height stacks at pipeline natural gas and simulated coal-gas system conditions.
- Demonstrate attainment of carbonate fuel cell stack performance and life goals.

A five-task program, where each task is dedicated to the realization of the above mentioned specific program objectives, was started in September of 1990 (as shown in Figure 1). In this program, parallel activities for market development, system development, stack manufacturing, balance-of-plant development, and stack technology development are being pursued aggressively.

## 5.0 RESULTS/ACCOMPLISHMENTS

In pursuit of commercialization, efforts are underway to: 1) advance the technology base by enhancing performance and demonstrating endurance, 2) scale up stack to the full area and height, 3) acquire stack manufacturing capability and experience, 4) establish capability as well as gain experience for power plant system testing of the full-height carbonate fuel cell stack, 5) and define power plant design and develop critical subsystem components.

All the major project objectives have already been attained. Over the last year, significant progress has been achieved in establishing the full-height stack design, gaining stack manufacturing and system integrated testing experience, and verifying the major equipment design in power plant system tests. In this paper, recent progresses on stack scaleup, demonstration testing, BOP verification, and stack endurance are presented.

Major accomplishments are detailed next.

### Stack Scaleup and Demonstration

ERC's full-height stack design, based on truck transportation consideration could be 3 to 4m tall, incorporating 250 to 300 cells. ERC's scaleup experience is shown in Fig. 2. The first scaleup step increased cell number from 20 to 54 in 1990[4]. In 1991, the cell number was further increased to 234 in a 70kW stack[5]. In 1992, cell area was also increased from nominal 4,000 to 6,000 $cm^2$[5]. More recently a nominal 120kW-size stack containing 246 cells of nominal 6,000-$cm^2$ area was evaluated in system integrated testing.

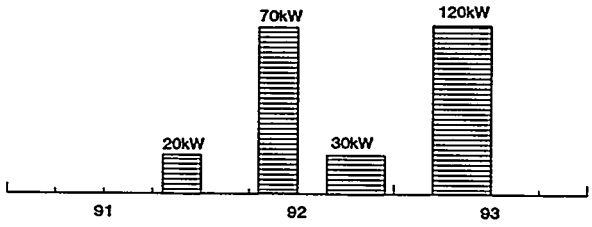


**Figure 2. ERC's Stack Size Has Been Successfully Scaled up to 246 Cells and 6,000 $cm^2$**

### 70kW Stack Test

During the past year, a testing of 70kW stack containing 234 cells of 4,000-$cm^2$ nominal cell area was performed. The stack was first successfully conditioned and pretested at ERC. The stack was thermally cycled twice at ERC following initial conditioning and low-power check-out. These initial results were already reported last year. The stack

was then cooled, crated and truck transported out to PG&E 100kW pilot plant in San Ramon, California. The stack was then operated in a system integrated mode using pipeline natural gas and output power connected to the utility grid. The stack performance characteristics at ERC was essential reproduced, verifying ERC's stack thermal cycling as well as stack transportation procedures. System integrated operation at PG&E was conducted for approximately 1,400 hours to give a total of 2,000 hours of testing for the stack. The majority of the testing was at approximately 65% load, and 70kW full-power output was also briefly demonstrated. A total 33MWh of electricity was generated and supplied to the utility grid. This test successfully demonstrated system integrated operation of ERC's first full-height stack.

### 120kW Stack Test

The full-height stack design was improved based on the 70kW stack experience. A stack pilot manufacturing facility was made fully operational this year and a 246-cell 120kW stack of 6000-$cm^2$ cell area using the improved design was built at the facility. This stack was the first full-size product from this FCMC (Fuel Cell Manufacturing Corporation) new manufacturing facility. The stack was transported from FCMC to ERC on a truck. A photograph of the 120kW stack taken during the transportation is shown in Fig. 3. The stack was tested at a newly built 100kW-Class test facility at ERC's Danbury site. The test facility matches power plant configuration and allows operation and evaluation of 100kW-Class stacks as well as power plant equipment in power plant integration mode. A photograph of the stack on test at this facility is shown in Fig. 4.

**Figure 3. 120kW Stack Enroute to ERC**
The stack manufactured at FCMC was brought to ERC for integrated testing

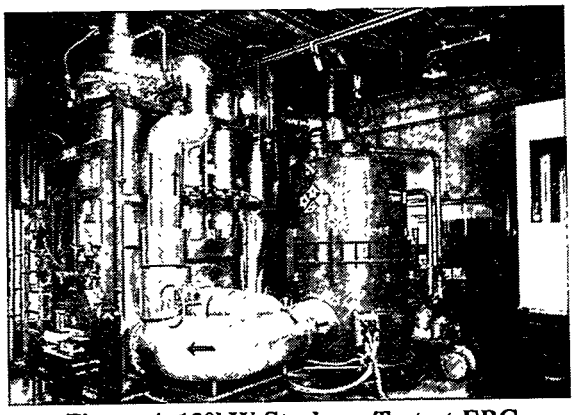

**Figure 4. 120kW Stack on Test at ERC**
The world highest carbonate fuel cell power of 123kW was produced in this test.

The stack was first conditioned and then started up smoothly incorporating field implementable startup procedures. The stack was tested for 250 hours, of which 100 hours was at 123kW (Fig. 5), the highest carbonate fuel cell power produced to date at any location. The stack performance at different load level is shown in Fig. 6. The stack produced a cell voltage of average 0.8 V/cell at the rated power which is consistent with BOL (beginning-of-life) performance goal of the Santa Clara Demonstration. The group-wise performance variation was only ±2.5%. At the 123kW operating point, the plant achieved greater than 50% overall efficiency level of natural gas energy conversion to direct-current electric power. This probably represents the highest electric generation efficiency ever achieved using natural gas in a single-cycle machine. The $NO_x$ and $SO_x$ emissions from the test were measured (Table 1). The emission levels were found very low. This represents a clean power production unmatched by any other fossil fuel based power conversion technology. This test demonstrate that ERC's basic cell design meets the goal of stack performance.

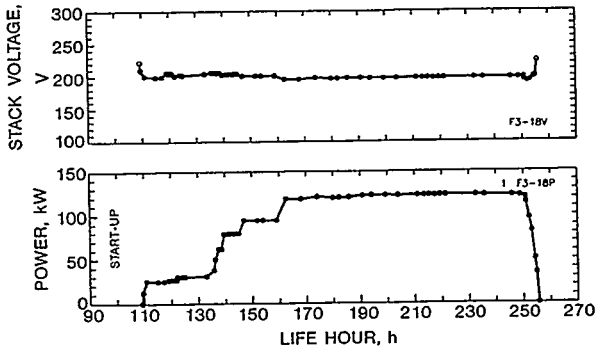


**Figure 5. Rated 120kW Power Operation Demonstrated in System Integrated Condition**

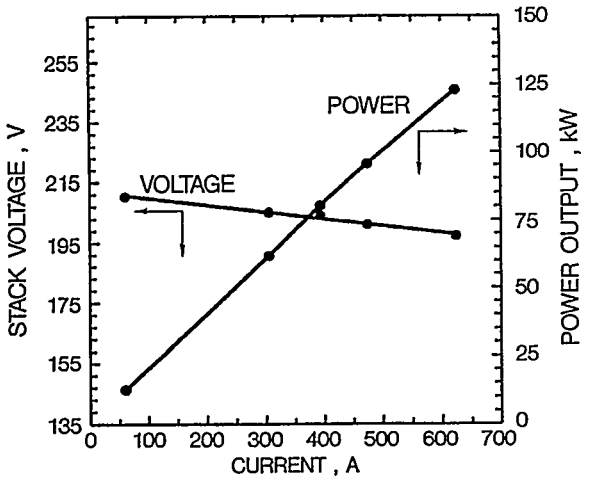


**Figure 6. 120kW Stack Performance (Natural Gas, 65% Fuel Utilization):**
The stack produced 800 mV/cell at 125 mA/cm², consistent with goal for demonstration

**Table 1**
**Environmental Emissions Verification:**
Low emission levels of $NO_x$ and $SO_x$ are verified

| SYSTEM TEST | $NO_x$† ppm | $SO_x$† ppm |
|---|---|---|
| 123kW ERC TEST | <1 | <4 * |
| 7kW ELKRAFT TEST | <1 | NOT MEASURED |

† VALUES CORRESPOND TO MINIMUM DETECTION LEVEL OF THE METHOD

* EXPECTED ~0.005 ppm

The test was shut down for evaluation and design correction after 250 hours of operation, following an incidence of sudden decrease in electrical power output of some cells in a section of the stack. The cause was traced to an external electric short not related to the active section of the stack and can be corrected easily. Consequently, the stack external hardware design was modified to eliminate the possibility of such an electric short.

After the correction to the external hardware, a hot test of the stack was subsequently conducted to qualify the important elements of the design correction and demonstrate electrical short-free operation. In this hot test the stack was tested for additional 380 hours with four thermal cycles. During three of these thermal cycles the stack was cooled to 200°C from the operating temperature. No performance degradation of the cells, excepting the ones physically damaged by the electric short, was noticed from thermal cycle tests. Manifold gas sealing efficiency was continuously monitored during this test and was compared with the goal for the Santa Clara Test. The results showed that the manifold sealing efficiency, even after four thermal cycles, was at least two times better than the BOL goal for the Santa Clara Test. Thus, this test has successfully qualified the design improvement, while providing additional test experience on the power plant system.

Improvements based on this 120kW test experience have been implemented in the design of a second 120kW full-height FCMC manufactured stack which is been assembled at his time. Testing of this stack is planed to start shortly; 1,500h testing is planned.

**Demonstration Testing of 30kW Stack with Gasifier Slip Stream**

A 30kW stack with scaled-up cell area of 6,000 cm² is planned to operate on a coal gas slip stream at Destec's coal-gasification plant in Plaquemine, Louisiana (Fig. 7)[6]. An endurance test of 4,000 hours is planned to evaluate the effects of coal-gas contaminants on stack endurance. A 100kW, system integrated pilot-plant has been constructed at the gasifier site for the test. The stack will be operated within an environmental enclosure which is maintained slightly above reactant pressure. This allows stack operation with higher downstream back pressure while controlling the pressure drop across the reactant manifold seals. The enclosure also serves as a weather-tight shipping container and shelter during operation. The stack was conditioned at ERC using natural gas as fuel. The stack produced 32kW power at 160 mA/cm² and the state-of-art and uniform performance was demonstrated. The stack was cooled down after the qualification testing and has been shipped to the Destec coal-gas facility site. The PAC test of the test facility is currently being performed; the stack testing is expected to start shortly. This testing will be the first one to date tested with actual coal gasifier gas.

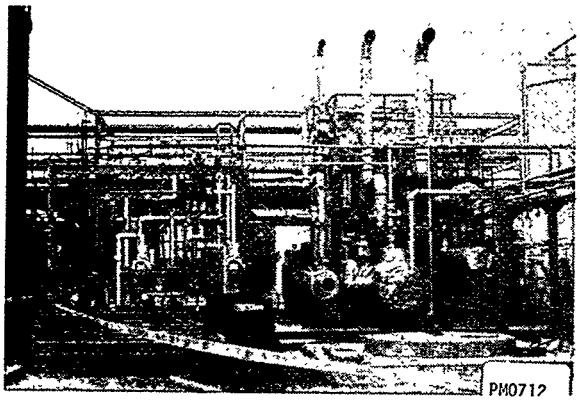


**Figure 7. Test Facility at Destec's Gasifier Site:**
30kW stack will be tested with gasifier slip stream

## Evaluation of Field Operating Procedures and Demonstration of BOP Equipment

The construction of a system integrated test facility was completed for the testing of 100kW-Class stacks and BOP equipment. A schematic diagram of the facility consisting of all the essential equipment for commercial fuel cell power plants (e.g., catalytic converter, high-temperature recycle blower, shift reactor) is shown in Fig. 8. The facility provides evaluation of both BOP equipment and field operating procedures.

The 120kW test performed to date have verified the operation of ERC's design for the following power plant key subsystems:

- Catalytic converter for $CO_2$ management and air preheating
- Steam generation subsystem
- Natural gas handling and preprocessing
- Fuel/oxidant hot isolation valve
- Commercial control and data acquisition system

The stack heatup and cooldown procedures were also successfully verified. A stack heatup rate consistent with the Santa Clara power plant goal has been successfully implemented. To date the facility has been operated for a total of 1,700 hours, including 800 hours of stack operation. The facility demonstrated flawless operation throughout the tests. Therefore, significant power plant equipment and operating experiences have been accumulated, which will ensure the success of designing and operating 2MW Santa Clara power plant system.

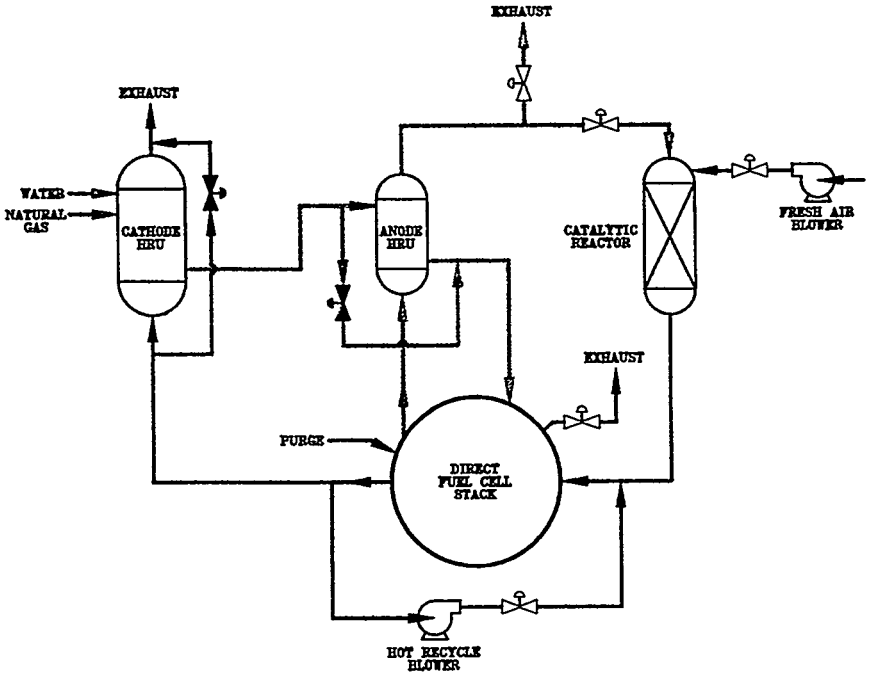


**Figure 8. 100kW-Class Facility Process Flow Diagram:**
100kW-Class stacks as well as BOP equipment can be evaluated

## Endurance Experience

Carbonate fuel cell stacks have demonstrated excellent performance, however long-term stack endurance needs to be demonstrated. A useful life of 40,000 hours is desired for large scale commercialization. Long-term stability of stack components against oxidation and hot corrosion is required, as well as electrolyte loss for long-term performance stability. During the past two years, ERC has tested five carbonate fuel cell stacks for 5,000 to 10,000 hours. Some test results were reported last year[5]. Detailed post-test chemical and metallurgical analyses have been performed this year on these stacks to evaluate endurance issues. The results of the analysis are used to predict the long-term behavior of ERC's stacks[7]. The results on hardware corrosion and electrolyte loss are reported here.

Metallographic analysis of the 316L cathode-side current collector has shown that the corrosion resistance of 316L appears acceptable for 40,000h use (Fig. 9). The 310S, due to its high Cr content, has shown better corrosion resistance than 316L. However, more electrolyte loss has been observed for 310S.

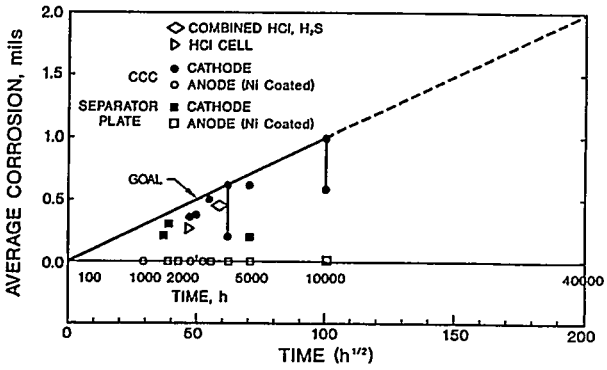


**Figure 9. Corrosion Characterization of Bipolar Plate Materials:**
The current ERC design is expected to meet life goal

Surface protection of stainless steels by Ni coating has generally been adopted by fuel cell developers. With the protection provided by the Ni coating, the anode-side bipolar plate has shown virtually no corrosion attack for up to 10,000h operation (Fig. 10). Consequently, no significant ohmic loss due to anode-side contact interfacial resistance was observed. Although a small amount of Cr-rich oxide forms at the grain boundaries of the Ni layer, no deleterious effect on the corrosion protection is observed. The interdiffusion profiles in the Ni coating during the 5,000-10,000h testing is shown in Fig. 11. The diffusion of Fe and Cr into the coating appears tolerable. Based on this information, the Ni thickness of 0.002" may be adequate for 40,000h use.

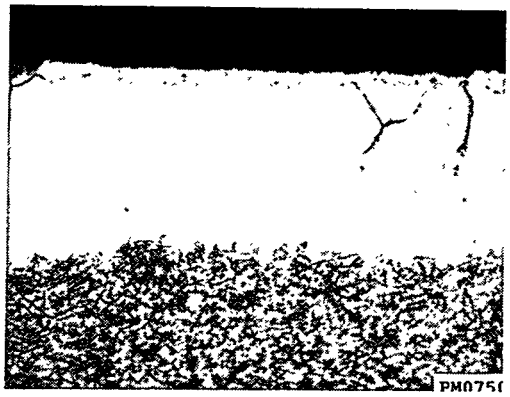


**Figure 10. Ni Coating After 10,000h Testing**
Excellent protection is provided ny Ni coating

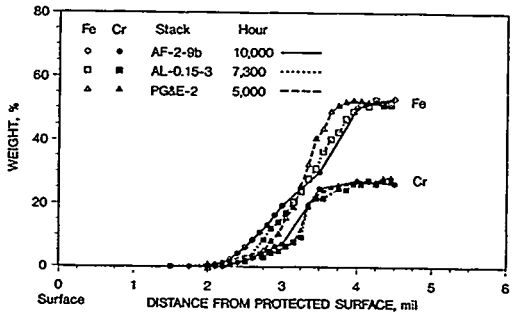


**Figure 11. Diffusion Profiles of Fe and Cr in Anode-Side Ni Layer:**
Two mil Ni protection appear adequate for 40,000h use

The aluminized coating for wet-seal protection has been shown to provide sufficient protection for the substrate stainless steels during a 5,000h out-of-cell and the 10,000h stack testing (Fig. 12). The X-ray microprobe analysis showed that the aluminized coating did not change significantly in

10,000h testing. Based on these results, it could be projected that the aluminized coating is sufficient for 40,000h use. The development drive now is to investigate various low-cost aluminizing processes for cost reduction. Based on the above post-test results, the stack hardware components appears adequate for 40,000h use.

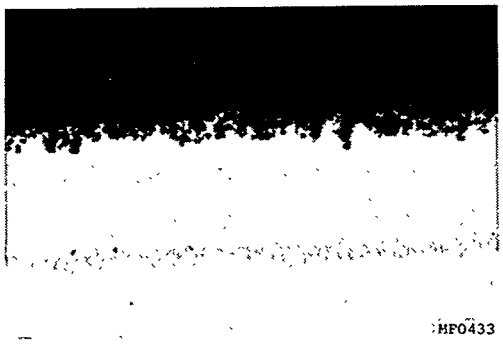


**Figure 12. Stability of Wet Seal:**
Wet-seal aluminized coating appears stable in 10,000h testing

Excessive electrolyte loss during operation may cause matrix and electrode drying, resulting in increased gas cross-over, electrode polarization and ohmic resistance. Analysis of post-test stacks has shown that electrolyte loss to the external hardware (manifold, end plates, etc.) and anode-side internal hardware to be very low (<5% of BOL inventory after 40,000 hours projected). On the other hand, electrolyte loss to the cathode-side internal hardware (mainly cathode current collector), either by creepage or by incorporation into the oxide scale contributes significantly to the total electrolyte loss (>20% of BOL inventory). The effect of cathode current collector surface area has also been evaluated. Larger surface area designs experienced proportionately larger total electrolyte loss. Therefore, current collectors of low surface area design are desired.

The continuous loss of electrolyte by evaporation in the fuel and oxidant streams has always been a concern as a possible cause of long-term performance loss. The major evaporated species is predicted as KOH. Using the calculated partial pressures, the evaporative loss from the anode side is estimated to be <3% of BOL inventory after 40,000h operation.

Based on these long-term stack endurance results, it is expected that the electrolyte inventory of the ERC's full-area cells (>5,000-cm$^2$) can be projected to be sufficient for more than 40,000h use.

**Conclusion**

ERC has made significant progress toward stack scaleup, and has demonstrated 100kW-Class stacks under power plant system operating parameters. The stack endurance testing has shown that ERC's stack hardware and electrolyte management schemes appears adequate for 40,000h life.

## 6.0 FUTURE WORK

The plan for the immediate future includes:

- Complete the testing of the second 120kW full-size stack.
- Test 30kW large area stack on a gasifier slip stream

## 7.0 ACKNOWLEDGEMENT

ERC would like to acknowledge the support of DOE, EPRI and PG&E for the stack and BOP development. Testing at ERC was conducted under DOE and EPRI contracts. Testing at PG&E was supported by PG&E, EPRI, California Energy Commission and GRI.

## 8.0 REFERENCES

[1] L. Paetsch, et al., "Molten Carbonate Fuel Cell Development," DOE Contract No. DE-AC03-76ET11304, Final Report, April, 1987.

[2] P. Patel, et al., "Internal Reforming for Natural Gas Fueled Molten Carbonate Fuel Cells," Final Report for the Period of May 1980 through June 1981 under GRI Contract No. 5080-344-0302.

[3] P. Patel, et al., "Internal Reforming Natural Gas Fueled Carbonate Fuel Cell Stack," Final Report for the Period of February 1982 through December 1983, under GRI Contract No. 5081-244-0545.

[4] M. Farooque, et al., "Development of Internal Reforming Carbonate Fuel Cell Stack Technology," Final Report for the Period of February 1988 through September 1990, under DOE Contract No. DE-AC21-87MC23274.

[5] M. Farooque, et al., "An Update of ERC's Carbonate Fuel Cell Development Program," Proc. 4th Annual Fuel Cells Contractors Review Meeting, P.19, Morgantown, WV, July, 1992.

[6] D. Rastler, et al., "Demonstration of a Carbonate Fuel Cell on Coal Derived Gas," 1992 Fuel Cell Seminar, P.186, November, 1992.

[7] C. Yuh, et al., "Carbonate Fuel Cell Endurance: Hardware Corrosion and Electrolyte Management Status," Proc. 3rd International Symp. Carbonate Fuel Cell Technology, P.158, PV93-3, The Electrochemical Society, 1993.

## 1.6 Simulated Coal Gas MCFC Power Plant System Verification

### CONTRACT INFORMATION


| | |
|---|---|
| **Contract Number** | DOE Contract No. DE-AC21-90MC27394 |
| **Contractor** | M-C Power Corporation<br>8040 S. Madison Street<br>Burr Ridge, IL 60521<br>(708) 986-8040 |
| **Contractor Project Manager** | E. H. Cámara |
| **Principal Investigators** | Thomas G. Benjamin<br>Elias H. Cámara<br>Leonard G. Marianowski<br>Vincent J. Petraglia<br>René M. Laurens |
| **METC Project Manager** | Dr. Mark C. Williams |
| **Period of Performance** | September 14, 1990 to September 14, 1994 |


### ABSTRACT


**Objective:** The overall program objective is the demonstration of a full-scale, full-height IMHEX® molten carbonate fuel cell stack in a 250-kW power plant test. Issues impeding development of manufacturing and testing facilities will be addressed in support of MCFC stack research and power plant development. Issues will be identified and resolved in engineering, manufacturing, assembling, cost, performance, and endurance of the stack repeat and non-repeat components. The tasks of the program are:

- TASK 1. Commercialization
- TASK 2. Power Plant Development
- TASK 3. Manufacturing Facilities Development
- TASK 4. Testing Facility Development
- TASK 5. Stack Research
- TASK 6. Advanced Research & Technology Development

**Participants:** The program is being executed by M-C Power (MCP) and several major subcontractors. M-C Power's role is to scale up the IMHEX® stack technology and fabrication techniques to commercial scale and to demonstrate progress in full-area stacks. Bechtel Corporation is responsible for power plant design, major equipment specification, and procurement and site erection. Stewart & Stevenson Services is responsible for detailed engineering, procurement, and assembly of skid-mounted equipment. UNOCAL will operate the power plant. The Institute of Gas Technology (IGT) will address stack technology development.

In addition to the DOE funding and the cost sharing of MCP, IGT, Bechtel, and Stewart & Stevenson, cost sharing is being provided by the Electric Power Research Institute (EPRI), Southern California Edison Company (SCE), Southern California Gas Company (SoCalGas), the South Coast Air Quality Management District (SCAQMD), and Union Oil of California (Unocal). The power plant system demonstration will be sited at Unocal's Science and Technology Center in Brea, California. Separate but integrated programs are also being funded by the Gas Research Institute (GRI) and San Diego Gas & Electric (SDG&E).

**Status:** Activities for the 250-kW demonstration are continuing for the stack and the Balance of Plant. Prototype active area manufacturing equipment has been commissioned and is being used to manufacture active components for the 250-kW Unocal stack. Upgrading for improved quality and increased throughput is continuing. The separator plates have been welded and are scheduled for aluminizing after post-weld inspection. Process flow diagrams and piping and instrumentation diagrams have been completed. Procurement and layout have begun.

Full-area stack testing comprises three stacks of 20 kW in addition to the 250-kW power plant system verification at UNOCAL. An additional 20-kW stack was operated in the spring of 1992 under the GRI and EPRI sponsorhsip. The second 20-kW stack was successfully operated at the end of 1992. The performance duplicated that of the first stack, indicating reproducibility of manufacturing and operating procedures. A third stack was started in June 1993 with components representative of those being manufactured for the 250-kW Unocal stack.

IGT has successfully tested numerous laboratory single cells to screen and evaluate advanced components, formulations, and fabrication processes. Several advancements are ready for scale-up: low-chromium nickel anodes (EPRI cost sharing), stabilized and strengthened cathodes, and clean binders. IGT endurance tested a 20-cell, 1 $ft^2$ stack. Over 7,150 hours of stable performance were logged.

**Future Work:** During the next 12 months, one 20-kW full-area stack will be tested at MCP. The detailed engineering of the 250-kW Balance of Plant will be completed and construction will begin. Design, commissioning, installation, and construction of the stack will also be completed and power plant operations will begin.

# FE Fuel Cells Conference

## Session 2

## *Solid Oxide Fuel Cells*

# 2.1 High Temperature Solid Oxide Fuel Cell Development Activities

## CONTRACT INFORMATION

| | |
|---|---|
| **Cooperative Agreement** | DE-FC21-91MC28055 |
| **Contractor** | Westinghouse Electric Corporation<br>1310 Beulah Road<br>Pittsburgh, Pennsylvania 15235-5098<br>(412) 256-2125 |
| **Contractor Program Manager** | Mr. Emerson R. Ray |
| **METC Project Manager** | Ms. Diane T. Hooie |
| **Period of Performance** | April 1, 1991 to November 30, 1995 |
| **Schedule and Milestones** | |

**FY1993 Program Schedule**

| | O | N | D | J | F | M | A | M | J | J | A | S |
|---|---|---|---|---|---|---|---|---|---|---|---|---|
| Market/User Assessment Studies | | | | | | | | | | | | |
| Reference Design | | | | | | | | | | | | |
| Base Cell Technology | | | | | | | | | | | | |
| 100 Cm Porous Support Tube (PST) Cell Dev. | | | | | | | | | | | | |
| 100 Cm Air Electrode Supported (AES) Cell Dev. | | | | | | | | | | | | |
| Alternate Process Development | | | | | | | | | | | | |
| 100 to 200 Centimeter Cell Development | | | | | | | | | | | | |
| Process Scale-up/Optimization/ Cost Reduction | | | | | | | | | | | | |
| Facility Construction/Field Test Gen. Support | | | | | | | | | | | | |
| Long Cell Test Station Design and Construction | | | | | | | | | | | | |
| Cell and Bundle Testing | | | | | | | | | | | | |
| Generator Development | | | | | | | | | | | | |
| Joint Field Unit Module Fabrication | | | | | | | | | | | | |
| Joint Field Unit Gen./System Fab./Test | | | | | | | | | | | | |

## OBJECTIVES

This paper presents an overview of the Westinghouse Solid Oxide Fuel Cell (SOFC) development activities and current program status. Our goal is to develop a cell that can operate for 50,000 to 100,000 hours. Progress toward this goal will be discussed and test results presented for multiple single cell tests which have now successfully exceeded 40,000 hours of continuous power operation at temperature. Curves are presented which demonstrate the improved cell performance and life obtained to date.

## BACKGROUND INFORMATION

Solid oxide fuel cells are highly efficient devices that convert chemical energy into electricity. They operate at atmospheric or elevated pressures at a temperature of approximately 1000°C to produce electricity using a variety of fossil fuels such as coal derived fuel gas, reformed natural gas, or reformed distillate fuel. The temperature of the exhaust gases from the cells varies between 600 to 900°C, a temperature which is attractive for cogeneration applications or for use in bottoming cycles for all-electric power plants.

The SOFC readily conducts oxygen ions from an air electrode (cathode), where they are formed, through a solid electrolyte to a fuel electrode (anode). There they react with carbon monoxide (CO) and hydrogen ($H_2$) contained in the fuel gas to deliver electrons and produce electricity. The state-of-the-art tubular SOFC (Figure 1) developed by Westinghouse features a porous air electrode made of strontium-doped lanthanum manganite. A gas-tight electrolyte of yttria-stabilized zirconia (approximately 40 microns thick) covers the air electrode, except in a strip about 9 mm wide along the entire active cell length. This strip of exposed air electrode is covered by a thin, dense, gas tight layer of magnesium-doped lanthanum chromite. This layer, termed the cell interconnection, serves as the electric contacting area to an adjacent cell or to a power contact. The fuel electrode is a nickel-zirconia cermet and covers the electrolyte surface except in the vicinity of the interconnection.

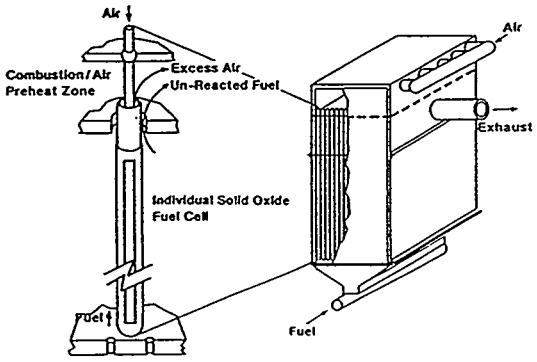


**Figure 1. SOFC Module**

For operation, air is introduced into the fuel cell through an air injector tube. The air, discharged from the injector tube near the closed end of the cell, flows through the annular space formed by the cell and its coaxial injector tube. Fuel flows on the outside of the cell. Typically, 85% of the fuel is electrochemically utilized (reacted) in the active fuel cell section. The gas-impervious electrolyte does not allow nitrogen to pass from the air side to the fuel side, hence the fuel is oxidized in a nitrogen free environment, averting the formation of NOx. At the open end of the cell, the remaining fuel is reacted with the air stream exiting the cell, thereby providing additional useful heat.

Because of the high generator temperature and because water vapor evolves on the anode side of the cell, reformation of natural gas and other hydrocarbon fuels can be accomplished within the generator, thus eliminating the need for an external reformer.

To construct an electric generator, individual cells are "bundled" into an array of series-parallel electrically connected cells forming a mechanically stress forgiving structure that is a basic generator building block. The individual bundles are connected in series to build generator voltage and to form submodules. The parallel electrical connection of the cells within a bundle enhances generator reliability. Submodules are further combined in series to form the generator module.

The performance of the basic module design has been demonstrated by the operation of eight generators, including those operated under field test conditions, presented in Table 1.

**Table 1.**
**Westinghouse SOFC Generators**

| System | Generator Rating | Number of Generators | Total Cells | Cell Length | Date |
|---|---|---|---|---|---|
| DOE | 5 kW | 1 | 324 | 30 | 1986 |
| Osaka Gas | 3 kW | 2 | 288 | 36 | 1987 |
| Tokyo Gas | 3 kW | 1 | 144 | 36 | 1987 |
| GRI | 3 kW | 1 | 144 | 36 | 1988 |
| DOE | 20 kW | 1 | 576 | 50 | 1990 |
| The UTILITIES | 25 kW | 1 | 1152 | 50 | 1992 |
| JGU | 25 kW | 1 | 1152 | 50 | 1992 |
| SCE* | 20 kW | 1 | 576 | 50 | 1994 |
| SCG* | 100 kW | 1 | 2016 | 100 | 1995 |

*in production.

Scaleup to multi-hundred kW and multi-MW commercial modules is the next step, and is now underway. Individual modules would produce, for example, 200 kW for on-site cogeneration applications. For larger applications, modules rated at several MW are planned. These modules, shown in Figure 2, would then be arranged in the power block concept shown in Figure 3. Any number of power blocks could then be installed to satisfy the specific requirement for large plants. Conceptual design studies have confirmed the practicality and economic feasibility of the power block concept in applications ranging up to several hundred megawatts.

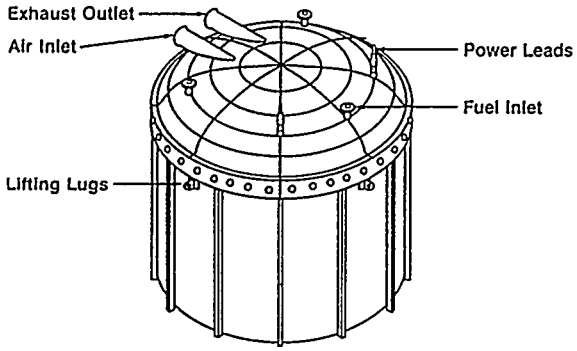


**Figure 2. SOFC Module**

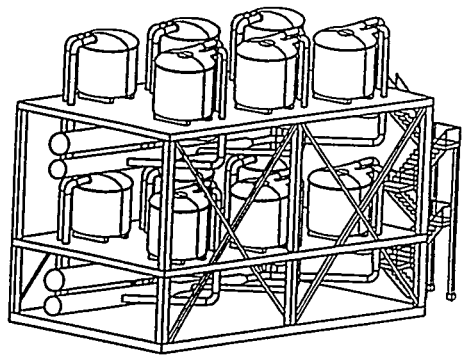

**Figure 3. SOFC Power Block**

## PROJECT DESCRIPTION

The development of the SOFC technology is being advanced under a five-year cooperative agreement between DOE-Morgantown Energy Technology Center, Ms. Diane T. Hooie, Program Manager, and Westinghouse. This program, extending from 1991 through 1995, is focused on continuing to develop, improve, and scale up the tubular SOFC technology. The primary objective of the program is the design, fabrication, and testing of multi-hundred kilowatt and multi-megawatt SOFC generators, both at Westinghouse and at customer sites. Testing at customer sites will provide operational feedback, field experience, and greater awareness of SOFC technology.

The successful commercialization of SOFC technology will depend on the ability to produce cost competitive systems that can operate for five to ten years before replacement of the SOFC module(s). Westinghouse is focusing its efforts on developing a thorough understanding of the parameters that limit cell and generator lifetime in order that new processes and/or materials, as may be needed, can be developed. Furthermore, a detailed understanding of the cost of manufacturing cells and generators is being pursued so that more cost effective processes and procedures can be implemented, and mass production facilities designed.

The Westinghouse goal is to develop a cell that can operate for 50,000 to 100,000 hours with a voltage degradation rate of less than 1/2% per 1000 hours. To date, Westinghouse has produced and operated for extended periods several thousand cells and has systematically improved cell performance, life, and voltage stability (see Figure 4). In August 1993 several test cells each surpassed 40,000 hours of power operation. These cells are the longest operating SOFCs in the world. Other long running cells have been shut down intentionally for detailed examination in order that improvements can be made in future cells. Still other advanced cells have been under test for up to three years with degradation rates as low as 0.5% per 1000 hours.

To enhance economic viability, Westinghouse is working to reduce the manufacturing costs of the cells and generators and to increase the power output per cell. Current programs are aimed at producing longer cells and

increasing power output per unit cell length so as to contribute to improved power plant economics. Over the past few years Westinghouse has focused on increasing the active length of the SOFC from 30 cm (in pre-1986 cells) to 100 cm with the results being a corresponding increase in power output per cell.

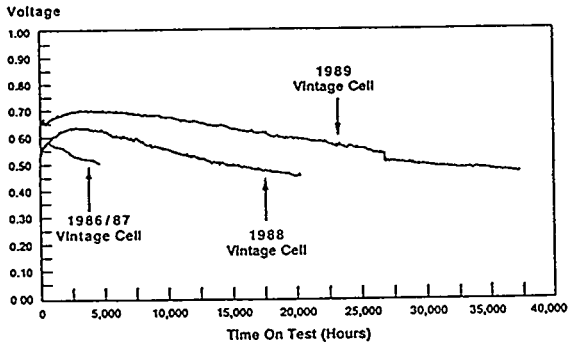


**Figure 4. SOFC Development Progress Increased Cell Stability**

In parallel with increasing the cell length, Westinghouse has also focused on eliminating the need for a porous support tube (PST) (see Figure 5). The early technology SOFCs had a PST with 2 mm wall thickness (defined as a thick-wall PST) that provided the support structure for the SOFC. Although sufficiently porous to allow oxygen ion diffusion to the air electrode, the PST still impedes diffusion and thus reduces performance. Efforts were successful in first reducing the PST wall thickness and ultimately in eliminating it altogether. To compensate for the PST, the air electrode thickness was increased to provide structural support for the cell. This new air electrode supported (AES) cell has improved cell efficiency and power production. The combined effects of increasing the cell length from 30 cm to 100 cm and eliminating the PST results in a six-fold increase in cell power output. Even longer cells of 1.5 to 2 meters long are currently being produced and evaluated to further improve SOFC economics, particularly for large central station electric utility power plants. Studies of advanced cells are also being pursued.

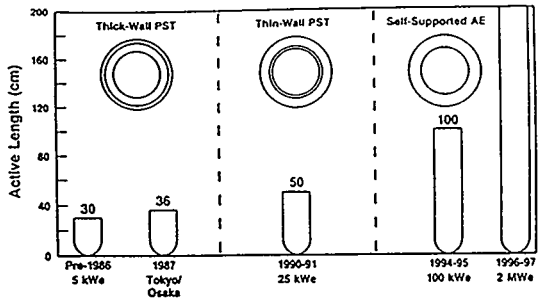


**Figure 5. Evolution of Solid Oxide Fuel Cell Design**

A major step in the commercialization program was construction of the 28,000 sq ft pre-pilot manufacturing facility (PPMF). This facility, located near Pittsburgh, provided the opportunity to move the technology from a laboratory environment to a manufacturing environment. It enables the processes and quality control programs to be put in place that will be required to commercialize the technology during the 1990's.

Bundle Test Four (BT4), the first SOFC test article fabricated at the PPMF, contained two bundles, each consisting of eighteen 50 cm long cells. This test article was fabricated in 1989 and was designed to demonstrate that the transfer of technology from the laboratory to the PPMF had been successfully accomplished. BT4 completed over 6800 hours of stable operation at 1000°C with eight planned thermal cycles (from room temperature to 1000°C and back to room temperature) for a total test period of over 8,000 hours. The successful thermal cycling tests indicate that the SOFC technology has the potential for numerous start-ups and shutdowns.

Another major milestone associated with the PPMF and the overall SOFC program was the fabrication of the multi-kilowatt generator (MKG) (Figure 6). The MKG, rated at 20 kW, contains approximately five hundred and seventy-six 50 cm long cells. The MKG was successfully started in November 1990 and operated for 1750 hours on pipeline natural gas, 900 hours on hydrogen, and an additional 750 hours on naphtha. NOx levels were measured at <0.5 ppm

in the generator exhaust. The design, fabrication, and testing of the MKG was a primary objective of the development contract with DOE during the 1980's.

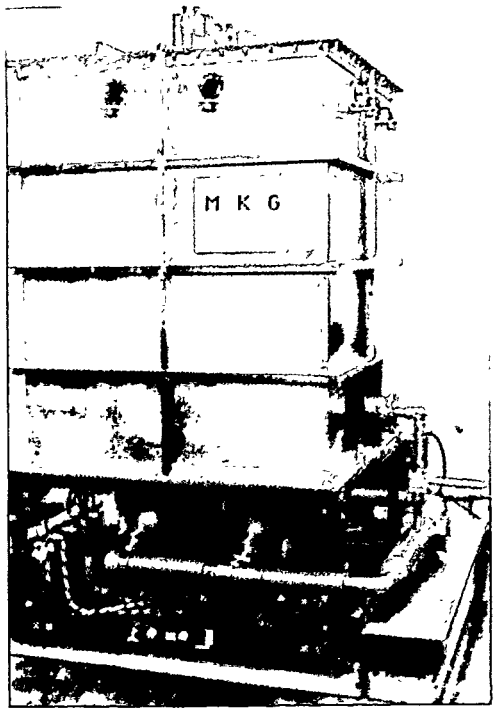


**Figure 6. 20 kW SOFC Module**

The MKG generator module subsequently has been replicated and used in 25 kW SOFC customer test units, the subject of a companion report.

The next larger SOFC generator, rated at 100 kW, is in the design stage. It will incorporate 100 cm AES cells and internal reforming of natural gas. The first of these units to be shipped to the field will be part of a 100 kW SOFC cogeneration system planned for operation at SCG's Pico Rivera site. A number of other 100 kW generators are planned and will undergo field tests at various other sites around the world.

A major step in our SOFC program is development of a megawatt class generator using the modules shown in Figure 2. Preliminary designs are now underway. These generators will use cells of 1.5 to 2 meters in length.

## RESULTS

In parallel with the SOFC technology development program, Westinghouse has performed numerous application studies to ensure that its development programs will result in a product that can satisfy the needs of various market sectors in the late 1990's and beyond. These studies help to define design requirements and establish the performance, economic, and development goals that the SOFC technology must achieve to reach commercialization. These studies are an important part of the Westinghouse Commercialization Plan for the SOFC technology.

SOFCs, with their high temperature exhaust, high efficiency, low emissions, fuel flexibility, and modularity, can be used in a broad spectrum of applications. Electric utilities have identified applications for the SOFC technology that include multi-megawatt size distributed electric power plants located near load centers, repowering of existing units, and large central station all-electric power plants. The gas utilities' interest in the SOFC technology is primarily for on-site power generation for commercial and small industrial applications.

## SUMMARY

A number of significant developments and accomplishments have been realized during the past two years of the tubular SOFC program:

- Four SOFCs have operated for more than 40,000 hours in single cell tests.
- Improved cell voltage stability (as low as 0.5% per 1000 hours degradation rate) has been achieved in single cell tests.
- Two 25 kW SOFC customer test units were delivered in 1992.
- A 20 kW SOFC system is being manufactured and will be operated by Southern California Edison (SCE) in 1995.

- A 100 kW SOFC cogeneration system project is underway for Southern California Gas (SCG).

- The porous support tube is being eliminated, thus reducing cell cost and increasing power output per cell.

- Fuel flexibility was demonstrated in a 20 kW SOFC module that operated on natural gas for 1750 hours, naphtha for 750 hours, and hydrogen for an additional 900 hours.

- Economically competitive system performance was confirmed in application studies of numerous types of SOFC plants: natural gas fueled cogeneration units of 50 kW to 20 MW and distributed power plants of 10-20 MW; 300 MW central stations fueled by natural gas and coal-derived fuel gas; and an existing steam turbine plant repowered by SOFCs.

- The next phase of the commercialization program is underway. The conceptual design of the megawatt class demonstration unit has been initiated for SCE.

- A notice of award has been received from DOD-ARPA concerning a program to test a tubular SOFC generator on logistic fuels (No. 2 fuel oil and JP-8).

## FUTURE WORK

The existing Cooperative Agreement between Westinghouse and the Department of Energy was initiated in April, 1991 and will continue through November 1995. This five year program includes considerable financial contributions from Westinghouse, from domestic and foreign utilities, and from other agencies, in addition to the U.S. Department of Energy. Under this program Westinghouse will continue development of the tubular solid oxide fuel cell technology and generator systems and plans for field testing of multi-hundred kilowatt and multi-megawatt rated generators during the mid to latter-1990's, The ultimate objective of this program is to develop tubular SOFC technology to the point of acceptable risk for private sector commercialization.

Development of the tubular solid oxide fuel cell technology is being supported by the Westinghouse Electric Corporation, the United States Department of Energy (DOE-METC), and various utility and industry sources. The Cooperative Agreement between Westinghouse and DOE is administered by the Morgantown Energy Technology Center (METC).

## 2.2 MSOFC Development Status

**CONTRACT INFORMATION**

| | |
|---|---|
| **Program Title** | MSOFC Technology Advancement For Coal-Based Power Generation |
| **Contract Number** | DE-AC-21-89MC26006 |
| **Contractor** | AlliedSignal Aerospace Systems & Equipment<br>2525 West 190th Street<br>Torrance, CA 90509 |
| **Contractor Project Manager** | Dr. Richard A. Gibson |
| **Principal Investigator** | Dr. Nguyen Q. Minh |
| **METC Project Manager** | Mr. Paul Micheli |
| **Period of Performance** | September 27, 1989 to December 30, 1993 |

**Schedule and Milestones**

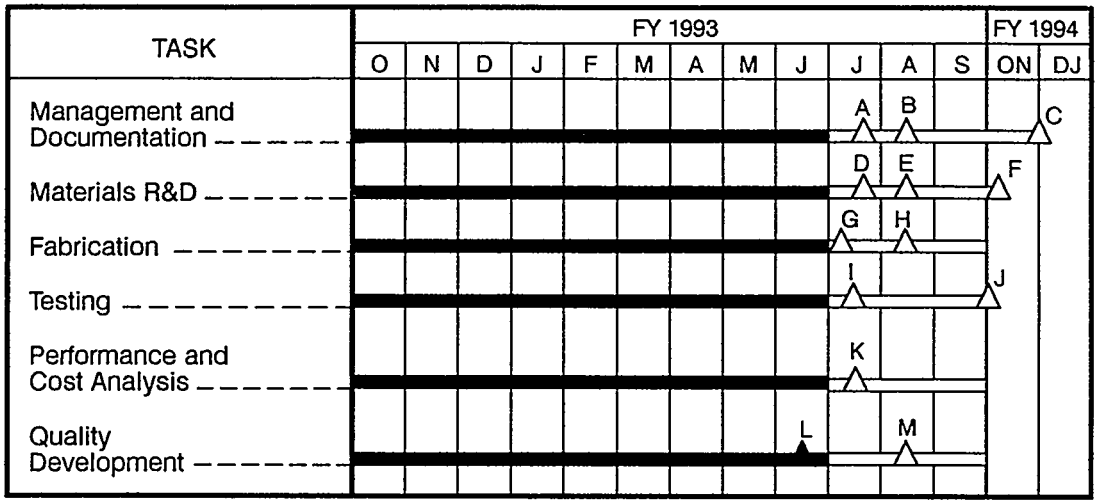


A - Topical Reports
B - Contractors' Review
C - Final Technical Report
D - Mechanical Properties Data Complete
E - New Test Fixture
F - Electrochemical Model Complete
G - 25-w Stack
H - 100-w Stack
I - 25-w Stack Test (Complete)
J - 100-w Stack (Complete)
K - MSOFC System Analysis Complete
L - Stack Stress Cool-down Model Complete
M - Stress Heat-up Model Complete

IG-18888

**Program Schedule**

## OBJECTIVES

The overall objective of this program is to advance materials and fabrication methodologies to develop a monolithic solid oxide fuel cell (MSOFC) system capable of meeting performance, life, and cost goals for coal-derived fuel applications. The technical effort of this program is aimed at creating a technology base that will be used to extend MSOFC development from proof of concept toward practical application. The program culminates in fabrication and testing of a 100-w stack.

## BACKGROUND INFORMATION

The MSOFC is an all-ceramic structure in which cell components are configured in a compact, corrugated array. The MSOFC produces a direct current by electrochemically combining fuel and oxidant across the zirconia solid electrolyte at an operating temperature of about 1000°C. There are two versions of the monolithic fuel cell, coflow (Figure 1) and crossflow (Figure 2). The crossflow approach is used in this program because it is more straightforward to manifold and fabricate. As can be seen from the figures, the MSOFC is made of two types of multilayer structures, each composed of three ceramics—anode/electrode/cathode and anode/interconnect/cathode. The anode/electrolyte/cathode composite represents a single cell. The function of the anode/interconnect/cathode composite is to connect the cells in electrical series to build voltage. In the MSOFC, the anode and cathode layers must be porous to allow gas

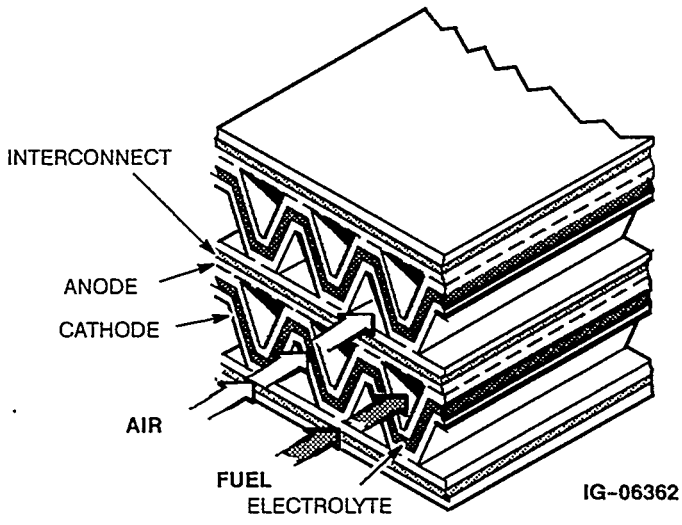


**Figure 1. Coflow MSOFC**

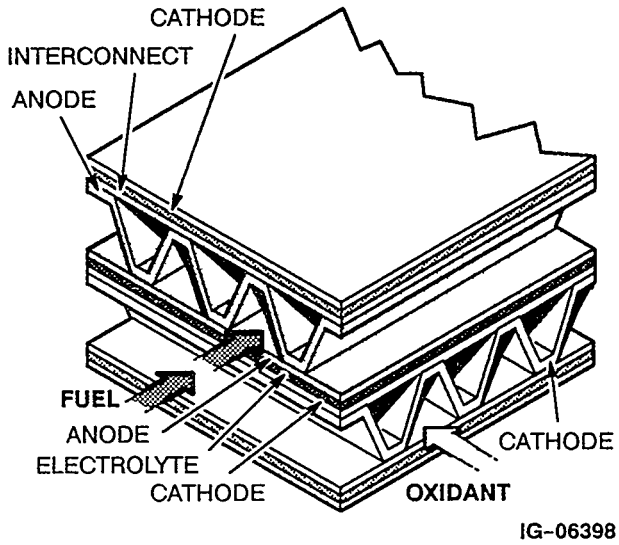


**Figure 2. Crossflow MSOFC**

transport to the reaction sites, while the electrolyte and interconnect layers must be dense to prevent gas mixing. Design goals for layer thicknesses and cell-to-cell distance are 5 to 100 μm and 1 to 2 mm, respectively. The MSOFC design eliminates inactive structural support, increases active surface areas, and lowers voltage losses due to internal electrical resistances. The monolithic fuel cell, thus, has high efficiency, excellent performance, and high power density. The MSOFC can be integrated with coal gasification plants and is expected to have high overall efficiency in the conversion of the chemical energy of coal to electrical energy.

The materials currently used for building the MSOFC are $Y_2O_3$-stabilized $ZrO_2$ for electrolytes, $Ni/Y_2O_3$-$ZrO_2$ cermet for anodes, doped $LaMnO_3$ for cathodes, and doped $LaCrO_3$ for interconnects. These materials are known to possess adequate levels of conductivity, and they are compatible and stable under cell operating conditions. The challenge is to develop ways to form the materials into thin components and to incorporate these components into the monolithic structure. A fabrication scheme for the MSOFC must incorporate each material such that none of the fabrication steps will diminish the desired material characteristics of any of the component layers. The fabrication of the MSOFC must achieve the following: (1) high-density electrolyte and interconnect, along with porous anode and cathode layers, (2) good interfacial bonding between adjacent layers, (3) insignificant reaction and interdiffusion between

neighboring layers, and (4) a defect-free structure. At present, the development of suitable materials and the fabrication of the intricate structure are the main foci of the MSOFC development effort.

## PROJECT DESCRIPTION

This program is performed by a team comprising the AlliedSignal Aerospace Systems & Equipment (ASE) and Argonne National Laboratory (ANL). The technical effort of the program is organized around five work tasks as follows:

(a) Materials research and development: This task concentrates on development of materials suitable for the unique MSOFC structure and environment. The work addresses several identified material issues such as interconnect sinterability, material stability and performance (especially in coal gas), and current collector materials.

(b) Fabrication: This task is aimed at demonstrating MSOFC fabrication and fabrication reproducibility and reliability. The fabrication process will be scaled up to produce MSOFC stacks of increasing power output. This effort also involves definition of optimal fabrication parameters, defect analysis, development of material and process specifications, and material supplier identification.

(c) Testing: This task verifies the performance and life of the MSOFC with coal-derived fuels. MSOFC cells and stacks are tested under specified conditions, and posttest analyses are carried out to provide information for explaining observed behavior and identifying degradation mechanisms.

(d) Performance and cost analysis: This task involves performance, system, and cost analysis of the MSOFC in coal-based applications. The emphasis of performance analysis is on development of an MSOFC performance model. System and cost analysis defines MSOFC system configurations and MSOFC manufacturing and system costs.

(e) Quality development: This task concentrates on developing methods for ensuring the quality of fabricated MSOFC stacks. This effort involves evaluation of NDE methods, stress analysis, and microcrack control.

The overall program is expected to resolve several material and fabrication issues and to result in a technology base that will be used to bring the MSOFC technology toward practical application.

## RESULTS

During the past year, AlliedSignal's effort has focused on development of the requisite technology for fabricating and testing multicell stacks. Due to the extraordinary promise of the thin-electrolyte technology developed within the past year, it has been incorporated as the baseline cell technology.

The fabrication sequence for the thin-electrolyte MSOFC is shown in Figure 3. A bilayer tape comprising anode and electrolyte tapes is formed by passing the tapes

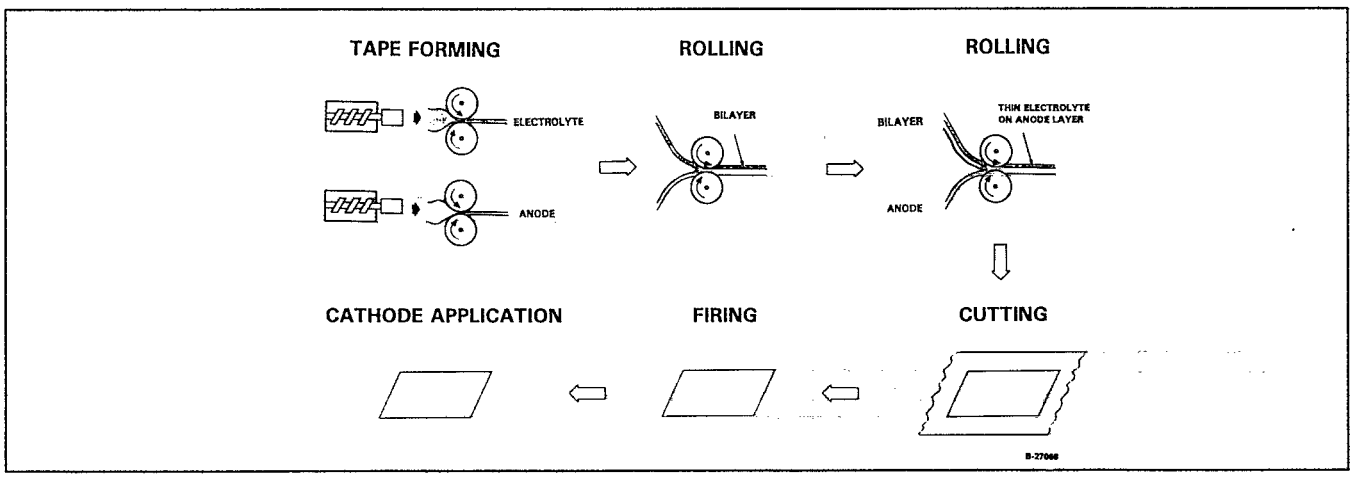


**Figure 3. Thin-electrolyte MSOFC Fabrication Sequence**

between counterrotating cylinders. This bilayer tape is then passed once again through the cylinders with an anode tape, forming a bilayer with an electrolyte of reduced thickness. This process is continued until the electrolyte layer thickness is reduced to less than 10 μ. The bilayer is fired, and then a cathode slurry is fired with the bilayer to form the trilayer cell. A fracture surface of a cell cross section (see Figure 4) shows a dense electrolyte positioned between porous anode and cathode. The element mapping shows essentially no interdiffusion of the materials. The electrochemical performance of a thin-electrolyte cell is displayed in Figure 5. At 1000°C, an area-specific resistance of 0.30 ohm-cm$^2$ is achieved, with a power density of more than 900 mw/cm$^2$.

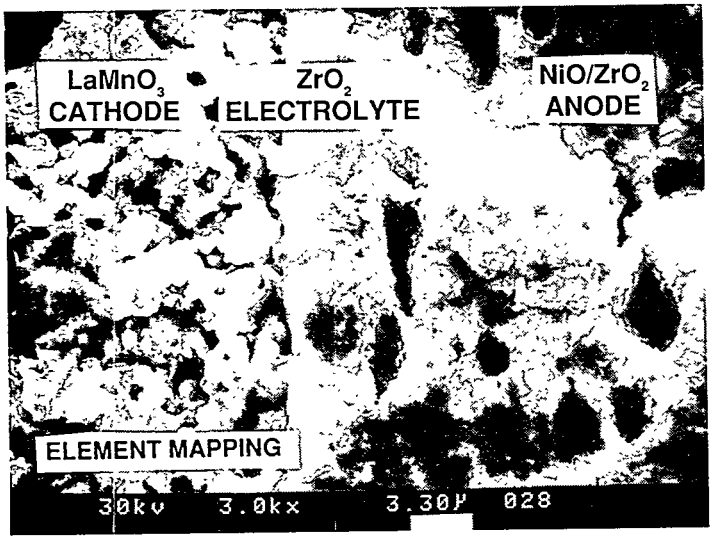


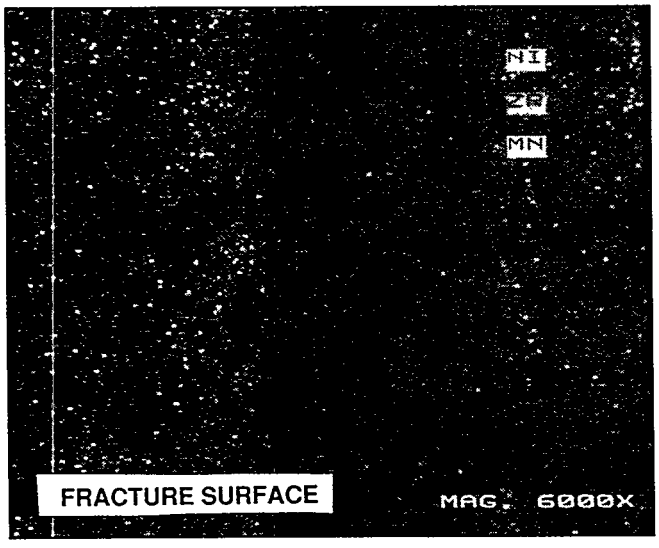


M-00365

**Figure 4. Thin-electrolyte Cell**

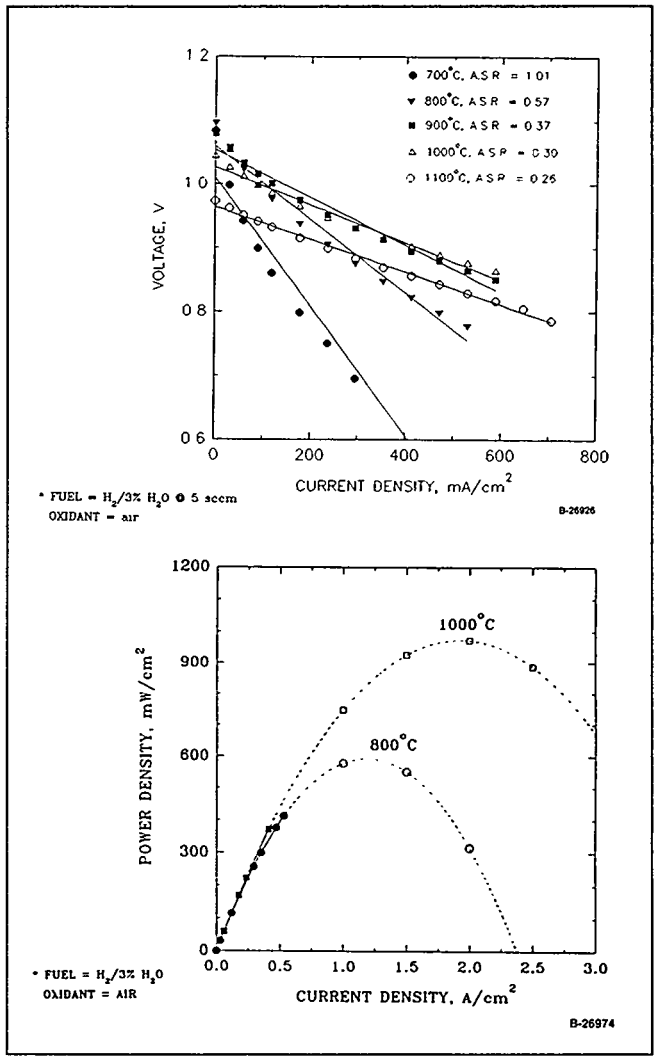


**Figure 5. MSOFC Performance Curves**

The anode/electrolyte bilayers have proved scalable to footprints larger than 8 by 8 in. (see Figure 6) with no evidence of performance-compromising defects.

Progress in fabricating high-performance stacks has been delayed due to three factors:

(a) The baseline anode formulation developed during the program shrinks when exposed to hydrogen, causing curvature of the cells. This leads to delamination of the stacks and must be avoided. New anode compositions which dramatically curtail anode-reduction-induced shrinkage are being developed (Figure 7).

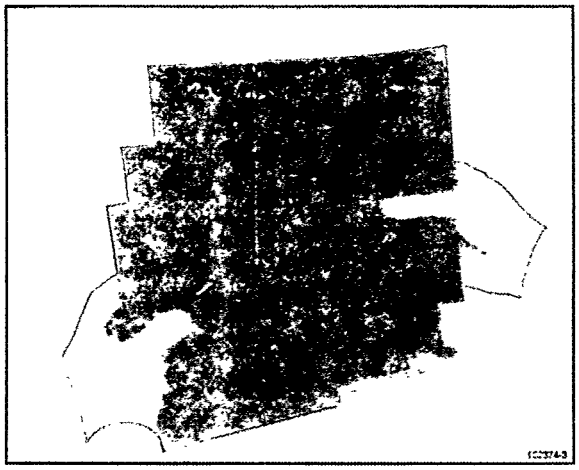

**Figure 6. Fabrication Scale-up**

(b) The manifold and sealant technologies are not sufficiently well developed, causing leakage and making thermal cycling infeasible. This is the focus of the effort at Argonne National Labs, where glass-ceramic sealant technology is being developed. Off-line testing of these sealants with the MSOFC components is progressing successfully, and a suitable sealant is expected to be developed in the near term.

(c) Component coefficient of thermal expansion mismatches may cause stresses sufficient to lead to internal fracturing and delamination, with concomitant high internal electrical resistance. The stack stress analysis model is being used to establish mechanical properties criteria, and minor modifications in material compositions are expected to lead to acceptable stress levels.

## FUTURE WORK

Future plans include fabrication of a 100-w stack and testing on hydrogen fuel for 600 hr and on natural gas for 24 hr. An updated assessment of the costs of producing MSOFC stacks will be performed, building on the study completed in the previous program, and incorporating a more detailed assessment of material costs. A system/performance analysis of a 200-Mw system will also be performed.

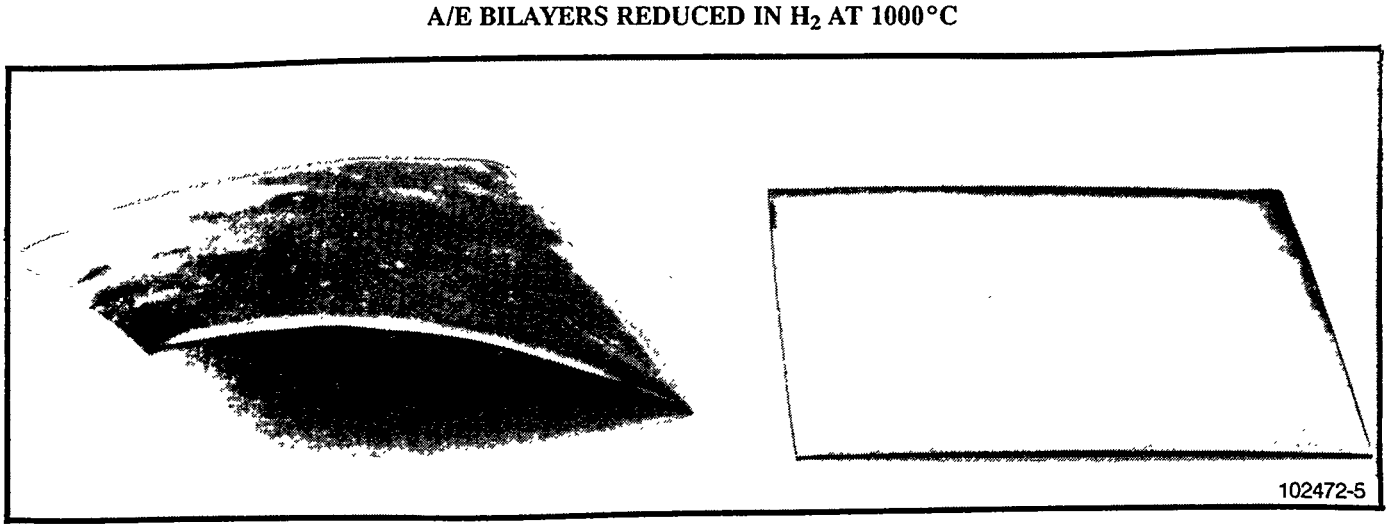


**Figure 7. New Anode Compositions Dramatically Curtail Anode-reduction-induced Shrinkage**

## 2.3 High Temperature Solid Oxide Fuel Cell - Customer Test Units

### CONTRACT INFORMATION

| | |
|---|---|
| **Contract Number** | DE-FC21-91MC28055 |
| **Contractor** | Westinghouse Electric Corporation<br>Science & Technology Center<br>1310 Beulah Road<br>Pittsburgh, PA 15235<br>(412) 256-1901 |
| **Contractor Project Manager** | Emerson R. Ray |
| **Principal Investigators** | Stephen E. Veyo |
| **METC Project Manager** | Diane T. Hooie |
| **Period of Performance** | April 1, 1991 to November 30, 1995 |

### CONTRACT INFORMATION

Customer test units are an integral part of the Cooperative Agreement between Westinghouse and the United States Department of Energy (DOE) for the development of tubular SOFC technology. The design and construction of the host systems for SOFC customer test units has been funded with customer and Westinghouse monies. DOE has participated in the customer test unit programs by providing the cells and in part, the stacks or generator modules. Test units have been operated by the customer entirely at customer expense with data shared with Westinghouse and DOE. Cells and generator modules are returned to Westinghouse at the completion of the customer test program.

### OBJECTIVES

The development of a viable fuel cell driven electrical power generation system involves not only the development of cell and stack technology, but also the development of the overall system concept, the strategy for control, and the ancillary subsystems. System development must maintain a customer focus in order to ensure that a viable commercial product evolves. Westinghouse has practiced the deployment of customer test units - fully integrated, automatically controlled, packaged power generation systems - utilizing our tubular SOFC technology, in order to demonstrate to customers first hand the beneficial attributes of the SOFC, to expose deficiencies through experience in order to guide continued development, and to garner real world feedback and data concerning not only cell and stack parameters, but also transportation, installation, permitting and licensing, start-up and shutdown,

system alarming, fault detection, fault response, and operator interaction.

## BACKGROUND INFORMATION

The deployment of customer test units began with the 400 W Westinghouse SOFC system tested by the Tennessee Valley Authority (TVA) in 1986. Subsequently, in 1987 to 1988, two 3 kW Westinghouse SOFC systems were tested in Japan, one by the Osaka Gas Company, and one by the Tokyo Gas Company. In 1992, testing of two 25 kW Westinghouse SOFC systems was initiated in Japan. The results of the 25 kW program are the principle focus of this report. Now under development for field deployment is a 100 kW SOFC system.

The evolution of cell and stack design used in the customer test units is shown in Figure 1. The cell has evolved from a thick wall porous support tube design nominally 16 mm in outside diameter and of 300 mm active length to a cell without the porous support tube and of 1000 mm active length. The maximum power output per unit of cell length has increased from about 0.7 W/cm. to approximately 1.3 W/cm. Cell design and manufacturing processes have been developed using funds provided by DOE and its predecessor agencies and by Westinghouse.

The 400 W and the 3 kW field units were fueled by a mixture of humidified hydrogen and carbon monoxide. The 25 kW field units are fueled directly by pipeline natural gas utilizing a prereformer that is thermally and hydraulically integrated with the stack. The principle of operation for the natural gas fired seal-less generator modules is shown schematically in Figure 2. Note that the required thermal energy to accomplish reforming is provided by the sensible heat in the SOFC exhaust and that the water vapor required to support reformation and suppress carbon deposition is provided by the recirculation of a portion of the anode exit gas. The prereformer is typically sized to reform approximately 75% of the incoming fresh fuel at peak power, with the balance reformed within the generator module. Reformer temperature is self regulated with the reformer inlet O:C (Oxygen to Carbon) atom ratio controlled by modulating PNG inlet pressure to the nozzle of the fixed geometry ejector used to recirculate anode exit gas. Development of the ability to directly use natural gas in the generator module has been supported by Westinghouse, DOE, and the Gas Research Institute (GRI).

The generator module used in the 25 kW SOFC customer test units is a near replica of the Multi-kW Generator (MKG) developed by Westinghouse for DOE. This module utilizes 576 cells of 500 mm active length arranged in four quadrants. Each quadrant is in essence a stretched version of the 3 kW generator module with integral prereformer developed with GRI support.

## PROJECT DESCRIPTION

There are three 25 kW class SOFC customer test unit programs. The first is sponsored by The UTILITIES, a confederation of The Kansai Electric Power Company, the Tokyo Gas Company, and the Osaka Gas Company. The second is sponsored by the Joint Gas Utilities (JGU), a consortium of the Tokyo Gas Company and the Osaka Gas Company. The third is sponsored by the Southern California Edison Company. All three systems are extensively instrumented and include a high speed data acquisition system and dedicated remotely located personal computer (PC) for interface and data archiving.

The UTILITIES' system consists of two independent dc generation systems, each incorporating a 576-cell, 20 kW class (MKG) stack. Figure 3 shows one of these systems. The package envelope houses the SOFC stack with integral reformers, the exhaust gas heat recovery heat exchanger (recuperator), the air supply system (centrifugal blower with motor and an electric air heater for start-up and low power operation), the fuel supply system (PNG compressor and valves for isolation and flow modulation), a power distribution module containing instrumentation power supplies, a silicon controlled rectifier (SCR) controller for the air heater, and variable frequency motor drives, and a controls module containing a programmable logic loop controller and a high speed data acquisition system. The package measures 2200 mm high by 1600 mm wide by 1800 mm deep. A dissipator for the dc power is housed in a separate rack panel cabinet. System parasitic power is supplied from the grid.

Figure 4 shows a flow schematic for The UTILITIES' system. It can be observed that the system is uncomplicated and simple in configuration. Start-up is accomplished using electric power for air heating and hydrogen as stack fuel until thermal conditions and adequate water evolution at the anode permit a transition to PNG fuel. The start-up process is semi-automatic requiring operator verification for state transition. After the transition to PNG fuel is accomplished, operation is fully automatic with no operator required. The system requires set point values for delivered dc current, stack temperature, fuel utilization, and air utilization. Fuel and air flow are automatically adjusted in proportion to the dc current. The control system will automatically shut the system down in response to either an operator command or the deviation of several critical parameters outside of the permitted value range.

The JGU system incorporates two 576-cell, 20 kW class (MKG) stacks connected in electrical series and integrated into a single system capable of cogenerating process steam. The monolithic enclosure, shown in Figure 5, measures 2200 mm high by 5000 mm wide by 2000 mm deep. The package includes both a high temperature and a low temperature recuperator plus an exhaust gas heat recovery steam generator (HRSG) and a dc-to-ac power conditioner. A flow schematic is shown in Figure 6. Of particular note is the location of the HRSG interposed between the high temperature and the low temperature recuperators. The steam generator is a once-through design that uses a set point value of steam superheat to modulate the feed water flow hence cogeneration thermal energy recovery. Air bypass valves around the recuperators are used to control the temperature of the air inlet to the SOFC stack. As with The UTILITIES' system, start-up is semi-automatic and normal operation automatic.

The 25 kW SOFC system for the Southern California Edison Company is identical in configuration to one of the system units supplied to The UTILITIES, but the stack incorporates the newer technology air electrode supported cells (no porous zirconia support tube).

## RESULTS

Assembly of The UTILITIES' 25 kW SOFC system was completed in November 1991 and after factory start-up and operational tests, the unit was shipped via overland truck and air freight to the Rokko Island Test Center for Advanced Energy Systems (near Kobe, Japan) operated by The Kansai Electric Power Company. Testing was initiated in February 1992, following installation and three weeks of pre-operation on-

site software and hardware verification directed toward licensing.

System start-up was accomplished easily demonstrating that automatic operation at nominally 1000°C is possible in less than eight hours after initiating the start-up process from ambient temperature. Subsequent shutdown was also achieved according to process design with the stack cooled to less than 100°C in six hours. Observed and predicted power versus current for the two system unit is shown in Figure 7.

Module A operated for 2529 hours at an average output of 16.8 kW dc, achieving a maximum output of 17.7 kW dc. The system was started from ambient temperature and cooled to ambient temperature four times and as a result of various system difficulties endured nine partial cool-downs. Testing spanned three distinct periods: from 11/29/91 to 12/13/91 at the Westinghouse factory, 2/25/92 to 5/1/92 and 6/13/92 to 7/12/92 at the Rokko Island test site. Test operation in Japan was interrupted by the need to repair a failed electric air heater which prevented a restart following an automatic stop induced by an instability in the dissipator control circuits. The final shutdown was also induced by current stability problems with the dissipator. A restart was not possible because of damaged cells and Module A was returned to the factory.

Module B operated for 1576 hours at an average output of 17.4 kW dc and achieved a maximum power of 19.2 kW dc. The system was started from ambient temperature twice and experienced two shutdowns to ambient temperature and three partial cool-downs. The final system shutdown occurred during a period of operational probing for maximum output. Subsequent post operation investigation showed that the unit was operated at excessively high fuel utilization as evidenced by a detachment of the fuel electrode from a few cells in quadrant 4. This event was due possibly to an internal fuel maldistribution caused by blocked fuel distribution ports (as observed), possibly exacerbated by cell leaks. The average fuel utilization in quadrant-4 based upon measurements is estimated at 91%. Locally, the fuel utilization was apparently much greater. Analysis of cool-down data indicated that only quadrant-4 had trouble. Module B was returned to the factory for repair. At the factory, quadrant-4 was replaced, but the remaining quadrants were not examined in great detail. A subsequent restart in October 1992 was aborted because of excessive internal temperatures. Subsequent post operation examination revealed that approximately six percent of the cells had cracked.

Module B was rebuilt with new cells and returned to Rokko Island without factory start-up. Installation and start-up took place during the last days of March 1993. Start-up was successful, but hampered by a lower than expected cell voltage and an instability in the output of the natural gas mass flow meter. Field modification of the control software during operation permitted completion of an extended start-up process. The repaired Module B operated for 1843 hours on PNG spanning the period from 4/1/93 to 6/17/93. Nominal output during this period was 17 kW dc. Shutdown was caused by a failure of the air supply system. Drive belts for the blower failed, and the motor bearings failed the day after belt replacement. The operational period was vexed by inadequate ambient temperature compensation in the air and PNG flow meters. Analysis of cool-down data indicates the existence of anomalous temperatures and a restart attempt has not been recommended.

Start-up of the JGU 25 kW SOFC cogeneration system in Japan in October 1992 was aborted because of a hot spot in one of the

stacks. In early December 1992 a field repair effort was initiated, but not completed, because a significant number of cells were found to be cracked. Initial factory tests of the JGU system were troubled by an air flow maldistribution which was caused by a manufacturing error in one of the stacks. Total operating time for the unit (at the factory) was 817 hours during which the unit endured four cold start-ups and shutdowns plus eight partial cool-downs. Observed and predicted power versus current are shown in Figure 8.

The 25 kW systems in general operated in a thermally self sustaining mode, with no fuel or electrical power consumed for temperature maintenance. Stack V-I performance was in general agreement with expectations based upon single cell tests. Projected overall system efficiencies for the 25 kW class machines, on a net ac/HHV basis, are about 33%. Measured NOx emissions are less than 1 ppm.

The installation and operational experience was positive. At a prepared site with cranes and rigging, unloading and physical installation can be accomplished easily in one day. The units could be started within eight hours, maneuvered across the load range, and stopped easily - as advertised. Data was available from both the data acquisition system and the control system via modem at any time. Instrumentation troubles (instability, zero drift, poor ambient temperature compensation), particularly with flow meters, were a continuous concern and were responsible for several unplanned shutdowns.

## FUTURE WORK

In early 1994 Westinghouse will deliver to the Southern California Edison Company a 20 kW class system utilizing air electrode supported (AES) cell technology in the stack and an AES repair module to the JGU. In 1995 Westinghouse will deliver a 100 kW SOFC system using the AES cell technology.

## ACKNOWLEDGEMENT

Westinghouse gratefully acknowledges the support of DOE for the continued development of the tubular SOFC. In addition, Westinghouse acknowledges the past, present, and future financial and programmatic support for the field unit test program of our commercial customers: the Tennessee Valley Authority; The Kansai Electric Power Company; the Tokyo Gas Company; the Osaka Gas Company; the Southern California Edison Company; and the Southern California Gas Company. A particular acknowledgement is due to personnel of The Kansai Electric Power Company for their competent and responsive installation and operation of The UTILITIES' 25 kW SOFC system.

## REFERENCES

Shinozaki, K. and Washio, S., 1993. Verification Test of a 25 kW Class SOFC Cogeneration System. In *Proceedings of the Third International Symposium on Solid Oxide Fuel Cells*, Volume 93-4, pp. 684-689.

Takeuchi, S., Kusunoki, A., Matsubara, H., Kikuoka, Y., Ohtsuki, J., Satomi, T., Shinozaki, K., 1993. A 25 kW Class SOFC Generation System Verification Test. In *Proceedings of the Third International Symposium on Solid Oxide Fuel Cells*, Volume 93-4, pp. 678-683.

Takeuchi, S., Kusunoki, A., Kikuoka, Y., Matsubara, H., Ohtsuki, J., Satomi, T., Shinozaki, K., Veyo, S.E., 1992. A 25 kW SOFC

Generation System Verification Test. In *1992 Fuel Cell Seminar Program and Abstracts*, pp. 354-357.

Shinozaki, K., Satomi, T., 1992. Verification Test of a 25 kW Class SOFC Cogeneration System. In *1992 Fuel Cell Seminar Program and Abstracts*, pp. 358-361.

| Year | Customer | Stack Rating (kW) | Stack Number | Cell Type | Cell Length (mm) | Cell Number | Oper. Time (Hrs) | Fuel |
|---|---|---|---|---|---|---|---|---|
| 1986 | TVA | 0.4 | 1 | TK-PST | 300 | 24 | 1760 | H2+CO |
| 1987 | Osaka Gas | 3 | 1 | TK-PST | 360 | 144 | 3012 | H2+CO |
| 1987 | Osaka Gas | 3 | 1 | TK-PST | 360 | 144 | 3683 | H2+CO |
| 1987 | Tokyo Gas | 3 | 1 | TK-PST | 360 | 144 | 4882 | H2+CO |
| 1992 | UTILITIES-A | 20 | 1 | TN-PST | 500 | 576 | 2595 | PNG |
| 1992 | UTILITIES-B1 | 20 | 1 | TN-PST | 500 | 576 | 1576 | PNG |
| 1993 | UTILITIES-B2 | 20 | 1 | TN-PST | 500 | 576 | 1843 | PNG |
| 1992 | JGU-1 | 20 | 2 | TN-PST | 500 | 576 | 817 | PNG |
| | | | | Future Work | | | | |
| 1994 | JGU-2 | 25 | 1 | AES | 500 | 576 | TBD | PNG |
| 1994 | SCE | 25 | 1 | AES | 500 | 576 | TBD | PNG |
| 1995 | SCG | 100 | 1 | AES | 1000 | 1512 | TBD | PNG |

PNG = pipeline natural gas
TK-PST = thick wall porous support tube
TN-PST = thin wall porous support tube
AES = air electrode supported

**Figure 1. Evolution in SOFC Cell and Stack Design**

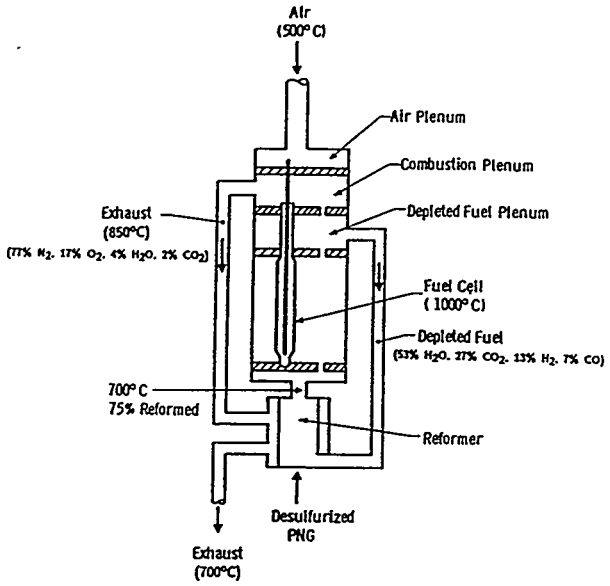


**Figure 2. Principle of Operation for PNG Fueled SOFC Stack**

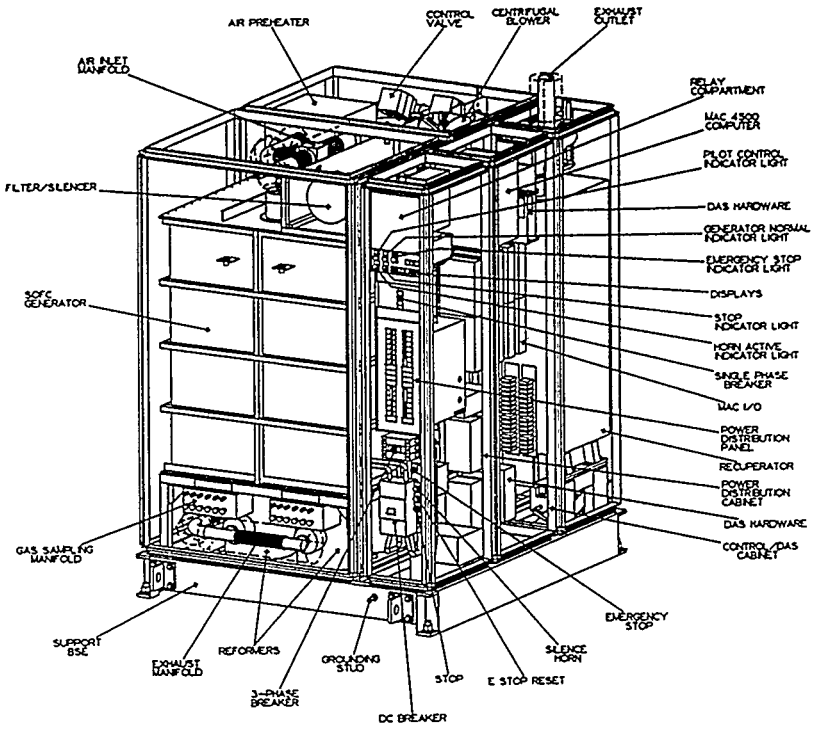


**Figure 3. 25 kW SOFC System**

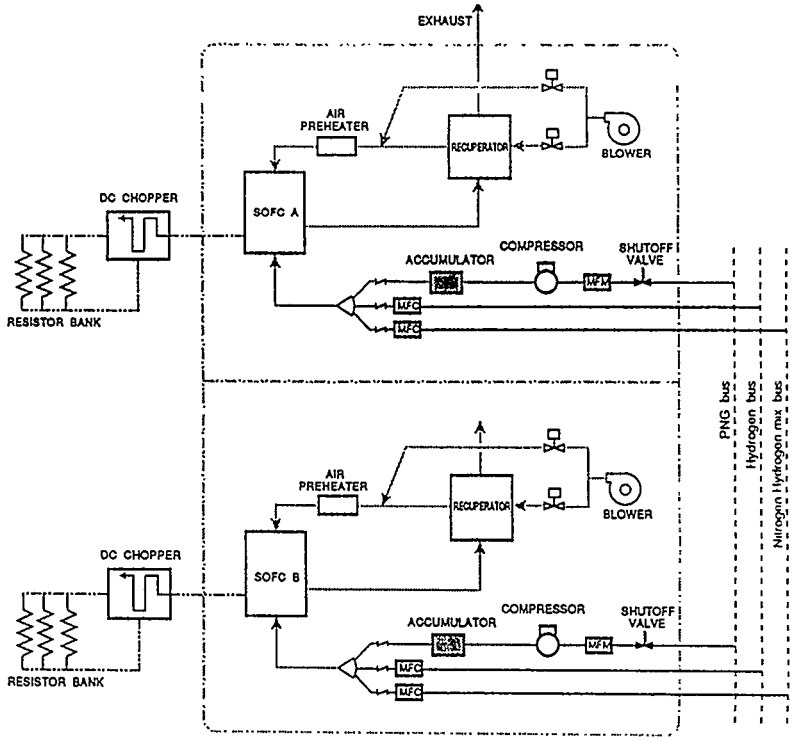


**Figure 4. Flow Schematic for The UTILITIES' 25 kW SOFC System**

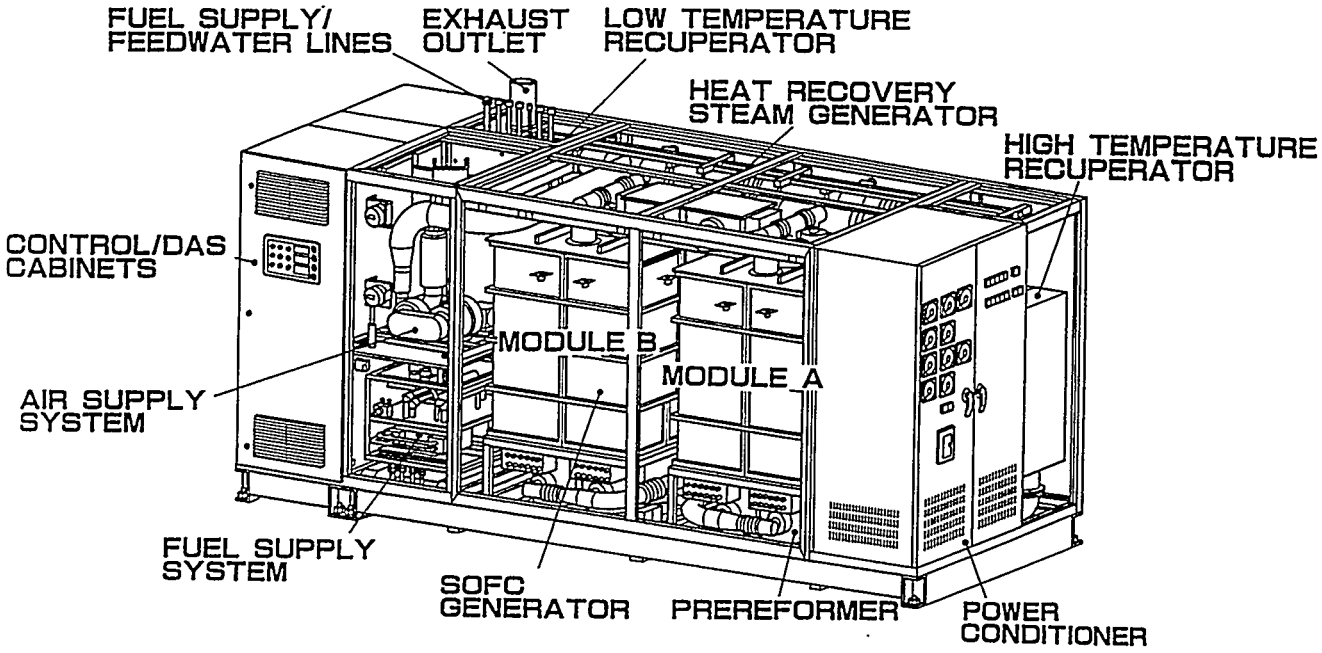


**Figure 5. 25 kW SOFC Cogeneration System**

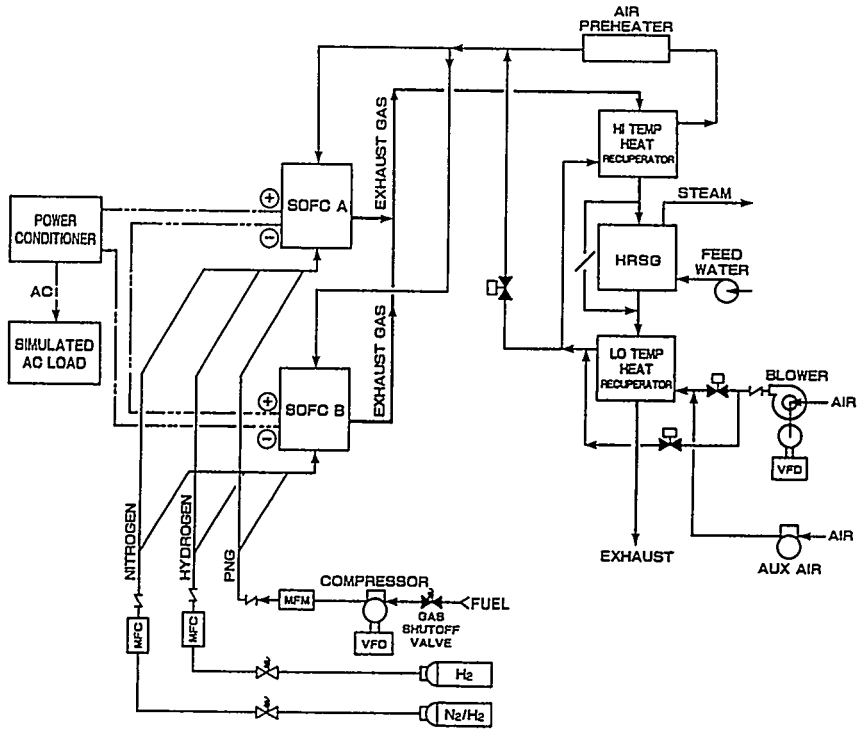


**Figure 6. Flow Schematic for 25 kW SOFC Cogeneration System**

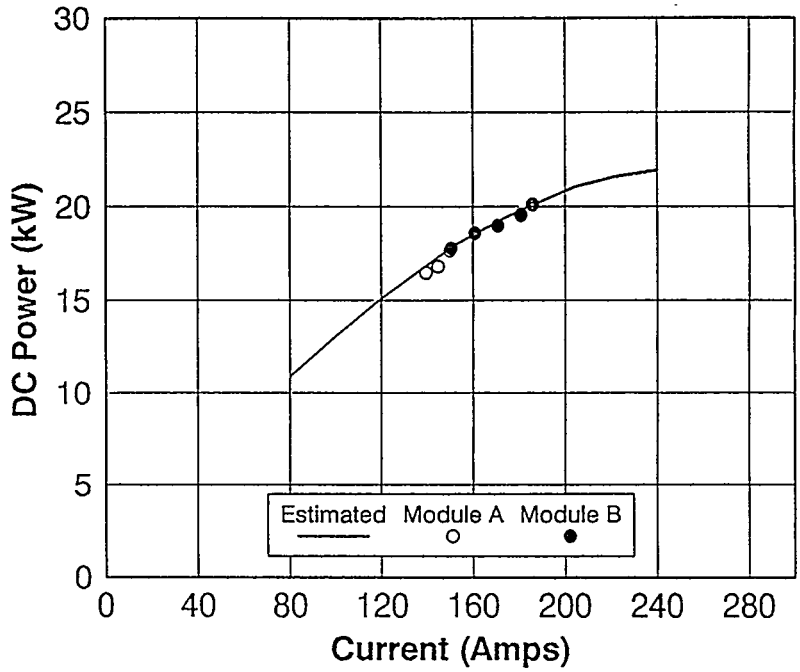


**Figure 7. DC Power vs. Current for The UTILITIES' System**

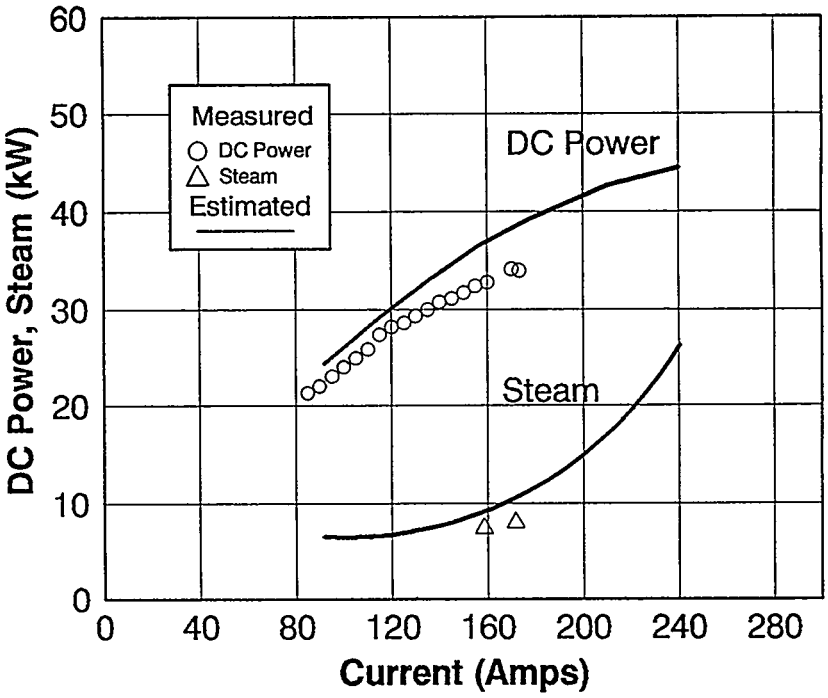


**Figure 8. DC and Steam Power vs. Current for the JGU System**

## 2.4 Contaminant Effects in Solid Oxide Fuel Cells

CONTRACT INFORMATION

| | |
|---|---|
| Contract Number | DE-AC21-89MC26355 |
| Contractor | Westinghouse Electric Corporation<br>Science and Technology Center<br>1310 Beulah Road<br>Pittsburgh, PA 15235-5098<br>(412) 256-2020 |
| Contractor Project Manager | Emerson R. Ray |
| Principal Investigator | Nicholas J. Maskalick |
| METC Project Manager | Diane Hooie |
| Period of Performance | June 1992 to June 1993 |

Schedule and Milestones

**Program Schedule**

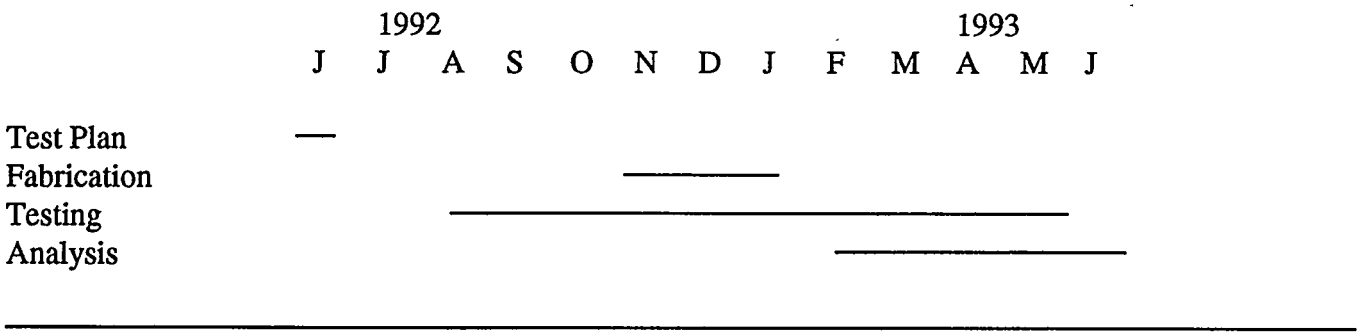


## OBJECTIVES

One objective of this study is to identify the long-term tolerance of solid oxide fuel cells (SOFC) to coal-derived fuel gas containing a mixture of three impurities: hydrogen sulfide ($H_2S$), hydrogen chloride (HCl) and ammonia ($NH_3$), with the SOFC operating at 350 mA/cm$^2$. Another objective is to learn whether the performance at 1000$^o$C of the SOFC at 350 mA/cm$^2$ would be affected by contact with silica ($SiO_2$), carried over as a hydrate. A third objective is to evaluate the effect on SOFC performance of zinc (Zn) impurity in coal-derived fuel gas, with and without HCl as a companion impurity. Post-test analyses are carried out to describe any interaction with the SOFC in terms of structural or chemical changes.

## BACKGROUND INFORMATION

These tests, which provide a basis for estimating the effects of operating the SOFC in the presence of specific amounts of the coal gas impurities $NH_3$, HCl, $H_2S$, $SiO_2$, and Zn, significantly relate to the Fossil Energy Program by:

- Providing information and guidance toward SOFC materials and designs that adapt best to coal gas impurities.
- Contributing to the development of an efficient and environmentally acceptable SOFC power generation system by establishing coal gas clean-up criteria for system engineering.

## PROJECT DESCRIPTION

Full-scale present-technology SOFCs are operated at 1000°C and 350 mA/cm$^2$, to demonstrate performance in fuel gas containing various coal-derived impurities. This report details testing of the effect of three impurities in combination: $NH_3$, HCl, and $H_2S$; and also the effects of the single impurities $SiO_2$ and Zn.

Table 1 fuel comprises the product gas composition obtained from a Texaco Entrained-Bed oxygen-blown coal gasifier at 413°C after external desulfurization. This fuel is employed in long-term life testing of the three combined impurities. It is also used in the initial tests evaluating $SiO_2$ and Zn as fuel impurities. In other increasingly severe tests involving the single impurity, $SiO_2$, the carryover of $SiO_2$ is enhanced by employing simulated partially reformed natural gas with progressively higher initial $H_2O$ concentrations as shown in Table 2.

**Table 1. Simulated $O_2$-Blown Coal Gas**

| Gas | Mole % |
|---|---|
| CO | 37.2 |
| $H_2$ | 34.1 |
| $CH_4$ | 0.3 |
| $CO_2$ | 14.4 |
| $H_2O$ | 13.2 |
| $N_2$ | 0.8 |

**Table 2. Simulated Natural Gas (Partially Reformed) Mole Fraction**

| Gas | Mole % | |
|---|---|---|
| | Comp. A | Comp. B |
| CO | 15.7 | 28.4 |
| $H_2$ | 36.2 | -- |
| $CH_4$ | 3.3 | 11.6 |
| $CO_2$ | 18.6 | 2.9 |
| $H_2O$ | 26.2 | 56.7 |

Time on test, Comp. A = 900 hours
Time on test, Comp. B = 2100 hours

Upon completion of testing, cells are examined in detail for evidence of physical or chemical damage. Experimental specifics of electrical testing and the theoretical basis of data interpretation are given in the Proceedings of the Third Annual Fuel Cells Contractors Meeting, pp. 109, 110.

## RESULTS

### Extended Testing (~5,000 hours) With $NH_3$, HCl, and $H_2S$ Impurities

Two full scale (50-cm length) SOFCs, each representative of generator cells in the field, were electrically connected in series; then operated at 1000°C and 350 mA/cm$^2$. An initial run of approximately 600 hours, including four thermal cycles to room temperature, served to establish base-line performance in 89% $H_2$, 11% $H_2O$ fuel

at 85% fuel utilization and 4 stoichs, air. Then, for approximately 70 hours, a similar base-line was established for operation in simulated coal gas fuel (Table 1). Finally, the three fuel impurity components were added. The cumulative effect on performance after ~300h is shown in Table 3.

These data reveal no strong association of cell resistance with cell performance change in the cases of $NH_3$ and HCl. When $H_2S$ is added, a rapid voltage decline occurs followed by a more moderate decline. Resistance increases account for a minor part of the 0.005V decline observed for each cell over the first 300 hours (Figure 1).

However, cell resistances after approximately 1000 hours change more rapidly, along with linearly declining voltages. In this latter phase, resistance accounts for a major part of each observed cell voltage decline. Table 3 shows these declines to be similar for each of the two cells. Figure 2 continues the performance curve begun in Figure 1. This figure also shows recovery, with HCl and $NH_3$, but without $H_2S$ for two extended periods of ~1100 and ~350 hours, followed by return to the original trend line when $H_2S$ flow is resumed.

**Overall Performance Loss with $NH_3$, HCl, and $H_2S$**

A good estimate of degradation attributable to impurity exposure in this test is given by examination of the resistance trend lines. Experience shows that these trends lines tend to remain relatively constant over periods of time typified by this experiment.

- The rates of resistance increase found are similar to those in cells operating on fuel gas without added impurities.
- $NH_3$, HCl and $H_2S$ do not cause significant resistance increases.
- $H_2S$ at 0.1 ppm is responsible for recoverable voltage losses experienced by this particular cell design but does not affect the rate of voltage degradation.
- The three impurities employed do not affect the running voltage to a degree that can be established by this test. These two cells show performance trends within the range exhibited by similar cells which have been shown to be capable of sustained operation, on "clean" fuel, for 38,000 hours.

**Table 3. Effect of Three Impurities on SOFC Operation at 1000°C and 350 mA/cm$^2$**

| Initial (300 hour) Voltage Drop (V) | | Long-Term V vs. t Trend Line (ΔV/1000 hrs) | | ΔV Due to Cell Resistance Index Change (ΔV/1000 hrs) | |
|---|---|---|---|---|---|
| Cell #1 | Cell #2 | Cell #1 | Cell #2 | Cell #1 | Cell #2 |
| 0.005 | 0.005 | 0.009 | 0.009 | 0.005 | 0.005 |

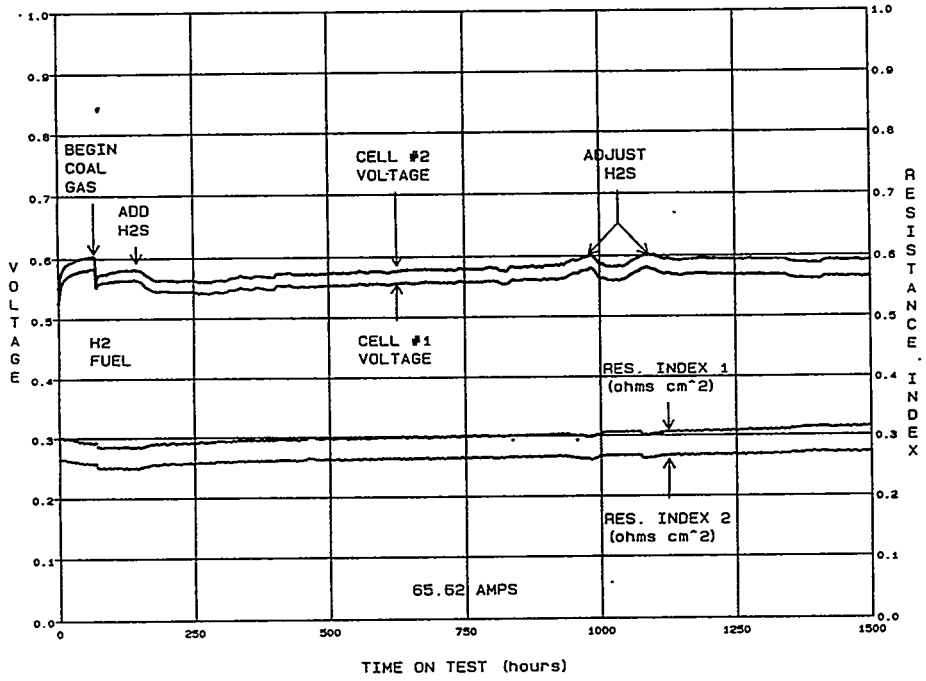


**Figure 1. The effect of $NH_3$, HCl, and $H_2S$ on initial performance of SOFC.**

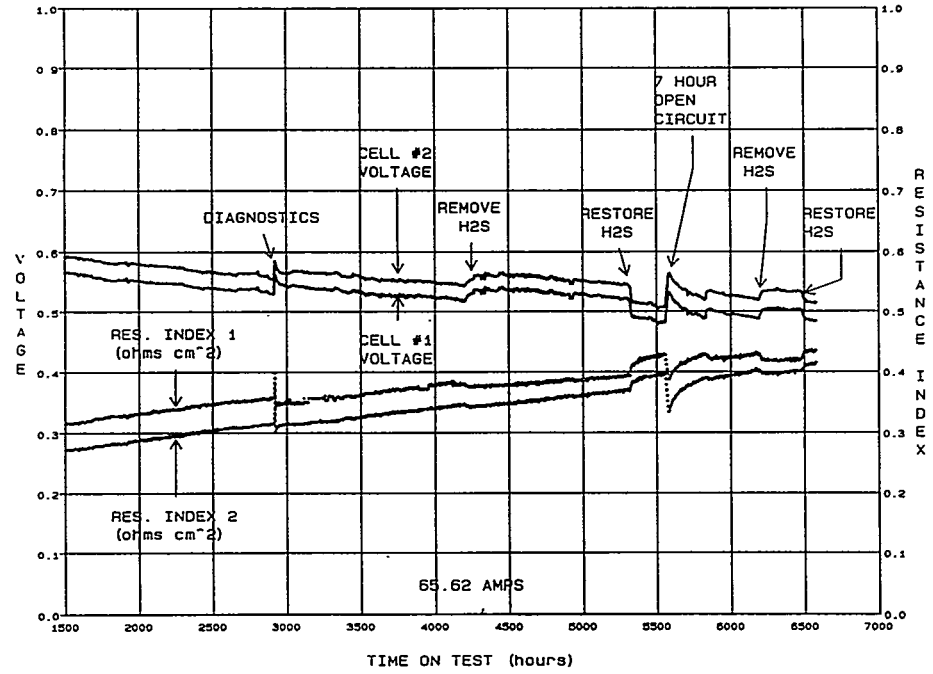


**Figure 2. The effect of $NH_3$, HCl and $H_2S$ on continued performance of SOFC.**

## SOFC Testing at 1000°C and 350 mA/cm$^2$ With Silica Impurity

Two full-scale (50 cm length) SOFCs show near-normal performance after approximately 2400 hours exposure to simulated coal gas (Table 1) contaminated with silica by permeation through a fixture held at 850-950°C; composed of "Duraboard", a porous material composed of 74% $Al_2O_3$ and 26% $SiO_2$. Some accumulation of silicon observed on exposed nickel in the fuel electrode (Figure 3) was insufficient to cause appreciable degradation.

## SOFC Testing at 1000°C and 350 mA/cm$^2$ Using Simulated Partially Reformed Natural Gas

A test employing fuel compositions simulating partially reformed natural gas investigated the effect of increasing $H_2O$ levels on silica transport. This test differs from the prior run with respect to the composition of the fuel permeating the "Duraboard". These experiments employ the two gas compositions and exposure times described in Table 2.

The accumulation of silicon (presumed to be silica) on the fuel electrode at 1000°C, 350 mA/cm$^2$, and 85% fuel utilization is shown in Figure 3. Protracted attempts to determine the type and degree of silica deposition resulted in only minor evidence of silica deposition.

Even though this test was longer (3000 hours versus 2400 hours) and employed higher $H_2O$ content in the inlet fuel, extensive electron beam microanalyses showed that silica deposited only in scattered places.

## Silica Carryover as a Fuel Contaminant

Silica transport may occur when the fuel contacts the silica present in the Duraboard fixture through which the fuel flows:

$$SiO_2(s) + 2H_2O(g) \rightarrow Si(OH)_4(g) \qquad (1)$$

As the $CH_4$ component in the fuel reforms farther downstream to CO and $H_2$, water is consumed:

$$CH_4 + nH_2O \rightarrow CO + 3H_2 + (n\text{-}1)\,H_2O \qquad (2)$$

which favors reversal of reaction (1):

$$Si(OH)_4(g) \rightarrow SiO_2(s) + 2H_2O(g) \qquad (3)$$

causing silica, $SiO_2(s)$ to deposit farther downstream; possibly on exposed nickel surfaces of the SOFC fuel electrode (Figure 3).

Coverage of nickel by silica would impede transport of $H_2$ fuel and decrease loaded voltage. Pore blockage has not been observed, but if it occurs, it will cause an increase in slow polarization due to counter diffusion of products and fuel.

Longer-term tests are required to determine if this effect is significant. In summary, contamination by silica to the degree that cell performance would be affected does not appear to be a concern, at least under conditions of these tests.

## SOFC Testing at 1000°C and 350 mA/cm$^2$ Using Coal-Derived Fuel Gas with Zinc Impurity

Two 50-cm length SOFCs were exposed to zinc contamination from an in-line zinc oxide (ZnO) bed placed immediately upstream of the cells and held at increasing temperature levels, up to 675°C. Except for initial voltage losses, the cells behaved normally for ~2800 hours (Figure 4) after an interruption to calibrate flowmeters.

Then, one cell was removed for destructive examination; the other cell was continued on test for ~1400 hours additional, showing the same trend lines, as before (Figure 5). HCl was then added to the Zr-containing fuel (Figure 6) for a final 200 hours. In an attempt to enhance the zinc transport without HCl, the test run described in Figure 4 consumed 0.67 gm ZnO. The follow-on tests (Figure 6) wherein HCl was added, consumed ~3.34 gm ZnO. Cell performance appeared to be unaffected over the test duration.

Electron beam microanalyses were completed on both samples. No zinc was detected.

Backscattered electrons.
Arrows indicate silicon-rich areas.

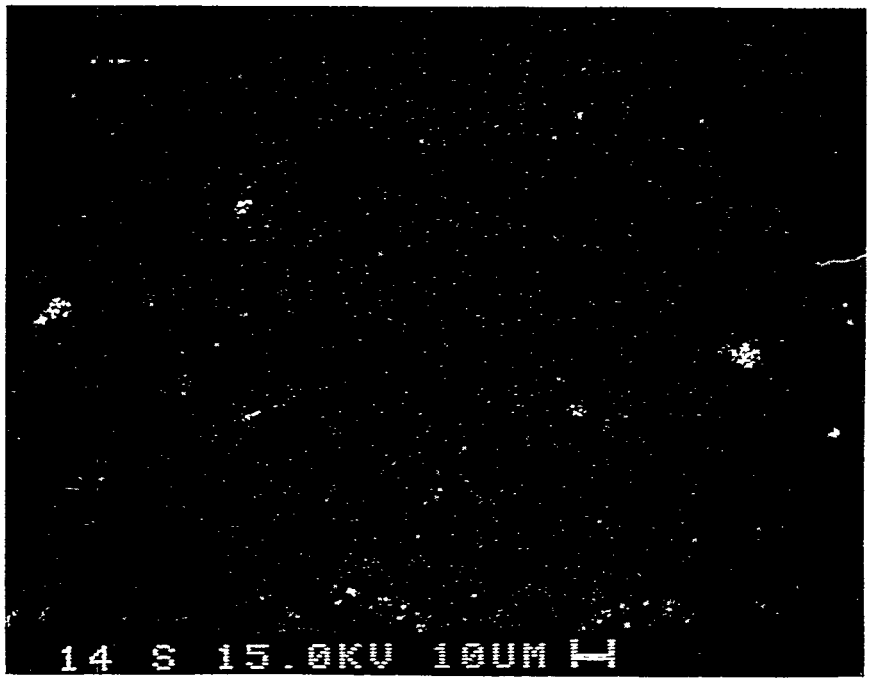


Silicon element map of area shown above.

**Figure 3a. Comparison of silicon-rich areas in nickel network of SOFC fuel electrode operated for 2400 hours in simulated coal gas (Table 1).**

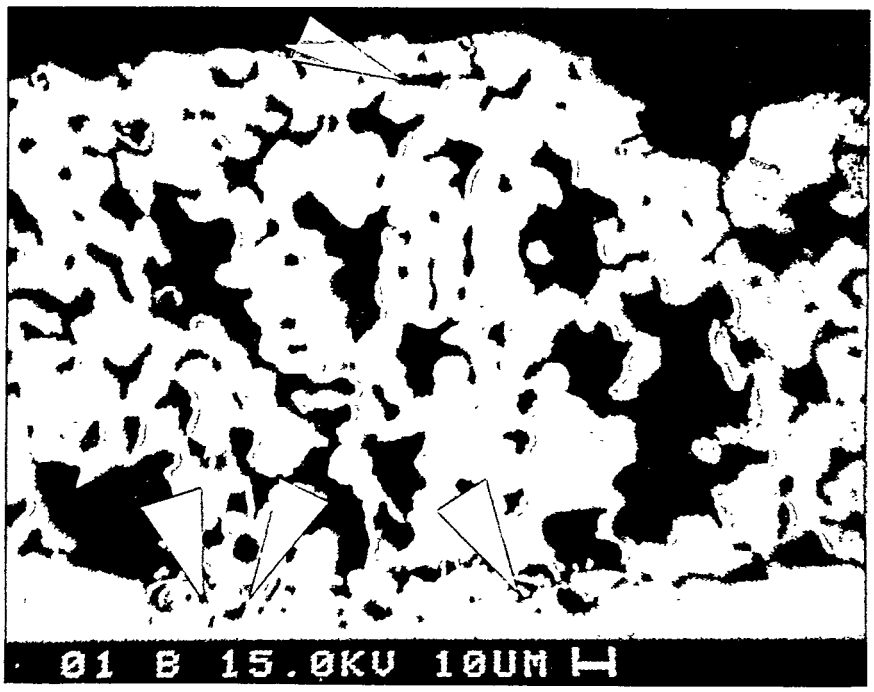


Backscattered electrons.
Arrows indicate silicon-rich areas.

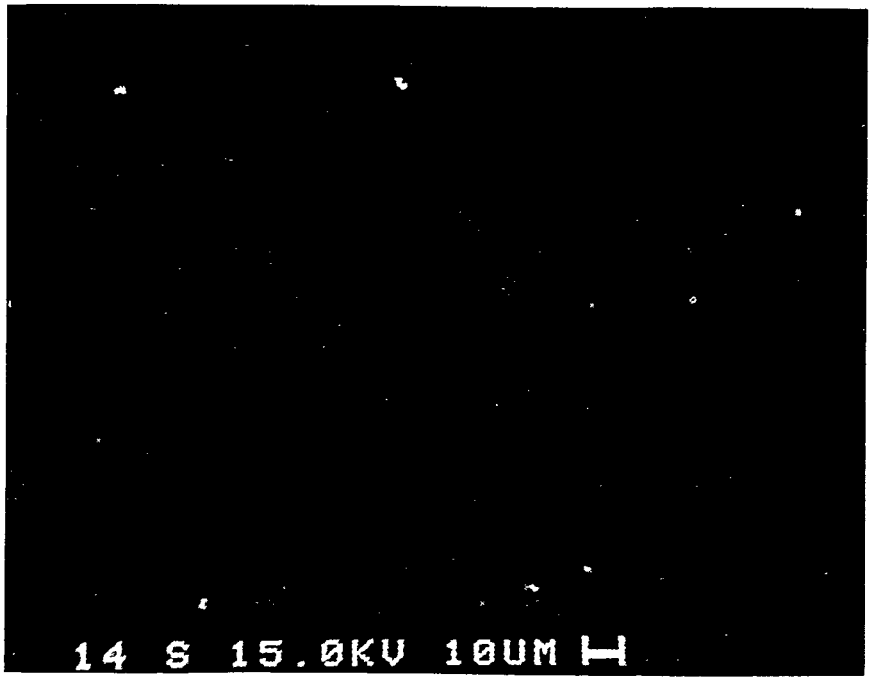


Silicon element map of area shown above.

**Figure 3b. Comparison of silicon-rich areas in nickel network of SOFC fuel electrode operated for 3000 hours in reformed natural gas (Table 2).**

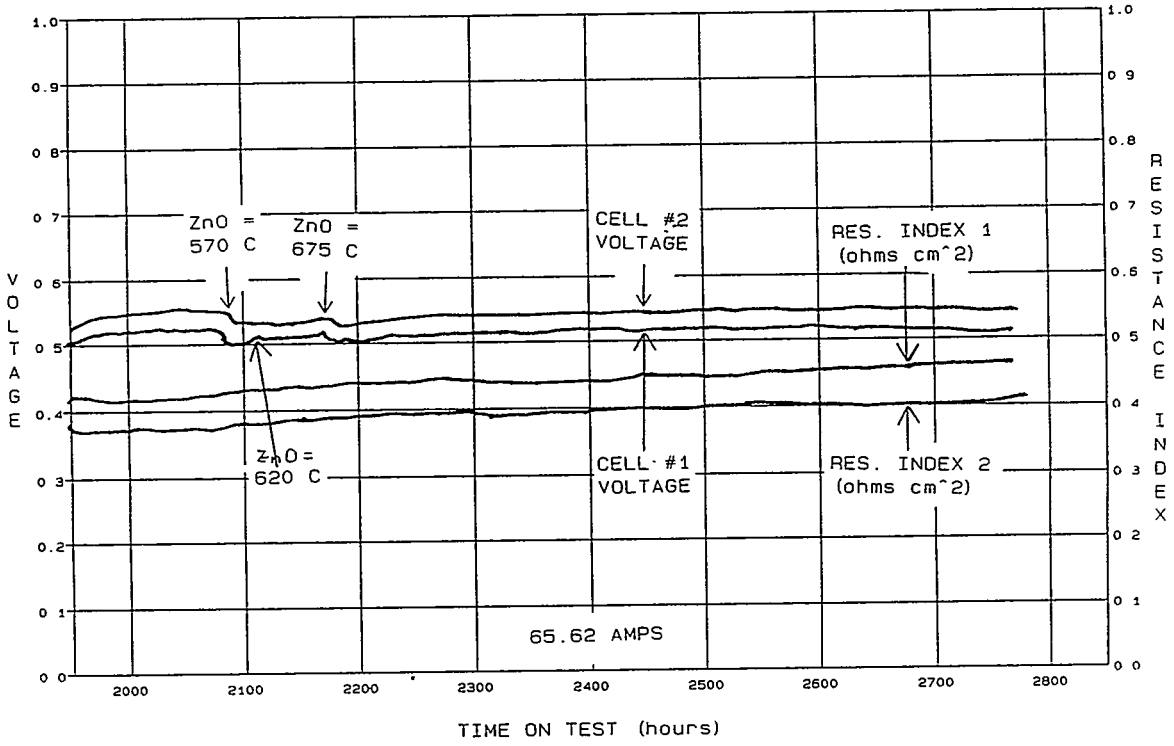


**Figure 4. The effect of Zn on SOFC performance. (continuation of prior 1950 hr run).**

## CONCLUSIONS

1) Ammonia impurity up to 5000 ppm in simulated coal gas does not present a measurable contribution to SOFC voltage degradation over approximately 6500 hours of testing. As testing time increases, $NH_3$ contaminant effects are expected to be nil.

2) HCl impurity at 1 ppm in simulated coal gas does not have a detectable effect on SOFC performance up to 6500 hours under the stated test conditions.

3) $H_2S$ impurity at 0.1 ppm in simulated coal gas fuel can be tolerated by state-of-the-art SOFCs, along with 5000 ppm $NH_3$ and 1 ppm HCl with no measurable non-recoverable voltage degradation over at least 5000 hours.

4) Silica impurity in coal gas can be carried over to the SOFC and deposited. The carryover is not perceptibly enhanced by up to 56% $H_2O$ content in the fuel. Silica is not expected to have a major effect on SOFC performance.

5) Zinc vapor impurity in coal gas, as generated over heated ZnO, may be carried over to the SOFC, but does not deposit. The carryover may be enhanced by HCl.

## FUTURE WORK

Continue a program to identify the long-term tolerance of the SOFC to simulated coal gas containing a mixture of the five impurities: $NH_3$, 5000 ppm, HCl, 1 ppm, and $H_2S$, 0.1 ppm, $SiO_2$ and Zn, with the latter impurities provided by in-line heated beds of $SiO_2$ and ZnO.

Initiate testing of SOFCs with modified fuel electrode materials or processes that may increase the $H_2S$ tolerance.

Initiate testing to identify short-term tolerance of the SOFC to other selected individual coal gas impurities. These other contaminants, including iron (Fe), aluminum (Al), potassium (K), and calcium (Ca) will be eventually included in a multi-impurity long-term test along with $NH_3$, HCl, and $H_2S$, $SiO_2$ and Zn.

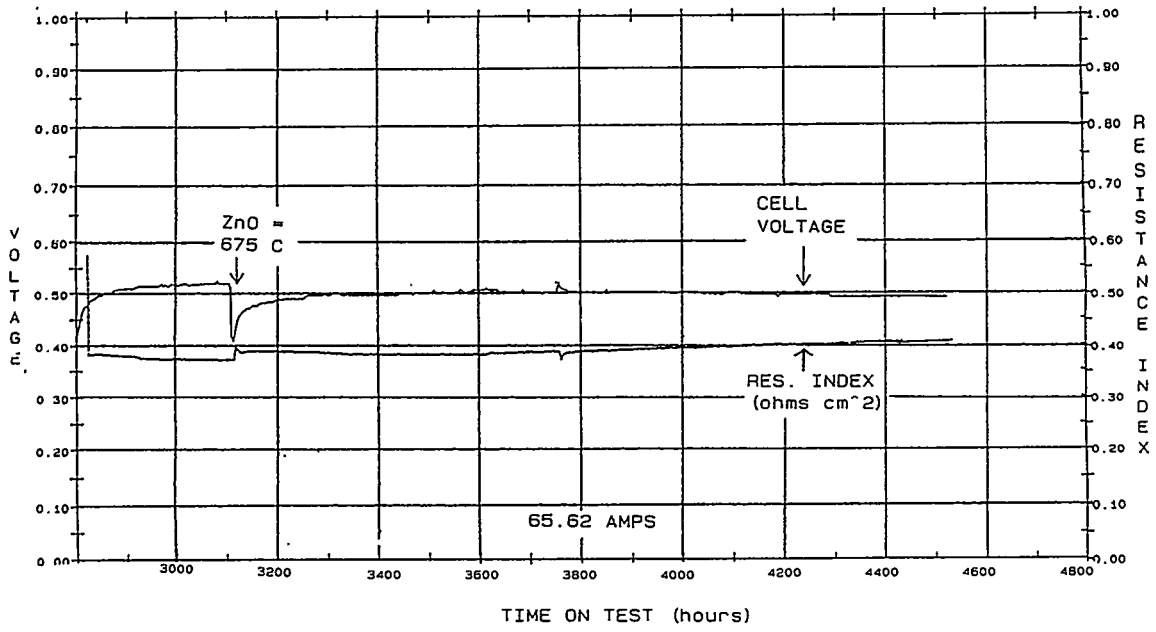


**Figure 5. The continued effect of Zn on performance of one SOFC.**

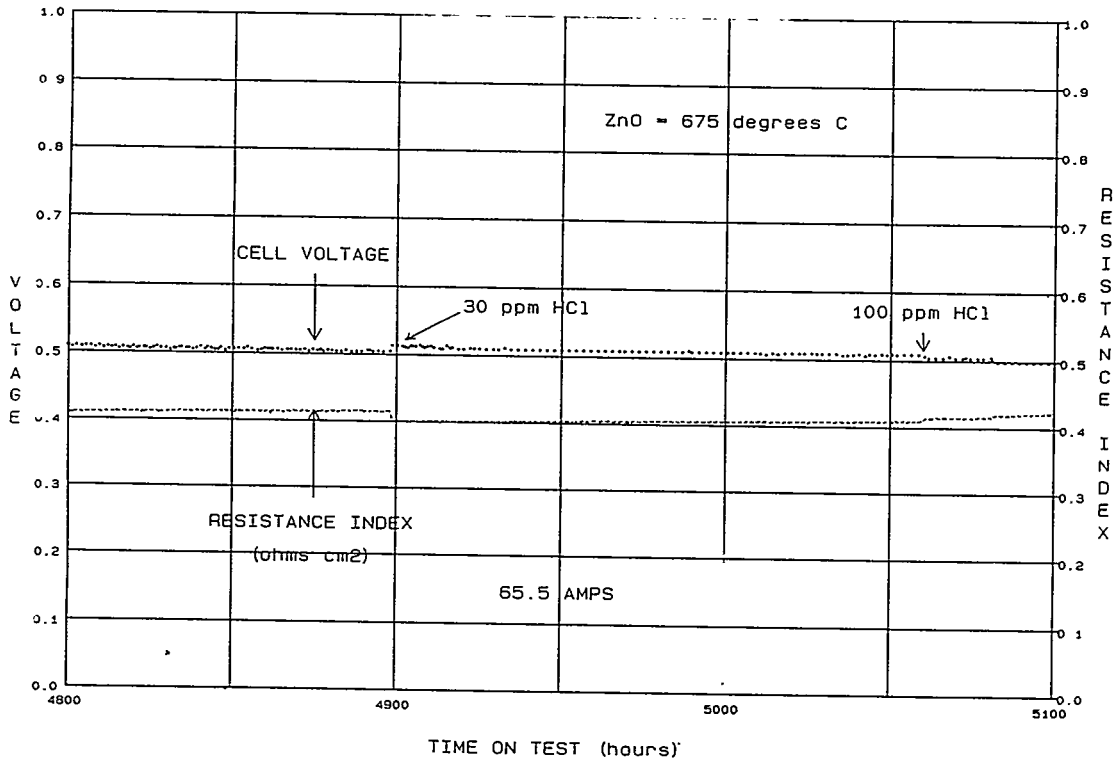


**Figure 6. The effect of Zn and HCl on SOFC performance.**

# Commercialization of Fuel Cells in the 21st Century

R. A. Figueroa
San Diego Gas & Electric
Presented at
Department of Energy
Morgantown Energy Technology Center
Advanced Turbine Systems and Fuel Cells Review Meeting
Commercialization of Fuel Cells Panel
August 5, 1993

## FUTURE GENERATION SCENARIO

Commercialization activities for fuel cell technology in general focus on today's guidelines of utility operation. That is meeting the repowering needs of tomorrow based on today's planning methods and guidelines. If we look at the year 2000, the utility industry may consist of a different type of organization and operation. One may expect to see the following advertisement in the local News Paper in New Jersey:

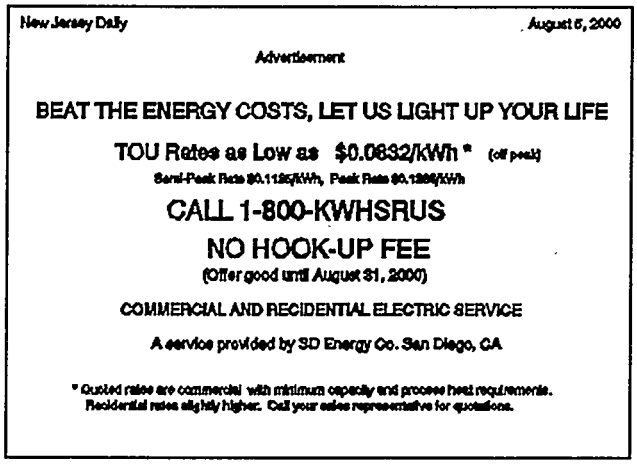
New Jersey Daily August 6, 2000

Advertisement

BEAT THE ENERGY COSTS, LET US LIGHT UP YOUR LIFE

TOU Rates as Low as $0.0632/KWh * (off peak)

Semi-Peak Rate $0.1135/KWh, Peak Rate $0.1366/KWh

CALL 1-800-KWHSRUS

NO HOOK-UP FEE

(Offer good until August 31, 2000)

COMMERCIAL AND RECIDENTIAL ELECTRIC SERVICE

A service provided by SD Energy Co. San Diego, CA

* Quoted rates are commercial with minimum capacity and process heat requirements. Residential rates slightly higher. Call your sales representative for quotations.

How does this relate to commercialization of fuel cells ? The utilities of the future may be very different from what we know today. The industry may undergo deregulation much like the telephone companies did thus, enabling power companies to compete across service areas and state lines. Under a deregulated environment a generation company could sell bulk power to transmission and distribution companies (DISCOS) as well as direct sales to customers in NJ, CO, AZ or wherever. The planning process for a generation company of the future is likely to use different criteria and methods.

Whatever the case may be however, whether a generation company is regulated or not the criteria for selecting generation technology is likely to be very similar to today's environment. This criteria for generation technology will be assessed on economic and external factors such as: first cost, operation and maintenance cost, modularity, reliability, short lead time, environmentally acceptable, high efficiency, etc.

## FUTURE UTILITY PERSPECTIVE

Will the utility of the future be based on the concept of distributed generation ? This concept has not clearly been defined as a benefit or detriment. The benefits of distributed generation may very well be utility specific and probably in a limited application. A number of studies are being conducted to evaluate the economic, operation, and system

benefits of distributed generation which could be an entry market for fuel cells.

Although environmental restrictions may be the single most valuable benefit for the commercialization of fuel cells, the issues of reliability, performance and cost are and will be significant drivers. Also, today's conventional materials for high temperature management lack the density required for compacting the technology. This presents an opportunity for technology transfer from the aerospace program to the fuel cell program. I don't propose or imply that DOE or DOD program funds be allocated in any way, but simply to explore opportunities of using space age technology to help the compacting of high temperature fuel cell technology.

For example, the space shuttle has glued tiles, which protect the fuselage from the heat generated at re-entry. Perhaps this or similar type of technology would help the heat management in fuel cells.

## ECONOMIC CHALLENGES

In today's environment as a learning tool a fuel cell with costs of $2,000/kW is likely to be acceptable to some utilities. Niche markets may develop in the customer site generation and transportation for technology less than 2MW. To penetrate the market of greater than 2MW however, fuel cell technology will compete with other available generation systems such as combustion turbines, which will present significant economic challenges.

In developing cost and commercialization schedules projections, fuel cell suppliers need to look carefully at their business plans and double check market projections. Ambitious statements resulting in significant delays on delivery, performance, and cost milestones is likely to have a negative effect on entry markets.

Suppliers of fuel cells have stated that material costs and volume are the key roadblocks to commercialization. My personal belief however, is that these roadblocks include stack manufacturing process, and stack and balance of plant (BOP) design issues. I feel that development of BOP is being underestimated by suppliers and this is an area that members of commercialization teams need to focus on.

## SUMMARY

Fuel cell suppliers face economic and technical challenges in a competitive power generation market. It is likely that a subsidy (in the form of tax deductions, government assisted programs to buy down the cost of materials, etc.) will be needed to ensure economic competitiveness in the 2000 time-frame.

Technology transfer from aerospace program may hold the key to breaking through some technical roadblocks in fuel cell technology. Therefore, DOE and DOD efforts in this area should be pursued.

# Poster Session

## *Heat Engines and Fuel Cells*

## P1 Particulate Control for Coal-Fueled Diesel Engine Exhaust

CONTRACT INFORMATION

| | |
|---|---|
| Contract Number | DE-FG02-91ER81187 |
| Contractor | LSR Technologies, Inc.<br>898 Main Street<br>Acton, MA 01720<br>(508) 635-0123 |
| Contract Project Manager | Dr. Leo A. Smolensky |
| Principal Investigators | Dr. Leo A. Smolensky<br>Dr. Bruce H. Easom |
| METC Project Manager | Mr. William C. Smith |
| Period of Performance | September 7, 1991 - July 5, 1994 |

Program Schedule

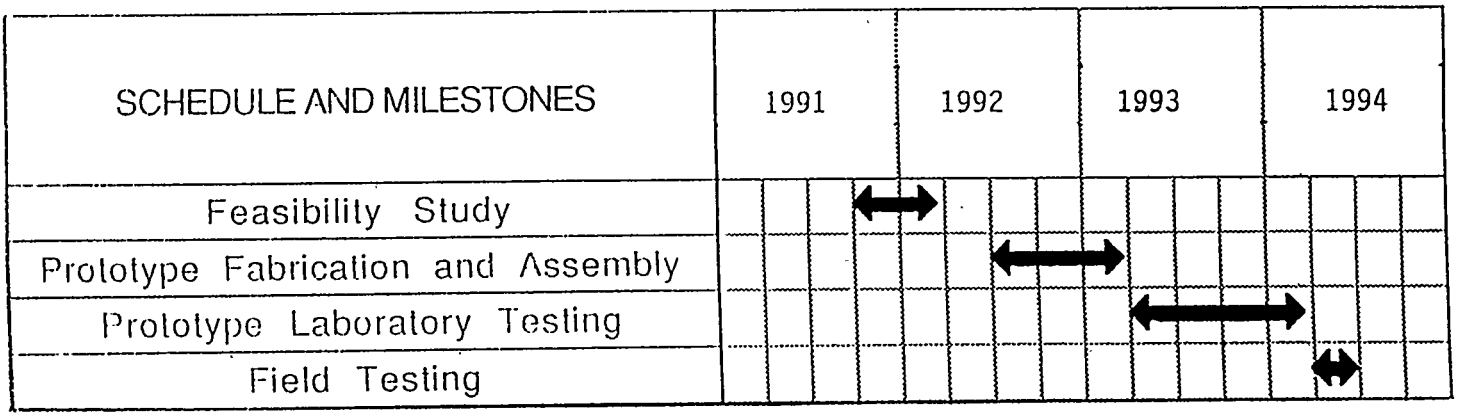

## OBJECTIVES

The overall goal of the program is to develop a viable control device for removing particulates from coal-fueled diesel engine exhaust. The separation concept utilizes the basic principles of the *Core Separator*, a mechanical particulate collector recently developed for treating low temperature flue gases. Specific performance and design goals of this control device are as follows:

- Collect up to 98% of Coal-Fueled Diesel particulates, if required
- Collect essentially all particles 5 μm and larger, if required
- Provide less than 10.0 inches (WC) total system pressure drop

## BACKGROUND INFORMATION

In this program, a high-temperature *Core Separator* system will be developed as a particulate control device for coal-fueled diesel engine exhaust. The *Core Separator* is a unique concept, which has been conceived and patented by LSR as a low-temperature mechanical collector. Several *Core Separator* configurations were tested at low temperatures in 1989 - 1991 within the scope of an SBIR program with the Department of Energy, Pittsburgh Energy Technology Center, and a contract with the Electric Power Research Institute. The device has the ability to extract fine particulates from gas streams and its performance significantly exceeds conventional cyclonic collectors. The *Core Separator* as a low-temperature mechanical collector is able to remove a substantial amount of submicron particles from flue gas and essentially all particles larger than 2 - 3 microns in diameter. In this regard, it is comparable to a medium efficiency electrostatic precipitator. Yet, the *Core Separator* retains most of the advantages of mechanical collectors, such as simplicity, self-cleaning ability, reliability, ability to handle high solids concentration, low capital and maintenance cost, etc.

The low-temperature *Core Separator* has already attracted considerable interest in industry. The technology was demonstrated at low temperature through several field prototypes, and more recently through commercial unit sales. It has been used to perform some difficult industrial separations, including minerals, coal flyash, glass, and chemical recovery processes.

## PROJECT DESCRIPTION

The program is being performed in collaboration with Arthur D. Little, Inc., a firm presently under contract to DOE/METC to develop coal-fueled diesel engines along with Cooper-Bessemer.

The program consists of two phases: in Phase I the goal is to conduct feasibility studies while the Phase II effort essentially involves refining the *Core Separator* design and scaling the unit to prototype size. In Phase I and II, both low and high temperature testing was conducted to evaluate several design configurations and characterize performance. Originally, a field experiment was planned at the site of a Coal-Fueled

Diesel Engine. A possible host site is the Cooper-Bessemer engine test facility in Mt. Vernon, Ohio. A full-scale *Core Separator* unit could be installed on the one cylinder test engine, as it is available. The test engine would be fueled with coal-water-slurry (CWS). Presently, this work will depend on the present testing at this site, and the effectiveness of the cyclone collectors in removing particulate matter.

Comparative analysis of different *Core Separator* design configurations is still under investigation. The basic concept of the *Core Separator* system is shown in Figure 1. It consists of three components. The key component is a special type of centrifugal separator, the so-called *Core Separator*. Its core is adjacent to the clean flow outlet and can be viewed as a 'potential flow' region. This region is free of vorticity or secondary flows which cause particle reentrainment. In addition to the *Core Separator*, the system includes two conventional components. One is a solids collector, in this particular case, a conventional cyclone, and the other a fan for flow recirculation.

The *Core Separator* is a cylindrical vessel having one tangential inlet and two outlets at the opposite end of the vessel. It contains an outlet for the clean flow and a second outlet for the recirculating flow. The solids-laden flue gas is introduced through a fan to the inlet of the *Core Separator*. Due to the swirling motion of the flow, solids move to the periphery as the central jet leaving the system through the central outlet is cleaned of particulates. The peripheral flow with most of the particles is exhausted to the cyclone and then recirculates back to the *Core Separator* by means of the fan.

The processes of separation and solids collection are accomplished separately and in different components. The *Core Separator* cleans the flow discharged from the system and detains solids within the system. If the *Core Separator* efficiency is high enough, particles cannot leave the system. They recirculate again and again until the cyclone finally collects them for removal. An analytical formula can be derived that defines the system performance.

$$E = \frac{E_c E_s}{1 - E_s(1 - E_c)},$$

where E, $E_c$, and $E_s$ are the system, collector, and *Core Separator* partial separation efficiencies respectively. Examination of this equation shows that the system efficiency remains high even with poor performance in the collector, as long as the efficiency of the *Core Separator* is high. For example, if $E_s$ is 99% and $E_c$ is 30%, the system efficiency is 96.7%.

## RESULTS

Phase I and several tasks of Phase II are complete, including: design and construction of a laboratory-scale test unit, the design, fabrication, assembling, and shakedown of the prototype-scale *Core Separator* system. Testing the prototype-scale *Core Separator* has been started.

The research has been focused on data analysis and the ability of the system to collect effectively fine particles. Particle separation

efficiency curves were generated as a result of measuring particle concentration and size distribution in the feed and outlet flow streams. A Universal Stack Sampler conforming to EPA Method 5 was used along with a University of Washington Mark 3 and Mark 5 Source Test Cascade Impactor. Fly-ash particles were obtained for use from Public Service Company of Colorado Commanche Station. Solids were introduced to the system through a feeder equipped with an air ejector to break-down loose agglomerates. The mean particle size diameter was 9.6 μm and the dust concentration was in the range of 1 - 30 grains/SCF.

In Phase I, twenty-four (24) test points were completed under ambient temperature conditions. The collection efficiency of the *Core Separator* ranged from a low of 94% to well above 99% over a given range of bleed flow rates. Under typical bleed flow conditions, 98% efficiency could be achieved. The cut point diameter ($d_{50}$) was determined to be well below 1.0 micron for the *Core Separator*, which is far better than the best high efficiency cyclones. In addition to this data, six high temperature test points were obtained at 1000 - 1050 °F. The collection efficiency under these conditions ranged from 93% to 98%. The separation efficiency at high temperature for a given bleed flow is lower than at ambient temperature, which is expected from the dynamic viscosity effect at elevated temperature.

The most challenging and ambitious goals of the Phase I research were to achieve at ambient temperature 95% collection efficiency at 1.0 μm and 50% at 0.1 μm. The research demonstrated that this level of performance can be obtained, if required. The pressure losses associated with this performance were approximately 10 inches W.C., which was also a performance goal. Dust concentrations of up to 30 gr/SCF were introduced to the system without operating difficulties.

In Phase II, the prototype-scale system comprising several *Core Separators* was constructed as shown in Figure 2. Recent test results have shown that this system is able to collect all particles larger than 3 μm. Photomicrographs shown in Figure 3 illustrate the size of the inlet ash particulates (A) as well as those penetrating in the clean outlet (B). At the same time, it should be pointed out that this system is quite sensitive to the flow distribution. Maldistribution of flow has been shown to have a significant detrimental effect on the system performance.

At the present time, Arthur D. Little, Inc. and Cooper-Bessemer have been interested in the *Core Separator* as an improvement over the cyclone collector in reducing turbocharger wear. Yet, if the *Core Separator* system can achieve separation efficiencies up to 98%, it would not only protect the turbocharger but also achieve the required NSPS emission level. Commercially-viable, engine-grade, CWS is expected to contain 1 to 2 wt % ash (dry basis). With the demonstrated high engine combustion efficiency (97 to 99% carbon burnout), uncontrolled particulate emissions have been measured at 1 to 3 lb/MM Btu. Achieving the NSPS level of 0.05 lb/MM BTU would require a reduction of the solids concentration by about 95 to 98%. The final

requirements of the *Core Separator* system will be formulated by A. D. Little/Cooper-Bessemer as a result of the field test analysis of the coal-fueled diesel engine.

## FUTURE WORK

Extensive laboratory testing of the prototype-scale *Core Separator* system over a wide range of parametric conditions will be continued over the next twelve months. The test data will be analyzed and the performance predictive model will be verified and calibrated. The program culmination will include testing of the *Core Separator* system with actual diesel exhaust if a test unit is available.

## REFERENCES

1. Benson, C.E., Staudt, J.E., Itse, D.C., Schaub, F., Rao, K. 1991. "Controlling Emissions From Stationary Coal-Fueled Diesel Engines", Proceedings of the Eighth Annual Coal-Fueled Heat Engines and Gas Stream Cleanup Systems Contractors Review Meeting, 449-458. DOE/METC - 91/6122. NTIS/DE91002091. Springfield, VA: National Technical Information Service.

2. Benedek, K.R., Menzies, K.T., Johnson, S.A., Wilson, R.P., Rao, A.K., Schaub, F.S., "Emission Characteristics and Control Technology for Stationary Coal-Fueled Diesel Engines", ASME, Journal of Engineering for Gas Turbines and Power, Vol. 111, pg. 507, July 1989.

3. Smolensky, L.A., Easom, B.H., Lin, Z., Wysk, S.R., "A *Core Separator* System for Fine Particulate Removal", Proceedings of the Eighth Annual Coal Preparation, Utilization, and Environmental Control Contractors Conference, pp. 630 - 637. July 27 - 30, 1991, Pittsburgh, PA.

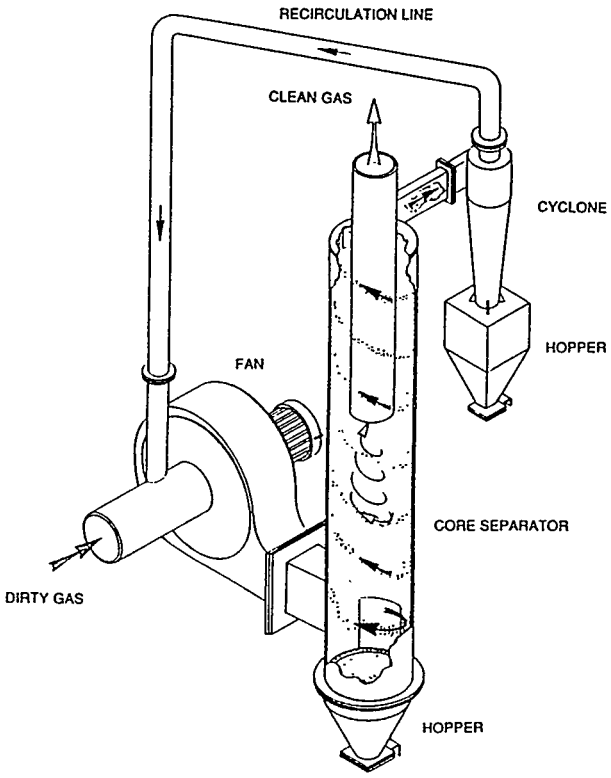


**Figure 1**
***Core Separator***
**Concept**

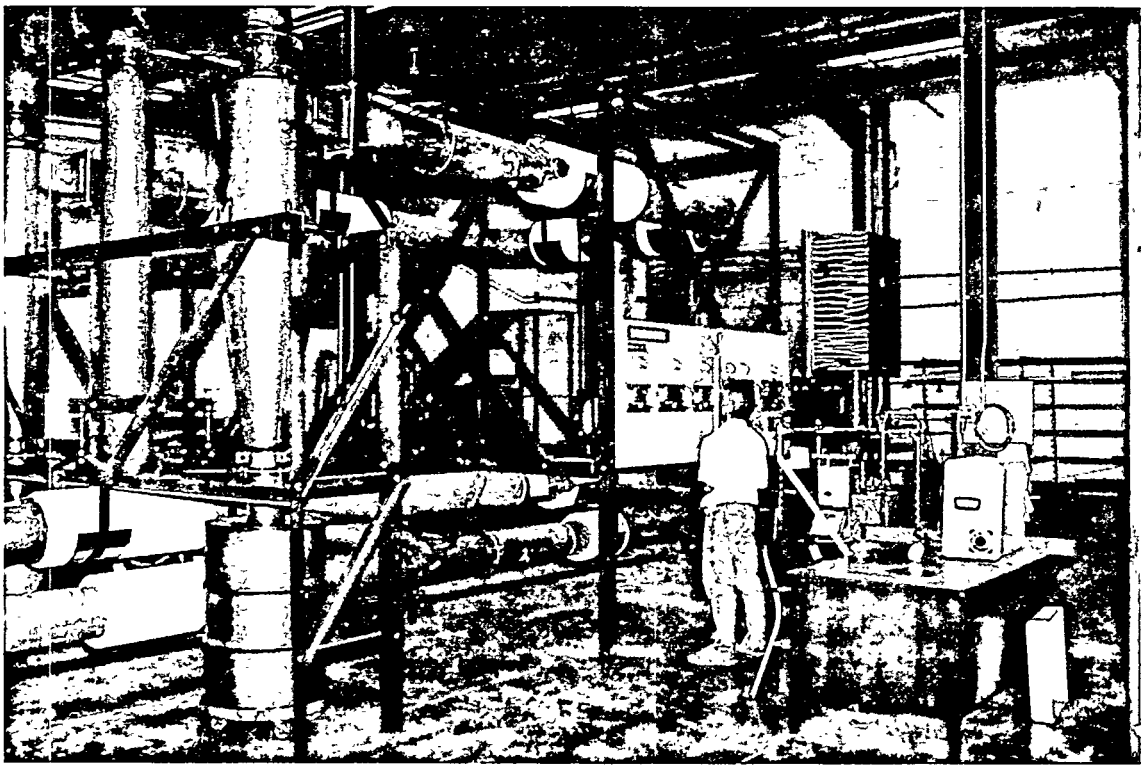

**Figure 2 Prototype Scale *Core Separator* System**

A

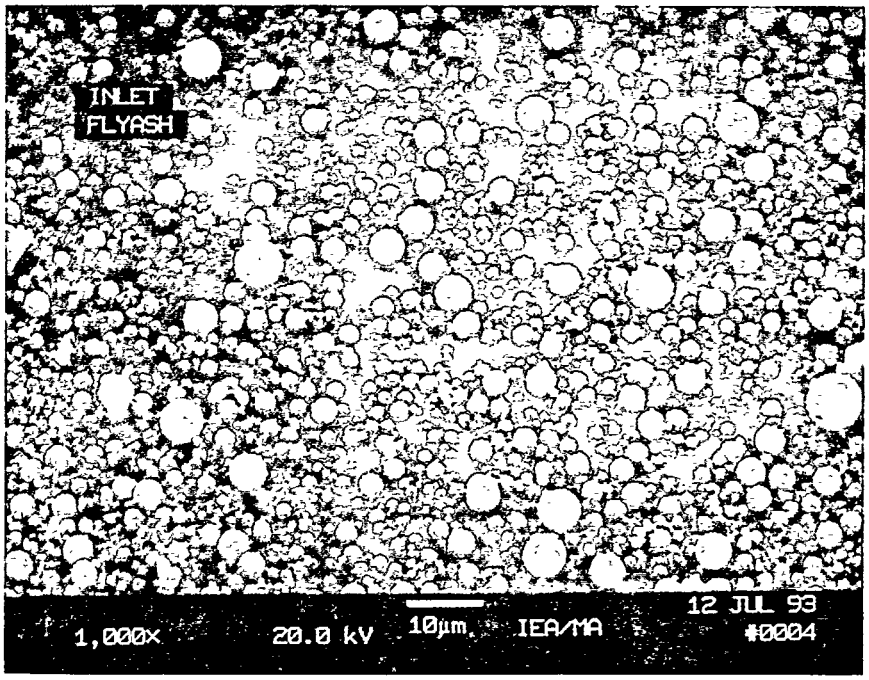


B

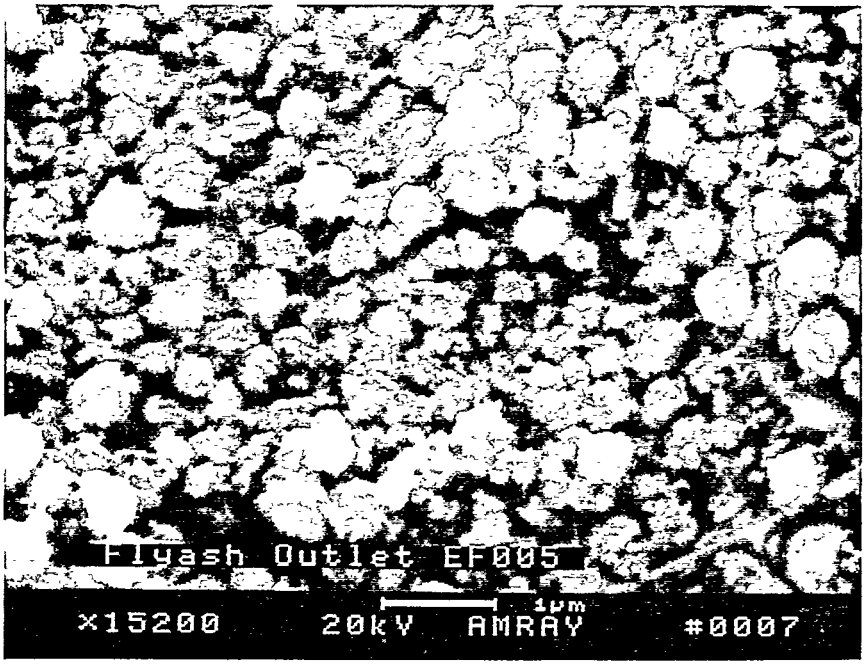


Figure 3. Photomicrographs of Particles Entering (A) and Exiting (B) Prototype-Scale Core Separator System

# P3 Sub-Scale Development of an Acoustically Enhanced Cyclone for PFBC

## CONTRACT INFORMATION

| | |
|---|---|
| **Contract Number** | DE-AC21-88MC25010 |
| **Contractor** | Solar Turbines Incorporated<br>P.O. Box 85375<br>San Diego, CA 92186-5376<br>(619) 544-2321 |
| **Contractor Program Manager** | Marlene A. Galica |
| **Principal Investigator** | Marlene A. Galica |
| **METC Project Manager** | Daniel C. Cicero |
| **Period of Performance** | Sept. 23, 1988 to Jan. 31, 1994 |

## ABSTRACT

Acoustically enhanced cyclone collectors offer the potential of achieving environmental particulate control standards under pressurized fluidized bed combustion conditions without the need for post turbine particulate control. The objective of this research program is to extend acoustic agglomeration technology from the laboratory scale up to the sub-pilot scale. The effects of high intensity sound on the agglomeration of fly ash particles are being investigated in a simulated PFBC effluent stream. The test facility consists of a variable residence time acoustic agglomeration chamber with a vitiating air preheat combustor, an ash injection system utilizing an auger feeder, a natural gas fired pulse combustor sound source, and a two-stage high temperature, high pressure cyclone. Fly ash for these tests has been obtained from the TVA Shawnee Station circulating fluidized bed combustor, as well as the Nucla CFBC, and Tidd AEP. Low frequency acoustic agglomeration tests are underway.

The acoustically enhanced cyclone collector is being evaluated with two distinct goals in mind: 1) determine the effects of the major operating parameters on acoustic agglomeration efficiency, and 2) optimize the agglomeration system performance for maximum particulate removal efficiency. The data obtained during these tests will provide direct information on the effects of sound intensity and frequency, particle residence time, ash loading, and pressure on the enhancement of cyclone collection efficiency with acoustic agglomeration. These data, in conjunction with results from an acoustic agglomeration computer model will be used to evaluate the economic and engineering feasibility of an acoustically enhanced cyclone collector for a full scale pressurized fluidized bed combustor.

# P4 Air Extraction in Gas Turbines Burning Coal-Derived Gas

## CONTRACT INFORMATION

**Contract Number** DE-AC-21-89MC26041

**Contractor**

Clemson University
Sponsored Programs, Administration
Brackett Hall
P.O. Box 345712
Clemson, SC 29634-5712
(803) 656-2424

**Contract Project Manager** Tah-teh Yang

**Principal Investigators**

Tah-teh Yang *
Ajay K. Agrawal
Jayanta S. Kapat

**METC Manager** Leland E. Paulson

**Period of Performance** October 1, 1992, to June 30, 1993

**Schedule and Milestones**

**FY 92-93 Program Schedule**

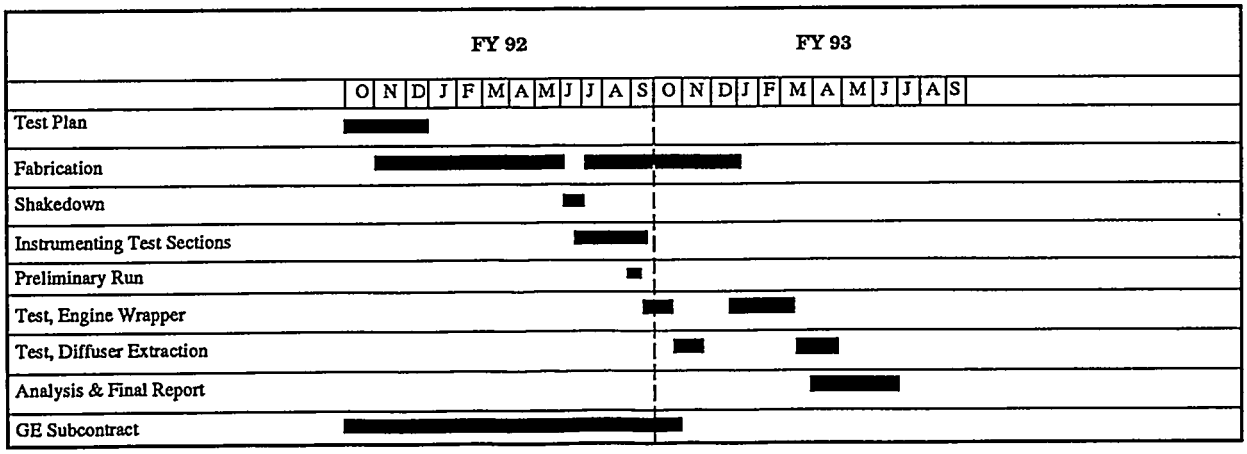


* Present Address:
School of Aerospace and Mechanical Engineering
The University of Oklahoma, Norman, OK 73019-0601

## OBJECTIVES

The primary objective of this study was to determine how extracting compressed air from a heavy-frame gas turbine affects (1) the total pressure loss in the compressor discharge casing (CDC), also referred to as the compressor/combustor pre- and dump diffusers; (2) the airflow distribution around the combustors and transition pieces; and (3) the pressure losses in the extraction manifold.

Another objective of this work was to characterize the flow field in the prediffuser and the dump diffuser for identifying the major pressure loss mechanisms. The final objective was to establish an experimental facility which can be used to assist the U.S. industry in improving the aerodynamic design of nonrotating components of heavy-frame gas turbines.

## BACKGROUND INFORMATION

In the first phase of this contracted research, a comprehensive investigation was performed. Principally, the effort was directed to identify the technical barriers which might exist in integrating the air-blown coal gasification process with a hot gas cleanup scheme and the state-of-the-art, U.S. made, heavy-frame gas turbine. The guiding rule of the integration is to keep the compressor and the expander unchanged if possible. Because of the low-heat content of coal gas and of the need to accommodate air extraction, the combustor and perhaps, the flow region between the compressor exit and the expander inlet might need to be modified.

In selecting a compressed air extraction scheme, one must consider how the scheme affects the air supply to the hot section of the turbine and the total pressure loss in the flow region. Air extraction must preserve effective cooling of the hot components, such as the transition pieces. It must also ensure proper air/fuel mixing in the combustor, hence the combustor exit pattern factor. The overall thermal efficiency of the power plant can be increased by minimizing the total pressure loss in the diffusers associated with the air extraction. Therefore, a study of airflow in the pre- and dump diffusers with and without air extraction would provide information crucial to attaining high-thermal efficiency and to preventing hot spots.

From structural considerations, air extraction at manholes of the engine wrapper might lead to the simplest design. Our concern was the adverse effects of air extraction on the impingement cooling of the transition pieces. An approximated analysis by Yang and Kapat (1991) substantiated that speculation. The research group at Clemson University suggested using a Griffith diffuser for the prediffuser and extracting air from the diffuser inlet. The present research establishes that the analytically identified problems in the impingement cooling flow are factual. This phase of the contracted research substantiates experimentally the advantage of using the Griffith diffuser with air extraction at the diffuser inlet.

## PROJECT DESCRIPTION

A brief description of the gas turbine test facility, developed as part of this experimental program, is given in the following sections.

## Experimental Facility

The major items designed, fabricated and installed for this test facility include (1) a 35% scale test model of a heavy-frame gas turbine to simulate airflow between the compressor discharge and the turbine expander inlet, (2) the main flow system to provide the desired airflow through the test model, (3) the manifold systems to collect a part of the compressor discharge air, and (4) the air extraction flow system to remove the desired airflow from the test model. The test facility also includes instruments and accessories for automated pressure and velocity measurements.

Figure 1 shows a schematic of the test model and the airflow path. In the prototype, the fuel enters the combustor can through several fuel nozzles on the combustor end plate. However, in the present cold flow tests, the room air was induced into the combustor can to simulate the fuel flow. A schematic of the extraction flow system that removed air from the prediffuser inlet is shown in Figure 2. The conical tubes on the manifolds passed between the adjacent combustor/transition piece assemblies. Further details of the flow systems and test model are given by Yang et al. (1992, 1993).

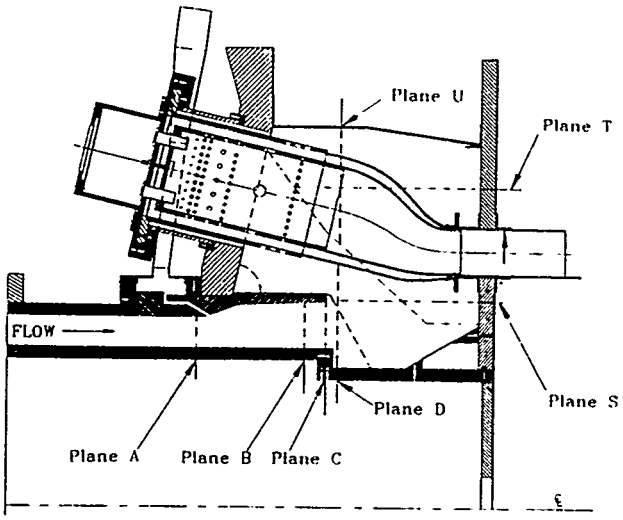


**Figure 1. A Schematic of the Test Model**

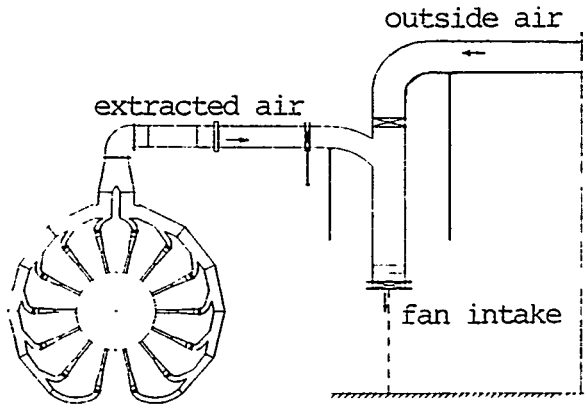


**Figure 2. A Schematic of the Extraction System for Air Removal from the Prediffuser Inlet**

## Computational Procedure

A closely approximated 3-D computational fluid dynamic analysis was performed to supplement the flow description. The airflow path was divided into two computational domains. These two domains share an interface region through which boundary condition data was communicated between the two domains and was updated during the computations.

The body-fitted, curvilinear coordinate system was used to incorporate the geometric details in the computational analysis. Internal solid objects, such as the support struts and the surface of the impingement sleeve, were simulated by blocking flow through grids representing these areas. Figure 3 shows the

computational grid in the two domains on a longitudinal plane between the support struts. The shaded grids in Figure 3 were impervious to the flow. Thus, they represent internal solid objects, such as the impingement sleeve and the transition piece. The computational grid in the lower domain consisted of 62,208 grids: 18 in the circumferential direction, 32 in the radial direction and 108 in the axial direction. The computational grid in the upper domain consisted of 63,648 grids: 18 in the circumferential direction, 52 in the radial direction and 68 in the axial direction.

## Measurement Plan

The experiments were conducted with the straight wall prediffuser and the modified prediffuser referred to as the Griffith diffuser. When the straight wall prediffuser was used, the air was extracted at the turbine wrapper. When the Griffith diffuser was used, the air was extracted at the prediffuser inlet. The maximum flow through the test section was 8,000 CFM, which also refers to the full load.

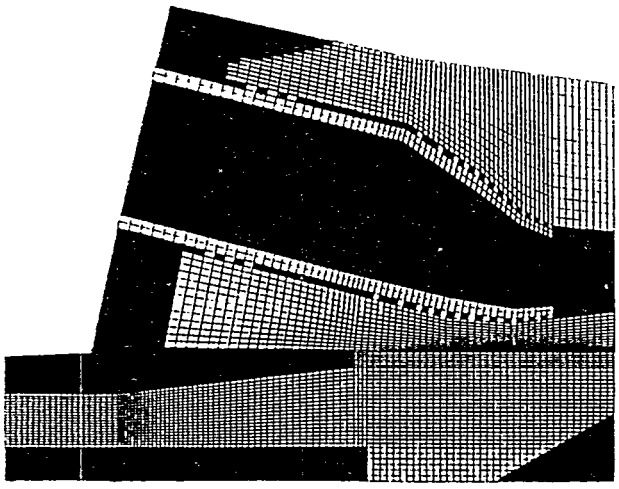

**Figure 3. Computational Grid in the Two Domains (between the Support Struts)**

Four tests with extractions of 0%, 20%, 12%, and 6% of the through flow were considered at 8,000 CFM or the full load. Twenty% air extraction (1,600 CFM) is referred to as the full extraction. Tests were also conducted at partial load, when the flow through the test section was 60% of that in the full-load operation (5,000 CFM). At partial load 3 tests with extractions of 0%, 20% and 12% of the through flow were considered. Thus, a set of 7 tests was conducted for each of the two prediffuser designs resulting in a total of 14 tests. While the pressure throughout the test model was measured for all 14 test runs, the detailed profiles for each of the two prediffusers were obtained only at full load with zero and full extraction.

The pressure was measured at more than 300 locations for the following reasons: (1) to establish the mass balance in the test model, (2) to study the prediffuser performance (3) to identify flow nonuniformity around the combustor casing and the impingement sleeve, (4) to determine static pressure loss/recovery in different regions of the test section, and (5) to determine pressure loss in the air extraction path.

One of the 14 combustor transition pieces was coated with lampblack. The air entered through the holes in the impingement sleeve and formed jets which impinged over the outer surface of this transition piece. These air jets removed the lampblack coating which, in turn, provided a flow pattern at the outer coated surface of the transition piece. These traces were lifted off the surface by a transparent tape.

Static pressure, total pressure and velocity profiles were measured to characterize the flow field in the pre- and dump diffusers. The pressure was measured with Kiel and pitot-

static probes. A single-wire, hot-film anemometer and a laser Doppler velocimeter measured the two components of velocities. These profiles were taken at longitudinal planes with circumferential symmetry to avoid 3-D effects. These symmetry planes were located between the struts and between the combustor/transition piece assembly. Figure 1 identifies 7 planes in the test model, A, B, C, D, S, T, and U, where detailed profiles were obtained.

## Experimental Procedure

The experimental procedure involved (1) establishing the test conditions, (2) the probe traverses, (3) the automated pressure measurements, (4) the automated velocity measurements using a hot-film probe and a laser Doppler velocimetry, and (5) the temperature measurements.

The test conditions were controlled to simulate a typical OD-peaked axial velocity profile at the prediffuser inlet, to obtain desired main flow, extraction flow and fuel nozzle flow, and to check the accuracy of the mass balance in the test model and the air extraction system.

Two computer-controlled, single-axis positioning devices were designed and built to move the probes during the profile measurements. A traverse system support was designed and fabricated to mount the traverse system, which carried the probes for profile measurements at stations A, B, C, and D in the test section. The only access to the flow at these stations was from the inside of the inner wall assembly. Figure 4 shows a schematic of the traverse system support secured coaxially inside the test section on one end at the junction of the test section and the upstream flow developing section and the other end on the metal turbine inlet assembly.

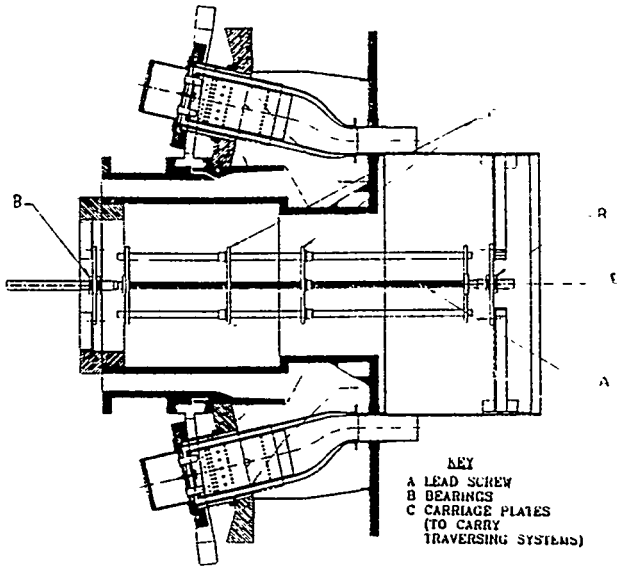


**Figure 4. A Schematic of the Traverse System Support**

A computer controlled pressure measurement system, Scanivalve MSS-48C, was used to measure pressure given by various probes. Each of the two pressure transducers in MSS-48C (+/-5.0 psig and a +/-2.5 psig) can accept a maximum of 48 pressure inputs. Computer programs were written for controlling the Scanivalve operation and for acquiring and storing data on the host computer.

A single-wire, hot-film probe was used to measure two components of the velocity. The hot-film probe was calibrated using a blow type wind tunnel. Since the hot-film probe is prone to breakage in any contact with a wall, an automated mechanism was devised and used during the experiments to detect the outer wall at the measurement location. The basic concept involves detecting the location of the outer

wall and ensuring that the probe never reaches this location.

A 2-component, 4-color fiberoptic LDV system was used to measure axial and circumferential velocity components at location UBC9. The probe accessed the measurement location through a transparent window on the turbine wrapper. A smoke generator burning oil-based smoke juice was built to provide the seeding necessary for LDV measurements. The smoke was introduced upstream of the prediffuser inlet through a port on the flow-developing section at the same circumferential location as station UBC9.

Twelve thermocouples mounted throughout the test section and flow systems were connected to an EXP-16 board attached to the DAS-20 board. Computer programs were written to control data acquisition and the storage of both voltage and temperature measurements.

## RESULTS

In this study, the profile measurements were limited to symmetry planes where the circumferential velocity was zero. Therefore, we used the computational results to furnish us the greater details of the flow field in the diffusers. The results from the two approaches are used in combination in our presentation and discussions.

### Flow Field

General characteristics of the flow at the midplane of the combustor/transition piece assembly (also in between the combustor support struts) are shown in Figure 5. The air in the prediffuser's outer region accelerates as it exits the prediffuser and then turns almost 180 degrees to enter the bypass holes on the combustor casing. This short-circuiting of the prediffuser flow is referred to as the sink effect of the combustor bypass holes on the flow field in the pre- and dump diffusers. Flow acceleration is detrimental to both the pre- and dump diffuser's performance because the primary function of a diffuser is to diffuse or decelerate the flow.

Another finding of this work is the recirculating region underneath the impingement sleeve close to the turbine inlet. The flow separates in the lower dump diffuser at the tip of the prediffuser's outer wall and in the space between the combustor casing and the prediffuser's outer wall. A recirculating flow dissipates the energy received from the main flow, thus contributing to frictional losses.

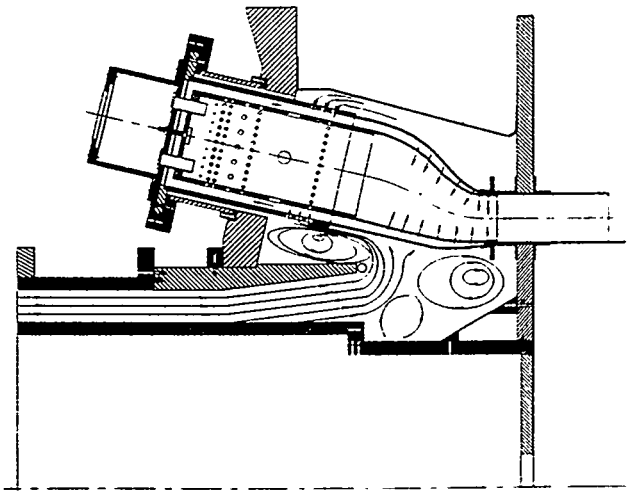

**Figure 5. A Schematic of General Flow Characteristics (between the Support Struts)**

**Comparison between Measurements and Computations.** Figures 6 and 7 compare the axial and radial velocity profiles measured by a single-wire, hot-film probe to the com-

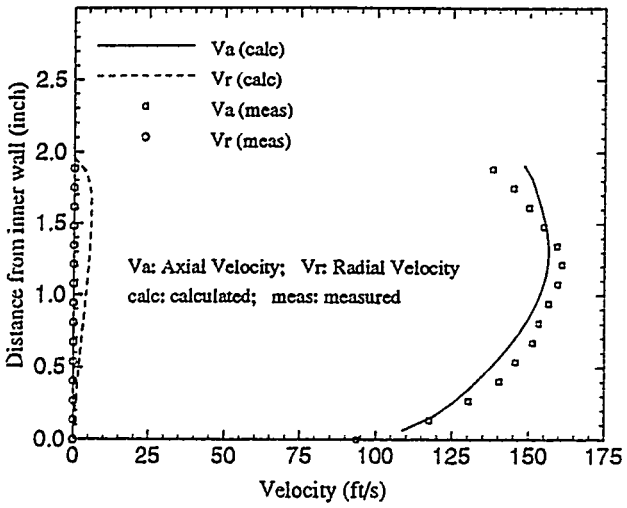


**Figure 6. Velocity Profiles at Plane A (between the Combustors) for a Base Line Configuration**

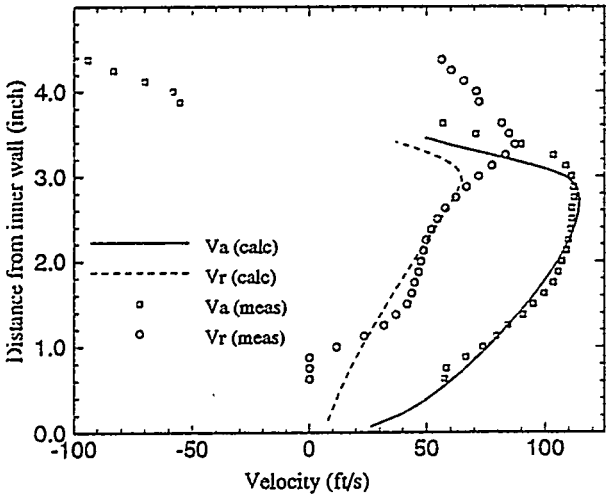


**Figure 7. Velocity Profiles at Plane D (between the Struts) for a Base Line Configuration**

puted results. The computed and measured axial velocity profiles compare well with each other. Even with the complexities involved, the correlation reached between the measurements and the computations is viewed as being from good to excellent.

The air extraction at the turbine wrapper had only a marginal influence on the flow field in the prediffuser and the lower portions of the dump diffuser. When the Griffith diffuser was used, the flow at the prediffuser inlet was directed radially upward.

## Overall System Performance

**Total Pressure Loss.** Table 1 summarizes the measured and computed pressure loss coefficients in the diffusers when the air is extracted from the test section. The total pressure loss coefficient in Table 1 is based on the mass flow rate passing through the dump diffuser. Both measurements and computations indicate a smaller pressure loss coefficient when the air is extracted at the prediffuser inlet because only 80% of the compressed air enters the dump diffuser. The total pressure loss coefficients thus obtained are related to the total pressure losses in the prototype. Table 2 provides a summary of these results and shows a difference of 0.5 percentage point between the overall thermal efficiencies of the two schemes.

**Table 1. Mass-Averaged Total Pressure Loss Coefficient with Air Extraction**

| | Measurements | | Computations | |
|---|---|---|---|---|
| | Turbine Wrapper | Prediffuser Inlet | Turbine Wrapper | Prediffuser Inlet |
| Prediffuser | 0.02-0.11 | 0.01-0.10 | 0.04 (4%) | 0.04 (6%) |
| Dump Diffuser | | | | |
| Lower Part | 0.08 | not available | 0.22 (22%) | 0.06 (9%) |
| Upper Part | <0.95 | <0.8 | 0.72 (74%) | 0.60 (85%) |
| Total | | | 0.98 (100%) | 0.70 (100%) |

**Table 2. A Summary of Results**

| | Base Case: No Extraction | Turbine Wrapper Extraction | Prediffuser Inlet Extraction |
|---|---|---|---|
| Total Pressure Loss Coefficient | 1.2 | 1.0 | 0.7 |
| Total Pressure Loss (%) | 2.2 | 1.8 | 1.3 |
| Thermal Efficiency (%) | 35.0* | 35.23 | 35.75 |
| Change in Thermal Efficiency (% point) | 0.0 | 0.23 | 0.75 |

* based on GE MS7001F

**Prediffuser Wall Static Pressure Recovery.** Figure 8 shows the measured and computed static pressure recovery coefficients along the inner and outer walls of the prediffuser for the straight wall prediffuser without air extraction (the base line configuration). Experimental data and computed results show similar trends, although the measured static pressure recovery is lower. The pressure increases linearly along the inner wall of the prediffuser. At an axial location of 6 inches from the prediffuser inlet, the $C_p$ values from the measurements and computations are 0.35 and 0.45, respectively. On the outer wall, the pressure decreases towards the exit of the prediffuser. The outer wall pressure decreases as the flow accelerates at the prediffuser exit because of the sink effect. The maximum $C_p$ values from measurements and computations are 0.27 and 0.42, respectively.

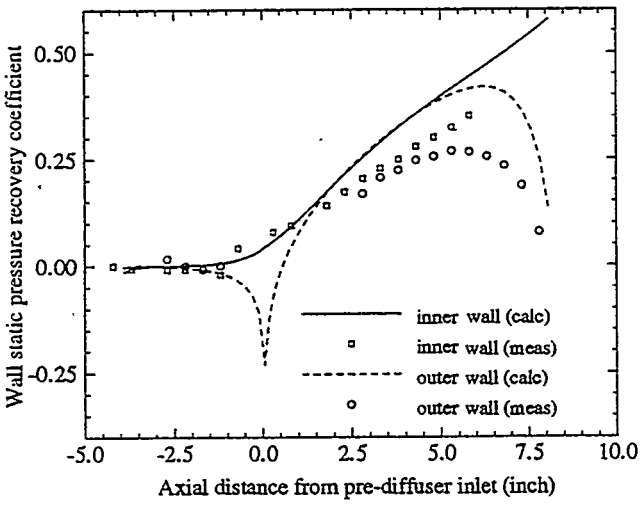


**Figure 8. Prediffuser Wall Static Pressure Recovery Coefficients for a Base Line Configuration**

## Flow Uniformity around the Combustor and Transition Piece

Table 3 summarizes the wall pressure measurements on the combustor casing and the impingement sleeve for the base line configuration at full through flow rate. Table 3 shows that the wall static pressure on the inside surface of the impingement sleeve is nearly the same in the circumferential direction. However, the wall static pressure on the outer

**Table 3. Wall Pressure Measurements on the Impingement Sleeve and the Combustor Casing (Inches of Water)**

| | Impingement Sleeve | | | | | |
|---|---|---|---|---|---|---|
| | Outer Surface | | | Inner Surface | | |
| 12 o'clock | -14.4 | -14.6 | -13.5 | -22.7 | -20.2 | -19.0 |
| 6 o'clock | -15.7 | -16.2 | -14.5 | -22.6 | -20.2 | -18.9 |
| 3 o'clock | -9.6 | -9.5 | -10.2 | -23.1 | -20.6 | -19.2 |
| | Combustor Casing | | | | | |
| | Outer Surface | | | Inner Surface | | |
| 12 o'clock | -14.9 | -14.4 | -14.1 | -26.0 | -21.9 | -21.0 |
| 6 o'clock | -14.5 | -14.5 | -13.3 | | | |
| 3 o'clock | -13.7 | -13.1 | -13.1 | | | |

surfaces of the combustor casing and the impingement sleeve varies in the circumferential direction. The circumferential variation is small on the combustor casing (near the bypass holes) but is significant around the impingement sleeve. The wall pressure is lowest at the 3 o'clock position (side panel) and highest at the 6 o'clock position (inner panel). The pressure is low at the 3'o clock position because of the venturi effect of the crossflow between adjacent combustor/transition piece assemblies. The venturi effect is more pronounced at the impingement sleeve where the crossflow area or the space between sleeves is small. The nonuniform pressure distribution would cause a lack of uniformity in the airflow that enters the bypass holes or cools the transition piece.

Table 3 also points to an increase in the circumferential nonuniformity of the wall pressure when the air is extracted at the turbine wrapper. Extracting air at the turbine wrapper increases the crossflow and hence the ventuti effect on the side panels (or 3 o'clock position) where the wall static pressure decreases. However, extracting air at the prediffuser inlet does not adversely affect the circumferential nonuniformity.

### Air Extraction Loss

In this study, 1 manifold system (M1) was tested with air extraction at the turbine wrapper, and 2 different manifold systems (M2 and M3) were tested with air extraction at the prediffuser inlet. The measured data indicated that the entrance loss of the collection branches is high compared to the loss in the manifold. For example, in the manifold system M3, the entrance loss is 11.2" of water head compared to a loss of 3.9" of water head in the manifold. Although the pressure loss in the manifold and collection branches reached a near optimum situation in the present design, the entrance loss still seems high. Further design improvements may be possible. The pressure loss associated with the two air extraction schemes are comparable.

## CONCLUDING REMARKS

From thermal-fluid considerations, it is recommended that the air be extracted at the prediffuser inlet. Air extraction at the turbine wrapper would distort flow distribution around the impingement sleeve and would result in a higher total pressure loss. In the air extraction path, the entrance loss of the collection branches of the manifold should be minimized by design optimization.

This study identified the pressure loss mechanisms in a compressor discharge casing of heavy-frame gas turbines. The total pressure loss can be minimized by a redesign of the prediffuser. In general, the area ratio of the prediffuser should be increased to the extent that the flow would not separate. The prediffuser length should be reduced to minimize the area of the "wetted surface" and perhaps to avoid the sink effect. Certain portions of the dump diffuser could be blocked off to reduce the region of the major recirculating flow.

## REFERENCES

Yang, T.T., and Kapat, J.S., 1991, "Effect of Manhole Air Extraction on the Performance of GE MS7001F Series Gas Turbines," Topical Report Vol. 7 to the Morgantown Energy Technology Center, US Department of Energy by Clemson University, Clemson, SC.

Yang, T.T., Agrawal, A.K., and Kapat, J.S., 1992, "Air Extraction and LBtu Coal Gas Combustion in Gas Turbines for IGCC Systems," In Proc. of the 9th Annual Coal-Fueled Heat Engines, Advanced Pressurized Fluidized-Bed Combustion, and Gas Stream Cleanup Systems Review Meeting, pp. 97-107, DOE/METC-93/6129, NTIS/DE93000232.

Yang, T.T., Agrawal, A.K., and Kapat, J.S., 1993, "Air Extraction from the Compressor Discharge of a Heavy-Duty Gas Turbine for an IGCC Systems Gasifier: Experiments and Analysis," Topical Report Vol. 8 to the Morgantown Energy Technology Center, US Department of Energy by Clemson University, Clemson, SC.

# P5 Development of a Dry-Feed System for a Coal-Fired Gas Turbine

## CONTRACT INFORMATION

**Contract Number** DE-AC21-86MC23165

**Contractor**

Allison Gas Turbine Division
General Motors Corporation
P.O. Box 420
Indianapolis, IN 46206-0420
(317) 230-2000

**Contractor Project Manager** John W. Rothrock Jr.

**Principal Investigators**

Craig F. Smith
John W. Rothrock Jr.

**METC Project Manager** Leland Paulson

**Period of Performance** August, 1986 to October, 1993

**Schedule and Milestones**

**FY93 Program Schedule**

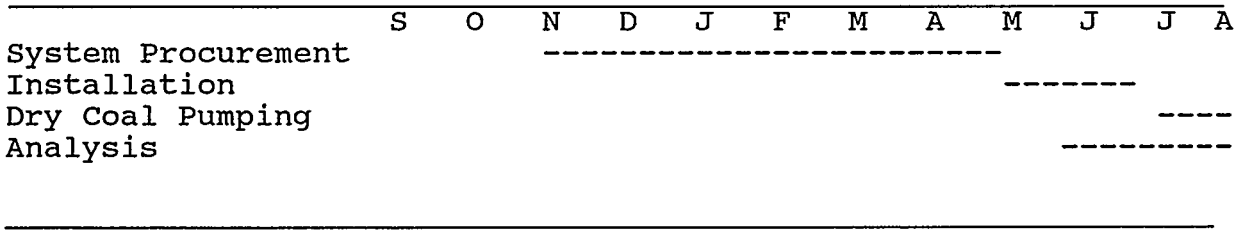


## OBJECTIVES

The objective of the reported work is to develop a dry coal feed system that provides smooth, controllable flow of coal solids into the high pressure combustor of the engine and all test rigs. The system must start quickly and easily, run continuously with automatic transfer of coal from low pressure hoppers to the high pressure delivery system, and offer at least a 3:1 smooth turn-down ratio. Cost of the equipment must be minimized to maintain the economic attractiveness of the whole system.

Before the current contract started some work was done with dry powder coal. For safety and convenience reasons, coal water slurry was selected as the fuel for all work on the program. Much of the experimental work, including running the Allison 501-

KM engine was done with coal slurry. Recent economic analysis led to a change to powdered coal.

## BACKGROUND INFORMATION

General Motors and Allison Gas Turbine Division have been working on dry coal feed systems for over 10 years. The initial use was a successful coal-fired gas turbine automobile demonstration project. Using General Motor's highly developed AGT-5 automotive gas turbine and a fuel system of novel design, a Cadillac El Dorado Coupe was equipped with the engine.

The dry fuel feed system used in the car is shown in schematic form in Figure 1. Essentially a "chain" pump, the coal was carried along in spaces between small metal disks strung on a steel cable. A vibrating hopper fed micronized coal into the line at ambient pressure. The coal was then carried through a zero-clearance seal across a pressure barrier and blown into the fuel line by compressor discharge air. Fuel flow rate was controlled by varying the speed of the DC electric motor driving the chain pulleys. This unit delivered about 60 pounds of coal per hour against 60 or 70 psi back pressure. It responded to control inputs from the driver (on the gas pedal) and was able to accelerate and decelerate the car as desired in traffic.

Although it would have been possible to scale this unit up by increasing element size and by use of parallel chains, it was thought likely that it would not be possible to seal the chain across a 160 psi pressure barrier as required by the Allison industrial gas turbine.

For this and safety reasons, all initial combustion work on this project was accomplished using coal water slurry, which allows the use of somewhat conventional pumps and valves. Ultra-fine ground coal water slurry has delightful and surprising characteristics of its own that make its use far from trivial.

The national market for coal slurries that was envisioned in 1986 as a replacement fuel for oil-fired boilers never developed. Companies that had planned large scale production of slurries either changed their plans or went out of business. Coal slurry fuels for the work on this project were made in barrel lots and were extremely expensive even for experimental use. The pressing economics of this made the decision to switch back to dry powder fuel inevitable.

## PROJECT DESCRIPTION

The work described in this paper was in support of Allison's Coal Fired Gas Turbine contract. Feed systems were needed both for the bench scale combustion rig and the full scale combustion rig and engine. The mass flow scale factor between these two units is ten to one. Nominally, the bench scale unit requires 500 pounds per hour of dry coal flow, and the full scale system needs 5000 pounds per hour. This variation in requirement meant no one feed unit could satisfy both.

Two separate units were specified and ordered. Ultimately, a third was acquired for the bench scale rig due to the failure of the first.

## RESULTS

While full scale engine testing continued on coal slurry, efforts were made to identify a supplier of coal conveying or metering equipment that could produce a unit that would operate properly at the high pressure required. The bench scale combustion rig operates at the same pressure as the full scale system.

Based on a survey of the industry, a pneumatic conveying system vendor was chosen and a purchase order was placed with them to design and build a bench scale fuel system. Figure 2 and 3 show photos of the completed system. Two parallel pressure vessels were employed, allowing continuous running by switching between them. The system conveyed coal in dense phase, the coal to air ratio being about 100 pounds of coal per pound of air. This necessarily leads to plug flow, and the fuel line was equipped with air injecting check valves every five feet to reduce the gaps between the plugs and even out the pressure distribution in the line.

Much time was spent trying to tune the booster valves and other parameters of this system to get smooth flow, but as Figure 4 shows, there was little success.

An outside consultant, Mr. Paul Solt of Pneumatic Conveying Consultants, was engaged to assist Allison with this problem. He recommended a change to dilute phase conveying in the line, and separate control of vessel air flow and pressure and line air flow and pressure. He also warned that the size of the unit might prevent accomplishment of the required flow and it might be necessary to change over to some sort of mechanical feeder at the point where coal entered the fuel line.

Following these recommendations, a small improvement in flow was noted. Figure 5 shows flow data against low back pressure and Figure 6 shows flow data against simulated combustor pressure. Two attempts to run a combustion test using the modified system were made but the burner was out of control for both tests. The best period of control showed a flow variation of +- 50 percent.

Meanwhile, a purchase order was awarded to another vendor of conveying equipment for the full scale rig fuel system. This vendor, Whirl-Air-Flow of Minneapolis, Minnesota, suggested that incorporation of their live bottom or aerated cone bottom on the existing pressure vessels of the bench scale rig might solve our problem. One of the two vessels was therefore taken out of the system and sent to the vendor for this modification.

After return to Allison and assembly further flow tests were made. No real improvement in performance was noted. Like the earlier system, the modified unit was prone to flow stoppages, most of which were due to "ratholing" of the coal in the pressure hopper. After a series of tests the pure pneumatic concept was abandoned for the bench scale rig.

Manufacturers of rotary and screw auger feeders were contacted and a handful thought their equipment could work at the required pressure. One of them sent actual flow data from a similar situation and with other considerations, won a purchase agreement from Allison for a pressurized bench scale dry coal screw feeder. This was Simon Air Systems of the United Kingdom.

While awaiting delivery of this unit, Whirl-Air-Flow completed assembly of the full scale feed system and began testing it on baking soda at low receiver pressure. Satisfied with the results, they then switched to anthracite coal for further testing. Their concern was one of safety in the handling of bituminous coal, since their facility was a manufacturing plant and not a test center. After discussion with Allison, a plan was developed to move the unit to the back of the factory where it could be vented to the outdoors in the event of explosion, and inerted with nitrogen when not in use. After making these changes, the unit was tested on Pennsylvania #8 bituminous coal ground to 15 microns average and 40 microns top size. It was necessary for Whirl-Air to develop a pneumatic device to prevent ratholes and install it in the pressure vessels to operate at the elevated pressure. Figure 7 is a photograph of the assembled system.

Figure 8 [test 32-6] shows a trace of coal flow versus time on this unit operating with 160 psig back pressure. The smoothness of the flow is encouraging. RMS variation of the smoothest section of the flow here is a low 1.6 percent. Figure 9 [test 32-2] shows a changeover from one pressure vessel to another. The two control valves for the vessels were not set for identical flows so there is a resulting step change in flow. The important parameter is the upset period of only 5 or 6 seconds. There was a small undershoot but no loss of flow. Further tuning of the setup should improve this. The minimum flow rate before stoppage was determined to be 14 pounds per minute using the 5/8 inch internal diameter fuel line. This rate, 840 pounds per hour, is more than the maximum required for the bench scale unit, which uses the same size fuel line.

Figure 10 [test 32-11] shows the pressure sensitivity of the system. The receiver pressure was varied while holding all parameters fixed on the delivery vessel and the change in coal flow was noted. The resulting plot shows an average sensitivity of about 1/2 pound per minute per psi of pressure change. This is small, but enough of a concern that the engine control system would have to monitor pressure and compensate for changes by modulating the control valves.

It appears that the full scale fuel system, with some tuning and control work, should provide an adequate fuel delivery system for engine testing at Allison.

The pressurized screw feeder from Simon-Air arrived at Allison in May and was promptly installed for flow testing. Figure 11 is a photograph of the screw feeder as installed in the Allison bench scale coal system.

This system incorporates a variable speed auger to convey coal out of a pressurized hopper to the fuel line. With independent control of pressurization air, convey air, and solids flow it is expected that the problems encountered in the pneumatic systems for bench scale work can be avoided.

## FUTURE WORK

Upon completion of the installation and check-out of the Simon Air Screw Feeder pumping tests will start. In these tests the actual fuel line, flow meter, fuel nozzle, and bench scale combustor will be used. Coal will be fed into the combustor held at its operating pressure but with no combustion taking place. Solids flowrate, air pressures and flows will be recorded for subsequent analysis. The unburned coal will be cleaned out of the combustor at the completion of the tests.

The feeder will be qualified for bench scale coal combustion testing upon satisfactory operation in this mode.

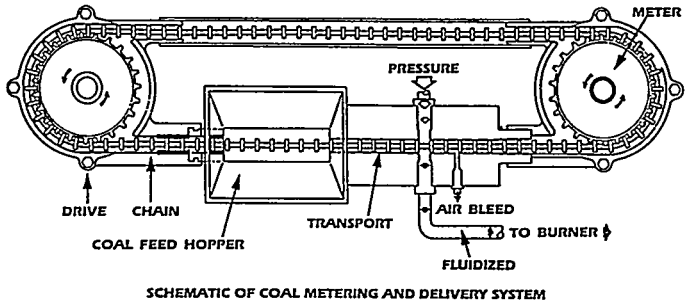


**Figure 1. Automotive Dry Coal Chain Pump**

**Figure 2. Allison Bench Scale Dry Coal Feed Test System**

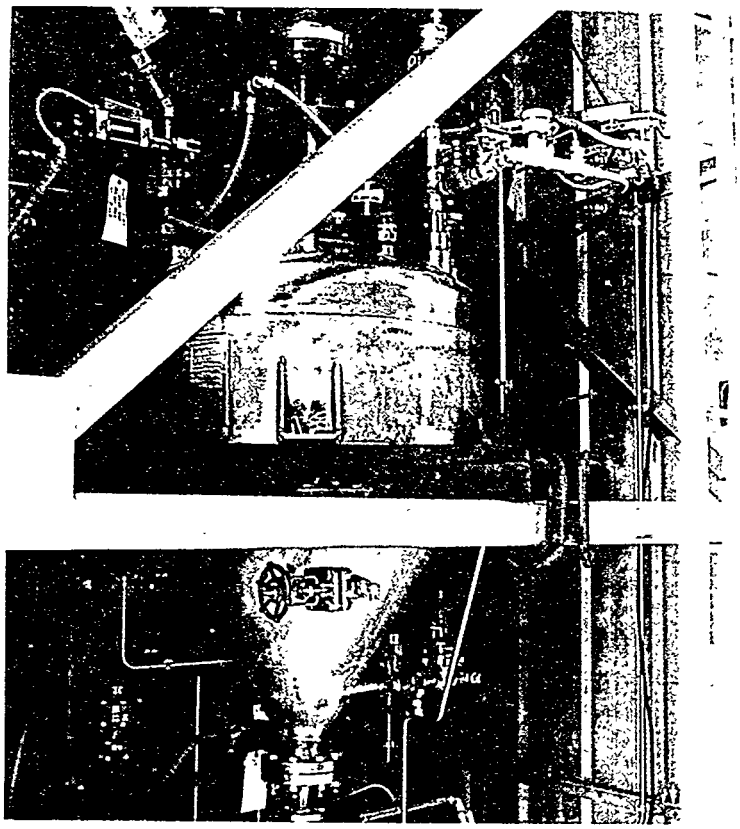

**Figure 3. Bench Scale Pure Pneumatic Dry Coal Feeders**

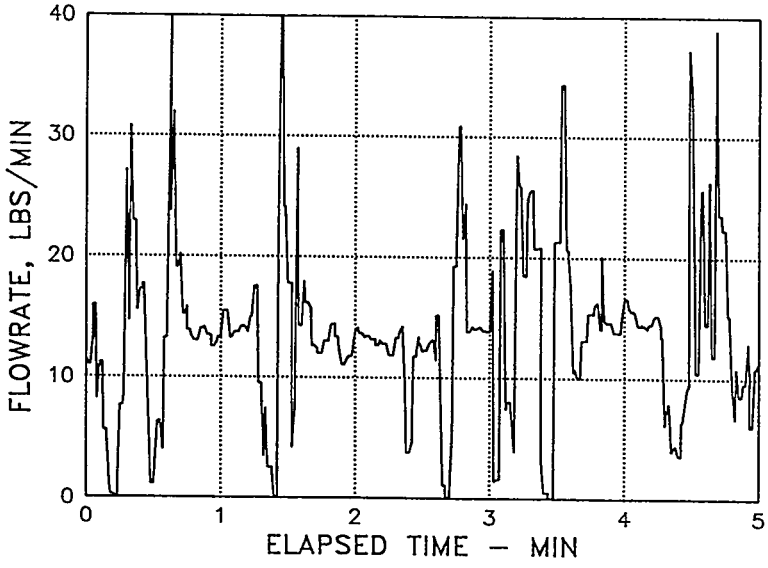


**Figure 4. Flow Data from Original Bench Scale Dense Phase System**

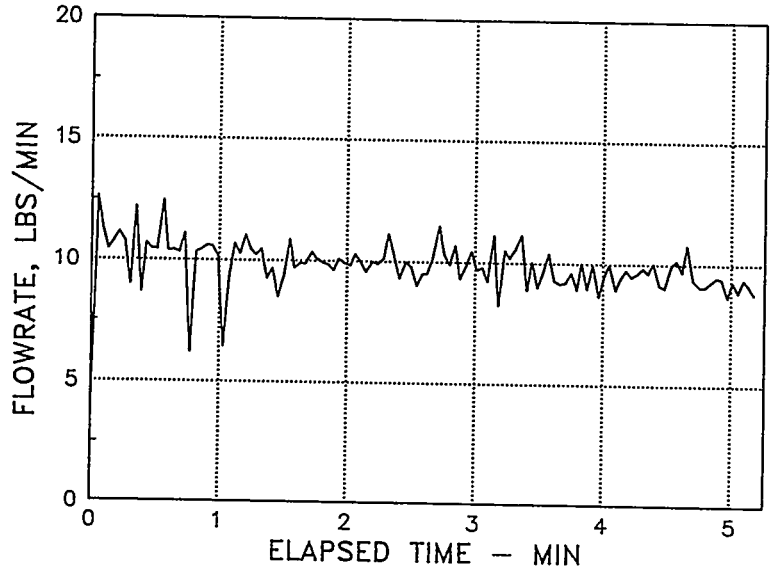


**Figure 5. Bench Scale Modified Dilute Phase Pneumatic System Low Pressure Flow Data**

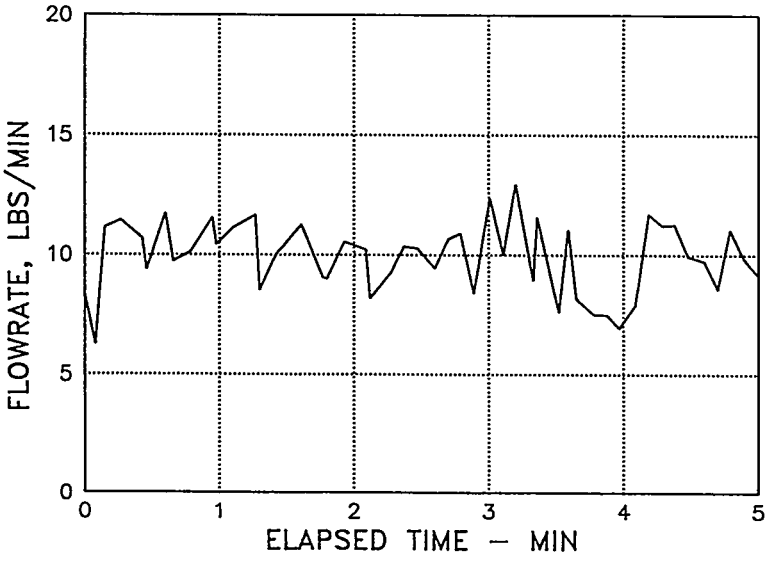


**Figure 6. Bench Scale Modified Dilute Phase Pneumatic System Flow Data**

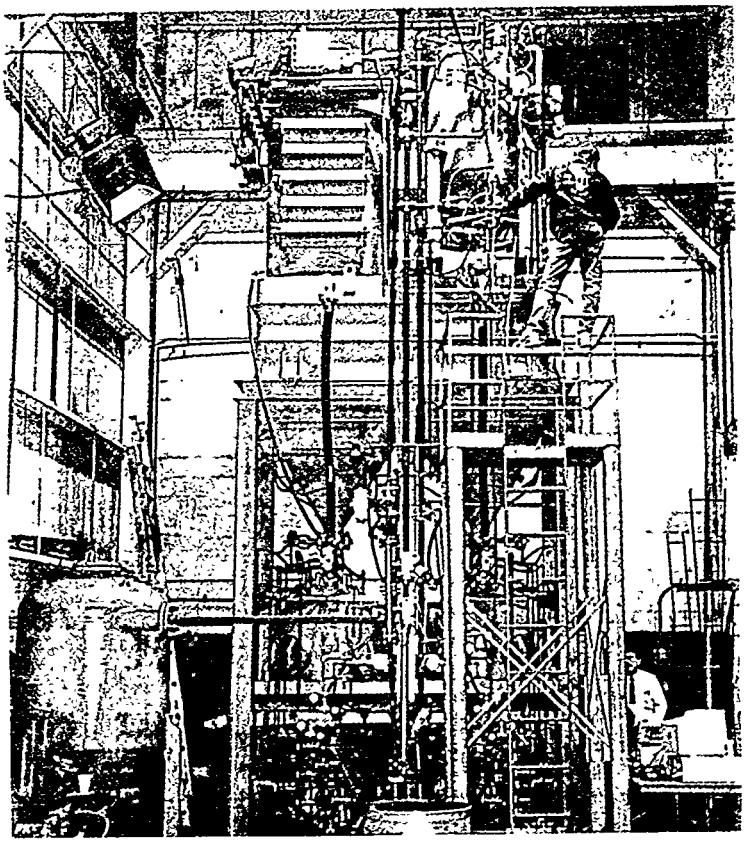

Figure 7. Full Scale Dry Coal Feeder

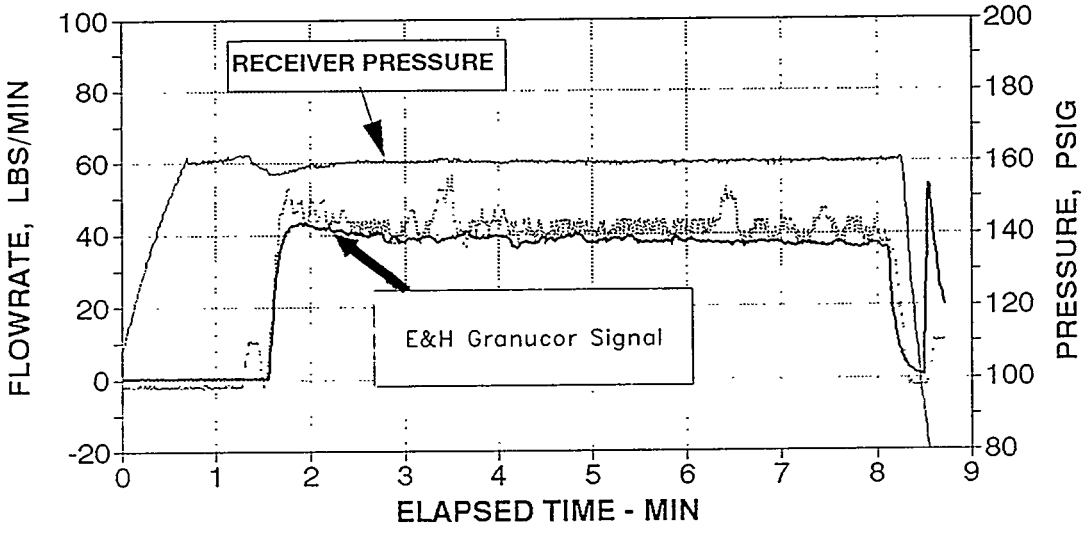


Figure 8. Full Scale Feeder Flow Data Demonstrating Smoothness of Flow

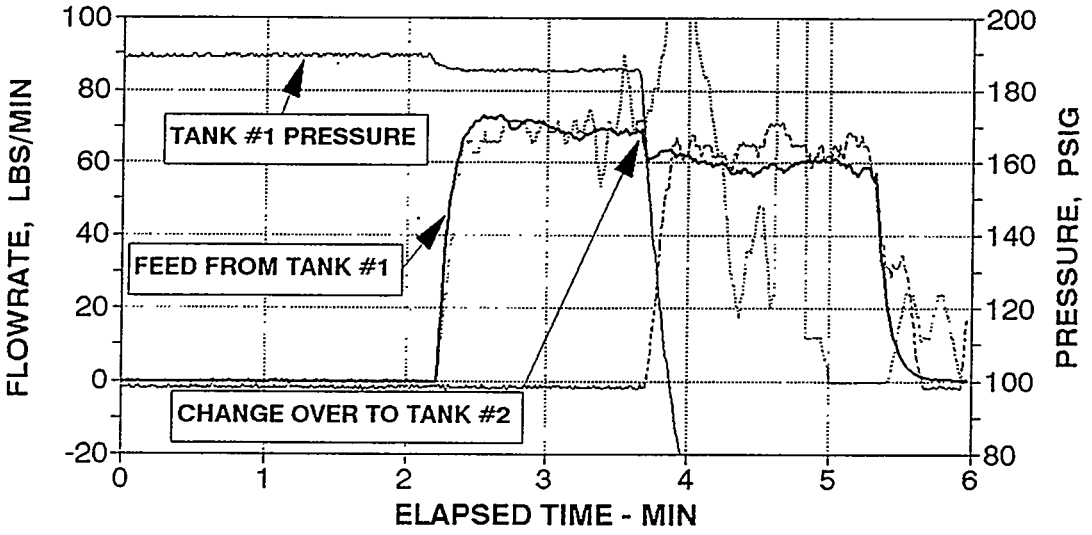


Figure 9. Full Scale Feeder Data Demonstrating Vessel Switch

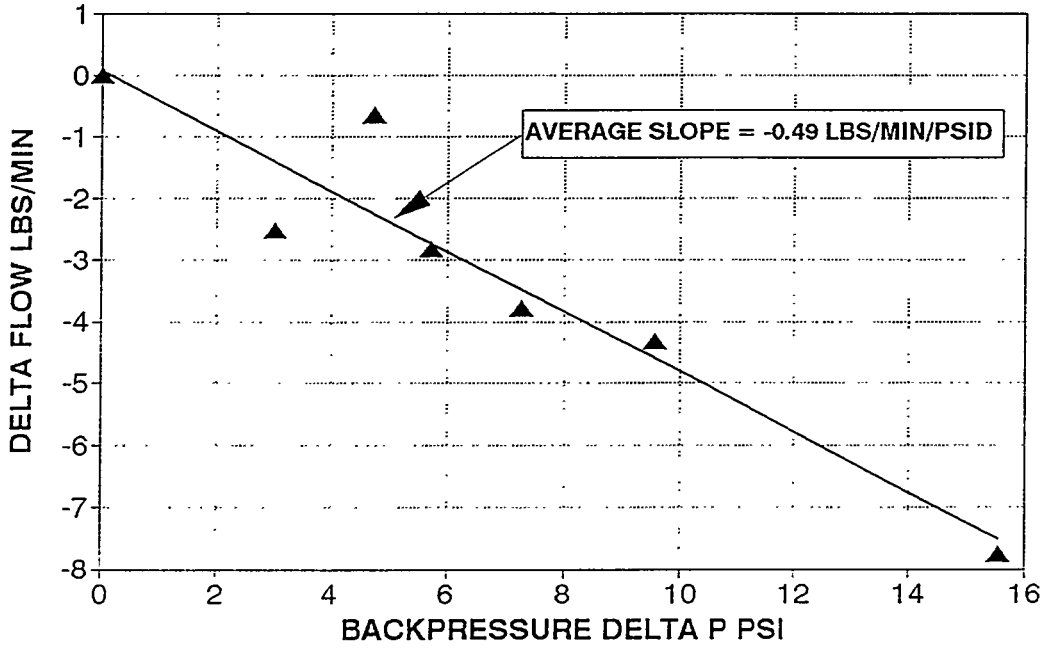


Figure 10. Full Scale Feeder Data Showing Pressure Sensitivity

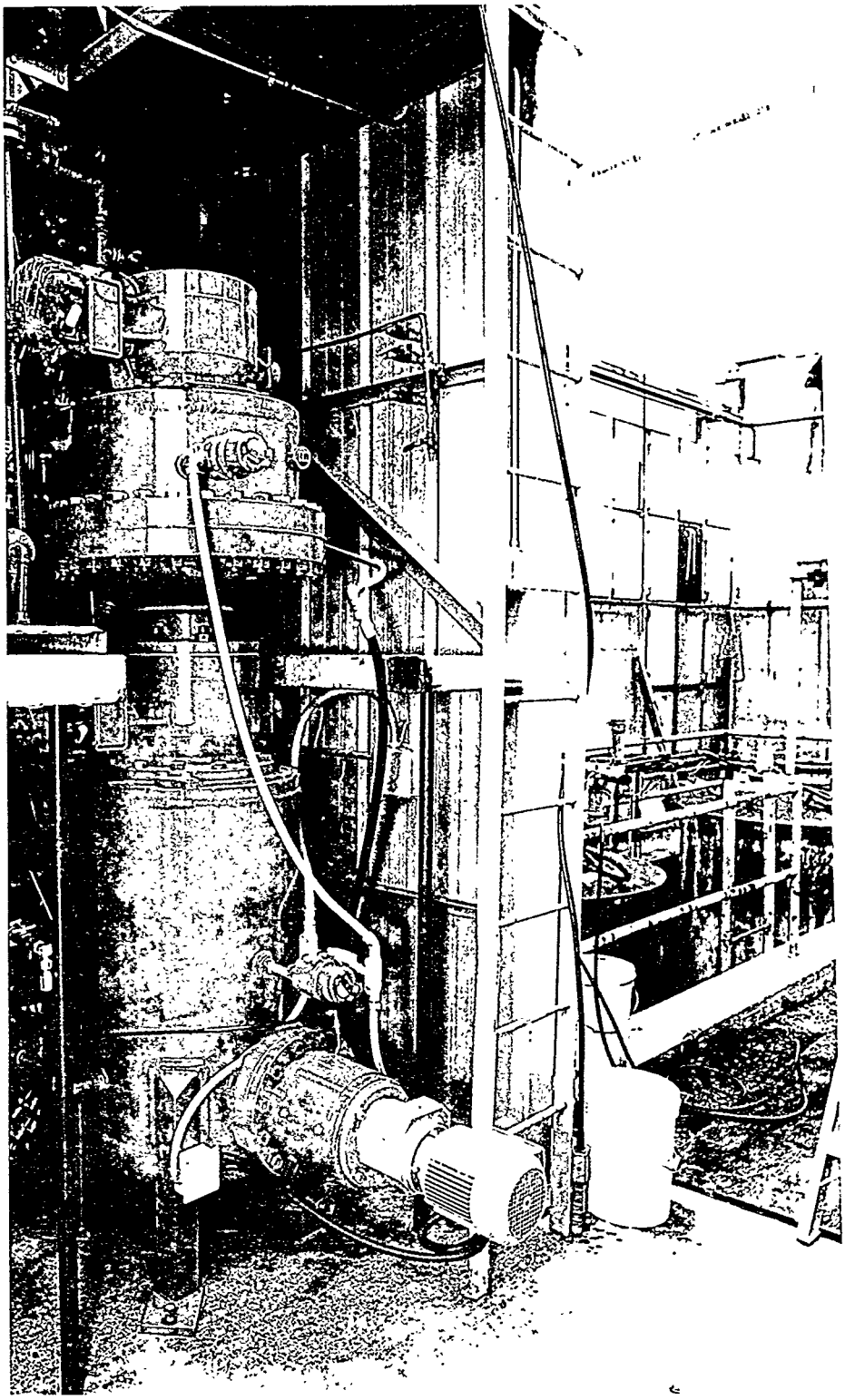

Figure 11. Bench Scale Pressurized Dry Coal Feeder

P6

# METC Research on Coal-Fired Diesels

Michael H. McMillian
Morgantown Energy Technology Center

Edward H. Robey
Richard E. Addis
EG&G Washington Analytical Services Center, Inc.

## ABSTRACT

The METC in-house Coal-Fueled Diesel Research project is part of the overall DOE effort to develop a technology base for diesel engines capable of operating on coal, shale oil or low-cost coal-derived fuels. The in-house effort started in 1985 as a test-bed for coal-derived liquid fuels and will end this fiscal year with the successful completion of METC's diesel R&D program. Currently METC in-house research and development efforts focus on pilot chamber combustion in METC's coal-water slurry (CWS) fueled diesel engine. A novel pilot chamber for a direct-injected, coal-fueled diesel engine has been designed and is being tested in METC's single cylinder research diesel engine. The pilot chamber configuration allows for operation at extended load and speed conditions using 100 percent CWS and no other pilot fuel. The concept involves the use of a small volume chamber exterior to the main cylinder in which approximately 5 percent of the total fuel energy at full load conditions is injected. Lower $NO_x$ levels may be obtained due to leaner burning as well as broader stable performance using only CWS fuel.

## INTRODUCTION

Development of Coal-Fueled diesels has been sponsored in the U.S. since 1949 (Robben 1983). The U.S. Department of Energy (DOE) Office of Fossil Energy has sponsored research in the coal-fueled diesel area since the late 1970s (McMillian and Webb 1989). To date, thousands of hours have been accumulated using coal-water slurry (CWS) fuel in engines of a broad size and speed range. These efforts have brought the technology to the demonstration stage as evidenced by the recent selection of Easton Utilities and Arthur D. Little, Inc. in DOE's Clean Coal Technology Program to demonstrate stationary, CWS-fueled diesel engines for production of power.

Although stationary applications of coal-fueled diesels have reached the demonstration stage, significant problems remain to be solved for transportation applications to be economical. In comparing the technology requirements of stationary coal-fueled diesels and diesels used in transportation applications, many differences come to mind. Some of the differences in CWS performance requirements are outlined in Table 1. Stationary diesel applications typically operate at constant speeds and steady or slowly changing loads. Engines in transportation applications, however, require stable combustion over a range of transient loads and speeds. The need for pilot-assisted combustion to stabilize CWS operation in diesel engines was identified early in DOE-sponsored development (Arthur D. Little, Inc. 1986). The need for a second fuel (typically diesel fuel) for a pilot diminishes the advantages of coal-fueled diesels in transportation applications.

Tests of a concept to eliminate the need for a second fuel are currently underway at DOE's

**Table 1. Comparison of Constraints on Combustion Performance of Stationary and Transportation-Based Diesel Engines**

| Characteristic | Stationary | Transportation |
|---|---|---|
| Engine Speed | Medium to slow speed (<250 rpm) engines | Medium to high speed (>1000 rpm) engines. Engine speeds may vary greatly during operation independent of load. |
| Engine Load | Engine loads are typically constant over long periods of time or may vary slightly. Engine transients are not a concern. | Engine loads vary greatly. Must have stable combustion over a wide range of engine loads. Transients are a concern for combustion and injection system performance and response. |
| Fuel | Fuel properties are established. Fuel is stored on site. | Fuel stability and handling more complicated. May require handling two fuels. Main fuel of CWS and pilot fuel typically diesel fuel. |

Morgantown Energy Technology Center (METC). METC's pilot chamber concept allows for 100 percent coal-fuel usage by allowing CWS to be used as a pilot fuel. Other similar designs have been proposed for applications with natural gas and for prechamber engines operating on natural gas and CWS (Kakwani and Kamo 1989). The uniqueness of the METC concept is its applicability to direct-injected diesel engines. The pilot chamber concept and a description of the test results to date are described below.

## BACKGROUND

Twenty (20) years ago it seemed implausible to run any but the slowest speed engines on CWS fuel due to the perceived requirements for combustion residence time (Anson et al. 1987). Engines have now been run, with ignition aids, at speeds up to 1800 rpm on CWS. In the beginning, it was also realized that many technology barriers existed in the path to commercialize coal-fueled diesel engines. Critical issues included fuels technology, combustion phenomena, fuel engine interaction and contaminate control. For stationary applications most of these problems have been solved.

The major barriers for stationary coal-fueled diesel engines have taken DOE-sponsored engine developers fifteen years to overcome. Wear issues have been addressed by using hardened materials in the injector nozzles, rings and liners, valves and turbochargers. Fuel handling has been addressed using special slurry formulations and specific hardware design constraints. Contaminant control has been addressed using off-the-shelf technology employing Selective Catalytic Reduction (SCR) for $NO_x$ control, sulfur capture with calcium-based sorbents and particulate control with low temperature particulate

filtering such as a baghouse. With the exception of the emissions technologies, due to size constraints, many of these technical solutions may be used in transportation applications. The need to carry a second fuel for use as a pilot remains a disadvantage of coal-fueled diesel engines in transportation applications.

For stationary applications, multifueling capability is desirable due to the long term instability of fuel prices and the ease of fuel storage. However, it must be noted that in the absence of fuel price and availability instabilities, should one purchase a coal-fueled diesel engine with its higher inherent initial costs due to hardened components, emissions controls, etc., low fuel cost would be the driving force in usage of transportation-based diesel engines. It would therefore be desirable to minimize use of more expensive fuels such as diesel fuel (DF2). CWS fuels would by definition be the only fuel of choice due to low fuel cost. In transportation applications in which fuel storage is a more prohibitive issue, the use and added baggage of a separate pilot fuel is also undesirable.

When considering hypothetical coal-fueled, transportation-based, diesel engines, the most probable scenario would be a locomotive engine. The economy of scale for hardened engine components in large transportation engines and the available space on a locomotive for emissions treatment are two of the primary reasons. GE has done extensive development of coal-fueled locomotive engines over the past ten years. In their 1989 economic analysis, they estimated that in an eastern average locomotive duty cycle, 16.5 percent of the total energy will come from DF2 pilot fuel, and in a western average duty cycle, 14.2 percent will come from DF2 (Slezinger 1989). Considerable cost savings could be realized should cheaper CWS be used not only as the main fuel but also as the pilot fuel in these scenarios.

METC's pilot chamber concept will eliminate the need to use diesel fuel as a pilot by replacing it with CWS. A hot, insulated chamber is maintained in connection with the engine cylinder. CWS injected into this hot chamber will ignite with the flame and products of combustion jetting into the engine cylinder to aid in ignition of the main CWS charge. The key features of this pilot chamber are described below.

## PILOT CHAMBER DESCRIPTION

The pilot chamber used in these studies is depicted in Figures 1 and 2. The chamber fits into the modified cylinder head shown in Figure 3. At full load conditions, approximately 3 percent of the total CWS fuel charge is introduced into the pilot chamber through the pilot injector. The pilot chamber represents 4.3 percent of the total clearance volume. At part load operation, fuel to the pilot chamber is constant, thus providing a steady combustion condition within the pilot chamber at all load conditions. The hot walls of the pilot chamber act to transfer heat to the incoming air charge and to provide an ignition source for the CWS fuel. The pilot chamber is fabricated from Inconel 625.

Two pilot chambers were constructed, one uninsulated and another insulated with a 1-mm external coating of partially stabilized zirconia (PSZ). Geometrical design considerations were influenced by the work of Radovanovic and Djordjevic (1979). The pilot chamber has been tested in the uninsulated mode with DF2 fuel. In the insulated mode, the pilot chamber is externally coated with a 1-mm layer of PSZ in order to retain heat to ignite the CWS. The PSZ coating has a thermal conductivity of 2 W/m K whereas Inconel 625 has a thermal conductivity of 50 W/m K. Although the pilot chamber wall thickness may exceed 6 mm in places, the conductive heat transfer is controlled by the zirconia layer. Energy stored in the Inconel walls of the

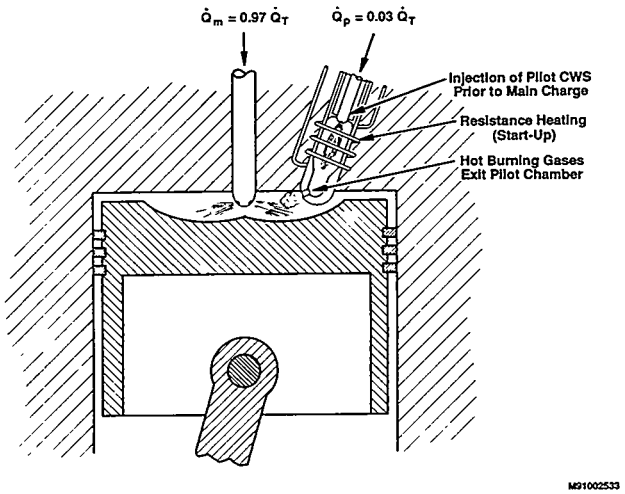


**Figure 1. Plot Chamber Schematic**

pilot chamber heats the incoming air and assists in ignition. The specific heat of the Inconel 625 is 410 J/kg K (0.095 Btu/lb °F). The specific heat of the incoming air compressed through the pilot chamber nozzle by the upward motion of the piston is approximately 1050 J/kg K (0.243 Btu/lb °F). The mass ratio of Inconel to air in the pilot chamber at TDC is approximately 1500. Assuming an air velocity in the throat of the pilot chamber of approximately 10 times the piston speed, the Reynolds number (Re) will exceed 150,000 ($Re_{ave}$> 75,000). From this we may estimate the conductive heat transfer coefficient ($h_c$) from $h_c = (Nu)k/L$ where Nu is the Nusselt number, k is the thermal conductivity and L is the throat diameter. The correlation (Heywood 1988) has been empirically derived for flow in straight pipes downstream of diesel exhaust valves:

$$Nu = 0.0483\ Re^{0.783}.$$

This gives an estimate convective heat transfer coefficient of 317 $W/m^2K$ and for the pilot chamber 0.68 W/K, which, for a wall temperature of 1000 K and air temperature of 600 K, 265 watts are available to the incoming air. At a 4-stroke engine speed of 25 rps, approximately 21 Joules are available per compression stroke.

## CWS FUEL SYSTEM DESIGN DESCRIPTION

The CWS fuel handling and injection system design for the pilot chamber and main chamber is depicted in Figure 4.

The CWS fuel is contained in two bladder-type accumulator vessels that set on separate weigh scales. The weight of the individual tanks are monitored for weight loss and hence fuel usage. One large ten gallon tank is used for the main slurry injector and a smaller one gallon tank is used for the pilot injector. The tanks are pressurized with nitrogen. The pressurized slurry is forced from the tanks through a check valve into the shuttle assemblies. The shuttle assemblies are used to separate the CWS fuel from the diesel fuel, which is used as a working fluid to pump the CWS into the engine. The shuttle assembly is depicted in Figure 5.

Diesel fuel is provided from a day tank to two fuel pumps, one each for the pilot injector and main injector. Diesel fuel is pumped from the fuel pumps to the shuttle assemblies. The small piston "shuttle" within the shuttle assembly is used to separate the working fluid (diesel fuel) from the CWS. During injection, the diesel fuel displaces the shuttle and thereby the CWS into either the main or pilot injector. The tolerance between the shuttle and the body of the assembly is tight (3 μm) to prevent coal particles from lodging between the two. An oil barrier is also used to prevent particle galling. Viscous oil is pumped at high pressure (>15,000 psi) to the cavity on the interior of the shuttle.

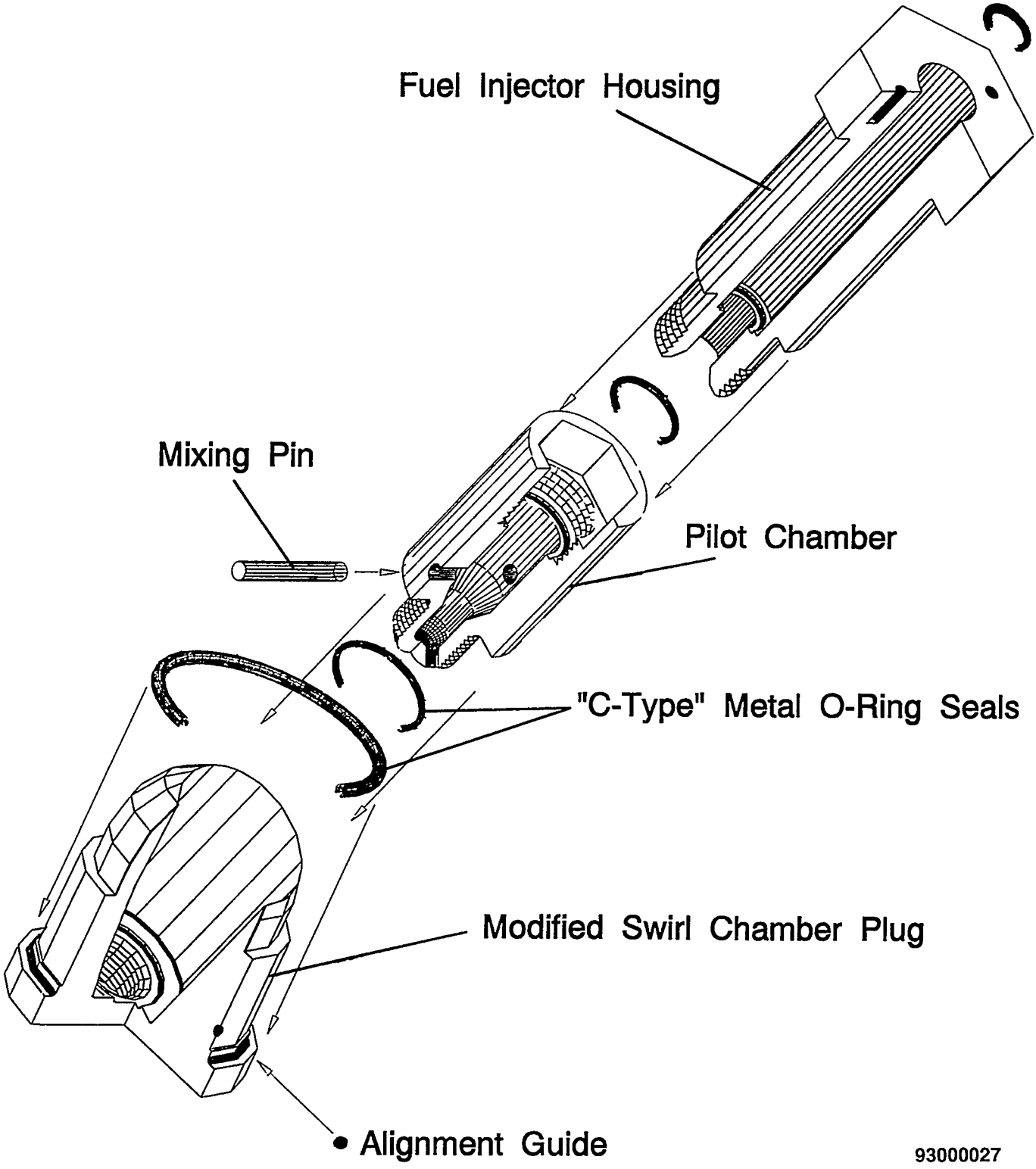


**Figure 2. Pilot Chamber Assembly**

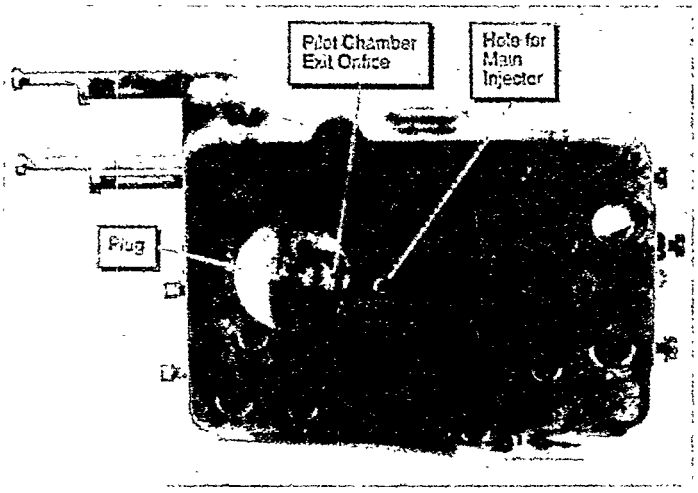


**Figure 3. Modified Cylinder Head**

This positive pressure aids in sealing the shuttle/body boundary from coal particles and also prevents mixing of diesel fuel and CWS. The two fuel pumps allow for independent control of injection timing and fuel quantity to the fuel injectors. This system is designed for startup on diesel fuel and changeover to CWS via a simple valving strategy. Properties of the CWS fuel to be used at METC are provided in Table 2.

## TEST ENGINE, INSTRUMENTATION AND OPERATING CONDITIONS

Baseline testing with diesel fuel was conducted at METC with a single cylinder research diesel engine. The engine, a Ricardo Proteus, and test bed were produced by G. Cussons Ltd. of Manchester, England. The design of this four-cycle engine was based on the Volvo TD120 with a toroidal combustion bowl in the piston. The engine has a bore and stroke of 130 mm (5.1 in) and 150 mm (6 in) respectively and a swept volume of 1.997 liters (122.4 cu in). The engine has a nominal compression ratio of

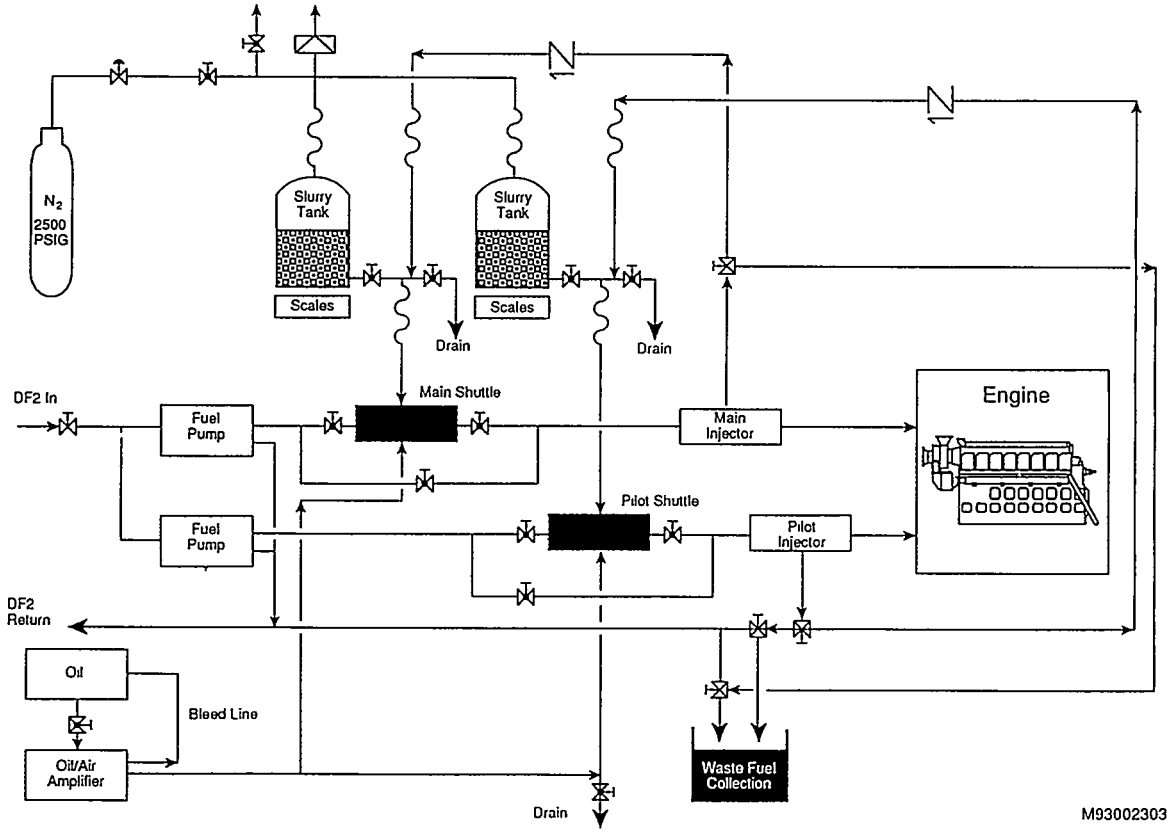


**Figure 4. Coal-Water-Slurry Handling System**

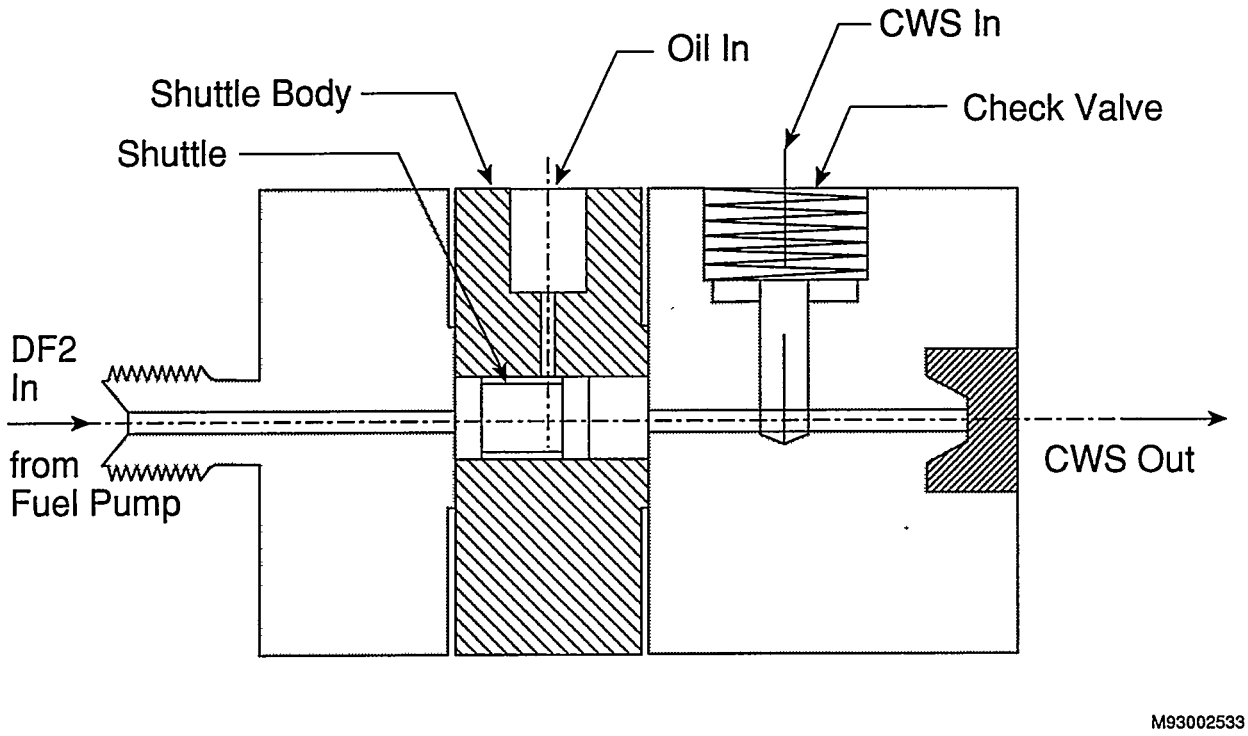


**Figure 5. CWS Shuttle Assembly**

**Table 2. CWS Fuel Specifications**

| | |
|---|---|
| Water (Wt%) | 49.04 |
| Coal (Wt%) | 50.43 |
| - Volatile Matter (Wt% Coal) | 35.66 |
| - Fixed Carbon (Wt% Coal) | 61.66 |
| - Ash (Wt% Coal) | 1.79 |
| - Sulfur (Wt% Coal) | 0.66 |
| - Heating Value (Btu/lb) | 15,101 |
| Additive Content (Wt%) | 0.51 |
| - Dispersant MCG92A-LS (Wt% Additive) | 97.00 |
| - Stabilizer Flocon 4800C (Wt% Additive) | 3.00 |
| Density (g/cc) | 1.13 |
| Mean Particle Diameter (Microns) | 13.25 |
| Diameter 100% less than (Microns) | 88.00 |
| Low Shear Viscosity @200/sec (cps) | 80.00 |

13.3:1 and a maximum power output of 55 kW (74 hp) at 36.7 rev/sec when operated in the unmodified direct injection build used prior to this work. Engine load is controlled by a

dynamometer. Turbocharger conditions were simulated by using a separate preheated pressurized air source and by using a back-pressure control valve in the exhaust.

The engine, when purchased from Cussons Ltd., was provided with an indirect injection build. The prechamber design was that of a swirl chamber in which approximately 68 percent of the total clearance volume was in the prechamber. This large cavity in the cylinder head was the ideal place to modify and locate our pilot chamber. The head had to be further modified to change it over to a direct-injected configuration. This was done by drilling and fitting a sleeve near the center of the head for the main injector. Because of restrictions in locating this hole, the main injector is now located off of center from the position that would be used in the standard direct-injected build. This off-center location was compensated for by altering the location and sizes of nozzle holes to provide similar penetration rates to all parts of the combustion volume. Correlations provided by Heywood (1988) were used to size the nozzle holes. For CWS application, a special nozzle is being designed that employs a tungsten carbide (WC) tip. Its design will be reported in the future.

Cylinder pressure and fuel line pressure were monitored at 0.25 crank angle degree increments by a Model CB-466 Ono Sokki Engine Analyzer. Cylinder pressure was measured by a piezo-electric transducer calibrated for 0-102 MPa (0-15000 psi). Other process data such as exhaust and intake air temperatures, fueling rates, and exhaust emissions were recorded once every second by data acquisition software on a PC/AT personal computer. A computer program was used to combine and summarize data collected by the engine analyzer, data acquisition software, and technician operators.

The concentration of $NO_x$ in the exhaust was measured with a Thermo Electron Model 10A Chemiluminescent $NO/NO_x$ gas analyzer. A Beckman Model 400 (flame ionization) analyzer was used to measure unburned hydrocarbons. Oxygen in the exhaust was monitored with a MSA Model 802 Oxygen analyzer. Concentrations of CO and $CO_2$ were measured with MSA LIRA Model 3000 infrared analyzers.

The operating conditions tested to date were chosen so that

1. The effects of the cylinder head modifications could be characterized.

2. The effects of additional volume from the pilot chamber on brake specific fuel consumption (BSFC), $NO_x$ and other operating parameters could be characterized.

3. The effects of pumping friction from the pilot chamber on engine efficiency could be characterized.

4. A baseline for future testing with diesel fuel and CWS to the pilot chamber could be established. (Future testing is discussed in the last section of this paper.)

Tests were conducted to date with diesel fuel using a "flat plug," a "recessed plug" and the pilot chamber itself without fuel flow or combustion taking place within the pilot chamber. The flat plug and standard piston provided a baseline for performance with the modified cylinder head. A recessed plug, which had a volume "cupped" out of the plug equal to the volume of the pilot chamber, was also tested. Comparisons of these test results with previous results with the flat plug provide insight to the effects of added combustion volume of the pilot chamber. Comparison of these results with tests

conducted with the pilot chamber installed but without fuel to the pilot chamber provide insight to frictional losses associated with the pilot chamber. These tests provide the baseline for future testing with pilot chamber fueling with diesel fuel and CWS in both uninsulated and insulated configurations.

A summary of the engine test conditions is provided in Table 3. The pilot chamber and other head components were tested at nine combinations of engine speed and boost air pressure. Back pressure on the exhaust was varied in conjunction with the boost air pressure to simulate turbocharging. For each cylinder head configuration tested, the engine was started at our baseline condition of 15 rps speed, 30 kPag boost pressure, 0 kPag exhaust pressure, 40 °C intake air temperature, start of combustion at 4° BTDC, and the rack set to produce 140 Nm torque. The engine was then operated over the nine conditions in Table 3 with the rack held constant and the load permitted to vary in response to changes in the other parameters. The loads shown in Table 3 are representative of those observed for the various head configurations. In addition to the parameters that were varied during the tests, two other operating parameters were held constant. The temperature of the intake air was held at 40 °C. Timing of fuel injection was adjusted for each condition to maintain the start of combustion at 4° BTDC.

## RESULTS AND DISCUSSION

Comparisons of Frictional Mean Effective Pressure (FMEP) during motoring tests are presented in Figure 6. Results for the flat plug were generally higher than that of the recessed plug or the pilot chamber. This is due to the relatively lower motoring pressure, or firing pressure, of the recessed plug and pilot chamber as illustrated in Figure 7. FMEP is a direct function of total pressure.

There was no significant difference in the FMEP between the motoring tests of the pilot chamber and recessed plug configured cylinder heads. These results are consistent with early results from Millington and Hartles (1982) that indicate that most of the pumping losses in prechamber diesel engines, unlike spark ignited engines, are due to heat transfer in the throat of the prechamber, which is a relatively minor frictional loss when compared to piston/crank assembly losses (Heywood 1988). Should pumping losses in this engine be related more to turbulent dissipation we would expect to see

**Table 3. Engine Test Conditions**

| Speed (rps) | Load[1] (N-m) | Boost Pressure (kPag) | Exhaust Pressure (kPag) |
|---|---|---|---|
| 10 | 118 | 3 | 0 |
| 10 | 164 | 79 | 23 |
| 10 | 180 | 155 | 46 |
| 17.5 | 114 | 3 | 0 |
| 17.5 | 149 | 79 | 23 |
| 17.5 | 160 | 155 | 46 |
| 25 | 112 | 3 | 0 |
| 25 | 139 | 79 | 23 |
| 25 | 144 | 155 | 46 |

[1] Rack setting adjusted to give 140 N-m torque at 15 rps.

| Cyl. Head Configuration | Engine Speed (Rev/Sec) | | |
|---|---|---|---|
| | 10 | 17.5 | 25 |
| Flat Plug | 1.62 | 1.86 | 1.65 |
| Recessed Plug | 1.33 | 1.71 | 1.52 |
| Pilot Chamber | 1.30 | 1.65 | 1.57 |

M93002378

**Figure 6. FMEP (bar) Measured During Motoring Tests (Boost = 79 KPag)**

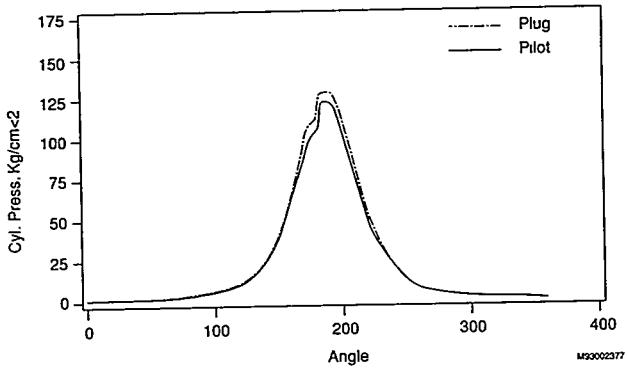


**Figure 7. Pressure Versus Crankangle**

more of an engine speed dependence. This trend may change at higher engine speeds where turbulent dissipation in areas such as the pilot chamber throat would become more significant.

With these results in mind, further differences in performance between the pilot chamber (with no fuel to the pilot chamber) and the flat plug configurations may be attributed to differences in clearance volume or compression ratio. Figures 8 and 9 below respectively compare Brake Specific Fuel Consumption (BSFC) and Specific $NO_x$ emissions of the flat plug configuration and the pilot chamber configuration. The pilot chamber configuration provides slightly better overall fuel consumption at all medium and high engine speed conditions and at low engine speed with high boost pressure. $NO_x$ levels are insignificantly different but are lower than that of the unmodified direct-injection engine configuration.

## CONCLUSIONS

Part of the baseline testing for pilot chamber operation in the METC diesel research engine was established. From these baseline data to date it is concluded that

1. Pumping frictional losses associated with the pilot chamber throat region are insignificant.

2. The effects of cylinder head modification have been partially characterized.

3. The effects of additional volume from the pilot chamber on brake specific fuel consumption (BSFC), $NO_x$ and other operating parameters have begun to be characterized.

4. A baseline for future testing with diesel fuel and CWS to the pilot chamber has begun to be established.

## FUTURE WORK

Future work will involve continued characterization of the pilot chamber's performance in the uninsulated and insulated configurations with both diesel fuel and CWS operation. The effects of engine parameter changes at constant Air/Fuel (A/F) ratio will be examined as will

| Speed | Intake Air Pressure | | | | | |
|---|---|---|---|---|---|---|
| | 3 kPag | | 79 kPag | | 155 kPag | |
| | Pilot | Plug | Pilot | Plug | Pilot | Plug |
| 10.0 RPS | 385 | 383 | 275 | 279 | 245 | 261 |
| 17.5 RPS | 335 | 381 | 265 | 283 | 256 | 265 |
| 25.0 RPS | 355 | 376 | 275 | 295 | 262 | 278 |

M93002350

**Figure 8. Comparison of Pilot Chamber With Flat Plug Test Results - BSFC (g/kWh)**

| Speed | Intake Air Pressure | | | | | |
|---|---|---|---|---|---|---|
| | 3 KPag | | 79 KPag | | 155 KPag | |
| | Pilot | Plug | Pilot | Plug | Pilot | Plug |
| 10.0 RPS | 0.7 | 0.6 | 0.9 | 1.0 | 0.6 | 0.7 |
| 17.5 RPS | 0.6 | 0.5 | 0.7 | 0.6 | 0.6 | 0.6 |
| 25.0 RPS | 0.6 | 0.5 | 0.7 | 0.6 | 0.7 | 0.7 |

M93002379

**Figure 9. Comparison of Pilot Chamber With Flat Plug Test Results - Specific $NO_x$ Emissions (LB/mBtu)**

temperature characterization of the pilot chamber during fueled operations. This effort will continue through September 1993.

MMCMIL\1:931680

## REFERENCES


Arthur D. Little, Inc. "Coal-Fueled Diesel Systems for Stationary Power Applications," DOE/MC/22182-2242 (DE87001080), September 1986.

Anson, D., S. A. Barber, H. F. Feldmann, and M. D. Gurney. "Development Plan for a Coal/Water Slurry Fired Diesel Engine for Cogeneration Applications," DOE/CE/40747-T1, July 1987.

GE Transportation Systems. "Coal Fueled Diesel Locomotive Conceptual System Economic Analysis," DOE/MC/23174-2844 (DE90009657), September 1989.

Heywood, J. B. "Internal Combustion Engine Fundamentals," McGraw-Hill, 1988.

Kakwani, R. M. and R. Kamo. "Combustion Characteristics of Dry Coal-Powder-Fueled Adiabatic Diesel Engine," DOE/MC/23258-2693 (DE89000978), January 1989.

McMillian, M. H. and H. A. Webb. "Coal-Fueled Diesels: Systems Development," Vol. 111, Journal of Engineering for Gas Turbines and Power, July 1989.

Millington, B. W. and E. R. Hartles. 1982. "Frictional Losses in Diesel Engines," SAE Paper No. 821576.

Radovanovic, R. S. and M. S. Djordjevic. 1979. "Diesel Precombustion Chamber Design and Its Influence on the Engine Performance and Exhaust Pollutants," SAE Paper No. 790496.

Robben, F. 1983. "Coal-Fueled Diesel Engines," SAE Paper No. 831747.

Slezinger, J. O. "A Life Cycle Cost Study of Six Advanced Coal-Fired Locomotive Concepts," EDR 14231, February 1989.

P7

# Pressure-Gain Combustion

George A. Richards  Joseph Yip
Randall S. Gemmen  Michael C. Janus
Thomas Norton
Morgantown Energy Technology Center

William A. Rogers
EG&G Washington Analytical Services Center, Inc.

Pulse combustion has been proposed for gas turbine applications in many early articles [1,2], and more recently has been demonstrated to produce so-called "pressure-gain" in a small gas turbine [3]. The basic concept is that the oscillatory combustion occurs as a constant-volume process, producing a gain in the stagnation pressure of air flowing through the combustor, rather than the pressure loss associated with conventional, steady combustion. If properly utilized, this pressure-gain could enhance simple-cycle gas turbine efficiency several percent, depending on the operating conditions.

In addition, pulse combustors have demonstrated relatively low $NO_x$ pollutant levels in some applications [4]. The combined potential for higher cycle efficiency and lower pollutant levels is the basis for the present investigation. Tests in progress at the Morgantown Energy Technology Center (METC) have considered a baseline pulse combustor configuration that has shown good oscillating performance, low $NO_x$ emissions, but disappointing results in terms of pressure-gain. However, a combination of numeric simulations and test data suggest that pressure-gain can be produced by a select combination of operating conditions and combustor geometry, but is especially sensitive to the combustor inlet geometry. Tests in progress will evaluate the effect of inlet geometry and operating pressure on both pollutant emissions and pressure-gain.

## EXPERIMENTAL INVESTIGATION

Current testing includes both an atmospheric pressure experiment and a high-pressure experiment. Figure 1 is a cutaway view of the atmospheric pressure pulse combustor. Measurements of pressure differences, dynamic pressures, and pollutant levels are recorded as a function of various operating and geometric parameters. Pollutant samples are collected by a sampling rake, which is centered in the exhaust duct, and is located 2 meters downstream of the mixing region. In the mixing region, dilution gas is added as a co-annular flow to the pulse combustor tailpipe gases. Mean and dynamic pressures are recorded at the combustion chamber, along with the mean pressure in the inlet plenum. The mean pressure difference between the inlet plenum and the pulse combustion chamber should give a measure of the pressure-gain achieved (up to the tailpipe inlet) during operation. Various inlet geometries can be attached to the pulse combustor inlet coupling; ideally these inlet geometries should favor flow in the forward direction, demonstrating "diodicity." Because of the diodicity, it is possible (in an unsteady flow) to achieve a net gain in pressure between the inlet plenum and the pulse combustion chamber. To date, measurements have shown that relatively simple straight (baseline geometry) or tapered inlet diffusers were not capable of producing pressure-gain.

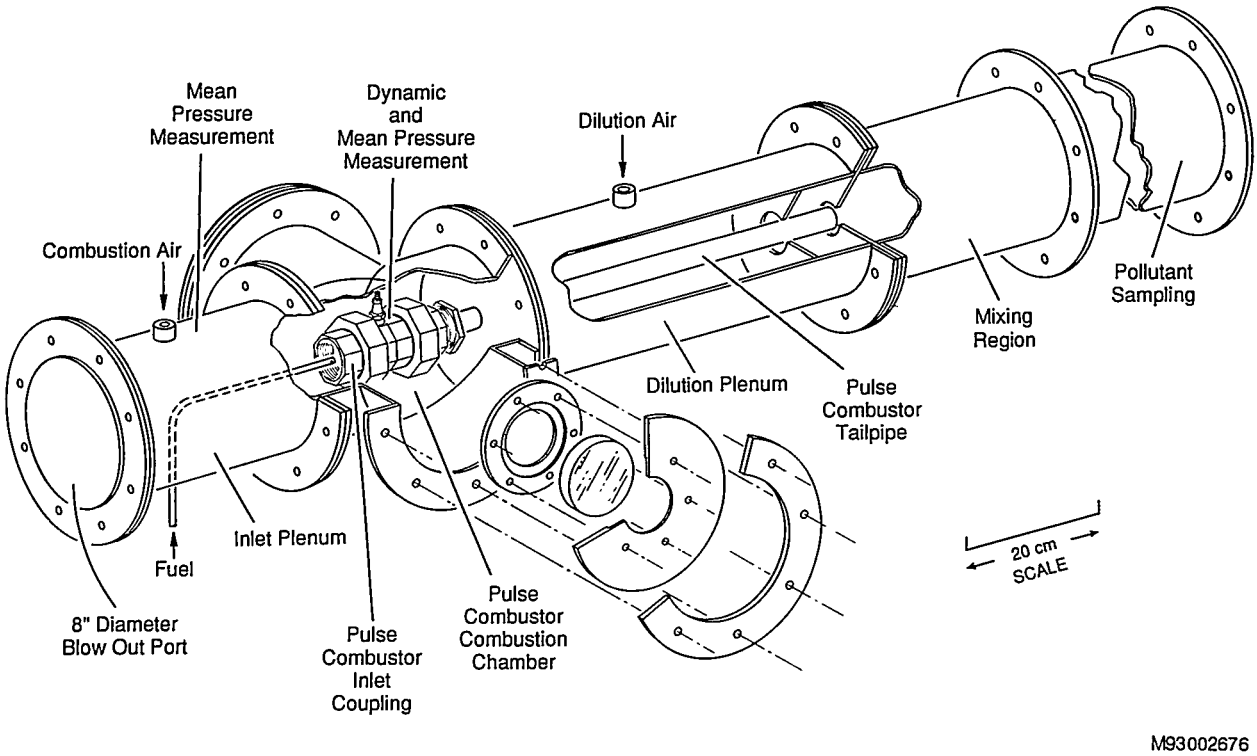


**Figure 1. Atmospheric Pressure Pulse Combustor Assembly**

Figure 2 is a plot of the measured pressure difference for the baseline geometry; the pressure drop across the inlet was smaller at lower flow rates. Notice that the drop extends above zero if extrapolated to lower flows, indicating that some pressure-gain might be achieved at the lowest flows. The laboratory combustor does not pulse at these lower flow rates, probably due to inadequate fuel-air mixing. The companion data on Figure 2 are the result of a bulk-flow numeric simulation (described below) for the baseline geometry. In comparison to the experimental data, there is a discrepancy in the magnitude of the predicted mean pressure difference, but notice that the predictions show the same trend as the lab data. Furthermore, the simulations predict a modest pressure gain at small flow rates. Unlike the laboratory combustor, the bulk flow model is run with a fixed mixing rate, such that pulsations are predicted even at the lowest flow rates. Taken together, these results suggest that a change in the flow rate (per combustor volume) is needed to produce pressure gain. This possibility is under investigation.

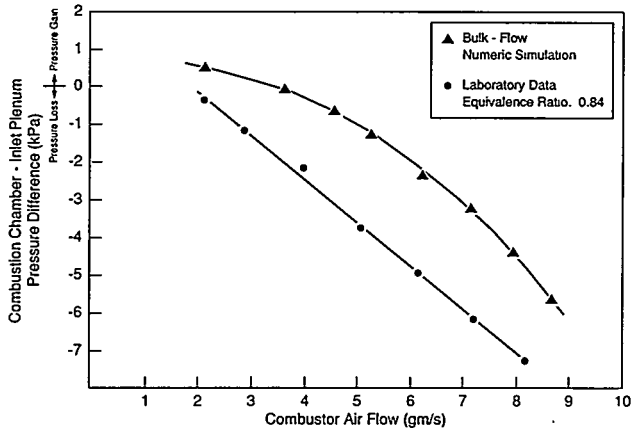


**Figure 2. Measured and predicted pressure differences between the inlet plenum and pulse combustion chamber. Positive values indicate pressure-gain.**

Figure 3 shows measurements of the pollutant levels produced in the combustor as a function of the combustor air flow and equivalence ratio. Pollutant results were obtained via analyses of grab-samples for $NO_x$, CO, and all other major species. A check on sample consistency was performed by calculating an elemental balance on the species to ensure that dilution levels were correct. Unburned hydrocarbons were detected at concentrations between 4 and 80 ppm. $NO_x$ levels were very low over the range of conditions studied, less than 10 ppm $NO_x$ at 15% oxygen. In a relatively small combustor, it would be expected that heat losses contribute to reduced $NO_x$ via associated low temperatures. However, such behavior would also result in relatively high levels of CO and unburned hydrocarbons, neither of which were recorded here. CO levels as low as 25 ppm (15% oxygen) were observed. This means that both low $NO_x$ and good combustion efficiency can be achieved under certain operating conditions.

In addition to the atmospheric pressure pulse combustor, a pressurized pulse combustor has just started operation in METC's Combustion Research Facility [5]. The pressurized combustor geometry is essentially an analogue of the atmospheric combustor experiment (Figure 4). Initial results have shown good oscillating performance at operating pressures ranging from 1 to 9 atmospheres. Measures of mean pressure differences, dynamic pressures, and pollutant level are being obtained over a range of operating pressures.

## NUMERIC SIMULATION

Numeric simulation of the pulse combustor is being carried out in several ways to complement experimental measurements, and to quickly identify parameters critical to producing pressure-gain. First, a bulk-flow model has been developed to quickly assess combustor operation as a function of major geometric and operating

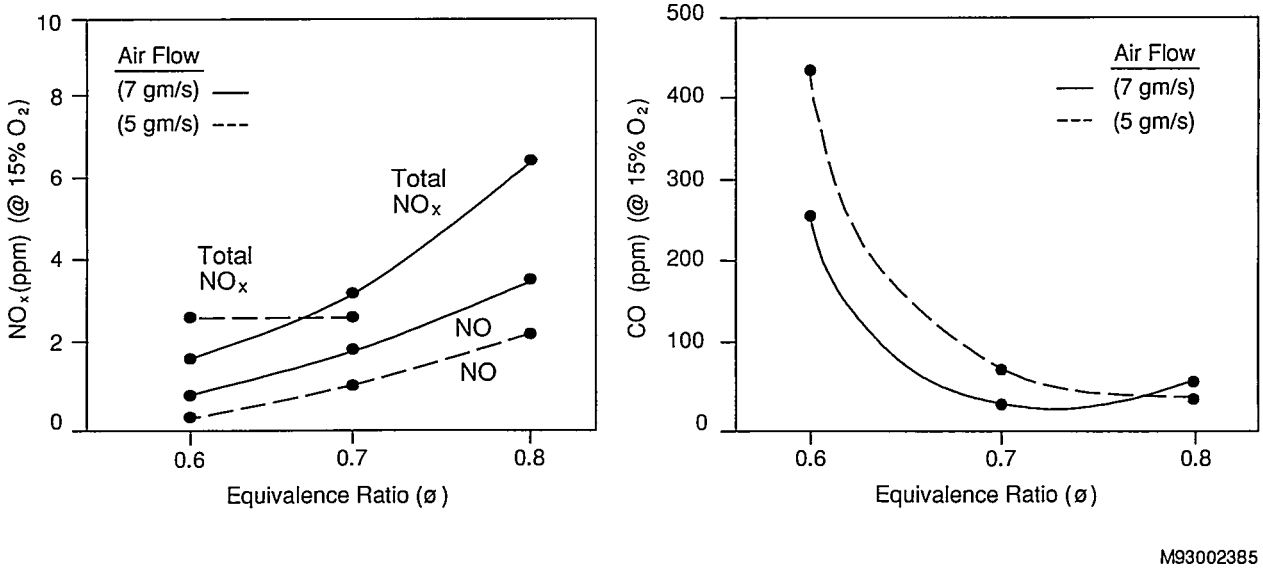


**Figure 3. Measured Pollutant Emissions From the Baseline Geometry Atmospheric Pressure Pulse Combustor**

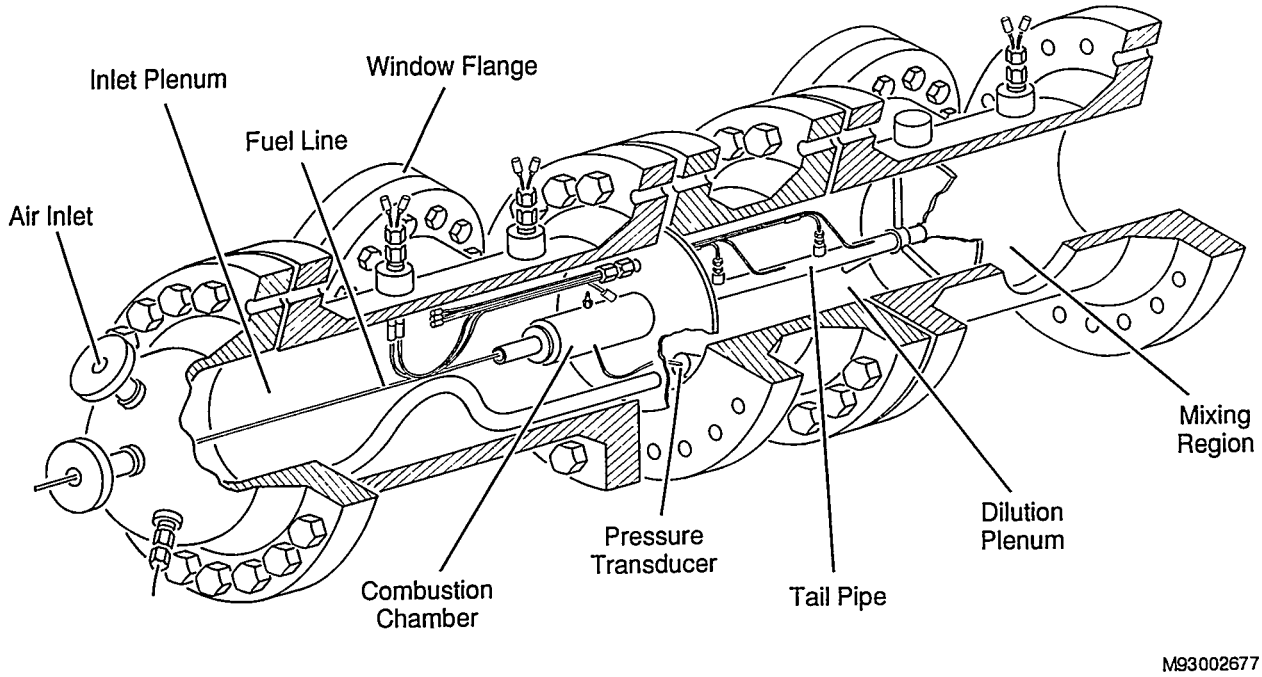


**Figure 4. Pressurized Pulse Combustor Assembly**

parameters. This bulk-flow model is essentially a control-volume analysis of the various combustor components (inlet, combustion chamber, and tailpipe), yet includes all the dynamics of mixing, chemical reaction, and flow oscillations. The model is a modification of an earlier METC approach [6] to include the mixing process in the description of the cyclic combustion. While the formulation of the model is too detailed to report here, Figure 5 shows the predicted oscillating pressure history (from start-up) in the combustion chamber. The five plots, from bottom up, demonstrate the difference in pressure history as the mixing delay is increased. The mixing delay is the time between the entry of fresh charge into the combustion chamber, and the initiation of rapid mixing between fuel and air. A noticeable difference in oscillating amplitude and frequency is evident, depending on the mixing rate. These results demonstrate the sensitivity of the oscillating performance to the mixing process; the implications for scale-up and pressure-gain are currently under study. As previously mentioned, the model has shown

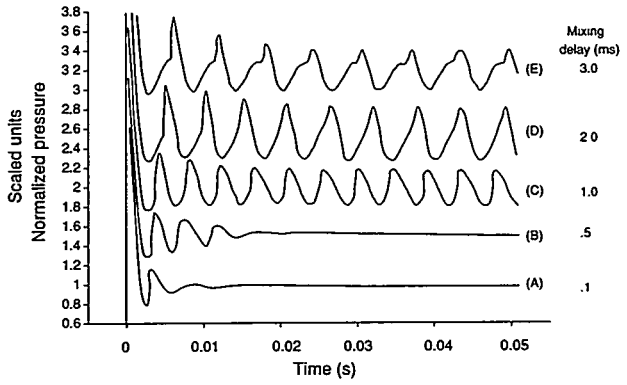


**Figure 5. Simulated Oscillating Pressure History in the Pulse Combustor From Start-up, and for Various Values of the Mixing Delay Parameter**

good qualitative agreement with laboratory measurements (Figure 2).

A more detailed quasi-one-dimensional gas dynamics simulation is being used to assess changes to the geometry of the pulse combustor inlet and exhaust. This simulation has been used to compare the effect of inlet and tailpipe geometries on the pressure-gain process. Figure 6 shows a comparison of measured laboratory pressure drop through the entire combustor (inlet plenum to mixing region) versus those predicted by the simulation for the baseline geometry; excellent agreement is obtained over the range of flow rates. Various parametric studies using this model are now underway to optimize the combustor performance.

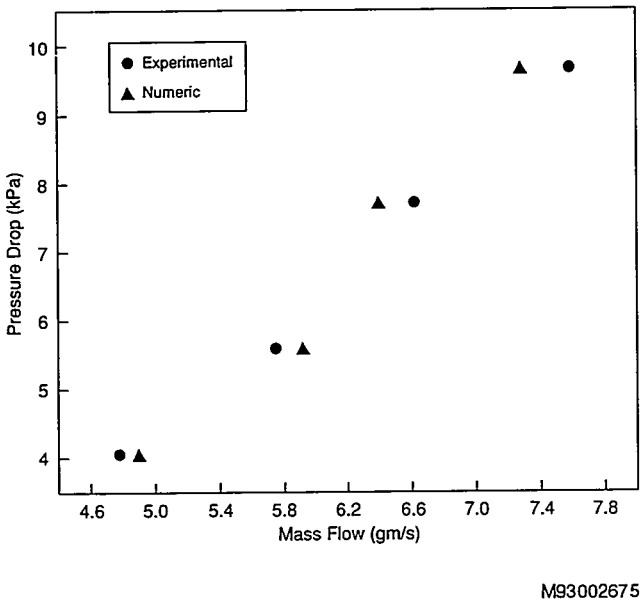


**Figure 6. Comparison of the Measured Versus Predicted Combustor Pressure Drop, from Inlet Plenum to the Mixing Region**

Finally, a commercial (FLUENT v 4.2) computation fluid dynamics (CFD) code is being used to assess the flow field in the mixing region of the exhaust duct, where dilution air is mixed with the gases exiting the tailpipe. (See Figure 1.) In any final application, the dilution air mixing process would need to be designed to utilize the oscillating flow energy where it mixes with the dilution air, and then direct this flow into a nozzle leading to the turbine. Numeric simulations of the present mixing region have been conducted in 2-dimensional axi-symmetric coordinates to gain confidence that commercial CFD codes can accurately describe this unsteady mixing process. With this confidence, eventual design concepts will be assessed numerically.

Figure 7 is a comparison of measured mean temperature profiles along the axis of the mixing region, versus those predicted by the FLUENT code. Figure 1 shows how dilution gases enter at the tailpipe exit plane in a co-annular fashion. Temperatures are normalized as indicated; distances are normalized with the tailpipe diameter. The prediction of these mean profiles is very good, suggesting that the numeric code will indeed be a useful tool to assess mean properties in various mixing geometries. Comparison of the code results to measurements of dynamic stagnation pressure is being performed as of this writing.

## FUTURE WORK

Continued work with the atmospheric pressure pulse combustor will evaluate several different inlet geometries, followed by a scale-up in size. Investigations of the pressurized pulse combustor will follow up on promising designs identified in the atmospheric pressure combustor. Measurement of pollutant emissions will be conducted at various pressure levels for the baseline geometry, and also on any design which shows promising pressure-gain performance.

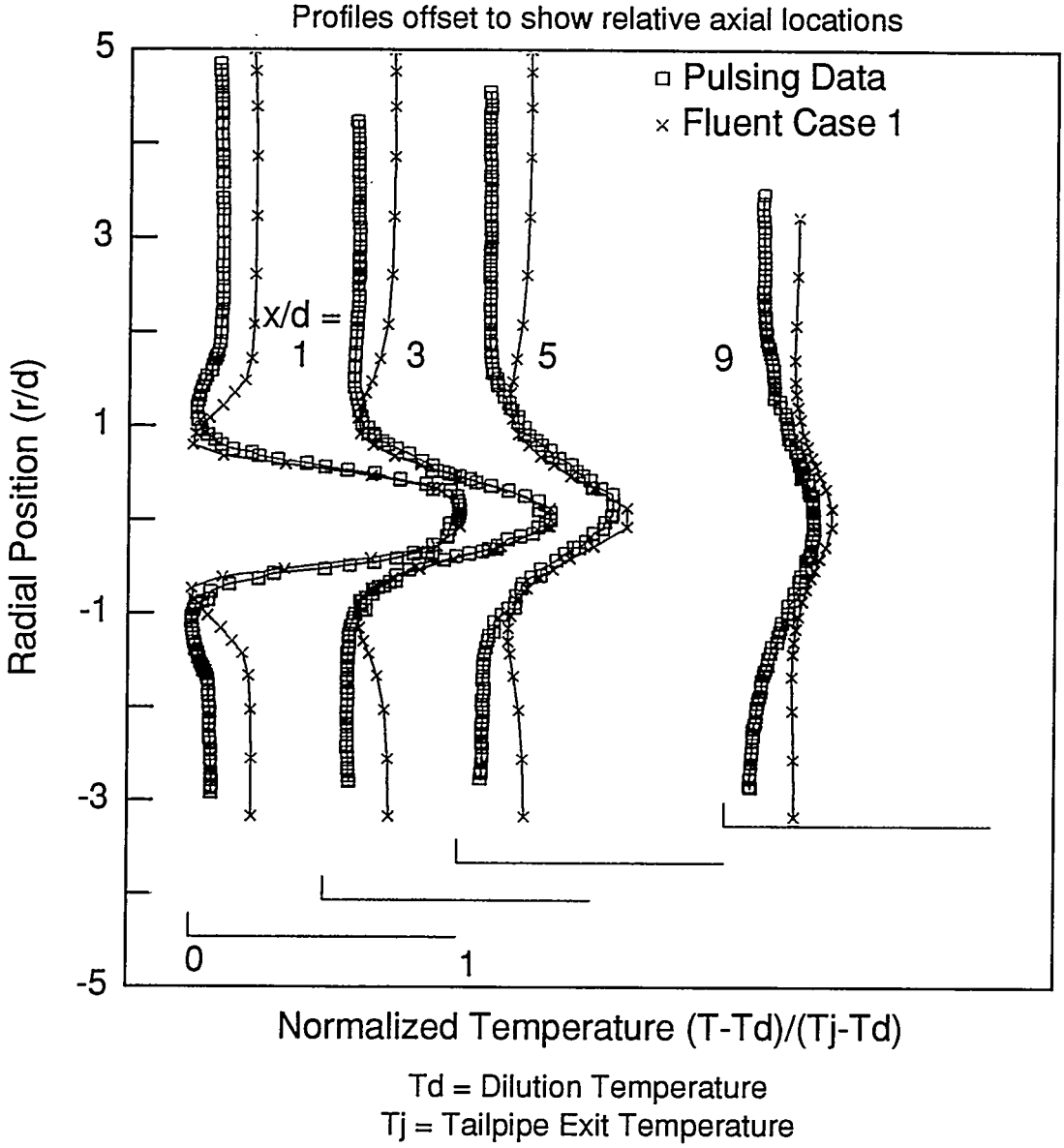


**Figure 7. Comparison of the predicted (mean) temperature profiles in the mixing region versus measurements. The x/d parameter is the axial distance measured from the tailpipe exit, normalized by the tailpipe diameter.**


1. Porter, C. D., "Valveless-Gas-Turbine Combustors with Pressure-Gain" ASME paper no. 58-GTP-11, (1958).

2. Muller, J. L., "Theoretical and Practical Aspects of Resonant Combustion Chambers in Gas Turbines," J. Mech. Eng. Sci., Vol 13, No. 3, pp. 137-150, (1971).

3. Kentfield, J. A. C., "Improvements to the Performance of a Prototype Pulse, Pressure-Gain, Gas Turbine Combustor," J. Engineering for Gas Turbines and Power, 112, pp. 67-72, January, 1990.

4. Corliss, J. M., A. A. Putnam, M. J. Murphy, and D. W. Locklin, "$NO_x$ Emissions from Several Pulse Combustors," ASME Paper 84-JPGC-APC-2, Presented at the 105th ASME Winter Annual Meeting, New Orleans (1984).

5. Halow, J. S., D. J. Maloney, G. A. Richards, "METC Combustion Research Facility," these proceedings, 1993.

6. Narayanaswami, L. L., G. A. Richards, "A Model for Aerodynamically-Valved Pulse Combustion," Central States Section of the Combustion Institute, Spring Meeting, Columbus Ohio, April 26 - 28, 1992.

# P8 Pressurized Burner Test Facility

Daniel J. Maloney
Thomas S. Norton
Mark A. Hadley
Morgantown Energy Technology Center

## OBJECTIVES

The Morgantown Energy Technology Center (METC) is currently fabricating a high-pressure burner test facility. The facility was designed to support the development of gas turbine combustion systems fired on natural gas and coal-derived gaseous fuels containing fuel-bound nitrogen. Upon completion of fabrication and shake-down testing in October 1993, the facility will be available for use by industrial and university partners through Cooperative Research and Development Agreements (CRADAs) or through other cooperative arrangements. This paper describes the burner test facility and associated operating parameter ranges and informs interested parties of the availability of the facility.

## BACKGROUND

$NO_x$ formation and removal are critical for selection of future power generation systems. Commercial vendors now offer "ultra-low $NO_x$" burners (less than 9 ppmvd $NO_x$) for gas turbine combustion systems fired on clean fuel gases (natural gas), but the demand for more efficient and cost effective power systems poses the challenge of increasing operating temperatures and pressures while burning lower quality, "dirty" fuel gases. Meeting these demands is particularly important for Integrated Gasification Combined Cycle (IGCC) and Advanced Pressurized Fluidized Bed Combustion (PFBC) Systems.

## PROJECT DESCRIPTION

The U. S. Department of Energy's METC has recently completed construction and commissioning of a new high-pressure combustion research facility. Utilities servicing the facility enable combustion tests at scales up to 3 MW (10 MM Btu/h) and pressures in excess of 3000 kPa (30 atm). These include a pre-heated, high-pressure air supply that can deliver up to 1.7 kg/s (3.7 lbs/s) of combustion air, and a high-pressure, natural gas compressor that can deliver 0.8 kg/s (.19 lbs/s). In the summer of 1994 METC's syngas generator is scheduled to come on line, at which time combustion tests on a range of fuel gases from low to medium to high heating values will be possible. The syngas generator will simulate a range of fuel gas compositions characteristic of coal gasification product streams.

As part of the combustion facility, a high-pressure burner test facility is currently being constructed to support the development of gas turbine combustion systems fired on natural gas and coal-derived gaseous fuels containing fuel-bound nitrogen. The facility, illustrated in Figure 1, is a 61-centimeter (24-inch) diameter, refractory-lined vessel of modular construction, offering the flexibility to test a variety of $NO_x$ control concepts. Burner test modules are sandwiched between gas inlet and sampling plenums with a maximum combustion test zone of 2.2 m (90 inches) in length. Modules are custom designed for specific burners or combustion cans

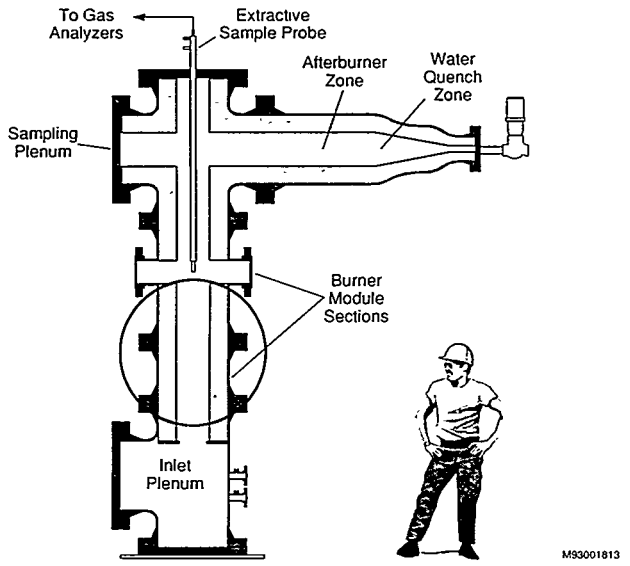


**Figure 1. Pressurized Burner Test Facility Assembly Drawing**

by varying the internal wall diameter and mating to the inlet gas plenum. Figures 2 and 3 are conceptual drawings illustrating test modules for studying a porous radiant burner and a small turbine combustion can. The facility is instrumented with an array of combustion gas analyzers for measurement of CO, $CO_2$, $O_2$, and unburned hydrocarbons, as well as NO, $NO_2$, and $N_2O$. Optical access ports are also available for advanced optical diagnostics.

Combustion tests can be conducted using either natural gas or simulated, coal-derived, low heating value gas mixtures at scales ranging from 0.03 to 3 MW (0.1 to 10 MM Btu/h) and pressures exceeding 3000 kPa (30 atmospheres). A bottled gas mixing system is included in the facility for simulating combustor fuel gases typical of IGCC or Advanced PFBC applications at scales up to 60 kW. In the summer of 1994, METC's syngas generator is scheduled to come on line, at which time the facility will be capable of operation on low heating value fuels at scales up to 2 MW.

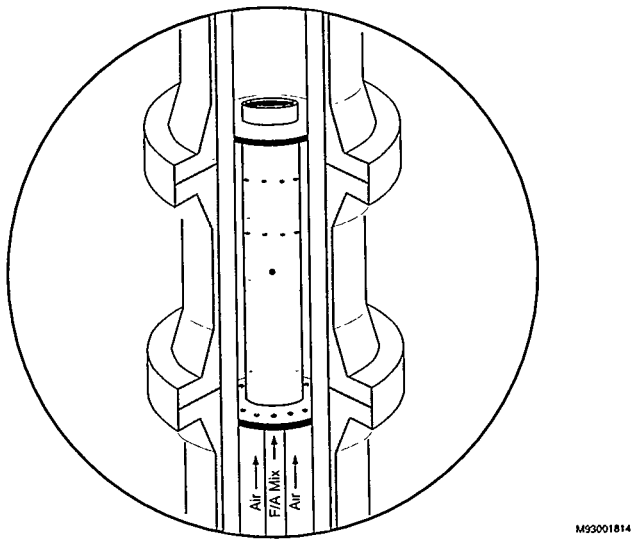


**Figure 2. Conceptual Drawing of Burner Module Configured for Small Can Combustor Tests**

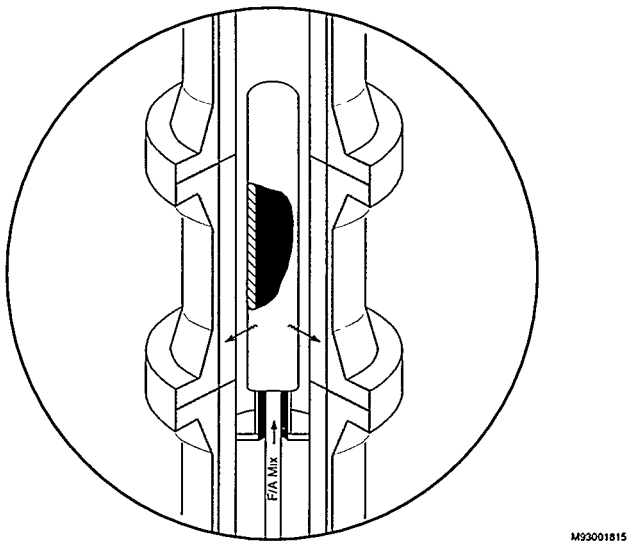


**Figure 3. Conceptual Drawing of Burner Module Configured for Porous Radiant Burner Tests**

Computational Fluid Dynamics (CFD) codes such as FLUENT and PCGC-3 are available at METC and are applied for simulation of flowfields, temperature, pressure, and chemical species distributions for proposed burner designs; evaluation of effects of burner design modifications on $NO_x$ and CO emissions; and evaluation of experimental results. In addition, reduced (simplified) chemical $NO_x$ formation mechanisms are being evaluated for inclusion in the CFD codes to improve $NO_x$ formation predictive capabilities.

## FUTURE WORK

Shakedown testing of the burner test facility is scheduled for October 1993. At present, discussions are in progress with two potential private-sector partners through cooperative research. Future plans include high-pressure combustion tests using some basic, flame holder designs, a porous radiant burner, and some small commercial, turbine combustion cans. The facility is available to industrial and university partners through CRADAs or other cooperative arrangements. Interested parties should contact one of the authors.

DMALON\3:931413a

# P9 Premixed Burner Studies of NOx Formation and Control

Kent H. Casleton
Doug L. Straub
Colleen Moran
Morgantown Energy Technology Center

James W. Stephens[†]
National Research Council

## OBJECTIVES

The overall goal of this lab-scale project is to support the accelerated development of low $NO_x$, low CO emissions combustors for heat engines burning natural gas or coal-derived fuels. This will be accomplished through a combination of lab-scale burner studies and chemical kinetic modeling activities. In this way, improved $NO_x$ control methodologies as well as more reliable instrumentation systems and techniques can be identified and implemented for larger scale systems.

## BACKGROUND INFORMATION

The demand for efficient, environmentally sound energy sources provides substantial incentive for the development of gas turbine systems with very low $NO_x$ emissions characteristics. Further, the development of low $NO_x$ burners that are capable of utilizing low-heating-value gases derived from coal-based systems is an essential component for a number of fossil energy technologies including IGCC and second-generation PFBC. However, the chemistry associated with $NO_x$ formation is complicated, and attempts to reduce these emissions often result in increases in other undesirable species such as CO or $N_2O$. In view of these complexities, it is useful to study $NO_x$ formation and control strategies in a well-controlled, lab-scale burner system. In this way, detailed knowledge about the intricate interrelationships between the various chemical pathways can be obtained and subsequently applied to bench-scale and larger systems. The current project involves both chemical kinetic modeling as well as experimental studies performed in a premixed burner system to generate these data.

## PROJECT DESCRIPTION

### Burner Studies

The burner system incorporates a commercially available flat flame burner, associated gas supply system, thermocouple and gas sample probes, and gas analyzers. A schematic drawing of the burner system is shown in Figure 1. The flat flame burner consists of a 6-cm diameter, porous sintered stainless steel disk surrounded by a 0.5-cm wide sintered-bronze shroud ring. Nitrogen is flowed through this outer ring to help contain the products of combustion and to prevent entrainment of room air in the post-flame gases. Reactant gases, in this case either methane and air or a synthetic fuel gas mix and air, are premixed and fed to the base of the burner. The mass flow rates of fuel and air are measured and controlled by means of calibrated mass flow controllers. At present all burner studies are performed at atmospheric pressure.

---

[†]Present address: National Institute of Occupational Safety and Health, Morgantown, WV, 26505

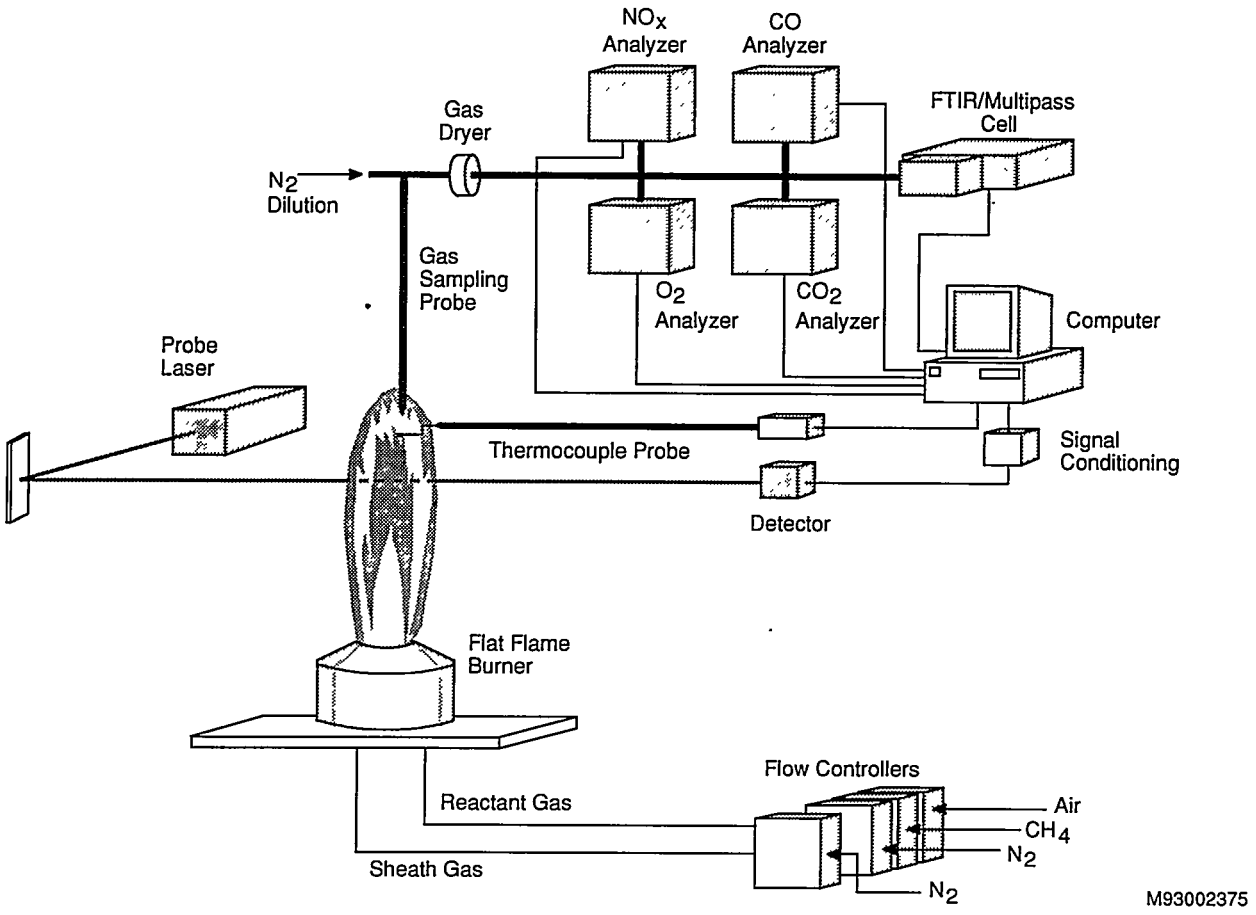


**Figure 1. Flat Flame Burner System**

Thermocouple and gas sampling probes are mounted on translation stages and extend into the zone of burned gases above the burner. Using these translation stages, the probes can be positioned in the horizontal, X-Y, plane above the burner. The burner is mounted on a computer-controlled, vertical translation stage to accurately control the height of the burner, Z, relative to the fixed heights of the thermocouple and gas sampling probes. By varying the distance between the thermocouple and gas sampling probes and the surface of the burner, different time-histories of the post-flame zone can be sampled and analyzed. By coupling the X-Y motion of the probes with the vertical motion of the burner relative to these probes, three-dimensional maps of temperature and species concentration profiles can be generated.

The temperature of the burned gases is measured using uncoated Pt-90% Pt/10% Rh thermocouples. These thermocouples are constructed from 28 ga. (0.33 mm-diameter) wire and have bead diameters in the 0.7 to 1.0 mm range. Temperature measurement errors due to radiative heat loss can be estimated using the formalism described by Lyons and Gracia-Salcedo (1989).

Gas samples are extracted from the burner exhaust through a water-cooled stainless steel gas sampling probe. Cooling water for the probe is typically maintained at temperatures near 80 to 90°C to minimize condensation of water vapor in the sample lines. Heat-traced 6.3-mm o.d. teflon tubing connects the outlet of the gas sample probe with a condenser. The cooling water to the condenser is maintained at approximately 2°C using a refrigerated water bath. A diaphragm pump draws the gas samples through the probe to supply the gas analyzers.

Analyses of gas samples extracted from the burner exhaust is performed using a number of continuous gas analyzers. Commercial analyzers are available to measure $O_2$, $CO_2$, CO, and NO/$NO_x$. Gas analyzers are calibrated by flowing appropriate calibration gas mixtures through the instruments prior to use in the burner experiments. A Fourier transform infrared (FTIR) spectrometer is also available for simultaneous determination infrared-active gases in batch samples withdrawn through the probe.

### Modeling Studies

In conjunction with the experimental studies performed with the burner, modeling studies are also performed to give insights regarding the chemical processes controlling the formation and removal of the contaminant species. The codes utilized here are a part of the CHEMKIN-family of chemical kinetic codes developed at Sandia National Laboratory (Kee and Miller 1986; Kee et al. 1989). These codes can be employed to simulate a variety of different applications including plug-flow reactors (CHEMKIN, SENKIN), well-stirred reactors (PSR), and premixed flames (PREMIX). By combining the predictions of these codes with detailed chemical species and temperature profile measurements obtained from the burner system, insights regarding the important chemical mechanisms can be found. This improved knowledge of the mechanisms that control these formation and removal processes can then be used to develop improved burner designs and $NO_x$ control strategies. In addition, a careful comparison of the model predictions of species profiles with the experimental measurements can be used in validation studies of various chemical kinetic $NO_x$ models that are found in the literature.

## RESULTS

One of the primary reasons for using this type of premixed, flat flame burner is that it is essentially one-dimensional (1-D), i.e., that important parameters such as temperature are nearly constant in regions near the central vertical axis of the burner for a fixed height above the burner surface. As a result of this 1-D nature, computer codes such as Sandia National Laboratory's PREMIX can be used to model the important chemical interactions involved in the combustion processes. These predictions can be compared with experimental measurements to gain valuable insight into the formation of nitrogen oxides.

The bulk of the burner experiments performed to date have been focussed primarily toward characterization of burner and the sample extraction and analysis system. All experiments thus far have been for methane/air flames at one atmosphere pressure. Figure 2 shows the burner centerline temperature profile for an equivalence ratio of $\Phi = 0.87$. The sharp peak in temperature near 0.3 cm corresponds to the luminous zone of the flame. The high temperature in the luminous zone shows an abrupt decay with increasing height above the burner. The temperature gradient in the non-luminous post-flame zone is much smaller, approximately 2.5°C decrease in temperature for each millimeter increase in height over the range of 1.3 to 4 cm above the burner. Radial temperature profiles have also been measured to assess the one-dimensional nature of this burner. Figure 3 shows radial temperature measurements for an

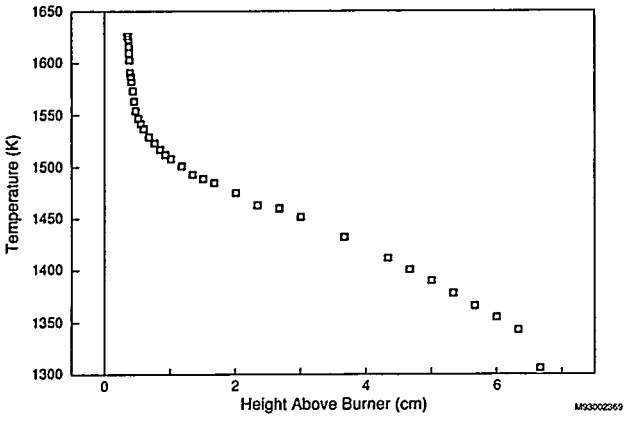


**Figure 2. Burner Centerline Temperature Profile**

array of three separate thermocouples for a $\Phi$ = 0.87 flame. This thermocouple rake was positioned at a particular height above the burner surface and temperatures recorded as a function of radial distance from the center of the burner. The central plateaus are quite flat with fluctuations in temperature of usually less than ±5°C. The flat plateau narrows with increasing height above the burner, probably due to flow instabilities as well as increased mixing of the sheath nitrogen with combustion products.

Concentration profiles have also been obtained for the species CO, $CO_2$, $O_2$, NO, and $NO_2$. These profiles can be compared with predicted profiles calculated by the PREMIX code. A modified version of the Miller and Bowman (1989) kinetic mechanism for $NO_x$ was used in these calculations. Figure 4 shows a comparison of model predictions and measured NO concentrations along the burner centerline for a $\Phi$ = 0.87 flame. Two important observations can be made. First, the model substantially underpredicts the NO concentration. This may be due to the overall low NO concentration. Most $NO_x$ kinetic models are developed and optimized for conditions appropriate to higher NO levels. Thus additional attention may be required to refine them for conditions appropriate to low-$NO_x$ combustion. Second, the measured NO profile rises to its maximum much more slowly than does the predicted curve. The model prediction for this set of experimental conditions suggests that essentially all the NO formation process is completed within the luminous flame zone with no significant variation in the NO level in the post-flame zone. In contrast, the experimental curve has a much slower rise with height above the burner, reaching its 1/e point at approximately 1.2 cm, well outside the flame zone.

As a result, measurements for this set of conditions were repeated. However, the gas velocity through the gas sampling probe was reduced to better approach isokinetic sampling conditions. This was thought to be important perhaps because of the relatively large size of the sampling probe (approximately 5 mm i.d.). Also the chemiluminescent $NO_x$ analyzer was operated in both the NO as well as the $NO_x$ mode to acquire profiles for NO and (NO+$NO_2$). Data obtained in this experiment are shown in Figure 5. The filled circles show the $NO_x$ (i.e., NO + $NO_2$) and NO curves, respectively. The difference between these two curves is labeled "$NO_x$ - NO". This should represent the $NO_2$ concentration reaching the $NO_x$ analyzer. While the NO curve exhibits the same slow increase in concentration with increasing probe height above the burner, now the $NO_x$ curve rises very sharply near the location of the luminous flame zone. This suggests that, while the orifice size of the sampling probe may have contributed to the large uncertainty in the point measured near the edge of the luminous zone near z = 0.35 cm, this is not likely the cause of the slow rise of the NO curve.

As seen previously, the peaks of the NO and $NO_x$ experimental curves are much higher

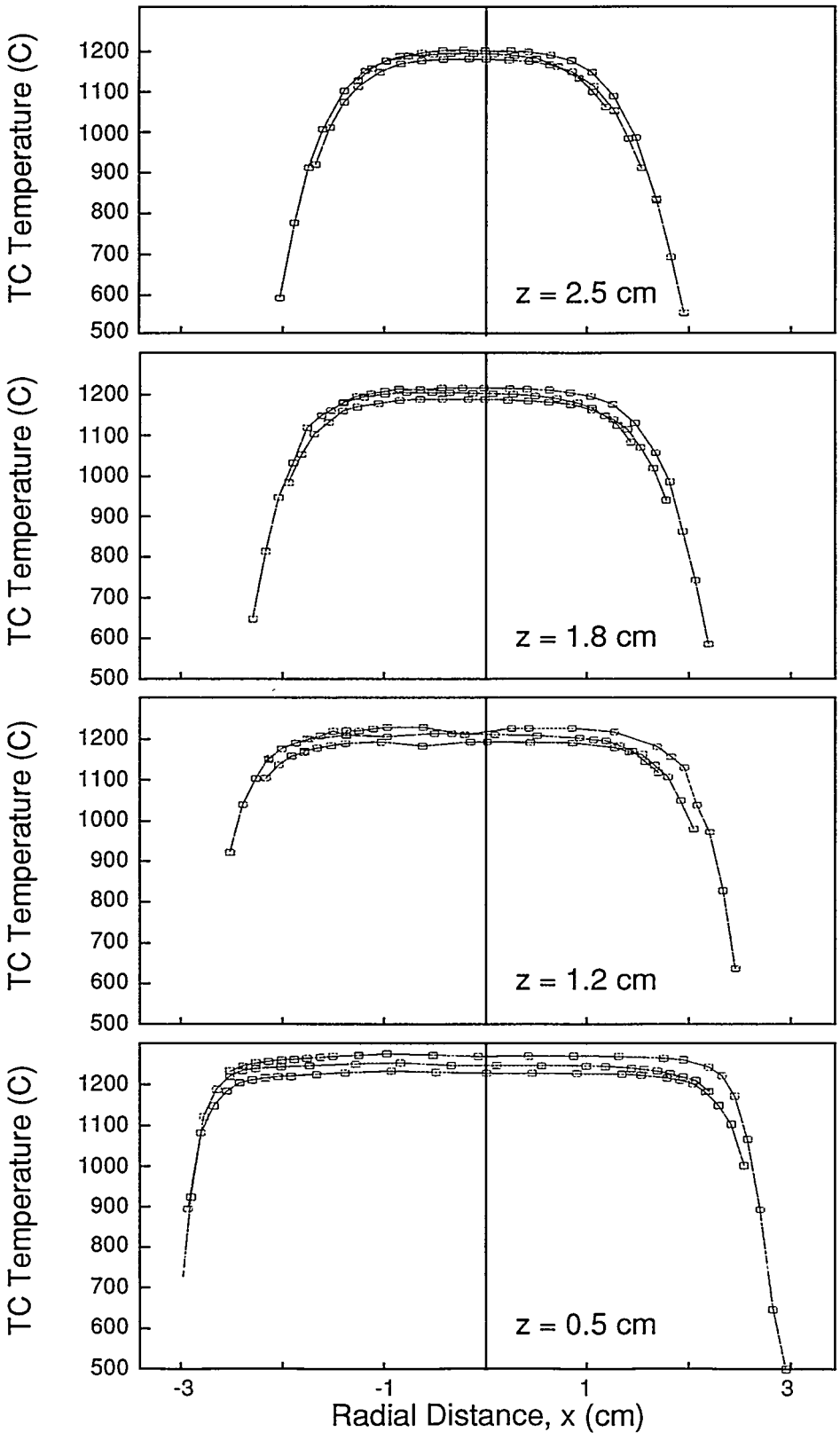


**Figure 3. Radial Temperature Profile Versus Height Above Burner**

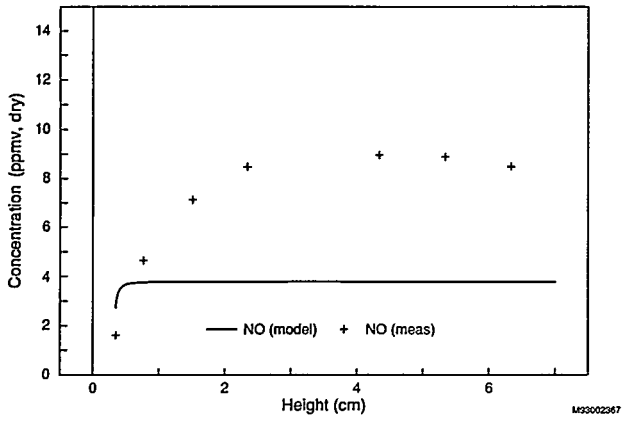


**Figure 4. NO Centerline Concentration Profile**

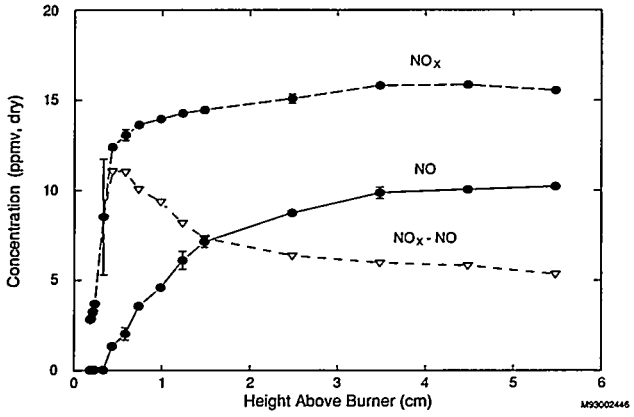


**Figure 5. $NO_x$ Concentration Profile**

than the model predictions. In fact most models typically predict only negligible amounts of $NO_2$ formed compared to NO for similar conditions. Several reports in the literature suggest that chemical conversions of NO to $NO_2$ and CO to $CO_2$ can occur in sampling probes (Kramlich and Malte 1978). It is generally believed that the conversion of NO to $NO_2$ occurs via the presence of $HO_2$ radical concentrations in the quenched gas samples.

To assess the magnitude of this effect for the present experimental conditions, the Sandia code SENKIN (Lutz et al. 1988) was used to calculate species concentration profiles within the sampling probe. An initial temperature of 1500 K, constant gas pressure of one atmosphere, and initial gas composition calculated by the PREMIX code were assumed. An entrance length calculation for flow in a uniform straight duct with convective cooling by constant-temperature walls was performed to estimate the fluid mean temperature distribution (White 1988). A relationship between mean gas temperature and reaction time was developed from this calculation and subsequently used in the SENKIN calculations. Preliminary results indicate that a large fraction of the initial NO may be converted to $NO_2$ in this type of gas sampling probe. However, the split between NO and $NO_2$ in the final calculated gas composition does not match well with the experimental results. Also, in contrast to previous studies indicating that total $NO_x$ is conserved in these sampling probes, these preliminary results suggest a large fraction of the initial NO is lost, presumably to $N_2$. A more detailed study of these issues is required.

## FUTURE WORK

Future activities will include the design, construction, and evaluation of a quartz microprobe for improved gas sampling. Sample probe effects in both probes will be further investigated. In particular, we wish to assess the validity of the initial results regarding the loss of $NO_x$ species in the water-cooled stainless steel probe. These conclusions may have a significant impact on directions taken in designing probes for larger-scale studies to be performed

in the Combustion Research Facility at METC. To test the validity of the CHEMKIN model predictions performed to date, other $NO_x$ models presently in the scientific literature will be utilized, and comparisons with experimental data will be made. Finally, additional experimental studies utilizing synthetic fuel gas mixtures will be initiated.

## REFERENCES


Kee, R. J., and J. A. Miller. 1986. *A Structured Approach to the Computational Modeling of Chemical Kinetics and Molecular Transport in Flowing Systems*. Sandia National Laboratories Report SAND86-8841.

Kee, R. J., F. M. Rupley, and J. A. Miller. 1989. *Chemkin-II: A Fortran Chemical Kinetics Package for the Analysis of Gas-Phase Chemical Kinetics*. Sandia National Laboratories Report SAND89-8009.

Kramlich, J. C, and P. C. Malte. 1978. Modeling and Measurement of Sample Probe Effects on Pollutant Gases Drawn from Flame Zones. *Combustion Science and Technology*. 18:91-104.

Lutz, A. E., R. J. Kee, and J. A. Miller. 1988. *A Fortran Program for Predicting Homogeneous Gas Phase Chemical Kinetics with Sensitivity Analysis*. Sandia National Laboratories Report SAND87-8248.

Lyons, V. J., and C. M. Gracia-Salcedo. 1989. *Determination of Combustion Gas Temperatures by Infrared Radiometry in Sooting and Nonsooting Flames*. NASA TP-2900, AVSCOM TR 88-C-008.

Miller, J. A., and C. T. Bowman. 1989. Mechanism and Modeling of Nitrogen Chemistry in Combustion. *Prog. Energy Combust. Sci.* 15:287-338.

White, F. M. 1988. *Heat and Mass Transfer*, 300-308. Reading, MA: Addison-Wesley.


KCASLE\1:931664

P10

# The DOE NEPA Process

Suellen A. Van Ooteghem
Morgantown Energy Technology Center

## OBJECTIVES

The National Environmental Policy Act (NEPA) declares that Federal agencies shall have a general commitment to "use all practicable means" to conduct their activities in a way that will promote "the general welfare where man and nature can exist in productive harmony." Within these general guidelines, the manner in which NEPA requirements are implemented may be somewhat different and unique from one Federal agency to the next.

A brief overview indicating the types of NEPA documents that are produced by the Department of Energy (DOE) in compliance with NEPA is shown in the figure. This figure indicates that the level of NEPA documentation required for any given project is graded and dependent on that project's size, complexity, and potential consequences to health and the human environment. More complex projects with potentially greater environmental impacts require a much more in-depth analysis to ensure that these potential consequences can be managed and/or mitigated, so that the proposed project can proceed in compliance with NEPA.

It is important to keep in mind the following points when conducting any project that involves Federal land, Federal monies, or Federal permits:

- Under these conditions (involvement of Federal lands, use of Federal monies, or requirement for Federal permits), some level of NEPA analysis and documentation is required.
- The NEPA process must be completed and a decision favorable to the proposed project must be supported by the NEPA analysis before that proposed project can fully expend Federal funds.
- Activities that cannot proceed until the NEPA analysis and decision-making process is completed are those that:

  1. Result in an adverse environmental impact (such as destroying the habitat of the spotted owl before considering the potential consequences of such an action) and/or

  2. Limit the choice of reasonable alternatives (such as destroying an archeological site before analysis of the potential losses that might result).

Based on the current experience at the Morgantown Energy Technology Center (METC), the level of NEPA documentation required for the preponderance of all METC projects is a Categorical Exclusion (CX).

A CX normally requires less than 2 months to complete. A certain number of more complex projects will, however, require Environmental Assessments (expected to take from between 8 months to more than 2 years to complete), and a few projects with the potential for complex environmental consequences will require an even greater depth of analysis, with development of an Environmental Impact Statement (usually requiring more than 2 years to complete).

# NEPA DOCUMENTATION FLOWCHART

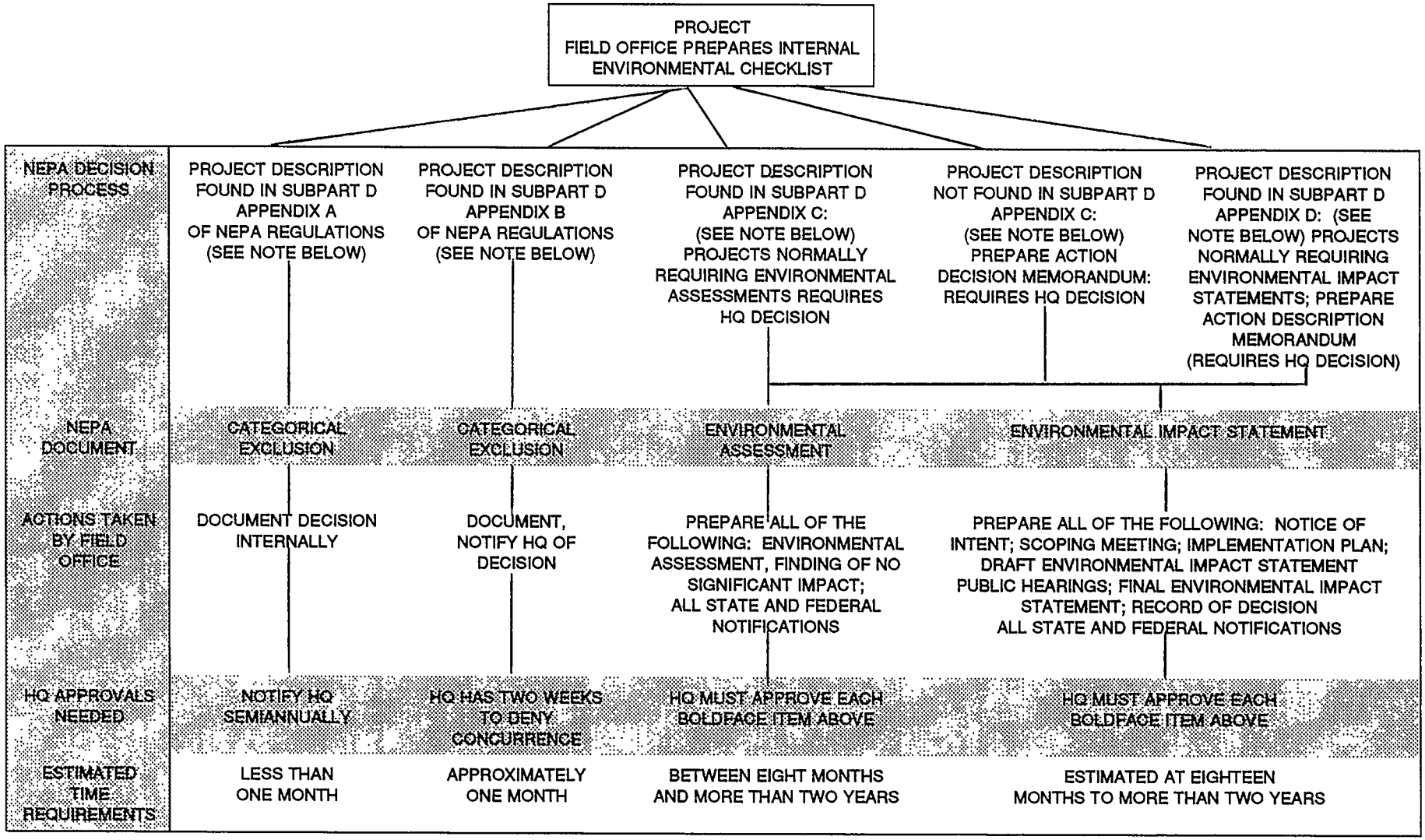


NOTE: DOE NEPA Implementation procedures are defined in the Federal Register (57 FR 15122, April 24, 1992).

Guidelines regarding the NEPA decision-making process and development of NEPA documentation can be obtained from DOE/METC environmental personnel, and additional information can be obtained from the references.

## REFERENCES


1. The National Environmental Policy Act of 1969, as amended, Pub. L. 91-190, 42 U.S.C. 4321-4327, January 1, 1970 as amended by Pub. L. 94-52, July 3, 1975, and Pub. L. 94-83, August 9, 1975.

2. Council on Environmental Quality-Regulations for Implementing NEPA Requirements, 40 CFR Parts 1500-1508.

3. Department of Energy, National Environmental Policy Act; Implementing Procedures and Guidelines Revocation; Final Rules, 10 CFR 1021.

## P11 Research and Development of Alternative Components at Argonne National Laboratory for Molten Carbonate Fuel Cells

### CONTRACT INFORMATION

| | |
|---|---|
| **Contract No.:** | **49943** |
| **Contractor:** | **Argonne National Laboratory<br>9700 S. Cass Avenue<br>Argonne, IL 60439<br>708 252-4038** |
| **Contract Project Manager:** | **K. M. Myles** |
| **Principal Investigators:** | **M. Krumpelt and G. H. Kucera** |
| **Co-Investigators:** | **M. Roche and E. Indacochea** |
| **METC Project Manager:** | **W. C. Smith** |
| **Period of Performance:** | **October 1, 1982 to Open** |

FY93 Program Schedule

FY93 PROGRAM SCHEDULE

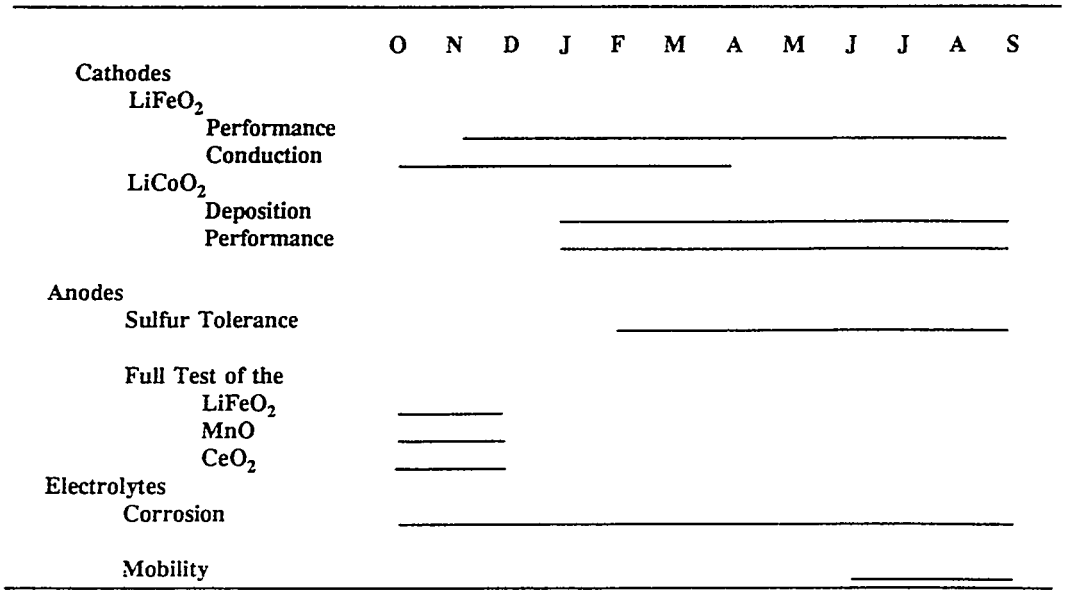

## OBJECTIVES

The objective of this project is to address the technical problems that limit the lifetime of the molten carbonate fuel cell (MCFC). The overall effort is focused on assessing electronically conductive ceramic oxides as electrode materials and determining the effectiveness of alternative electrolyte formulations at reducing nickel oxide solubility, minimizing differential electrolyte migration, and reducing component corrosion.

## BACKGROUND INFORMATION

Many of the technical problems associated with the lifetime of molten carbonate fuel cells are materials related. In earlier work at ANL (1), various ceramic materials were identified as being stable in the anode and/or cathode environment. These materials were selected for development as alternatives to the NiO cathode and Ni/Cr anode presently used in the MCFC. For cathode use, because these ceramic materials are poor conductors, dopants are added to improve their electronic conductivity. For anode use, many of the materials have good, inherent conductivity, and dopants are added to further enhance that conductivity. For the progression from conductive material to electrode, fabrication processes have been developed to form elongated agglomerates which can be tape cast into structures with the desired bimodal pore distribution and porosity for electrode use.

Lithium ferrate ($LiFeO_2$) and lithium cobaltate ($LiCoO_2$) were selected as promising candidates for the cathode materials. In previous work (2), $LiFeO_2$ cathodes with individual dopants of Co, Ni, Mn, and Cu were tested in half cells to determine any possible effects on performance due to the chemical nature of the dopant or the electrical conductivity of the material. With the standard laboratory oxidant of 14% $O_2$-28% $CO_2$-58% $N_2$ at ~100 kPa pressure and an operating temperature of 650°C, the performance of these doped $LiFeO_2$ cathodes was similar. However, the best performing electrode was still about 225 mV poorer than a state-of-the-art NiO cathode. When the oxygen partial pressure was increased from ~15 to ~70 kPa, the best performing electrode (Co-doped $LiFeO_2$) is now only about 60 mV poorer than the NiO performance. These data suggest that Co-doped $LiFeO_2$ has promise as a cathode under high pressure operation, where the oxygen partial pressure could reach as high as 150 kPa.

To understand the factors influencing the behavior of these electrodes, Seebeck coefficients were measured as a function of temperature and oxygen partial pressure. Of the four doped materials, only Ni-doped and Co-doped $LiFeO_2$ showed the desired positive Seebeck coefficient. In addition, this coefficient was relatively insensitive to temperature. The positive coefficient is indicative of a p-type conductor in which holes are the primary charge carriers. This type of conductor undergoes an enhancement in the number of charge carriers with increasing oxygen partial pressure, and this enhancement could account for the improvement in cell performance.

Cathodes of undoped $LiCoO_2$ were studied in a manner similar to that of the $LiFeO_2$ cathodes. The half-cell performance was good, with overpotentials similar to those of NiO. The Seebeck coefficient was positive and insensitive to temperature. In general, these characteristics suggest that this material has promise as a substitute for NiO. However, this material, like NiO, dissolves in the electrolyte and deposits in or near the anode. Nevertheless, because the solubility of $LiCoO_2$ is less than that of NiO, it remains a candidate for use as a MCFC cathode.

Of the various potential anode materials identified, several doped and undoped $LiFeO_2$ anodes and a Mg-doped MnO anode were tested in 25-$cm^2$ full cells against a NiO cathode. The $LiFeO_2$ dopants were Mn, Co, Ni, and Nb. None of these alternative anodes performed as well as a state-of-the-art Ni/Cr anode. In addition, none was able to support current densities greater than about 80 $mA/cm^2$. Post-test analysis of these cells showed that all of the anodes suffered from at least some chemical instability. Other potential anode materials are under test; these include Nb-doped $CeO_2$, undoped $Li_2TiO_3$, and Mo-doped $Li_3VO_4$.

Fundamental molten-salt theories, used to predict NiO solubilities in binary alkali metal carbonate melts, were expanded to include ternary salt systems (3-5). The calculations indicate that the addition of an alkaline earth carbonate to binary alkali metal carbonate melts would lower the NiO solubility. The addition of about 20 mol% $CaCO_3$ to 70 mol% $Li_2CO_3$-30 mol% $K_2CO_3$ was found to reduce the NiO solubility at 650°C from about 9.5 wppm to about 3 wppm. A similar effect was seen when $CaCO_3$ was added to $Li_2CO_3$-$Na_2CO_3$, where the NiO solubility was reduced to 1 wppm. Thermal analyses of the ternary mixtures have shown that Li/K/Ca melts have liquidus temperatures $\leq 550^0$C, whereas the Li/Na/Ca melt has a liquidus temperature of about $610^0$C, making it unsuitable for use in an MCFC (operating temperature, ~650°C). The effect of the new electrolyte on other cell components has yet to be determined.

## PROJECT DESCRIPTION

This project consists of work in several areas of MCFC component development: alternative cathodes and anodes are being evaluated in 25-$cm^2$ full cells, and alternative electrolytes, shown to possess a low NiO solubility and a low liquidus temperature, are being studied.

Full-cell tests are being carried out with Co-doped and doubly-doped $LiFeO_2$ cathodes and with undoped $LiCoO_2$ cathodes. The performance of these cathodes is being studied as a function of oxygen partial pressure and carbon dioxide partial pressure at ambient pressure, as well as under simulated high pressure operation. In addition, post-test analyses are underway to assess the chemical composition of the electrode, the electrode morphology, and the cobalt loss as a function of test duration.

Ceramic anodes are being developed as alternatives to the current Ni/Cr and Ni/Al electrodes. The ceramic anodes are expected to provide better tolerance to sulfur-containing fuel gases. Ceramic anodes consisting of Nb-doped $CeO_2$ were tested in full cells against a NiO cathode. The sintering characteristics and electronic conductivity of Mo-doped $Li_3VO_4$ are also being studied. In addition, an anode half-cell test stand has been designed and operated with standard Ni/Cr anodes to verify the apparatus design and merits of the results obtained.

Alternative electrolytes are being developed as another approach to solving the dissolution/precipitation problem of the NiO cathodes. Melt compositions that have low NiO solubility and low liquidus temperatures have been identified. However, other requirements must also be met for any new electrolyte to be considered for use in a fuel cell. The cathode polarization, corrosion properties, and the differential ion migration must still be considered. Currently, the corrosion properties and the cathode polarization are under study.

## RESULTS AND ACCOMPLISHMENTS

### Cathode Development

In previous work, the half-cell performance of several doped $LiFeO_2$ cathodes was reported (2) as a function of oxygen partial pressure and carbon dioxide partial pressure. The data suggested that the performance differences at high oxygen partial pressure might have been due to the relative catalytic activities of the various dopants or to the type of charge carriers. Seebeck-coefficient measurements, made to determine the dominant charge carrier type, showed that the cathode that exhibited the greatest improvement in performance with increasing oxygen partial pressure (Co-doped $LiFeO_2$) was a p-type conductor with little or no component attributable to electrons. The results of the earlier work also suggested that the Co-doped $LiFeO_2$ cathode would be a good electrode for use under pressurized fuel cell operation, where the oxygen partial pressure would be significantly higher than in ambient-pressure cells. To determine how great the effect of higher oxygen and carbon dioxide partial pressures would be on performance, full cells were operated with Co-doped $LiFeO_2$ cathodes under simulated pressurized conditions. The data also suggested that an electrode possessing the p-type characteristics exhibited by the Co-doped $LiFeO_2$ have potential for good cell performance. Undoped

$LiCoO_2$ and doubly-doped $LiFeO_2$ both have the desired characteristics and are being tested in full cells under ambient pressure, as well as simulated pressurized conditions.

The performance of a Co-doped $LiFeO_2$ cathode in a full cell, with a standard laboratory oxidant of 14% $O_2$-28% $CO_2$-58% $N_2$ at 100 kPa, is shown in Fig. 1. The performance at 120 kPa

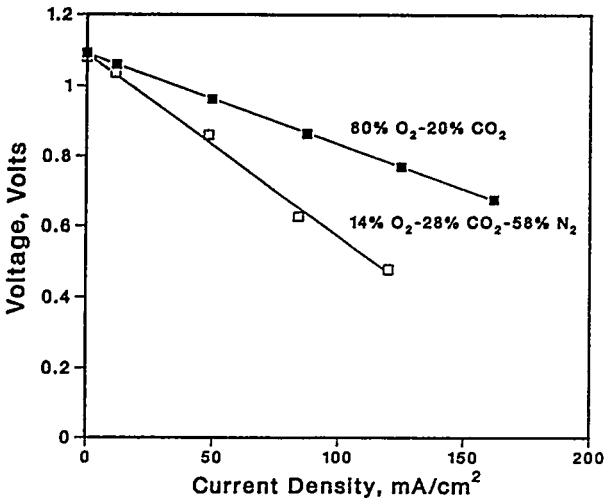


Fig. 1. Voltage vs. Current Density for an MCFC with a LiFe(Co)$O_2$ Cathode in 80% $O_2$-20% $CO_2$ or 14% $O_2$-28% $CO_2$-58% $N_2$

$mA/cm^2$ was about 400 mV worse than that of a NiO cathode under similar conditions. When an oxygen-rich gas of 80% $O_2$-20% $CO_2$ was used, the performance of the Co-doped $LiFeO_2$ cathode at this same current density improved by 300 mV (see Fig. 1). The area specific resistance (ASR) of the electrode decreased dramatically between the two operating conditions, going from 4.8 ohm-$cm^2$ with standard oxidant to 1.5 ohm-$cm^2$ with the oxygen-rich gas mixture. The ASR of this electrode was examined in greater detail as a function of $O_2$-to-$CO_2$ ratio. The data showed a pronounced minimum at an $O_2$ mole fraction of 0.8 and a $CO_2$ mole fraction of 0.2. This cell was operated with the oxygen-rich gas for about 1000 h with no decline in performance. However, the unusual polarization characteristics with respect to $O_2$-to-$CO_2$ ratio are not desirable and have led to the study of doubly-doped $LiFeO_2$.

From the above data, it was apparent that the electrode characteristics had to be altered to include a positive response to increasing $O_2$ and an ASR of about 1 ohm-$cm^2$ that remained constant over a broad range of $O_2$-to-$CO_2$ ratios. The guidance for the choice of dopants in the doubly-doped $LiFeO_2$ came from the performance curves obtained in earlier studies in half cells (2). The performance of two doubly-doped $LiFeO_2$ cathodes has been measured in full cell tests as a function of current density and $O_2$-to-$CO_2$ ratio. The results of these tests demonstrated the merits of using a doubly-doped electrode; the electrode ASR remained constant at about 1.3 ohm-$cm^2$ for $O_2$-to-$CO_2$ ratios ranging from about 4 to 0.8. Thus, the sensitivity to $CO_2$ was eliminated over a broad range of oxidant compositions. These data, along with similar data for a $LiCoO_2$ cathode (discussed below), are shown in Fig. 2. In addition, the performance of the doubly-doped $LiFeO_2$ cathode early in cell life was about 100 mV higher at 160 $mA/cm^2$ than that of a cell containing a Co-doped $LiFeO_2$ cathode. The long-term performance of the doubly-doped $LiFeO_2$ electrode remains to be demonstrated.

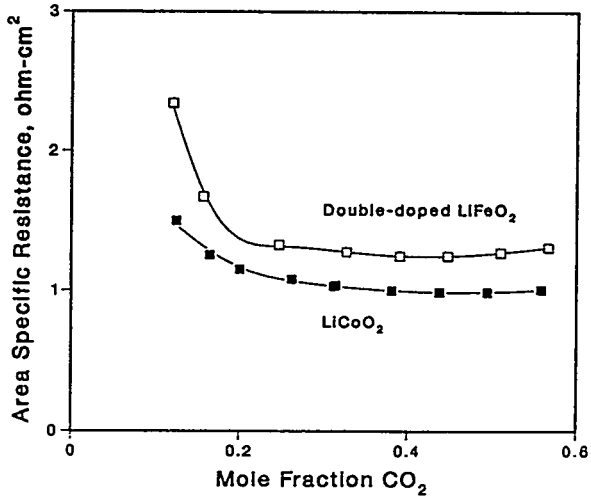


Fig. 2. Electrode ASR Values in an MCFC Employing a Double-doped $LiFeO_2$ or a $LiCoO_2$ Cathode with Various $CO_2$-$O_2$ Mixtures (Current Density 160 $mA/cm^2$)

In addition to the $LiFeO_2$ cathodes, $LiCoO_2$ cathodes are being evaluated in full cells. The performance curves as a function of current density for the standard laboratory oxidant and for an oxygen-rich gas mixture (58% $O_2$-42% $CO_2$) are shown in Fig. 3. The data show that the performance at a current density of 160 mA/cm$^2$ improved by about 100 mV with the oxygen-rich gas. The performance of this electrode is compared with that of the doubly-doped $LiFeO_2$ electrode in Fig. 4. The data show similar performances for these electrodes. The sensitivity of the $LiCoO_2$ electrode to $CO_2$ was also evaluated by measuring the electrode ASR as a function of the $O_2$-to-$CO_2$ ratio. The data, shown in Fig. 2, indicate that the ASR of the $LiCoO_2$ electrode is similar to that of the doubly-doped $LiFeO_2$ electrode. The results of the cell tests with the doped $LiFeO_2$ and undoped $LiCoO_2$ cathodes have been encouraging, but long-term studies and post-test analyses are required to ascertain the stability of the $LiFeO_2$ electrode with respect to the dopants and the stability of the $LiCoO_2$ with respect to cobalt deposition.

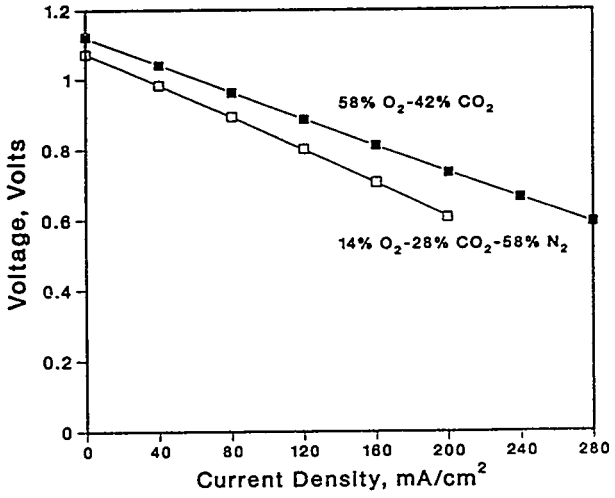


Fig. 3. Voltage vs. Current Density for an MCFC with a $LiCoO_2$ Cathode in 58% O-42% $CO_2$ or 14% $O_2$-28% $CO_2$-58% $N_2$

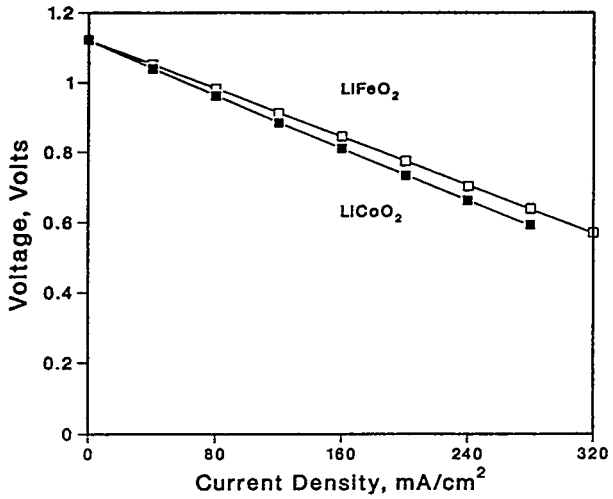


Fig. 4. Voltage vs. Current Density for an MCFC with a Double-doped $LiFeO_2$ Cathode or a $LiCoO_2$ Cathode in 58% $O_2$-42% $CO_2$

## ANODE DEVELOPMENT

Niobium-doped $CeO_2$ anodes have been tested in 25-cm$^2$ full cells using an oxidant of 14% $O_2$-28% $CO_2$-58% $N_2$ and a fuel of 80 % $H_2$-20% $CO_2$ humidified at 60$^0$C. The initial polarization curves for this anode showed that it suffered from the same problem encountered with the $LiFeO_2$ anodes (2), namely, it was not possible to maintain a stable voltage at current densities above 80 mA/cm$^2$. Unlike the $LiFeO_2$ anodes, the cell potential did not recover when the current density was reduced. This suggested that unfavorable changes in the charge donor/acceptor ratio had occurred. If, during the fuel oxidation reaction, $Ce^{4+}$ accepted any electrons, then the $Ce^{3+}$ concentration could increase to such a level that too few charge acceptors remained. To test this, the $CeO_2$ anodes were exposed to an oxidizing gas. After the oxidizing gas was purged from the cell and fuel gas was restored, current densities of about 140 mA/cm$^2$ were possible. The performance curves of the as-prepared electrode and of the treated electrode are shown in Fig. 5; the performance curve of a standard Ni/Cr anode is also included. It was possible to maintain a current density of 140 mA/cm$^2$ at a stable voltage for about 20 h. After this, the cell voltage again

began to decrease. The polarization data suggest that with the appropriate doping this electrode could give a performance equivalent to that of a Ni/Cr anode.

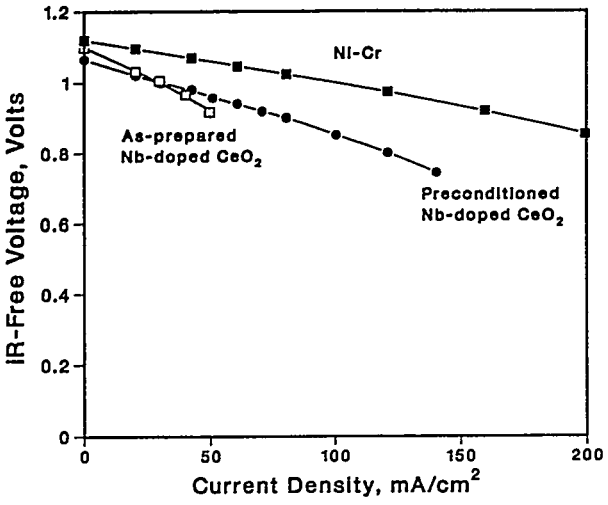


**Fig. 5. Voltage (iR Free) vs. Current Density for Oxidant-Conditioned and As-prepared Nb-doped $CeO_2$ Anodes (Ni-Cr Anode for Comparison)**

Although the performance of the cerium oxide-based anode looked promising, the post-test analysis gave discouraging results. Examination of the electrolyte structure by scanning electron microscopy and energy dispersive spectrometry showed that cerium dissolved in the electrolyte and moved toward the cathode. This indicates that $CeO_2$ has greater stability in the cathode environment than in the anode environment. The rate of deposition is unknown at this time. Therefore, it has not been established if this material could be used as an alternative anode should the appropriate charge carrier relationships be achieved.

In addition to full-cell testing of the alternative anodes, some emphasis has been placed on developing the capability of measuring the changes in performance as a function of material properties and of separating the chemistry of the anode from that of the cathode. Therefore, a half cell was designed, and the first tests using a standard Ni/Cr anode were successful. In the future development of the anodes, both full and half cells will be operated.

## ELECTROLYTE DEVELOPMENT

It was reported previously (2) that alternative electrolytes in the alkali metal/alkaline earth carbonate systems are effective in reducing the solubility of NiO and have liquidus temperatures of about $550^0$C. In this report period, we evaluated the effect of a new electrolyte, consisting of 20 mol% $CaCO_3$ in a 70 mol% $Li_2CO_3$-30 mol% $K_2CO_3$ melt, on other cell components and on the performance of standard electrodes. Corrosion tests on Type 310 and 316L stainless steel exposed to both the binary and the ternary melt for 1500 h showed that the addition of $CaCO_3$ has beneficial effects. Both types of stainless steel showed significant decreases in the thicknesses of their corrosion layers. The mechanism by which the $CaCO_3$ lowers the corrosion rate is not yet understood. It was expected that the corrosion products would contain a $CaO/Fe_2O_3$ layer, but none was found.

Earlier half-cell studies, using the new electrolyte and a NiO cathode, showed a minor decline (10 mV) in cathode performance. Full cells are currently being operated to determine if other losses in performance will occur as a result of using the new electrolyte. Two full cells containing standard electrodes (NiO cathode and Ni/Cr anode) and electrolyte structures consisting of 46 wt% $LiAlO_2$ and 54 wt% electrolyte are in operation. The electrolyte in one cell is the new electrolyte (20 mol% $CaCO_3$-56 mol% $Li_2CO_3$-24 mol% $K_2CO_3$), while that in the other cell is the standard binary electrolyte (70 mol% $Li_2CO_3$-30 mol% $K_2CO_3$). These cells have only recently been started, so no data are available.

## FUTURE WORK

Because of the significant performance improvements seen with the doubly-doped $LiFeO_2$ cathodes under simulated pressurized conditions, it is planned to operate cells with these cathodes to study the effect of longer term (~2000 h) operation on the performance and on the physical and compositional characteristics of the electrode. The focus will be on electrode morphology and on the dopant concentration in the post-test cathode. Tests of similar duration are planned for cells using $LiCoO_2$ cathodes to determine the rate of cobalt metal deposition in the anode environment.

The development of alternative anodes will continue, with the emphasis being placed on those materials that show more tolerance to sulfur-containing fuels. The performance of the alternative anodes will continue to be evaluated in both full and half cells.

The significant decrease in NiO solubility in both the Li/K and Li/Na binary melts with the addition of $CaCO_3$ offers another option for solving the problem of NiO dissolution/precipitation. The long-term (~2000 h) effects of these electrolytes on the various cell components will continue to be studied. In addition, the relative cation mobilities of promising ternary-electrolyte mixtures will be determined.

## ACKNOWLEDGEMENT

This work was performed under the auspices of the United States Department of Energy, under Contract number W-31-109-Eng-38.

## REFERENCES

1. J. L. Smith, G. H. Kucera, and A. P. Brown, "Development of Cathode Materials and Structures for the Molten Carbonate Fuel Cell," Proc. Second Symp. Molten Carbonate Fuel Cell Technology, eds., J. R. Selman, D. A. Shores, H. C. Maru, and I. Uchida, Electrochemical Society, Vol. 90-16, pp. 226-246 (1990).

2. G. H. Kucera, A. P. Brown, M. F. Roche, D. Chu, and E. Indacochea, "ANL's Research and Development of Alternative Components for MCFCs," Proc. Fourth Annual Fuel Cells Contractors Review Meeting, ed., W. J. Huber, DOE/METC-92/6127, pp. 31-41 (1992).

3. M.-L. Saboungi and M. Blander, J. Chem. Phys. 63, 212 (1975).

4. M. Blander, M.-L. Saboungi, and P. Cerisier, Metall. Trans 10B, 613-622 (1979).

5. M. Blander and A. D. Pelton, "Calculations of the Solubilities of Oxides in Molten Carbonates," Proc. Seventh Symp. on Molten Salts, Electrochemical Society, 177th Meeting, pp. 18-29 (1990).

# P12 Sealant Research for Solid Oxide Fuel Cells

## CONTRACT INFORMATION

| | |
|---|---|
| **Contract Number** | **49638** |
| **Contractor** | **Argonne National Laboratory<br>9700 South Cass Avenue<br>Argonne, IL 60439<br>(708) 252-4516** |
| **Contractor Project Manager** | **Kevin M. Myles** |
| **Principal Investigators** | **Ira Bloom and Michael Krumpelt** |
| **Co-Investigators** | **Kevin L. Ley, Stephen E. Dorris and Arun S. Wagh** |
| **METC Project Manager** | **William C. Smith** |
| **Period of Performance** | **April 1, 1992 to June 2, 1993** |

## OBJECTIVE

The objective of this work is to develop sealing materials for solid oxide fuel cells (SOFCs). A suitable sealant must form strong, dense bonds with SOFC components, be chemically and mechanically compatible with the components, be stable at 1000°C in the operating environment of the SOFC ($H_2$ and $H_2O$ on the anode side, $O_2$ on the cathode side), and be electronically insulating.

## BACKGROUND

Advanced flat-plate and monolithic SOFC designs offer high electrochemical performance because of their short current paths. In these designs, gas-tight seals must be formed at the edges of the cells and between the stack and fuel and air manifolds.

In general, the sealant must be compatible with the cell components and the cell environment. Further, the bonding material can be exposed to both oxidizing and reducing conditions simultaneously at high temperature. Reactions between the sealant and cell gases are clearly undesirable; the reactions can lead to cell failure. This program seeks to develop materials that are chemically stable toward the cell gases and that form adherent bonds to cell components.

For the intended application, the sealant must be electrically insulating. Since the sealant can contact both the anode and cathode, any electronic conductivity in the sealant will short circuit the cell.

The thermal properties of the sealant must match its application. At the cell edge, the sealant must be compatible with the thermal expansion behavior of, at most, two ceramics. For example, in the cathode compartment, the sealant must be matched to the behavior of yttria-stabilized zirconia (YSZ) electrolyte and $La(Sr)MnO_3$ cathode material. Rigid or compliant sealants are appropriate here. Along the stack-to-manifold junction the thermal requirements are different. Due to the number of different ceramics present (anode, cathode, electrolyte, interconnect, and the manifold) and the long sealing distances, compliant sealants may be necessary.

## PROJECT DESCRIPTION

Two types of sealants are being developed in this program: rigid for the cell edge, and compliant for stack-to-manifold joining.

For rigid sealants, the approach is to start with known cements. The desired chemical compatibility and stability and thermal expansion characteristics can then be obtained by altering the composition.

For compliant sealants, glasses and glass-ceramics are the starting point. Since the viscosity of these materials is a stronger function of temperature than that of crystalline ceramics, the sealant can be soft at 1000°C. Due to the temperature-dependence of viscosity, glass-based materials would develop expansion-mismatch-induced stresses over only a fraction of the cooling cycle, hence minimizing the stresses produced. Therefore, the temperature at which stresses begin to build should be as low as possible. At the same time, the viscosity at 1000°C should be above $10^3$ Pa-s (below which glass sags under its own weight).

As the first test of a sealant, its ability to bond to YSZ electrolyte, porous NiO/YSZ anode, and porous $La(Sr)MnO_x$ cathode (LSM) is determined qualitatively. This aspect of testing can be complicated because the bond quality may depend on temperature, composition, and method of application. Materials that form strong bonds are subsequently examined by microscopy to determine the level of porosity and nature and extent of the chemical interaction. Selected sealants are tested for chemical stability toward humidified $H_2$ and humidified $CO_2$ at 1000°C for extended periods of time; these exposure tests approximate the conditions found in the anode compartment of the SOFC.

The physical compliance of the sealant, that is, its tolerance to thermal expansion mismatch, is tested by bonding two substrates with a large difference in their coefficients of thermal expansion (CTEs), such as LSM and alumina (about a 20% mismatch in CTEs). After the bonded structure is sealed and thermally cycled, the bonded area is examined under the scanning electron microscope for cracks and evidence of delamination.

Finally, the effectiveness of the sealant is measured using a small electrochemical cell consisting of YSZ electrolyte and platinum electrodes. The cell is sealed to a housing with the sealant. Deviations from the Nernst potential and changes in the EMF with time are direct indications of how leak-tight and stable the sealant is, respectively.

## RESULTS

**Rigid sealants.** Magnesium ammonium phosphate-based cements are being explored as rigid sealants. The cements are known to set at room temperature and form strong bonds to common substrates. After the powder is mixed with water, the cement sets, but during the curing process (1-5 days at room temperature), some water is given off.

After curing followed by firing at 1300°C, samples of the original cement were found to be porous. The composition of the cement was altered to introduce a high-temperature liquid phase which enhanced diffusion. Density increased from 53% to 92% of theoretical.

The cement was applied to coupons of YSZ, porous NiO/YSZ, and LSM. After allowing for cement curing and firing at 1300°C, adherent bonds were formed to all substrates as well as to alumina. Examination by scanning electron microscopy showed the interfacial reaction zones to be small, about 10-μm thick on the YSZ, LSM, NiO/YSZ, and alumina substrates.

Samples of the cement (1-cm long, 4 x 4 mm) were exposed to humidified $H_2$ and humidified $CO_2$. After a 120-h exposure at 1000°C, negligible change in sample weights was observed, and no change in the physical appearance of the samples was seen.

When applied to a monolithic SOFC stack and fired, the cement exhibited vertical, evenly spaced cracks. Likely causes of these cracks include CTE mismatch between the materials involved and consolidation shrinkage of the cement during firing. We measured the CTE and shrinkage of the cement by itself. The thermal expansion coefficient of the cement, 10.2 x $10^{-6}$/°C, is close to that of the SOFC component ceramics (10-11 x $10^{-6}$/°C), but the cement shrinks about 30 vol% during firing. This shrinkage will be addressed before proceeding to other characterization tests.

**Compliant sealants.** Borate-based compositions were chosen initially for several reasons: they are electrical insulators, possess the desired combination of viscosity and expansion coefficient in the temperature region of interest, and contain no mobile ions. A borate-based material was preferred over a silica-based one since, in addition to elimination of any possible $SiO_2$ reduction, target viscosities in the desired temperature range could be achieved without loss of compositional flexibility.

Fabrication of the glass-ceramic sealant involved calcination of metal nitrates, oxides, and boric acid, melting of the mixture at high temperature, followed by quenching. After the melt-quenched material was milled to a fine powder, it was cast in the form of a flexible tape.

After firing at 1000°C, the sintered sealant consists of a refractory, crystalline phase and a glassy matrix phase. Differential thermal analysis showed that the glass in the material has a glass transition temperature of 780°C. The measured thermal expansion coefficient of the sealant at room temperature to 780°C is 11.5 x $10^{-6}$/C.

Application of this glass-ceramic to coupons of YSZ, NiO/YSZ, and LSM yielded extremely adherent and mechanically durable bonds. The glass-ceramic also bonded very well to disks of alumina. No obvious signs of interfacial reactions, such as phase formation, were observed between the glass-ceramic material and any of the bonded substrates. Sealant/substrate composites were thermally cycled twice between room temperature and 1000°C to gauge the thermal compatibility of the sealant with substrate materials. No delamination or cracking was observed.

To test the stability of these glass-ceramic materials in humidified fuel, pellets of sealant (2.5-cm dia, 4-6 mm thick) were exposed to flowing, humidified $H_2$ and humidified $CO_2$ at 1000°C for 120 h. No changes in the physical appearance of the sample were seen. There was insignificant change in sample weight and little X-ray diffraction evidence of any reduction products.

To test for compliance, a tape of the glass-ceramic material was bonded to a monolithic SOFC stack and an alumina disk. This composite

structure was thermally cycled between room temperature and 1000°C twice. Even though there was an estimated mismatch in thermal expansion of at least 20% between the two components, the bonds were strong and dense. Under the optical microscope, some isolated large pores were seen in the sealant, which were attributed to removal of the binder. The sealant/alumina and sealant/stack interfaces were sharp and showed no signs of reaction. In addition, no visible signs of bond delamination were evident.

Examination by scanning electron microscopy showed that the bonding phase at all interfaces consists of glass. Energy dispersive X-ray spectroscopy of the alumina/seal interface indicated that there is diffusion of aluminum ions into the glassy component, producing a composition gradient. Hence, a seal with a graded thermal expansion profile may have been formed at this interface, thus minimizing the interfacial stresses.

The sealing ability of the glass-ceramic was tested in an electrochemical cell consisting of a 500-μm-thick YSZ disk with platinum screen electrodes on either side. A 1-mm-thick, O-ring gasket of the glass-ceramic was used as the seal. The sealing operation itself consisted of pre-shrinking the gasket at 800°C and then using the gasket to bond the zirconia tube to the disk at 1000°C. The bonded cell was thermally cycled once between room temperature and 1000°C with no cracking.

The cell was then tested for electrochemical performance. Flowing, humidified 5% $H_2$ in helium (ca. 135 mL/min) served as the fuel gas and the stagnant furnace air as the oxidant. The cell EMF was measured at 800, 900, and 1000°C. The EMF values were recorded over a 72-h period at test temperature and are given in Table 1 along with the theoretical values. As shown in the table, the measured values are between 86% and 90% of theoretical. No significant change in EMF values was seen with time at temperature.

While the cell was operating, the fuel gas flow was periodically shut off, and the resulting change in EMF values was recorded as a function of time. The $\Delta EMF/\Delta t$ values were 1, 21, and 115 mV/h at 800, 900 and 1000°C, respectively.

For the case of molecular permeation involving no dissociation of gas molecules at the solid surface, the total amount of material, q (in $cm^3$ at STP), permeating a membrane at constant temperature is given by [1]:

$$q=\frac{KAt(p_1-p_2)}{d}$$

where K is the permeation velocity constant; A, the area of membrane exposed ($cm^2$); t, time (s); $p_1$, the gas pressure on the high side (cm Hg); $p_2$, the gas pressure on the low side (cm Hg); and d, the membrane thickness (mm). Using the $\Delta EMF/\Delta t$ data, values of permeability were calculated (Table 2).

In the literature, the value of K quoted for oxygen permeating through fused $SiO_2$ at 700°C is under $10^{-15}$ mm-$cm^3$/(s.$cm^2$.cmHg). For oxygen moving through crystalline quartz at the same temperature, one would expect a K value of about $10^{-22}$ mm-$cm^3$/(s.$cm^2$.cmHg), since permeation through crystalline solids can be expected to be $10^7$ times slower [1]. The data above are consistent with the fact that the glass-ceramic is an elastic, rigid solid composed primarily of crystalline material at 800°C. The higher permeation rates at 900°C and 1000°C can be explained by the smaller but significant amount of glassy component. At the higher temperatures, the glass is soft and affords another permeation path.

## FUTURE WORK

The shrinkage of the rigid sealant needs to be reduced. Efforts are now underway to control shrinkage by changing synthesis conditions and processing parameters.

Further testing of compliant sealants is underway. These tests include additional thermal cycling and time-at-temperature tests, determination of effectiveness of the sealant materials versus temperature, and measurement of the sealant conductivity.

## REFERENCES

1. Kohl, W. H., *Handbook of Materials and Techniques for Vacuum Devices*, Reinhold Publishing Co., New York, 1967, pp. 10-13.

---

This work is supported by the U.S. Department of Energy under contract no. W-31-109-Eng-38.

**Table 1. Measured and Theoretical EMF Values from Cell Sealed with Compliant Sealant**

| Temperature, °C | Measured EMF, mV | Theoretical EMF, mV |
|---|---|---|
| 800 | 967±3 | 1070 |
| 900 | 938±2 | 1060 |
| 1000 | 911±2 | 1050 |

**Table 2. Calculated Permeability Velocity Constant, K, as a Function of Temperature**

| Temperature, °C | K, mm-cm$^3$ (at STP)/(s.cm$^2$.cmHg) |
|---|---|
| 800 | $2.19 \times 10^{-23}$ |
| 900 | $6.91 \times 10^{-20}$ |
| 1000 | $5.46 \times 10^{-17}$ |

## P13 Alternative Materials for Solid Oxide Fuel Cells: Processing and Interactions of Materials

### CONTRACT INFORMATION

| | |
|---|---|
| **Contract Number (FTPA)** | 13822 |
| **Contractor** | Pacific Northwest Laboratory<br>Operated for the<br>U.S. Department of Energy by<br>Battelle Memorial Institute<br>under contract DE-AC06-76RLO 1830<br>P.O. Box 999<br>Richland, Washington 99352<br>(509) 375-3938 |
| **Contractor Project Managers** | Dr. J. Lambert Bates<br>Dr. Timothy R. Armstrong |
| **Principle Investigators** | Dr. Larry A. Chick<br>Dr. Timothy R. Armstrong<br>Dr. J. Lambert Bates |
| **METC Project Manager** | Diane Hooie |
| **Period of Performance** | April 1, 1993 to June 30, 1993 |

**Schedule and Milestones**

**FY93 Program Schedule**

| | S O N D J F M A M J J A S |
|---|---|
| Materials Development and Property Evaluation | ---------- |
| Materials Synthesis | ---------- |
| Materials Processing and Fabrication | ---------- |
| Electrochemical Processes | ---------- |

## OBJECTIVES

The purpose of this research is to develop alternative materials for solid oxide fuel cell (SOFC) interconnections and electrodes with improved electrical, thermal, and electrochemical properties. Another objective is to develop synthesis and fabrication methods for these materials whereby they can be processed in air into SOFCs. The approach is to (1) develop modifications of the current, state-of-the-art materials used in SOFCs, (2) minimize the number of cations used in the SOFC materials to reduce potential deleterious interactions, (3) improve thermal, electrical, and electrochemical properties, (4) develop methods to synthesize both state-of-the-art and alternative materials for the simultaneous fabrication and consolidation in air of the interconnections and electrodes with the solid electrolyte, and (5) understand electrochemical reactions at materials interfaces and the effects of component composition and processing on those reactions.

## BACKGROUND INFORMATION

Solid oxide fuel cells (SOFCs) continue to develop as promising, clean, and efficient technology for the direct conversion of hydrogen and fossil fuels to electrical energy. Standard materials we use in state-of-the-art designs are: the air electrodes, La(Sr)$MnO_3$; the fuel electrode, $ZrO_2$•Ni cermet, the interconnection, La(Mg)$CrO_3$ or La(Sr)$CrO_3$, and the electrolyte, $Y_2O_3$-stabilized $ZrO_2$. The use of these different material combinations of manganite, chromite, zirconia, and nickel in state-of-the-art SOFCs pose several materials fabrication and performance related problems.

New alternative materials with improved properties that can be more easily fabricated into fuel cells are needed for the further development of cost efficient and improved performance SOFCs. An important key is the development of a SOFC interconnection material that can be sintered in air to a high density at temperatures less than 1500°C. It should have a good thermal expansion match with and intimately bond to both the air and the fuel electrodes, without forming deleterious interactions at the interfaces. At present time this has not been attained with the state-of-the-art $La_{1-x}Sr_xCrO_3$ interconnections.

## PROJECT DESCRIPTION

The overall approach for this research and development is to:

- Minimize the number of cations in the electrode, electrolyte, and interconnection by developing yttrium compounds, such as Y(Ca)$CrO_3$ as the interconnection, and Y(M')$MnO_3$ as the air electrode.

- Develop advanced synthesis and fabrication processes for air sintering, below 1500°C, of chromite interconnections through (1) the use of sintering aids; and (2) the synthesis of sub-micrometer powders.

- Establish methods for the simultaneous processing and consolidation of air-sinterable powders.

- Electrochemically evaluate interface reactions (in reproducible and controlled laboratory tests) for both the alternate and state-of-the-art materials and cell components developed under this program.

- Evaluate the chemical reactivity and interdiffusion effects that take place between the various fuel cell components: electrolyte/cathode, interconnect/cathode, and interconnect/anode.

This paper describes a comprehensive study that assessed the processing of air-sinterable chromites, the sintering mechanism of chromites, and the chemical reactivity and interdiffusional effects between the interconnect, air, and fuel electrodes. Materials evaluated were $La_{0.7}Ca_{0.31}CrO_3$ (LCC31), $La_{0.7}Ca_{0.29}CrO_3$ (LCC29), $(Y_{0.6}Ca_{0.4})_{1.05}Cr_{0.95}O_3$ (YCC105), $La_{1-x}Sr_xMnO_3$ (LSM), $La_{1-x}Ca_xMnO_3$ (LCM), $Y_{1-x}Ca_xMnO_3$ (YCM), and $Y_{1-x}Sr_xMnO_3$ (YSM).

## RESULTS

### Experimental Procedure

The required compositions were prepared by the glycine-nitrate process using a stoichiometric molar ratio of glycine-to-nitrate[1,2]. The powder was calcined at 650°C for 0.5 hr. Reaction couples were formed to study the migration of cations and anions between the SOFC materials and to determine if any secondary phases developed at the interface. The two materials for each interaction couple were fabricated into a bilayer configuration using a two-step process. First, one powder was placed into a die and lightly compacted by uniaxial pressing. The second powder was added to the die and the two were consolidated (no binder) by uniaxial pressing at 35 MPa. This step was followed by isostatically pressing the disks, 21 mm diameter by 2 mm thick, at 140 MPa. The pellets were sintered in an electric resistance furnace by heating 5°C/min to 1300°, 1400°, and 1500°C and soaking for 1 hour in air. These temperatures were chosen because they cover a broad range over which SOFCs may be thermally processed. A cross-section of each sample was mounted, polished, and examined by scanning electron microscopy. Energy dispersive spectroscopy (EDS) was used to measure the cation diffusion distances.

Phase formation during co-sintering was investigated by thoroughly mixing the as-synthesized powders (1:1 ratio) and uniaxially pressing the powder into disks. The samples were heated following the same schedule used for sintering, except they were quenched after soaking for 1 hr at temperature. The disks were ground in a mortar and pestle and analyzed by x-ray diffraction (XRD) to determine the reaction products.

### Tape Casting of Glycine-Nitrate Powders

Tape casting studies included evaluations of dispersants, binders, and plasticizers. The powders used in this study were $La_{0.7}Ca_{0.31}CrO_3$ and $(Y_{0.6}Ca_{0.4})_{0.99}Cr_{1.01}O_3$ prepared by the glycine-nitrate process. The solvent used was an azeotropic mixture of 66% methyl ethyl ketone and 34% ethanol. Acrylic binders were chosen for the study due to their wide commercial acceptance, and for most of the study phosphate esters were used as the dispersant.

Figure 1 shows the viscosity versus concentration of dispersant curves for suspensions containing 45 wt% solids of as-synthesized LCC31. The minimum viscosity was achieved with a 1 wt% PS-21A (aliphatic phosphate ester) and 3.5 wt% for the CS-1361 (aromatic phosphate ester) addition. These results are similar to those reported by Chartier[3] in which he concluded that the aromatic ester adsorbs more slowly, possibly because of its large size with respect to that of the aliphatic ester. No distinct minima was observed in the viscosity when Menhadden fish oil was used. When a shear stress was applied to the slip they showed pseudo-plastic behavior at all dispersant concentrations except at the minimum for PS-21A, where the slip displayed Newtonian behavior. The other dispersants showed only pseudo-plastic behavior at all dispersant levels.

The average particle size of the as-synthesized powder was ≈60 nm and the average agglomerate size was 30 μm. The powders were coarsened by heat treating at 800°C and 1000°C for 2 hours. The average particle sizes after treatment at 800°C and 1000°C were ≈150 nm and 800 nm, respectively. The agglomerate size of the heat treated powders decreased to 17 μm and 15 μm. These powders were ball milled to determine the amount of milling necessary to break up the agglomerates without destabilizing the suspension. The studies carried out showed that no more than 5 hours of milling was needed to break up the agglomerates. The average agglomerate size, after milling, decreased to 1 μm and 3.5 μm for powders coarsened at 1000°C and 800°C. The LCC31 coarsened at 650°C had a bimodal distribution after milling with one maxima at 3 μm and the second at 0.8 μm.

Figure 2 shows the viscosity versus concentration dispersant curve for a suspension with 65 wt% (20 vol%) LCC31, dispersed with PS-21A, and ball milled for 5 hours. The three curves show the effect that particle size and agglomerate size have on the slip viscosity. LCC31 heat-treated at 650°C requires nearly 8 times more dispersant than the same powder heat-treated at 1000°C, that had a larger particle size and smaller agglomerate size.

Figure 3 shows the viscosity versus concentration dispersant curve for suspensions composed of LCC31 coarsened at 1000°C, dispersed with PS-21A, and ball milled for 5 hours. The curves displayed in Figure 3 show that as the solids loading increases from 65 wt% (20 vol%) to 80 wt% (35 vol%) the viscosity increased from 10 centipoise to 400 centipoise and the amount of dispersant needed to disperse the powder increased from 0.25 wt% to 0.75 wt%.

The best results for dispersing LCC31 and YCC99 were achieved using aliphatic phosphate esters. Suspensions with 85 wt% solids loading have been tape cast using ≈1.0 wt% dispersant. Acrylic binders with low glass transition temperatures have been used as binders with polyglycol and benzyl butyl phthalate as plasticizers.

## Chromite Sintering

The SOFC interconnect must be sintered to high density so that it will provide a gas-tight seal between the electrodes. Furthermore, decreasing the cost of SOFC manufacturing to the point that the technology is economically competitive may require that the ceramic components are sintered together in one step. In order to prevent decomposition of the manganite cathode, such co-sintering would have to be performed in air at temperatures near or below 1400°C, conditions that are not favorable to chromite densification. For these reasons, a substantial effort has been devoted to developing air-sinterable chromites. Recently, it has been shown that chromite densification can be substantially improved by slightly enriching the overall concentration of A-site relative to B-site[4-16]. We have focused our recent investigations on the reasons for the substantially improved densification of LCC31 relative to that of LCC29.

As discussed previously[17], the sintering shrinkage curves for LCC29 and LCC31 heated at 2°C/min, both exhibit periods of rapid shrinkage. However, there are two characteristic differences between the curves; the first rapid-shrinkage event starts almost 100°C lower in LCC31 than in LCC29 (about 950°C versus about 1040°C). Also, LCC31 exhibits a second rapid-shrinkage event, starting near 1150°C, that takes the sample

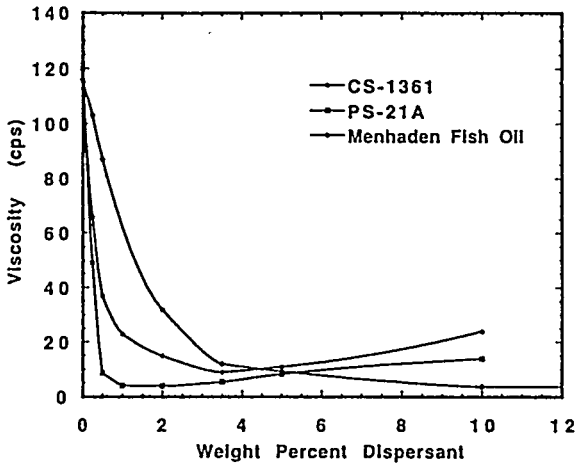


**Figure 1. Viscosity versus dispersant concentration for different dispersants. Suspension contained 45 wt% LCC31.**

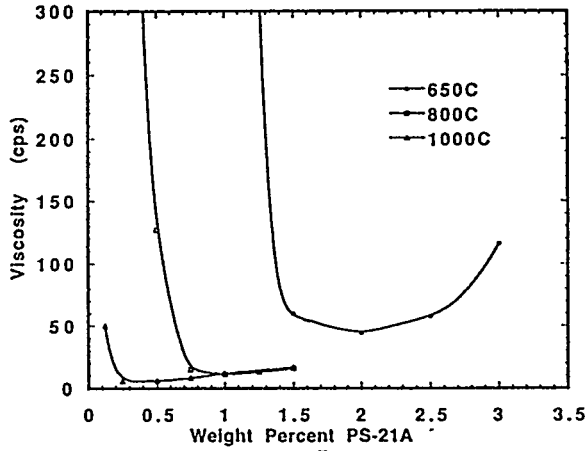


**Figure 2. Viscosity versus dispersant concentration for LCC31 coarsened at 650°, 800°, and 1000°C. Suspension contained 65 wt% LCC31, dispersant was PS-21A.**

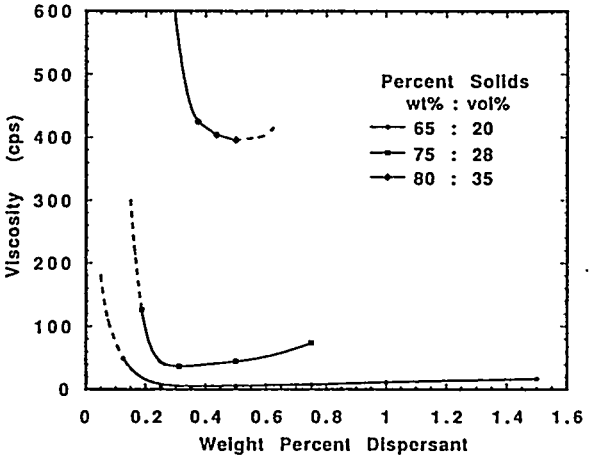


**Figure 3. Viscosity versus dispersant concentration for different solids loadings of LCC31. Dispersant was PS-21A, phosphate ester.**

to near full density by 1300°C. The same characteristic differences are exhibited between chromium-enriched and chromium-depleted compositions in the $Y(Ca)CrO_3$ system.

In order to investigate the phase changes associated with the rapid-shrinkage events, a series of quenched samples was prepared. These samples were heated at 2°C/min, then air quenched from various peak temperatures. Results of XRD analyses on the quenched pellets are listed in Tables 1 and 2. The fraction of Ca in the perovskite phase was estimated from the perovskite orthorhombic unit cell volume, which was determined from XRD. In addition to the perovskite phase, samples quenched from temperatures up to 1126°C were found to contain $CaCrO_4$. The concentration of $CaCrO_4$ in each sample was estimated based on comparison of major peak intensities. The LCC29 sample that was quenched from 1067°C also contained approximately 0.5 wt% of $\beta$-$CaCr_2O_4$. No additional crystalline phases were detected in any of the other samples, however, the presence and quantity of x-ray amorphous material was inferred by performing a material balance to account for the total amounts of cations introduced during synthesis. This x-ray amorphous material, which was present in all samples up through 1126°C, may consist of poorly crystallized phases or the glassy remnants of liquid phases. The material balance calculations indicated that the X-ray amorphous material in LCC31 samples had slightly more Ca than Cr, with the atom ratio, Ca/Cr = 0.53/0.47. The corresponding ratio for the LCC29 samples was Ca/Cr = 0.48/0.52.

These XRD results clearly establish that over half of the Ca resides in non-perovskite phases at the onset of sintering (926°C). Although the glycine-nitrate synthesized chromites are composed of a single perovskite phase after combustion, much of the Ca is exsoluted from the perovskite during calcination, forming the $CaCrO_4$ and other minor phases. This exsoluted Ca, along with the associated Cr, dissolves back into the perovskite phase during sintering. In Figure 4, the Ca concentrations determined for the perovskite phase are plotted along with the dilatometer shrinkage curves. This plot shows that, for both samples, dissolution of the Ca into the perovskite proceeds at roughly constant rates up to 1126°C, then more rapidly proceeds to completion at 1207°C. The more rapid dissolution is concurrent with the second rapid-shrinkage event in LCC31. Both materials experience rapid dissolution of Ca in this temperature interval, however, only LCC31 exhibits rapid densification.

The binary phase diagram between Ca and Cr oxides in air is relevant to the transitory conditions involved in chromite densification because the non-perovskite material is mainly composed of these two components. The most recent version of this diagram is published by Adendorff et al.[18] from de Villiers et al.[19]. This diagram shows a eutectic on the Ca-rich side of $CaCrO_4$ (Ca/Cr = 0.55/0.45, atom basis) at 1061°C. As discussed above, the X-ray amorphous portion of LCC31 probably has a Ca/Cr ratio near that of the eutectic and thus could be expected to melt almost completely by 1150°C. Therefore, it seems plausible that the second densification event in LCC31, near 1150°C, is due to liquid-phase sintering. In contrast, the X-ray amorphous portion of LCC29 probably has a Ca/Cr ratio that places it in the "$\beta$-$CaCr_2O_4$ + liquid" phase region at 1150°C, as indicated by the detection of $\beta$-$CaCr_2O_4$ along with $CaCrO_4$ at 1067°C. Therefore, the non-perovskite material in LCC29 might be expected to melt incongruently, retaining substantial solid phase at 1150°C. Nevertheless, *both* materials could be expected to form some liquid phase near 1061°C.

It is well known that A-site enriched chromites contain liquid-phase remnants after sintering, but evidence of liquid formation has not been reported in A-site depleted samples, although these have been found to contain isolated Cr-rich deposits[8,10,14]. However, an LCC29 sample quenched from 1400°C contained isolated Cr-rich inclusions which, upon examination by SEM in polished cross section, were found to consist of rounded perovskite-like grains embedded in a matrix of essentially pure Cr oxide. This matrix phase may be a liquid-phase remnant that was progressively isolated and enriched in Cr as most of the original liquid was dissolved into the perovskite.

This leaves the problem of explaining why the LCC29 material does not densify even though a

**Table 1. Results of XRD analyses of $La_{0.7}Ca_{0.29}CrO_3$ samples heated at 2°C/min in air to peak temperature, then quenched.**

| Peak Temp.°C | Ca Concentration in Perovskite Phase (x) | Mole Fraction $La_{1-x}Ca_xCrO_3$ Phase | Mole Fraction $CaCrO_4$ Phase | Mole Fraction X-Ray Amorphous Phase |
|---|---|---|---|---|
| 800 | 0.07 | 0.75 | 0.13 | 0.12 |
| 926 | 0.12 | 0.79 | 0.11 | 0.10 |
| 1015 | 0.15 | 0.83 | 0.09 | 0.09 |
| 1067 | 0.17 | 0.85 | 0.04 | 0.11 |
| 1126 | 0.17 | 0.86 | 0.03 | 0.12* |
| 1207 | 0.30 | 1.00 | --- | trace |
| 1296 | 0.30 | 1.00 | --- | trace |
| 1530 | 0.30 | 1.00 | --- | trace |

* Includes ≈0.5 wt% of $\beta$-$CaCr_2O_4$ (JCPDS-ICDD #9-146).

**Table 2. Results of XRD analyses of $La_{0.7}Ca_{0.31}CrO_3$ samples heated at 2°C/min in air to peak temperature, then quenched.**

| Peak Temp.°C | Ca Concentration in Perovskite Phase (x) | Mole Fraction $La_{1-x}Ca_xCrO_3$ Phase | Mole Fraction $CaCrO_4$ Phase | Mole Fraction X-Ray Amorphous Phase |
|---|---|---|---|---|
| 800 | 0.08 | 0.75 | 0.13 | 0.12 |
| 926 | 0.13 | 0.79 | 0.11 | 0.10 |
| 1015 | 0.17 | 0.84 | 0.08 | 0.09 |
| 1067 | 0.18 | 0.85 | 0.05 | 0.09 |
| 1126 | 0.20 | 0.87 | 0.04 | 0.09 |
| 1207 | 0.31 | 1.00 | --- | trace |
| 1296 | 0.31 | 1.00 | --- | trace |
| 1530 | 0.31 | 1.00 | --- | trace |

liquid phase is formed. In the case of LCC31, Figure 4 indicates that densification may not result directly from liquid formation, but rather from the subsequent dissolution of the liquid into the perovskite. This might indicate that the liquid does not adequately wet the solid perovskite in LCC31 until dissolution begins [20]. However, substantial Ca dissolution also takes place in the LCC29 material within the same temperature range; why does this not also lead to densification? The simple answer might be that liquid does not form in the LCC29 material, even though the present XRD analysis and the binary phase diagram indicate that it should.

It has been proposed that vapor-phase transport plays a role in preventing densification of the A-site depleted materials, such as LCC29[4,8]. Yokokawa et al.[2] argue that the presence of minor quantities of $Cr_2O_3$ will substantially increase the vapor pressure of $CrO_3$, causing vapor-phase transport and formation of $Cr_2O_3$ at intergranular necks, thus preventing further densification. This theory is supported by the work of Meadowcroft and Wimmer[21], whose data indicate that pure $Cr_2O_3$ vaporizes at a much higher rate than does $LaCrO_3$.

A key experiment was completed that clarifies the role of vapor-phase transport in chromite

sintering. The experiment is shown schematically in Figure 5. Pellets of LCC31 were placed in the furnace either in the open (air) atmosphere or contained within a double crucible arrangement in which the solid powder controlled the atmosphere surrounding the sample. As seen in, Figure 6, the sample in air and those surrounded by $Al_2O_3$ or $La_2O_3$ powders reached high density. However, when $Cr_2O_3$ powder controlled the atmosphere, the sample did not sinter well. This implies that the presence of substantial $CrO_3$ vapor in the atmosphere destroys the effectiveness of the liquid phase, perhaps by affecting the wetting angle of the liquid.

## Material Interactions

### Interconnect/Cathode Interactions

X-ray diffraction analysis of mixtures of LCC31 and LSM10 indicated that a solid solution formed between the two materials at all temperatures studied. The resulting crystal structure of the solid solution was determined to be orthorhombic. The only evidence of complete solid solution formation in the YCC/YCM system occurred when YCC105 and YCM60 were heat treated at 1500°C. The crystal structure and lattice parameters of the solid solution indicated orthorhombic symmetry similar to that of yttrium chromites. X-ray diffraction data collected from the solid solutions corresponds well with earlier work reported by Koc et. al.[22].

Figure 7 shows a YCC105/LSM10 reaction couple sintered at 1400°C for 1 hour. The interface in these samples is characterized by a dense reaction zone approximately 90 μm, the majority of which resides on the interconnect side. This dense interfacial region is enriched with calcium and chromium and its thickness was found to be invariant with temperature. Aside from the interface the remainder of the interconnect and cathode are porous. Calcium and chromium migration into the cathode was observed approximately 100 μm and 80 μm beyond the dense interfacial region.

Figure 8 shows a YCC105/LCM20 reaction couple sintered at 1400°C for 1 hour. The interfacial region in these samples is similar to

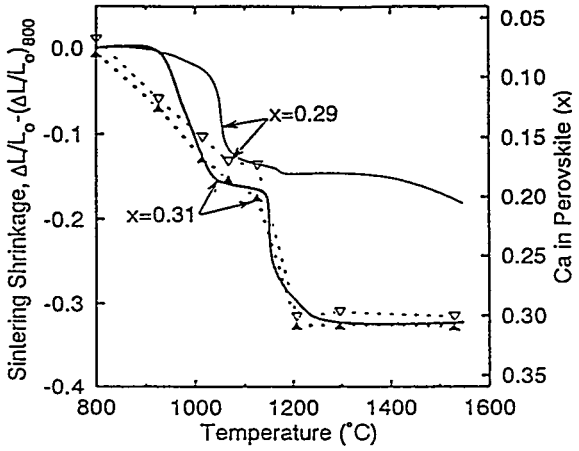


**Figure 4. Sintering shrinkage curves for LCC31 and LCC29. Triangular symbols are estimated levels of Ca in the perovskite phase.**

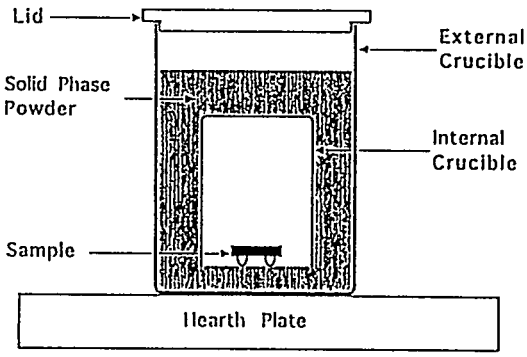


**Figure 5. Schematic of solids controlled atmosphere setup.**

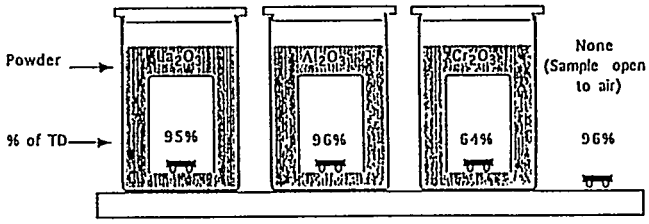


**Figure 6. Effect of solid phase-controlled atmosphere on sintering of LCC31 at 1300°C /1 hr.**

those observed between YCC and LSM, shown in Figure 7. The samples sintered at 1400° and 1500°C had a dense reaction zone at the interface approximately 80 μm thick. This region is again enriched in calcium and chromium with chromium migrating 70 μm past the dense region into the cathode at the temperatures observed. Again, as in the YCC/LSM reaction couples the interconnect only densified near the interface. EDS analysis of the interface indicated some distinct differences in microchemistry. Areas of the interface on the interconnect side were found to have a higher concentration of calcium and chromium than other areas within the dense region, indicating possible melting and migration of $CaCrO_4$. On the cathode side of the interface, the material was enriched in calcium and depleted in chromium. The composition of the interface is similar to the composition of the dispersed phase within the reaction zone. These calcium rich regions were not found in samples sintered at lower temperatures.

Figure 9 shows a LCC31/LSM10 reaction couple sintered at 1400°C. In these interaction couples there is no distinct interface. An interfacial zone can be approximated in the region where there is formation of a second phase between LCC31 and LSM, indicated by arrows in the micrograph. EDS of the dispersed phase indicates that it is a calcium rich $(La,Ca)(Cr,Mn)O_3$ phase, while the surrounding material is $(La,Ca)(Cr,Mn)O_3$ solid solution. $(La,Ca)(Cr,Mn)O_3$ solid solutions are reported to have a lower electrical conductivity than LSM[22], but this should not lead to an increase in the interfacial resistance between these two materials because the relative amount of the calcium rich second phase is minimal and does not form a continuous barrier.

Sintering at 1500°C does not result in an increase of second phase material observed at the interface. The only change observed in the microstructure with increased sintering temperature is further densification of the LSM. The characteristics of these couples are nearly ideal, the LCC is dense, the LSM is porous, and the interfaces are relatively free of low conducting second phases. In the LSM/LCC31 couples no manganese diffusion into LCC31 is observed at

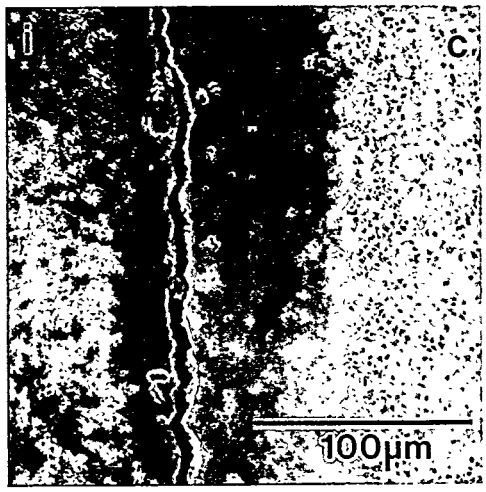


**Figure 7. YCC105/LSM10 reaction couple sintered at 1400°C/1 hr.**

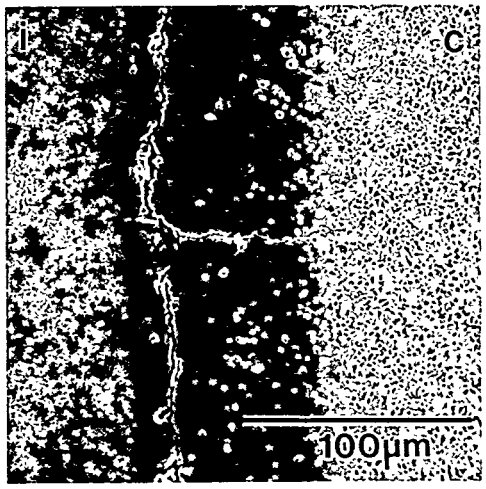


**Figure 8. YCC105/LCM20 reaction couple sintered at 1400°C/1 hr.**

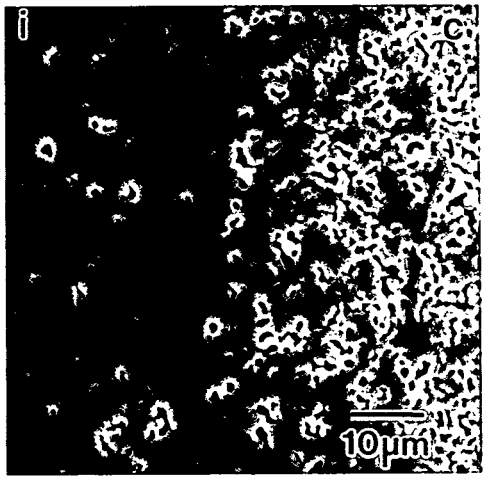


**Figure 9. LCC31/LSM10 reaction couple sintered at 1400°C/1 hr.**

the temperatures studied, however, the distance both calcium and chromium diffused into the LSM increased with increasing sintering temperature.

Figure 10 is a reaction couple composed of LCC31 and LCM20 sintered at 1400°C for 1 hour. These interfaces are clean with the only noticeable feature being a porous region at the interface. Otherwise the interconnect is dense and the cathode porous. Sintering at higher temperatures results in increased densification of both the interconnect and cathode. Chromium migration into the cathode is limited to approximately 65 μm.

In this study six different combinations of interconnect/cathode were evaluated. The results for the samples in which YCC105 was used as the interconnect material were not encouraging. Large interfacial regions rich in calcium and chromium formed in the sample. When YCC was adjacent to YCM60 the interface was porous, in contrast to the dense interfacial region that formed when adjacent to LSM or LCM. However, the formation of these wide interfacial regions indicates that a liquid phase is forming and migrating during the sintering process. The extensive migration of chromium into the cathode in these samples is a result of both liquid and vapor phase transport. The majority of the liquid collects at the interface forming wide continuous interfacial layers. However, it has yet to be determined if these layers and reactions lead to increased interfacial resistance.

Similar reaction couples were prepared with LCC31 as the interconnect. Nearly ideal interfaces resulted adjacent to LCM or LSM. When the LCC was next to YCM, $CaMnO_3$ formed noncontinuous dense regions. Continuous interfacial layers formed when samples were sintered at 1500°C. No other dense interfacial region was observed in any of these samples. The interconnect was dense in all the samples, indicating that migration of the liquid phase is limited. The data suggests that the presence of yttrium in the calcium and chromium rich liquid phases may change their wetting characteristics, resulting in the formation of dense interfacial layers. The presence of yttrium in the liquid phase is supported by evidence that yttrium

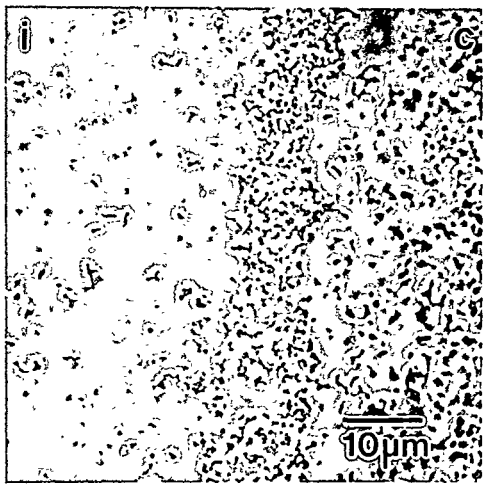


**Figure 10. LCC31/LCM20 reaction couple sintered at 1400°C/1 hr.**

migrated from the YCM cathode into the LCC interconnect.

### Interconnect/Anode Interactions

A phase equilibria study was carried on the $La_{1-x}Ca_xCrO_3/NiO{\cdot}ZrO_2$ system to determine the compositional and temperature ranges over which phases form between the two components. Figure 11 shows the resulting phase diagram. No reaction phases were formed when the Ca content was less than 13 mole percent. Between 13 and 33 mole percent Ca, $NiCr_2O_4$ forms, and above 33 mole percent Ca, both $NiCr_2O_4$ and $CaZrO_3$ form. At low Ca concentrations (10 mole percent) $NiCr_2O_4$ forms at temperatures as low as 975°C. The formation temperatures decrease to 925°C as the Ca concentration increases to 30 mole percent.

These studies indicate that both the lanthanum and yttrium chromites react with the anode to form dense interfacial layers when sintered at temperatures greater than 1400°C. However, when temperatures less than 1400°C are used, the interfacial reaction area is no longer dense, but neither is the interconnect. It appears that the liquid phase needed to densify the interconnect wets the anode well.

## Conclusions

These studies indicate that interfacial reactions occur between SOFC materials when either

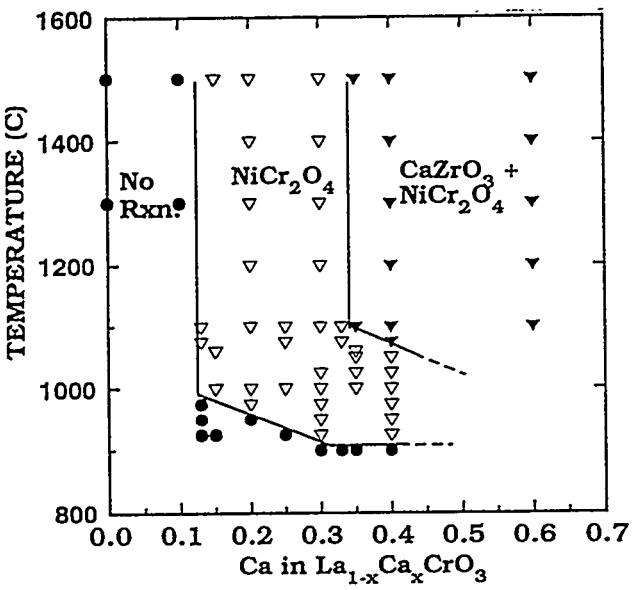


**Figure 11. $La_{1-x}Ca_xCrO_3/NiO{\cdot}ZrO_2$ phase diagram.**

yttrium chromite is used as the interconnect or yttrium manganite is used as the air electrode material. The exact reason why yttrium chromite or manganite leads to more extensive reactions upon sintering in unknown. However, it may be due to modification of the wetting characteristics of the liquid phase by yttrium.

More severe reactions occur between the interconnect and the anode than anticipated. It appears from these preliminary studies that the liquid phase generated by the interconnect wets the anode well, leading to enhanced densification of the anode and decreased densification of the interconnect.

It was established that A-site enriched chromites sinter to high density below 1300°C in two rapid shrinkage stages, whereas their A-site depleted counterparts only exhibit the first of these rapid shrinkage events and dot reach high density. Phase changes are similar between A-site depleted and A-site enriched materials; over half of the Ca has been exsoluted into non-perovskite phases by the onset of sintering, and this Ca, along with associated Cr, dissolves back into the perovskite phase during sintering.

## FUTURE WORK

The emphasis of this project over the next several years will be co-sintering and interactions between SOFC materials, including both state-of-the-art and alternative compositions. Issues involved in co-sintering and interactions between couples of these materials and with the YSZ electrolyte will be investigated. Emphasis on thermal expansion and sintering shrinkage tolerances for the sintering of thin-layer composites. These composites will be fabricated by conventional low cost processing techniques, diffusion of additive cations, and wicking of transient liquid phases into adjacent components, formation of deleterious crystalline interaction phases between components, and effects of interlayers to prevent limit or prevent diffusion of cations.

In addition to the interactions between components that occur during fabrication and sintering, this program will address mechanisms and effects of interactions that occur during SOFC operation. One of the goals of this work will be to develop valid accelerated testing techniques to predict the long-term performance of SOFC components.

The fabrication and processing of SOFC materials will be further emphasized. These efforts will be integrated with the activities of other DOE and GRI SOFC contractors.

## REFERENCES

1. LA Chick, LR Pederson, GD Maupin, JL Bates, LE Thomas, and GJ Exarhos, Mater. Lett., **10** (1990) 6.

2. LA Chick, JL Bates, LR Pederson, and HE Kissinger, in Proceedings of First International Symposium on Solid Oxide Fuel Cells, ed. S. C. Singhal, The Electrochemical Society, Pennington, NJ (1989).

3. T Chartier, E Streicher, and P Boch, Am. Ceram. Soc. Bull. **66** [11] (1987) 1653.

4. H Yokokawa, N Sakai, T Kawada, and M Dokiya, J. Electrochem. Soc. **138** [4] (1991) 1018-27.

5. M Dokiya, N Sakai, T Kawada, H Yokokawa, T Iwata and M Mori, in Proceedings of the First International Symposium on Solid Oxide Fuel Cells, ed. by SC Singhal. Electrochemical Society, Pennington, NJ. (1989) 325 -336.

6. N Sakai, T Kawada, H Yokokawa, and M Dokiya, J. Mat. Sci. **25** (1990) 4531.

7. N Sakai, T Kawada, H Yokokawa, M Dokiya and T Iwata, Solid State Ionics **40/41** (1990) 394-397.

8. LA Chick, JL Bates and GD Maupin, in Proceedings Second International Symposium on Solid Oxide Fuel Cells, ed. by F Grosz, P Zegers, SC Singhal and O Yamamoto, EUR 13564. Athens Greece. Commission of the European Communities, Luxembourg. (1991) 621-628.

9. H Yokokawa,N Sakai, T Kawada, and M Dokiya, *ibid.*, 663-670.

10. N Sakai, T Kawada, H Yokokawa, and M Dokiya, *ibid.*, 629-636.

11. M Mori, N Sakai, T Kawada, H Yokokawa, and M Dokiya, Denaki Kagaku 59 [4] (1991) 314-319.

12. JL Bates, LA Chick and WJ Weber, Solid State Ionics **52**, (1992) 235-242.

13. H Yokokawa, N Sakai, T Kawada, and M Dokiya, *ibid.*, 43-56.

14. T Kawada, N Sakai, H Yokokawa, M Dokiya and I Anzai, Solid State Ionics **50** (1992) 189-196.

15. LA Chick, GD Maupin and JL Bates, in Proceedings of the Fifth Annual Conference on Fossil Energy Materials, Oak Ridge, TN, May 2, 1992 (in press).

16. LA Chick, TR Armstrong, DE McCready, GW Coffey, GD Maupin and JL Bates, in Proceedings of the Third International Symposium on Solid Oxide Fuel Cells, ed by S.C. Singhal and H Iwahara. Proc. Vol. 93-4, The Electrochemical Society, Pennington, NJ. (1993) 374-84.

17. JL Bates and LA Chick, (last year's METC report from the Fourth Fuel Cell Contractor's Meeting)

18. KT Adendorff, JPR de Villiers and GJ Kruger, J. Am. Ceram. Soc. **75** [6] (1992) 1416-22.

19. JPR de Villiers J Mathias and A Muan, Trans. Inst. Metall. Sect. C, **96** (1987) C55-C62.

20. IA Aksay, CE Hoge and JA Pask, J. Phys. Chem. **78** [12] (1974) 1178-1183.

21. DB Meadowcroft and JM Wimmer, Bull. Am. Ceram. Soc. **58** (1979) 610-615.

22. R Koc, HU Anderson, and SA Howard, in Proceedings of First International Symposium on Solid Oxide Fuel Cells, ed. SC Singhal, The Electrochemical Society, Pennington, NJ (1989).

23. T Kawada, N Sakai, H Yokokawa, and M Dokiya, Solid State Ionics, **50** (1992) 189 .

## P14 Low Cost, Radial Flow, Solid Oxide Fuel Cell

### CONTRACT INFORMATION

| | |
|---|---|
| **Contract Number** | **DE-FG02-92ER81453** |
| **Contractor** | **Technology Management Incorporated**<br>9718 Lake Shore Boulevard<br>Cleveland, Ohio 44108<br>(216) 541-1000 |
| **Contract Project Manager** | Michael A. Petrik |
| **Principal Investigator** | Michael A. Petrik |
| **METC Project Manager** | Dr. Diane T. Hooie |
| **Period of Performance** | July 27, 1992 to March 31, 1993 |

### OBJECTIVES

Current development of solid oxide fuel cell (SOFC) technologies suffer from problems associated with high operating temperatures and harsh operating environments. The need to match coefficients of thermal expansion constrains materials choices and can requires high cost fabrication techniques. The Interscience Radial Flow (IRF) SOFC technology was designed specifically to minimize problems associated with high temperature operation and for manufacture by available and low cost fabrication techniques. The three key physical characteristics of the IRF design are its planar, non-sintered construction, the use of particulate materials to form porous electrodes, and the internal radial flow.

The objective in this phase of the research was to demonstrate the feasibility of multi-cell stack operation. The performance milestone was 15% DC HHV efficiency with hydrogen at power densities greater than 50 mW/cm$^2$ in runs longer than 100 hours.

### BACKGROUND INFORMATION

The Interscience Radial Flow (IRF) Solid Oxide Fuel Cell (US Patent Number 4,770,955) was conceived and developed in the mid 80's by Standard Oil of Ohio (SOHIO), now BP Research (Cleveland, Ohio). The original development objectives were to design a new, planar geometry, solid oxide fuel cell which could incorporate current advances in fuel cell materials, and utilized simpler cell fabrication and automated stack manufacturing techniques.

TMI has designed its technology to be successful in the marketplace, as well as at the bench. Based on optimization of the overall systems module for manufacture at low cost per kilowatt ($/kW), by two independent consultant studies (Battelle (Columbus) in 1988 and Michael A. Cobb and Company in 1992) that a power density target of 100 mW/cm$^2$ (using natural gas fuel at a 43% HHV efficiency) correlates to a manufactured cost for a complete system approaching $500/kW. The cell and stack designs also reflect TMI's objective to manufacture using available equipment and known fabrication methods and techniques.

The cell, approximately 5 cm (2 inches) in diameter, is full commercial scale. Figures 1 and 2 show an expanded and a cross-sectional schematic, respectively, of the IRF unit cell. Each cell is constructed of three layers: (1) tape cast or pressed, porous, nickel -zirconia cermet anode, (2) tape cast and sintered, non-porous, yttria-stabilized zirconia electrolyte, (3) tape cast or pressed porous, strontium-doped, lanthanum

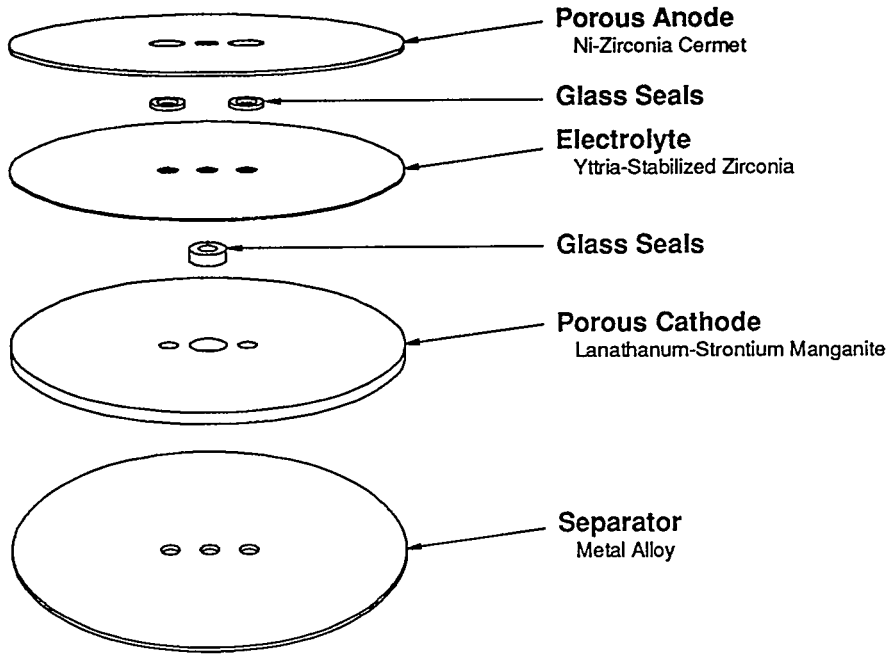


Figure 1. IRF Cell Schematic (Exploded)

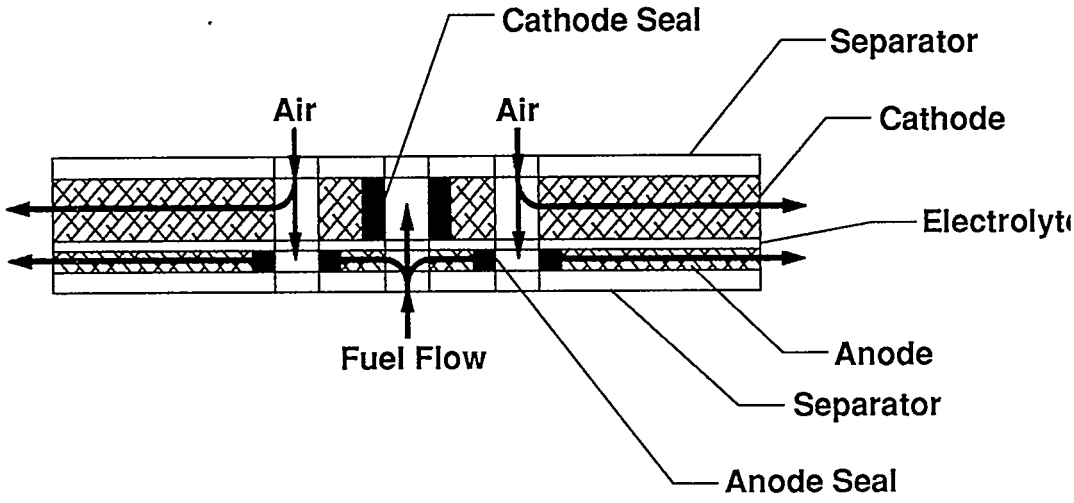


Figure 2. IRF Cell Schematic (Cross Section)

manganite cathode, and a stamped, high-temperature, metal alloy separator.

Figure 3 shows a schematic of the IRF stack. Cells are bipolar and connected in series to obtain higher voltage outputs. Stacks of 600 to 1000 cells will produce approximately 2 kW to 3 kW of power. Spring loaded stack assemblies accommodate both thermal expansion and any gradual size changes of the cells themselves. Physically, a complete 100-kW system module, including a power unit of approximately 80 stacks, will fit into an insulated box, 1 meter by 1 meter by 1.5 meters. System modules can be connected for higher power outputs.

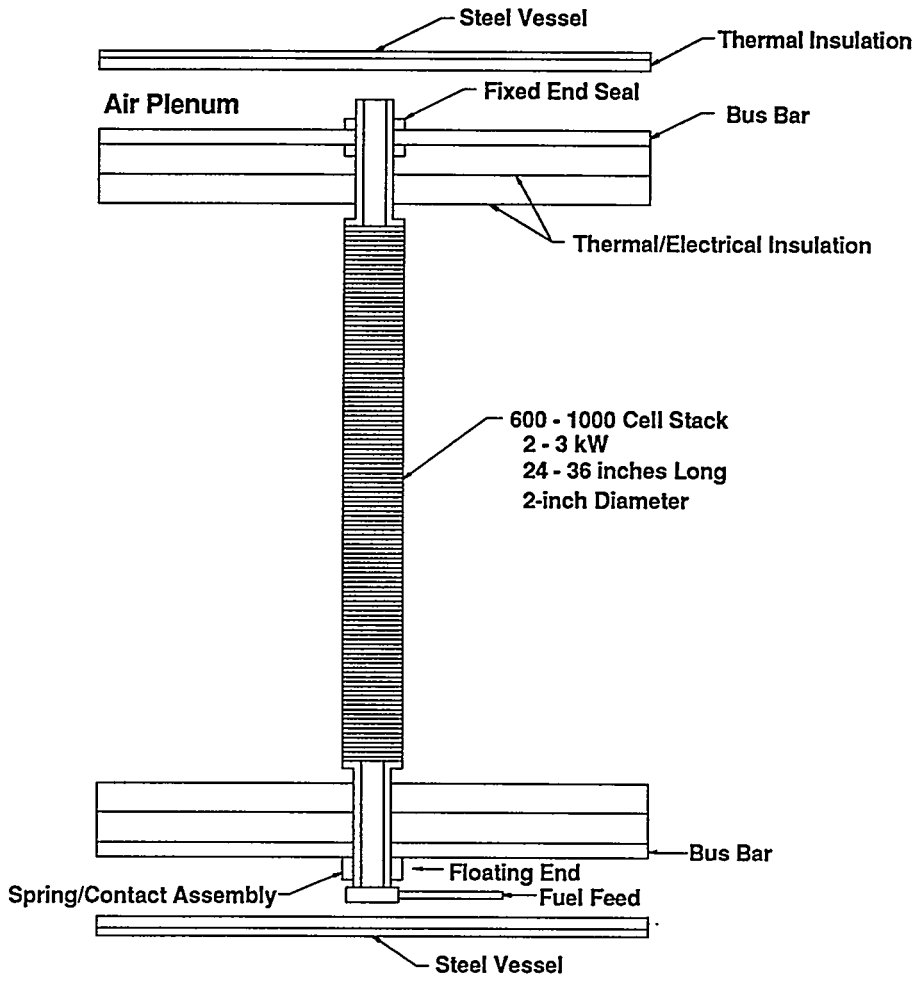


**Figure 3. IRF Stack Schematic**

The key physical characteristics of IRF design are the porous, particulate electrodes and the radial design. Fuel and oxidant, usually air, are supplied through the internally-manifolded holes and flow radially outward on either side of the non-permeable electrolyte. Intimate mixing of the fuel with the high surface area nickel catalyzes the reforming reaction. The plug flow through the particulate bed also gives rise to high fuel utilization (90% to 95%) with a single pass.

The novel use of particulate electrodes eliminates problems caused by thermal expansion coefficient mismatches at the sintered boundaries in other SOFC designs. The loose particles in the electrodes allow the separator, seals, and electrolyte to expand at different rates and change position with respect to the electrode without loosing electrical contact. A "micro slip" occurs between the particles, separators, and electrolytes. Because of this characteristic, metallic separators, which are cheaper and easier to manufacture than ceramic separators, can be used. Metal separators also serve to contain any crack propagation in a stack, and prevent catastrophic failure due to cracks.

The radial design allows internal manifolding of the fuel and oxidant inlet streams. Internal manifolding minimizes the seal areas

Ceramic materials were not investigated for this initial study due to the gasket-like viscosity requirement.

IRF manufacturing contemplates using green anodes and cathodes in the stacks and firing in situ. Using green electrodes minimizes the number of process steps required and increases the handling strength of the electrodes. Similar techniques can be used for seal preforms. The use of green seals also increases the flexibility in seal design and testing. The green seal preforms were more flexible and resistant to stresses than fired preforms, easier to handle, and had decreased likelihood of damage during assembly.

MULTI-CELL STACKS

Two and three cell stack tests have been completed, using the newly developed techniques for electrode and seal fabrication. Stacks are initially started under open circuit conditions. After the stack open circuit voltage stabilizes the stack is switched to closed circuit operation. Hydrogen and air flows are varied to investigate efficiency, fuel utilization and power output.

MANUFACTURING COST ANALYSIS

In conjunction with other supported development, an extensive manufacturing cost analysis was conducted by Michael A. Cobb and Company (MAC&Co). Previous manufacturing cost analyses had been performed by BP and Battelle (Columbus) in the late 1980's. Cobb was engaged by TMI to provide an independent review of the previous work, update costs to reflect 1992 dollars, and to incorporate recent revisions to the original manufacturing plan. MAC&Co reviewed the basic methodology and assumptions used in the previous estimates for logic and completeness and verified and updated costs using supplier-provided materials and equipment quotations, literature prices and inflation factors, and up to date labor rates.

## RESULTS AND ACCOMPLISHMENTS

SEALS

Seal preforms testing, using green seal preforms, has been quite successful. Cathode seal dimensions have been determined so that the seals hold pressure and in some instances they have survived thermal cycling to room temperature and back to 1000 C. Optimization of the anode seals has proven to be more difficult, mostly due to problems of fracturing of the YSZ electrolyte beneath the seals.

A series of anode seal tests done in single hole fuel cell tests (without a cathode seal) were performed. Different seal wall thicknesses, sealing temperatures and applied loads were also tested. The open circuit voltages ranged from 0.66 to 0.96 V for the series of tests. The results showed that a number of seal thicknesses could be used successfully, using the open circuit voltage, Voc, as a measure of the effectiveness of the seal. However, fracture of the YSZ electrolyte occurred in all but one test.

The open circuit voltages of 3-cell stacks ranged from 0.08 to 2.46 V for a series of six stack tests. Fracturing of the YSZ, in varying degrees, was a problem in all six tests. The issue of the electrolyte strength is now being addressed.

MULTI-CELL STACKS

The ultimate objective in this phase of the research was to show the feasibility of IRF stack operation and achieve the first stack performance milestone of 15% DC HHV efficiency with hydrogen at power densities greater than 50 $mW/cm^2$ in runs longer than 100 hours. The performance targets have been met in both three cell and two cell stacks. The best three cell stack performance had a peak power density (based on active anode area) of 80.7 $mW/cm^2$ at 20.2 % DC HHV efficiency. The stack performed at greater than 51 $mW/cm^2$ for 93 hours and for 117 hours at greater than 45 $mW/cm^2$. The most successful two cell stack operated for more than 435 hours, with a maximum power density of 68 $mW/cm^2$ at a DC HHV efficiency of 17.4 %. The highest combined power density and efficiency in a two cell stack was 82 $mW/cm^2$ and 15.7 % efficiency.

MANUFACTURING COST ANALYSIS

In the economic evaluation, MAC&Co found that the Battelle estimate generally gave an accurate accounting of the raw materials, processes, and equipment. Using the revised and updated Battelle numbers as the basis, manufacturing process changes were then implemented. The revised manufacturing

processes identified by TMI were generally lower cost alternatives to those estimated by Battelle. Therefore MAC&Co adjusted the manufacturing costs to reflect the changes.

Based on the improved manufacturing processes and the required materials and balance of system parts costs, labor and overhead expenses, and capital equipment charges, MAC&Co estimated that the total manufacturing cost of the complete IRF SOFC power module would **approach $500/kW as production levels increased to mature levels.**

MAC&Co indicated that the low manufacturing costs were supported by :

- Thin layers and low per unit area materials content. Projected materials costs is obtained using performance levels already achieved in single cells.
- Planar design with simple repeating units is well suited to automation.
- Internal manifolds and radial flow design without exhaust manifolds minimize the number of additional external components required, and minimize the operations required to build a stack.
- Cost reduction potential exists with improved cell performance (increased power densities) and improved fabrication techniques, particularly in the area of electrolyte sintering.
- The inverter, the most expensive balance of plant element, offers potential for cost reduction as technical developments are made in similar power conversion applications.

MAC&Co also identified several factors which help to minimize the development risk of the IRF SOFC:

- Current experimental test cells and stacks use commercial-size components, reducing scale-up risks. This allows greater confidence in production cost estimates and projected cell performance.
- Cell layers are not sintered together, eliminating precise thermal expansion matching requirements. Improved higher performance materials can be easily substituted.
- Key process steps can be tested effectively at the bench scale allowing early identification of potential problems and the opportunity to develop alternatives.

## FUTURE WORK

The IRF system requires study in the area of materials and fabrication to improve cell electrical characteristics, performance reproducibility, and long term performance. Optimization of seal fabrication and geometry, electrode fabrication, electrolyte strength and fabrication, and startup procedures are key tasks in improving stack performance and development. Key technical development milestones which must be demonstrated to achieve commercial success include:

- Electrodes fabricated using the proposed production processes must be tested and proved. Current electrode fabrication efforts being done in this area.
- Improved electrolyte fabrication and sintering schemes must be proved. Preliminary demonstration can be obtained using simulated firing cycles in batch furnaces. Continuous operation must then be demonstrated.
- Glass sealing must be demonstrated. Seal testing is currently in progress.
- Automated assembly processes must be demonstrated. Assembly processes can be initially demonstrated individually during the early production phases. Integration of these processes does not afford high technical risk, but requires a complex engineering effort.
- The enclosure, bus bars, stack support components, and the air, water, and fuel supply systems must be designed and tested. Though expected to follow the normal technical development cycle, these components are intimately tied to the stack and inverter and should evolve in parallel with them.

between fuel and air ports and removes the need for exhaust manifolds at the outer radius of the cell stack. At the outer radius, the spent fuel and excess oxidant mix, burning the remaining fuel.

Battelle (Columbus) was commissioned by BP America to evaluate the IRF fuel cell technology. Their final report, submitted in 1988, included a complete manufacturing cost analysis, including detailed material balances, and determination of equipment, manpower, facilities, and other factors required for mass production of the IRF fuel cell system. Battelle concluded that the IRF design concept was unique, had excellent potential for low cost manufacture, and the economic potential to compete with combustion-based electricity generating technologies, such as gas turbines. Battelle's cost analyses and conclusions were based on a power density of 100 $mW/cm^2$ at good efficiencies, a performance level exceeded by BP in the laboratory in 1988 (and repeated in 1992 by TMI).

## PROJECT DESCRIPTION

The Phase I R&D effort involved five major areas: test stand fabrication, IRF cell component development or procurement (anode, cathode, electrolyte, and separators), seal development, IRF multi-cell testing, and economic analysis. The major focus of the research was directed toward identifying promising sealing materials and determining proper dimensional requirements of seals for stack operation. The ultimate test of successful seals was the demonstration of IRF multi-cell stack operation. The stack performance milestone was 15% DC HHV efficiency with hydrogen at power densities greater than 50 $mW/cm^2$ in runs longer than 100 hours.

### TEST STAND

In the IRF seal and stack tests, the cell or stack is held in compression between two metallic air and fuel manifolds. These manifolds act as both the gas distribution system (for fuel on one side and air on the other) and electrical contacts. The test stands were designed to accomplish all three activities (gas flow, electrical contact, and compression loading) while holding the cell (or stack) at 1000° C.

### ELECTRODES

Anode and cathode geometric uniformity is critical to evaluate seal dimensions. To shorten the overall development timeline, the decision was made to initiate development of the electrode fabrication process proposed for commercial electrode manufacture. Originally, electrodes were to be individually fabricated by powder pressing. The commercial forming technique also allows greater control of electrode dimensions and therefore better uniformity.

Electrodes were fabricated using a proprietary forming technology developed by BP. Formulations were initially devised by substituting the binder system used for powder pressing with the BP binder system.

### SEALS

Seal studies were initiated to identify and quantify the variables which most directly affect successful stack operation. Materials properties were studied such as thermal expansion, shrinkage, viscosity, etc. Fabrication techniques were developed for preparation of seal preforms of various dimensions, and testing was conducted to determine dimensional limits and ranges for successful sealing.

The IRF SOFC design requires a glass seal which functions more like a gasket than a cement to allow for dimensional changes in the electrode materials. The glass should wet both the YSZ and the metal separator and should not decompose in reducing or oxidizing atmospheres. Though not critical, a CTE close to YSZ or the metal separator is preferred.

Two glass compositions were identified and tested in fuel cells during Phase I. The primary difference between the two materials was that Composition A softened at a lower temperature and thus had a lower viscosity at lower temperatures than Composition B. Preliminary testing in two cell stacks indicated the viscosity of Composition A was excessively low at the operating temperature causing the seal material to flow and block air and fuel manifold openings. Composition B was chosen for continued study during this phase of the work.

# P15 Processing of $LaCrO_3$ for Solid Oxide Fuel Cell Applications

## CONTRACT INFORMATION

| | |
|---|---|
| **Contract Number** | DE-FG21-93MC29224 |
| **Contractor** | University of Missouri - Rolla<br>Ceramic Engineering Department<br>222 McNutt Hall<br>Rolla, MO 65401<br>(314) 341-6129 |
| **Contractor Project Manager** | Wayne Huebner |
| **Principal Investigators** | Wayne Huebner<br>Magdi M. Nasrallah<br>Harlan U. Anderson |
| **METC Project Manager** | Diane T. Hooie |
| **Period of Performance** | April 16, 1993 to April 15, 1994 |

**Schedule and Milestones**

**FY93 Program Schedule**

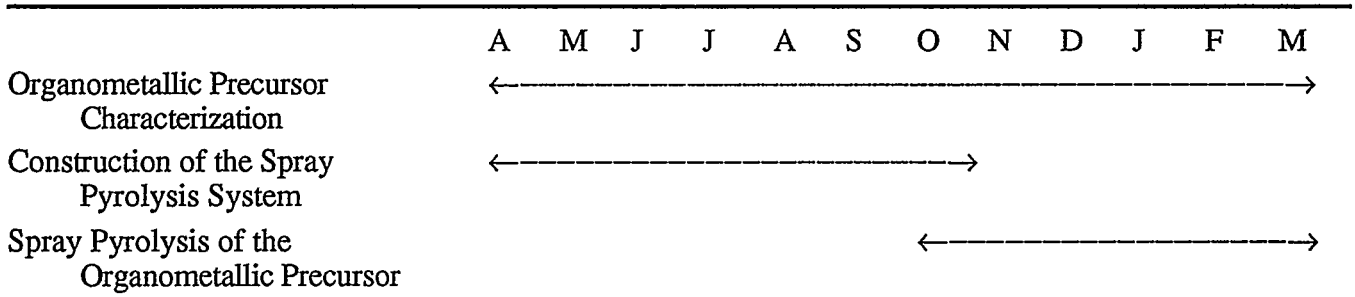


## OBJECTIVES

The University of Missouri-Rolla has recently embarked on a 5 year research program dedicated towards the development of $LaCrO_3$-based interconnect powders which densify when in contact with anode and cathode materials for solid oxide fuel cells (SOFC). During a previous DOE-METC program (DE-FG21-89MC26015) we developed and characterized potential cathode and interconnect materials.[1] During the course of this program we investigated compositions within the pseudo-ternary $LaCrO_3$-$LaMnO_3$-$LaCoO_3$ system. Results indicated that some of the compositions in this system exhibited the requisite electrical

conductivity and stability towards reduction, and could be sintered in air at temperatures less than 1450°C.

In this research program we will expand our studies on the processing and sintering of $LaCrO_3$ to make dense interconnects using $LaCrO_3$-based oxides at temperatures less than 1500°C in an air atmosphere and in contact with both anode and cathode oxides. The specific objectives of this research program are to:

- Develop a novel technique which reproducibly yields $LaCrO_3$-based powders with the desired particle characteristics
- Fully understand the liquid phase sintering mechanism
- Clearly identify the reason why $LaCrO_3$ does not densify in the presence of electrolyte and cathode materials
- Systematically solve this problem through judicious control over the liquid phase.

## BACKGROUND INFORMATION

Despite years of intensive research, one of the primary factors limiting the commercial application of solid oxide fuel cells is the lack of fully-understood microstructural evolution ↔ property relationships of the $LaCrO_3$-based interconnect. Indeed, the inability to co-sinter $LaCrO_3$-based compounds in air at T<1550°C with other SOFC components leads to unacceptable interfacial reactions, and resultant losses in efficiency. Many researchers have addressed this problem, yet progress has been hindered due to recognized difficulties in repeatable processing. Phase development, stoichiometry, particle size/distribution, agglomerate/ aggregate formation, volatility of components, and their dependence on dopant levels and sintering temperature, time and atmosphere are very difficult to systematically take into account. Even chemical preparation techniques such as the "Pechini" process[2] and more recently, the "Glycine Nitrate"[3-4] process, do not readily allow for the controlled synthesis of multicomponent perovskite powders with the desired characteristics.

In many regards, the key issue is related to an intermediate synthesis stage which involves the presence of multiple cations in an amorphous precursor. More often than not, intermediate oxides or hydroxides of the cations present nucleate and grow instead of the desired phase. Phase development past this stage is identical to the traditional mixed oxide approach, except for the advantage that the scale is greatly diminished. For most systems the best situation is to directly nucleate the desired perovskite at the lowest temperature possible since this minimizes the primary particle size. However, with regard to $LaCrO_3$ it appears that minimizing the primary particle size, and hence increasing the driving force for densification is not sufficient. It is likely that the existence of an intermediate phase, which leads to liquid phase sintering, is the key to low temperature densification in air.

Thus the results of our work and other investigators[3-11] has lead us to the conclusion that the densification of $LaCrO_3$-based oxides is controlled by the ability for mass transport (sintering) to occur under conditions which minimize Cr oxide volatilization (Cr activity, $a_{Cr}$). We demonstrated that this could be accomplished by sintering at temperatures >1750°C and oxygen activities of about $10^{-10}$ atm[11], but clearly these sintering conditions are not compatible with the stability of other SOFC components. Another approach to reduce $a_{Cr}$ is to lower the sintering temperature with liquid fluxes, which was initially pursued by Argonne National Labs[7]. Although the high mobility of the fluoride fluxes detrimentally affected the other cell components, their work showed that liquid phase sintering with a more compatible transient phase would be an attractive approach.

In our earlier DOE-METC program we showed that additions of Ca and Co to $LaCrO_3$ and $YCrO_3$ allowed densification to take place in air at temperatures below 1450°C. However further studies showed that interactions during cofiring between the transient liquid phase (mixture of CaO-CoO and $Cr_2O_3$) and the electrolyte and cathode prevent densification of the $LaCrO_3$.

Recent sintering studies on Ca-and Sr-doped $LaCrO_3$ suggest that the ability to densify these compounds in air at T<1550°C may be related to the presence of a transient liquid phase formed from the melting of chromates ($CaO$-$CoO$-$Cr_2O_3$ system)[1,13]. If this is true, then in order to co-sinter this system with other SOFC components, detailed knowledge concerning the composition, source, stability range, and wetting behavior of the liquid phase is required. With this information we can vary the parameters which will allow for the densification of the interconnect when cofired with the other SOFC components. Successful completion of the proposed objectives will be a major step towards the commercialization of SOFC.

## PROJECT DESCRIPTION

This project is divided into three primary objectives:

#1 Reproducible Powder Synthesis

#2 Sintering of $LaCrO_3$-based Powders

#3 Co-sintering of $LaCrO_3$-based Powders with Cathode and Electrolyte Materials

A summary statement of the goals, tasks, and anticipated results for each of these objectives is presented at the beginning of each of the following sections, followed by details concerning the justification and procedure for the experiments to be performed.

### #1 Reproducible Powder Synthesis

Goal: Develop a technique of synthesizing $(La_{1-x}Ca_x)(Cr_{1-y}Co_y)O_3$; A:B = 0.99 to 1.01 powders which reproducibly yields the desired composition, size/distribution, morphology, and surface area.

Approach: Spray pyrolysis of organometallic precursors

Specific Tasks:

A. Characterization of the Organometallic Precursor
   - ♦ Rheology
   - ♦ Decomposition
   - ♦ Phase Development (nucleation & crystal growth)

B. Construction of the Spray Pyrolysis System

C. Spray Pyrolysis of the Organometallic Precursor
   - ♦ Particle formation studies - control over particle characteristics via aerosol T/t/atm, and precursor rheology & concentration

Anticipated Results:

A. Reproducible powder processing

B. Answer to key questions regarding the chromate phases:
   - ♦ Is the chromate present as a result of exsolution due to metastability, or is it simply the first phase to nucleate from amorphous precursors ?
   - ♦ Is the solubility of dopants higher in the chromate phase due to its tetragonal structure and higher molar volume ?
   - ♦ What is the distribution and connectivity of the chromate phase ? - Is it homogeneously precipitated on powder surfaces or does it form as a discrete phase ?

Key to the success of this project is the reproducible synthesis of powders with very specific attributes. Phase development, stoichiometry, particle size/distribution, agglomerate/aggregate formation, volatility of components, and their dependence on dopant levels and sintering temperature, time and atmosphere must be systematically taken into account.

In this project we will directly convert Pechini-derived precursors into dense, spherical

powders by **spray pyrolysis**. Figure #1 summarizes the overall process. This approach utilizes the advantages of the Pechini-precursor, yet circumvents the significant problem of agglomerate/hard aggregate formation associated with the high "local" temperature achieved during combustion of the residual organics. Spray pyrolysis is a well-established technique which inhibits aggregation since phase and particle development are confined to the droplet scale. In addition, by controlling the precursor characteristics and spray pyrolysis conditions we can not only prepare particles with a wide variation in particle sizes and morphologies, but we can also directly control the phase distribution of the chromates which nucleate or exsolve at low temperatures.

To spray-pyrolyze the Pechini precursor we need to characterize: 1) its rheological behavior, and 2) phase development. The Pechini precursor is of particular interest since its viscosity is variable through solvent concentration, limited esterification, and temperature control (it is thermoplastic). This ability to modify the viscosity allows for the systematic variation of the droplet size/distribution, which directly controls the final particle size/distribution. In this study we will vary the rheology by changing the [cations]/$cm^3$, the ethylene glycol:citric acid ratio, extent of esterification, and temperature.

In parallel with these studies a series of thermal analyses will be performed to characterize the decomposition and phase development stages. We are interested in knowing the temperature/time/atmosphere conditions which yield single phase components. A unique advantage of spray pyrolysis is that we are not limited in any way as to the temperature → the particles remain separated during the high temperature sequences, eliminating the potential of aggregation. DTA/TGA on the precursors with varying $\eta$ coupled with XRD analyses will yield the desired information.

A unique aspect of spray pyrolysis is that the phase distribution and connectivity can be controlled to a certain extent, i.e.:

→ If the chromate nucleates first, then spray pyrolysis will yield an ultrafine dispersion of this phase intimately mixed with the nucleated perovskite.

→ If the chromate nucleates first and then melts (a high temperature calcine), then a wetting liquid phase will result in uniformly-coated powders.

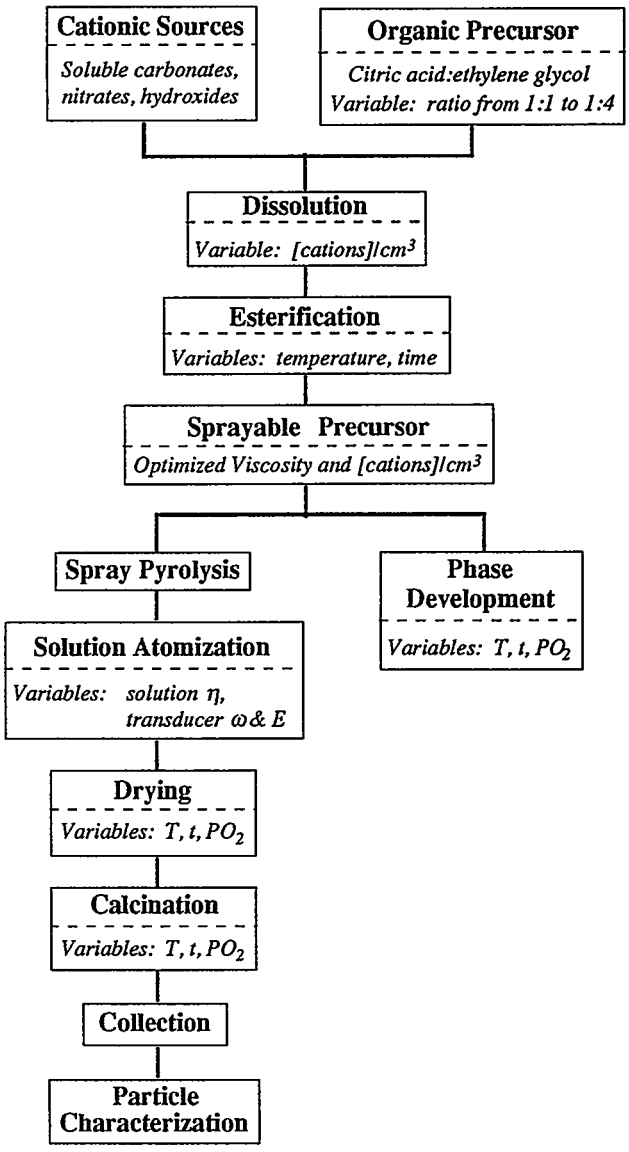


**Figure 1. Experimental Overview**

→ If the chromate exsolves we need to determine if this is strictly a surface reaction or if precipitation occurs throughout the bulk. If nucleation occurs within the bulk then spray pyrolysis is still advantageous with regard to prevention of aggregation, but poses no special advantages with regard to phase distribution. If it exsolves on the surface, then spray pyrolysis will inhibit segregation and growth of the chromate, again resulting in a uniform, fine distribution. If the chromate exsolves and then melts, again we have the potential for uniformly coated individual particles.

## Spray Pyrolysis System

During the proposed studies on the precursor, we will build the spray pyrolysis system schematically illustrated in Figure 2. This system is comprised of three subsystems: 1) aerosol production, 2) furnace, and 3) collection. The aerosol will be produced using a piezoelectric atomizer. The diameter of a droplet, D, produced by ultrasonic atomization is given by:

$$D = 0.34\left[\frac{8\pi\gamma}{\rho f^2}\right]^{1/3}$$

where $\gamma$ is the surface tension, $\rho$ is the liquid density, and f is the driven transducer frequency. $\gamma$ will be a function of the viscosity of the precursor. The viscosity of the Pechini precursor can be varied by orders of magnitude. $\rho$ will primarily depend upon the cation concentration in solution, but cannot be changed by orders of magnitude. The driving frequency can be varied several orders of magnitude ($\approx$ 1kHz to 1 MHz) with a Kepco high voltage supply and oscillator.

Once the precursor is atomized it is carried to a furnace chamber in a gas stream. To minimize coagulation during this step the droplet concentration must be kept below $10^7/cm^3$.

At this point particle development begins: the drying and firing stages are important to control. For this project the ideal particle is solid as compared to hollow. Thus, during the drying stage we need to slowly collapse the droplet by

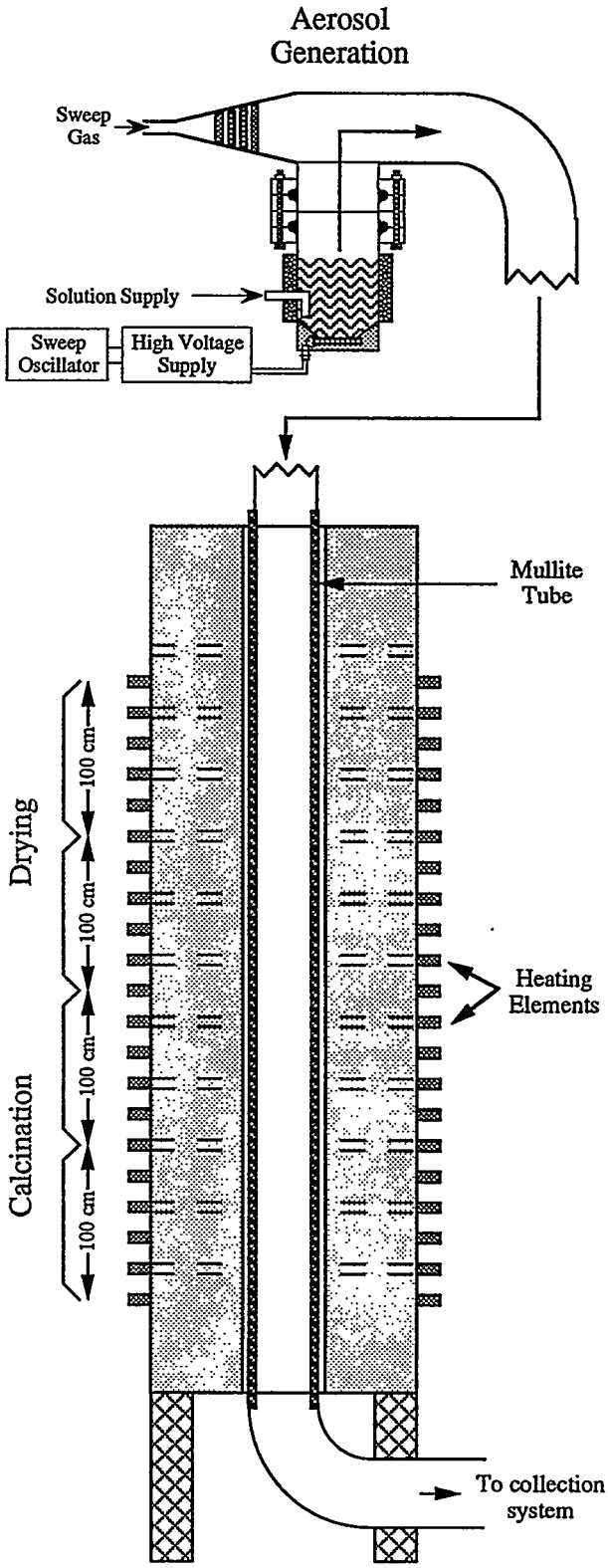


**Figure 2. Spray Pyrolysis System**

solvent evaporation with precipitation or the formation of a rigid shell which would result in either a hollow particle, or an "explosion" which would blow apart the particle into fragments due to internal pressure. As we recently showed during spray pyrolysis of a mixed conductor and the YBC superconductor[14], the Pechini precursor is ideally suited as the high viscosity prevents precipitation, and the rapid esterification which occurs with temperature/time allows for solid particle development. From these studies we concluded that a precursor with a high degree of polymerization is an important requirement for the formation of "solid" particles by spray pyrolysis.

Once the particles are dried they are calcined to remove the organics and nucleate and grow the desired phase. Phase development results from the initial stages of the research will set the temperature/time/atm needed to obtain particles with the desired phase purity (or inhomogeneity if the chromate second phase is needed). We can easily control the $PO_2$ with the sweep gas, and the residence time with the flow rate. After calcination the powders will be collected with a simple gore-tex filtration system.

## #2 Sintering of $LaCrO_3$-based Powders

Goal: To better understand the sintering mechanism of $(La_{1-x}Ca_x)(Cr_{1-y}Co_y)O_3$ in air at T≤1450°C.

Specific Tasks:

A. Reproducible Green State Synthesis via Tape Casting

- Develop the tape casting system & characterize the dispersive behavior of the spray-pyrolyzed powders in the binder system.

B. Characterization of the Chromate Liquid Phase

- Composition
- Volume fraction
- Viscosity as a f(T, composition)
- Temperature stability
- Wettability on $LaCrO_3$-based powders (contact angle measurements)

C. Microstructural Evolution with Spray-Pyrolyzed Powders

- Temperature/time/atmosphere ($pO_2/a_{Cr}$) studies and as a f(volume fraction liquid)
- Compositional studies: effect of Ca, Co content, the Ca:Co ratio, and the volume fraction of liquid.

Anticipated Results:

1. A $LaCrO_3$ composition which sinters in air at T≤1450°C.

2. Answer to key questions concerning the sintering mechanism:

   - What is the composition and viscosity of the liquid phase ?
   - How are these affected by the A:B, Ca:Co ratios ?
   - When does it form ?
   - Why is it metastable ?
   - What role does it play in the densification process ?, i.e. does it:
     - → wet
     - → cause particle rearrangement
     - → go into solid solution at higher temperatures
     - → phase separate upon cooling, and if so, where ?

Microstructural evolution in monolithic specimens prepared using the spray-pyrolyzed will be systematically studied with the goal of achieving fully dense, homogeneous, single phase components with a controlled microstructure. Our primary objective is to study the powder processing/phase stability relationships for the development and commercialization of $(La_{1-x}Ca_x)(Cr_{1-y}Co_y)O_3$ perovskite powders for solid oxide fuel cell interconnects.

The initial stage of this portion of the research will focus on reproducible "green state" synthesis by tape casting. Although some of the studies in this section can be made using simple pressed disks, research on understanding the dispersion of the spray-pyrolyzed powders in organic vehicles suitable for tape casting will establish an important practical database. Measurements of the rheological behavior of optimized powders dispersed in a commercial binder system will be performed, with the goal of maximizing the green density. This stage of the research is very important, as many of the irreproducibility problems cited by previous researchers may be traced to poor green state synthesis.

Once this database is established, studies will proceed to further our understanding of the role the chromate phase plays in the densification behavior of $LaCrO_3$-based powders. With regard to the chromate phase we are particularly interested in characterizing its composition, volume fraction, viscosity as a function of temperature and composition, temperature stability range, and wettability on $LaCrO_3$. These are by no means easy tasks, and will require extensive TGA/DTA, XRD, SEM, TEM, rheological and Sessile drop measurements.

In parallel with these studies a comprehensive investigation of microstructural evolution of the spray-pyrolyzed powders will be performed. Experimental parameters including temperature, time, atmosphere ($PO_2$ and $a_{Cr}$) will be studied, in addition to compositional parameters such as the volume fraction of the liquid phase, and the A- and B-site dopant levels. We have the facilities to perform dilatometric studies under these conditions, and thus will perform shrinkage and density measurements for each composition. These measurements will be used as a guide leading to compositions which have the optimum densification characteristics. Microstructural, thermal expansion coefficient, electrical conductivity and thermal stability measurements will also be performed.

## #3 Co-sintering of $LaCrO_3$-based Powders with Cathode and Electrolyte Materials

Goal: Understand why LCC and YCC do not densify when in contact with $ZrO_2$ or LSM

Specific Tasks:

A. Identify the Underlying Cause

- Contact angle measurements of liquid phase on LSM and $ZrO_2$
- Diffusion couples
  - → dense & porous specimens
  - → microstructural analysis of the interface (microprobe)

B. Develop Approaches to Solve the Co-Sintering Problem

- If $Ca^{2+}$ segregation (surface diffusion, preferential migration):
  - → decrease the Ca activity gradient ($\Delta a_{Ca}$) by using Ca-doped $LaMnO_3$ and $ZrO_2$
  - → Buffer zone to block $Ca^{2+}$ migration (e.g. $CeO_2$-based materials - an electronic conductor)
- If wicking:
  - → alter pore size distributions to diminish the driving force - this knowledge will come out of consideration of the viscosity of the melt & the contact angles - the pore size needed to prevent wicking can then be calculated.
  - → alter wetting behavior via dopants to the liquid phase (changes in viscosity - incorporation of ions that bond well to $Cr^{3+}$ compared to $Mn^{3+}$ or $Zr^{4+}$ )
- Develop new materials through this and parallel research projects that will outperform the $LaCrO_3$-based approach to the interconnect.

Anticipated Results:

A. A $LaCrO_3$-type composition which sinters in air at T≤1450°C when in contact with other SOFC components.

This portion of the research program is the most important, as progress in cofiring $LaCrO_3$-based compositions when in contact with LSM or $ZrO_2$ is hindering progress in the application of SOFC. Thus the primary goal of this aspect of the program is to understand the underlying cause. Our approach will be understand what occurs at the interface during cofiring, and then take steps to circumvent the problem. We anticipate that the problem is related to either 1) wicking of the liquid phase responsible for densification away from the LCC, or 2) preferential $Ca^{2+}$ and/or $Co^{2+}$ segregation from the LCC to LSM and/or $ZrO_2$.

We will initially perform experiments to evaluate the interaction of the liquid phase identified in Task #1 with LSM and $ZrO_2$. The first studies will be DTA/TGA analyses on powder mixtures to evaluate potential reactions (i.e. is there eutectic liquid formation at $T<T_m^{liquid}$), and contact angle measurements on dense LSM and $ZrO_2$. The contact angle will be determined using the Sessile drop approach shown in Figure 3.:

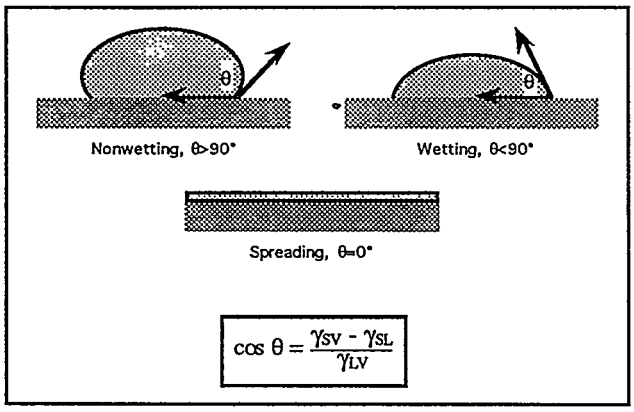


**Figure 3. Sessile Drop Experiment**

From these measurements we will be able to directly identify how well the liquid phase wets LSM and $ZrO_2$. If it turns out that the liquid phase wets LSM and $ZrO_2$ better than LCC, then a series of studies will be initiated to understand the influence of the atmosphere and composition of the liquid phase on the wetting behavior. If the driving force for preferential wicking is due to differences in capillary forces, we need to consider how to manipulate these forces to minimize or eliminate the wicking. Using Poiseulle's law the penetration distance, L, of a liquid into a porous tube (i.e. continuous porosity) is:

$$L^2 = \frac{\gamma \cos\theta}{2\eta} r$$

where: $\theta$ = contact angle
$\gamma$ = surface tension of the liquid
$\eta$ = viscosity
r = pore radius
t = penetration time

Hence effective strategies for minimizing preferential wicking is to increase the viscosity by appropriate additives, minimize the time over which the liquid can penetrate, develop a system which has a lower contact angle on the LCC than either the LSM or $ZrO_2$, or increase the pore size of the anode/cathode compared to the LCC. Compositional alterations of the liquid phase which would change the viscosity and the wetting characteristics will be studied (e.g. $Co^{2+}$ additions, and other ions such as $Mn^{2+}$, $Al^{3+}$ and $Fe^{2+}$). Altered pore size distributions can be easily achieved through variation of the size distribution of the starting powders. It may also be possible to modify the interface, or surface of the anode/cathode powders to alter $\theta$, yet not affect the requisite electrical properties of the interface. In all cases, microstructural evolution of cofired tapes will be studied to see if the potential solutions were successful. In a parallel study, the effect of particle size, firing temperature and binders on the porosity of LSM tapes is being investigated.

To address the diffusion/segregation issue we will synthesize diffusion couples from laminated tapes, and then perform a series of T/time studies on quenched specimens to evaluate the presence/extent of $Ca^{2+}$ and $Co^{2+}$ interdiffusion. Diffusion experiments will be carried out using a) $LaCrO_3$ doped with a wide range of Ca and Co contents (between 5-30%) and A:B ratio, coupled with b) $LaMnO_3$ doped with up to 20% Sr or up to 40% Ca, and $ZrO_2$ stabilized with either Y or Ca. In addition, chromium rich or depleted compounds will be synthesized and the impact of changing chromium activity on sintering of the couples will be investigated. We're looking for extensive $Ca^{2+}$

diffusion prior to the onset temperature of densification of the LCC. If this is the cause, then several approaches may be possible to eliminate the problem. It is well known that Ca-doped $LaMnO_3$ and $ZrO_2$ exhibit electrical characteristics which make their use as fuel cell materials feasible. Hence, if the anode and cathode were synthesized from Ca-doped materials this would decrease the $Ca^{2+}$ activity gradient ($\Delta a_{Cr}$) and hopefully allow cofiring. Alternately, a material could be used as a buffer zone to prevent $Ca^{2+}$ interdiffusion. This layer should satisfy the materials requirements of the SOFC, hence its development is by no means an easy task. For instance, $CeO_2$ is being studied as a potential buffer for preventing interactions at the electrolyte/cathode interface. If migration of the Ca occurs via grain boundary diffusion, then it is expected that altering grain boundary area will affect the rates of diffusion. This can be accomplished by coarsening the starting powders.

If none of these solutions prove to be suitable, then a modified composition needs to be developed. For example, if $Ca^{2+}$ cannot be retained due to preferential segregation, a substitute such as $Sr^{2+}$ may be needed to serve the same purpose (forming lower melting eutectics) but does not migrate. Our studies indicate that compositions with lower sintering temperatures can be developed by appropriate additions. Efforts by our group through this and other ongoing activities as well as those of others will hopefully resolve the critical materials problems that hinder the commercialization of SOFC's.

## RESULTS

This program has been in place for three months, which is why this proceedings paper was written as a Project Description rather than being results-oriented. To date we have begun construction of the spray pyrolysis system , and have initiated studies on the organometallic precursor.

## REFERENCES


1. H.U. Anderson and M.M. Nasrallah, "Development of Improved Cathodes for Solid Oxide Fuel Cells," Proc. of the 2nd Annual Fuel Cell Contractors Review Meeting, ed. W.J. Huber, pp 171-78, DOE/METC-90/6112.

2. M.P. Pechini, "Method of Preparing Lead and Alkaline Earth Titanates and Niobates and Coating Method Using the Same to From a Capacitor," U.S. Patent #3,330,697 (1967).

3. J.L. Bates, L.A. Chick, and W.J. Weber, "Alternative Materials for Solid Oxide Fuel Cells," Proc. of the 1st Annual Fuel Cell Contractors Review Meeting, ed. W.J. Huber, pp 54-63, DOE/METC-89/6105.

4. L.A. Chick, J.L. Bates, L.R. Pederson and H.E. Kissinger, "Synthesis of Air-Sinterable Lanthanum Chromite Powders," pp 170-187, Proc. 1st Intl. Symp. SOFC, ed. S. Singhal, Electrochem. Soc., Pennington, N.J. (1989).

5. N. Sakai, T. Kawada, H. Yokokawa and M. Dokiya, "Sinterability and Electrical Conductivity of Ca-doped $LaCrO_3$," *J. Mater. Sci.*, **25**:4531-34 (1990).

6. N. Sakai, T. Kawada, H. Yokokawa and M. Dokiya, "Low Temperature Sintering Characteristics of Ca-doped $LaCrO_3$," Proc. 2nd Intl. Symp. on Solid Oxide Fuel Cells, eds. F. Grosz, P. Zegers, S. Singhal, and O. Yamamoto, Athens, Greece, July 1991, pp. 629-636.

7. M. Mori, N. Sakai, T. Kawada, H. Yokokawa and M. Dokiya, "Low Temperature Air-Sinterable Lanthanum Calcium Chromite with Chromium Deficit for SOFC Separator," to be published in Denki Kagaku.

8. B.K. Flandermeyer, R.B. Poeppel, J.T. Dusek and H.U. Anderson, "Sintering Aid for Lanthanum Chromite Refractories," U.S. Patent #4,749,632, 1988.

9. H.U. Anderson, J.D. Carter, R. Koc, and M.M. Nasrallah, "Air Sinterable Solid Oxide Fuel Cell Interconnects," Fuel Cell Seminar, Phoenix, AZ November 1990, pp. 141-44.
10. L.A. Chick, J.L. Bates and G.D. Maupin, "Air-Sinterable Mechanisms of Chromites," Proc. 2nd Intl. Symp. on Solid Oxide Fuel Cells, eds. F. Grosz, P. Zegers, S. Singhal, and O. Yamamoto, Athens, Greece, July 1991, pp. 621-628.

11. J.D. Carter, M.M. Nasrallah and H.U. Anderson, "Properties of Liquid Phase Sintered $LaCrO_3$ and $YCrO_3$," Ceramic Society Meeting, Cincinnati, OH, April 1991.

12. H.U. Anderson, Processing of Crystalline Ceramics, pp. 469-477, eds. H. Palmour, R. Davis and T. Hane, Plenum, New York (1978).

13. L.A. Chick and J.L. Bates, "Synthesis and Processing of Air-Sinterable Chromite Powders as Interconnections," Proc. of the 2nd Annual Fuel Cell Contractors Review Meeting, ed. W.J. Huber, pp 159-70, DOE/METC-90/6112.

14. S.C. Zhang, G.L. Messing and W. Huebner, "$YBa_2Cu_3O_{7-x}$ Superconductor Powder Synthesis by Spray Pyrolysis of Organic Acid Solutions," accepted for publication in the *J. Aerosol Science* (1991).

# P17 Advanced Research and Technology Development of MCFCs

## CONTRACT INFORMATION

| | |
|---|---|
| **Contract Number** | DE-AC21-90MC27394 |
| **Contractor** | M-C Power Corporation<br>8040 S. Madison<br>Burr Ridge, IL 60521<br>(708) 986-8040 |
| **Contractor Project Manager** | Thomas G. Benjamin |
| **Principal Investigators** | Robert J. Remick<br>Rafael A. Donado |
| **METC Project Manager** | Mark C. Williams |
| **Period of Performance** | Oct. 1, 1990 to Sept. 30, 1993 |

**Schedule and Milestones**

**FY93 Program Schedule**

| | S | O | N | D | J | F | M | A | M | J | J | A | S |
|---|---|---|---|---|---|---|---|---|---|---|---|---|---|
| Test Cell Modification | -(Completed FY91)- | | | | | | | | | | | | |
| Baseline Data Test | -(Completed FY92)- | | | | | | | | | | | | |
| Application of Ferrite | XXXXXXXXXXXXXXX | | | | | | | | | | | | |
| Evaluation of Ferrite | | | | | XXXXXXXXXXXXXXXXXXXXXXXXXXXXXXX | | | | | | | | |

## OBJECTIVES

The objective of this work is to evaluate methods for forming protective oxide layers of lithium ferrite *ex-situ* on the cathode-side stainless steel hardware of a molten carbonate fuel cell prior to cell/stack assembly. It is expected that once this *ex-situ* process is identified, it also will be possible to dope the protective oxide layer and achieve higher electrical conductivity and lower contact resistances than are experienced with the protective oxide layers that form *in-situ* when the cell/stack is first heated to operating temperature.

## BACKGROUND

The molten carbonate fuel cells (MCFCS) currently under development use either 310S or 316L stainless steel for the bipolar separator plate and the cathode current collector. Although both of these materials exhibit resistance to corrosion by the alkali carbonate, significant chemical processing of the exposed surface of the metal takes place during the first 1000 hours of operation. This chemical processing results in chromium and manganese being leached out of the surface oxide and into the electrolyte. Metallic and ionic diffusion

within the protective oxide coating causes segregation of the cations into several distinct oxide layers and in the case of 316L contributes to spalling of the surface oxide during thermal cycling. If the top surface of the exposed stainless steel can be protected from corrosive attack by the alkali carbonate, endurance of the separator plate will be improved, the purity of the electrolyte will be preserved, and changes in contact resistance over time could be kept to a minimum.

## PROJECT DESCRIPTION

The objective of this work is to develop methods to lower contact resistance losses associated with the protective oxide layer that forms on the surface of stainless steel in the MCFC cathode environment. The approach being taken is to coat the top surface of the stainless steel with a thin film of iron oxide to slow the chemical processing of the surface by the molten alkali carbonate.

## RESULTS

### Molten Salt Corrosion

Samples of 316L stainless steel sheet metal were coated with a 3-micron thick layer of $Fe_2O_3$ by the Jet Process Corporation using jet vapor deposition (JVD). A 25 mm by 25 mm square of the coated sample was placed in a tube furnace with the coated side up and a square 17 mm by 17 mm of lithium aluminate supported alkali carbonate matrix from a MCFC was placed on top. The alkali carbonate was present in a 38 mole-percent potassium carbonate, 62 mole-percent lithium carbonate ratio. The tube furnace was heated to 650°C and a gas mixture of 70% air/30% carbon dioxide was passed through the tube at a rate of about 100 cc per minute. Although the alkali carbonate melts at about 490°C, the lithium aluminate support, which is 50% porous and has a sub-micron mean pore size, acts as a sponge holding the molten electrolyte in place. This corrosion experiment was conducted for a period of 1000 hours. The tube furnace was then cooled and the sample recovered.

Visual inspection of the sample indicated that the iron oxide film on which the matrix rested had performed its function in protecting the underlying stainless steel from corrosive attack by the alkali carbonate. The lithium aluminate supported matrix was still white in color. Had corrosive attack on the stainless steel occurred, the matrix would have been colored yellow to orange by the dissolved chromium. Furthermore, no spalling of the surface oxide occurred on cool down of the apparatus.

The sample was mounted, cross sectioned and examined by SEM/EDX. Figure 1 is a photomicrograph of the cross section. What was not apparent from the visual inspection but is apparent from this cross section is that the final oxide layer is very much thicker than expected. The initial JVD coated iron oxide layer was only 3-microns thick. The oxide layer appearing in Figure 1 is over 20-microns thick.

EDX analysis of nine locations in the cross section, labeled A through I in the photomicrograph, was also performed. Results for locations A through G are listed in Table 1. Locations G, H, and I all have the same composition

corresponding to the composition of the unoxidized stainless steel metal.

The EDX analysis of the JVD sample cross section holds some surprises. First, it is not possible to unequivocal identify the original iron oxide layer applied by JVD. Second, the data in Table 1 suggests the presence of two, possible three, iron oxide layers corresponding to locations A, B, and C. Third, the chromium oxide layer at locations D and E contains substantial amounts of iron and nickel. Finally, there appears to be no chromium depletion layer in the metallic substrate. It is also important to note that manganese appears to be concentrating in the middle of the iron oxide layer at location B. This is important since a manganese doped iron oxide layer is the goal of this work.

The nature of the corrosion process which took place in this experiment is essentially unknown. However, one possible mechanism that can explain the results observed with the JVD iron oxide sample is ionic diffusion of iron ions through the oxide layer. Access of oxygen and molten electrolyte to the underlying bulk metal is restricted by the iron oxide layer. If the growth of the oxide layer is by cationic diffusion of iron from the bulk metal, through the iron oxide layer to the top surface, we would expect the top layer to be nearly pure iron oxide, as is the case. We might also expect that the layer immediately under the iron oxide to be depleted in iron and enriched in chromium. Chromium oxide has a higher free energy of formation than iron oxide. Therefore, we would expect that chromium oxide would form at the interface between the iron oxide and the chromium metal by way of a solid state reaction between chromium and iron oxide with the result that iron in a lower oxidation state, iron (II), would be present adjacent to the chromium oxide layer. In other words, the chromium oxide layer that formed at Locations D and E in Figure 1, were formed by the solid state reduction of $Fe_2O_3$ to FeO. If this is the case, then the iron oxide layer present in Location C immediately above the chromium layer is iron (II) oxide not iron (III) oxide. This would help account for the difference in gray scale color in the SEM between Locations B and C despite the two locations having similar elemental compositions.

The rate at which the oxide layer grows in this experiment is controlled by the rate of ionic diffusion of iron through the protective oxide layer rather than by oxygen diffusion to the bulk metal. One of the key indicators that oxygen diffusion through the protective oxide layer is slow is the absence of a nickel rich region immediately below the chromium oxide layer at Location F. In samples of stainless steel heated in air in the absence of molten salt oxygen access to the bulk metal is initially high. A dense protective oxide layer forms at the oxide/metal interface with the metal side being depleted in chromium and rich in nickel. Such is not the case here. The chromium and nickel content at Location F is only slightly different than that at Location G, which has the standard composition of 316 stainless steel. This supports the contention that the iron oxide film protected the underlying metal from corrosive attack by the molten electrolyte and also slowed the oxidation process as well.

**Conductivity Measurements**

Three of the laboratory-scale MCFC test stands were converted for use as dual-atmosphere conductivity test stands. Conversion consisted of little more than removing the reference electrodes and disconnecting the potentiostat circuit. The dual-atmosphere corrosion test cell which were used in the conductivity experiments has the same approximate configuration as a standard 3-$cm^2$ MCFC with the exception that the a sample of separator plate material has been substituted for the electrolyte matrix. Figure 2 is a schematic of the conductivity cell configuration. The cell is assembled with aluminum foil rings above and below the test sample. The outer ceramic gas manifold tubes, not shown in Figure 2, press on the aluminum foil rings creating a soft seal that serves the same purpose as the wet seal in the standard MCFC. The viability of this approach to sealing the cell was proved in preliminary experiments.

After assembly, but before heat up, crystals of the lithium/potassium carbonate eutectic are placed on the top of the stainless steel current collector. As the cell heats up, the carbonate crystals melt and wick into the NiO electrode. The lithium in the eutectic lithiates the NiO making it into a good electronic conductor. Sufficient carbonate is added to the cell to fill 40% of the void volume of the NiO electrode. This carbonate also wets the surface of the stainless steel sample and is responsible for the corrosive attack on the sample. The physical and chemical conditions existing at this NiO/stainless steel interface are identical to those at the cathode/cathode current collector interface in the MCFC. The Ni/Cr electrode at the bottom of the sample is operated in the dry condition. This electrode sees only fuel gases and does not oxidize but remains a good electrical conductor throughout the 1000-hour experiment. A current of one amp is passed through the conductivity cell and the voltage drop between the ends of the connecting rods is monitored as a function of time.

It is important to note that all current carried through the cell is electronic. The molten salt in the NiO electrode does not participate in carrying the current. No electrochemistry occurs in this cell. Fuel is not oxidized and oxidant is not reduced. By assembling two cells using identical components, except for the separator material, and by using iron oxide coated 316L and a sample of uncoated 316L as a control, it should be possible to determine differences in the interfacial contact resistance between the samples without the need to determine the electrical resistance of the other components.

Two conductivity cells, one with the iron oxide coated 316L sample as a separator and one with a uncoated 316L sample as a separator were assembled and operated for 1000 hours. A constant current of 1-amp (333 $mA/cm^2$) was applied during the test. The voltage drop across the cell was measured once every 24 hours. Figure 3 is a plot of the voltage drop data as a function of time for the uncoated control. The rapid change in resistance observed during the first 50 hours is associated with lithiation of the NiO electrode which is formed in-situ through oxidation of porous nickel metal. As a consequence of the change in resistance due to the lithiation process, the

voltage drop at the completion of the 1000 hours was used to make comparisons between the cells.

The resistance of the cell having only a 316L separator was 0.116 Ohm, and the resistance of the cell having the iron oxide coated 316L separator was 0.124 Ohm. Note that at a constant current of 1-amp, a voltage drop of 1-Volt corresponds to a cell resistance of 1-Ohm. We see that the oxide layer on the JVD coated sample contributes another 0.008 Ohm or 0.024 Ohm/cm$^2$ to the total resistance.

## FUTURE WORK

All that remains is to complete the analysis of the iron oxide coated sample retrieved from the conductivity cell and verify that the oxide layers formed in the conductivity cell are identical in nature to the out of cell test.

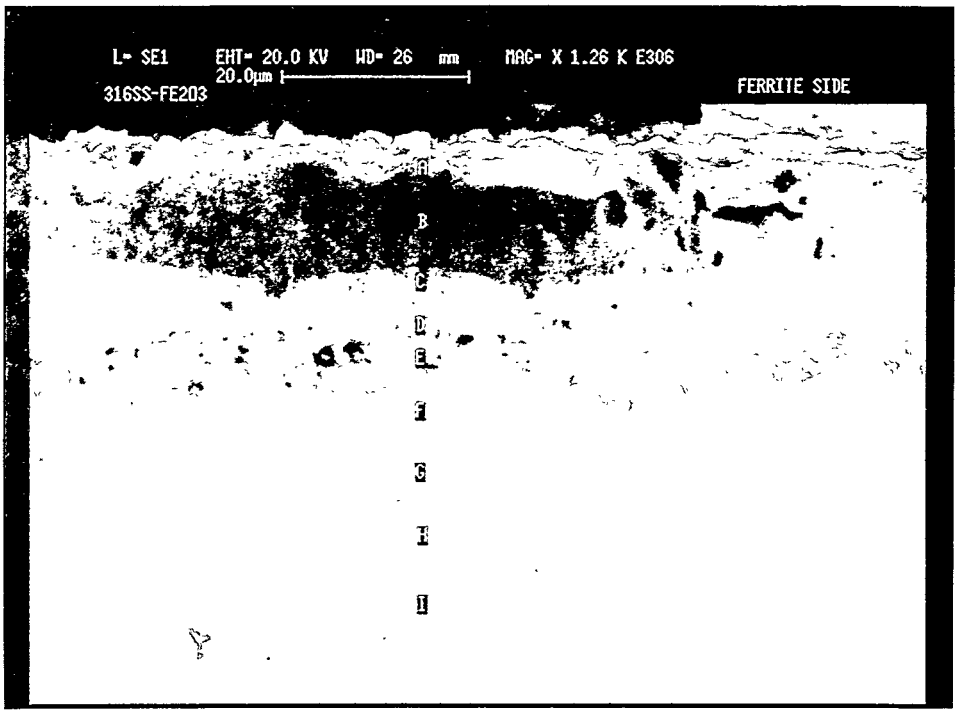


Figure 1. SCANNING ELECTRON MICROGRAPH OF IRON OXIDE COATED SAMPLE CROSS SECTION

| Table 1. EDX ANALYSIS OF JVD SAMPLES CROSS SECTION | | | | | | | |
|---|---|---|---|---|---|---|---|
| | Weight/Percent by Location | | | | | | |
| Element | A | B | C | D | E | F | G |
| Cr | 0.4 | 1.1 | 2.1 | 56.2 | 57.1 | 17.8 | 18.5 |
| Mn | 0.3 | 3.4 | 1.2 | 0.6 | 1.3 | 1.9 | 1.6 |
| Fe | 97.3 | 90.4 | 91.7 | 35.7 | 32.1 | 67.3 | 67.4 |
| Ni | 2.0 | 5.2 | 5.1 | 7.5 | 9.5 | 13.0 | 12.6 |

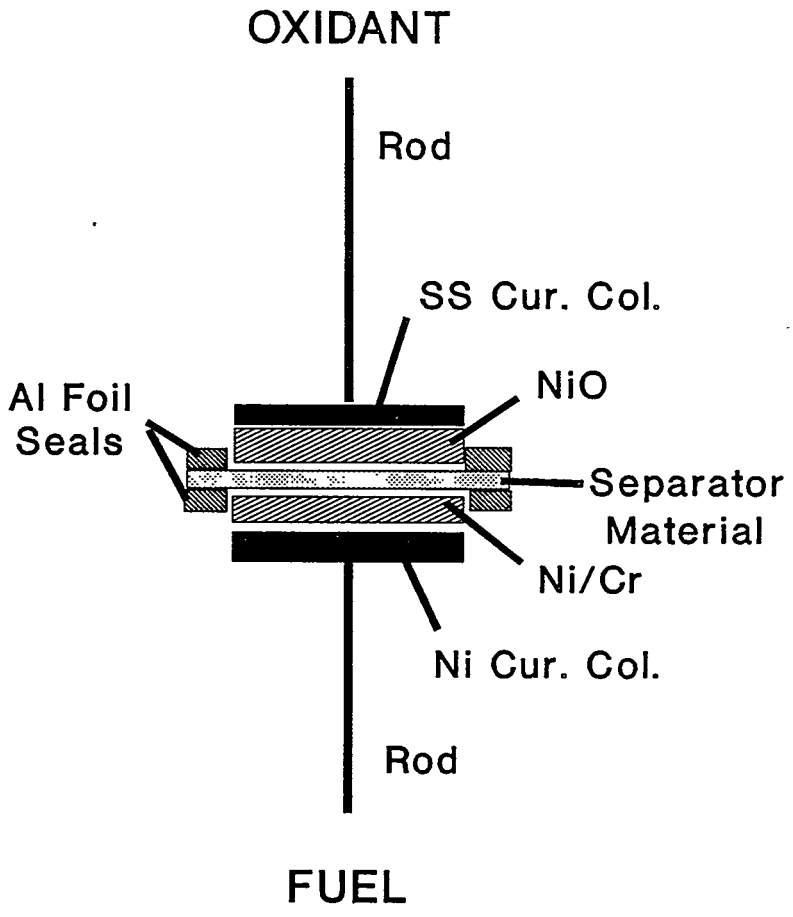


Figure 2. SCHEMATIC OF CONDUCTIVITY CELL CONFIGURATION

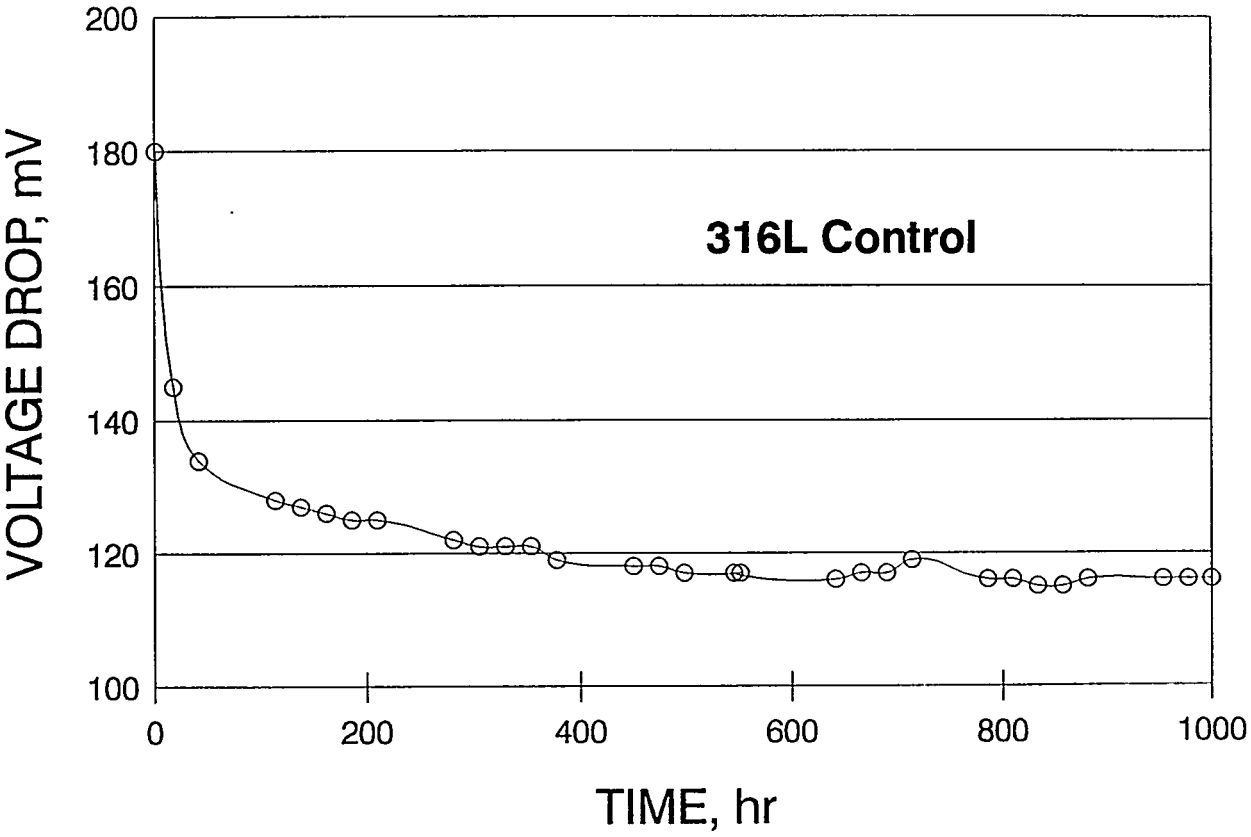


Figure 3. VOLTAGE DROP AS A FUNCTION OF TIME FOR 316L CONTROL SAMPLE

## P18 Fuel Cell Handbook Update

### CONTRACT INFORMATION

| | |
|---|---|
| Contract Number | DE - AC01 - 88FE61684 |
| Contractor | Gilbert/Commonwealth, Inc.<br>P.O. Box 1498<br>Reading, PA 19603<br>(215)775-2600 |
| Contractor Project Manager | William R. Owens |
| Principal Investigators | John H. Hirschenhofer<br>Ronald R. Engleman Jr.<br>David B. Stauffer |
| METC Project Manager | Diane T. Hooie |
| Period of Performance | June 15, 1992 to June 25, 1993 |

### OBJECTIVES

The objective of this work was to update the 1988 version of DOE's Fuel Cell Handbook. Significant developments in the various fuel cell technologies required revisions to reflect state-of-the-art configurations and performance. The theoretical presentation was refined in order to make the handbook more useful to both the casual reader and fuel cell or systems analyst. In order to further emphasize the practical application of fuel cell technologies, the system integration information was expanded. In addition, practical elements, such as suggestions and guidelines to approximate fuel cell performance, were provided.

### BACKGROUND INFORMATION

In 1980 the Institute of Gas Technology (IGT) published the "Handbook of Fuel Cell Performance" under a DOE contract. This document was later revised in 1988 under another DOE contract by Lawrence Berkeley Laboratory to become "Fuel Cells, A Handbook". These previous publications serve as the basis for this latest version.

The current version has the same format and organization of the 1988 handbook. Specific information from the 1988 handbook was also retained where applicable. It was determined, however, that the scope of the handbook should be adjusted for an expanded audience. The increased interest in fuel cells by those not directly familiar with the technology or those interested in potentially using the technology requires a more practical and applications oriented approach.

Some of the more detailed electrochemical information that appeared in the 1988 handbook was removed. The theoretical background that was emphasized in the 1988 handbook was replaced by information concerning performance predictions of fuel cell technologies. The use of experimentally based equations to clearly define important operating parameters was drawn from the 1980 version of the handbook. Recent experimentally derived data was used to update the coefficients of these equations. Data was gathered from a variety of sources

which included fuel cell contractors and published information from both domestic and international sources.

In order to provide additional information on technology application for potential users desiring to assess the technology, the presentation on fuel cell systems was expanded. Issues related to system integration were described. A series of typical power plant designs were included to illustrate operating characteristics.

## PROJECT DESCRIPTION

The research and analysis involved in this update included personal interviews of researchers involved in fuel cell material , component and system testing. Additional information was gathered through an extensive literature search of fuel cell papers published since 1988. These papers outlined domestic research in fuel cells as well as both European and Japanese efforts.

Each fuel cell type was essentially treated as a separate technology. The most promising developments in materials and design configurations for each fuel cell type were described in order to give an overview of current technology development. This overview also gives the likely course of future research as these technologies continue to approach commercialization. The inherent strengths and weaknesses of each technology were emphasized throughout to assist in determining possible application scenarios.

Recent experimental data was used to update or develop equations describing the performance of the various fuel cell types. The equations are theoretically based and define the change in cell voltage as a result of an increase or a decrease in a specific parameter. The following operational variables are the key parameters used in these equations: pressure, temperature, oxidant and fuel utilizations, contaminant level, current density and operational life.

The effect of each parameter essentially needed to be determined independently of the others. Data showing the effect on performance by changing only one parameter at a time was used. Data from different sources was analyzed in order to provide a more balanced depiction of typical cell performance. Comparing data from different sources, however, was often difficult due to variations in base operating conditions. This data needed to be normalized as best as possible in order to provide for a more direct comparison. Linear regression was used to determine standard performance curves. Data from these performance curves was then used to calculate the constant coefficients of the equations. The coefficients for these equations is what reflects the current state-of-the-art performance of the particular fuel cell type.

The system integration material that was added outlined typical conceptual designs of fuel cell power plants. This material was based on ASPEN/SP simulation code. Performance and flow characteristics were described and a system schematics were included.

## RESULTS

The primary result of working on the handbook was the updating of equations which describe the performance of the different fuel cell technologies. A summary of these equations, as well as the variable ranges for which they are applicable, appears in Tables 1, 2 and 3. The best estimate of the coefficients for these equations is included. The text of the handbook presents other possible coefficients for these equations when the data was difficult to normalize and a direct comparison could not be made between different sources. These coefficients, along with operating information, were presented as possible alternatives to the ones found in the tables.

The three most advanced fuel cell technologies, PAFC, MCFC and SOFC, appear in the tables. Experimental data for polymer electrolyte fuel cells (PEFC's) was also reviewed. It was determined, however, that

more extensive test data is required before typical performance equations could be defined. Recent data for PEFC's describing the effect on performance from changes in operating variables was summarized in the text of the handbook.

**Table 1. Summary of PAFC Performance Equations**

| Parameter | Equation | Comments |
|---|---|---|
| Pressure | $\Delta V_P(mV) = 146 \log (P_2/P_1)$ | 1 atm$\leq$P$\leq$10 atm<br>177°C$\leq$T$\leq$218°C |
| Temperature | $\Delta V_T(mV) = 1.15 (T_2-T_1)$ | 180°C$\leq$T$\leq$250°C |
| Oxidant | $\Delta V_c(mV) = 148 \log (P_{O2})_2/(P_{O2})_1$<br>$\Delta V_c(mV) = 96 \log (P_{O2})_2/(P_{O2})_1$ | $0.04 \leq P_{O2}/P_{Total} \leq 0.20$<br>$0.20 < P_{O2}/P_{Total} < 1.0$ |
| Fuel | $\Delta V_a(mV) = 55 \log (P_{H2})_2/(P_{H2})_1$ | $0.55 \leq P_{H2}/P_{Total} \leq 0.65$ |
| CO Poisoning | $\Delta V_{CO}(mV) = -11.1 ([CO]_2 - [CO]_1)$<br>$\Delta V_{CO}(mV) = -6.14 ([CO]_2 - [CO]_1)$<br>$\Delta V_{CO}(mV) = -3.54 ([CO]_2 - [CO]_1)$<br>$\Delta V_{CO}(mV) = -2.05 ([CO]_2 - [CO]_1)$<br>$\Delta V_{CO}(mV) = -1.30 ([CO]_2 - [CO]_1)$ | 163°C<br>177°C<br>190°C<br>204°C<br>218° |
| Current Density | $\Delta V_J(mV) = -0.53 \Delta J$<br>$\Delta V_J(mV) = -0.39 \Delta J$<br>$\Delta V_J(mV) = -0.74 \Delta J$<br>$\Delta V_J(mV) = -0.45 \Delta J$ | $100mA/cm^2 \leq J \leq 200mA/cm^2$, 8.2 atm<br>$200mA/cm^2 < J \leq 650mA/cm^2$, 8.2 atm<br>$50mA/cm^2 \leq J \leq 120mA/cm^2$, 1 atm<br>$120mA/cm^2 < J \leq 215mA/cm^2$, 1 atm |
| Life Effects | $\Delta V_{lifetime}(mV) = -4$ mV/1000 hours | |

**Table 2. Summary of MCFC Performance Equations**

| Parameter | Equation | Comments |
|---|---|---|
| Pressure | $\Delta V_P(mV) = 76.5 \log (P_2/P_1)$ | $1\ atm \leq P \leq 10\ atm$ |
| Temperature | $\Delta V_T(mV) = 2.16\ (T_2-T_1)$<br>$\Delta V_T(mV) = 1.40\ (T_2-T_1)$<br>$\Delta V_T(mV) = 0.25\ (T_2-T_1)$ | $575^oC \leq T < 600^oC$<br>$600^oC \leq T \leq 650^oC$<br>$650^oC < T \leq 700^oC$ |
| Oxidant | $\Delta V_c(mV) = 250 \log (P_{CO2}P_{O2}^{1/2})_2/(P_{CO2}P_{O2}^{1/2})_1$<br>$\Delta V_c(mV) = 99 \log (P_{CO2}P_{O2}^{1/2})_2/(P_{CO2}P_{O2}^{1/2})_1$ | $0.04 \leq P_{CO2}/P_{O2}^{1/2} \leq 0.11$<br>$0.11 < P_{O2}/P_{O2}^{1/2} \leq 0.38$ |
| Fuel | $\Delta V_a(mV) = 173 \log (P_{H2}/P_{CO2}P_{H2O}^{1/2})_2/(P_{H2}/P_{CO2}P_{H2O}^{1/2})_1$ | $3.8 \leq P_{H2}/P_{CO2}P_{H2O}^{1/2} \leq 17.5$ |
| Current Density | $\Delta V_J(mV) = -1.21\ \Delta J$<br>$\Delta V_J(mV) = -1.76\ \Delta J$ | $50 mA/cm^2 \leq J \leq 150 mA/cm^2$<br>$150 mA/cm^2 < J \leq 200 mA/cm^2$ |
| Life Effects | $\Delta V_{lifetime}(mV) = -5$ mV/1000 hours | |

**Table 3. Summary of SOFC Performance Equations**

| Parameter | Equation | Comments |
|---|---|---|
| Pressure | $\Delta V_P(mV) = 59 \log (P_2/P_1)$ | $1\ atm \leq P \leq 10\ atm$ |
| Temperature | $\Delta V_T(mV) = 1.31\ (T_2-T_1)$<br>$\Delta V_T(mV) = 0.41\ (T_2-T_1)$ | $800^oC \leq T < 900^oC$<br>$900^oC \leq T \leq 1000^oC$ |
| Oxidant | $\Delta V_c(mV) = 92 \log (P_{O2})_2/(P_{O2})_1$ | $0.16 \leq P_{O2}/P_{Total} \leq 0.20$ |
| Fuel | $\Delta V_a(mV) = 159 \log (P_{H2}/P_{H2O})_2/(P_{H2}/P_{H2O})_1$ | $1.39 \leq P_{H2}/P_{H2O} \leq 6.87$ |
| Current Density | $\Delta V_J(mV) = -0.73\ \Delta J$ | $50 mA/cm^2 \leq J \leq 400 mA/cm^2$<br>1 atm |
| Life Effects | $\Delta V_{lifetime}(mV) = -10$ mV/1000 hours | |

## FUTURE WORK

The current version of the fuel cell handbook is in draft form and is being reviewed by DOE and others independent parties. This draft will be revised according to the suggestions and comments obtained through this review process. Upon approval from DOE a final version will be submitted as both a hard and electronic copy. This electronic copy will assist in the efficient update of this handbook in the future.

## REFERENCES

*Fuel Cells, A Handbook* (DRAFT), Contract No. DE-AC01-88FE61684, 1993.

*Fuel Cells, A Handbook*, DOE/METC-88/6096, NTIS-DE88010252

*Handbook of Fuel Cell Performance*, Contract No. EC-77-C-03-1545, 1980.

# P19 Macrocyclic Redox Promoters for Methanol Oxidation

## CONTRACT INFORMATION

| | |
|---|---|
| **Contract Number** | DE-FG02-91ER81186 |
| **Contractor** | ICET, Inc.<br>916 Pleasant St., Unit 12<br>Norwood MA 02062<br>(617)769-6064 |
| **Contractor Project Manager** | Shantha Sarangapani |
| **Principal Investigator** | Shantha Sarangapani |
| **METC Project Manager** | Venkat K. Venkataraman |
| **Period of Performance** | Sep 1991 - June 1993 |

## OBJECTIVES

The overall goal of this program is to develop catalyst promoters that will result in longer and better performance of the presently used platinum catalysts for methanol oxidation. The specific technical objectives of this program are:

1) To synthesize several inorganic macrocyclic complexes that will act as promoters for methanol oxidation
2) To improve the reactivity of the promoter core by a) incorporating a mixture of promoters and b) by covalent attachment of the promoters to the carbon substrate
3) To conduct physical and electrochemical characterization of the complexes
4) To conduct basic electrochemical studies of the role of promoters
5) To conduct half-cell screening studies with the above complexes using liquid phase or gas phase methanol feed
6) To conduct direct methanol fuel cell experiments using polymer electrolyte membrane fuel cells.

## BACKGROUND

Direct methanol fuel cell (DMFC) powered vehicles are foreseen as the choice of the future, because of its environmentally benign combustion products, potential for high efficiency and above all for its unlimited supply within United States. The major obstacle in the development of methanol fuel cell is the methanol electrode, particularly, a catalyst for the oxidation of methanol. No stable and active catalysts exist that can oxidize methanol for long periods of time without the loss of efficiency. Unless a better understanding of the methanol oxidation and the surface conditions for the removal of adsorbed poisoning intermediates is achieved, no effort in the design and engineering of the DMFC systems is worth undertaking.

This paper discusses the development of contaminant resistant platinum coated carbon anodes containing a bonded core of redox mediators. Unlike the oxide mediators which more often show irreversible behavior, these promoter molecules are characterized by well defined, highly reversible redox and stable coordination chemistry; they also possess an affinity for CO and small organic species. It is hoped that this study will provide a predictive base based on the electronic interactions between the intimately bound oxidized promoter atom and the Pt. Correlation between the redox potentials, structure and reactivity of the promoter species to revive the poisoned Pt could prove highly useful in building a model system for metha-

nol oxidation.

It is well understood at this point that a promoter metal capable of oxygen transfer to the platinum or that could oxidize the adsorbed residues from methanol oxidation ideally should improve the performance of the methanol oxidation electrode. The best catalysts for this reaction must have the ability to adsorb water at potentials close to the operating potential for methanol oxidation. In the presence of alloys such as Pt-Ru, the following mechanism is invoked to explain the remarkable promoting effect of ruthenium (Fritts and Sen, 1988).

$$CH_3OH + 3\,Pt \text{-----} > HCO\text{-}Pt + 3\,H\text{-}Pt$$

$$3\,H\text{-}Pt \text{-----} > 3\,Pt + 3\,H^+ + 3\,e^-$$

$$H_2O + Pt\text{-}Ru \text{-----} > HO\text{-}Pt\text{-}Ru + H^+ + e^-$$

$$HCO\text{-}Pt + HO\text{-}Pt\text{-}Ru \text{-----} > Pt + Pt\text{-}Ru + CO_2 + 2\,H^+ + 2\,e^-$$

Dissociative water adsorption on Pt alone occurs at about +0.8V vs NHE at 50°C and this is why Pt alone is not a good catalyst for methanol oxidation. The reaction rate of methanol oxidation in the presence of promoting alloy atoms is assumed to be proportional to the number of Ru sites located at the nearest neighbor. So far, macrocyclic complexes of well defined stereochemistry and redox potentials have not been explored as promoters for methanol oxidation in the presence of Pt . Considerable amount of work has been done in the area of oxygen electrocatalysis and lithium batteries using metallomacrocycles as electrocatalysts.

The advantages of the approach presented here are that a)the promoter species at a given potential is well defined unlike the case of oxides of ruthenium, tin or molybdenum where complications exist in exactly identifying the oxidation state of the metal. b) The intimately bound carbon linked metallo macrocycle undergoing reversible, well defined redox changes under a Pt layer would allow facile redox reactions in comparison to promoter oxides simply mixed with carbon. c) If a good model catalytic system is discovered through this effort, possibilities of achieving multimetal sites covalently bound to carbon using highly stable bifunctional ligand systems exist. Thus more efficient, tailor-made systems could be constructed.

## PROJECT DESCRIPTION

### Task1. SYNTHESIS OF COMPLEXES

Sub task a: Synthesis of gram quantities of several Phase I complexes
Sub task b: Preparation of some new complexes.

### Task 2. PROMOTER CORE FABRICATION

Sub task a: Preparation promoter cores on substrate carbon.
Sub task b: Preparation of promoter cores using covalent bonding
Sub task c: Variation of metal to complex ratios.
Sub task d: Preparation of promoter cores containing mixtures of promoters

**Task 3.** Platinization of promoter cores prepared in Task 2 above.

### Task 4. PHYSICAL AND ELECTROCHEMICAL CHARACTERIZATION

Sub-task a: Elemental analysis, FTIR, and pyrolysis mass spectroscopy of the complexes and surface bound complexes on carbon respectively.
Sub-task b: Cyclic voltammetric investigation of promoter core in the presence and absence of methanol.
Sub-task c: Polarization studies of platinized, promoter modified electrodes.
Sub-task d: Basic electrochemical studies - methanol adsorption measurements and kinetics of oxidation of adsorbed intermediates.

**Task 5.** Half-cell experiments with Teflon bonded electrodes in a gas diffusion type test apparatus.

### Task 6. EVALUATION OF ICET PROMOTER CATALYSTS IN IFC's PEM FUEL CELLS

Sub-Task 1: Fabrication of Membrane Electrode Assemblies (M&EA) using ICET Promoted Direct Methanol Oxidation Cata-

lyst

Sub-Task 2: Evaluation of ICET Promoted Direct Methanol Oxidation Catalyst in a PEM Fuel Cell
Sub-Task 3: Fabrication of Membrane Electrode Assemblies using ICET Optimized Promoted Direct Methanol Oxidation Catalyst
Sub-Task 4: Evaluation of ICET Optimized Promoted Direct Methanol Oxidation Catalyst in a PEM Fuel Cell

**Task 7:** Preparation and delivery of quarterly and final reports.

## EXPERIMENTAL:

All experiments were carried out either in 1 M $H_2SO_4$ or 1 M $H_2SO_4$ and 1M $CH_3OH$. Oxygen free nitrogen bubbled through a presaturator containing the same solution as in the cell was used to deaerate the solutions. A thermostatted cell was used to maintain 60°C for the polarization experiments during Phase I. In Phase II, all experiments were conducted at 80°C. The cell and electrode holder that were used for the electrochemical experiments are shown in **Fig. 1 a&b**. An EG & G 273 A potentiostat was used for all measurements and was interfaced with a 386SX computer. Model M270 data acquisition software was used to acquire data. Reference electrodes were either DHE or $Hg/Hg_2(SO_4)$. All electrodes were wetted with a few drops of methanol prior to immersion into the electrolyte and care was taken to exclude any unabsorbed methanol prior to immersion. The electrodes were then cycled between 0 and 1.4 V vs. RHE, at 100 mV/s for 100 cycles followed by two 10 mV/s sweeps. The polarization studies were conducted at constant current; steady state potentials were recorded one minute after a given current was applied. The potential recovery curves were obtained by applying a 10 mA current to the electrode; after the potential reached a steady value, usually within a minute, the current was interrupted and the recovery of potential to open circuit was recorded using the M270 software. The potential step experiments were performed using the chronoamperometric mode of the M270 software. The potential of the working electrode is switched to 500 mv vs. RHE from its open circuit value and the current decay recorded as a function of time. For most electrodes the decay was recorded for a maximum of 2147 seconds. All potentials (except those referring to the redox chemistry of the complexes) are referred to RHE. The exposed electrode area in all our experiments were 0.95$cm^2$.

## RESULTS

***Polarization Studies:*** The polarization data for various promoters are compared to the platinum on Vulcan control in **Figs. 2 a&b**. The polarization curves have two clear segments, a high slope region at low current densities (0.1-1 mA/sq.cm) and a low slope, high current density region (1-30 mA/sq.cm). The Tafel plots for the high current density region are shown in **Figs. 3 a&b** along with the regression lines. The slopes for the two regions and the exchange current densities calculated by extrapolating the regression lines for the high current density region are shown in **Table I.**

The rapid rise in the E-logi curve in the 0.1-1 mA c.d. range can be attributed to the classical porous electrode doubling effect. Since the current is not proportional to $\sqrt{\eta}$, we can rule out a chemical step as the r.d.s. (Tilak et al., 1989). Some of these slopes are anomalously high (500-800 mV), and no proper explanation is available at the present time. A limiting process of some sort (kinetic or diffusional) for this step may be the reason for this high slope behavior. A more detailed basic investigation, perhaps with complementary techniques such as AC impedance have to be conducted to find out the behavior of the electrodes in this region.

In the current density region 1-30 mA/$cm^2$, the Tafel slopes range from 79-158 mV, with most of the samples showing a slope of $\sim$ 100 mV. The exchange current density for control is comparable to that reported in the literature (Kadirgan et al., 1981) for the plain platinum. All promoters show an improvement with the best showing 2-3 orders of magnitude higher values. Among the promoters with the same Tafel slope ($\sim$100mV), #04 has the highest exchange current density

and is clearly the best. #13, although has the highest $i^o$ of all, is ranked only as the second, due to its high Tafel slope. #12, although has only a 4x improvement in $i^o$, is ranked equal to #13, due to its lowest Tafel slope.

***Potential Step Experiments***: The current decay behaviors of the different electrodes when subjected to a 500 mV (vs. RHE) step are shown in **Fig. 4.** The currents and charges for the different promoters are presented in **Table II.**

It is clear from the above data that the I-t transient responses strongly depend on the type of promoter used. The charge passed during the period at 0.5 V RHE far exceeds that for reactions such as

$$CH_3OH \text{ -----> } ¦COH + 3\,H^+ + 3e$$
$$CH_3OH \text{ -----> } CO_{ads} + 4H^+ + 4e$$

at least for the several promoters. This conclusion is based on the assumption that the platinum surface area is not less than 80 $m^2/g$ and the analytical data on actual loadings of Pt on these electrodes. Therefore, at least for the case of promoter modified catalyst, the reaction must involve the oxidation of the carbon residues.

***Current Step Experiments***: The potential time behavior of our promoted catalysts were compared with Pt control using a galvanostatic pulse of 105 mA/sq.cm at 80°C with a solution of 1M methanol in 1M sulfuric acid. The IR corrected values are shown in **Figure 5.** The performance of the two promoted electrodes are ~150 mV better than the control electrode. The slope of the control electrode is 9.3 $\mu$V/s, whereas , the two promoted electrodes show 5.3 & 8.1 $\mu$V/s. Thus the promoted electrodes not only show a lower polarization, but their performance decay with time is lower than that of unpromoted platinum.

Analysis of data obtained above and correlation with the Pt and macrocycle loading parameters reveal the following trends:
i) Based on Tafel slopes and exchange current densities, the following order of methanol oxidation activity is better for several promoters.
ii) In general, 150-200 mV gain over the platinum control is observed for the macrocycle promoted Pt on carbon. The voltage decay with time is better for promoted catalysts than the control platinum.

iii) Potential step experiments indicate that for the promoter modified catalysts, the net reaction must involve the oxidation of carbon residues.

**REFERENCES**

Fritts S.D. and R.K.Sen DOE report PNl- 6077-ul-95
Kadirgan, F.K., B.Beden, J.M.Leger and C.Lamy, J. Electroanal.Chem., 125, 89(1981)
Tilak B.V. etal J.Electrochem. Soc., 136, 1977(1989)

**TABLE I. KINETIC PARAMETERS FOR ELECTROOXIDATION OF METHANOL (1M) IN $H_2SO_4$ (1M) at 60°C.**

| Promoter | code | Tafel slope(mV/decade) 0.1-1 mA | 1-30 mA | $i_o^!$ * $A/cm^2$ |
|---|---|---|---|---|
| | 01 | 480 | 94 | $6.8 \times 10^{-8}$ |
| | 04 | 780 | 99 | $1.7 \times 10^{-6}$ |
| | 13 | 280 | 158 | $3.4 \times 10^{-5}$ |
| | 12 | 480 | 79 | $2.4 \times 10^{-7}$ |
| | 10 | 550 | 95 | $5.1 \times 10^{-7}$ |
| | 11 | 500 | 97 | $4.5 \times 10^{-7}$ |

* : apparent exchange current densities based on geometric area, obtained by extrapolation of the regression line to 50 mV RHE (Kadirgan et al., 1981)

**TABLE II. ANALYSIS OF POTENTIAL STEP EXPERIMENTS**

| Promoter | Code | Current (mA) at 600s | 2147 s | Charge (C) at 600 s | 2147 s |
|---|---|---|---|---|---|
| | 01 | 5.6 | - | 3.2 | - |
| | 04 | - | 33 | 26 | 80 |
| | 13 | 23.7 | 21.2 | 15 | 50 |
| | 10 | 20.7 | - | 13 | 36* |
| | 11 | 12.8 | - | 8 | 26 |

*: current and charge at 1800 s. Electrode area in all cases = 0.95 $cm^2$

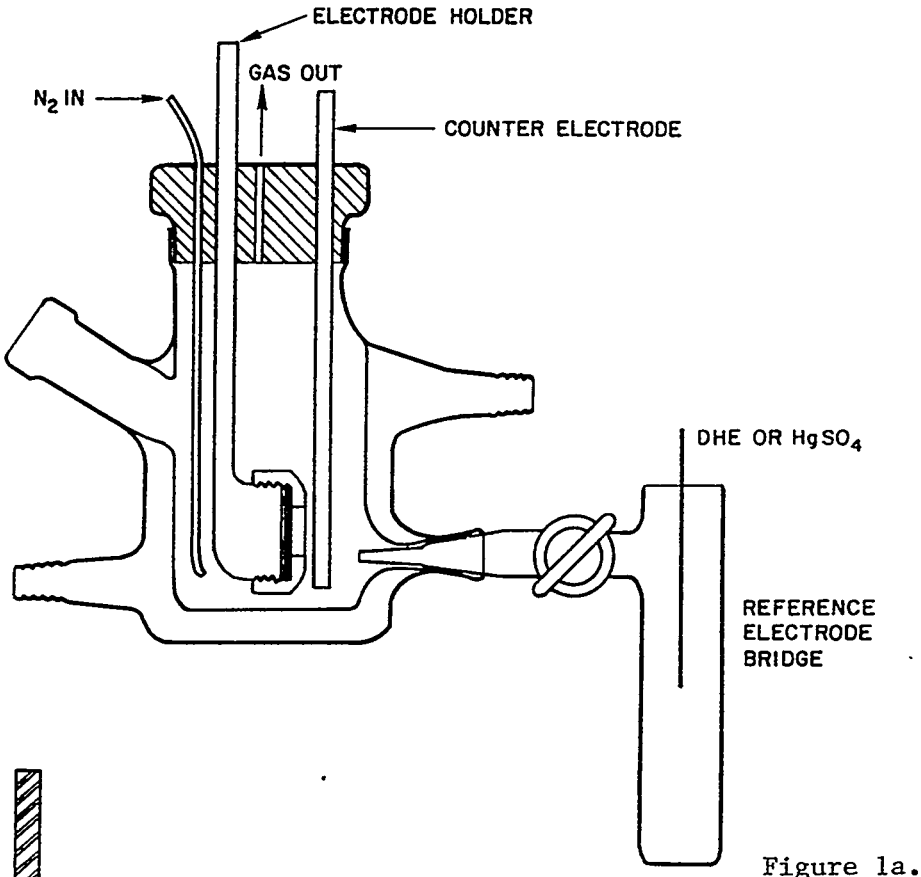


Figure 1a. Experimental cell set-up for polarization studies.

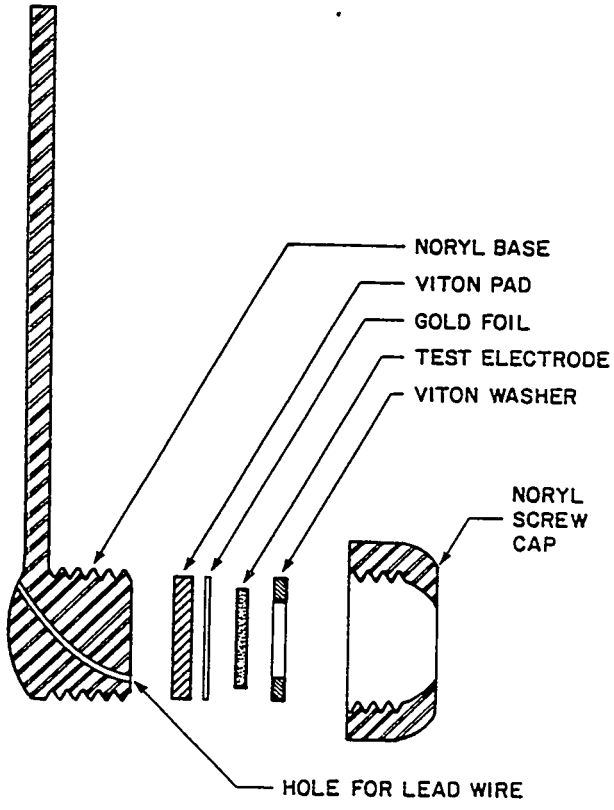


Figure 1b. Electrode holder

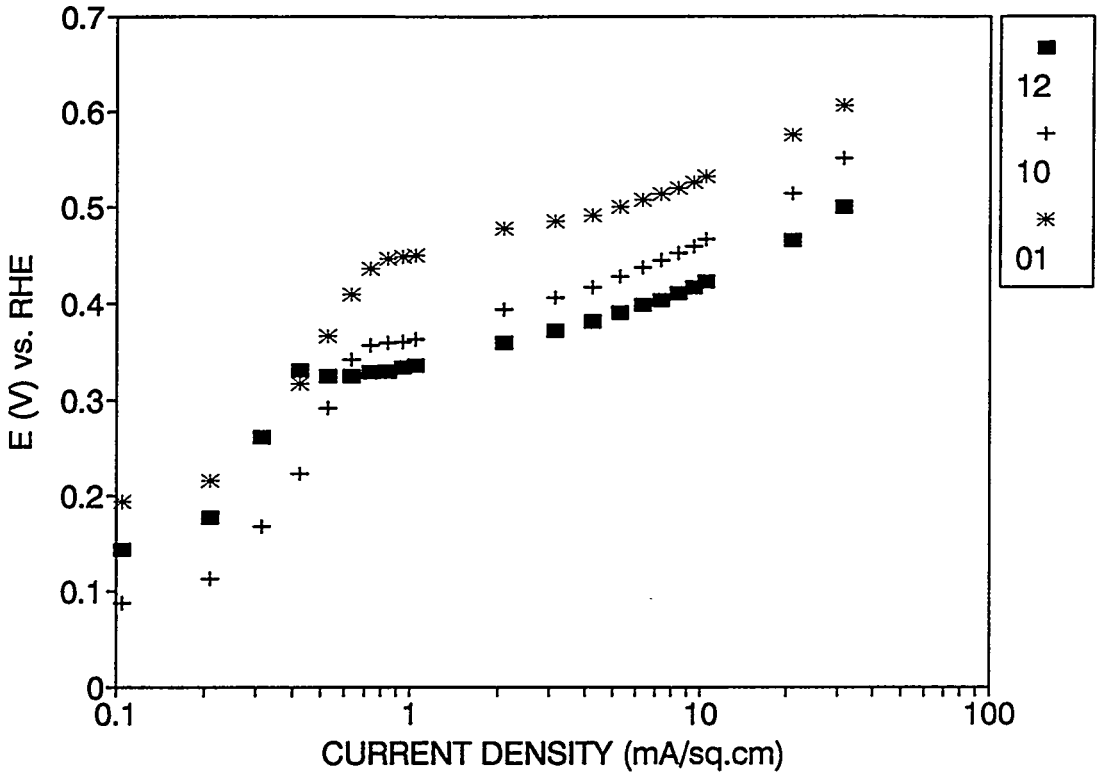


Figure 2a (above) and 2b (below). Polarization data for methanol oxidation in 1M sulfuric acid at 60° C for various promoters.

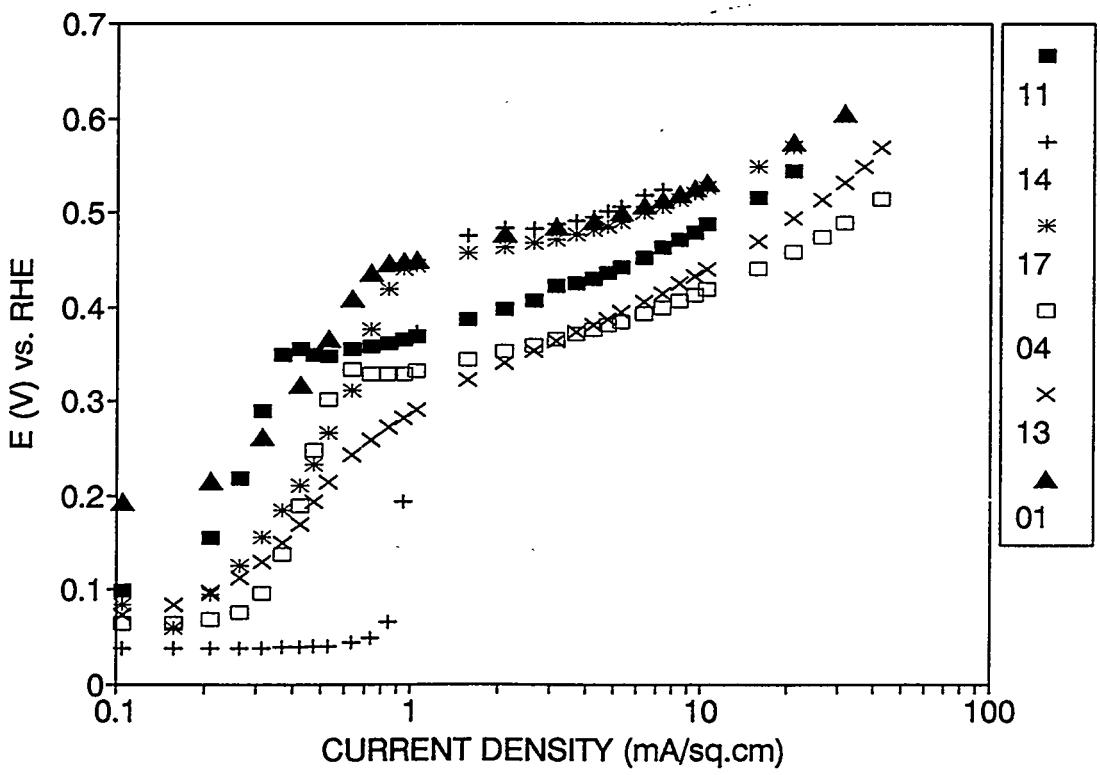

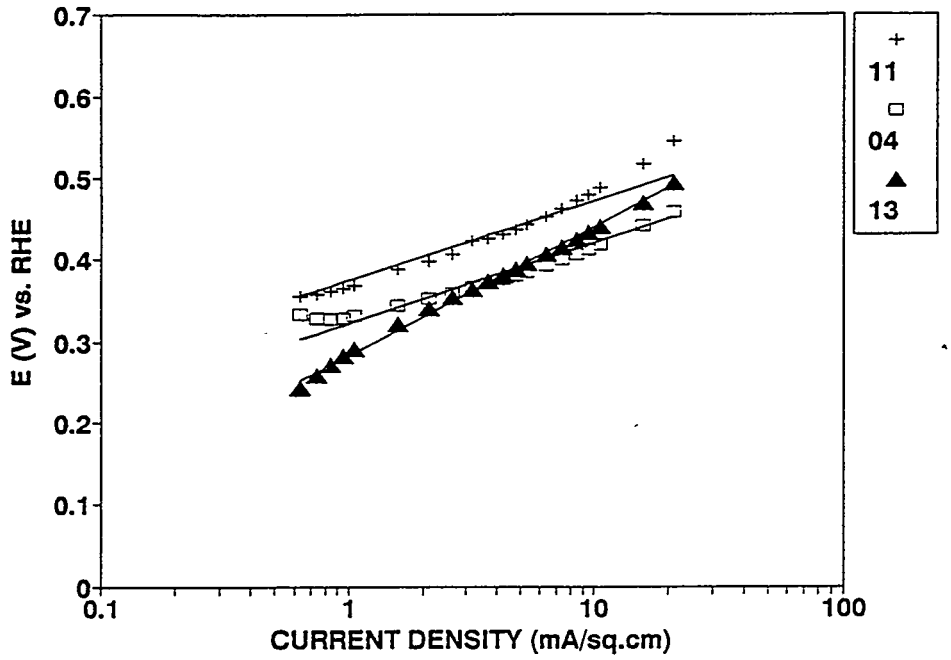


Figure 3 a &b. Tafel plots of data shown in Figures 2a & 2b.

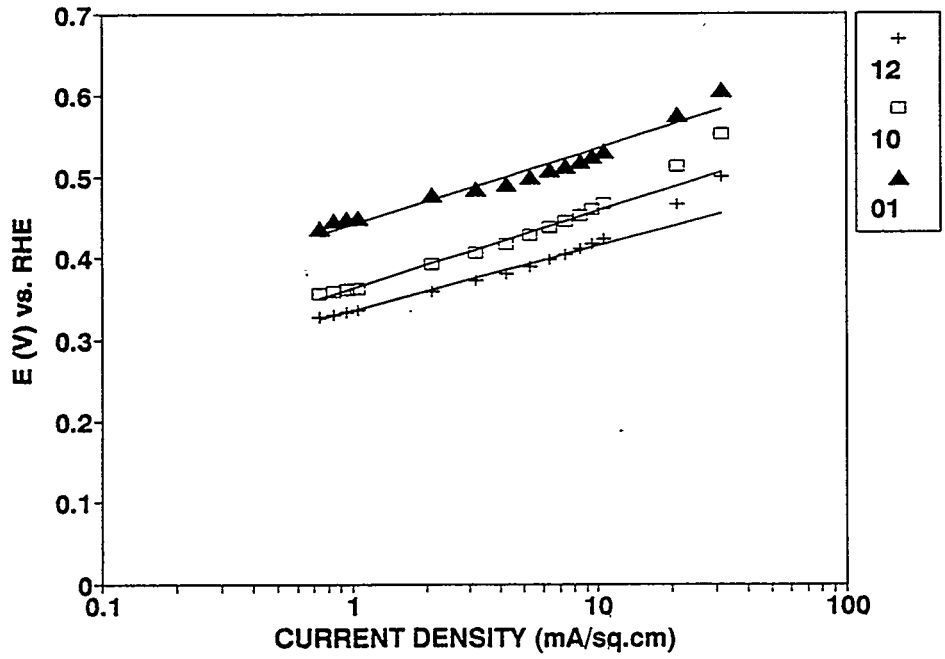

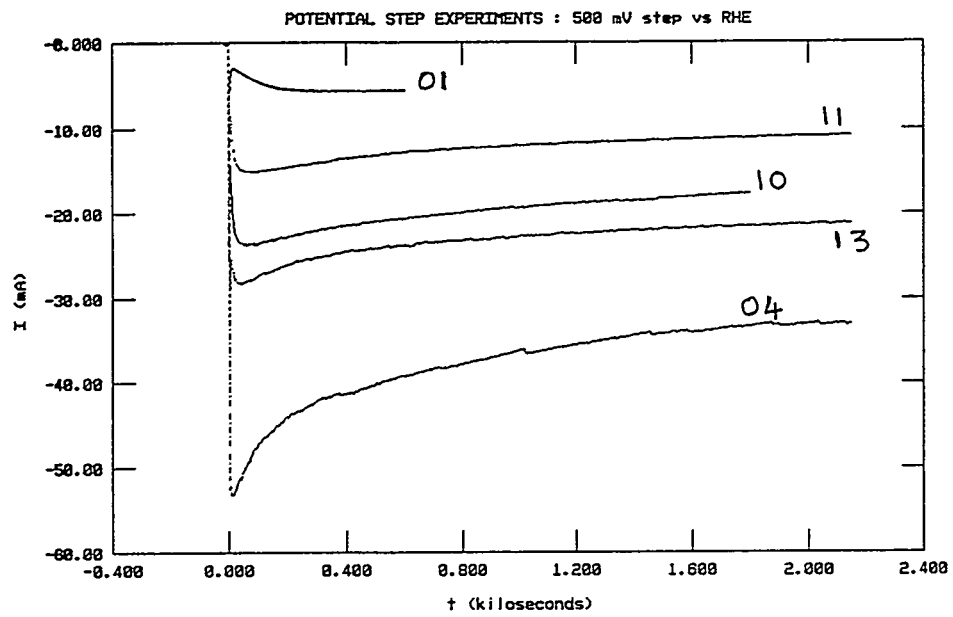


Figure 4. Potential step experiments - Current decay curves for methanol oxidation recorded as a function of time after the potential is stepped from the OCV to 500 mV vs. RHE. Temperature: 60° C.

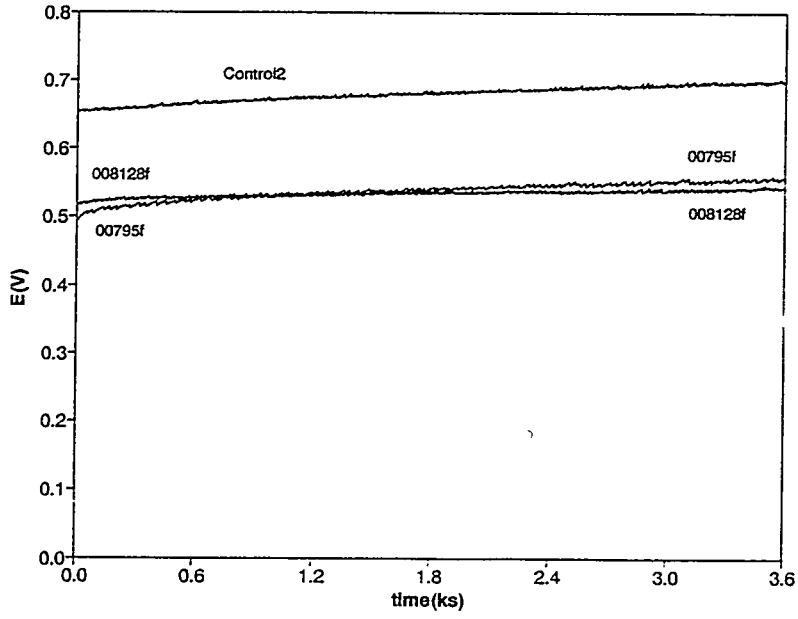


Figure 5. Potential-time response of two promoter electrodes compared with an unpromoted platinum control. The promoted electrodes 00795f and 008128f show lower polarization and lower slope for an input of 100 mA. 1M methanol in 1M sulfuric acid at 80° C.

# P20 Optical Sensor Development for MCFCs: HCl Detection Through Wavelength Modulation Diode Laser Absorption Spectroscopy

## CONTRACT INFORMATION

| | |
|---|---|
| **Contract Number** | A198 |
| **Contractor** | Los Alamos National Laboratory<br>P.O. Box 1663<br>Los Alamos, NM 87545<br>(505) 667-5061 |
| **Contractor Project Manager** | Robert Hanold |
| **Principle Investigators** | David J. Funk<br>Byron A. Palmer<br>Richard C. Oldenborg |
| **METC Project Manager** | Norman T. Holcombe |
| **Period of Performance** | October 1, 1992 to July 30, 1993 |

**Schedule and Milestones**

**FY93 Program Schedule**

| | O | N | D | J | F | M | A | M | J | J | A | S |
|---|---|---|---|---|---|---|---|---|---|---|---|---|
| HCl Uptake Measurements | | | | | | | X | X | X | X | X | X |
| HCl Field Test @ ERC | | | | | | | | | | X | X | X |
| HCl Interaction Model | | | | | | | | | | | | X |
| HCl Prototype Development | X | X | X | X | X | X | X | X | | | | |
| HCl Final Report | | | | | | | | | | X | X | X |

## OBJECTIVES

The Molten Carbonate Fuel Cell (MCFC) provides an attractive option for the extremely efficient conversion of coal-derived gas and/or natural gas to electricity. However, several technical issues need to be addressed before this option can be realized for use with coal-derived gas. In particular, contaminants found in coal gas can seriously degrade the performance of the cells through both reversible and irreversible processes.[1] For example, side reactions with contaminants enhance the movement of the carbonate (electrolyte) and reduce the lifetime of the cell. There presently exist no *in situ* techniques for monitoring contaminants and/or for studying the underlying chemical kinetics and mechanisms behind fuel cell degradation. This program seeks to provide diagnostics for the understanding of the movement of the carbonate in the cell and the contamination processes that

effect the operation of the fuel cell. We hope this understanding will facilitate better cell design and enable much improved prediction of performance and lifetime of the MCFC. Emphasis is placed upon optical diagnostics that permit nonintrusive, sensitive, and structure specific monitoring of MCFC chemistry. We are developing sensors for measuring, *in situ*, the atomic and molecular species to provide: 1) continuous contaminant monitors that will allow industrial partners to gauge the expected lifetime of a particular fuel cell as it operates; 2) tools for understanding the physical and chemical mechanisms behind fuel cell degradation and thereby creating opportunities for development of technologies to address and eliminate problematic contaminants.

In FY'93, we have developed a laser diode sensor capable of detecting, *in situ*, HCl gas at levels of part-per-million and below on time scales of under one minute (using 25 *cm* path lengths). HCl poses problems to MCFCs since it can react with the carbonate and undergo an exchange reaction forming KCl, which at the fuel cell operational temperature is volatile and will leave the cell. After sufficient contamination and resulting selective depletion of $K^+$ cations, the fuel cell will no longer contain the necessary eutectic mole fraction ratios and will solidify, shutting down the flow of current. This scenario has been confirmed by equilibrium calculations performed by us (Los Alamos National Laboratory) and Energy Research Corporation (ERC; Danbury, CT) using two independent codes and experiments performed at ERC.[2] Development of our HCl diagnostic will enable us to determine the kinetic rates of HCl uptake which will then provide evidence for or against the use of equilibrium codes as an accurate description of this chemical process.

## BACKGROUND INFORMATION

It is well established that there are many contaminants contained in coal gas that can harm MCFC fuel cells in both reversible and irreversible manners.[1] These contaminants include, but are not limited to, HCl, $H_2S$, $H_2Se$, $AsH_3$, $NH_3$, Zn, tar, and other trace metals. This years work has been devoted to development and application of an *in situ* monitor for HCl detection and the paper will be devoted primarily to this topic.

HCl, which is present in coal gas, can cause serious problems in MCFCs. HCl is absorbed into the carbonate forming alkali chlorides, which at 923 K, volatilize and leave the fuel cell predominantly as KCl. This depletion has two major effects. The depletion reduces the amount of carbonate present (which is a thin layer for efficiency and space considerations), causing holes to form in the carbonate layer and allowing mixing of the anode and cathode gases. The largest effect, however, is the selective removal of the potassium ion. The depletion of potassium ions from the carbonate melt alters its ionic conductivity, gas solubility and diffusivity, as well as the solubility of the NiO electrode. Furthermore, if the potassium depletion is allowed to continue, the composition of the mixture will change to a point where it is no longer a eutectic at normal operating temperature, resulting in a solidifying of the melt and a shut down of the affected cell area.

Secondary effects due to the vaporization of the alkali chloride have also shown up in test cells. In particular, the condensation of the alkali chlorides in cooler regions of the cell can cause significant blockages of critical passageways. For example, the plugging of tubes leaving the fuel cell anode has been observed, as well as plugging of the tubes in which gas is recirculated to the cathode side.

Because the effects of HCl contamination are only readily apparent after long exposure times, early work on MCFCs did not identify the seriousness of the HCl problem. The depletion of the alkali atoms from the carbonate exhibits only a small effect on the efficiency of the cell and therefore does not show up in short tests. Even when the cells were operated with large HCl loads for a few thousand hours, the problems were still not apparent. Calculations and longer test runs have, however, demonstrated that HCl is a problem to commercial fuel cells where long lifetimes are needed to be economically feasible. The estimates of maximum continual loading

concentrations for HCl has been reduced repeatedly as the problem became more apparent. Given the present knowledge and fuel cell design, the expected maximum continual loading is now only 100 ppb. Measuring fuel gases for HCl at these concentration levels is difficult as is cleaning the gas to this limit, and we have been developing laser based techniques to make these measurements and provide assessment of scrubbing methods.

## PROJECT DESCRIPTION

Our general approach has been to employ established optical techniques to investigate contamination processes in MCFCs. Optical diagnostics are chosen for their ability to provide direct, nonintrusive, *in situ,* sensitive, temporally and spatially resolved probes of MCFC processes. We have investigated other methods,[2] but optical methods have proven to be superior for the current diagnostic needs. Our emphasis will be on developing these techniques, establishing industrial collaborations to implement the techniques, and to directly address the contaminant issue. By taking this approach, we do not have to reinvent the technology involved in the fuel cells and the transfer of our techniques to industry occurs more rapidly.

We have chosen Wavelength Modulation Diode Laser Absorption Spectroscopy for i*n situ* detection of HCl contaminants in coal gas. We use diode lasers for generation of extremely monochromatic (10 MHz) middle infra red light. This monochromaticity provides us with the necessary selectivity for species specific detection. To increase our sensitivity (which would not be provided by direct absorption) we move our detection frequencies away from laser 1/f noise through the use of modulation techniques. In our case, since we are modulating with kHz frequencies, we are in the regime denoted as wavelength modulation, where the frequency of the modulation (kHz) is much less than the half width of the molecular resonance (GHz).[3] In addition to reduction of laser 1/f noise, laser modulation helps eliminate baseline changes found in most diode lasers, further increasing sensitivity (though in principle these could be addressed in other ways). Moreover, wavelength modulation is in a frequency range that couples well to diode lasers (in the frequency modulation regime, one needs .1 to 1 GHz modulation frequencies which do not couple well to the diodes) that can be performed with off the shelf components to provide reduced expense. Furthermore, this technique has sufficient dynamic range to provide *in situ* detection of trace species in the sub ppm to hundred ppm range, with optimized systems capable of providing ppm detection on second time scales, making this technique useful for detecting contaminant concentration spikes (fast continuous detection).

In addition to construction of the HCl monitor, we have taken the monitor to Energy Research Corporation (ERC; Danbury, CT) and operated it on a working fuel cell. Demonstration of the HCl technique in an operating fuel cell is important in that it has given us confidence in the technique as well as clarified unanticipated problem areas. These measurements will be used to verify the predictions of the model that we and ERC have developed for the HCl-carbonate interaction.

Experimental:

The output of a liquid nitrogen cooled Mid-IR lead-salt diode (Laser Photonics) tuned to the P10, v'=1, rovibrational line of HCl (2651.976 $cm^{-1}$) is collimated using an f/0.67 offaxis parabolic mirror and directed into two arms (by a beam splitter and mirror) carrying input to and output from a test fuel cell fitted with sapphire windows (Fig. 1). The laser is driven by an ILXLightwave Ultra-low Noise current source running an internal ramp for wavelength control while being externally modulated (the wavelength modulation) with a sine wave running at 30 kHz using a digitally synthesized frequency generator (Stanford Research System Model DS335). The laser output from the cell arms is imaged onto two liquid nitrogen cooled InSb detectors (InfraRed Associates) fit with Anti-Reflection (AR) coated germanium windows and amplified using two home built amplifiers based on Analog Devices ultra low noise precision Op Amp (AD OP-27). The detector outputs are then passed to two

Stanford Research Systems Lock-In Amplifiers (Model SR510) where the signals are mixed and demodulated at the second harmonic to provide an input to a digital oscilloscope (LeCroy 9310). The reference signal to the lock-ins is provided by the TTL sync output of the frequency generator isolated by a Monsanto optoisolator (MCT2). The spectrum is repetitively swept and then linearly averaged using the scope to provide enhanced S/N ratios. The output of the scope is transferred to a Macintosh Powerbook 170 through National Instruments SCSI to GPIB adapter where data are evaluated and stored.

The fuel cell is a standard ERC 7 cm x 7 cm fuel cell equipped with a methane reformation catalyst. The cell was run on primarily 72% $H_2$/18% $CO_2$/10% $H_2O$, with capabilities for addition of test gases as required for experiments. The cell was equipped with two optical access tubes capped with AR coated sapphire conflat windows mounted on wedged copper gaskets. The AR coating and the wedged gaskets were to minimize the etalons resulting from constructive/destructive interference of the laser between the windows as it is swept in frequency space. HCl was added using permeation tubes held at a fixed temperature (Dynacal), in which a known amount of HCl permeates a Teflon membrane over time. A ten percent side stream was flowed over the permeation tube and mixed with the standard fuel gas before entering the input optical access tube. Actual HCl concentrations were determined by weighing the tubes before and after each set of experiments. Alternatively, HCl was added using a diluted mixture of 1000 ppm HCl/$N_2$ and adding it directly to the fuel gas. This was found to be less reliable due to inaccuracies in our flow measurement.

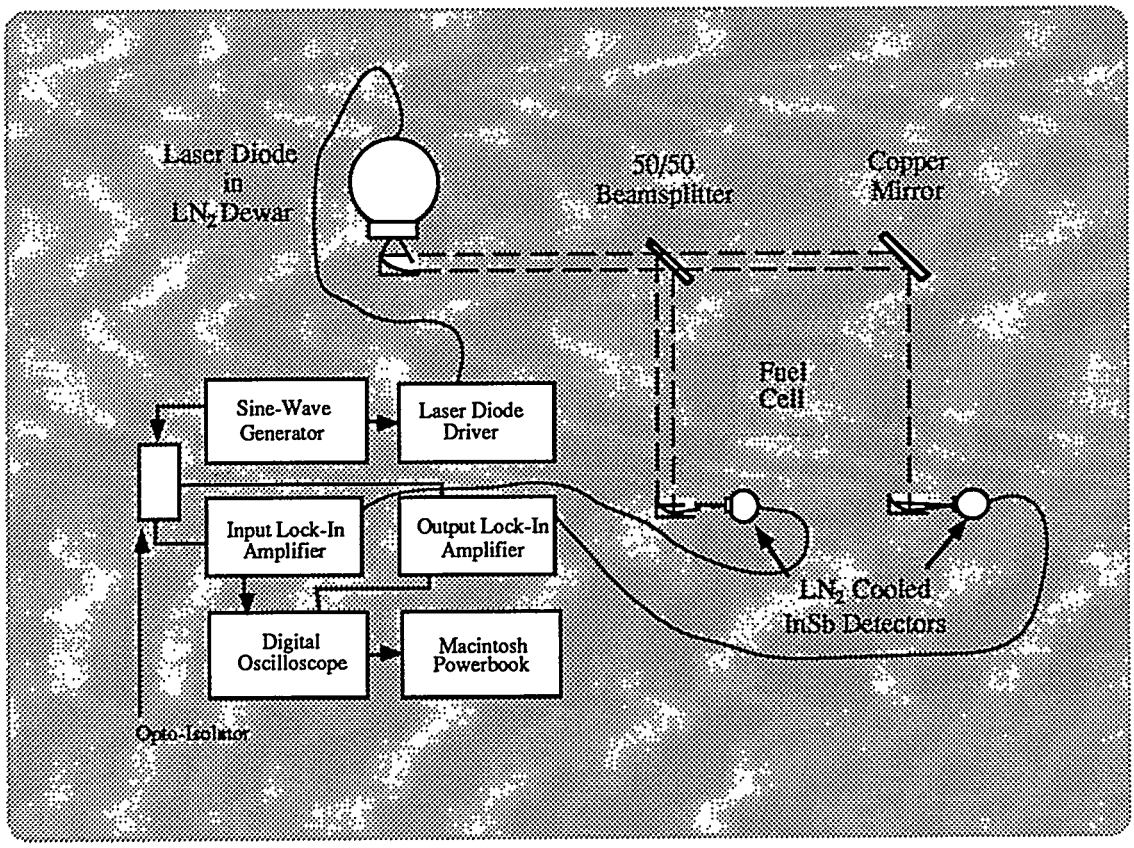


Figure 1. Schematic of the wavelength modulation spectrometer coupled to an operating fuel cell.

Concentrations are determined from the resulting spectra by matching them to computationally simulated spectra. The modulation frequency on the diode laser can significantly alter the observed spectral lineshapes, and this is accounted for in the simulation using the method described by Arndt.[4] In addition, we must correct our data for etalon effects, pressure broadening, line shifts, and nonlinear frequency sweeps of our laser. As stated previously, etalons are generated by the constructive and destructive interference of the laser caused by reflections at each interface. Optical components and cell designs are such that the effects of etalons are minimized. It is not always possible however, to mitigate such etalons completely; our principle source of etalons in the data presented here is due to the AR coated Ge window attached to the detector; our assumption that the AR coating would be sufficient to remove this etalon was incorrect. Etalon correction is performed when possible by fitting the characteristically curved background to a simple sine function and subtracting from the data. We are presently looking into other active/passive etalon reduction techniques to eliminate this effect and resulting data manipulation.

Pressure broadening and line shifts (rather, incorrect line positions) are taken account of through both experimental determinations and modeling. The experimental results provide us with information regarding both line widths and line positions (the laser is inherently narrow compared to the molecular absorptions; there is some additional broadening induced by the modulation and is accounted for in the theoretical framework of Arndt[4]). Initial line positions and cross sections are taken from the HITRAN database of infra red activity for atmospheric molecules.[5] This data, and subsequent experimental data is used in our spectral simulations. We are presently modeling the data shown below, and the best fit parameters will be used in all subsequent data reductions.

Finally, the diode current controller that we are presently using scans the diode in frequency space nonlinearly in time. We use a one inch cylinder of germanium for our etalon with a Free Spectral Range (FSR) of 0.047952 $cm^{-1}$. This provides a relative frequency guide with which to correct the spectra.

## RESULTS

Shown in Figure 2 is a representative scan of fuel gas contaminated with approximately 2.2 ppm HCl, taken at ERC on July 23, 1993. There are several things to note in the figure relevant to the rest of the data. First, we note that the spectrum is complicated by interferences from isotopic variants of $H_2O$ and $CO_2$. In fact, as will be shown later, the unexpected position and intensity (absorption strength) of the $^{18}OCO$ isotope limits our sensitivity with this method. We also point out the unwanted background curvature due to the etalon generated by the Ge window on the detector. The curvature corresponds to an etalon with an FSR of approx. 1.25 $cm^{-1}$ matching the thickness of our detector window (FSR=1/2nl; n=index, l=pathlength). We are looking into correcting this problem by fitting the detector with AR-coated wedged windows. Also, note the second derivative line shape of the HCl absorption feature. Wavelength modulation spectroscopy is often known as derivative spectroscopy, since in the limit of small modulation index (m), the line shape is directly proportional to the $n^{th}$ derivative, where n is the detection harmonic.[3,4] Finally, note the changing period of the germanium etalon fringes, indicating the nonlinear scan in frequency of this diode requiring the correction described above.

Shown in Fig. 3 is data taken at ERC on test cell 7-377. The data was taken by adding a small side stream of 1000 ppm $HCl/N_2$ to the fuel gas. The absolute flow of this side stream was not continuously monitored and changes in the flow may cause the large discrepancy between the calculated and experimental values (6.5 ppm vs. 12 ppm). The left peak is due to singly deuterated water, while the right peak is a convolution of HCl and $^{18}OCO$. Note the large S/N ratio of this scan (approx. 50-100), which corresponds to a detection of approximately $3*10^{-3}$ absorbance units (base e). In the absence of interferences, detection of 100 ppb HCl requires sensitivity of approximately $5*10^{-5}$ absorbance units, which we approach.

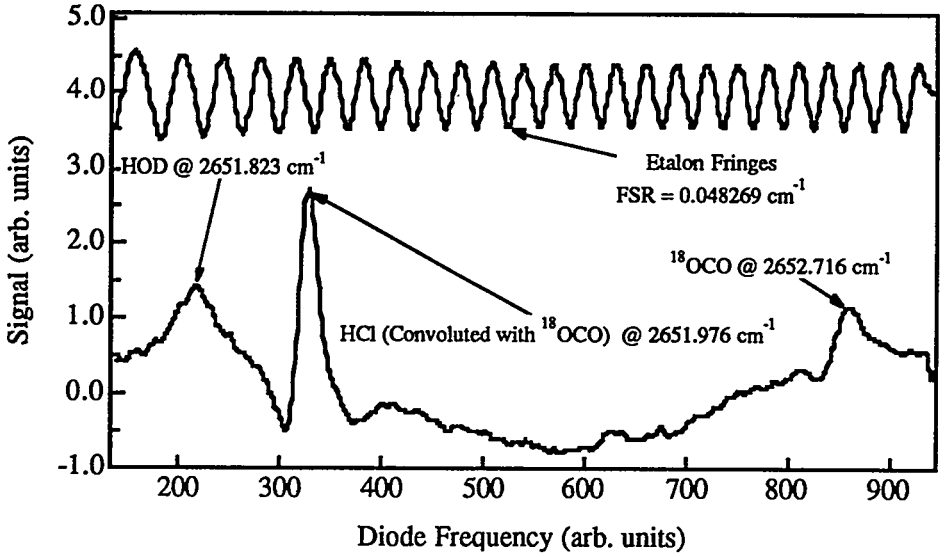


Figure 2. Representative scan showing spectral interferences, etalons, and nonlinear frequency scans. Data of fuel gas with 2.2 ppm HCl contaminant.

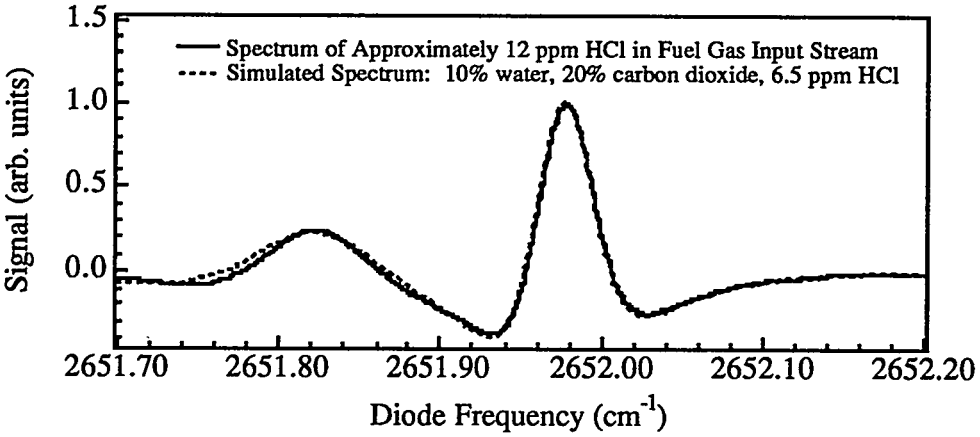


Figure 3. Spectrum and simulated spectrum of data taken at ERC. Flow was approximately 6.5 cc (STP) of 1000 ppm $HCl/N_2$. Total fuel gas flow was 556 cc (STP), yielding calculated contaminant concentration of 12 ppm. See text.

Shown in Figure 4 is a background spectrum taken of the input fuel gas consisting of 72% $H_2$/18% $CO_2$/10% $H_2O$. The left hand peak is the expected absorption due to the singly deuterated from of $H_2O$, HOD. The right hand peak, however, is absorption due to the oxygen-18 isotopic variant of $CO_2$, $^{18}OCO$. To even come close to simulating the measured spectrum, we had to arbitrarily shift the position of the $^{18}OCO$ by -0.032 $cm^{-1}$ and to scale the cross section by a factor of twenty. We were disturbed by this, because the magnitude and location of this absorption interferes with our ability to sensitively detect HCl, and we returned to the original literature, assuming that the error lay in the

database. Unfortunately, we found the same cross section as listed in the database. We are presently investigating the source of this discrepancy, and will use the scaled value in all of the following simulations. Also, we note the presence of unidentified absorptions (or possibly Residual Amplitude Modulation; RAM) located at 2652.1 and 2652.2 $cm^{-1}$ respectively and are pursuing their origin.

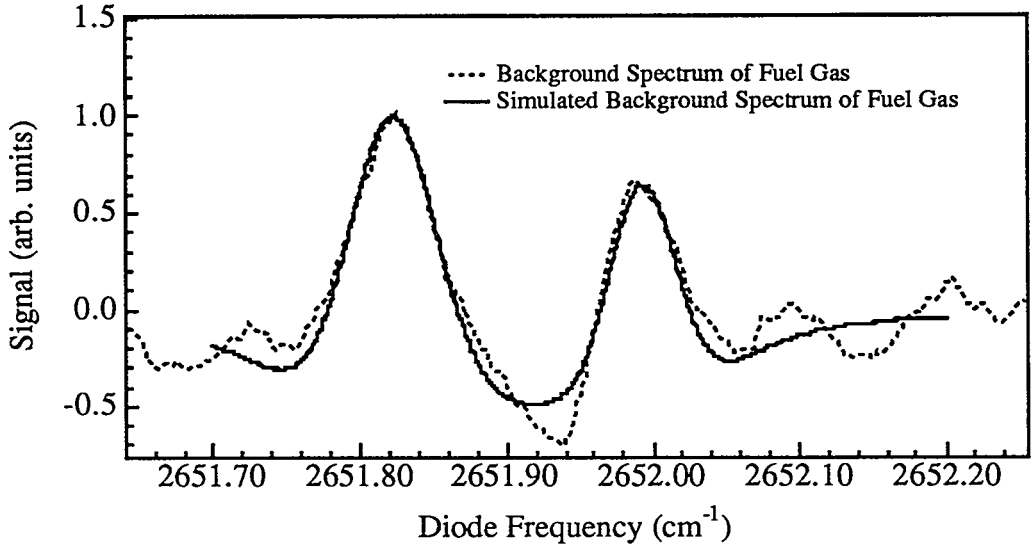


Figure 4. Background spectrum taken of HCl free fuel gas. The peak located at 2651.99 $cm^{-1}$ has been assigned to the oxygen-18 isotope of $CO_2$, and limits our sensitivity.

The data shown below (Fig. 5) is a spectrum of 72% $H_2$/18% $CO_2$/10% $H_2O$ with 2.2 ppm HCl contaminant taken of the anode input at ERC on test cell 7-377. The left peak is due to singly deuterated water, while the right peak is due to absorption by $^{18}OCO$ convoluted with HCl. We note that for the simulated

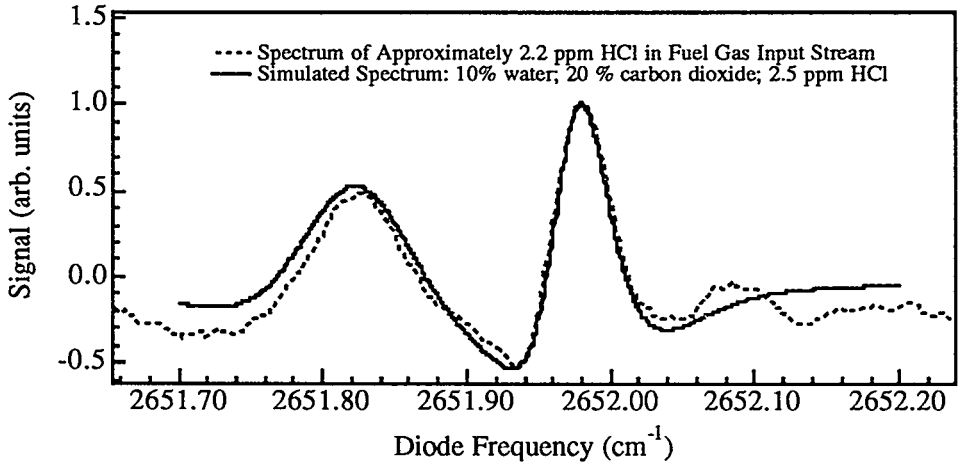


Figure 5. Spectrum of fuel gas contaminated with approximately 2.2 ppm HCl. Note the intensity change of only a factor of two compared to the previous figure, which has implications for our ultimate sensitivity.

spectrum, we used the scaled absorption cross section for $^{18}OCO$ shown previously. In comparing this spectrum to the HCl free spectrum listed above, we note that the absolute magnitude of the 2.2 ppm signal is only approx. a factor of two larger than the isolated $^{18}OCO$ line.

Shown in Figure 6 is a spectrum taken of the exit stream of the fuel cell anode. Note the increase in HOD absorption intensity relative to the $CO_2$. This is a result of the larger fractional increase in mole fraction of the HOD relative to the $CO_2$. Within our detection limits (determined to be approx. 250 -500 ppm; see below) we do not see HCl making it out of the fuel cell. This is consistent with previous data and equilibrium calculations which predict complete conversion of HCl to KCl, followed by KCl vaporization and removal from the fuel cell.

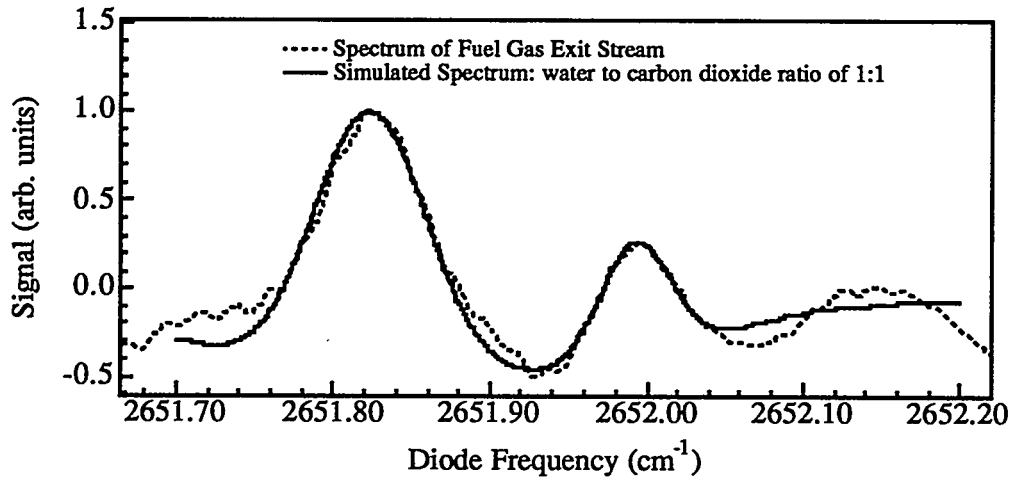


Figure 6. Spectrum and simulated spectrum of fuel cell anode exit stream.

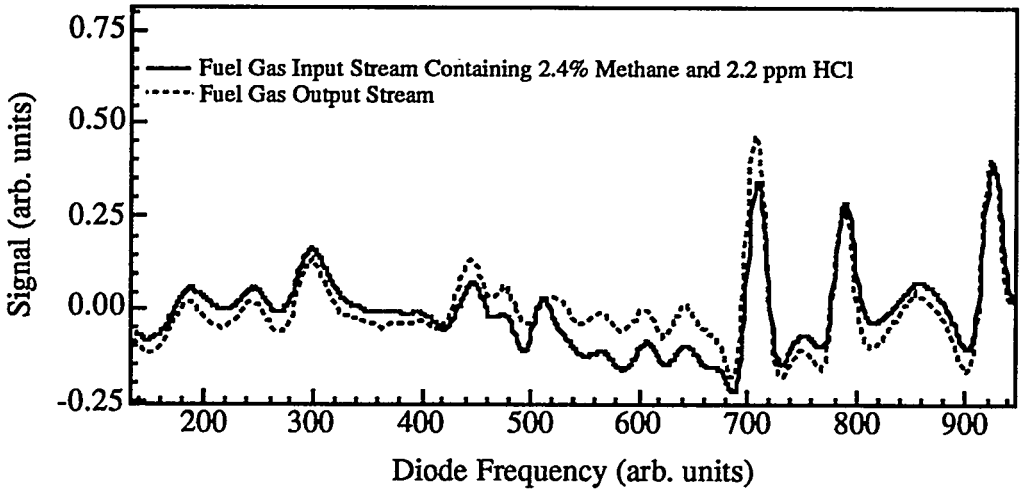


Figure 7. Spectra of fuel cell anode input and exit streams with addition of 2.4% $CH_4$. Fuel cell is running open circuit with a voltage of 1.043 V.

Shown in Fig. 7 are input and exit spectra taken of the addition of 2.4% $CH_4$ to the anode fuel gas stream. The cell is equipped with a methane reformer catalyst, and under normal operation the fuel cell uses up the added methane. In the spectrum taken below the cell was beingrun with no load (open circuit) and as a result, the methane was not being consumed. Note that the only difference in the spectra occurs at approximately point 510. The difference is attributable to the 2.2 ppm HCl being added to the fuel stream.

Shown in Figure 8 is a set of spectral simulations demonstrating the interference expected from $^{18}OCO$ under typical fuel cell operating conditions. Observe that the HOD peak is not greatly affected by the varying HCl concentration, and that the spectral signature of the $^{18}OCO$ only becomes significantly modified at HCl concentrations of 300 ppb and greater. With our present S/N ratios, we feel that this is the limit of our sensitivity at this time.

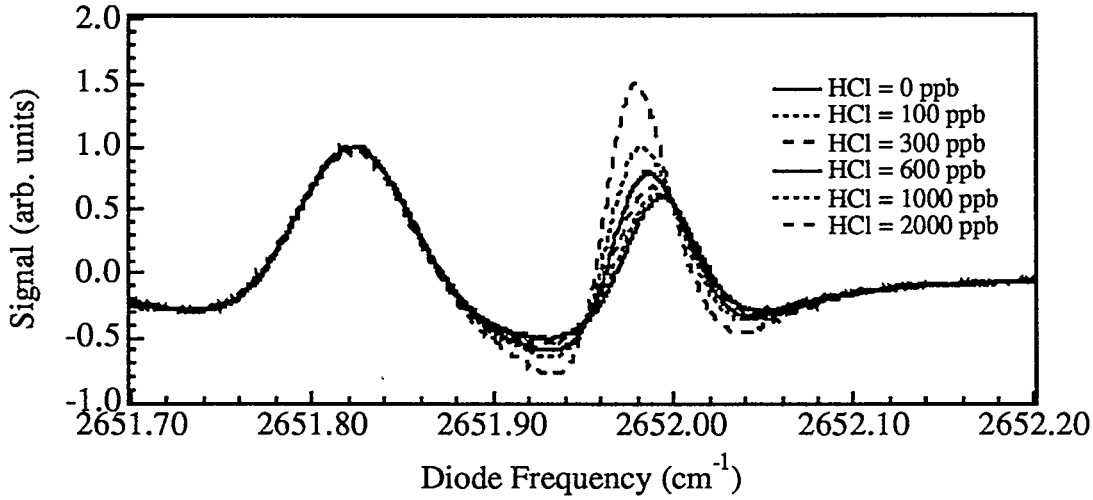


Figure 8. Spectral Simulations showing the change in spectral signature near $^{18}OCO$ as a function of HCl concentration.

## FUTURE WORK & CONCLUSIONS

We have stated previously, that due to the unexpected intensity and overlap of $^{18}OCO$ with P10 transition of HCl, that we are some what limited in our sensitivity because of our limited S/N ratios. We intend to improve the S/N ratio of our absorption spectrometer by eliminating all etalon effects. In addition, we will look for alternative HCl lines that may possibly provide reduced spectral interference. If such lines are found, we will record high resolution spectra of fuel cell constituents at temperature (923 K) to identify unforeseen spectral interferences.

In addition, we would like to demonstrate long-term application of the diagnostic on an operating fuel cell. The system is currently setup at ERC and is presently recording data.

We will also investigate the viability of this technique for detection of $H_2S$ and $H_2Se$ on real coal gas streams. We will identify the spectral region of each species with the necessary absorption strength and spectral "cleanliness" to provide a useful diagnostic. We then plan to conduct high resolution scans to identify possible spectral interferences.

In related preliminary work, we have found that room temperature Li/K carbonate can act as a prefilter for HCl contaminants. This was determined by monitoring the relative concentration drop across a nickel boat containing a Li/K carbonate mixture. We observed a one thousand fold drop in HCl concentration across

this boat. We are planning to investigate sodium carbonate as a high temperature HCl trap; sodium is chosen because the exchange reaction should generate NaCl, which will not have the volatility that KCl has and should not contaminate the fuel cell. In addition, we have setup an apparatus to assist us in measuring the absolute sticking coefficient of HCl with molten carbonate, that is, the probability an HCl molecule will stick upon collision with a carbonate surface. This data will provide the beginnings of a physical and chemical model to describe the kinetics of this process.

We also intend to pursue technology transfer of our diagnostic. The diagnostic would be much more useful if an industrial partner took the concept and marketed an affordable product.

In conclusion, we have demonstrated an *in situ* wavelength modulation spectrometer coupled to an operable fuel cell, and demonstrated the versatility of our diode laser technique for simultaneous detection of trace and major species. Unfortunately, we also determined that there is a large spectral interference due to $^{18}OCO$ at a spectral position and intensity that was not anticipated. Even so, we are close to the detection limit required of 100 ppb; we need to eliminate major sources of noise to achieve this goal (RAM and etalons).

## REFERENCES


1. K. Kinoshita, F. R. McLarnon, and E. J. Cairns, Fuel Cells: A Handbook, USDOE Report DOE/METC-88/6096 (1988).

2. B. A. Palmer, D. J. Funk, R. C. Oldenborg, "MCFC Diagnostics: HCl Detection," Fourth Annual Fuel Cells Contractors Review Meeting, Editor W. J. Huber (1992). A. Pigeaud, "Effects of Coal-Derived Trace Species on Performance of Molten Carbonate Fuel Cells," USDOE Final Report No. DE-AC21-88MC25009, Energy Research Corporation (1992).

3. D. S. Bohmse, A. C. Stanton, and J. A. Silver, "Frequency Modulation and Wavelength Modulation Spectroscopies: Comparison of Experimental Methods Using a Lead-Salt Diode Laser," Appl. Optics, **31**(6), 718 (1992).

4. R. Arndt, "Analytical Lineshapes for Lorentzian Signals Broadened by Modulation", J. Appl. Phys. **36**, 2522-2524 (1965)

5. L. S. Rothman et al., "The HITRAN Database: 1986 Edition", Appl. Opt. **26**(19) 4058 (1987).

## P21 Perovskite Solid Electrolytes for SOFC

CONTRACT INFORMATION

| | |
|---|---|
| Contract Number | DE-FG02-90ER80910 |
| Contractor | Eltron Research, Inc.<br>2830 Wilderness Place<br>Boulder, CO 80301<br>(303) 440-8008 |
| Contract Project Manager | Anthony F. Sammells |
| Principal Investigator | Anthony F. Sammells |
| METC Project Manager | Kamalendu Das |
| Period of Performance | July 23, 1990 to May 19, 1994 |

Schedule and Milestones

FY93 Program Schedule

| | O | N | D | J | F | M | A | M | J | J | A | S |
|---|---|---|---|---|---|---|---|---|---|---|---|---|
| Electrolyte Preparation | | | | | | | | | | | | |
| Electrolyte Characterization | | | | | | | | | | | | |
| SOFC Testing | | | | | | | | | | | | |

### OBJECTIVES

The object of this program is to experimentally determine the utility of selected perovskite related solid electrolytes for application in SOFC's operating at intermediate temperatures (600-750°C). Specific technical objectives addressed in this program include:

- Gaining useful insight into those crystallographic and thermodynamic parameters which influence both activation energy ($E_a$) for ionic transport and the population of ionic charge carriers.
- Synthesizing selected perovskite related solid electrolyte powders expected to possess i) low $E_a$ for ionic conduction and ii) an intrinsically high population of ionic charge carriers.
- Preparing sintered solid electrolyte disks and determine their ionic conductivity.
- Incorporating solid electrolytes demonstrating acceptable ionic conductivity into small research size SOFC's operating at intermediate temperatures and determine their electrochemical performance.
- Determining the long-term stability of selected solid electrolyte materials incorporated into SOFC's.

## BACKGROUND INFORMATION

Because of the relatively high activation energy $E_a$ for ionic conduction in yttria stabilized zirconia (YSZ) corresponding to $\cong 0.8eV$, it is necessary to operate fuel cells incorporating this material at 1000°C where this oxygen anion conducting solid electrolyte possesses a sufficiently high ionic conductivity an ionic conductivity of $2 \times 10^{-1} Scm^{-1}$.

As a consequence of the above, there are strong incentives to identify alternate solid electrolytes possessing sufficiently high ionic conductivities to facilitate practical fuel cell operation at lower "intermediate" temperatures. Research towards this goal is addressing development of an approach for clarifying the dependency between $E_a$ for ionic conduction in perovskite related lattice and parameters relating to i) metal oxide lattice dimensions, ii) the nature and sizes of ionic lattice constituents, iii) thermodynamic parameters relating to perovskite stability and iv) the intrinsic lattice polarizability or "flexibility" towards facilitating ionic mediation. Such an approach is currently evolving at Eltron Research, Inc. (Eltron) for the systematic selection of perovskite related solid electrolytes with the potential for achieving ionic conduction significantly larger than currently found with YSZ based materials.

## PROJECT DESCRIPTION

Perovskite solid electrolytes being selected for preparation into sintered disks and subsequent fabrication into SOFC's were based upon rationale currently under evolution at Eltron which is showing trends[1-7] between activation energy ($E_a$) for ionic conduction and the respective parameters: 1) the average perovskite metal-oxygen energy and associated enthalpy of formation $\Delta H_f$, 2) the lattice free volume (FV) obtained by subtracting the ionic volumes of lattice constituents in unit cell from the overall unit cell volume, 3) the parameter $r_{critical}$ ($r_c$) which corresponds to the radius of an opening between two A site cations and one B site cation, through which the mobile ion must pass, and 4) the lattice polarizability $\alpha$.

The expression for ionic conductivity ($\sigma$) in a solid electrolyte, as derived from random walk theory, may be given by:[8,9]

$$\sigma T = A \exp(-\Delta H_m/KT) \quad (1)$$

where

$$A = (Z\lambda^2 e^2/6\upsilon_o K)C(1-C)\upsilon_o \exp(\Delta S_m/K) \quad (2)$$

and $-\Delta H_m$ (equivalent to $E_a$) and $\Delta S_m$ are, respectively, enthalpies and entropies for activation, C is the fraction of available sites occupied by mobile ions, $\lambda$ the jump distance, Z the number of jump directions, $\upsilon_o$ the molar volume, K the Boltzmann constant and e the electronic charge.

Examining relationship (1) above, we see that overall ionic conductivity $\sigma$ is influenced both by an exponential and a preexponential term A. Performing a study on the influence of perovskite lattice parameters and ionic constituents upon $E_a$ only addresses the exponential component of this relationship. The preexponential term A is related to the number of charge carriers present in the solid-state lattice.

As a consequence, experimental investigations were extended to also include perovskite related lattice where a high population of oxygen vacancies were intrinsic, thereby contributing to the possibility of high ionic conductivity. This general approach resulted in our investigating materials based upon the brownmillerite structure $A_2B_2O_5$, which may be considered to be derived from the perovskite structure by removing 1/6 of the unit cell oxygen atoms.

Both stoichiometric and non-stoichiometric perovskite related solid electrolyte compositions are being studied.

## RESULTS

Recent work in our laboratory has been directed towards developing a rational approach for the selection of perovskite and perovskite-related solid electrolytes. This approach has resulted in identifying[6] the highly conducting perovskite $BaTh_{0.9}Gd_{0.1}O_3$. Unfortunately, this material does not possess long-term phase stability under intermediate temperature fuel cell operating conditions. This work has also led us to choose to study perovskite-related brownmillerite phases as potential solid electrolytes due to their inherently larger population of oxygen vacancies available for ionic conduction. Here, we report the synthesis and ionic conductivity of new brownmillerite phases of composition $Ba_2GdIn_{1-x}Ga_xO_5$ (x = 0,0.2,0.4). The x = 0.2 phase exhibits an extremely low activation energy ($E_a$) for ionic conduction, $E_a$ = 0.35 eV. This result supports the premise that brownmillerite compounds provide a suitable structure for achieving high ionic conductivity.

Compounds were prepared from stoichiometric powders of $BaCO_3$, $Gd_2O_3$, $In_2O_3$ and $Ga_2O_3$. These were initially thoroughly mixed and ball-milled for several hours in a polyethylene container with zirconia grinding media. Powders were then heated to 1200°C for 12 h in alumina crucibles and again ball-milled and reheated at 1400°C for 12 h. Resulting powders were again thoroughly ball-milled. Solid electrolyte disks were prepared by pressing approximately 1.2g of dry powder in a 1/2" diameter die at 20,000 psi and sintered at 1450°C for 4 h. For x = 0.2 and 0.4 phases, sintered disk densities were 92 and 88% of theoretical, respectively. Attempts to prepare sintered disks of the x = 0 phase were unsuccessful. X-ray diffraction was performed on both powders and sintered disks using a Rigaku Miniflex CN2005 diffractometer. No evidence for decomposition was noted during the sintering process. Lattice parameters were determined using Micro-Index from Materials Data, Inc.

Figure 1 shows the X-ray diffraction pattern of $Ba_2GdInO_5$. The pattern could be fitted to an orthorhombic cell with parameters a = 6.10Å, b = 17.26Å, and c = 6.00Å. Observed reflections are consistent with the brownmillerite structure in space group Ibm2. Lattice parameters are slightly larger than those reported[10] for the brownmillerite $Ba_2In_2O_5$ (a = 6.08Å, b = 16.79Å, c = 5.89Å). For the x = 0.2 and 0.4 phases, the patterns were similar to the x = 0 phase with lattice parameters a = 6.08Å, b = 17.20Å, c = 6.01Å and a = 6.02Å, b = 17.04Å, c = 6.00Å, respectively. The decreases in lattice parameters with increase in Ga content is consistent with the smaller[11] ionic radius of $Ga^{3+}$ relative to $In^{3+}$.

Ionic conductivities were determined from fuel cells of configuration:
$H_2,(3\%H_2O)Ni/Ba_2GdIn_{1-x}Ga_xO_5/Ag(3\%H_2O),O_2$
which were prepared using techniques previously discussed.[2] Ni (anode) and Ag (cathode) electrodes were prepared from metal epoxies. Open circuit potentials were within a few percent of theoretical indicating that the measured conductivities were primarily ionic. Conductivities up to $5 \times 10^{-3}$ $Scm^{-1}$ at 600°C were observed. We were not able to unequivocally confirm whether the conducting species were protons or oxide ions.

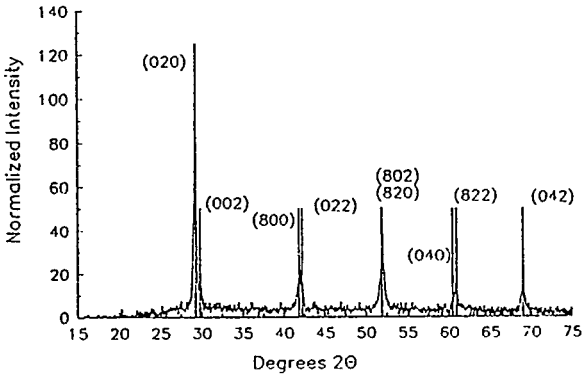


Figure 1. X-ray diffraction pattern of $Ba_2GdInO_5$ using $CuK_\alpha$ radiation. The pattern is indexed in the space group Ibm2 with lattice parameters a = 6.10, b = 17.26, and c = 6.00 Å.

However, it was noted that conductivities tended to increase upon operating the fuel cell and typically stabilized after approximately one day. This behavior had been observed previously[6] in $BaTh_{0.9}Gd_{0.1}O_3$ and was attributed to protonic conductivity. This may also be true for compounds under study here.

$E_a$ was calculated from measured conductivities as a function of temperature. Figure 2 shows plots of $\ln(\sigma T)$ vs. 1000/T for $Ba_2GdIn_{0.8}Ga_{0.2}O_5$ and $Ba_2GdIn_{0.6}Ga_{0.4}O_5$ with $E_a$ = 0.35 and 0.45eV and ln A = 3.9 and 6.0 $Scm^{-1}K$ for respective phases over the temperature range 550-700°C. Fuel cell conductivities were stable over several days with no direct evidence of materials instability.

An $E_a$ of 0.35eV is unusually low when compared[10] to the brownmillerite $Ba_2In_2O_5$ ($E_a$ = 0.75eV), the related brownmillerite intergrowth phase $Ba_3In_2ZrO_8$ ($E_a$ = 0.60eV), and the related perovskite[6] conductors $BaTh_{0.9}Gd_{0.1}O_3$ ($E_a \approx 0.4$eV) and $BaCe_{0.9}Gd_{0.1}O_3$ ($E_a$ = 0.52eV). A low value of $E_a$ for proton conduction, 0.37eV, in the latter compound has also been reported.[13]

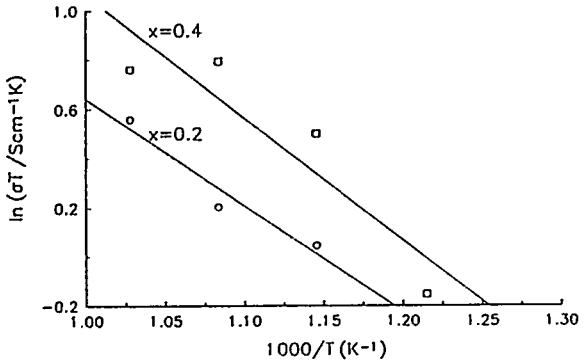


Figure 2. Plots of $\ln(\sigma T)$ vs. 1000/T for $Ba_2GdIn_{0.8}Ga_{0.2}O_5$(○) and $Ba_2GdIn_{0.6}Ga_{0.4}O_5$ (□) in the temperature range 550-700°C.

Despite the low $E_a$ measured for $Ba_2GdIn_{0.8}Ga_{0.2}O_5$, the absolute ionic conductivity is lower than that obtained for $BaTh_{0.9}Gd_{0.1}O_3$ exhibiting[6] a higher $E_a$. This result may arise from two causes. The first may be that the Meyer-Neldel rule:

$$\ln A = aE_a + b \qquad (2)$$

which governs the relationship between $E_a$ and A and has been shown to be valid within a given class of solid electrolyte materials[14,15] is not valid in this instance. However, not enough conducting brownmillerite compounds have been characterized to determine whether this rule also holds for brownmillerites.

On a more fundamental level, Equation 1 shows that conductivity is governed by two terms, the $E_a$ and the preexponential term A. According to random walk theory[16,17] A has a C(1-C) dependence, where C corresponds the fraction of available sites, *i.e.* the number of vacancies available for ionic conduction. Therefore, since $E_a$ is relatively low in this phase, the conductivity may be limited by lack of available charge carriers.

The situation in $Ba_2GdIn_{0.8}Ga_{0.2}O_5$ is somewhat different from that in $Ba_2In_2O_5$. In the latter compound, an order-disorder transition among the anion sites at ≈900°C leads to a decrease in $E_a$ with a subsequent increase in conductivity, while $Ba_2GdIn_{0.8}Ga_{0.2}O_5$ exhibits an inherently low $E_a$. Our previous work has pointed out that a correlation exists between $E_a$ and "free volume" (the difference between the measured volume and the volume calculated using ionic radii) in perovskites. This has found that larger free volume generally gives lower $E_a$ values. The free volume for $Ba_2GdIn_{0.8}Ga_{0.2}O_5$ is calculated to be 265.2Å$^3$ while for $Ba_2In_2O_5$ is only 242.8Å$^3$. It is then not surprising that $E_a$ for $Ba_2GdIn_{0.8}Ga_{0.2}O_5$ is lower than for $Ba_2In_2O_5$.

## SUMMARY

We have synthesized a new series of brownmillerite solid electrolyte phases $Ba_2GdIn_{1-x}Ga_xO_5$ (x = 0,0.2,0.4) with the x = 0.2 phase exhibiting an unusually low $E_a$ relative to both the observed ionic conductivity in this phase and to $E_a$s observed in similar compounds. We attribute measured ionic conductivities to a lack of available charge carriers in $Ba_2GdIn_{0.8}Ga_{0.2}O_5$. However, the low $E_a$ supports the premise that brownmillerite solid electrolyte structures are suitable for supporting high ionic conductivity. Current work is focusing on enhancing the amount of charge carriers in these materials by systematically introducing disorder into the brownmillerite lattice.

## FUTURE WORK

This is being addressed by i) optimization of perovskite related solid electrolytes, ii) optimize preparation techniques for perovskite solid electrolytes and other components to be incorporated into the intermediate temperature fuel cell, iii) perform an in-depth electrochemical study on fuel cells incorporating preferred selected solid electrolytes and electrocatalysts, and iv) incorporate preferred components into a fuel cell stack which will be subjected to extensive performance testing at intermediate temperatures.

## REFERENCES

1. A.F. Sammells, R.L. Cook, J.H. White, J.J. Osborne and R.C. MacDuff, Solid State Ionics, 52, 111, (1992).
2. M. Schwartz, B.F. Link, and A.F. Sammells, J. Electrochem Soc., 140 L62 (1993).
3. A.F. Sammells, Proceedings of a Presentation given at the International Fuel Cell Conference, Makuhari, Japan, February 3 (1992).
4. A.F. Sammells, Presentation given at U.S. DOE/Japan AIST Fuel Cells Subcommittee & Technical Meeting, January 27-28, Tokyo, Japan (1992).
5. A.F. Sammells, R.L. Cook, J.H. White, J.J. Osbourne and R.C. MacDuff, Solid State Ionics, 52, 111 (1992).
6. R.L. Cook, J.J. Osborne, J.H. White, R.C. MacDuff and A.F. Sammells, J. Electrochem Soc., 139, L19 (1992).
7. R.L. Cook and A. F. Sammells, Solid State Ionics, 45, 311 (1991).
8. P. McGeehin and A. Hopper, J. Mater. Sci., 12, 1 (1977).
9. J.B. Goodenough, Proc. Royal Soc., (London) A393, 215 (1984).
10. J.B. Goodenough, J.E. Ruiz-Diaz, and Y.S. Zhen, Solid State Ionics, 44, 21 (1990).
11. R.D. Shannon, Acta Cryst., A32, 751 (1976).
12. N. Bonanos, B. Ellis, K.S. Knight, and M.N. Mahmood, Solid State Ionics, 35, 179 (1989).
13. R.C.T. Slade and N. Singh, J. Mater. Chem., 1, 441 (1991).
14. A.S. Nowick, W.K. Lee, and H. Jain, Solid State Ionics, 28/30, 89 (1988).
15. D.P. Almond and A.R. West, Solid State Ionics, 23, 27 (1987).
16. P. McGeehin and A. Hopper, J. Mater Sci., 12, 1 (1977).
17. J.B. Goodenough, Proc. Roy. Soc., (London), A393, 215 (1984).

# Appendices

# Appendix A



## Joint Contractors Meeting

## FE/EE Advanced Turbine Systems Conference
## FE Fuel Cells and Coal-Fired Heat Engines Conference
## August 3-5, 1993

## AGENDA
TUESDAY, AUGUST 3, 1993

### FE/EE ADVANCED TURBINE SYSTEMS (ATS) CONFERENCE

8:00 a.m. Registration/Continental Breakfast

### OPENING SESSION

Co-chairpersons: William P. Parks and Edward L. Parsons

8:30 a.m. *Opening Announcements, Introduction of Keynote Speakers*
William T. Langan
Morgantown Energy Technology Center

*Keynote Addresses*

8:35 a.m. Jack S. Siegel, Acting Assistant Secretary, Office of Fossil Energy

8:55 a.m. Robert L. San Martin, Acting Assistant Secretary, Office of Energy Efficiency and Renewable Energy

### PANEL DISCUSSION -- PERSPECTIVES ON THE ATS PROGRAM

9:15 - 9:55 a.m. Prepared Remarks

| | | |
|---|---|---|
| Ronald H. Wolk<br>EPRI | Donald K. Walter<br>DOE/EE | Paul Stolpman<br>EPA |
| Stephen Freedman<br>GRI | George Rudins<br>DOE/FE | |

*Tuesday*

**FE/EE Advanced Turbine Systems Conference**

9:55 a.m. Panel Discussion -- Moderator: Edward L. Parsons

10:30 a.m. BREAK

## SESSION 1 -- STUDIES AND CONCEPTUAL DESIGN

Chairperson: Donald W. Geiling

10:50 a.m. 1.1 *Development of Advanced Gas Turbine Systems*
Ronald L. Bannister
Westinghouse Electric Corporation

11:15 a.m. 1.2 *GE Power Generation Technology Challenges for Advanced Gas Turbines*
John G. Nourse
GE Environmental Services

11:40 a.m. 1.3 *Gas Fired Advanced Turbine System*
David J. White
Solar Turbines Incorporated

12:05 p.m. 1.4 *Advanced Turbine Systems - Scoping and Feasibility Study*
Dale W. Mukavetz
Allison Gas Turbine Division
General Motors Corporation

12:30 p.m. LUNCH

Chairperson: Charles T. Alsup

1:30 p.m. 1.5 *Advanced Turbine Systems - Studies and Conceptual Design*
Septimus van der Linden
ABB Power Generation Inc.

1:55 p.m. 1.6 *METC Combustion Research Facility*
John S. Halow
Morgantown Energy Technology Center

## SESSION 2 – INDUSTRIAL SYSTEMS

Chairperson: Stephen Waslo

| | | |
|---|---|---|
| 2:20 p.m. | 2.1 | *Ceramic Retrofit Project*<br>Mark van Roode<br>Solar Turbines Incorporated |
| 2:45 p.m. | 2.2 | *Materials/Manufacturing Element of the Advanced Turbine Systems Program*<br>Michael A. Karnitz<br>Oak Ridge National Laboratory |
| 3:10 p.m. | | BREAK |

## SESSION 3 – RELATED PROGRAMS

Chairperson: Holmes A. Webb

| | | |
|---|---|---|
| 3:30 p.m. | 3.1 | *Collaborative Advanced Gas Turbine Project*<br>Arthur Cohn<br>Electric Power Research Institute |
| 3:55 p.m. | 3.2 | *U.S. Navy Intercooled Recuperated (ICR) Engine*<br>Thomas L. Bowen<br>Naval Surface Warfare Center |
| 4:20 p.m. | 3.3 | *Integrated High Performance Turbine Engine Technology Initiative*<br>G. D. Turner<br>United States Air Force |
| 4:45 p.m. | 3.4 | *Industry/University Consortium for ATS Research*<br>Lawrence P. Golan<br>South Carolina Energy Research and Development Center |
| 5:10 p.m. | | ADJOURN |
| 6:30 p.m. | | SOCIAL HOUR AND BARBECUE<br>Lakeview Resort and Conference Center |

## ATS UNIVERSITY WORKSHOP
Room G-4

**Workshop held concurrently with Heat Engines Meeting**

### OPENING SESSION

Chairperson: Paul L. Micheli

8:15 a.m. *Welcome - ATS University Workshop*
Lawrence P. Golan, Director
South Carolina Energy Research and Development Center

8:20 a.m. *University Participation in the ATS Program*
Roy P. Allen, Director
Advanced Gas Turbine Systems Research
South Carolina Energy Research and Development Center

### UNIVERSITY PRESENTATIONS

8:50 a.m. W1 *Combustion Modeling in Advanced Turbine Systems*
Paul O. Hedman
Brigham Young University

9:05 a.m. W2 *Ultra-Low Gas Turbine Emissions Using Catalytic and Noncatalytic Porous Combustors*
Robert W. Dibble
University of California at Berkeley

9:20 a.m. W3 *Reduction of Turbine Endwall Total Pressure Loss and Heat Transfer Using the Iceformation Design Method*
Ronald S. LaFleur
Clarkson University

9:35 a.m. BREAK

10:00 a.m. W4 *Functionally Gradient Materials for Thermal Barrier Coatings in Advanced Gas Turbine Systems*
Arnold R. Marder
Lehigh University

## *Wednesday*

**ATS University Workshop**

| | | |
|---|---|---|
| 10:15 a.m. | W5 | *Vortex-Generator Induced Enhanced Heat Transfer in Gas Turbine Blade Coolant Channels With Rotation*<br>Sumanta Acharya<br>Louisiana State University |
| 10:30 a.m. | W6 | *Life Prediction of Advanced Materials for Gas Turbine Applications*<br>Sam Y. Zamrik<br>The Pennsylvania State University |
| 10:45 a.m. | W7 | *NOx Abatement in Advanced Gas Turbines*<br>Paul E. Sojka<br>Purdue University |
| 11:00 a.m. | W8 | *Advanced Turbine Cooling, Heat Transfer, and Aerodynamic Studies*<br>J. C. Han<br>Texas A&M University |
| 11:15 a.m. | W9 | *NOx and CO Emissions Models for Gas Fired, Lean Premixed Combustion Turbines*<br>A. M. Mellor<br>Vanderbilt University |
| 11:30 a.m. | W10 | *Advanced Combustion Technologies for Gas Turbine Power Plants*<br>S. Desu<br>Virginia Polytechnic Institute |
| 11:45 a.m. | | ADJOURN |

## WEDNESDAY, AUGUST 4, 1993

### FE COAL-FIRED HEAT ENGINES CONFERENCE

8:00 a.m. Registration/Continental Breakfast

8:15 a.m. *Introductory Remarks*
Holmes A. Webb

### SESSION 1 – COAL-FUELED TURBINES

Chairperson: Leland E. Paulson

8:25 a.m. 1.1 *Interface Between a Gas Turbine and PFBC*
Arthur W. McGuigan
Westinghouse Electric Corporation

8:50 a.m. 1.2 *Full-Scale and Bench-Scale Testing of a Coal-Fueled Gas Turbine System*
Richard T. LeCren
Solar Turbines Incorporated

9:15 a.m. 1.3 *High Pressure Ceramic Air Heater for Indirectly-Fired Gas Turbine Applications*
Nelson J. Orozco
Hague International

9:40 a.m. BREAK

10:00 a.m. 1.4 *Direct Coal-Fired Gas Turbines for Combined Cycle Plants*
Richard A. Wenglarz
Allison Division of General Motors Corporation

10:25 a.m. 1.5 *Heavy Duty Gas Turbine Combustion Tests Using Simulated Low-Btu Coal Gas*
Thomas E. Ekstrom
General Electric Company

10:50 a.m. 1.6 *Combustion Tests of a Turbine Simulator Burning Low Btu Fuel From a Fixed Bed Gasifier*
Alan S. Feitelberg
GE Environmental Services, Inc.

## SESSION 2 – COAL-FUELED DIESELS

Chairperson: William C. Smith

| | | |
|---|---|---|
| 11:15 a.m. | 2.1 | *Commercialization of Coal Diesel Engines for Non-Utility and Export Power Markets*<br>Robert P. Wilson<br>Arthur D. Little, Inc. |
| 11:40 a.m. | 2.2 | *Coal-Fueled Diesel Engines for Locomotive Applications*<br>Bertrand D. Hsu<br>GE Transportation Systems |
| 12:05 p.m. | 2.3 | *Coal-Fueled High-Speed Diesel Engine Development*<br>Ramish M. Kakwani<br>Detroit Diesel Corporation |
| 12:30 p.m. | | LUNCH |

## FE FUEL CELLS CONFERENCE

### OPENING SESSION

Co-chairpersons: Manville J. Mayfield and Edward L. Parsons

1:30 p.m.

*Welcome & METC Perspective*
Manville J. Mayfield

*EPRI Perspective*
Ronald H. Wolk

*GRI Perspective*
Michael Whelan

### SESSION 1 – MOLTEN CARBONATE FUEL CELLS

Chairperson: Mark C. Williams

2:00 p.m. 1.1 *Overview of ERC's Carbonate Fuel Cell Development Program*
Donald R. Glenn
Energy Research Corporation

2:25 p.m. 1.2 *Overview of M-C Power's MCFC Power Generation System*
Richard R. Woods
M-C Power Corporation

2:50 p.m. 1.3 *MCFC Product Development Test*
Ashok K. Kush
Energy Research Corporation

3:15 p.m. BREAK

Chairperson: Tom J. George

3:35 p.m. 1.4 *Molten Carbonate Fuel Cell Product Development Test*
Joseph A. Scroppo
M-C Power Corporation

| | | |
|---|---|---|
| 4:00 p.m. | 1.5 | *MCFC Power Plant System Verification*<br>Mohammad Farooque<br>Energy Research Corporation |
| 4:25 p.m. | 1.6 | *Simulated Coal Gas MCFC Power Plant System Verification*<br>Thomas G. Benjamin<br>M-C Power Corporation |
| 4:50 p.m. | | ADJOURN |

## POSTER SESSION -- HEAT ENGINES AND FUEL CELLS

4:50 - 6:15 p.m.

Heat Engines Technologies

P1 *Particulate Control for Coal-Fueled Diesel Engine Exhaust*
Leo A. Smolensky
LSR Technologies, Inc.

P2 *Ames Assay of Particulates From Coal-Fueled Diesel Engines*
William E. Wallace
National Institute of Occupational Safety and Health

P3 *Sub-Scale Development of an Acoustically Enhanced Cyclone for PFBC*
Marlene A. Galica
Solar Turbines Incorporated

P4 *Air Extraction in Gas Turbines Burning Coal-Derived Gas*
Tah-teh Yang
Clemson University

P5 *Development of a Dry-Feed System for a Coal-Fired Gas Turbine*
John W. Rothrock, Jr.
Allison Gas Turbine Division
General Motors Corporation

P6 *METC Research on Coal-Fired Diesels*
Michael H. McMillian
Morgantown Energy Technology Center

P7 *Pressure-Gain Combustion*
George A. Richards
Morgantown Energy Technology Center

P8 *Pressurized Burner Test Facility*
Daniel J. Maloney
Morgantown Energy Technology Center

P9 *Premixed Burner Studies of NOx Formation and Control*
Kent H. Casleton
Morgantown Energy Technology Center

P10 *The DOE NEPA Process*
Suellen A. Van Ooteghem
Morgantown Energy Technology Center

Fuel Cells Technologies

P11 *Research and Development of Alternative Components at Argonne National Laboratory for Molten Carbonate Fuel Cells*
Gene H. Kucera
Argonne National Laboratory

P12 *Sealant Research for Solid Oxide Fuel Cells*
Ira Bloom
Argonne National Laboratory

P13 *Alternative Materials for Solid Oxide Fuel Cells: Processing and Interactions of Materials*
Timothy R. Armstrong
Pacific Northwest Laboratory

P14 *Low Cost, Radial Flow, Solid Oxide Fuel Cell*
Michael A. Petrik
Technology Management, Inc.

P15 *Processing of $LaCrO_3$ for Solid Oxide Fuel Cell Applications*
Wayne Huebner
University of Missouri - Rolla

P16 *Econominization of SOFCs*
David P. Bloomfield
Analytic Power

P17 *Advanced Research and Technology Development of MCFCs*
Leonard G. Marianowski
Institute of Gas Technology

P18 *Fuel Cell Handbook Update*
John H. Hirschenhofer
Gilbert/Commonwealth, Inc.

P19 *Macrocyclic Redox Promoters for Methanol Oxidation*
Shantha Sarangapani
ICET, Inc.

P20 *Optical Sensor Development for MCFCs: Wavelength Modulation Diode Laser Absorption Spectroscopy*
David J. Funk
Los Alamos National Laboratory

P21 *Perovskite Solid Electrolytes for SOFC*
Anthony F. Sammells
Eltron Research, Inc.

## THURSDAY, AUGUST 5, 1993

8:00 a.m. Registration/Continental Breakfast

8:20 a.m. *Welcome Back*
Manville J. Mayfield

### SESSION 2 – SOLID OXIDE FUEL CELLS

Chairperson: Diane T. Hooie

8:25 a.m. 2.1 *High Temperature Solid Oxide Fuel Cell Development Activities*
Emerson R. Ray
Westinghouse Electric Corporation

8:50 a.m. 2.2 *Development of a Monolithic Solid Oxide Fuel Cell*
Richard A. Gibson
AlliedSignal Aerospace

9:15 a.m. 2.3 *High Temperature Solid Oxide Fuel Cell - Customer Test Units*
Stephen E. Veyo
Westinghouse Electric Corporation

9:40 a.m. 2.4 *Contaminant Effects in Solid Oxide Fuel Cells*
Nicholas J. Maskalick
Westinghouse Electric Corporation

10:05 a.m. BREAK

## PANEL DISCUSSION -- COMMERCIALIZATION OF FUEL CELLS

Moderator: Manville J. Mayfield

10:25 - 11:25 a.m.

Industrial & Manufacturing

William J. Lueckel
International Fuel Cells Corporation

Bernard S. Baker
Energy Research Corporation

Elias H. Camara
M-C Power Corporation

Walter J. Dollard
Westinghouse Electric Corporation

Steve Huval
Stewart and Stevenson

Christopher R. Bentley
Fuel Cell Manufacturing Corporation

Utilities

John D. Leeper
Southern California Edison

Al Figueroa
San Diego Gas and Electric

David D. Moard
Southern California Gas

Sam Clowney
Tenneco

11:25 a.m. CLOSING REMARKS

11:30 a.m. CONFERENCE ADJOURNS

# Appendix B

## Meeting Participants


Sumanta Acharya, Professor
Louisiana State University
Mechanical Engineering Department
Baton Rouge, LA 70803
504-388-5809, (FAX) 504-388-5990

Sanjay K. Agarwal, Research
Chemical Engineer
Research Triangle Institute
P.O. Box 12194
Research Triangle Park, NC 27709
919-541-8024, (FAX) 919-541-8000

Ajay Agrawal, Assistant Professor
University of Oklahoma
Aerospace & Mechanical Engineering
Norman, OK 73019-0601
405-325-5011, (FAX) 405-325-1088

Annette Ahart, Customer Service Manager
EG&G WASC, Inc.
P.O. Box 880, MS A02
Morgantown, WV 26507-0880
304-291-4463

David S. Alcorn, Chairman & CEO
Donlee Technologies, Inc.
693 North Hills Road
York, PA 17402
717-755-1081, (FAX) 717-755-0020

Sy Ali, Manager
Industrial Engine Tech.
Allison Gas Turbine
General Motors
P.O. Box 420, W16
Indianapolis, IN 46206-0420
317-230-6864, (FAX) 317-230-5600

Roy Allen, Director
Gas Turbine Research
South Carolina Energy Center
386-2 College Avenue
Clemson, SC 29634
803-656-1418, (FAX) 803-656-0142

David H. Archer, Professor
Carnegie Mellon University
114 Kentzel Road
Pittsburgh, PA 15237-2816
412-268-6808, (FAX) 412-268-3348

Tim Armstrong, Senior Research Scientist
Pacific Northwest Laboratories
Battelle Boulevard, P.O. Box 999
Richland, WA 99352
509-375-3938, (FAX) 509-375-2186

Stan Arrigotti, Research Engineer
Energy International
127 Bellevue Way, S.E., Suite 200
Bellevue, WA 98004
206-453-9595, (FAX) 206-455-0981

Carol J. Bailey, Fuel Cell Program Manager
Southern California Gas Company
555 W. Fifth Street, M.L. 19 E0
Los Angeles, CA 90013
213-244-5328, (FAX) 213-244-8191

Richard A. Bajura, Associate
Provost for Research
West Virginia University
617 North Spruce Street
Morgantown, WV 26506
304-293-3449

Bernard S. Baker, President
Energy Research Corporation
3 Great Pasture Road
Danbury, CT 06813
203-792-1460, (FAX) 203-798-2945

Ronald L. Bannister, Manager
Gasification Programs
Westinghouse Electric Corporation
4400 Alafaya Trail, MC 381
Orlando, FL 32826-2399
407-281-3270, (FAX) 407-281-5014

Eric A. Barringer, Group Supervisor
Babcock & Wilcox
Lynchburg Research Center
P.O. Box 1165
Lynchburg, VA 24506-1165
804-522-6191, (FAX) 804-522-6196

Paul Bautista, Project Manager
Gas Turbine
Gas Research Institute
8600 W. Bryn Mawr Avenue
Chicago, IL 60631
312-399-5460, (FAX) 312-399-8170

Dan Beishon, Senior Engineer
British Gas
Gas Research Centre
Ashby Road
Loughborough
United Kingdom

Christopher R. Bentley, President
Fuel Cell Manufacturing Corporation
318 Industrial Lane, P.O. Box 0538
Torrington, CT 06790
203-496-1111, (FAX) 203-496-2222

Jeffrey M. Bentley
Arthur D. Little, Inc.
Acorn Park
Cambridge, MA 02140-2390
617-498-5820, (FAX) 617-498-5000

Frank P. Bevc, Manager
Emerging Technologies
Westinghouse Electric Corporation
4400 Alafaya Trail
Orlando, FL 32826
407-281-3393, (FAX) 407-281-5014

Ed Beyma, Program Manager
U.S. Department of Energy
FE-73/Germantown
Washington, DC 20585
301-903-2828, (FAX) 301-903-2713

Richard Biljetina, Vice President
Product Technology
Institute of Gas Technology
3424 South State Street
Chicago, IL 60077
312-890-6418, (FAX) 312-890-6419

Ben Bingham, Executive Director
AGTMA
1825 Eye Street, N.W., Suite 400
Washington, DC 20006
202-429-6833, (FAX) 202-857-5209

Samuel Biondo, Deputy Director
Office of Spec. Tech.
U.S. Department of Energy
Washington, DC 20585
301-903-2700, (FAX) 301-903-2713

Joseph Blanford, Executive
MTCI
5570 Sterrett Place, Suite 206
Columbia, MD 21044
410-730-0445, (FAX) 410-997-6980

Ira Bloom
Argonne National Laboratory
9700 S. Cass Avenue
Argonne, IL 60438
708-252-4516, (FAX) 708-252-4176

Thomas L. Bowen, ICR Program Manager
U.S. Naval Surface Warfare Center
3A Leggett Circle, Code 80B
Annapolis, MD 21402
410-267-2723, (FAX) 410-267-3491

Thomas J. Bradish, Manager
R&D
Pennsylvania Electric Company
1001 Broad Street
Johnstown, PA 15907
814-533-8593, (FAX) 814-533-8591

David Breeden, Patent Advisor
U.S. Department of Energy
Oak Ridge Field Office
P.O. Box 2001
Oak Ridge, TN 37831-8751
615-576-1080

Warren W. Bunker, Program Manager
U.S. Department of Energy.
FE-231
Washington, DC 20585
301-903-2824, (FAX) 301-903-2406

Linus B. Buss, Chief Engineer
Allied Signal Aerospace Company
2525 W. 190th Street, P.O. Box 2960
Torrance, CA 90504-6099
310-512-4525, (FAX) 310-512-3974

Elias Camara, Senior Vice President
M-C Power
830 Fox Hill Road
Chatham, MA 02633
708-986-8040, (FAX) 508-945-4120

Harold A. Carlson, Marketing Consultant
Hague International
11 Golf Green Lane
Salem, SC 29676
803-944-2115, (FAX) 803-944-2115

Peter A. Carroll, Vice President
Government Affairs
Solar Turbines, Inc.
1730 Pennsylvania Ave., N.W., Suite 750
Washington, DC 20006
202-783-1833, (FAX) 202-783-2055

Ismail Celik, Professor
West Virginia University
Mechanical & Aerospace Engineering
Morgantown, WV 26506
304-293-3111, (FAX) 304-293-6689

S. H. Chan, Professor
University of Wisconsin
P.O. Box 784
Milwaukee, WI 53201
414-229-5001

Ravi Chandran, Principal Scientist
MTCI
6001 Chemical Road
Baltimore, MD 21226
410-354-0420, (FAX) 410-354-0471

Alex Chang, Research Engineer
NOXSO Corporation
P.O. Box 469
Library, PA 15129
412-854-1200, (FAX) 412-854-5729

Tan-Ping Chen, Manager
Coal & Gas Conversion
Bechtel Corporation
50 Beale Street
San Francisco, CA 94105-1895
415-768-1419, (FAX) 415-768-3580

Dennis Cheney, Program Manager
EG&G Idaho, Inc.
P.O. Box 1625
Idaho Falls, ID 83415
208-526-9557

Tsu-Wei Chou, Professor
Center for Composite Materials
University of Delaware
Newark, DE 19716
302-831-2904, (FAX) 302-831-8525

M. A. Choudhry, Professor
West Virginia University
Electrical & Computer Engineering
Morgantown, WV 26505
304-293-6371, (FAX) 304-293-5024

Larry Christner, Vice President
Fuel Cell Manufacturing Corporation
318 Industrial Lane
P.O. Box 0538
Torrington, CT 06790
203-496-1111, (FAX) 203-496-2222

Arthur Cohn, Technical Manager
Electric Power Research Institute
P.O. Box 10412
Palo Alto, CA 94303
415-855-2525, (FAX) 415-855-8501

Nancy Cole, Program Manager
Oak Ridge National Laboratory
P.O. Box 2008
Oak Ridge, TN 37831
615-574-4824

Charles S. Cook, IGCC Technology Leader
GE Power Generation
1 River Road, Building 53-225
Schenectady, NY 12345
518-585-9421, (FAX) 518-385-5041

John R. Cooper, Engineer
R&D
Allegheny Power Service Corporation
800 Cabin Hill Drive
Greensburg, PA 15601
412-830-5688, (FAX) 412-830-5008

James C. Corman, General Manager
Advanced Technology
General Electric Company
1 River Road, Building 53, Room 417
Schenectady, NY 12345
518-385-7779, (FAX) 518-385-0404

Steve C. Datsko, Research Specialist
Babcock & Wilcox
1562 Beeson Street
Alliance, OH 44601
216-829-7528

Keith G. Davidson, Director
Power Generation
Gas Research Institute
8600 West Bryn Mawr Avenue
Chicago, IL 60631
312-399-8246, (FAX) 312-399-8170

Frank G. Davis, Office Manager
Allied Signal Aerospace Company
7550 Lucerne Drive, Suite 203
Middleburg Heights, OH 44130
216-826-0330, (FAX) 216-826-0333

Michael R. Delallo
DOE - Programs Manager
Gilbert/Commonwealth, Inc.
P.O. Box 1498
Reading, PA 19603
215-775-2600, (FAX) 215-775-2670

Victor Der, Director
Office of Special Tech.
U.S. Department of Energy
Washington, DC 20585
301-903-2700, (FAX) 301-903-2713

Jack Devan, Engineer
Senior Research Staff
Oak Ridge National Laboratory
P.O. Box 2008, Building 4500S, MS-6156
Oak Ridge, TN 37354
615-574-4451, (FAX) 615-574-5118

Robert W. Dibble, Professor
University of California
Department of Mechanical Engineering
Berkeley, CA 94720
510-642-4901, (FAX) 510-642-6163

Walter J. Dollard, General Manager
Westinghouse Electric Corporation
Science & Technology Center
1310 Beulah Road
Pittsburgh, PA 15235
412-256-5300, (FAX) 412-256-2002

Rand Drake, Mechanical Engineer
Naval Energy & Environmental Support
1001 Lyons Street, Suite 1
Port Hueneme, CA 93043-4340
805-982-3514, (FAX) 805-982-5388

Raymond D. Dunlop, Manager
Protection & Planning
New England Electric
25 Research Drive
Westborough, MA 01582
508-366-9011, (FAX) 508-389-3218

Suren Dwivedi, Professor
West Virginia University, ESB 333
Morgantown, WV 26506
304-293-3111

Paul Eggerstedt, Director of R&D
Industrial Filter
5900 Ogden Avenue
Cicero, IL 60650
708-656-7800, (FAX) 708-656-7806

Thomas E. Ekstrom, Program Manager
General Electric Company
1 River Road, Building 53-303
Schenectady, NY 12345
518-385-5418, (FAX) 518-385-5041

Ron Engleman, Systems Engineer
Gilbert/Commonwealth, Inc.
19644 Club House Road, Suite 820
Gaithersburg, MD 20879
301-869-9191, (FAX) 301-977-7507

Erek J. Erekson, Senior Chemical Engineer
Institute of Gas Technology
3424 South State Street
Chicago, IL 60616
312-949-3898, (FAX) 312-949-3700

Thomas Erickson, Research Associate
UND Energy & Environ. Research Center
P.O. Box 9018, University Station
Grand Forks, ND 58202-9018
701-777-5000

Mike Fabian, Aeronautical Engineer
University of Notre Dame
P.O. Box 6713
South Bend, IN 46660
219-289-9695

Mohammad Farooque, General Manager
CFC Development
Energy Research Corporation
3 Great Pasture Road
Danbury, CT 06813
203-792-1460, (FAX) 203-798-2945

Benjamin Fasano, Senior Engineer
IBM Corporation
40 E. 1580, Route 52
Hopewell Junction, NY 12533
914-894-9632, (FAX) 914-892-6256

Lanny Feder, Assistant Director
Program Development
Institute of Gas Technology
1825 K Street, N.W., Suite 503
Washington, DC 20006
202-785-3511, (FAX) 202-223-4625

Alan S. Feitelberg, Chemical Engineer
GE Corporate R&D
1 River Road
Building K-1, Room ES-103
Schenectady, NY 12301
518-387-5737, (FAX) 518-387-7258

Jerry Feret
Westinghouse
RD 5, Box 87
Greensburg, PA 15601
412-834-8795

R. A. (Al) Figueroa, Senior Engineer
San Diego Gas & Electric
P.O. Box 1831
San Diego, CA 92112
619-696-1924, (FAX) 619-696-1940

Thomas H. Fletcher, Associate Professor
Brigham Young University
350 Clyde Building
Provo, UT 84602
801-378-6236, (FAX) 801-378-7799

Anthony G. Fonseca, Director
Coal Utilization
Consol, Inc.
4000 Brownsville Road
Library, PA 15129
412-854-6797, (FAX) 412-854-6613

Chris A. Forbes, Manager
Program Development
Westinghouse Electric Corporation
Science & Technology Center
1310 Beulah Road
Pittsburgh, PA 15235-5098
412-256-2022, (FAX) 412-256-2002

Steven Freedman, Executive Engineer
Gas Research Institute
8600 West Bryn Mawr Avenue
Chicago, IL 60015
312-399-8390, (FAX) 312-399-8170

Charles E. French, Group Manager
Energy Conv.
Gas Research Institute
8600 West Bryn Mawr Avenue
Chicago, IL 60631
312-399-8243

David J. Funk, Technical Staff Member
Los Alamos National Laboratory
Group CLS-4, MS J567
Los Alamos, NM 87545
505-665-7566, (FAX) 505-665-4817

Marlene A. Galica, Combustion Engineer
Solar Turbines, Inc.
P.O. Box 85376, 2200 Pacific Highway
San Diego, CA 92186-5375
619-544-2321, (FAX) 619-544-5500

Chuck Garrett, Program Manager
U.S. Department of Energy, FE-72
Washington, DC 20585
301-903-2819, (FAX) 301-903-8350

Richard Gibson, Sr. Engineering Specialist
Allied Signal Aerospace Company
2525 West 190th Street
Torrance, CA 90509
310-512-3310, (FAX) 310-512-3974

Bruce B. Gillies, Programs Manager
Energy Technology Engineering Center
Rocketdyne Division, Rockwell
P.O. Box 7930
Canoga Park, CA 91309
818-586-5948

Donald R. Glenn, President
Fuel Cell Engineering Corporation
1627 K Street, N.W., Suite 403
Washington, DC 20006
202-785-9321, (FAX) 202-331-1403

David E. Godfrey, President
Manufacturing Resources, Inc.
9700 Rockside Road, Suite 110
Cleveland, OH 44125
216-524-9334

Lawrence P. Golan, Director
South Carolina Energy Center
Development Center, Clemson University
386-2 College Avenue
Clemson, SC 29634
803-656-2267, (FAX) 803-656-0142

Richard (Rocky) Goldstein, Manager
Fuel Cell Technology
Electric Power Research Institute
3412 Hillview Avenue, P.O. Box 10412
Palo Alto, CA 94303
415-855-2171, (FAX) 415-855-8501

Arnold Gordon, President
IGR
11000 Cedar Avenue, Suite 449
Cleveland, OH 44106
216-721-5511

George A. Graves, Jr., Senior
Research Engineer
University of Dayton Research Institute
300 College Park, KL 165
Dayton, OH 45469-0172
513-229-4415, (FAX) 513-229-3433

Sigmund Gronich, Program Manager
U.S. Department of Energy
1000 Independence Avenue
Washington, DC 20585
202-586-1623

Jeff A. Gunsher, Project Manager
The Dow Chemical Company
2030 Dow Center
Midland, MI 48674
517-636-0411, (FAX) 517-636-8127

C. Paul Gunzelman, Principal Engineer
Baltimore Gas & Electric Company
1000 Brandon Shores Road
Baltimore, MD 21226
410-787-5242, (FAX) 410-787-5299

J. C. Han, Professor
Texas A&M University
Mechanical Engineering Department
College Station, TX 77843
409-845-3738

W. R. Haney, Director of Marketing
Parker Hannifin Corporation
6507 Foxboro Drive
Mayfield Village, OH 44143
216-461-9763

Jim Hansen
Oak Ridge National Laboratory
P.O. Box 2003, MS 7294
Oak Ridge, TN 37831
615-241-2102, (FAX) 615-574-8481

Robert J. Hansen, Chief Scientist
Applied Research Laboratory
Penn State University, P.O. Box 30
State College, PA 16804
814-865-1419, (FAX) 814-865-1615

Robert Hanson, Principal Program Manager
EG&G Idaho, Inc.
P.O. Box 1625, MS 3885
Idaho Falls, ID 83415
208-526-9701

Bruce Harkins, Senior Research Engineer
Solar Turbines, Inc.
2200 Pacific Highway
San Diego, CA 92101
619-544-5398

Douglas P. Harrison, Alumni Professor
Louisiana State University
Department of Chemical Engineering
Baton Rouge, LA 70803
504-388-3066, (FAX) 504-388-1476

Robert Harrison, Consultant
ORNL
414 Waterburgy Circle
Cincinnati, OH 45231
513-771-3152

Paul O. Hedman, Professor
Brigham Young University
Chemical Engineering Department, 350 CB
Provo, UT 84602
801-378-6238, (FAX) 801-378-7799

Jack R. Hill
Turbine Metallurgical Engineer
A. Finkl & Sons
P.O. Box 4279
Greenville, SC 29608
800-635-8872, (FAX) 803-271-7997

Al Himy
Westinghouse/U.S. Navy
P.O. Box 18249
Pittsburgh, PA 15236
412-382-7883, (FAX) 412-382-7870

John H. Hirschenhofer, Project Manager
Gilbert/Commonwealth, Inc.
P.O. Box 1498
Reading, PA 19603
215-775-2600, (FAX) 215-775-2670

Gene Hoffman, Manager
National Materials Programs
Oak Ridge National Laboratory
Oak Ridge, TN 37831-6269
615-576-0735

Nate Hoffman, Senior Staff Scientist
Energy Tech Engineering Contractor
P.O. Box 7930
Canoga Park, CA 91309
818-586-5531

Robert S. Holcomb, Development Engineer
Oak Ridge National Laboratory
P.O. Box 2009
Building 9108, MS 8088
Oak Ridge, TN 37831-8088
615-574-0273, (FAX) 615-574-2102

Keith Hollingsworth, Assistant Professor
University of Houston
Department of Mechanical Engineering
Houston, TX 77204
713-743-4534, (FAX) 713-743-4503

John Holmgren, Interim Director
West Virginia University
617 N. Spruce Street, P.O. Box 6064
Morgantown, WV 26506-6064
304-293-2867, (FAX) 304-293-3749

Ivan Howell, Principal Engineer
Westinghouse Electric Corporation
P.O. Box 18249
Pittsburgh, PA 15236-0249
412-382-7676

Bertrand D. Hsu, Coal-Fueled
Locomotive Manager
GE Transportation Systems
2901 East Lake Road, Building 14-3
Erie, PA 16531
814-875-2110, (FAX) 814-875-3633

Michael Hsu, President
ZTEK Corporation
460 Totten Pond Road
Waltham, MA 02154
617-890-5665

Wayne Huebner, Associate Professor
University of Missouri - Rolla
222 McNutt Hall
Rolla, MO 65401
314-341-6129, (FAX) 314-341-6934

Steve Huval, Director of Operations
Stewart & Stevenson Services
16415 Jacintoport Boulevard
Houston, TX 77015
713-457-7867, (FAX) 713-452-7550

Mounir Ibrahim, Professor
Cleveland State University
Mechanical Engineering Department
Cleveland, OH 44115
216-687-2580

Carl Irwin, Research Director
West Virginia University
NRCCE
P.O. Box 6064
Morgantown, WV 26506-6064
304-293-7318

Daniel C. Itse, Chief Engineer
Physical Sciences, Inc.
20 New England Business Center
Andover, MA 01810
508-689-0003

Michael Izsak, Engineer
Burns & Roe Services Corporation
P.O. Box 18288
Pittsburgh, PA 15236
412-892-4190, (FAX) 412-892-4736

Eric Jumper, Professor
University of Notre Dame
Aerospace & Mechanical Engineering
South Bend, IN 46530
219-631-7680, (FAX) 219-631-8355

Ramish M. Kakwani, Senior
Technology Engineer
Detroit Diesel Corporation
13400 Outer Drive, West
Speed Code A07
Detroit, MI 48239-4001
313-592-5000

Doohee Kang, Senior Principal Engineer
Air Products
7201 Hamilton Boulevard
Allentown, PA 18103
215-481-8311, (FAX) 215-481-4566

Jayanta Kapat, Visiting Assistant Professor
Clemson University
Mechanical Engineering Department
P.O. Box 340921
Clemson, SC 29634-0921
803-656-3470, (FAX) 803-656-4435

Roger W. Karn, Senior Engineer
Pennsylvania Electric Company
1001 Broad Street
Johnstown, PA 15907
814-533-8395, (FAX) 814-533-8591

Mike Karnitz, Program Manager
Oak Ridge National Laboratory
P.O. Box 2008, Building 4515, MS 6065
Oak Ridge, TN 37831-8088
615-574-5150, (FAX) 615-574-6098

George Kassianides, Manager
Propulsion Systems
Westinghouse Machinery Tech.
P.O. Box 18249
Pittsburgh, PA 15236-0249
412-382-7652, (FAX) 412-382-4975

George B. Kenney, Associate Director
Massachusetts Institute of Technology
Materials Processing Center
77 Mass Avenue, Room 12-007 D
Cambridge, MA 02139
617-253-3244, (FAX) 617-258-6900

John Kessinger, General Manager
Westinghouse Electric
4400 Alafaya Trail
Orlando, FL 32817
407-281-2511

Ashok C. Khandkar, Senior Scientist
Ceramatec
2425 South 900 West
Salt Lake City, UT 84119
801-972-2455, (FAX) 801-972-1925

Mark J. Khinkis, Associate Director
Applied Combustion
Institute of Gas Technology
3424 South State Street
Chicago, IL 60616
312-890-6445, (FAX) 312-890-6460

Richard Kieffer, Engineer
Praxair Surface Technologies
P.O. Box 1705
Stow, OH 44224
216-688-1989, (FAX) 216-688-3440

S. G. Kimura, Manager
Combustion & Heat
GE Corporate R&D
1 River Road, Building K-1, ES-142
Schenectady, NY 12301
518-387-6653, (FAX) 518-387-7258

Robert B. King, Senior Program Engineer
NASA - Sverdrup
21000 Brookpark Road
Cleveland, OH 44135
216-433-6122

Carey A. Kinney, Program Manager
U.S. Department of Energy
FE-231
Washington, DC 20545
301-903-2827, (FAX) 301-903-2406

Josiah D. Knight, Associate Professor
Duke University
Mechanical Engineering Department
P.O. Box 90300
Durham, NC 27708-0300
919-660-5337, (FAX) 919-660-8963

T. Korakianitis, Assistant Professor
Washington University
Campus Box 1185, One Brookings Drive
St. Louis, MO 63130-4899
314-935-4346, (FAX) 314-935-4014

Jacob Korenberg, Vice President
Donlee Technologies, Inc.
693 North Hills Road
York, PA 17402
717-755-1081, (FAX) 717-755-0020

Jerry Koupal, Manager
Fossil Resource Group
Bechtel Power Corporation
9801 Washingtonian Boulevard
Gaithersburg, MD 20879
301-417-4042, (FAX) 301-216-1482

L. Krishnamurthy, Professor
Florida Institute of Technology
150 W. University Boulevard
Mechanical & Aerospace Engineering
Melbourne, FL 32901-6988
407-768-8000, (FAX) 407-984-8461

Michael Krumpelt
Argonne National Laboratory
9700 S. Cass Avenue
Argonne, IL 60439
708-252-8520

Gene H. Kucera, Chemist, Group Leader
Argonne National Laboratory
9700 South Cass Avenue
Argonne, IL 60439
708-252-4038, (FAX) 708-252-4176

Romesh Kumar, Group Leader
Argonne National Laboratory
9700 South Cass Avenue
Argonne, IL 60439
708-252-4342, (FAX) 708-252-4176

Ashok K. Kush, Technical Director
Fuel Cell Engineering Corporation
3 Great Pasture Road
Danbury, CT 06813
203-792-1460, (FAX) 203-798-2945

Ronald S. Lafleur, Assistant Professor
Clarkson University
P.O. Box 5725
Potsdam, NY 13699-5725
315-268-3823, (FAX) 315-268-6938

B. Lakshminarayana, Professor
Penn State University
153 J. Hammond Building
University Park, PA 16802
814-865-5551, (FAX) 814-865-7092

John A. Latcovich, Jr., Principal Engineer
ABB Power Generation, Inc.
1200 Willis Road
Richmond, VA 23237
804-743-4042, (FAX) 804-743-4018

Francis Lau
Process Development
Institute of Gas Technology
3424 South State Street
Chicago, IL 60616
312-949-3692, (FAX) 312-949-3700

Richard T. Lecren, Consulting
Combustion Engineer
Solar Turbines, Inc.
2700 Pacific Highway, P.O. Box 85376
San Diego, CA 92186-5376
619-544-5531, (FAX) 619-544-5500

Benson P. Lee
Technology Management, Inc.
9718 Lake Shore Boulevard
Cleveland, OH 44108-1049
216-541-1000, (FAX) 216-541-1000

Minyoung Lee, R&D Staff
GE Corporate R&D
P.O. Box 8
Schenectady, NY 12301
518-387-6455, (FAX) 518-387-7007

John D. Leeper, Senior Research Engineer
Southern California Edison
6090 North Irwindale Avenue
Irwindale, CA 91702
818-812-7543, (FAX) 818-812-7320

Anthony Leo, Manager of Engineering
Fuel Cell Engineering Corporation
3 Great Pasture Road
Danbury, CT 06813
203-792-1460, (FAX) 203-798-2945

Gary Leonard, Advanced Products Manager
GE Marine & Indust. Gas Turbine
1 Neumann Way
Cincinnati, OH 45246
513-552-6093, (FAX) 513-552-5008

William J. Lueckel, Jr., Vice President
Government Programs
International Fuel Cells
P.O. Box 739
South Windsor, CT 06074
203-727-2225, (FAX) 203-727-2319

Wayne L. Lundberg, Principal Engineer
Westinghouse Electric Corporation
Science & Technology Center
1310 Beulah Road
Pittsburgh, PA 15235-5098
412-256-2418, (FAX) 412-256-2002

Thomas M. Maloney, Supervisor
Sverdrup Technology, Inc.
21000 Brookpark Road, MS 309-1
Cleveland, OH 44135
216-433-6137, (FAX) 216-433-6160

Philip C. Malte, Professor
University of Washington
Mechanical Engineering, FU-10
Seattle, WA 98195
206-543-5486, (FAX) 206-685-8047

A. R. Marder, Associate Director
Energy Research Center
Lehigh University
117 Atlss Drive
Bethlehem, PA 18015
215-758-4095, (FAX) 215-758-5959

Mark A. Mares, Controller
Office of Budget
U.S. Department of Energy
1000 Independence Avenue, S.W.
Washington, DC 20585
202-586-4508

L. G. Marianowski, Director
Energy Conversion
Institute of Gas Technology
3424 South State Street
Chicago, IL 60616
312-949-3687, (FAX) 312-949-3700

Donald L. Maricle, Manager
Materials Engineering
International Fuel Cells
195 Governors Highway
South Windsor, CT 06074
203-727-2278, (FAX) 203-727-2319

Hans C. Maru, Executive Vice President
Energy Research Corporation
3 Great Pasture Road
Danbury, CT 06813
203-792-1460, (FAX) 203-798-2945

Nicholas J. Maskalick, Fellow Engineer
Westinghouse Electric Corporation
Science & Technology Center
1310 Beulah Road
Pittsburgh, PA 15235-5098
412-256-2020, (FAX) 412-256-2002

Arthur McGuigan, Senior Project Engineer
Westinghouse Electric Corporation
Power Generation Business Unit
4400 Alafaya Trail
Orlando, FL 32826-2399
407-281-3382, (FAX) 407-281-5014

G. B. Kirby Meacham, Associate
Michael A. Cobb & Company
18560 Parkland Drive
Shaker Heights, OH 44122
216-731-9005, (FAX) 216-731-8980

A. M. Mellor, Centennial Professor
Vanderbilt University
Box 1592, Station B
Nashville, TN 37235-1592
615-343-6214, (FAX) 615-343-6687

Donna J. Michalek, Assistant Professor
Michigan Technological University
ME-EM Department
1400 Townsend Drive
Houghton, MI 49931
906-487-2551, (FAX) 906-487-2822

Nguyen Q. Minh
Allied Signal Aerospace Company
2525 W. 190th Street
Department 93140, T-41
Torrance, CA 90504-6099
310-512-3515, (FAX) 310-512-2476

Thomas Modrak, Mechanical Engineer
Raytheon Engineers & Consultants
30 S. 17th Street
Philadelphia, PA 19301
215-422-3342, (FAX) 215-422-4241

Kevin Moore, Analyst
EG&G WASC, Inc.
P.O. Box 880, MS M02
Morgantown, WV 26507-0880
304-291-4018

George Mosinskis, Manager
Technology Development
American Gas Association
1515 Wilson Boulevard
Arlington, VA 22209
703-841-8572, (FAX) 703-841-8677

Vahid Motevalli, Assistant Professor
Worcester Polytechnic Institute
Mechanical Engineering Department
Worcester, MA 01609
508-831-5124, (FAX) 508-831-5680

Joel W. Muehlhauser, Administrator
Energy Conversion R&D
University of Tennessee Space Institute
B. H. Goethert Parkway
Tullahoma, TN 37388
615-393-7286, (FAX) 615-455-7266

Dale Mukavetz, Supervisor
Preliminary Design
Allison Gas Turbine
2001 S. Tibbs Avenue, Plant 8, T12A
Indianapolis, IN 46206-0420
317-230-2575, (FAX) 317-230-3009

David J. Najewicz, Manager
Energy & Environmental
GE Corporate R&D
1 River Road, Building K-1, ES-201
Schenectady, NY 12301
518-387-6427, (FAX) 518-387-7258

Dan Nathanson, Vice President
ZTEK Corporation
468 Totten Pond Road
Waltham, MA 02154
617-890-5605, (FAX) 617-890-3731

Mohammad Nawaz, Engineering Specialist
Bechtel Corporation
50 Beale Street
San Francisco, CA 94105-1895
415-768-0780, (FAX) 415-768-3580

Charles Neulander, Principal
Chemical Engineer
Fluor Daniel
3333 Michelson Drive
Irvine, CA 92730
714-975-3755, (FAX) 714-975-5742

Richard A. Newby, Principal Engineer
Westinghouse Electric Corporation
Science & Technology Center
1310 Beulah Road
Pittsburgh, PA 15235
412-256-2210

Richard L. Newland, Manager of
Engineering Sales
Haldor Topsoe, Inc.
P.O. Box 58767
Houston, TX 77258-8767
713-480-2600, (FAX) 713-480-3371

Grady B. Nichols, Vice President
Environmental Sciences
Southern Research Institute
P.O. Box 55305
Birmingham, AL 35255-5305
205-581-2361, (FAX) 205-581-2448

John G. Nourse, Manager
Advanced Technology
General Electric Company
1 River Road, 53-425
Schenectady, NY 12345
518-385-9191, (FAX) 518-385-4314

Robert L. Novak, Manager
Materials Technology
Westinghouse PGBU
4400 Alafaya Trail
Orlando, FL 32826
407-281-3185, (FAX) 407-281-2080

John O'Sullivan, Manager
Fuel Cells
Electric Power Research Institute
P.O. Box 10412, 3412 Hillview Avenue
Palo Alto, CA 94303
415-855-2292, (FAX) 415-855-8501

Richard Oldenborg, Deputy Group Leader
Los Alamos National Laboratory
Group CLS-4, MS J567
Los Alamos, NM 87545
505-667-2096, (FAX) 505-667-0440

Nelson J. Orozco, Project Engineer
Hague International
3 Adams Street
S. Portland, ME 04106
207-799-7346, (FAX) 207-799-6743

Rachid Oukaci, Research Assistant Professor
University of Pittsburgh
1249 Benedum Hall
Chemical Engineering Department
Pittsburgh, PA 15261
412-624-4754, (FAX) 412-624-9639

William R. Owens, Sr. Program Manager
Gilbert/Commonwealth, Inc.
19644 Club House Road, Suite 820
Gaithersburg, MD 20879
301-869-9191, (FAX) 301-977-7507

George L. Padgett, Manager
Advanced Product Development
Solar Turbines, Inc.
2200 Pacific Highway
San Diego, CA 92186-5376
619-544-5708, (FAX) 619-544-2682

David H. Pai, President
Foster Wheeler Development Corporation
12 Peach Tree Hill Road
Livingston, NJ 07039
201-535-2309, (FAX) 201-535-2242

Walter G. Parker, Manager
Applications Engineering
Westinghouse Electric Corporation
Science & Technology Center
1310 Beulah Road
Pittsburgh, PA 15235-5098
412-256-2417, (FAX) 412-256-2002

Bill Parks, Program Manager
U.S. Department of Energy
1000 Independence Avenue, S.W.
Washington, DC 20585
202-586-2093

Charles Pax, Program Manager
U.S. Department of Energy
FE-73/Germantown
Washington, DC 20585
301-903-2832, (FAX) 301-903-2713

Michael A. Petrik
Technology Management, Inc.
9718 Lake Shore Boulevard
Cleveland, OH 44108-1049
216-541-1000, (FAX) 216-541-1000

John Plunkett, Engineer
EG&G WASC, Inc.
P.O. Box 880, MS M02
Morgantown, WV 26507-0880
304-291-4605

Duane H. Pontius, Head
Particulate Science Division
Southern Research Institute
P.O. Box 55305
Birmingham, AL 35255-5305
205-581-2268, (FAX) 205-581-2448

Dennis Raden, Senior Program Manager
Radian Corporation
P.O. Box 201088
Austin, TX 78720-1088
512-454-4797, (FAX) 512-343-1833

Adrian S. Radziwon, Senior Engineer
Burns & Roe Services Corporation
P.O. Box 18288
Pittsburgh, PA 15236
412-892-4672, (FAX) 412-892-4736

Massood Ramezan, Principal Engineer
Burns & Roe Services Corporation
P.O. Box 18288
Pittsburgh, PA 15236
412-892-6451, (FAX) 412-892-4736

A. K. (Kam) Rao, Project Manager
Cooper Bessemer
1050 Lincoln Avenue
Grove City, PA 16127-1898
412-458-3550, (FAX) 412-458-3525

Asok Ray, Professor
Penn State University
205 Mechanical Engineering Building
University Park, PA 16802
814-865-6377, (FAX) 814-863-4848

Emerson R. Ray, Manager
Agency Programs
Westinghouse Electric Corporation
Science & Technology Center
1310 Beulah Road
Pittsburgh, PA 15235-5098
412-256-2125, (FAX) 412-256-2002

Michael M. Reischman, Associate Dean
Graduate Studies
Penn State University
College of Engineering
101 Hammond Building
University Park, PA 16802
814-865-4542, (FAX) 814-863-0497

A. John Rezaiyan, Program Manager
K&M Engineering
2001 L Street, N.W., Suite 500
Washington, DC 20036
202-728-0390

Ivan G. Rice, Consultant
Gas Turbines & Rotating Equipment
P.O. Box 233
Spring, TX 77383
713-353-5040, (FAX) 713-353-5040

Thomas J. Richards, Staff Engineer
Caterpillar, Inc.
Technical Center - Building A
P.O. Box 1875
Peoria, IL 61656-1875
309-578-8597, (FAX) 309-578-6988

Jeffery H. Richardson, Division Leader
Lawrence Livermore National Laboratory
P.O. Box 808, MS L-326
Livermore, CA 94550
510-423-5187, (FAX) 510-422-3360

Irven H. Rinard, Professor
City College of CUNY
349 West 21st Street
New York, NY 10011
212-645-1519, (FAX) 212-650-6660

Thomas Risley, Manager
Turbomachinery
Westinghouse Electric Corporation
P.O. Box 18249
Pittsburgh, PA 15236-0249
412-382-7676

Larry Roe, Assistant Professor
Virginia Tech
Mechanical Engineering Department
Blacksburg, VA 24061
703-231-7295, (FAX) 703-231-9100

David A. Rohy, Director
Development Engineer
Solar Turbines, Inc.
2200 Pacific Highway
San Diego, CA 92138
619-544-5078

Charles M. Rose, Vice President and
General Manager
Environmental Energy Systems
811 Route 51 S.
Large, PA 15025
412-382-7124, (FAX) 412-382-4927

Tom Rosfjord, Senior Project Engineer
United Technologies Res.
MS 16
East Hartford, CT 06108
203-727-7418, (FAX) 203-727-7669

John W. Rothrock, Project Manager
Allison Gas Turbine
P.O. Box 420, Mail Stop W-16
Indianapolis, IN 46206-0420
317-230-3057, (FAX) 317-230-5600

George Rudins, Acting Deputy
Assistant Secretary
U.S. Department of Energy
19901 Germantown Road, FE-23
Germantown, MD 20585
301-903-3991

Robert Ruhl, Consultant
Technology Management, Inc.
9718 Lake Shore Boulevard
Cleveland, OH 44108-1049
216-541-1000, (FAX) 216-541-1000

Thomas W. Ryan, Manager
Combustion Technology
Southwest Research Institute
6220 Culebra Road
San Antonio, TX 78228
210-522-3192, (FAX) 210-522-5720

Anthony F. Sammells, President
Eltron Research, Inc.
2830 Wilderness Place, Suite E
Boulder, CO 80301-5455
303-440-8008

Robert San Martin, Acting Assistant
Secretary for Energy
U.S. Department of Energy
1000 Independence Ave., S.W.
Room 6C-016
Washington, DC 20585
202-586-9220, (FAX) 202-586-9260

S. G. Sankar, President
Advanced Materials Corporation
100 N. Bellefield Avenue
Pittsburgh, PA 15213
412-268-5649, (FAX) 412-268-3101

Domenic Santavicca, Professor
Penn State University
132 Research Building E
University Park, PA 16802
814-863-1863, (FAX) 814-865-3389

Srinivasan Sarangapani, Vice President
ICET, Inc.
916 Pleasant Street, Unit 12
Norwood, MA 02062
617-769-6064, (FAX) 617-769-6064

Augustine J. Scalzo, Technical Director
Westinghouse Electric Corporation
4400 Alafaya Trail, MC 205
Orlando, FL 32826
407-281-2030, (FAX) 407-281-5633

Frank Schora, Consultant
M-C Power
830 Fox Hill Road
Chatham, MA 02633
508-945-9034, (FAX) 508-945-4120

Garland E. Scott, Jr., CEO
RSI Associates, Inc.
1580 N. Claremont Blvd., Suite 101
Claremont, CA 91711
909-626-4120, (FAX) 909-624-6356

Joseph Scroppo, Senior Project Manager
M-C Power
830 Fox Hill Road
Chatham, MA 02633
508-986-8040, (FAX) 508-945-4120

Daniel J. Seery, Senior Program Manager
UTRC
411 Silver Lane
East Hartford, CT 06105
203-727-7150

Jack S. Siegel, Acting Assistant
Secretary for Energy
U.S. Department of Energy
Forrestal, FE-20
Washington, DC 20585
202-586-1650

Terrence W. Simon, Professor
University of Minnesota
M.E. Department
111 Church Street, S.E.
Minneapolis, MN 55455
612-625-5831, (FAX) 612-624-1398

Raj N. Singh, Professor
University of Cincinnati
Department of Materials Science
498 Rhodes Hall
Cincinnati, OH 45221-0012
513-556-5172, (FAX) 513-556-2569

Alok Sinha, Associate Professor
Penn State University
Mechanical Engineering Department
University Park, PA 16802
814-237-1867

Andrew Skok, Manager
Facilities Development
Energy Research Corporation
3 Great Pasture Road
Danbury, CT 06813
203-792-1460, (FAX) 203-798-2945

Robert E. Smith, Project Engineer
U.S. Naval Surface Warfare Center
Code 824, CDNSWC
Annapolis, MD 21402
410-267-2148, (FAX) 410-267-3553

Leo A. Smolensky, Technical Director
LSR Technologies, Inc.
898 Main Street
Acton, MA 01720
508-635-0123, (FAX) 508-635-0058

Paul E. Sojka, Associate Professor
Purdue University
School of Mechanical Engineering
West Lafayette, IN 47907-1003
317-494-1536, (FAX) 317-494-0530

William (Bill) Sowa, Associate Director
UCICL
University of California, Irvine
UCI Combustion Laboratory
Irvine, CA 92717
714-856-8452, (FAX) 714-856-7423

Sree Srinivasan, Lead Research Engineer
Air Products
7201 Hamilton Boulevard
Allentown, PA 18103
215-481-5848, (FAX) 215-481-4566

Stuart Starrett, Director
Mechanical Research
Southern Research Institute
P.O. Box 55305
Birmingham, AL 35255-5305
205-581-2452, (FAX) 205-581-2448

Peter Steiner, Vice President
Foster Wheeler Development Corporation
12 Peach Tree Hill Road
Livingston, NJ 07039
201-535-2314, (FAX) 201-535-2242

Paul Stolpman, Acting Director
EPA
401 Street, S.W., Mail Stop 6201 (J)
Washington, DC 20460
202-260-2090

Alan J. Streb, Deputy Assistant Secretary
U.S. Department of Energy
1000 Independence Avenue, S.W.
Washington, DC 20585
202-586-9232, (FAX) 202-586-9234

Franz Stuhlmuller
Dipl. - Ing.
Hammerbacher Str.
P.O. Box 32 20
Erlangen, 91058
Germany

C. S. Subramanian, Associate Professor
Florida Institute of Technology
150 W. University Boulevard
Melbourne, FL 32901
407-768-8000, (FAX) 407-984-8461

Yutaka Sugiyama, Electrical Engineer
Naval Civil Engineering Lab
560 Laboratory Drive, Code L72
Port Hueneme, CA 93043
805-982-1608, (FAX) 805-982-1409

Jim C. Swinler, Support Coordinator
EG&G WASC, Inc.
P.O. Box 880, MS M02
Morgantown, WV 26507-0880
304-291-4681

Paul B. Tarman, President
M-C Power
8040 S. Madison Street
Burr Ridge, IL 60521
708-986-8040, (FAX) 708-986-8086

Walter G. Taschek, Chief
Systems Assessment Team
U.S. Army Belvoir RDE Center
SATBE-FEA
Fort Belvoir, VA 22060
703-704-2633, (FAX) 703-704-3794

Owen S. Taylor, Manager
Westinghouse Electric Corporation
1310 Beulah Road
Pittsburgh, PA 15235
412-256-2270, (FAX) 412-256-1948

Heinz Termuehlen, Chief Engineer
Dir. Product Plan
Siemens Power Corporation
2001 U.S. Highway 301
Palmetto, FL 34221
813-723-4145, (FAX) 813-723-4177

Bruce Thomson, Manager
Business Development
Textron Specialty Materials
2 Industrial Avenue
Lowell, MA 01851
508-934-7519, (FAX) 508-934-7593

George Tsatsaronis, Professor
Tennessee Tech University
Mechanical Engineering Department
P.O. Box 5032
Cookeville, TN 38505
615-372-3681, (FAX) 615-372-3898

G. D. Turner, Deputy Director
Turbine Engines
United States Air Force
WL/P02 Building 18, 1950 5th Street
Wright Patterson AFB, OH 45433
513-255-4100

Niels R. Udengaard, Manager
Process Engineering
Haldor Topsoe, Inc.
P.O. Box 58767
Houston, TX 77258-8767
713-480-2600, (FAX) 713-480-3371

Septimus Van Der Linden, Vice President
ABB Power Generation, Inc.
1460 Livingstone Avenue
N. Brunswick, NJ 08902
908-932-6319, (FAX) 908-932-6463

Mark Van Roode, Consulting
Research Scientist
Solar Turbines, Inc.
P.O. Box 85376, 2200 Pacific Highway
San Diego, CA 92186
619-544-5549, (FAX) 619-544-2836

U. Vandsburger, Professor
Virginia Tech
Mechanical Engineering Department
Blacksburg, VA 24061-0238
703-231-4459, (FAX) 703-231-9100

Suresh Venkatesan, Chemical Engineer
EG&G WASC, Inc.
P.O. Box 880, MS M02
Morgantown, WV 26507-0880
304-291-4962

Stephen C. Verikios, Program Manager
U.S. Department of Energy
FE-231
Washington, DC 20585
301-903-2824, (FAX) 301-903-2406

Ron Walecki, Business Development
Manager
Ceramic Components
2525 W-190th Street
Torrance, CA 90509-2960
310-512-5916, (FAX) 310-512-5901

Donald K. Walter, Director
Office Waste Reduction
U.S. Department of Energy
CE-22
Washington, DC 20585
202-586-4679, (FAX) 202-586-7114

Ting Wang, Associate Professor
Clemson University
Department of Mechanical Engineering
Box 340921
Clemson, SC 29634-0921
803-656-5630, (FAX) 803-656-4435

Stephen Waslo, Program Manager
U.S. Department of Energy
Field Office-Chicago
4900 South Cass Avenue
Argonne, IL 60439
708-252-2143

Richard A. Wenglarz, Senior Staff
Research Scientist
Allison Gas Turbine
P.O. Box 420, Speed Code T14
Indianapolis, IN 46206-0420
317-230-2185, (FAX) 317-230-3691

Michael P. Whelan, Manager
Cogeneration & Fuel Cells
Gas Research Institute
8600 West Bryn Mawr Avenue
Chicago, IL 60631
312-399-8339, (FAX) 312-399-8170

David J. White, Manager
Advanced Development
Solar Turbines, Inc.
2200 Pacific Highway, P.O. Box 85376
San Diego, CA 92186-5376
619-544-5542, (FAX) 619-544-2681

Thomas F. Widmer, Consultant
AES Corporation
17 Spring Street
Westerly, RI 02891
401-596-6806

Sunil Wijeyesekera, Research Leader
Dow Chemical
CR-ACL, 1776 Building
Midland, MI 48674
517-636-8402, (FAX) 517-638-9716

John Wills, Director
Business Development
Rolls-Royce, Inc.
Industrial Power Marketing
11911 Freedom Drive
Reston, VA 22090
703-318-9008, (FAX) 703-318-9009

Robert P. Wilson, Vice President
Combustion & Fuels
Arthur D. Little, Inc.
20 Acorn Park
Cambridge, MA 02140
617-498-5806

John Wiss, Professor
Carnegie Mellon University
5000 Forbes Avenue
Pittsburgh, PA 15213-3890
412-268-2337, (FAX) 412-268-3797

Joseph A. Woerner, Project Engineer
U.S. Naval Surface Warfare Center
Code 824, CDNSWC
Annapolis, MD 21402
410-267-2148, (FAX) 410-267-3553

George T. Wolff, Engineer
Consolidated Edison Company
4 Irving Place, Room 1428
New York, NY 10003-2418
212-460-2909, (FAX) 212-529-8511

Ronald H. Wolk, Director
AFPS Department
Electric Power Research Institute
P.O. Box 10412
Palo Alto, CA 94303
415-855-2000

Richard R. Woods, Marketing Manager
M-C Power
830 Fox Hill Road
Chatham, MA 02633
708-986-8040, (FAX) 708-945-4120

Randy Wotring, Vice President and
Group Director
EG&G WASC, Inc.
P.O. Box 880, MS D02
Morgantown, WV 26507-0880
304-291-4298

S. Ronald Wysk, Managing Director
LSR Technologies, Inc.
898 Main Street
Acton, MA 01720
508-635-0123, (FAX) 508-635-0058

Rich Yetter, Research Scientist
Princeton University
Department of Mechanical & Aerospace
Engineering
Princeton, NJ 08544
609-258-2947, (FAX) 609-258-1939

Edward F. Young, Visiting Asst. Professor
University of South Carolina
Mechanical Engineering Department
Sumwalt Building, Room 103
Columbia, SC 29208
803-777-0084

Sam Y. Zamrik, Professor of
Engineering Mechanics
Penn State University
121 Hammond Building
University Park, PA 16802
814-865-5241

Fred H. Zerkel, Vice President
Institute of Gas Technology
1825 K Street, N.W., Suite 503
Washington, DC 20006
202-785-3511, (FAX) 202-223-4625

Qian Zhou, Research Engineer
NOXSO Corporation
P.O. Box 469
Library, PA 15129
412-854-1200, (FAX) 412-854-5729

Bernard M. Ziemianek, Fuel Cell
Issues Manager
Pennsylvania Power & Light Company
344 South Poplar Street
Hazleton, PA 18201
717-459-7303, (FAX) 717-459-7478

# Appendix C

## METC Participants

Chuck Alsup, Project Manager
304-284-5432, MS D06

Rodney Anderson, Physical Scientist
304-291-4709, MS B05

Rita A. Bajura, Division Director
304-291-4109, MS D01

Thomas F. Bechtel, Director
304-291-4931, MS C02

Robert C. Bedick, Division Director
304-291-4505, MS E06

Justin L. Beeson, Chemical Engineer
304-291-4671, MS C04

Louis H. Berkshire, Program Analyst
304-291-4189, MS E01

John W. Byam, Jr.
International/Domestic Business Development
304-291-4064, MS A05

Cliff Carpenter, Mechanical Engineer
304-291-4041, MS D06

Kent H. Casleton, Research Chemist
304-291-4573, MS N05

Mingking K. Chyu, Mechanical Engineer
304-284-5461, MS L07

Daniel Cicero, Project Manager
304-291-4826, MS C04

Floyd Crouse, General Engineer
304-291-4535, MS D01

Kamalendu Das, Physical Scientist
304-291-4065, MS C05

Randy Dellefield, PFBC Product Manager
304-291-4725, MS D01

John Duda, Petroleum Engineer
304-291-4217, MS E01

Donald W. Geiling, Project Manager
304-291-4784, MS D06

Randall Gemmen, Mechanical Engineer
304-291-4536, MS N05

Tom George, Project Manager
304-291-4825, MS D06

Madhav R. Ghate, Division Director
304-291-4135, MS C04

Robert W. Gross, Mechanical Engineer
304-291-4235, MS C05

Hugh D. Guthrie, General Engineer
304-291-4632, MS B06

Mark A. Hadley, Mechanical Engineer
304-291-4929, MS N05

Jack S. Halow, Division Director
304-291-4114, MS N06

Thomas J. Hand, Chemical Engineer
304-291-4642, MS E01

Larry Headley, Division Director
304-291-4314, MS B05

Norman Holcombe, Project Manager
304-291-4829, MS C05

Diane Hooie, Project Manager
304-291-4524, MS D06

Lisa Jarr, Patent Advisor
304-291-4555, MS A03

Chuck Komar, Staff Engineer
304-291-4107, MS B05

Wu K. Lan, Project Manager
304-291-4044, MS C05

William T. Langan, Division Director
304-291-4519, MS D04

William Lawson, Division Director
304-291-4173, MS A03

Abbie Layne, Petroleum Engineer
304-291-4603, MS E01

Patrick Le, Mechanical Engineer
304-291-4324, MS E01

George Lee, Chemical Engineer
304-291-4824, MS E01

Hsue-Peng Loh, Chemical Engineer
304-291-4546, MS E01

James Longanbach, Project Manager
304-291-4659, MS C04

Kanwal Mahajan, General Engineer
304-291-4965, MS E01

Daniel J. Maloney, Physical Scientist
304-291-4629, MS N05

Kenneth E. Markel, Jr., Deputy Associate Director
304-291-4364, MS B06

Manville J. Mayfield, Fuel Cells Product Manager
304-291-4847, MS D01

Heather M. McDaniel, Mechanical Engineer
304-284-5430, MS C04

Ted McMahon, General Engineer
304-291-4865, MS C04

Mike McMillian, Mechanical Engineer
304-291-4669, MS N05

Paul Micheli, Project Manager
304-291-4625, MS D06

Darren Mollot, Project Manager
304-284-5447, MS C04

M.J. Moran, ORAU Faculty Fellow
304-284-5461, MS L07

Harvey Ness, Branch Chief
304-291-4172, MS C04

Thomas S. Norton, Mechanical Engineer
304-291-4617, MS N05

John E. Notestein, Chief Engineer
304-291-4232, MS A05

Edward L. Parsons, Jr., Branch Chief
304-291-4533, MS D06

Leland E. Paulson, Project Manager
304-291-4074, MS D06

Kelly D. Pearce, Mechanical Engineer
304-284-5424, MS B05

Lawrence Rath, Branch Chief
304-291-4094, MS E01

George A. Richards, Mechanical Engineer
304-291-4458, MS N05

Luke H. Rogers, Engineer
304-291-4231, MS N05

Louis A. Salvador, Associate Director
304-291-4147, MS B06

Dale Schmidt, IGCC Product Manager
304-291-4359, MS D01

Harold D. Shoemaker, Project Manager
304-291-4715, MS E06

William Cary Smith, Project Manager
304-291-4260, MS D06

Larry D. Strickland, Division Director
304-291-4494, MS N04

Fred Sudhoff, Chemical Engineer
304-291-4560, MS E01

Brad Tomer, General Engineer
304-291-4692, MS E01

Suellen Van Ooteghem, Acting NEPA Group Leader
304-284-5443, MS N02

John Vanosdol, Mechanical Engineer
304-284-5446, MS D06

Venkat K. Venkataraman, Project Manager
304-291-4105, MS C05

Holmes A. Webb, Product Manager
304-291-4724, MS D01

Paul Wieber, Associate Director
304-291-4544, MS B05

Mark Williams, General Engineer
304-291-4747, MS D06

John S. Wilson, Deputy Director
304-291-4259, MS A05

John Wimer, Mechanical Engineer
304-291-4124, MS N04

Anthony Zammerilli, Petroleum Engineer
304-291-4641, MS E01

Charles M. Zeh, Product Manager
304-291-4265, MS D01